A Thesis Entitled

SYNTHESIS OF ALLYLIC MONOMERS AND POLYMERS CONTAINING SULPHUR AND PHOSPHORUS FUNCTIONALITIES FOR SOLID STATE NUCLEAR TRACK DETECTION

Submitted to Goa University for the Award of the Degree of

DOCTOR OF PHILOSOPHY

In

CHEMISTRY

By

Mr. DIPTESH GURUDAS NAIK

M. Sc.

Under the Guidance of

PROF. VISHNU S. NADKARNI

Department of Chemistry

GOA UNIVERSITY

Taleigao Plateau, Goa 403206

INDIA

APRIL 2017

A Thesis Entitled

SYNTHESIS OF ALLYLIC MONOMERS AND POLYMERS CONTAINING SULPHUR AND PHOSPHORUS FUNCTIONALITIES FOR SOLID STATE NUCLEAR TRACK DETECTION

Submitted to Goa University for the Award of the Degree of

DOCTOR OF PHILOSOPHY

In

CHEMISTRY

By

Mr. DIPTESH GURUDAS NAIK

M. Sc.

Under the Guidance of

PROF. VISHNU S. NADKARNI

Department of Chemistry

GOA UNIVERSITY

Taleigao Plateau, Goa 403206

INDIA

APRIL 2017

DEPARTMENT OF CHEMISTRY

CERTIFICATE

This is to certify that the thesis entitled, "**Synthesis of allylic monomers and polymers containing Sulphur and Phosphorus functionalities for Solid State Nuclear Track Detection**" submitted by Mr. **DIPTESH GURUDAS NAIK**, is a record of research work carried out by the candidate during the period of study under my supervision and that it has not previously formed the basis for the award of any degree or diploma or other similar titles.

Goa University   **Prof. Vishnu S. Nadkarni**
April 2017   Research Guide
                                                     Department of Chemistry
                                                     Goa University

DECLARATION

I hereby declare that the work embodied in the thesis entitled "**Synthesis of allylic monomers and polymers containing Sulphur and Phosphorus functionalities for Solid State Nuclear Track Detection**" is the result of investigations carried out by me under the guidance of **PROF. VISHNU S. NADKARNI** at Department of Chemistry, Goa University and that it has not previously formed the basis for the award of any degree or diploma or other similar titles.

In keeping with the general practice of reporting scientific observations, due acknowledgement has been made wherever the work described is based on the findings of other investigators.

Goa University   **Mr. Diptesh G. Naik**
April 2017   Ph.D. Student
                                                   Department of Chemistry
                                                   Goa University

ACKNOWLEDGEMENT

Undertaking this Research work has been a truly life-changing experience for me and it would not have been possible to do without the support and guidance that I received from many people, so I would like to thank all the people who have supported me throughout my journey of Ph. D. work.

First and foremost, I would like to express my sincere gratitude towards my guide, **Prof. Vishnu S. Nadkarni**; who has supported me throughout my research with his exquisite guidance, knowledge and vision of research. The work presented would have not been accomplished without his enthusiasm to motivate me in every step of my research. Without his guidance and constant feedback, this PhD would not have been materialized. I am thankful for the patience he has shown during my difficult times and also allowing to work independently. I will be forever grateful to him throughout my life.

I would like to thank my Subject Expert, **Prof. Santosh G. Tilve**, *Professor, Department of Chemistry, Goa University,* Goa for re-evaluating my research work periodically.

I wish to thank **Prof. Varun Sahni***,* Vice-Chancellor, Goa University and *Prof. Y. V. Reddy*, Registrar, Goa University, for their valuable support. Also, I would like to thank *Prof. Satish Shetye*, former Vice-Chancellor, Goa University and *Prof. Vijayendra Kamat,* former Registrar of Goa University.

My sincere thanks to **Prof. B. R. Srinivasan**, Head, Department of Chemistry, Goa University, and former heads *Prof. S. G. Tilve*, *Prof. A. V. Salkar*, for their constant support during my research work. I also thank **Prof. A. V. Salkar**, Dean, faculty of Natural Science and former Deans, *Prof J. Disa* and *Prof. J. B. Fernandes*. Heartfelt thanks goes to all the teachers from Department of Chemistry, *Prof. S. G. Tilve, Dr. V. M. S. Verenkar,*

help and support. I am also obliged to all Chemistry Research Scholars namely; *Dattaprasad, Daniel, Mira, Sagar, Prajesh, Shambhu, Satu, Durga, Dr. Madhavi Naik, Mayuri, Mithil, Rita, Savita, John, Vishnu, Chandan, Rahul, Sudesh, Kedar, Pooja, Celia, Apurva, Madhavi Shet, Prajoyti, Pratibha and Sudarshana* for making the entire PhD. research work at the University more lively, more scientific and memorable one.

Special thanks to my dear friends *Rohit Naik and Pranav Naik* who always supported me during hard times in my life.

This journey of Research work would have not been possible without the support and prayers of my parents. Words are at short to convey my feelings towards my beloved parents, ***Gurudas Naik*** and ***Pushpa Naik*** for their unconditional love, support and sacrifices to give me best possible life. I am very much indebted to my family who supported me in every possible way to see the completion of this work. I thank them whole heartedly for their efforts. I also thank my elder brother ***Mr. Vasudev G. Kavlekar***, my soul mate *Mrs. Shraddha Naik* and all the *family members* for their support.

Above all I owe it to Almighty GOD for granting me the wisdom, health and strength to undertake this research work and enabling me to its completion.

||Hare Krishna||

Mr. DIPTESH GURUDAS NAIK

Dedicated

To

My Beloved

Parents

TABLE OF CONTENT

GENERAL REMARKS

◆   Commercial reagents were used without further purification.

◆   Solvents were distilled prior to use and dried whenever necessary using standard procedures.

◆   Petroleum ether refers to the hydrocarbon fraction collected in the boiling range 60-80 °C.

◆   Thin layer chromatography (TLC) was carried out on silica gel 60 F254 aluminium plates purchased from Merck.

◆   Chromatographic purification was conducted by column chromatography using silica gel (60-120 mesh size) or by flash chromatography using silica gel (230-400 mesh size) on Combiflash Companion instrument.

◆   All the melting points and boiling points were recorded using Thiele's tube and are uncorrected.

◆   The compounds numbers, figure numbers, scheme numbers and reference numbers are referred to the particular chapter.

◆   IR spectra were recorded on Shimadzu FT-IR spectrophotometer.

◆ ^{1}H (400 MHz) and ^{13}C (100 MHz) NMR spectra were recorded on Bruker AVANCE 400 MHz instrument and the multiplicities of carbon signals were obtained from DEPT experiment.

◆   High-resolution mass spectra (HRMS) were recorded on a MicroMass ES-QTOF Mass spectrometer (at IISc. Bangalore).

◆   Gas Chromatograph was recorded on Nucon 5700 Gas Chromatographer using capillary column.

◆   Optical glass plates from Schott, Germany and Teflon^{TM} sheets were used for preparation of polymer molds. Polymerization was carried using a polymerization bath controlled using microprocessor-based electronic temperature controller F25 HP from M/s Julabo, Germany.

ABBREVIATIONS

1. General Abbreviations

aq.	Aqueous	Equiv.	Equivalent
b.p.	Boiling point	*cat.*	Catalytic
conc.	Concentrated	*TLC / tlc*	Thin layer chromatography
dil.	Dilute	*atm.*	Atmospheric
Eq.	Equation/s	RT / rt	Room temperature
fig.	Figure	sat.	Saturated
g	Gram/s	*et al.*	Et alia (and others)
h	Hour/s	*psi*	Pounds per square inch
hv	Irradiation	*MS*	Molecular sieves
lit.	Literature	*p*	Para
m.p.	Melting point	Expt.	Experiment
mg	Milligram/s	Temp.	Temperature
mL	Millilitre	anhyd.	Anhydrous
mmol	Millimol	*Calcd.*	Calculated
Min.	Minute/s	°C	Degree Celcius
%	Percentage	DTD	Dielectric track detectors
w/w	weight by weight	EM	Electron microscope
sec	Second/s	V_t	Track etch rate
DP	Degree of polymerization	θc	Critical angle of etching
CE	Chemical etching	c	Velocity of light
ECE	Electrochemical etching	m	Mass of the particle
OM	Optical microscope	Tg	Glass transition temperature
V_b	Bulk etch rate	V	Velocity of charged particle
S	Sensitivity		

2. Spectroscopic Abbreviations

δ	Delta (Chemical shift in ppm)	*m/z*	Mass to charge ratio
$CDCl_3$	Deuterated chloroform	dd	Doublet of doublet
$DMSO-d_6$	Deuterated dimethyl sulfoxide	td	Triplet of a doublet
DEPT	Distortionless Enhancement by Polarization Transfer	HRMS	High Resolution Mass Spectrum
cm^{-1}	Frequency in wave number	t	Triplet
$\tilde{v}$	Frequency maximum	d	Doublet
Hz	Hertz	br	Broad
HPLC	High Performance Liquid Chromatography	Cq	Quaternary carbon
IR	Infrared	s	Singlet
MHz	Megahertz	*J*	Coupling constant
NMR	Nuclear magnetic resonance	m	Multiplet
ppm	Parts per million	M^+	Molecular ion
UV	Ultra violet	q	Quartet

3. Compound Abbreviations

AA	Allyl alcohol	ADC	Allyl diglycol carbonate
ATC	Allyl thiodiglycol carbonate	ADS	Allyl diglycol sulphite
SDAC	2,2'-sulfonyldiethanol bis(allyl carbonate)	PEBDP	Pentaerythrityl bis (diallylphosphoramidate)
BP	Benzoyl peroxide	CN	Nitocellulose (cellulose nitrate)
CHPC	Cyclohexyl peroxydicarbonate	DEG	Diethylene glycol
CR-39	ADC polymer (Trademark of PPG Industries, UK)	DEAS	Diethylene glycol bis(allyl sulfonate)
DAC	Diallyl carbonate	DAS	DiaIly1 sulphite
DVS	Divinyl sulfone	DOP	Dioctyl phthalate
IPA	Isopropyl alcohol	IPP	Isopropylperoxydicarbonate
LR-115	(Trademark) CN SSNTD film manufactured by Kodak Pathe, France	NADAC	N-(Allyloxycarbonyl) diethanol amine bis(ally1 carbonate)
NAAAC	N-Allyloxycarbonyl ammediol bis(allyl carbonate)	PETAC	Pentaerythritol tetrakis(ally1 carbonate)
DMPDDP	2,2-dimethylpropan-1,3-diyl diallylphosphoramidate	PeAC	Pentanediol bis(ally1 carbonate)
SR-86(10)	Copolymer of CR-39:DEAS 9:1 w/w	SR-86(20)	Copolymer of CR-39:DEAS 8:2 w/w
PC	Polycarbonate	BP-1	Barium phosphate glass
PET	Polyethylene terephthalate	PP	Polypropylene
TBPB	t-butyl peroxy benzoate	AIBN	Azobisisobutyronitrile
SSNTD	Solid state nuclear track detection	SSNTD's	Solid State Nuclear Track detectors
TAP	Triallyl phosphate		

ABSRACT OF THESIS

For last five decades, Solid State Nuclear Track Detection (SSNTD) technique has developed an immense interest in many fields of science and technology. The disciplines where track detectors are frequently in use are nuclear physics, nuclear imaging, nuclear technology, space physics, microanalysis, mine safety, environmental research, uranium prospecting, biomedical sciences, for cancer treatment by radiation therapy (BNCT), material sciences, and geological sciences which have made this technique more versatile and popular. Commercial CR-39 polymeric detector is the only detector vastly used for neutron dosimetry and dosimetry of heavy ions and radon. Although materials like bisphenol-A polycarbonate (Lexan/Makrofol), nitrocellulose (LR-115) etc. could be used as charged particle detectors; there is no replacement available so far for the PADC detector due to its superiority in many aspects. During the course of research work, our efforts were directed towards designing and developing more efficient track detectors than CR-39.

The thesis entitled "Synthesis of allylic monomers and polymers containing Sulphur and Phosphorus functionalities for Solid State Nuclear Track Detection" comprises of four chapters.

The *first chapter* incorporates the introduction and literature review about SSNTD technique. In this chapter origin of radiation, its hazardous effects and different types of radiation detectors used earlier for radiation detection have been discussed. Also advantages, important features and applications of SSNTD technique have been discussed here.

The ***second chapter*** includes the designing and development of phosphorus containing polymers for SSNTD applications. Here, we considered development of some phosphate, phosphoramidate containing monomers/ polymers for our study. Out of which triallyl phosphate (TAP) has been homopolymerized and also copolymerized with allyl diglycol carbonate to generate polymeric film detectors (Scheme 1).
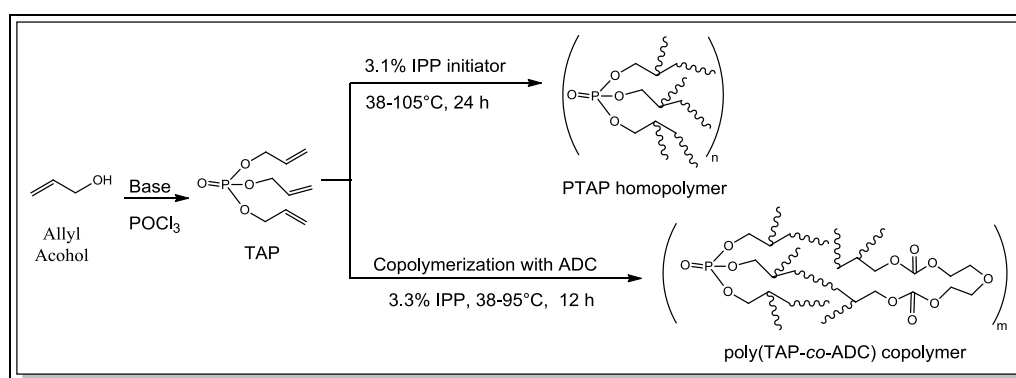
Scheme 1

Initial studies of PTAP and poly (TAP-*co*-ADC) as track detectors were carried out. PTAP homopolymer hardly detected any alpha tracks. But, Poly (TAP-*co*-ADC) polymeric film revealed tracks and has been optimized as per the protocol proposed for systematic development of polymeric track detectors. The alpha sensitivity as well as alpha track detection efficiency of optimised poly (TAP-*co*-ADC) polymer were compared with commercial CR-39 and indigenously prepared PADC detectors. Copolymers poly (TAP-*co*-PETAC) and poly (TAP-*co*-NADAC) have also been prepared and successfully tested for nuclear track detection.

The ***third chapter*** describes design and development of sulfur containing monomers/ polymers for SSNTD applications. Here we have reported the synthesis of monomers containing sulfide, sulfoxide, sulfonamide, and sulfone functionalities. Attempts were made to cast polymerize the synthesized monomers.

Allyl thiodiglycol carbonate
(ATC)

CAS No. 128809-87-0

(M1)

3,6-dithiaoctan-1,8-diol bis
(allyl carbonate)

CAS No. 128809-89-2

(M2)

5,5'-oxybis(3-thiapentan-1-ol)
bis(allyl carbonate)   **OR**
3,9-dithia-6-oxa-undecane-1,11-diol
bis(allyl carbonate)

(M3)

2,2'-sulfinyldiethanol
bis (allyl carbonate)

(M4)

2,2'-(ethane-1,2-
diyldisulfonyl)diethanol bis
(allyl carbonate)

(M5)

2,2'-(3-oxapentane-1,5-
diyldisulfonyl)diethanol bis
(allyl carbonate)

(M6)

2,2'-sulfonyldiethanol
bis(allyl carbonate) (SDAC)

(M7)*

N,N-diallylprop-2-ene-1-sulfonamide

CAS No. 1852256-21-3

(M8)

Allyl Sulfone

CAS No. 16841-48-8

(M9)

*Note: Compound **M7** has also been referred as Allyl Thiodiglycol Sulfone Carbonate (ATSC) by us in some other communications.

Out of several monomers, process of casting detector films from 2,2'-sulfonyldiethanol bis(allyl carbonate) (SDAC) monomer was optimized as per the protocol mentioned above. Polymerization kinetics for PSDAC as well as poly (SDAC-*co*-ADC) was studied to generate 12 h constant rate polymerization profile. Time required for track development, alpha sensitivity, alpha track efficiency, alpha to fission fragment ratio as well as neutron sensitivity of homopolymer PATSC and copolymers poly (SDAC-*co*-ADC) were studied. PSDAC and poly (SDAC-*co*-ADC) detectors showed alpha sensitivity values of 1.95 & 2.75 respectively which is higher than that of CR-39 (1.28). These new polymers could also detect recoil proton tracks from fast neutrons. It was interesting to note that the PATSC and poly (SDAC-*co*-

ADC) detectors reveal alpha, fission or proton tracks within a few minutes whereas CR-39 requires a few hours for the same.

The *fourth chapter* deals with the development of PADC polymeric track detector for the personnel neutron dosimetric analysis and an attempt towards its commercialization. Although PADC detectors are widely used for monitoring thermal neutron doses due to its sensitivity towards neutrons through (n, p) reactions, and excellent optical properties but, these detectors are not manufactured in India and are obtained only through import procedure (i.e. commercial CR-39 detectors). So with this view in mind, we have successfully scaled up the synthetic process to prepare ADC monomer and cast polymerized ADC monomer to obtain polymeric films of size upto 10" x 10". Synthesis of ADC was carried out using two methods i.e. transesterification process (scheme 2) and condensation process (scheme 3).

Scheme 2

Scheme 3
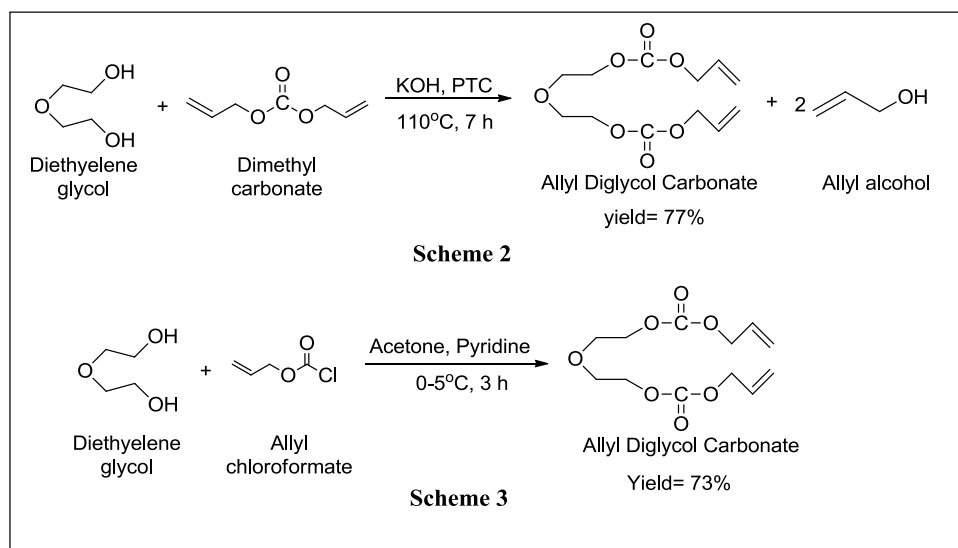
Process to cast PADC sheets of 10" X 10" was developed and the PADC detectors were tested for the dosimetric parameters such as minimum dose limit (MDL value), sensitivity and signal to noise ratio. Based on these parameters, improvements in polymerization process were carried out to develop a dosimetry grade PADC detector sheet.

LIST OF PUBLICATIONS

International peer reviewed journal publications:

1. R. Pal, V. S. Nadkarni, **D. G. Naik**, *et. al.,* Development and dosimetric characterization of indigenous PADC for personnel neutron dosimetry. Nuclear technology and radiation protection, 30(3), 175-187, **2015**.

    http://dx.doi.org/10.2298/NTRP1503175P

2. **D. G. Naik** and V. S. Nadkarni, Poly (triallyl phosphate) and its copolymers with allyl diglycol carbonate as Solid State Nuclear Track detectors. Designed monomers and polymers, 19(7), 643-649, **2016**.

    http://dx.doi.org/10.1080/15685551.2016.1187445

3. **D. G. Naik** and V. S. Nadkarni, Poly (sulfone-carbonate) detectors for rapid detection of nuclear tracks by chemical etching (*manuscript under communication*).

4. **D. G. Naik** and V. S. Nadkarni, Polyphosphates and poly (phosphate-*co*-carbonate) polymeric materials for Solid State Nuclear Track Detections (*manuscript under preparation*).

Patent filed:

1. V. S. Nadkarni and **D. G. Naik**, *Indian Patent No. 201621021793*, entitled "Allyl Thiodiglycol Sulfone Carbonate, polymers thereof and their use in detection of ionizing radiations."

Papers presented/ attended at National/ International conferences:

1. **D. G. Naik** and V. S. Nadkarni, Polytriallyl phosphate (PTAP) and its copolymers for solid state nuclear track detection; *18ᵗʰ National symposium on SSNTD's and their applications*, organized by Aggarwal College Ballabgarh Faridabad, Haryana during October 18-20, 2013.

2. **D. G. Naik** and V. S. Nadkarni, Polymerization of Triallyl Phosphate (TAP) and mixture of (ADC-TAP) and Application in Solid State Nuclear Track Detection; *ACT NCCT-2014 National conference on "Emerging Area in Chemical Education & Research and National Convention on Chemistry Teachers"*, organized by The IIS University, Jaipur on 16-18 October 2014.

3. **D. G. Naik** and V. S. Nadkarni, Development of Novel poly (TAP-*co*-PETAC) and poly (TAP-*co*-NADAC) polymeric materials for solid state nuclear track detection studies; *National Symposium on "Materials Characterization and Manufacturing (MCM-2016)"*, organized by P. C. College of Engineering, Verna, Goa in collaboration with Department of Physics, Goa University, Goa held on 18ᵗʰ and 19ᵗʰ August 2016.

4. **D. G. Naik**, V. S. Nadkarni, "Phosphorus containing polymeric materials for solid state nuclear track detection- A brief review" *in International conference and exhibition on Polymer Chemistry at Atlanta, USA accepted for E-poster presentation* held on 14ᵗʰ -16ᵗʰ November 2016.

5. **D. G. Naik**, V. S. Nadkarni, "Poly (sulfone-carbonate) Polymers for Swift Detection of Charged Particle Tracks: A Replacement for Commercially available PADC Nuclear Track Detectors", (Oral presentation) at *20ᵗʰ National conference on SSNTDs and their applications,* organized by VVIET, Mysuru on October 26-28, 2017.

6. Attended one day workshop entitled "IPR and National Innovation system in India" organized by NRDC New Delhi & co-organized by Goa university Goa on 13th December 2013.

7. Participated in the conference on "Chemical Industrial Disaster Management (CIDM): Chemical, Pharmaceutical & Hydrocarbon Industry" organized by Federation of Indian Chambers of Commerce and Industry at Cidade De Goa, Goa on 29th September – 1st October 2014.

8. Participated in the International Conference on Green Chemistry in Goa University, Goa on 22nd - 24th January 2015.

9. Participated in the National Conference at IXth J-NOST Conference for Research Scholars in IISER-Bhopal, Madhya Pradesh on 4th - 6th December 2013.

CHAPTER 1

Introduction and Literature review regarding Solid State Nuclear Track Detection (SSNTD)

CHAPTER 1

1.1   Origin of Radiations:

"It seemed at first a new kind of invisible light. It was clearly something new, something unrecorded." **- WILHELM RÖNTGEN**

The origin of radiation chemistry is contemporary with the X-rays and uranic ray discoveries. This started in the late years of 18th century, with Sir Wilhelm Röntgen's[1] invention of invisible radiations called "X-rays". In the year 1895, while performing various experiments with electrical discharge in evacuated glass tubes (Hittorf-Crooke's vacuum tube) covered with black cardboard in dark room, he noticed some invisible rays penetrating through the board to react with barium platinocyanide solution on a screen that showed a faint flickering greenish fluorescent light which was placed nearby. Röntgen verified that the source of a new kind of radiation was the tube itself, these radiations were invisible but revealed its existence upon hitting the luminescent screen. So he named it as "X-rays". The existence of x-ray emission was earlier postulated by Henry Poincare[2] but was rejected. Henry Becquerel[3,4] discovered another form of penetrating radiation which was named as radioactivity or natural phosphorescence soon after 114 days of invention of X-rays. He demonstrated that the potassium uranyl sulfate spontaneously emitted energetic radiation similar to those of Roentgen rays without any light excitation. He soon observed that these uranic radiations could reduce silver ions on photographic plates and ionize the air[5]. The discovery of radioactivity by Henri Becquerel 120 years ago initiated a new field of research for mankind. He was awarded with Nobel Prize in Physics (1903) for the discovery of spontaneous radioactivity process. The innovation of radiation had a massive influence in motivating major advances in fundamental science. In 1897, Marie curie extensively utilized the very sensitive piezoelectric quartz electrometer designed by Pierre and

Jacques Curie[6] to investigate quantitatively the ionizing properties of uranic radiations. Subsequently in the year 1898, Marie Curie[7] and Pierre Curie discovered two new radioactive elements viz. radium and polonium from pitchblende and chalcholite ores, which was found to be more radioactive than uranium. In 1903, Pierre Curie and Marie Curie both were awarded with Nobel Prize in physics in recognition of the extraordinary services[8] they have rendered by their joint researches on the radiation phenomena discovered by Prof. Henri Becquerel. Again in 1911, Marie curie was awarded with Nobel Prize in Chemistry for her discovery of Radium and Polonium radioactive elements.

Sir Wilhelm Röntgen   Prof. Henri Becquerel   Madam Marie Curie   Prof. Pierre Curie

Pioneers of Radioactivity and Radiation Chemistry

1.1.1 Radiations, Nuclear particles and their hazardous effects[15]:

Radiation is a route by which energy is released either in the form of particles or waves. Radiation can take form of sound, light, or heat. Scale of electromagnetic radiation is shown in figure 1.1 below. Basically they are classified as ionizing radiation and Non-ionizing radiation. Non-ionizing radiation like microwave, infrared, radio wave energy has less energy than ionizing radiation and it does not hold enough energy to ionize. Whereas ionizing radiations are capable of ionizing atoms or molecules to produce ions. These radiations are produced naturally and by

man-made materials. The radiations of primary concern originate from atomic or nuclear processes. They are grouped into four types as follows (1) Fast electrons that include beta particles emitted in nuclear decay; (2) Heavy charged particles such as alpha particles, protons, fission fragments or the products of many nuclear reactions; (3) Electromagnetic radiation includes x-rays, gamma rays and (4) Neutrons produced in different nuclear reactions which is further classified as slow neutrons and fast neutrons. Fast electrons and heavy charged particles are charged particulate radiations while electromagnetic radiation and neutrons are uncharged radiations. These are hazardous radiation, can cause cancer like diseases and even death.
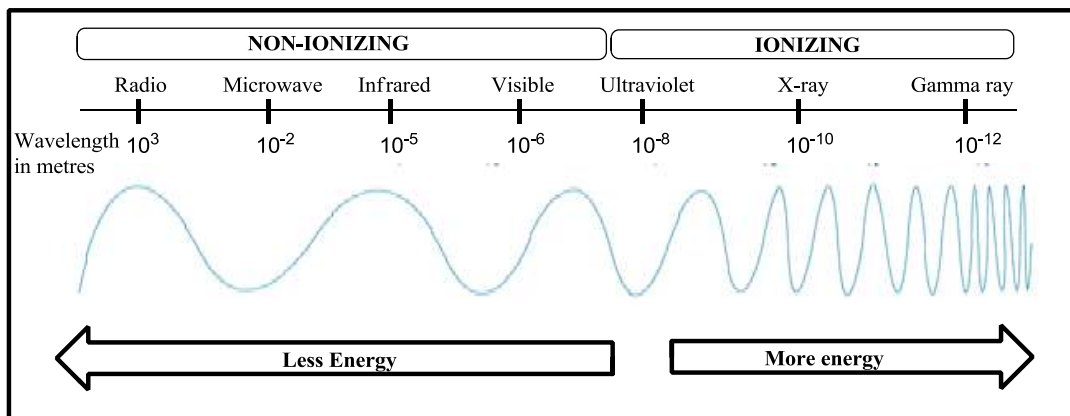
Figure 1.1: The electromagnetic radiation scale showing types of ionizing and non-ionizing radiation.

1.1.2 Biological effects of radiation: Shortly after the discovery of radiations, it was recognized that ionizing radiations can have harmful health effects[9]. The harmful effects were perceived in individuals who had been exposed to large and continuous doses of ionizing radiations. Radiations were found to impede cell division and could therefore be used to stop cancer growth. Radiations applied locally causes lesions, leading to cancer. In 1906, Bergonie and Tribondeau[10] made hypothesis regarding biological effect of radiation that "Biological effects are directly proportional to

mitotic index and mitotic future of the exposed cell, and inversely proportional to the degree of differentiation. Mitosis refers to natural division of cell nucleus during cell reproduction; differentiation means the cell degree of specialisation to perform a specific function in the organ". These radiations cause severe damage to living things including the mankind. They may have varying effects depending on the dose received and a type of tissues exposed. The long term exposure to ionizing radiation leads to alteration in DNA within the cells. In early years[11], many serious accidents took place as a result of the use of radiation before sufficient understanding of its biological effects. By 1922, around 100 radiologists died due to biological radiation damage. The effect of very large doses of radiation to complete body leads to radiation sickness and early death. Genetic and non- genetic effects can be seen in a person due to high dose of radiation exposure. Cancer is the most prominent long term deterministic effect. Leukemia and bone cancer occurs in person who is exposed to strontium-90 radioactive element. The acute radiation exposure of 25-50 rem (roentgen equivalent man) leads to noticeable decrease in lymphocyte counts, with symptoms like alopecia, skin erythema, hematopoietic damage, gastrointestinal damage, central nervous system damage with increasing radiation dose[12]. Acute radiation exposure of 150-350 rem in a person leads to Acute Radiation Syndrome causing fatigue, hair loss, nausea, and skin reddening.

1.1.3 History of Radiation detectors[13]: The detection of ionizing radiation depends upon the measurement of its effects in medium and the history of emergence of radiation detectors is closely associated with invention of radiation and radiation effects. Although ionizing radiation has been there in nature all over human history and remained unnoticed till 130 years ago. Human and animals have no specific

sense which could have responded to these radiations and there were no instruments developed for amplifying human response. In the year 1895, Roentgen after performing several experiments to discover X-rays, replaced fluorescent screen by a photographic plate to monitor X-rays and thus gave a tool for recording X-ray photographs. Roentgen also examined that air would conduct electricity when crossed by ionizing radiations. This effect was then used as principle for many radiation detectors. In 1903, Crookes invented Spinthariscope instrument that was able to detect individual radiations. In 1908, Rutherford and Geiger[14] designed the first cylindrical electrical counter for alpha particles. It was further improved to detect beta particles. In 1911, another instrument i.e. Cloud chamber was designed by C. T. R. Wilson that made single radiation events visible. In the year 1923 and 1930, the cloud chamber was used extensively for large number of major discoveries. In 1928, Geiger and Muller invented a new kind of gas-filled counter called GM counter for detecting ionizing radiation with high level output signal. In 1950s, bubble chamber was discovered that made particle trails visible in liquid medium. But still GM counter is often used because of its simplicity and ease of operation. In 1940, Frisch developed another gas filled counter, the ionization chamber for alpha particles. The proportional counter was also developed in same year which amplified the charge initiating in the gas. Further it was realized that instead of gas filled detectors, solid state detectors can have more advantage in radiation detection application. Crystal counters was soon reported by Jaffe in 1932 and by Van Heerden in 1945. Many semiconductor detectors were then developed soon after invention of solid state nuclear track detectors by D. A. Young in 1958.

1.1.4 Types of Radiation Detectors:

The occupational workers who are handling such radioactive materials at the nuclear reactors and nuclear research centres must be monitored for radiation protection and thus it becomes necessary to have techniques for radiation detection. Radiation exposure to individual can be classified as internal exposure and external exposure. External exposure monitoring refers to measuring of radiation levels around work areas; around radiotherapy equipments or source containers and measuring of equivalent doses received by individuals working with radiations. This monitoring is carried out to assess workplace condition and personal exposure; to ensure safety and satisfactory radiological conditions in workplaces; and also to keep records of monitoring for long period of time and for good practices. The radiation monitoring devices are used both for area monitoring and for individual monitoring. Devices used for area monitoring are either gas filled or solid state detectors like scintillators, semiconductor detectors. Individual monitoring is the measurement of radiation dose received by individuals at workplaces. The most widely used individual monitoring systems are based on film dosimetry, Radio photoluminescence (RPL), Optically Stimulated Luminescence (OSL). Other dosimeters like Albedo dosimeters, nuclear emulsions, self-reading pocket dosimeters and Electronic Personal Dosimeters (EPDs) are used as personnel monitoring systems. Few detectors used in early years are given in table 1.1.

Table 1.1: Different types of detectors used earlier.

Detectors	Counters type	Interaction	Medium
Ionization Counter	Signal	Ionization	Gas
Proportional Counter	Signal	Ionization	Gas

Geiger counter	Signal	Excitation of electronic levels and associated production of photons	Gas, liquid and solids
Scintillation Counter	Signal	Excitation of electronic levels and associated production of photons	Gas, liquid and solids
Semiconductor Counters	Signal	formed of electrons and holes	Solid
Cerenkov Counter	Signal	photons produced by Cerenkov effect	Gas, liquid and solids
Photographic Emulsion (1940)	Track	Ionization	Solid
Cloud Chamber (1911)	Track	Ionization	Gas
Bubble Chamber (1952)	Track	Ionization	Liquid
Spark Chamber (1930)	Track	Ionization	Gas and solid
Dielectric particle detector (1958)	Track	Ionization	Solid, tracks developed by etching

As stated above many detection techniques[15, 16] were developed for quantitative measurements of nuclear particles. Details of detection techniques are as follows.

1.   Cloud chamber[17]: The cloud chamber also called Wilson chamber is a particle detector used for detecting charged particles. It played an outstanding role in the experimental particle physics from 1920 to 1950. A cloud chamber consists of a sealed environment having supersaturated vapour of water or alcohol. When ionizing radiation interacts with supersaturated vapour, it is ionized and the supersaturated alcohol vapours condenses along the path behind the charged particles/ radiation. A tangential light source illuminates the white droplets formed by tracks and due to

black background it can be viewed easily from horizontal position. The cloud chamber is usually operated in a uniform magnetic field. When uniform magnetic field is applied to the cloud chamber, charged particles get deflected and the quantity of deflection depends upon the energy of charged particles.

2. **Bubble chamber:** This detector was discovered by Donald A. Glaser[18] in 1952. In 1962, he was awarded the Nobel Prize in physics for his innovation. The bubble chamber is a large cylindrical vessel filled with a superheated transparent liquid like liquid hydrogen which can be used to detect electrically charged particles moving through it. It works on the same principles as that of cloud chamber only difference is here in bubble chamber, superheated liquid is used instead of supersaturated vapours. Bubble chamber consists of bulkier cylinder with volume of thousands of litres and hybrid systems of supplementary detectors for particle identification. When a charged particle enters the chamber, it creates an ionization track around which superheated liquid vaporizes forming tiny microscopic bubbles. Density of bubbles formed around the track is directly proportional to particle's energy. The bubbles size can be increased by expanding chamber. The chamber is subjected to constant magnetic field that makes the charged particles to move in helical paths. Their time resolution is very deprived. Evaluation of bubble chamber data is giant task and requires human and computing resources.

3. **Spark chamber:** It is a particle detector used for detecting electrically charged particles in particle physics. The spark chamber is a reservoir of thin, parallel, metal plates separated by gaps of few millimetres containing noble gas like helium, neon or their mixture at atmospheric pressure. It can be further improved by

changing the stack of metal plates with a large number of wire grids placed in a sealed box filled with noble gas. When a cosmic ray traversed through the box, the gas between the plates gets ionized. And if a high voltage is applied to each pair of plates before the ionization disappears, the sparks can be produced along the path of the ray and thus the cosmic ray becomes visible as a line of sparks. The limited time resolution of the bubble chamber is overcome in the spark chamber.

4.   Ionization Chambers[19]: The ionization chamber is the first and simplest of all gas filled detector which is most widely used in nuclear physics for radiation detection. The types of interaction involved in the chamber are ionization and excitation of gas molecules along the path of particle. The majority of gas filled detectors depends on sensing direct ionization by the channel of the radiation. Normal operation of ion chamber is based on gathering all the charges formed by direct ionization within the gas by using electric field. Ion chambers can work in current as well as pulse mode. This detector consists of a closed container containing an ionization media and electrodes at different electrical potentials. The ionization media is made of gas or semi conducting solids. The incident radiations ionize the gas between the electrodes creating ion pairs. These ions travel to the electrodes of opposite sign, producing current which can be amplified and measured.

5.   Proportional counters[20]: The proportional counter is a type of gas-filled detector that was introduced in the late 1940s. It is a gaseous ionization detector used to determine ionizing radiation. The characteristic feature of this detector is its capacity to evaluate the energy of incident radiation, by generating a detector output that is proportional to the radiation energy; hence the name as proportional counter's

for the detector. The detector chamber consists of a mixture of 90% argon and 10% methane. An inert gas in the chamber is ionized by incoming incident radiation while 10% methane 'a quench gas' ensures that each pulse discharge ceases. Ionizing radiation enters the chamber where it collides with an inert gas atom and ionizes it to generate an electron and a positively charged ion, called "ion pair". The charged particle leaves a track of ion pairs along its path when it travels through the chamber. If the charged particle is fully stopped within the gas, then the energy of the particle is given by the number of ion pairs. Typically around 30,000 ion pairs are generated when 1 MeV particle are stopped within gas chamber. Oftenly these detectors are operated in pulse mode. These detectors depend on the phenomenon of *gas multiplication* for amplification of the charge corresponds to the original ion pairs formed within the gas. Such counters can be useful to condition in which the ion pairs generated by the radiation are too small to allow acceptable action in pulse-type ion chambers. One chief application of proportional counters has therefore been in the detection and spectroscopy of low-energy X-radiation. They are also widely applied in the detection of neutrons.

6.   Geiger Muller counters[19, 21]: The Geiger-Mueller counter (also known as the G-M counter or Geiger tube) is one of the oldest radiation detector which is still in use. G-M counter is a type of gas-filled detector used to detect ionizing radiation. It was been introduced by Geiger and Mueller in 1928. It is very simple, low costing and easy to operate which made these detectors to continue the usage in the present time. It can measure/ detect ionizing radiation such as alpha particles, beta particles and gamma rays using the ionization effect created in a Geiger Muller

tube[22]. They are widely used in applications such as radiation dosimetry, radiological protection, experimental physics and the nuclear industry.

A G-M counter consists of a Geiger tube filled with an inert gas like helium, neon; the radiation sensing element which detects radiation and the processing electronics, which gives the output result. Like proportional counters, it makes use of gas multiplication to significantly intensify the charge symbolized by the unique ion pairs formed along the radiation path, but in a basically diverse way. A Geiger tube can therefore function only as a simple counter of radiation induced actions and cannot be applied in direct emission spectroscopy since all information on the quantity of energy deposited by the incident radiation is vanished. Besides the lack of energy information, a main shortcoming of G-M counters is their abnormally large dead time, which significantly exceeds that of any other frequently used radiation detector. These detectors are therefore limited to comparatively low counting rates, and a dead time correction must be applied to circumstances in which the counting rate would otherwise be regarded as fair.

7.   Scintillation detectors: This is one of the oldest and most reliable technique which was first discovered by Lucas[23]. A scintillation counter is a detector used for measuring ionizing radiation by the excitation effect of incident radiation on a scintillators material, and spotting the consequential light pulses. Scintillation counting in the gaseous phase has been broadly used for the purpose. They are generally used in radiation protection, analysis of radioactive materials and in physics research as they can be prepared economically with good quantum efficiency, and can determine both the intensity and the energy of incident radiation. They are also used to measure radiation in a range of applications comprising hand

held radiation survey meters, radiometric assay, medical imaging, personnel and environmental examining for radioactive contamination, nuclear safety and nuclear plant protection. The device is a glass vessel internally enclosed with scintillating substances like Zinc Sulfide ZnS (for alpha particles), Cesium iodide CsI (for protons and alpha particles), Sodium iodide NaI with thallium (for gamma wave detection), Lithium iodide LiI (used in neutron detectors) that produces photons with respect to incident rays, a photomultiplier tube (PMT) converts the light to an electrical signal and the signal is further processed by electronics. The tiny flashes created by hitting of α-particles on the phosphor can be noticed by a light amplifier. Sensitivity of this detector depends on the time of counting of ionizing radiation. The device can directly collect ^{218}Po atoms on the detector[24] . Introducing α-emitter rich filter in front of the scintillation screen[25] the scintillation can be viewed upon subsequent filtering radon progeny. A more superior version of the Lucas cell is the one which offers the multiple scintillation of time with better quality response[26]. This type of apparatus was devised by Madnick and Sherwood[27], which consist of several light tight chambers in which scintillation counting of radon and its progeny is executed. A plastic scintillators and photomultiplier detector detects the β-radiation emitted from the particle bearing area**.**

8. **Semiconductor diode detectors:** This detector is employed for very high resolution energy measurement. It works as a solid state ionization chamber. Silicon and Germanium are commonly used semiconductor materials. Functioning of semiconductor counters is quite similar to that of ionization counters. In this detector, the radiation generates electron-hole pairs and their collection at the electrodes causes the electric signal. Because of presence of DC current in a single

crystal of semiconductor material like Si or Ge, it will not create a right counter. Random change of this current may create pulses like the radiation-induced pulses. To decrease this current a p-n junction in reverse bias is utilized.

9.   **Nuclear or photographic emulsions:** This type of detectors has high sensitivity to record even high energy electrons. In a photographic emulsion, the ionization generated by a photon or a charged particle escort the conversion of some Ag+ to Ag atoms. This link together to shape complexes which catalyses the reduction of a whole AgBr grain to metallic Ag under the action of the developer. In the final stage the fixer breaks away the entire undeveloped small pieces. A particle track is therefore imaged as collection of black Ag grains.

10.   **Silver halide Crystals:** This detector depends on the precipitation of metallic silver crumb along the trail of a charged particle in AgCl or AgBr single crystal. Some processes causing track formation in the crystals are not completely known and understood, but there are some similarities with nuclear emulsions. This type of detection was first observed in the early 1960s, by Childs and Slifkin. The AgCl crystals were first irradiated with charged particles and exposed to an ultra violet light followed by pulsed electric field for 2 hours to measure ionizing radiation. This type of crystals (AgCl) have many useful properties like they are more sensitive than etched-track detectors, they don't require any wet chemical development methods of emulsions. These detectors are more complex than the simple dielectric track detectors. As far as particle identification is concerned, they are still in development stages. These detectors have limited attention and applications.

CHAPTER 1

1.2 Introduction to Solid State Nuclear Track detection (SSNTD) technique:

Solid State Nuclear Track detectors (SSNTDs) fall in the category of particle track detectors and are essentially dielectric insulating solid materials that are permanently damage by energetic/ charged particles forming narrow intense damaged trails of ~ 30-100Å diameter along the path of the particle. These trails/ tracks could be subsequently developed by processes like electrochemical or chemical etching and could be conveniently observed using optical microscope. These tracks could be retained permanently on detectors as solid record. The ionizing radiations passing all the way through the detector material, cause trail of damaged molecules due to energy transfer. A particle tracks consist of region of atomic displacement formed by ionizing process. Such narrow damaged region in solid with different physical and chemical properties than the undamaged bulk material of the solid is called the "Latent Tracks" which are tiny and cannot be observed with naked eyes. These latent tracks can be observed directly with Transmission Electron Microscope (TEM). The latent tracks upon chemical or electrochemical etching creates conical etch pits called Tracks. These tracks are enlarged to few microns and can be viewed under optical microscope. The damaged region of the materials could be etched with appropriate etchant at faster speed as compared to undamaged matter.

For last more than three decades the SSNTDs have established applications in almost all branches of science and technology[28]. They are the most extensively employed detectors for low as well as high energy ionography. These dielectric materials mainly consist of natural, volcanic and man-made glasses viz. phosphate, granite, silica, soda lime, obsidian, tektite, flint, etc. It also includes minerals like aragonite, sphene, apatite, garnet, allanite, quartz, epidote, feldspar, zircon, diopside, mica etc. and plastics such as certain cellulosics, vinylics, polyesters, polycarbonates

etc. Basically solid state nuclear track detectors are categorized as inorganic crystals, inorganic glasses and high polymers (plastics). Out of which plastic materials are the most sensitive group that have broad applications in the study of heavy ions, neutron dosimetry, cosmic rays and radon dosimetry etc. Radon dosimetry in indoor environment is based on the detection of α-particles. In crystals, the latent trails are due to atomic displacements whereas in plastics, the damaged trails are because of broken molecular chains which produce active free radical sites etc.

At present, the SSNTDs technique have been developed to such an extent that there is hardly any area of science and technology where it is not used [16, 29]. The SSNTDs are extremely simple to use as compared to other detectors like cloud, spark chambers, bubble, nuclear emulsions etc. Almost all the materials used in track detection are made-up as insulators for their application in broad range of everyday objects[16].

1.2.1 Historical background to SSNTD[30]: The era of nuclear tracks commenced in 1958 when D. A. Young working at the Atomic Energy Research Establishment at Harwell published an extraordinary note in Nature[31] regarding the discovery of etch pits in LiF crystals. According to this, the LiF crystals were irradiated with thermal neutrons which were placed in contact with uranium foil (U_3O_8) after subsequent chemical etching to developed small etch pits. He briefly explained possible mechanism of track formation whose principle is alike to what some models afterwards proposed for track formation mechanism in inorganic detectors. Further examination of the crystals illustrated a complete connection between the numbers of etch pits and the approximate number of fission fragments which would have recoiled into the crystals from the uranium foil. The elongated etch pits observed in

the crystals were later called 'tracks'. This led to discovery of new field of radiation measurement and detection called SSNTD. Similar study was carried out independently by two scientists E.C.H. Silk and R.S. Barnes working at Atomic Energy Research Establishment at Harwell (England) in 1959 who first observed the damage trails produced by fission fragments and they observed nuclear tracks in mica sheets using Transmission Electron Microscope (TEM)[32] microscopy. Their explanation provided a chain of ideas about the discovery of particle tracks and has assisted to construct an aura of stimulation and attraction for particle tracks in solids. Another group of scientists working at General Electric Research Laboratory in Schenectady, New York, applied this technique to investigate use of different types of materials like crystals, glasses, minerals, and mica sheets in track detection study[33, 34]. They repeated the interpretation of some previous workers. Successively, they scrutinized that the damaged trails in mica can be etched preferentially in a suitable etchant and can be viewed under an optical microscope[35]. They observed that the spontaneous fission of the small quantity of uranium present in rocks would leave similar latent tracks in crystals lattice. They also showed that the nuclear tracks could be etched and viewed in glasses, minerals and also in plastics. Thus the new field of 'Trackology' was established by Fleischer, Price and Walker and the idea on the prospects of applications of SSNTDs in science and technology was put forward. Because of their excellent properties like durability, simplicity, flexibility and their specific nature of response to various radiations, they established rapid applications in various fields of science and technology. The first review paper by Fleischer *et al.*[34], made different scientists to work on SSNTDs for their applications in different laboratories of the world. Thus, the development of basic knowledge and

technological applications of 'Trackology' based on ionographic registration in SSNTDs was established[36].

1.2.2 Development of SSNTD technique research in India:

In the year 1965, Professor P. B. Price visited the Tata Institute of Fundamental Research (TIFR), Mumbai. This caused the beginning of SSNTD research activity on cosmic ray prehistory using meteorite samples at TIFR which was led by Prof. D. Lal and 'Nuclear Track Society of India's (NTSI) founder president, Prof. S. Biswas[37]. In 1969, SSNTD work was initiated at Kurukshetra University by late Professor K.K. Nagpaul where he pioneered the research in the areas of fission track dating and microanalysis[38]. In 1968, R. H. Iyer at the Bhabha Atomic Research Centre (BARC) Trombay, Mumbai started the experimental work using SSNTDs. Using Lexan polycarbonate track detector[39], he at first detected fission fragments from the thermal neutron fission of ^{235}U. He slowly and steadily extended his work over the years to cover many aspects of the fission process[40, 41] and applications like trace analysis, monitoring of radon and thoron, uranium analysis[42] etc. In 1972, the fundamental research on heavy ion ranges, track length and etching kinetics was started at the Indian Institute of Technology (IIT), Kanpur. Several other Indian Universities and Research Institutes started experimental work using SSNTDs at the same time or a little later and now these are emerging centres of brilliance in "Trackology". The versatile and inexpensive nature of the technique attracted most of the Indian Universities and Research Institutes to Trackology. Presently, there are many research groups and specialized centres in India engaged in research and development work concerning SSNTDs. These include: IIT Kanpur; Gauhati University, Guwahati; Saha Institute of Nuclear Physics (SINP), Kolkata; Bose

Institute, Kolkata; Defence Research Laboratory, Jodhpur; North-Eastern Hill University (NEHU), Shillong; Nuclear Science Centre (NSC), New Delhi; Wadia Institute of Himalayan Geology, Dehradun; H.N.B Garhwal University, Tehri Garhwal; Arunachal University, Itanagar; University of Mysore, Mysore; Banaras Hindu University (BHU), Varanasi; Punjab University, Chandigarh; Guru Nanak Dev University (GNDU), Amritsar; Mangalore University, Mangalore; Osmania University, Hyderabad; IIT, Kharagpur; Aligarh Muslim University (AMU), Aligarh; Physical Research Laboratory, Ahmedabad and Calicut University, Calicut, UDCT, Mumbai (1992-95) and Goa University, Goa, since 1996. BARC played a very important role in bringing together different groups working in the field of SSNTDs[43].

1.2.3 Important features and advantages of solid state nuclear track detectors[30, 44]: The track formation in SSNTDs is associated with the ions or charged particles which make the damage in a solid lattice, exceeding certain threshold unit such that the damaged made leaves the permanent track along the path of the ions. This characteristic feature of the track detector is one of the key advantages in particle detection. The threshold quality is an important tool in many applications in physical sciences and contributes appreciably to the establishment of SSNTD. The intensity of ionization damage produced by charged particle is directly proportional to the square of its charge and roughly contrariwise proportional to the square of its velocity. This feature of charged particles for detector material was used effectively by different workers in the study of cosmic ray particles through nuclear track detection. Sensitivities of nuclear particles for diverse materials found to be different for different ions theoretically and experimentally. Organic polymeric materials/

CHAPTER 1

Plastics are found to be most sensitive materials. Some of the commonly utilized plastic materials with their sensitivities are given in table 1.2.

Table 1.2: Sensitivities of some of the commonly used polymeric detector materials

Polymeric materials	Chemical composition	Least viewed ion
Cellulose nitrate (Diacel)	$C_6H_8O_9N_2$	0.55MeV ^{1}H
Cellulose nitrate (LR-115)	$C_6H_8O_9N_2$	0.1 MeV ^{1}H
Bisphenol-A polycarbonate (Lexan, Makrofol)	$C_{16}H_{14}O_3$	0.3 MeV ^{4}He
Allyl diglycol carbonate (PADC, CR-39)	$C_{12}H_{18}O_7$	1 MeV ^{1}H
Amber	$C_2H_3O_2$	Fission fragments
Polyethylene	CH_2	Fission fragments
Polyimide (Pyralin PI-2550 or PI2540)	$C_{11}H_4O_4N_2$	36 MeV ^{16}O
Polyoxymethylene (Delrin)	CH_2O	28 MeV ^{11}B
Polypropylene	CH_2	1 MeV ^{4}He

SSNTDs have a lot of useful superiority over other conventional nuclear charged particle detectors like ionization chamber, cloud chamber, scintillation counter, proportional counter, spark counter, Geiger Muller counter, nuclear emulsion, bubble chamber, and semiconductor detectors etc. Some vital characteristics of solid state nuclear track detectors over conventional detectors are specified as follows:

1.   SSNTD's are relatively simple in construction and can be obtained in very small as well as in very large sizes. They are very simple to use, durable, rough. They are economical and can be conveniently used.

2.   They are practically insensitive to background radiations like light, x-rays, β-rays, γ-rays and could be used for radiation detection in presence of background radiation.

3.   The nuclear radiation damages the detector in such a way that the tracks formed in these detectors can be viewed after several years depending upon shelf life of the detector material. The detectors record tracks permanently in them which can be left or stored for very long period unattended under stringent environmental conditions like high temperature, pressure, humidity, radiation background and extreme mechanical vibrations.

4.   These detectors do not require any careful handling. They could be utilized in any remote and difficult areas where other techniques fail.

5.   If the detectors are placed in direct contact with fission fragment sources, a very high efficiency and sensitivity can be achieved.

6.   These detectors also have the charge and energy bias properties. Recently, it has been reported that the resolution for high charged particles obtained with plastic detectors is superior to nuclear emulsions.

7.   These detectors are particularly useful in angular distribution measurements as they have a substantial amount of geometric flexibility.

8.   To learn nuclear interactions in these detectors, high spatial and time resolutions may be achieved using electron microscope.

9.   As compared to nuclear emulsions, the revelation of tracks in these detectors via special chemical etching process is very fast.

10.   Out of all SSNTDs, some solids themselves can be used as both target and detector. Like in plastics while measuring neutron flux recoil nuclei; glasses and

mica in neutron fluence measurement using fission fragments. Fission fragments arise because of presence of impurities like ^{235}U

11.   There are some naturally forming materials like minerals, crystals and surface materials of celestial bodies that can act as SSNTDs. From these materials, even natural records of geological and cosmological dealings can be exposed. Unlike other instrumental techniques, SSNTDs does not need any electrical energy during recording of the nuclear tracks.

12.   SSNTD detectors are threshold type detectors and the best use of this feature is for the revealing of heavy ions like fission fragments which can be determined and distinguished from a very high background of light charged particles like ^{4}He, ^{2}H, ^{1}H β-particles, X-rays, γ-rays and also neutrons.

1.2.4   Disadvantages of the SSNTDs:

Although there are many advantages of SNTDs, still they suffer from some disadvantages with them as follows.

1.   When charged particles pass through these detectors and upon subsequent etching, only a part of the total track length of the particle trajectory can be observed leaving the part that has been etched off.

2.   Even though charge and mass resolution of charged particles have been feasible with these detectors, precise energy resolution has still not been achievable.

3.   Recording of blank experimental readings may be required.

After assessment of the properties of SSNTDs with other detectors, it can be observed that in general, SSNTDs have a lot of advantages over other detectors. Light charged particles like ^{1}H, ^{2}H, ^{3}He, and ^{4}He are detected using SSNTDs and

efforts were also made to construct some practical estimates of their energies. However, later they found broad applications in heavy ion and cosmic ray studies.

1.2.5   Applications of SSNTD techniques:

This technique has turned out to be more popular and well recognized technique of measurements[36] in different fields like fission and nuclear chemistry/ physics, astrophysics, in the study of lunar and meteoritic samples, cosmic rays, particle accelerators and reactors, in archaeology, medical physics, dosimetry[16, 29, 33, 45] and also for biomedical and cosmological studies[16, 46] etc. There are some technological applications like in the biological filters, sensors, cancer therapy, information technology, medical diagnosis, biomedical sciences, biotechnology, radon mapping, material sciences, nuclear technology, nanotechnology, and ion track etching dosimetry, magneto resistive sensors and many more[47]. Apel, P.Y. et al., have reported much interesting work regarding the development of nanostructure via etched track pores[48]. Almost all types of dielectric materials, photographic emulsions, crystals, glasses, and plastics were used as SSNTD or DTD (for dielectric track detector) as the density of these materials is higher and charged particles could leave all its energy while passing through it to generate damage alongside the pathway, thus allowing detection of the charged particle. The topics of more importance to the current track detector workers are environmental studies and health effects. The nuclear track detectors are utilized in following different fields

1.   **Environmental and health physics:** The nuclear track detectors have been used extensively in the field of personnel protection dosimetry. The areas of interest includes

CHAPTER 1

a) Radon dosimetry: A Radon level measurement to check and manage indoor radioactive pollution continues to be an important activity followed by the workers of SSNTDs. It becomes important to recognize the radon rich areas for construction purposes. Radon monitoring and measurements in soil, natural water and tap water are important for uranium and thorium point of view[49]. Radon detection in mines and other underground places is also important issue for radiological protection of miners[50].Prediction of earthquakes can also be done by monitoring radon level in underground water or in deep wells. It increases suddenly and considerably before earthquake could occur[51].

b) Neutron dosimetry: To evaluate neutrons exposure at nuclear reactors and other reactor places using track detectors has turn out to be of great importance. To avoid risk of neutron exposure at the reactor sites and to monitor the neutron flux in irradiation chambers of a nuclear reactor are major uses of SSNTDs.

c) Exposure at spacecrafts: During the visits at global space station, lunar landings and other flybys the cosmonauts are exposed to a range of radiations sources like ultra heavy, interplanetary dust particles, cosmic rays and solar flare particles. As we know that nuclear track detectors are handy to measure dose levels of charged particles, they can be used to measure the dose levels of such types of particles.

2. Nuclear Physics and Technology: This technique of track development has been widely utilized in the field of nuclear physics and technology. Some of the uses are as follows.

a) Astrophysics and cosmic rays: To study the elemental and isotopic composition of primary galactic cosmic rays, the SSNTDs technique have been used widely.

b) Thorium and Uranium investigation: Uranium and thorium can be explored by radon dosimetric technique. Radon gas is evolved during uranium decay which

diffuses to some distance in soil and surrounding through the cracks in the rocks. Alpha particles from radons are detected and counted using the detector upon subsequent etching. The alpha track efficiency provides the radon concentration in the soil[52].

c) Alpha estimation in waste water fields: Plastic track detectors can be used to analyse the alpha activity in the waste water from radioactive source which contains alpha activity below 0.04 Bq/ml.

d) Fission track dating: This technique is also used for archaeological dating by fission track dating method. In nature all the minerals have small quantity of uranium. This uranium radiate fission fragments by spontaneous fission reaction which can be stored on a track detector and later can be counted upon etching.

e) Heavy ion reactions: The nuclear track detectors are used to study the reactions induced by heavy ions of low energy as well as of high energy. The product track analysis gives projectile charges, mean free path of ion fragments and other vital information.

f) Search for super heavy elements: The technique can be utilized for studying heavy ion reactions. It can also be used to find super heavy ions of natural origin or in simulated conversion reaction.

3.   Biomedical and Technological science:

a) Boron neutron capture therapy: The most important application of SSNTD technique is BNCT. This therapy is employed to examine and destroy malignant brain tumours. In this therapy, a boron containing drug is injected into the patient's body which travels through blood to the tumour cells where it is absorbed by tumour cells. Tumour containing part of the body is then irradiated with thermal neutrons and energy released by (n, α) reaction destroys the tumour cells. The spatial division

of alpha particles formed by the reaction ^{10}B (*n*, α) ^{7}Li can be studied for research and treatment purposes.

b) Alpha content of blood: The blood samples of the workers of the uranium mines and reactors can be examined by dipping the detectors in to frozen blood for radioactive substance by their alpha activity.

c) Lead content in bones: Bones and teeth can also be analysed by SSNTDs technique for lead content.

d) Nucleopore filters: By irradiating thin polycarbonate films and etching upto desire pore size, different filters can be prepared with cylindrical holes in the detector material. These filters can be used to examine bacteria, algae and other microscopic organisms[53]. These filters have also been used for diagnostics of blood cancer. As the cancer cells are bigger and rigid then normal cells, these cancer cells are separated from blood using Nucleopore filters[54].

1.3 Track formation in SSNTDs:

As discussed earlier, the solid state nuclear track detectors work on the principle that when ionizing radiation passes through the material, it causes ionization of the material and latent tracks are formed along the path of charged particle. When an alpha particle with energy of 6 MeV traverses through a cellulose nitrate track detector, it creates around 150,000 ion pairs[55]. Due to the primary ionization, free radicals and other chemical species are formed along the trail of the alpha particle. This zone with free radicals and other chemical species is called a latent track. Under suitable conditions the resulting radiation damaged area may be practically continuous all along the particle trajectories which can be developed to a suitable size to view under an optical microscope. The detector with these latent

tracks is treated with etching media like aqueous NaOH or hydrofluoric acid at elevated temperature. At these active sites, the chemical reactions will occur at faster rate. The track etch rate V_t is higher as compared to bulk etch rate V_b (chemical etching at surface) (see section 1.3.4) leading to a track which can be viewed under an optical microscope. These etchable tracks may be formed in any kind of electrically insulating materials like crystalline, glassy or polymeric. Figure 1.2 gives the detailed process of track formation in insulating material.
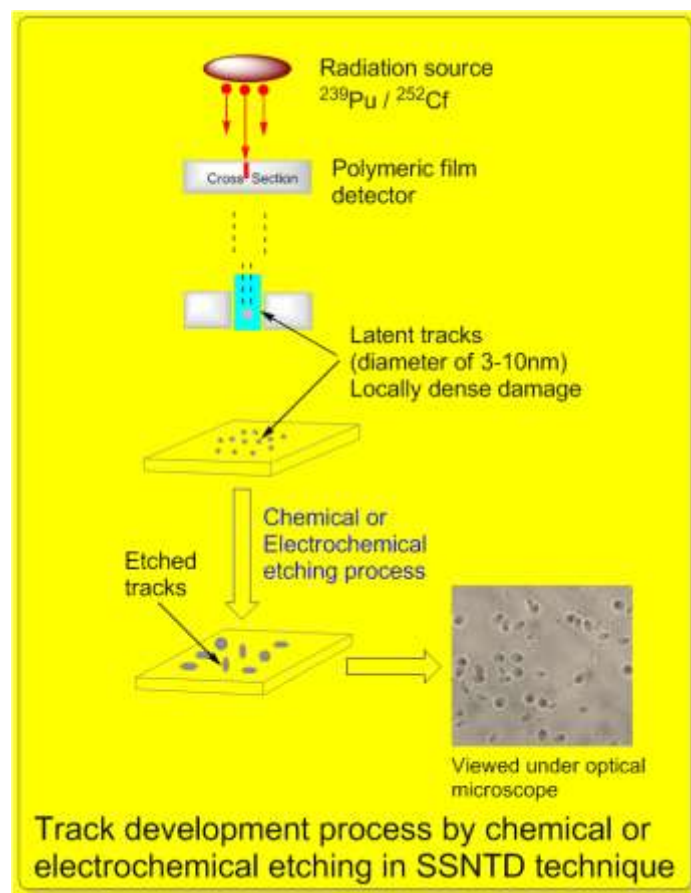

Figure 1.2: Track development process by chemical etching in SSNTD technique.

1.3.1   Characteristics of nuclear tracks: Following are characteristics of the latent tracks formed by charged particle in dielectric materials,

i. The latent tracks primarily consist of damaged region along the pathway of the particle because of displaced atoms.

ii. The latent tracks are reactive centres to chemical reagents.

iii. The latent tracks are stable and can be viewed under optical microscope upon etching whenever required.

iv. The track region is continuous along the trail with a diameter of around 3-10 nm.

v. The damaged track length is equal to the particle range in the material under study.

Dielectric materials with electrical resistivity greater than 2000 Ωcm can accumulate the tracks. Cellulose nitrates or different polycarbonates having long chain polymeric backbone are most suitable for this application. Such effect is also observed in some amorphous materials like glasses, etc. Metals and semiconductors do not form the stable latent tracks and cannot store tracks as the course of recombination of the unstable nuclei takes place rapidly. Materials with high degree of electrical resistance can hold tracks with maximum efficiency.

1.3.2 Theory of track formation: The track formation signifies the processes by which the charged particle modifies the solid along its pathway to create damaged track. Ionizing particles passing through dielectric materials form intense trails of damage on atomic scale. The damage formed by irradiation of solids depends on the intrinsic properties of incident particles like mass, charge, velocity and the material composition of the detector itself. Particle tracks are produced in many insulating materials and some semiconductors. The latent tracks in solids are fine (<50 A radius), stable and chemically reactive centres of damage that are mostly made of displaced atoms rather than electronic imperfection[36]. The heavy ion drops energy while slowing down in a solid and it is very significant in understanding the track formation mechanism. The track forming property of the detector depends on the

sensitivity of material. Various materials have diverse critical rates of energy loss for track formation[44, 56].

In plastics, ionizing radiations directly generates ionized and excited molecules and electrons. Excitation energy can also be moved from one molecule to another. Electrons are entrapped at different sites or can merge with molecules to form negative ions or recombine with positive ions yielding energized molecules. Both ions and excited molecules may obtain considerable vibrational energy and suffer bond break to form a complex collection of radical ions, stable molecules and free radicals.

In case of inorganic crystals, the effect of radiation on the material is to generate ionization and excitation of atoms or molecules. Electrons are moved up across the forbidden energy band. Few may arrive to the valence band via luminescence centres with the release of radiation, while few after diffusing from the crystal will either be trapped at various imperfections sites or will return via non radiative transitions to positive ions.

1.3.3 Mechanisms of Track formation models:

Different models have been proposed for explanation of the track formation and other characteristics of the track formation in inorganic materials and plastics. Some of the successful models are:

1. Thermal spike model

2. Displacement spike model

3. Ion explosion spike model

4. Restricted energy loss model

CHAPTER 1

1. Thermal spike model: The thermal spike mechanism can be utilized to elucidate track formation in inorganic insulating materials. When an energetic particle passes through a detector material it generates lots of heat in localized region of the crystal lattice. The localized heat elevates the region to a higher temperature level and then cools through heat conduction to the surrounding. If the temperature is adequately high, it can cause permanent change thus generating tracks[57]. This technique damages the lattice structure of the material by different atomic processes. This model explains the track formation in insulating materials and inability of metals to reveal tracks. According to this model, charged particle first provides energy to the electrons of the solid then it is transported to the atom by electron-phonon collisions which cause thermal motion. Due to this the incident charged particle displaces the crystal lattice and generates strong heating in some part of the solid where particles are traversed. Metals can drive away the heat formed very rapidly due to the presence of huge number of electrons in the conduction band. In insulators, the electron interacts with the different types of vibrations and the excitation is corresponding to the lattice more conveniently. This model failed to relate sensitivities of the various materials in any standard way with a known melting, softening or transformation temperature of detectors[57c]. Also it could not differentiate suitably between the materials in which tracks might be formed and those in which the tracks might not be produced.

2. Displacement spike model: According to this model particle changes the solid alongside the passageway by moving atoms in the particle nuclei collisions. But this model failed to explain why the tracks were not produced in metals and hence it was discarded. According to it tracks should be more common near the end of the range

of charged particles. This is because of the fact that the loss of energy by particle-nuclei collisions becomes more competent as the velocity of particle diminishes.

3. Ion Explosion Spike model[34,55]: Ion explosion spike model was proposed by Fleischer et al. which successfully and satisfactorily explained the track formation mechanism in dielectric solids. According to this model, a positively charged particle knocks out the orbital electrons of the atom lying in and around the pathway of it, creating a region full of positive ions along the route of ionizing particle. These positive ions repel one another, distressing the regular lattice of a crystalline solid, generating a similar cylindrical region of ion (Figure 1.3). In organic polymer, the charged particles rupture the long molecular chains by ionization and excitation thus forming new species are formed which are highly chemically reactive. These latent damage tracks can be viewed at high magnifications using transmission electron microscope. These damaged tracks can be developed by using suitable etching process as used earlier by D. A. Young. The necessity of track formation in the ion-explosion spike model is that the coulomb repulsive forces within the ionized region should be enough to overcome the lattice bonding forces, in other words, the electrostatic stress should be higher than the mechanical strength or bonding strength.
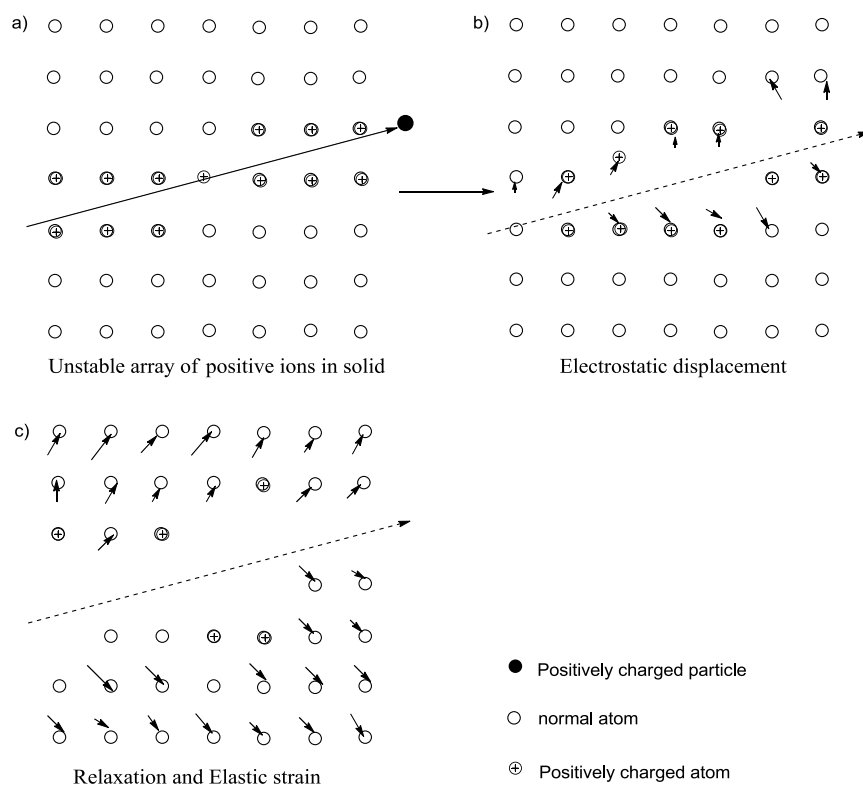
**Figure 1.3:** Schematic diagram of Ion Explosion spike model

4. Radiochemical damage mechanism[30]: Track development in organic solids (polymers) is based on radiochemical damage mechanism. Radiation damage in polymers involves breakage of cross-linking of molecular chains. The time of the polymer dissolution is improved by decrease in molecular weight caused by scission. This prototype of scission and dissolution is followed by the polymeric track detectors. According to this model, etchable tracks are generated by radiolytic breakage of long polymeric chains into fragments and reactive products which are easily dissolved by etching media as compared to the undamaged part. The tracks have been seen in cross linking polymers like poly (allyl diglycol carbonate). The cross-linking can make a polymer less soluble but in the region of radiochemical damage, the etchants attacks the polymer more quickly. The composition of some etch product of polymers which degrade by chain breakage indicates that the

chemical reaction with the molecules plays a part in superior termination. The chain crosslinking ability of a polymer on irradiation can be explained by an empirical rule[58]. The rule says that chain breakage on irradiation is likely in polymers with general formula:
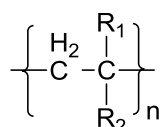
while those with cross links are of the type
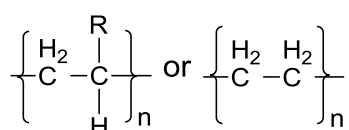
Radiation damage in polymers can generate free radicals by breaking C-C backbone bonds and C-H bond.

1.1

1.2
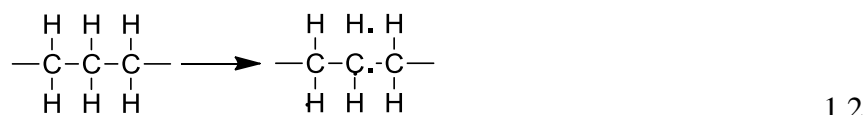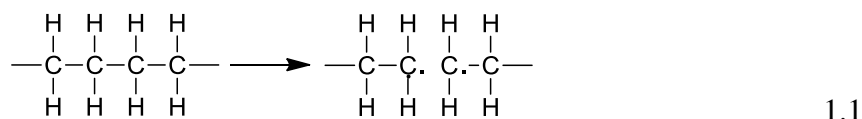
In first stage, the free radicals can readily recombine in case of polyethylene as the broken ends do not require any specific orientation to approach each other before recombination. In doubly substituted molecules, the probability of recombination is decreased slightly because of formation of stable end groups. The stabilization of the breaking event is observed in poly isobutylene as shown below.

1.3
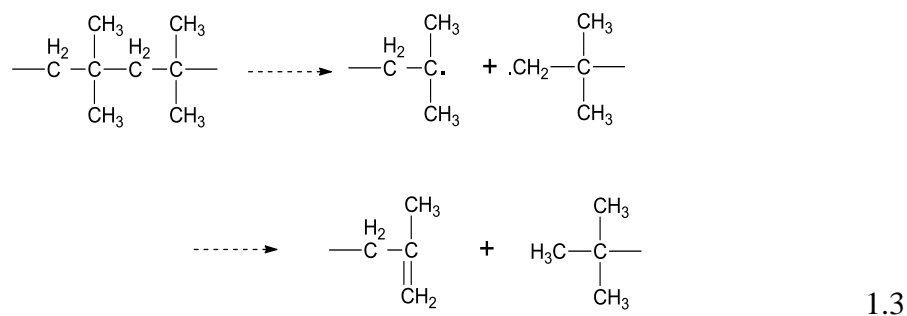
Thus, the damage process in polymeric track detectors could have many stages. It is possible that the mechanisms propagating from the damage at the track exists leading to a lower primary ionization density necessary for etchability. In case of polycarbonates, damage mechanism is available in addition to the ion explosion spike. Polymers can be degraded at energies below that required for ionization. The lower energies necessary for polymer degradation mean that the delta rays also contribute considerably to the damage leading to improved etching rates reasonably remote from the track core in which the ion explosion mechanism dominates.
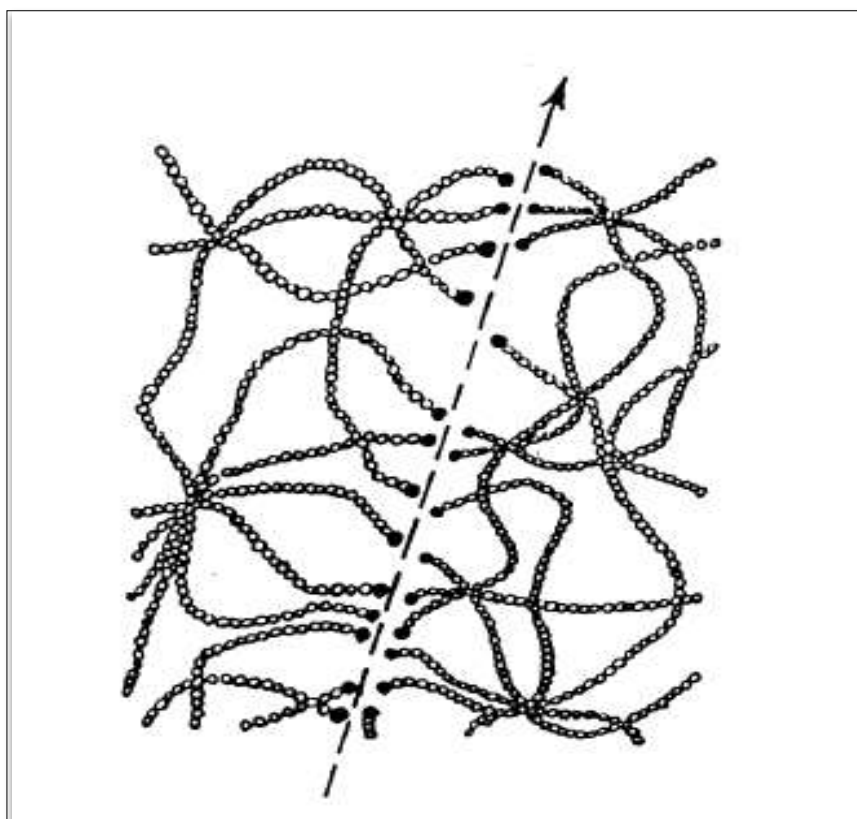

Figure 1.4: Radiochemical damage mechanism.

Thus, the penetration of charged particle creates a range of free radicals along its route as shown in Figure 1.4. The creation of free radicals can lead to chain breakage, degradation of side groups into low molecular weight species and the

formation of cross links thus forming a latent track. Chemical reagents like alkalis are capable of degrading these regions of the latent track predominantly.

1.3.4   Geometry and Criteria of track formation[46a]:

During exposure to charged particle source, numerous latent tracks are created along the path of the ions. After irradiation, the material is subjected to etching process to reveal preferentially the latent ion tracks. The geometry of track development is shown below in figure 1.5(a, c) where the ionizing radiation incidents at an angle perpendicular to the surface of detector and at critical angle above which tracks are registered. When the charged particle incidents at angle below critical angle θ_c, no tracks are registered as the surface is removed at faster rate than normal component V_t (figure 1.5 b).
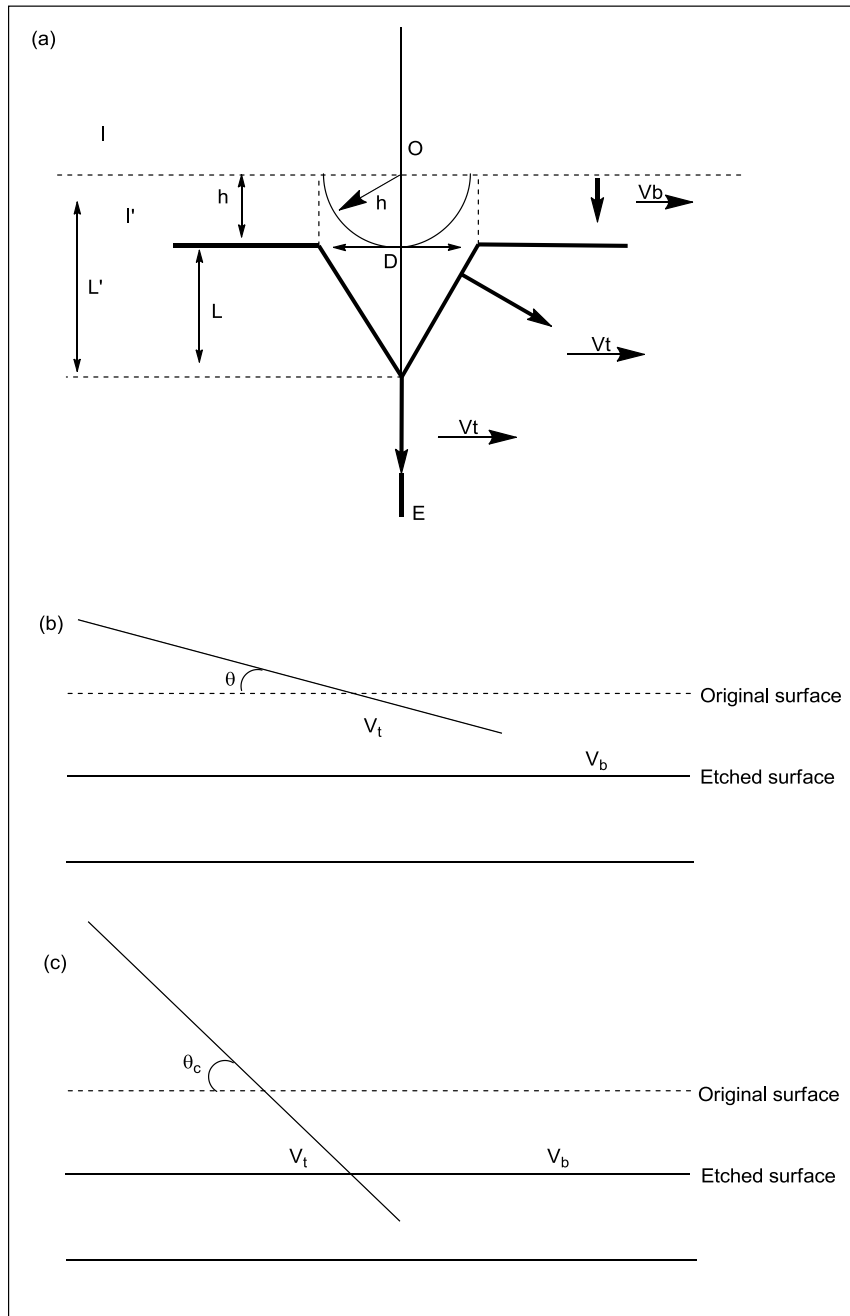
Figure 1.5: (a) Geometry of track formation when charged particle incident at right angle to surface of detector (when $V_b/V_t < 1$); (b) No etchable track formation occur when charged particle incident at an angle below critical angle ($\theta < \theta c$). (c) When charged particle incidents at critical angle θc above which tracks are registered which will have different shapes.

Here, the simple case of track development is considered wherein the incident particle enters a detector perpendicular to the detector surface as shown in Figure 1.5(a). In this figure, the initial detector surface is represented as I, I' is surface after etching, V_t is the track etch rate along the particle pathway, V_b is the etch rate of undamaged area of the detector i.e. bulk etch rate, the entrance point of particle corresponds to O and the end point of a particle in the detector material is given by E, and the range of particle in the detector material is given by OE. The thickness of the layer removed by etching is the distance between I and I' which is equal to h, the total distance traversed by the etching solution along the particle track is L', and the track depth is given by L. Diameter of the etched track is D.

During the study of chemical etching process, the shape and size of the etched track is determined. During this process, the most significant experimental parameter is the "Track etch ratio" which is the ratio between the track etch rate (V_t) and the bulk etch rate (V_b). Development of any tracks in dielectric material is governed by the ratio $V = V_t/V_b$. If the track etch ratio V is smaller than or equal to 1 then the track will not be seen after etching. That means to form an etchable track in detector; the condition $V > 1$ must be fulfilled. The feature of the etching process is proportional to the energy deposition density of the ion along its path, also on the radiation sensitivity of the material, on the storage conditions of the irradiated material before etching, and on the etchant.

In three dimensions, the geometry of track formed is conic and depending on the angle of incidence track geometry can be altered.

Bulk etch rate (Vb)[16]**:** The bulk etch rate V_b is the rate at which the undamaged surface of the detector is taken away during chemical etching. Some molecules of the

detectors are removed because of the chemical reaction between the etchant and the detector material. The final effect is the exclusion of the material from the detector surface. During etching process, the material is removed layer by layer and the detector thickness becomes smaller and smaller. The bulk etch rate is probably the most oftenly measured quantity concerning track detectors.

Track etch rate (V_t)[16]: The rate at which the latent track is etched is called track etch rate in other words it is the rate of etching of detector along the trail of charged particle. This process involves attack of the etchant along the trajectory of track. Track etch rate depends on the extent of damage located in the trace core region. As mentioned earlier, that the track etch rate should be always greater than the bulk etch rate for efficient track viewing under optical microscope.

Critical angle of incidence (θ_c): The surface of some detectors dissolves at a finite etching rate and tracks incident at a very shallow angle in these detectors will not be noticeable. For each and every detector materials, there exists critical angle of incidence[46 (b)] (θ_c) as shown in table 1.3 below. At any angle below θ_c, no etchable track will be seen after etching process although condition $V_t > V_b$ is satisfied, as the surface would dissolve at a faster rate before the track material was etched out[59]. To understand it, consider a ionizing radiation strikes the detector surface at an angle θ (figure 1.5), After etching for time t', $V_t \cdot t'$ and $V_b \cdot t'$ be the thickness of removed bulk material. The tracks recorded will be seen only if the component $V_t \cdot t' \sin\theta$ is larger than $V_b \cdot t'$

So, critical angle is given by,

$V_t \cdot t' \sin\theta_c = V_b \cdot t'$ (considering $\theta = \theta_c$)

i.e. $\theta_c = Sin^{-1} (V_b/V_t)$

Table 1.3: Critical angle of incidence in different NTDs

Material	Critical angle of incidence $\theta_c(^o)$
1. Minerals	0-7
2. Glasses	
soda, borosilicate, flint, Obsidian *etc*.	20-70
Phosphate glass	1-5
Silica glass	13-19
3. Plastics	
Nitrocellulose	>2
Lexan	2.5
Makrofol	3

From the θ_c values given above, it may be observed that plastics are certainly more efficient, because of its lower value of θ_c.

1.3.5 Criteria for track formation: The chief condition for track formation is that the, track etch rate must be always higher than the bulk etch rate for efficient track development. The legitimacy of this condition has been scrutinized by many theories put forward by different track detector employees. A track formation must define a parameter X, having an exact and distinct limit X_c, below which a non-etchability limit occurs. These criteria's are discussed in many reports. Few are listed as follows

i. Total Energy Loss rate (dE/dx) criterion[60]: This criterion was first proposed by Fleischer, Price, Walker and Hubbard in 1967. If rate of energy loss by the charged particle is above the critical value then the charge particle track is formed in a detector material which is characteristic of the material. That means the rate of energy loss per unit length dE/d_X by the attacking particle must surpass a critical value, $(dE/dx)_c$. This criterion was successful for particle velocities over a constricted region. But it failed when it applied to relativistic particles. This is because the relativistic bombarding particles generate many energetic delta rays

which scattered away from the latent track region leaving their energy away from the path of the primary particle. Therefore this criterion was rejected by Fleischer *et al.* in 1967.

ii. Restricted Energy Loss (REL) criteria[61]: The charged particle falling on to the detector loses its energy because of distant collisions with electrons of the stopping material which is called restricted energy loss. According to this criterion, latent track can be formed only if REL of the particle surpasses a critical value characteristic of the detector material. This energy loss includes both the energies of primary ionization as well as higher order ionizations. This criteria works well when the incident particle energy is greater than 3.5MeV/nucleon.

iii. Radius restricted energy loss (RREL) criteria[62]: All the measures of energy deposition occurring within a radius 'r' around the passing particle are accounted in the RREL criteria. This criterion highlights the track region and strives to consider only that part of energy of delta rays, which really gets deposited in the interior region irrespective of the energy of the delta rays.

iv. The primary ionization criterion (PI)[63]: When charged particles go through a detector material, powerful ionization takes place and the particle is stripped off of its electrons. If the primary ionization occurs at higher rate than its critical value, etchable track will be formed. However, this criterion does not consider the δ rays and their ionizations.

v. The delta-ray criterion by Katz and Kobetich[64]: According to this criterion, to form etchable tracks, the secondary electrons should deposit critical energy at critical distance. This approach is exactly opposite to that of the total energy loss and the primary ionization criterion. To calculate the spatial energy distribution, the δ ray energy spectra and the range energy relation in the vicinity of the particle track were

combined. This criterion fails as it neglects the contributions of the primary excitations.

vi. The delta-ray criterion by Monin[65]: This approach is analogous to that of Katz and Kobetich. This criterion does not consider any critical radius initially as the dose deposited within the cylindrical area is calculated. A traversing particle is thus believed to produce an etchable track when the absorbed dose surpasses the specific value within a cylinder of certain radius.

1.4   Track visualization techniques and its evaluation:

The commonly used techniques for track visualization are as follows:

1.   Electron microscopy: The charged particle tracks in an unetched detector are not visible under an optical microscope but, can be seen directly by transmission electron microscopy successfully. TEM was first used by Silk et al to view latent tracks in crystalline detector material like mica[32]. This technique can be useful only to exceptionally thin (< 3000 Å) detector samples with quite high track density (10^5 tracks/ cm^2).

2.   Selective chemical etching[66]: The most extensively used method among the track detection workers for track visualization is the chemical etching method. The latent track of nuclear particle is a region of enhanced activity towards chemically aggressive reagents. The detector with latent track is immersed into a solution called 'etchant' which degrades the latent track at much faster rate than the surrounding bulk region. This process enlarges the latent tracks in detector. When the size of the tracks become similar to that of the wavelength of visible light they act as strong scattering center which appears black in normal bright field illumination and white in a dark field under the optical microscope. This process of chemically increasing

the dimensions of the latent track damages to visible tracks under the optical microscope is termed as chemical etching. Once the chemical etching process is finished, the detector is removed from the etchant and washed with distilled water. The detector is dried under an IR lamp before observing under optical microscope. Typical chemical etching methods for some detectors are summarized in table 1.4 below.

Table 1.4: Etching conditions used for etching latent tracks in different detector materials.

Category	Track detector material	Etching conditions
Crystal	Feldspars	33% aq. NaOH solution, reflux.
	Olivine	KOH solution at 160 ºC for 6 min.
	Mica	48 % HF solution at 20-25 °C for 3 seconds- 40 min.
	Quartz	KOH solution at 210 ºC for 10 min.
Glass	Soda lime glass	48 % HF solution at 20 - 25 °C for 3 sec.
	Phosphate glass	48 % HF solution at 20 - 25 °C for 3 sec.
Plastics	CR-39	1 - 12 N NaOH at 40 - 70 °C for 1-4 hrs.
	Polycarbonate	6 N NaOH at 50 °C for 60 min.
	Cellulose nitrate	3-6 N NaOH at 50 °C for 40 min.

There are a vast number of etchants which can be used for track revelation. The plastic track detectors are normally etched by using strong alkali hydroxides such as NaOH, KOH etc. To amplify the effectiveness of attack of these aqueous etchants, etch promoters like ethanol, methanol, propanol is supplemented into the solution. These organic solvents speed up the rate of dissolution of the degraded polymer fragments produced during etching process. Detergents are also added in some cases which can be utilized for creating cigar-like shapes of the tracks[67].

Oxidizing agents like $KMnO_4$, $K_2Cr_2O_7$ have also been attempted. However, these etchants leads to highly resistant deposits of partially reduced metal oxides of low solubility. The chromium attaches to polymers by covalent bonds and cannot be removed easily. For minerals and glass track detectors acids like H_2SO_4, H_3PO_4, HF, HI, HCl, glacial acetic acid etc are utilized as etchants.

3.   **Electrochemical etching (ECE)[68]:** The chemical etching process is enhanced by using high voltage electric fields. The process enhances the size of the tracks so that they can be counted by low magnification device. This method is more useful for light particles like protons, alphas at low intensities. The process makes track counting easier and faster. The process of ECE starts with the development of conical tracks with a sharp tip analogous to the tracks obtained by chemical etching. Under these conditions the influence of electric field at the conductive tip can be many times larger than that applied to the remaining surface of the detector material. The chemical action of the etchant combined with the electrical phenomena initiated by very high localized stress gradients leads to formation of tree shaped track at the tip, the process is called treeing. The process can be visualized from the Figure 1.6 below.
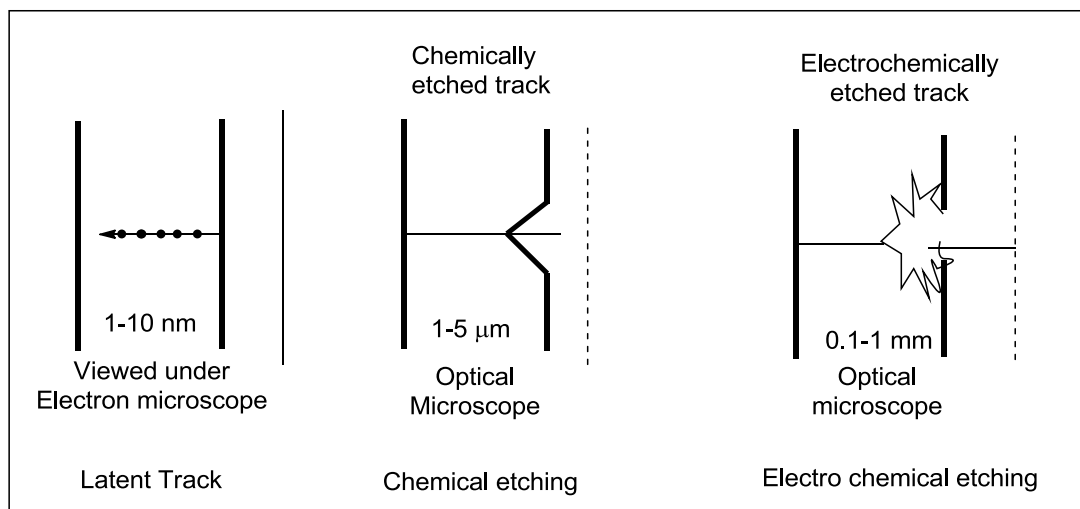

Figure 1.6: Electrochemical etching process.

The ECE process consists of two volumes of electrolytes which are separated by the detector material. One of the electrolytes is the etchant used for chemical etching of the detector. The two electrodes are dipped in the two electrolytes and alternating current of high voltage is applied across the foil. The ECE electrical field ranges from 20-40kVcm^{-1}with the frequency values of the order of kHz. The detector film behaves as insulator between the two electrolytes. The AC voltage also leads to electrical phenomena that lead to electrical stress in the polymer. The high voltage produces the thermal phenomenon which increases the etch rate of the detector. The etching process is carried out at a temperature between 25-70°C. In the ECE process the first step is the formation of a cone as is the case in chemical etching. Once a conical track is formed the tip of the needle shaped track attains a high electric field than that of the remaining detector. The high electrical field generates a local stress and can initiate electrical phenomenon which when combined with chemical action of the etchant produce a tree shaped track and the process is called treeing. A typical ECE assembly is showed in the Figure 1.7 below.
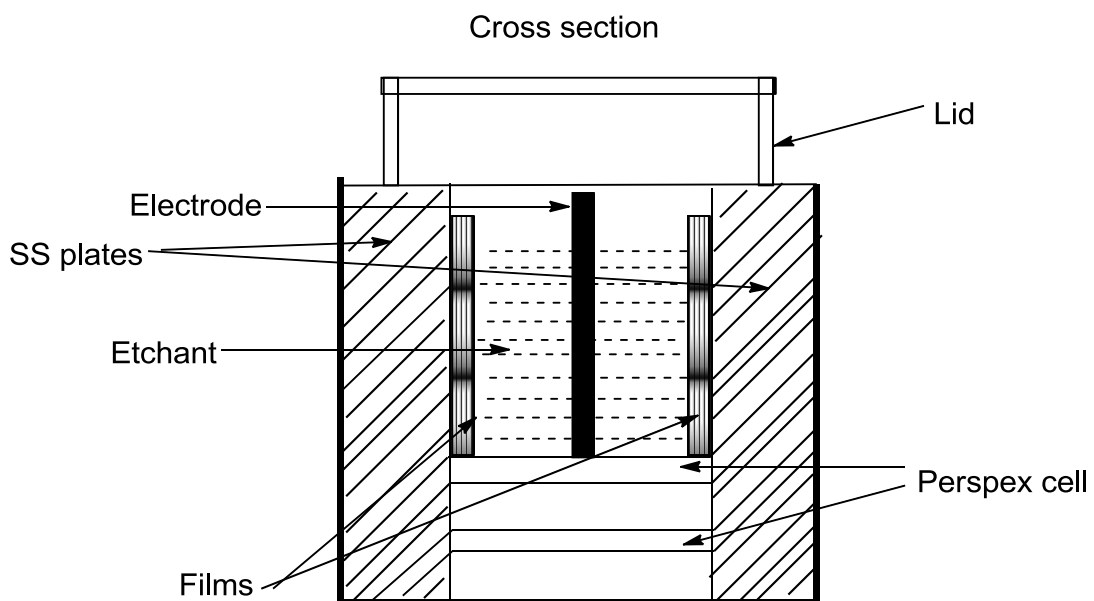

Figure 1.7: Electrochemical etching assembly.

This technique has been found to be better than conventional chemical etching as it gives large amplification of the tracks that can be seen by naked eyes. This technique has principally found to work with polymers with general properties like good electrical properties, low water absorptivity, low value of dissipation factor or dielectric loss factor and polar nature of the materials.

The disadvantages of the technique are that the presence of high track density (above $10^3 cm^{-2}$) makes the technique incompatible due to intersecting track geometries. Secondly, the specific information of the track is lost upon EC etching. Moreover, tracks analogous to radiation particle tracks are obtained if the detector contains defects or contaminants.

4. **By optical microscope:** The optical microscope is the most appropriate equipment utilized for track visualization and tracks counting in SSNTD. Tracks formed by chemical etching are usually viewed by an optical microscope using different magnifications. Tracks counting in each graticule can be carried out by using hand tally counter. Track parameters such as track length, track diameter etc can be measured with the help of a micrometer eye piece. This technique is not suitable when a detailed structural analysis of an individual etched channel is desired.

5. **By naked eyes:** In 1966, the Aluminium backed plastic detector technique was suggested by Fleischer et al.[69]. In this technique an opaque coating of aluminium is made on one side of the thin film of detector. The thickness of the detector should be less than the expected length of the particle track. After irradiation, only the detector side is etched. Thus the etchant (hydroxide solution) dissolves the thin layer of aluminium along the track site and creates large holes in it. The holes are easily visible by naked eye. Another technique of detecting holes in thin plastic sheets was

developed by Cross and Tommasino[70] in 1967 which could detect upto 10^3 tracks/cm^2. In 1969, Block et al.[71] developed yet another technique in which ammonia gas was made to pass through the track path from one side of the plastic track detector to form a replica of track pattern on a sensitized paper. It is useful only for very low track densities.

1.4.1   Factors influencing etch rate of a detector during etching process:

The factors affecting the etch rate of polymer are

i) Etching conditions: Different etching conditions used during track revelation effects the bulk etch rate. The elevation in temperature has a significant effect on the bulk etch rate. The speed of etching increases exponentially with the increasing temperature for the plastic track detectors. Different alkali hydroxide solutions are used for etching process of the plastic track detectors. The bulk etch rate of a polymeric detector enhances with increase in ionic radii of alkali metal ion used[72]. Figure 1.8 and 1.9 shows change in the bulk etch rate with the type of alkali and concentration respectively.
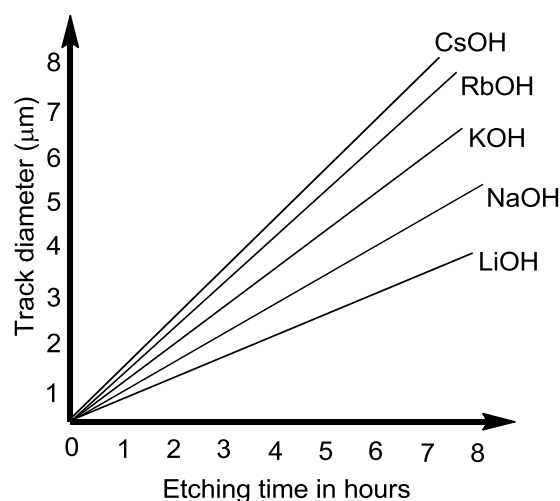

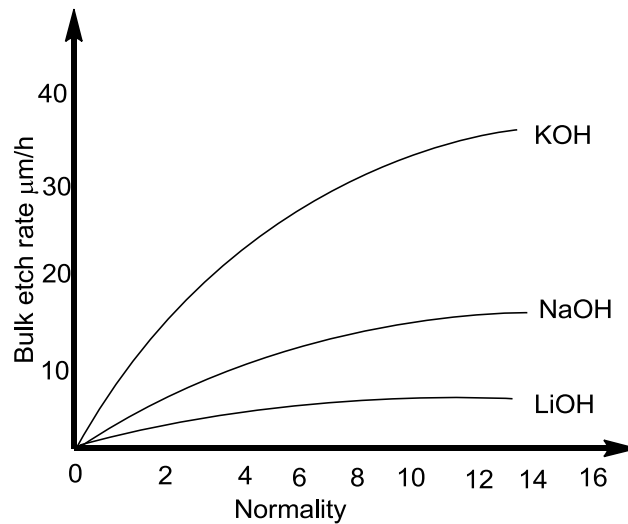**Figure 1.8:** Effect of different alkali hydroxide on the track etching rate of a polycarbonate.

Figure 1.9: Effect of etchant concentration on the bulk etch rate of LR-115 detector at 50°C.

From figure 1.9, it is clear that with increase in the concentration, the bulk etch rate was increased exponentially. The stirring speed of the etchant solution also plays crucial role in etching process. The rate of etching decreases when detectors are etched without stirring of etchant media[72(b)].

ii) Effect of homogeneity[73]: According to thermal spike model, the latent tracks are produced due to rapid thermal stopping of the bombarding charged nucleus by an amorphous ion track core. The removal of the amorphous component selectively leads to the development of track and is the major step in ion track etching. Crystalline solids are therefore, preferably suited for ion track etching, but, large mono crystals seldom occur. Muskovite, Mica and Quartz are some of the mono crystals which are used. These systems are very promising detectors for research, due to their high homogeneity down to the atomic scale, they facilitate well-defined nanostructures down to less than 10 nm. Displacement and marked grain boundaries

will challenge the latent tracks during track etching process in case of polycrystalline solids and hence are barred.

iii) Detector ageing effect: The aging of polymer film ageing can affect the etching properties of the material. The detector ageing depends on the storage conditions. The moisture content in storage places of some detectors can affect the bulk etch rate of water sensitive polymers like LR-115[16]. Natural degradation of CR-39 detector may occur by auto-oxidation. Peroxides may be formed due to attack of oxygen on the tertiary hydrogen of allylic part of the polymer[74]. The peroxides formation on the substrate will preferentially take place with tertiary hydrogen atoms in the structure[75].
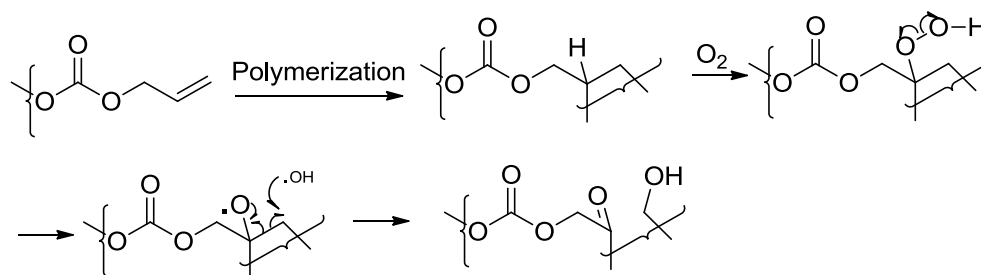
A nitrogen atmosphere reduces the track etching rate. Detectors older than 5 years show abnormal activities of bulk etch rate which reduces upon increased age.

iv) Irradiation effect of detector before etching[46]: There is enhancement in the bulk etch rate of the detector if irradiated with certain radiations before etching. Before etching if the detector materials are irradiated with radiations such as, gamma radiation, electrons, proton beams, ultraviolet and infrared radiation it increases the bulk etch rate. Polymer surface undergo different changes on exposure to radiation i. e. it causes either localized hardening/bulk surface hardening or softening. The hardening caused by heating leads to decrease in bulk etch rate, while softening can lead to enhanced etch rate.

The increase in the gamma dose on the detector increases the bulk etch rate as well as the sensitivity of the material[76]. The effect of gamma dose on PADC bulk etch rate was not intense till a dose of 10^4 Gy as V_b was unaffected. But, further increase in dose increased the V_b[77]. The ultraviolet radiations, proton beams, the infrared radiation and electrons also enhanced the etching rate. This was due to the chain scission/ breakage of the polymer matrix during irradiation.

1.4.2 Mechanism of surface degradation in detectors[36, 78 (a)]:

The mechanism of track development in polymers is entirely different than that of inorganic materials. Here, the etchant actually attacks the functional groups present in the polymer and degrades the material. The polymers containing different functional groups can be etched as follows.

i) The carbonate containing polymers (CR-39): The polymers with carbonate moieties are very frequently used as plastic nuclear track detectors. The commonly used carbonate containing detector is PADC or CR-39. The polymer degrades in alkali solution as follows
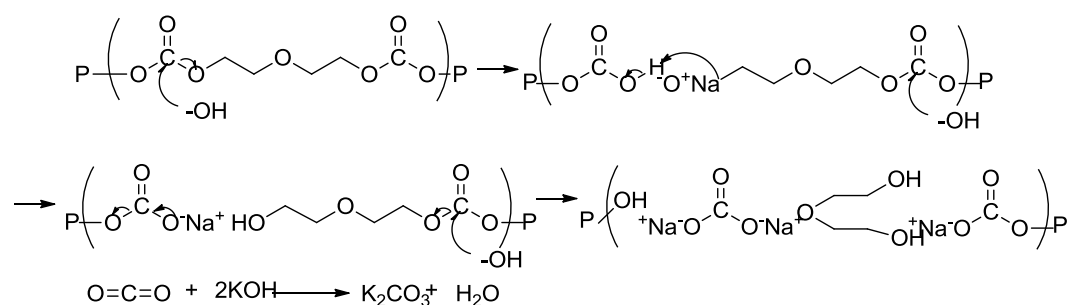

Initially, the base interacts with the carbonate functionality thus leaving the bridged ethylene glycol free into the solution. Further, the carbonate moiety gets decarboxylated and the liberated carbon dioxide is absorbed in the alkali hydroxide solution completing the dissolution process. Also, the ethylene glycol along with the

carbonate moiety can be eliminated as a single fragment. Similar mechanism exists in all the other polymers having carbonate moieties.

ii) Polypropylene (PP): This monomer does not have any reactive functional group but under oxidizing etchant condition, acetic acid is formed as one of the etch products. It is etched in acidic CrO_3 etching media. Here, the tertiary carbon is attacked by strong oxidizers breaking the carbon hydrogen bond. This creates peroxides or hydroperoxides and later carbon-carbon bonds adjacent to the tertiary carbon are cleaved.

iii) The ester moiety in Polyethyleneterephtalate (PET): In case of PET, disodium terephthalate and ethylene glycol are generated during hydrolysis of the polymer as the end products. The products can be accounted for, only if, the points of etch attack are the partially charged ester groups, which are hydrolyzed by alkali.
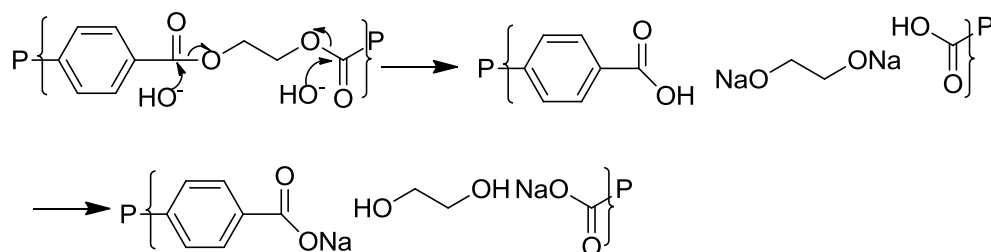

Track etch ratio above ten thousand have been observed for polycarbonates[98(b)]. And it can be reduced by adding organic solvents, like methanol, ethanol or propanol into etchant for PET. For example, these cones can be placed on both ends of a cylindrical track section. In general, heavier ions lead to more specifically defined ion tracks.

iv) Nitrocellulose / Cellulosic's: Nitrocellulose polymeric detectors have numerous applications because of its easy formulation procedure, low cost and its sensitivity to practically all nuclear radiations like alpha, protons and neutrons. High energy

charged particles causes modification of bonds in polymers. Many radicals, reactive sites in the latent tracks region are formed when radiations strikes the polymer. In cellulosics, the cleavage occurs at the bond with least strength like at acetate or nitrate linkages. The radicals formed due to cleavage can undergo oxidation with nitric or acetic acid. Nitric acid is good oxidizing agent as compared to acetic acid. Nitrocellulose (CN) is well-known to undergo fast hydrolysis. During the hydrolysis process of nitrocellulose, nitrate groups are reduced to nitrite and CO_2 gas is formed which was studied by Kenyon and Gray[78(c)]. It was supported well by Berthlot [78(d)] who suggested the route shown in Eq. 1 and Klason[78(e)] who gave process shown in Eq. 2. Formation of aldehyde and ketone from primary and secondary nitrates respectively was confirmed by Honeyman[78(f)] (Eq. 1, 2 and 3).
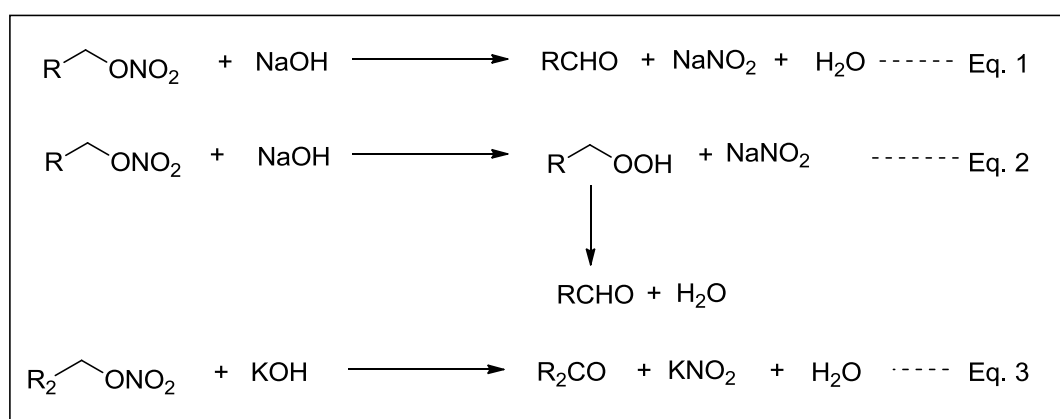
Further, Lucas and Hammett postulated processes[78(g)] (Eq. 4-7) regarding the mechanism of CN that also supported the observations of Kenyon. During base catalyzed reaction, benzyl nitrile undergoes first order reactions (Eq. 4 and Eq. 5). This was extrapolated to CN and degradation study was explained (Eq. 6 and Eq. 7). In reaction Eq. 6, nitrocellulose undergoes simple ester hydrolysis. Three possibilities of cleavage can exist in second case i.e. formation of (a), (b) or (c) or both (b) and (c) (shown in Eq. 7). A rapid hydrolysis will occur at 2-keto and 6-CHO

groups which are beta to 4-glucosidic link. So, ketonic bond formation over cellulose chain helps in its sensitization to alkaline attack.
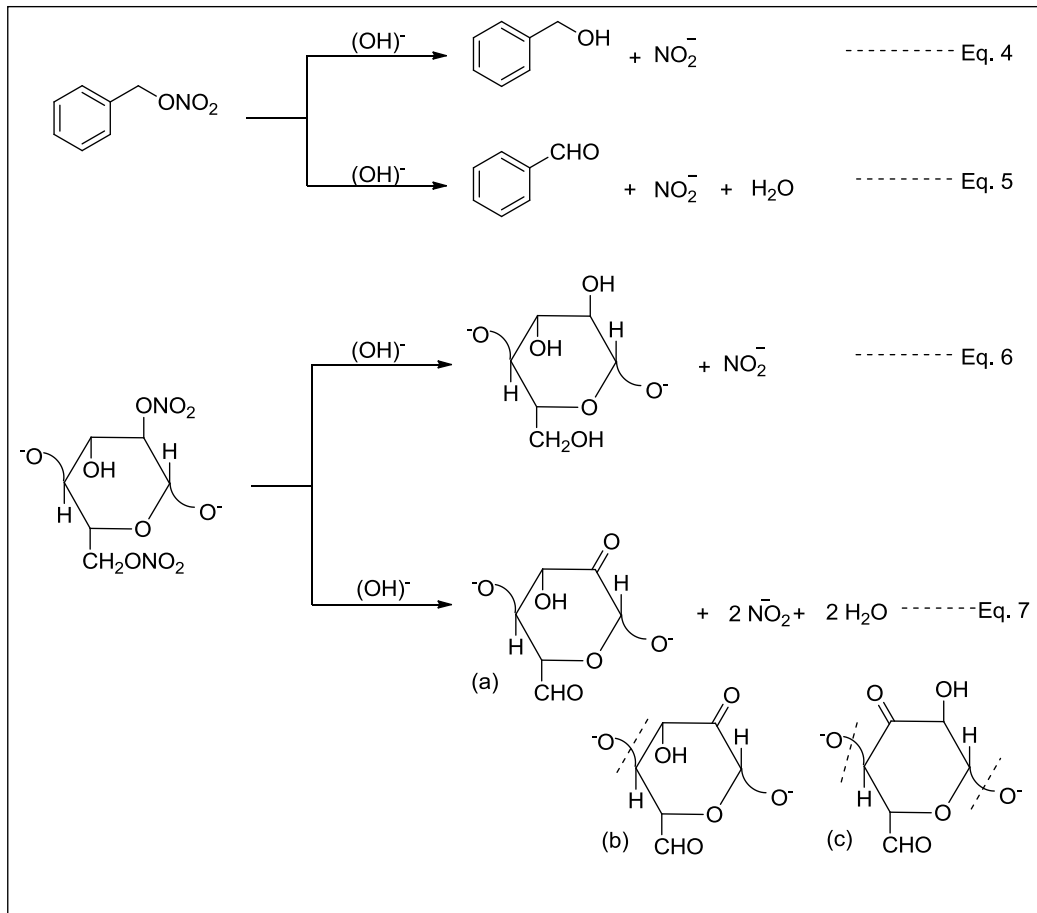
1.4.3 Techniques to improve track visibility:

Development of tracks by chemical etching process and their observation under optical microscope can be enhanced by following techniques.

i) The track visibility can be improved by using polarized light and a crossed polarizer. The light scattered from track surfaces can be easily detected by crossed polarizer[79].

ii) A thin layer (8-12 μm) of red-dyed cellulose nitrate is coated over polyester film which on etching, holes of particle tracks is seen over a red background. These tracks

can be consequently enlarged and recorded permanently on high contrast film or photographic paper[80].

iii) If fibre optic is used to introduce light at edge of detector film, bright tracks on a dark background can be viewed on a film. The tracks can then be effortlessly counted against a dark background[81].

iv) The track detector surface is coated with silver layer which reflects the light and the reflected light can be utilized to illuminate the tracks and help counting purposes[82].

v) Tracks can be viewed under ultraviolet light by using a fluorescent dye to penetrate etched tracks[46 (b)].

vii) If the holes in a detector film are exposed simultaneously to HC1 gas on one side and NH_3 gas on the other then the reaction produces white NH_4C1 crystals at each hole and tracks can be viewed and counted easily [83].

Visual counting of tracks is usually a difficult and lengthy procedure and requires automatic techniques when evaluation of many detectors or of large areas, speed and high accuracy is concerned.

1.5   Literature review on nuclear track detectors:

The technique of SSNTD was commenced in the year 1960, when ionizing radiation tracks were developed by suitable etching process by D. A. Young at AERE, Harwell. Different materials can be used as nuclear track detectors after appropriate calibration. Various natural minerals, glasses and plastics are utilized as track detectors. As per the scifinder report, there are around 6595 research papers, articles etc. that have been published by researchers and scientists from this field

during the period of 1964-2017. Approximately 3309 articles were published on solid state nuclear track detectors for the period of 2000-2017.

According to early reports, during the period of 1964-1994, around 2462 articles were published on nuclear track detectors[84] as searched over scifinder by terms "Solid state nuclear track detectors" OR "particle track detectors" OR "Polymeric track detectors" OR "SSNTDs" NOT "Solid state". And there are only 484 articles related to polymeric track detectors published for past 5 decades. Out of which only few were dealt with design and preparation of new polymeric detector films.
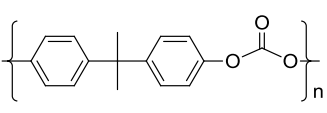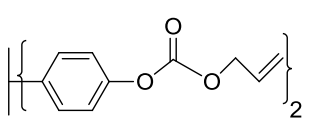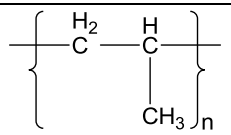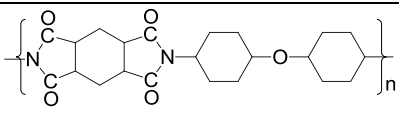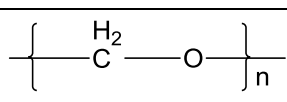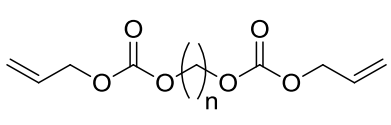
1.5.1 Polymeric track detectors: During early years, cellulose acetates, cellulose nitrates, bisphenol-A polycarbonates were used as plastic track detectors until the introduction of aliphatic polycarbonate CR-39 as nuclear track detectors. The use of CR-39 as track detector was a milestone in the field of solid state nuclear track detection. CR-39 polymeric material showed outstanding performance both in track sensitivity, homogeneity and optical properties. It could detect charged particles $Z/\beta \geq 6$[85]. The polymer was widely utilized in neutron dosimetry, measurement of traces of uranium in different materials and cosmic radiations study.

Table 1.5 gives the details of few monomeric/ polymeric materials that have been tested as plastic track detector.

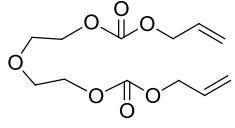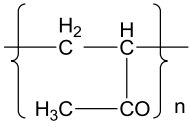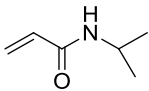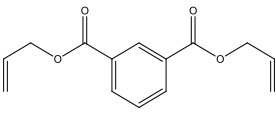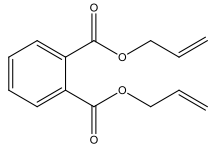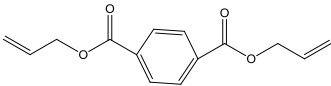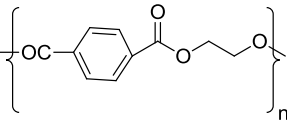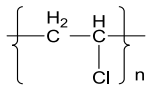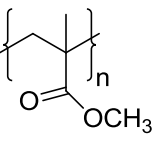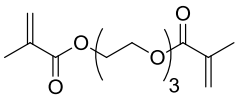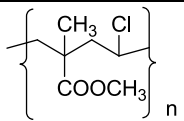**Table 1.5:** Some monomers/ polymers that have been tested as plastic track detectors

Sr No	Name of monomer with CAS registry number	Monomer or CRU	Trade name
1 2	Cellulose acetate {9004-35-7} $R^1 = R^2 = H, R^3 = -COCH_3$		
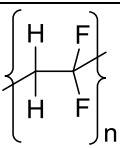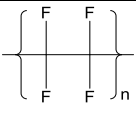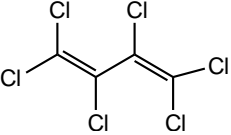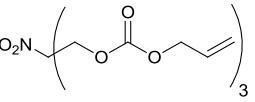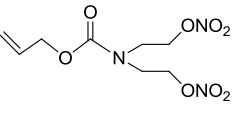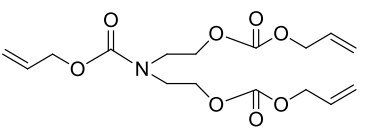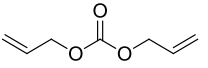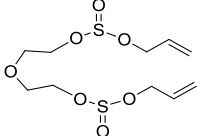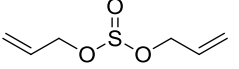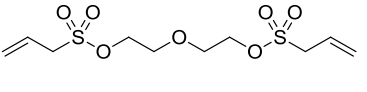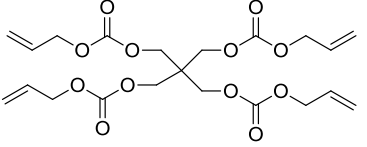
	Cellulose acetate butyrate {9004-36-8} R^1= H, R^2= -COC_3H_7, R^3= -$COCH_3$		
3	Cellulose diacetate {9035-69-2} R^1= H, R^2= R^3= -$COCH_3$		
4	Cellulose triacetate {9012-09-3} R^1= R^2=R^3=-$COCH_3$		Triafol-TN
5	Cellulose nitrate {9004-70-0} R^1= R^2=R^3=-NO_2		LR-115, CN-85, Daicel
6	Bisphenol-A polycarbonate {9002-88-4}		Lexan, Makrofol
7	Bisphenol-A- bis (allyl carbonate) [88] {84000-75-9}		CR-73
8	Poly(propylene) [56(b)] {9003-07-0}		Propene polymer
9	Poly(imide) [46(b)]		
10	Poly (oxymethylene) {9002-81-7}		Formaldehyde polymer
11	Alkanediol bis allyl carbonate [86] Propanediol when n= 3; Butanediol when n=4 ; and Pentanediol when n=5		

12	Allyl diglycol carbonate[45(d)] {142-22-3}		CR-39
13	Poly (vinyl acetate) {9003-20-7}		Poly(1-acetoxyethylene)
14	N-isopropyl acrylamide[87] {2210-25-5}		Copolymer with CR-39 used as track detector
15	Poly diallyl isophthalate[88] {25035-78-3}		Diallyl isophthalate polymer
16	Poly diallyl phthalate[89] {25053-15-0}		
17	Diallyl terephthalate[90] {959-26-2}		AW-15
18	Polyethylene terephthalate {25038-59-9}		Lavasan, Mylar, Melinex-O
19	Poly(ethylene) {9002-88-4}	$\{CH_2\}_n$	Poly(methylene)
20	Poly (vinyl chloride)[91] {9002-86-2}		Poly(1-chloroethylene); Myraform
21	Poly (methyl methacrylate)[98(a)] {9011-14-7}		Methyl methacrylate polymer; PMMA
22	Triethylene glycol bis (methacrylate)[88] {109-16-0}		
23	Methyl methacrylate vinyl chloride		Viniproz
24	Tetrafluoroethylene-	$-\{CF_2CF_2-\}_n-\{CH_2CH_2-\}_m-$	PTFE-E

	ethylene copolymer		
25	Poly(vinylidene fluoride)[92] {24937-79-9}		Poly(1,1-difluoroethylene); PVDF
26	Poly(tetrafluroethylene)[93] {9002-84-0}		Teflon
27	Hexachlorobutadiene[94] (gets copolymerized with ADC monomer)		Actually used as additive in PADC polymer
28	Tris-(2,4-dioxa-3-oxohept-6-1-yl) nitromethane[98(a)] (TDONM) {119845-30-6}		
29	Allyl bis-(2-nitroxy-ethyl) carbamate[98(a)] (ABNEC)		
30	N-Allyloxycarbonyloxy-diethanolaminebis-(allyl carbonate)[95] (NADAC) {869885-52-9}		
31	Diallyl carbonate (DAC)		
32	Poly (ADC-co-SO$_2$)[96]	Copolymer of ADC with SO$_2$.	
33	Allyl diglycol sulfonate (ADS)[98(b)] {121752-04-3}		
34	Diallyl sulphite (DAS)		
35	Diethylene glycol bis(allyl sulfonate)[97, 98 (b)] (DEAS)		SR-86
36	Pentaerythritol tetrakis (allyl carbonate)[98(b)] (PETAC)		

From the literature, it was observed that, in most of the cases only commercially available plastic films are analysed as SSNTDs. Columbian Resin CR-39 was explored in detail. There have not been any special attempts worldwide in designing and developing newer polymers were made leaving few materials. The primary focus of research has always been in the enhancement of the process for CR-39 track detectors. CR-39 is the only polymeric material commercially available to track workers and most of the research is involved in improving this commercially available CR-39 detector only. To some extent, LR-115 plastic detector is also used for track detection. Both CR-39 and LR-115 detectors have been used in many applications, particularly for radon, thoron and their descendant's measurements.

LR-115 detector[99, 100]**:** LR-115 type-II plastic detector has been used worldwide for measurement of radon, thoron and their progeny. This detector is made up of a thin film of cellulose nitrate having thickness of around 12 μm deposited on 100 μm thick clear polyester base substrate. This detector has been commonly used for the long-term integrated measurements as it is sensitive to α-particles, and offers less expansive method. These are of two types, pelleculable and non-pelleculable. In non-pelleculable detectors, the tracks can be counted by using an optical microscope. Tracks in the pelleculable detectors can be counted with the help of a Spark Counter.

CR-39 detector: The CR-39 detector is most versatile, sensitive, and widely used SSNTD till date. In 1978, Cartwright and his colleagues used CR-39 for the first time as a track detector[45(d)]. In 1940, Columbia Resin 39th sample is abbreviated as CR-39. It is an amorphous polymer with three dimensional networks containing carbonates and diethylene glycol groups[101]. The CR-39 detector is very sensitive for α-particle detection and also for tracing the radon daughters in the energy range of

around 1–60 MeV. CR-39 detector is etched at 70 ^{o}C for about 6–10 h in 6N NaOH solution and used in neutron, heavy ion and radon dosimetry.

After investigating CR-39, some reports suggested few important parameters that may be used in devising new track detectors. They are,

1.5.2   Effect of radiation sensitive groups: The sensitivity of detectors is mainly depends on the functional moiety present in the monomer/polymer. As per the reports[97], monomers having sulfonate/ nitrate groups are more sensitive as compared to that with carbonate moiety. Chemical etching process of such polymers occurs be at faster rate. So by using functional groups with lower binging energy into the thermosetting polymer will enhance the sensitivity of radiation.

1.5.3   Effect of chain bridging the functional groups[86]: In CR-39, two carbonate groups are linked together by a ethylene diglycol bridging chain. This chain/linker also enhances the radiation sensitivity. When sensitivity of PADC was compared with that of Pentanediol bis(allyl carbonate) polymer (PPeAC), it was found that later have less sensitivity due to presence of pentane chain as bridging chain between two carbonates where as   PADC have 4 time higher sensitivity as compared to PPeAC polymer.

1.5.4   Sulfur containing allylic monomers and compounds: The term allyl derived from the allium product or onion family compound allyl sulfide. Allyl compounds are represented by general formula CH2=CH-CH2- X. In polymer industries, sulfurous compounds have been in use from mid 19th century. The sulfur containing polymers found extensive use. The polymers with sulfonic group find extensive applications in industrial and water treatments. They are used as functional polymers as they can be tailored into different groups like sulfonic acids and their

sodium salts, sulfonates, sulfonyl chlorides, sulfonamides, etc. Also they can be used as ion exchangers, polymer supports, etc. Few commonly used monomers are listed below.

1. Allyl isothiocyanates: Sodium thiocyanate reacts with allyl halides in mild conditions to give allyl thiocyanate which rearranges readily to form allyl isothiocyanates.[102]
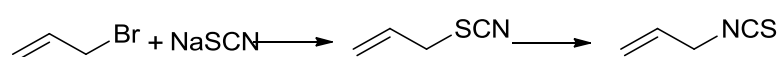
Allyl isothiocynate is used as war gas. This gas is acute and chronic irritant. Also it causes watery eyes, sneezing and asthma.

2. Allyl sulfonic acid: This monomer can be synthesised by thermal elimination reaction.[103] It can also be synthesized in high yields by elimination of sodium hydroxyethyl sulfonate using orthophosphoric acid[95].Sodium salt of acid monomer acts as emulsifying agent and stabilizes the polymeric emulsion. Sodium allyl sulfonate is used in nickel electroplating as a brightener. It is also used as a dye site monomer in acrylic fibre and also in synthetic polymer applications as a performance monomer.
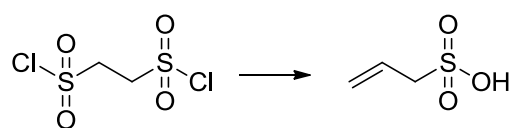
3. N-allyl-vinyl sulfonamide: This monomer was synthesised by condensing allyl amine with vinyl sulfonyl chloride in presence of base as shown below. Poly (cyclic sulfonamide)[104] can be prepared by using N-allyl-vinyl sulfonamide monomer.
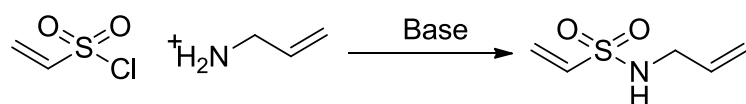
A soluble polymer can be formed using azobisisobutyronitrile (AIBN) initiator at 45 °C. The radical polymerization was carried out in benzene which was relatively faster than other N-alkyl vinyl sulfonamide.
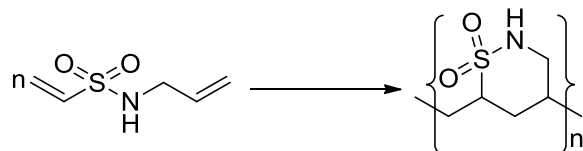
4. p-styrene sulfonic acid: From this monomer polystyrene sulfonic acid can be prepared. It can also be prepared by treating polystyrene with conc. sulphuric acid at higher temperature[105]. Block copolymers of p-styrene sulfonic acid with hydrophobic component have many major applications like ion exchange resins, blood compatible materials etc[105(b)]. Also composite of polyaniline with poly (p-styrene sulfonic acid) have been used as active materials in rechargeable lithium battery[105(d)].
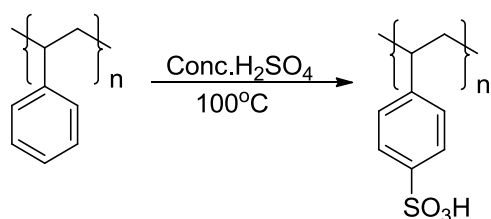
5. Diallyl sulfide: Allyl halides on treatment with potassium or sodium sulfide give allyl sulfide[106]. It naturally occurs in garlic oil, which can be obtained by steam distillation of garlic oil. During suspension polymerization of vinyl chloride, small amount of diallyl sulfide is added. Diallyl sulfide reacts with SO_2 to give equimolar sulfone composition[107].
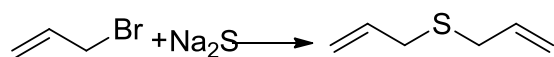
6. Allyl sulfoxides and sulfones: Diallyl sulfoxide and diallyl sulfone can be obtained from oxidation of diallyl sulfide using benzoyl peroxide[108]. They can also be prepared using hydrogen peroxide as shown in scheme below. Diallyl sulfoxide is hygroscopic solid while diallyl sulfone is liquid[109].
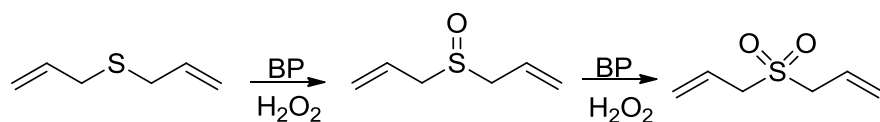
Reaction of cyclic trimethylene sulfone with allyl chloride gives diallyl trisulfone. It can be polymerized by heating the monomer solution in dimethyl formamide and diethylene glycol. Hexallyl trimethylene sulfone has been recommended as crosslinking agent for acrylic acid in manufacture of high viscosity mucilage.[110]
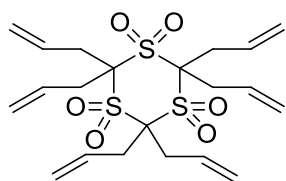
7. Allyl thiourea: Allyl thiourea can be synthesised by reacting allyl isothiocyanates with ammonia. This compound is used in developing photographic films. N, N'-diallylthiourea was prepared by reacting allyl isothiocyanates with allyl amine[111].
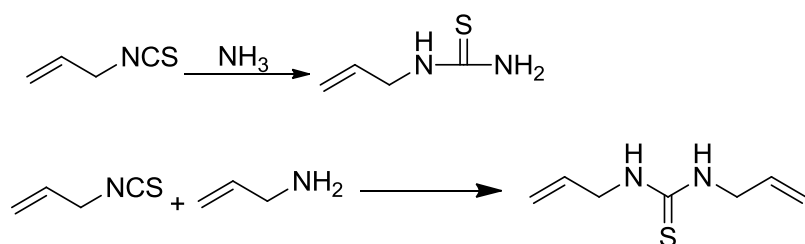
8. Sodium allyl sulfonate: Sodium Allyl sulfonate can be synthesised by reacting allyl halide with aq. sodium sulfite. It can be copolymerized with methyl acrylate to give high polymers having sulfonate functionalities[112].
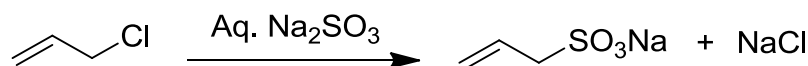
1.5.5 Allylic phosphorus containing monomers/polymers:

Phosphorus containing polymeric materials are also used for wide range of technological[113] and biomedical applications[114]. They are extensively employed in industries[115]. Phosphorus based polymers have attractive complexing properties[116]

and are utilized as corrosion inhibiting agents, dispersant[117]. Some of the commonly used monomers and polymers are enlisted below.

1. **Phosphonate PEG polymers:** Phosphonate-PEG polymers[118] made of phosphonate (4-chlorophenyl dichlorophosphonate) as a linking agent with poly(ethylene glycol) (PEG) were prepared to increase segmental motion to assist the ion transport and ionic conductivity at ambient temperatures. Phosphonate-PEG polymers were prepared by solution polycondensation of 4-chlorophenyldichlorophosphonate as a linking agent and poly (ethylene glycol)s with different molecular weights in the presence of triethylamine or 1-methylimidazole as acid scavenger.
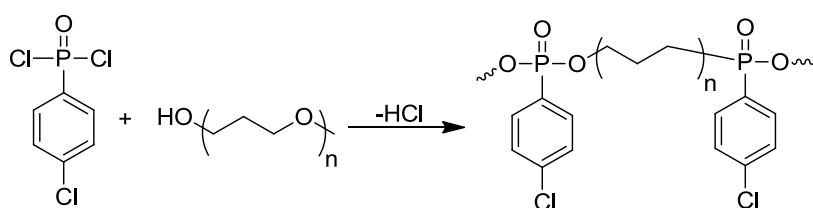
2. **Allyl phosphonate[119]:** 5-(allyloxymethyl)-5-ethyl-2-oxo-1,3,2-dioxaphosphorinane was homopolymerized by using 2, 2'-azobisisobutyronitrile (AIBN) initiator at 70 °C temperature.
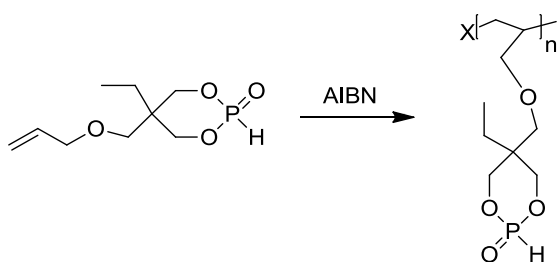
3. **Allyl diphenyl phosphine oxide (ADPPO)[120]:** It was obtained by reacting triphenyl phosphine with allyl bromide in presence of sodium hydroxide base according to Michaelis-Arbuzov rearrangement.
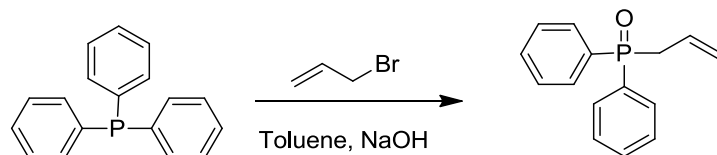
4. **Bis{4-(allyloxy)phenyl}(phenyl)phosphine (DAPPO)[91]:** DAPPO was prepared by reacting aromatic phosphine 4,4'-(phenylphosphinediyl)diphenol with 2 equivalents of allyl bromide in presence of potassium carbonate as shown in below.
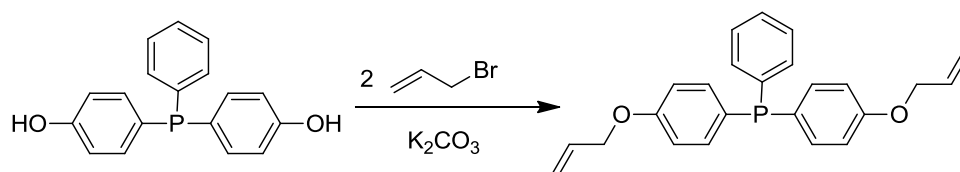
Both monomers ADPPO and DAPPO were separately cured by UV radiation using epoxy acrylate resin and photoinitiator.

5. **Nitrogen and phosphorus containing allylic monomers[121]:** homopolymerization of such types of monomers were carried out using radical method in aqueous media. Phosphonated oligoallylamines were obtained by radical polymerization as shown below. The polymers formed have zwitterionic functions which can be utilized in many applications. Commercially available azo-phosphonates like phosphazenes, phospham or phosphorimides are used as flame retardants. Vinyl polymers having phosphorus and nitrogen groups can also be used as flame retardants.
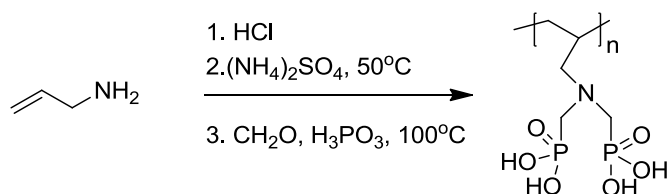
Nitrogen and phosphorus containing monomer shown below was synthesized by Huang et al.[122] and was mixed with acrylate adhesive resin to form polymer having flame retardant properties.
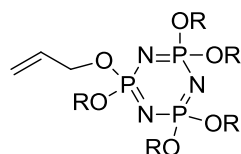
6. **Diethyl allyl phosphonate (AP)[123]:** AP monomer was synthesized by reacting allyl bromide with triethyl phosphite via Arbuzov rearrangement[124] i.e. isomerization of $P(OR)_3$ to $(RO)_2P(O)R_o$ (where R_o is an allyl group). This rearrangement gives the quantitative yield of AP monomer.
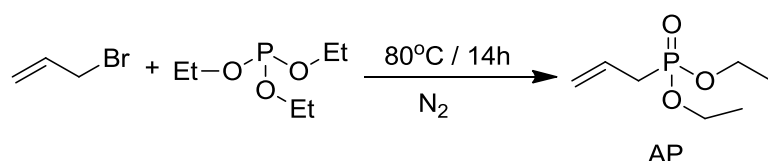
7. **Dimethyl allyloxymethylphosphonate (AOP)[94]:** AOP monomer was synthesized by reacting equimolar amount of allyl bromide with primary alcohol bearing phosphonate group. Reactant dimethyl hydroxymethylphosphonate was prepared by reacting dimethyl phosphonate with paraformaldehyde and anhydrous potassium carbonate[125].
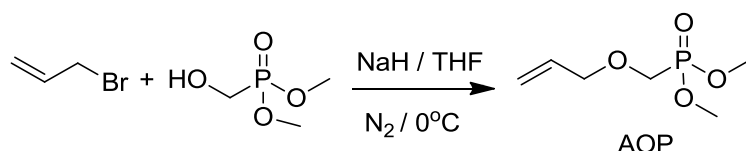
These monomers (AP and AOP) were copolymerized using free radical polymerization in presence of maleic anhydride.

1.6   Statement of objectives: -

The study of different polymers as SSNTDs is of prime interest to us for obtaining better detectors for alpha and fission particle detection. We envisaged that introduction of hetero-atoms through sulphur and phosphorus containing functional groups in a polymer frame work may give better detectors.

CHAPTER 1

We noted that commercial CR-39 detector requires longer time (2-3 hours) for alpha track development by chemical etching. For today's rapid world, we require a detector that develops tracks by chemical etching in shorter time period. We noted that some sulphur containing materials are known to be more sensitive than CR-39. As sulfonates and sulphites were earlier studied by our group, we decided to try groups like sulfoxide, sulfones, and sulfonamides.

We had also noted that no phosphorus containing monomers/ polymers have been studied for track detection so far. Hence, we decided to study some phosphates $(P(=O)(OR)_3)$ and phosphamide as track detectors, as these are analogous to carbonate $(O-C(=O)O-)$ and carbamate $(N-C(=O)O-)$.

Thus, following objectives were considered.

1. Synthesis of allylic monomers containing different functional groups like phosphate, phosphamide, sulfonamide, sulfoxide and sulfone.

2. Cast polymerization to prepare of thin films (~550-650 microns) from such monomers.

3. Study of kinetics of polymerization by extending Dial's kinetics model of allylic polymerization to obtain a constant rate polymerization profile wherever possible.

4. Copolymerization of the synthesized monomers with ADC, and some other known monomers to get more crosslinked polymers.

5. Optimization of track detectors based on the protocol generated earlier by our laboratory for systematic development of polymeric track detector.

6. To make preliminary assessment of the new polymers as track detectors in comparison to PADC/CR-39^{TM} based on following studies.

      i. ^{239}Pu Alpha particles and ^{252}Cf fission particle track detection characteristics.

      ii.   Bulk and track etch rates.

      iii.   Optimization of etching conditions.

      iv.   Alpha sensitivity studies.

      v.   Alpha track detection efficiency

      vi.   Neutron sensitivity studies of some promising polymers

7.   Standardization of PADC detector films for personnel neutron dosimetric analysis application.

1.7   References:

1.   Glasser, O. *Dr W. C. R. Roentgen;* Charles C. Thomas Publisher: Springfield, 1958; *2nd edn.*

2.   Poincaré H. *Rev Gén Sci*. **1896**, *7*, 52–59

3.   Becquerel, H. *Compt. Rend. Acad. Sci.* **1896**, *122*, 420-421.

4.   Becquerel, H. *Compt. Rend. Acad. Sci.* **1896**, *122*, 501-503.

5.   Becquerel H. *Compt. Rend. Acad. Sci.* **1896**, *122*, 559–561.

6.   (a) Curie, M. *La Radioactivité*; Hermann & Cie: Paris, 1935**;** Vol. 1–2. (b) Sklodowska-Curie, M. *Rev Gén Sci.* **1899**, *10*, 41–50. (c) Sklodowska-Curie, M. *Chemik Polski.* **1904**, 4, 141–241.

7.   Curie, P.; Curie, M. S.; Belmont, G. *Compt. Rend.* **1898**, *127*, 1215-1217.

8.   (a) Curie, P; Desains, P. *Compt. Rend*. **1880**, *90*, 1506. (b) Curie, M. *Compt. Rend.* **1898**, *126*, 1101. (c) Curie, M.S.; Curie, P. *Compt. Rend.* **1898**, *127*, 175. (d) Curie, M.S.; Curie, P.; Bémont, G. *Compt. Rend.* **1898**, *127*, 1215.

9.   Alpen, E. L. *Radiation Biophysics;* Englewood Cliffs: Prentice-Hall, 1990.

10.   Bergonié, J.; Tribondeau, L. Interpretation of some results of radiotherapy and test of fixation of a rational technique; *Weekly Proceedings of the Academy of Sciences*, **1906***,* 143, 983–985.

11.   (a) Morgan. K. Z.; Turner, J. E. *In Principles of radiation protection;* John Wiley and Sons: New York, 1967. (b) Rees, D. J. *In Health Physics, Principles of radiation protection;* Butterworth: London, 1967. (c) Bacq, Z. M.; Alexander, P. *Fundamentals of radiobiology;* Pergamon Press: 1961, 2nd edition.

12.   Kamiya, K.; Sasatani, M. *Nihon Rinsho.* **2012**, *70 (3),* 367-374.

13.   Flakus, F. N. *IAEA bulletin*. **1981**, *23(4)*, 31-36.

14.   (a) Etter, L. E. *In The science of ionizing radiation*; Charles C Thomas: Springfield, Illinois, USA 1965. (b) Bromley, D. A. *Nucl. Instr. Meth.* **1979**, *162*, 1-8.

15.   Knoll, G. F. *In Radiation detection and measurement*; John Wiley and Sons publisher: 1999, 3rd edn.

16.   Durrani, S. A.; Bull, R. K. *In Solid State Nuclear Track Detection Principles Methods and Applications;* Pergamon press: 1987; Vol. 111.

17. Das Gupta, N. N.; Ghosh, S. K. *Reviews of Modern Physics*. **1946**, *18 (2)*, 225–365.

18. Glaser, D. A. *Physical Rev.* **1952**, *87 (4)*, 665–665. doi:10.1103/PhysRev.87.665

19. (a) Rossi, B. B.; Staub, H. H. *In Ionization Chambers and Counters;* McGraw-Hill: New York, 1949. (b) Wilkinson, D. H. *In Ionization Chambers and Counters;* Cambridge University Press: Cambridge, 1950. (c) Sharpe, J. *In Nuclear Radiation Detectors;* Methuen and Co.: London, 1964; 2nd edn. (d) Price, W. J. *In Nuclear Radiation Detection;* McGraw-Hill: New York, 1964; 2nd edn. (e) Boag, J. W. *In Ionization Chambers, in Radiation Dosimetry;* Academic Press: New York, 1966. (f) Palladino, V.; Sadoulet, B. *Nucl. Instrum. Meth.* **1975***, 128*, 323-335.

20. Campion, P. J. *Int. J. Appl. Radiat. Isotopes,* **1968***, 19*, 219-224. (b) Bambynek, W., *Nucl. Instrum. Meth.* **1973**, *112 (1-2)*, 103-110.

21. (a) Attix, F. H.; Roesch, W. C. In *Radiation Dosimetry;* Academic Press: New York, 1966; Vol. 2. (b) Wilkinson, D. H. *Nucl. Instrum. Meth. A.* **1992,** *321*, 195-210. doi:10.1016/0168-9002(92)90388-K (c) Wilkinson, D. H. *Nucl. Instrum. Meth. A.* **1996**, *383 (2-3)*, 516-522. (d) Wilkinson, D. H. *Nucl. Instrurn. Meth. A.* **1996**, *383 (2-3)*, 523-527. (e) Matsuda, K.; Sanada, J. *Nucl. Instrurn. Meth. A.* **1990**, 294, 268-270.

22. Rutherford, E.; Geiger, H. An electrical method of counting the number of α particles from radioactive substances. *Proceedings of the Royal Society Series A,* London, **1908**, *81(546)*, 141–161.

23. Lucas, H. F. *Rev. Sci. Instrum.*, **1957**, *28*, 680–683.

24. Bochicchio, F.; Risica, S. *In proc. Intern. Workshop, Trieste,* World Scientific: Singapore, 1990; Vol. 211.

25. (a) Bovi, M.; Boldassini, P.; Porcu, I. Italian Patent, 3,588,190,900,704; 1993. (b) Japanese Patent, 930,427; 1993 (c) Canadian Patent, 05,7259,690,329; 1969 (d) Powell, B. British Patent, 019, 214, 790, 601; 1979.

26. Demel, F. Czeckoslovak Patent 8, 604, 867, 880, 615; 1988.

27. Madnick, P. A.; Sherwood, R. W. U. S. Patent 4, 894, 535, 900,116; 1990.

28. Durrani, S. A. *Radiat. Meas.* **2001**, *34*, 5–13.

29. Ilic, R.; Durrani, S. A.; Annunziata, M. F. L. *In Solid state nuclear track detectors: Hand-book of radioactivity analysis*; Academic Press: Amsterdam, **2003**; 2nd edn.

30. Bhagwat, A. M. *Solid State Nuclear Track detection: Theory and Applications,* Indian Society of Radiation Physics: Kalpakkam, 1993.

31. Young, D. A. *Nature*. **1958**, *182*, 375-377.

32. Silk, E. C. H.; Barnes, R. S. *Philos. Mag.* **1959**, *4*, 970-972.

33. Fleischer, R. L.; Price, P. B.; Walker, R. M. *Annu. Rev. Nucl. Sci.* **1965**, *15*, 1-28.

34. Fleischer, R. L.; Price, P. B.; Walker, R. M. *Science*. **1965c,** *149*, 383-393.

35. (a) Fleischer, R. L.; Price, P. B. *Science.* **1963a**, *140*, 1221-1222. (b) Fleischer, R. L.; Price, P. B. *J. Appl. Phys.* **1963b,** *34*, 2903-2904.

36. Fleischer, R. L.; Price, P. B.; Walker, R. M. *In Nuclear tracks in solids: Principles and applications*; University of California press: Berkley, 1975.

37. Lal, D.; Goswami, J. N. *Nuclear tracks, researches in space physics, geophysics and nuclear physics*. Indian academy of sciences, Bangalore, India, 5–7, 1981.

38. Nagpaul, K. K.; Goswami, J. N. Fission tracks geochronology of India, *Nuclear tracks,* Indian Academy of Sciences: India, 1981.

39. Iyer, R. H. *Nucl. India*, **1971**, *9 (11)*, 4–7.

40. Chaudhuri, N. K.; Natarajan, V.; Sampathkumar, R.; Sagu, M. L.; Iyer, R. H. *Nucl. Tracks*, **1979,** *3*, 69–81.

41. Iyer, R. H. *Proc. of Indian Academy of Sci. and Earth Planet. Sci.* **1981**, *90 (3)*, 437–460.

42. Iyer, R. H.; Rao, V. V. *Nucl. India*, **1976**, *15(1)*, 1–8.

43. Iyer, R. H.; Dwivedi, K. K. *Radiat. Meas.* **2003**, *36*, 63–72.

44. Fleischer, R. L.; Price, P. B.; Walker, R. M. *J. Geophys. Res.* **1965b**, *70*, 1497-1502.

45. (a) Durrani, S. A. *Nucl. Tracks.* **1982**, *6*, 209–228. (b) Durrani, S. A.; Ilic, R. *In Radon Measurements by Etched Track Detectors: Applications in Radiation Protection, Earth Sciences and the Environment;* World Scientific: Singapore, 1997. (c) Fleischer, R. L. *Tracks to Innovation: Nuclear Tracks in Science and Technology*; Springer: 1998. (d) Cartwright, B. G.; Shirk, E. K.; Price, P. B. *Nucl. Instruments Methods.* **1978**, *153*, 457–460.

46. Yu, K. N.; Nikezic, D. *Mater. Sci. Eng. R,* **2004**, *46(3-5)*, 51-123.

47. Price, B. *Radiat. Meas.*, **2003**, *40(2–6)*, 146–159.

48. (a) Apel, P. Y.; Blonskaya, I. V.; Dmitriev, S. N.; Mamonova, T. I.; Orelovitch, O. L.; Sartowska, B.; Yamauchi, Y. *Radiat. Meas.* **2008**, *43(1)*, S552–S559. (b) Guo, W.; Xue, J. M.; Zhang, W. M.; Zou, X. Q.; Wang, Y. G. *Radiat. Meas.*, **2008**, *43 (1)*, S623–S626.

49. (a) Chavez, A.; Monnin, M.; Segovia, N.; Seidel, J. L.; Pena, P.; Moreno, A.; Balcazar, M. *Radiat. Meas.* **1997**, *27(4)*, 587–591. (b) Farid, S. M. *J. Environ. Radioact.* **1997**, *34(1)*, 29–36. (c) Tayyeb, Z. A.; Kinsara, A. R.; Farid, S. M. *J. Environ. Radioact.* **1998**, *38(1)*, 97–104.

50. (a) Qureshi, A. A.; Kakar, D. M.; Akram, M.; Khattak, N. U.; Tufail, M.; Mehmood, K.; Jamil, K.; Khan, H. A. *J. Environ. Radioact.* **2000**, *48(2)*, 203–209. (b) Tomasek, L.; Müller, T.; Kunz, E.; Heribanova, A.; Matzner, J.; Placek, V.; Burian, I.; Holecek, J. *Intern. Cong. Ser.* **2002**, *1225*, 239–245. (c) Tomasek, L.; Kunz, E.; Müller, T.; Hulka, J.; Heribanova, A.; Matzner, J.; Placek, V.; Burian, I.; Holecek, J. *Sci. Tot. Environ.* **2001**, *272(1–3)*, 43–51. (d) Jamil, K.; Ali, S. *J. Environ. Radioact.* **2001**, *54(3),* 415–422. (e) Lubin, J. H.; Boice, J. D. *J. Natl. Cancer Inst.* **1997**, 89(1): 49–57.

51. (a) Ulomov, V. I.; Zakharova, A. I.; Ulomova, N. V. *Geophys.*, **1967**, *177*, 567– 570. (b). Ulomov, V. I.; Mavashev, B. Z. *Dokl. Akad. Sci. USSR, Earth Sci. Sect.* **1968**, *176(1–6)*, 9–11. (c) Monnin, M. M.; Seidel, J. L. *Nucl. Instrum. Meth. Phys. Res. A*, **1992**, *314(2),* 316–330. (d) Wakita, H. *Geochemical challenge to earthquake prediction;* Proc. Natl. Acad. Sci. USA, **1996**, *93*, 3781–3786. (e). Zmazek, B.; Todorovski, L.; Dzeroski, S.; Vaupotic, J.; Kobal, I. *Appl. Radiat. Isot.* **2003**, *58(6)*, 697–706. (f) Ioannides, K.; Papachristodoulou, C.; Stamoulis, K.; Karamanis, D.; Pavlides, S.; Chatzipetros, A.; Karakala, E. *Appl. Radiat. Isot.* **2003**, *59(2–3)*, 205–213.

52. Iyer, R. H. *Science Today.* **1977**, *37*, 8.

53. (a) Christner, B. C.; Mosley-Thompson, E.; Thompson, L. G.; Reeve, J. N. *Environ. Microbiol.* **2001**, *3*, 570-577. (b) Price, P. B. *Radiat. Meas.,* **2005**, *40*, 146-159.

54. Seal S. *Cancer,* **1964**, *17*, 549 - 568.

55. Hepburn, C; Windle, A. H. *J. Mater. Sci.* **1980**, *151*, 279.

56. Fleischer, R. L.; Price P. B. *Geochim. Cosmochin Acta.* **1964**, *28*, 1705-1712.

57. (a) Chadderton, L. T.; Montagu-Pollock, H. M. *Proc. Roy. Soc.* **1963**, *A274*, 239-252. doi:10.1098/rspa.1963.0127. (b) Chadderton, L. T.; Morgan, D. V.; Torrens, I. M.; Van Vliet, D. *Phil. Mag.* **1966**, *13*, 185-195. (c) Desauer, F. *Z. Physik.* **1968**, *38*, 107.

58. Miller, A. A.; Lawton, E. J.; Bafwitt, J. S. *J. Polymer Sci.* **1954**, *14 (77),* 503-504.

59. Somogyi, G.; Szalay, A. S. *Nucl. Instrum. Methods.* **1973**, *109 (2)*, 211-232.

60. Fleischer, R. L.; Price, P. B.; Walker, R. M.; Hubbard, E. L. *Phys. Rev.* **1964**, *133,* 1443-1449.

61. Benton, E. V. *Charged particle tracks in polymers;* USNRDL-TR-67-80, 1967; Vol. 4.

62. Paretzke, H. G. *Radiat. Eff. Defects.* **1977**, *34*, 3-8.

63. Fleischer, R. L.; Price, P. B.; Walker, R. M.; Hubbard, E. L. *Phys. Rev.* **1967**, *156*, 353-355.

64. Katz, R.; Kobetich, E. J. *Phys. Rev.* **1968**, *170*, 391-396.

65. Monin, M. *PNCF.,* **1968**, *68*, RI-9.

66. Bhagwat, A. M. *Solid State Nuclear Track detection: Theory and Applications,* Indian Society of Radiation Physics: Kalpakkam, 1993.

67. Apel, P. Y.; Blonskaya, I. V.; Didyk, A. Y.; Dmitriev, S. N.; Orelovitch, O. L.; Root, D.; Samoilova, L. I.; Vutsadakis, V. A. *Nucl. Instrum. Methods B.* **2001**, *179(1)*, 55-62.

68. Tommasino L., *In Electrochemical Etching of Damaged Track Detectors by H. V. Pulse and Sinusoidal Waveform;* Internal Repot-Lab. Dosdimetriae Standardizzaaione, CNEN Casaccia: Rome, 1970.

69. Fleischer, R. L.; Price, P. B.; Walker, R. M.; Hubbard, E. L. *Phys. Rev.* **1966b**, *143*, 943-946.

70. Cross, W. G.; Tommasino, L. *Health Phys.* **1967**, *13*, 932.

71. Block J.; Humphery, J. S.; Nicholas, G. E. *Rev. Sci. Inst.* **1969**, *40*,509.

72. (a) Gruhn, T. A.; Li, W. K.; Benton, E. V.; Cassou, R. M.; Johnson, C. S. *Proceedings of the 10th Conference on Solid State Nuclear Track Detectors,* Lyon, 1979. (b) Yip, C. W. Y.; Ho, J. P. Y.; Koo, V. S. Y.; Nikezic, D.; Yu, K. N. *Radiat. Meas.* **2003**, *37*, 197–200.

73. Spohr R. *European Research Training Network EuNITT;* Report M 2.1, 2001, 3.

74. Portwood, T.; Henshaw, D. L.; Stejny, J. *Nucl. Tracks. Radiat. Meas.* **1986**, *12(1-6)*, 109-112.

75. Siems, M.; Freyer, K.; Treutler, H. C.; Jonsson, G.; Enge, W. *Radiat. Meas.* **2001**, *34*, 81-84.

76. Abu-Jarad, F.; Hala, A. M.; Farhat, M.; Islam, M. *Radiat. Meas.* **1997**, *28*, 111-114.

77. Sinha, D.; Ghosh, S.; Srivastava, A.; Dedgaonkar, V. G.; Dwiwedi K. K. *Radiat. Meas.* **1997**, *28,* 145-148.

78. (a) Apel P. *In Track Membranes, Contribution to IAEA Consultant's Meeting;* JAERI: Takasaki, 1999. (b) Apel, P. Y. Direct communication; Joint Institution of Nuclear Reactions: Berkeley, Dubna, 1975. (c) Kenyon, W.O.; Gray, H. L. G. *J. Am. Chem. Soc.* **1936**, *58*, 1422- (d) Berthelot, *Compt. Rend.* **1900**, *131*, 519. (e) Klason, P.; Karlson, T. Ber. 1906, 39, 2752. (f) Honeyman, J. *Advances in Carbohydrate Chem.* **1957**, *12*, 130. (g) Lucas, G. R.; Hammett, L. P. *J. Am. Chem. Soc.* **1942**, *64,*1928.

79. Morley, J. A. *Trans. Am. Nucl. Soc.* **1972**, *15,*120-122.

80. (a) Varnagy, M.; Szabo, I.; Juhasz, S.; Csikai, I. *Nucl. Instr. Meth.* **1973**, *106*, 301-305. (b) Kodak, P. Instructions for the Use of CA80-15 Film and LR-115 Film*,* type I and type II.

81. Dixon, G. P.; Williams, J. G. *Nucl. Instr. Meth.* **1976**, *135*, 293-298.

82. Seitz, M. G.; Walker, R. M.; Carpenter, B. S. *J. AppI. Phys.* **1973**, *44*, 510-512.

83. Geisler, F.; Phillips, P. R. *Rev. Sci. Instrum.* **1972**, *43*, 283-284.

84. Nadkarni, V. S. *Ph.D. Thesis,* University of Mumbai, 1996.

85. Kalsi, P.C.; Ramaswami, A.; Manchanda, V. K. *BARC Newsletter.* 2005, *257*, 6-15.

86. Fujii, M.; Yokota, R. *Nucl. Tracks.* **1986**, *12 (1-6)*, 55-58.

87. Ogura, K.; Asano, M.; Yasuda, N.; Yoshida, M. *Nucl. Instr. Meth. B.* **2001**, *185* 222-227.

88. Fujii, M. *Nucl. Instr. Meth. A.* **1985**, *236*, 183-186.

89. Tsuruta, T. *Radiat. Meas.* **2000**, *32*, 289-297.

90. Schulz, A.; Siegmon, G.; Enge, W. *Nucl. Tracks. Radiat. Meas.* **1991***, 19 (1-4),* 117-120*.*

91. Kovalenko, L. M.; Gaichenko, L. N.; Lavrentovich, Y. I.; Kabakchi, A. M. *Atomnaya Energiya.* **1971**, *31(5)*, 510-519.

92. Komaki, Y.; Ishikawa, N.; Morishita, N.; Takamura, S. *Radiat. Meas.* **1996**, *26(1)*, 123-129.

93. Shirkowa, V. V.; Tretyakova, S. P. *Radiat. Meas.* **2001**, *34*, 177-180.

94. Fujii, M.; Nishimura, J. *Nucl. Instr. Meth.* **1984**, *226,* 496-500.

95. Mascarenhas A. A. A.; Kolekar, R. V.; Kalsi, P. C.; Ramaswami, A.; Joshi, V. B.; Tilve, S. G.; Nadkarni, V. S. *Radiat. Meas.* **2006**, *41(1)*, 23-30.

96. Stejny, J.; Portwood, T. *Nucl. Tracks.* **1986**, *12 (1-6)*, 59-62.

97. Fujii, M.; Yokota, R.; Atarashi, Y. *Nucl. Tracks. Radiat. Meas.* **1990**, *17(1)*, 19-21.

98. (a) Mascarenhas, A. A. A. *Ph.D. Thesis,* Goa University, 2007. (b) Mandrekar, V. K. *Ph.D. Thesis*, Goa University, 2010.

99. Fujii, M.; Yokota, R.; Kobayashi, T.; Hasegawa, H. *Radiat. Meas.* **1995**, *25*, 141–144.

100. Nikezic, D.; Janicijevic, A. *Appl. Radiat. Isot.* **2002**, *57*, 275–278.

101. Singh, S.; Prasher, S. *Nucl. Instrum. Meth. B.* **2004**, *222,* 518–524.

102. (a) Gerlish, G. *Ann.* **1875**, *178*, 85. (b) *US Pat.* 2462433, 1963.

103. *US Pat.* 2597696, 1952.

104. Goethals, E. J.; Bomberke, De Witte, J. E. *Makromol. Chem.* **1967**, *108*, 312-314. doi:10.1002/macp.1967.021080131.

105. a) Hart, R.; Janssen, R. *Makromol. Chem.* **1961**, *43*, 242-244. (b) Chen, C. H.; Hammett, L. P. *J. Am. Chem. Soc.* **1958**, *80*, 1329-1331. (c) Whicher, S. J.; Brash, J. L. *J. Polym. Sci. Part A, Polym. Chem.* **1981**, *19*(8), 1995-2006. (d) Tsutsumi, H.; Yamashita, S.; Oishi, T. *Synthetic Metals*, **1997**, *85*(1-3), 1361-1362.

106. Rheinboldth, H.; Diepenbruck O. *Ber.* **1926**, *59*, 1311.

107. *US Pat.* 3072616, 1963.

108. Lewin, L. N. *J. Prakt. Chem.* **1930**, *127(1)*, 77-91.

109. Ford-moore, A. H. *J. Chem. Soc.* **1949**, 2433-2440.

110. *US Pat.* 2958679, 1960.

111. Wheeler, H. L.; Jamieson, G. S. *J. Am. Chem. Soc.* **1903**, *25*, 719-722. (b) Hecht, O.; *Ber.* **1890**, *23*, 287.

112. *US Pat.* 2849330, 1958.

113. Huang, S. W.; Zhuo, R. X. *Phosphorus, Sulfur Silicon, Relat. Elem.*, **2008**, *183, 340*-348.

114. Monge, S.; Canniccioni, B.; Graillot, A.; Robin, J. J. *Biomacromolecules*. **2011**, *12*, 1973-1982.

115. (a) Clearfield, A. *Curr. Opin. Solid State Mater. Sci.* **1996**, *1*, 268-278. (b) Clearfield, A. *Curr. Opin. Solid State Mater. Sci.*, **2002**, *6*, 495-506. (c) Clearfield, A. *J. Alloys Compd.* **2006**, *418*, 128-138. (d) Essahli, M.; Colomines, G.; Monge S.; Robin, J. J.; Collet, A.; Boutevin, B. *Polymer.* **2008**, *49*, 4510-4518.

116. Knepper, T. P. *Trends Anal. Chem.* **2003**, 22, 708-724.

117. Herrera, L.; Guzmenn, M.; Neubecker, K.; Goethlich, A. *PTC Int. Appl.* **2008**, *28.*

118. Iliescu, S.; Zubizarreta, L.; Plescu, N.; Macarie, L.; Popa, A.; Ilia, G. *Chemistry Central Journal*, **2012**, *6(1)*, 132.

119. Negrell-Guirao, C.; Boutevin, B. *Macromolecules*, **2009**, *42*, 2446-2454.

120. Kahraman, M. V.; Kayaman-Apohan, N.; Arsu N.; Guengoer, A. *Prog. Org. Coat.* **2004**, *51*, 213-219.

121. Negrell-Guirao, C.; Carosio, F.; Boutevin, B.; Cottet, H.; Loubat, C. *J. Polym. Sci. Part B: Polym. Phys.* **2013**, *51*, 1244-1251.

122. Huang, J.; Yuan, D.; Tang, A.; Liao X. (Sichuan EM Technology), *China Patent*, 102719206, **2012**.

123. Negrell-Guirao, C.; David, G.; Boutevin, B.; Chougrani, K. *J. Polym. Sci., Part A: Polym. Chem.* **2011**, *49*, 3905-3910.

124. Yu, Z.; Zhu, W. X.; Cabasso, I. *J. Polym. Sci., Part A: Polym. Chem.* **1990**, *28*, 227-230.

125. El Asri, Z.; Chougrani, K.; Negrell-Guirao, C.; David, G.; Boutevin, B.; Loubat. C. *J. Polym. Sci., Part A: Polym. Chem.* **2008**, *46*, 4794-4803.

CHAPTER 2

Development of Phosphorus containing polymeric materials for SSNTD Applications

CHAPTER 2

2.1   Introduction

For the last many years, it has been observed that phosphorus containing monomers and polymers have gained extensive demand for many uses from healthcare and medicine to energy and environmental applications. These types of materials have been used in industries because of their ability to bind metals[1]. Phosphonate based polymeric materials are used for corrosion inhibition[2]. They are also used for flame retardancy[3]. Phosphorus containing polymers are widely used in biomedical field for dental applications[4], tissue engineering, also for drug delivery applications[5]. Some of the monomers listed in figure 2.1 below have been used for dental applications. Also for tissue engineering, phosphonated polymers are being used. Figure 2.2 shows some monomers/polymers that are used in tissue engineering. These materials are also used in fuel cells[6], and also in waste water treatment[7]. The polymers from triallyl phosphate, diallyl phthalate-triallyl phosphate materials have properties similar to that of concrete and can be used for the polarization optical study of the stress deformation state of steel-reinforced structures. In recent years, rechargeable lithium batteries based on solid copolymeric films of polyphosphoesters with poly (ethylene oxide), poly (propylene oxide), etc as an electrolyte are also being used extensively[8].
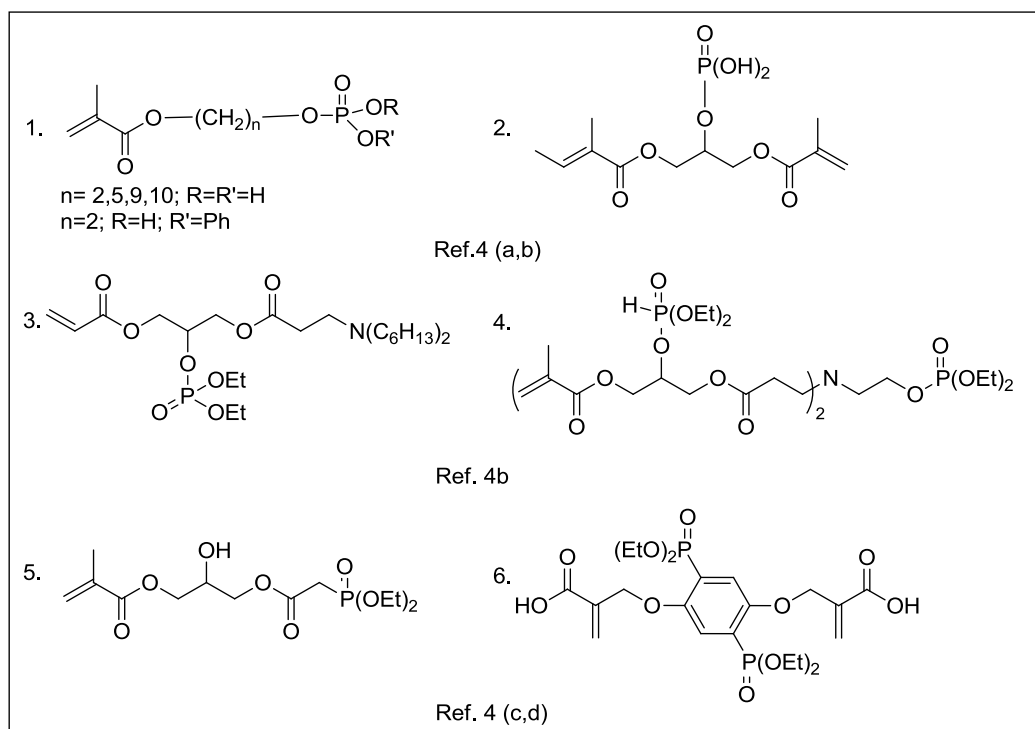
Figure 2.1: Some phosphate/ phosphonate containing monomers used for dental applications
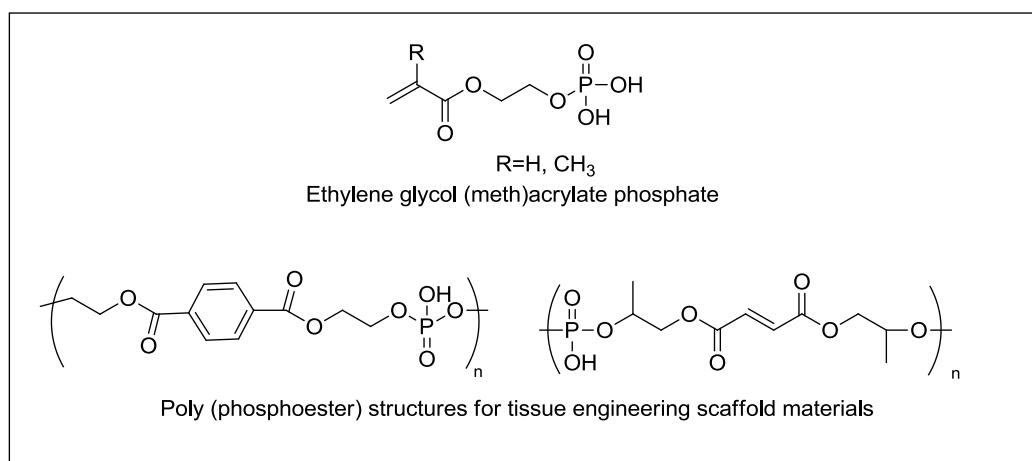
Figure 2.2: Some phosphorus containing polymeric materials used in tissue engineering.

Phosphate containing glass detectors were also known in the literature. Many scientists have studied phosphate containing glass as solid state nuclear track

detectors. In 1966, A. Becker[9] for the first time used phosphate glass (make Toshiba Co. Ltd.) for thermal and fast neutron dosimetry in mixed radiation field. He also discussed different methods for optical assessment of the fission track density in glasses. Also, he studied the effect of foil radioactivity and the neutron fission fragments on the glass radio photoluminescence. In the year 1987, Price *et al.* reported a very sensitive phosphate glass detector[10] called VG-13. But, it had many disadvantages due to its uranium content and it easily corroded in air. This was followed by Wang *et al* who developed barium phosphate glass (BP-1) with high charge resolution and sensitivity among glasses[11]. They made an efficient search of phosphate glasses of various compositions which were free from uranium. BP1 glass material was colorless and transparent, composed of P_2O_5 (65), BaO (25), NaO (5) and SiO_2 5wt. % and no uranium. This material was more sensitive to ionizing particles as compared to that of VG-13. Further R. Bonetti et *al* have carried out calibration of a phosphate glass BP-1 due to its high sensitivity comparable to that of some polymers[12]. BP-1 glass detector was used in different cluster radioactivity study to detect carbon or oxygen ions. They also have calibrated LG750 phosphate glass with heavy ion beams, as it is known previously that, LG750 phosphate glass is suitable to detect cluster radioactivity because of its very high tolerance of alpha dose[13]. However, polymeric track detectors are handy and more sensitive compared to glasses and find maximum applications. Though, polymeric track detectors are known to be sensitive compared to glasses and find maximum applications, there are no reports about the use of phosphorus containing polymers for nuclear track detection. Hence, we considered development of some phosphate, phosphamide containing monomers/ polymers for our study. Following monomers (Figure 2.3) containing -O-PO-O- or -O-PO-N linkages which are analogues to -O-CO-O- or -O-

CO-N respectively, were considered for our study and syntheses of the same were carried out. It may also be noted that these monomers are expected to result in polymers with highly 3-D cross-linked structures.
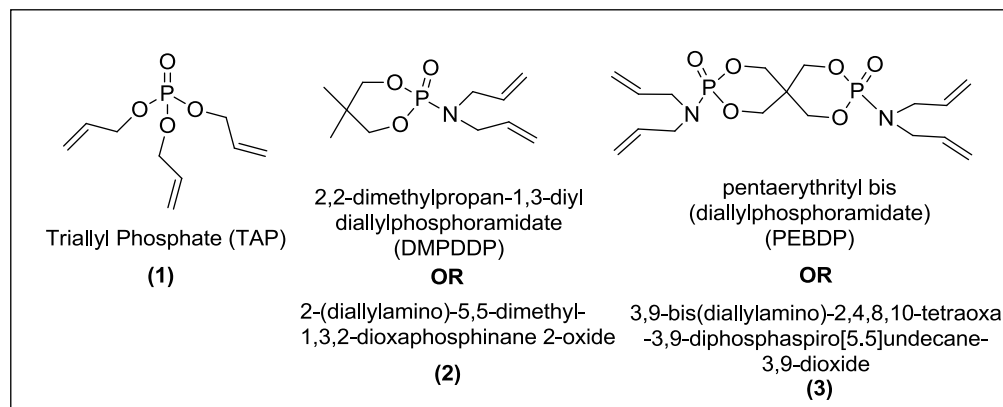
Figure 2.3: Some phosphorus containing allylic monomers for SSNTD application

It is known that copolymers of allyl diglycol carbonate (ADC) show better alpha sensitivity and track detection property as compared to that with homopolymer PADC, So the synthesis of monomers like ADC, N-(Allyloxycarbonyl) diethanolamine bis (allyl carbonate) NADAC, pentaerythritol tetrakis allyl carbonate PETAC, N-Allyloxycarbonyl ammediol bis(allyl carbonate) (NAAAC) were also carried out so as to prepare copolymeric films with phosphate containing monomers (Figure 2.4) and check its track detection property.

2.2   Experimental

2.2.1   Materials and Methods:

All the chemicals were obtained from M/s Loba Chemie, India, M/s Qualigens Fine Chemicals, India, M/s Molychem, India and M/s Spectrochem, India. Most of the chemicals were first purified and dried (wherever required) by standard procedure[14].

Solvents used during reactions and also during column chromatography were first distilled. Reagents viz. ICl in acetic acid, starch solutions, sodium thiosulfate solution, sodium hydroxide solution etc. were freshly prepared and used whenever required. Reactants like allyl chloroformate, phosphoryl chloride, allyl alcohol, Ammediol, diethylene glycol, pentaerythritol were supplied by Spectrochem Pvt. Ltd. and used directly without further purification.
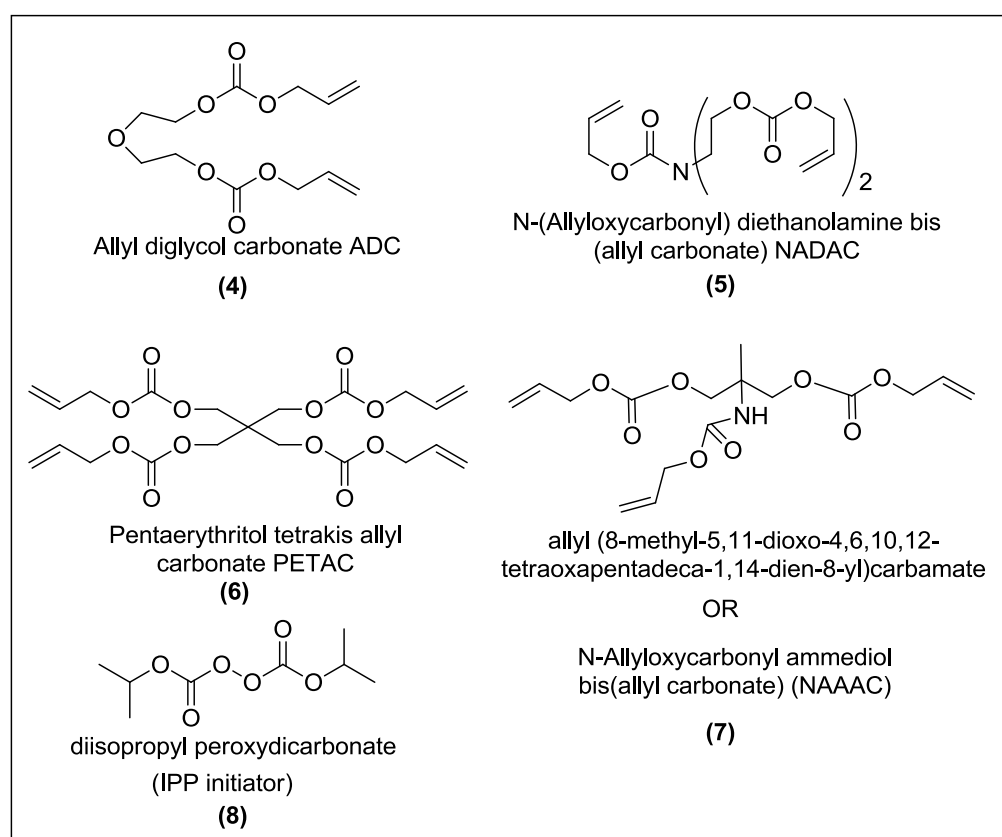
Figure 2.4: Other allylic monomers for copolymerization and IPP initiator

Monomers: All the monomers utilized in the study were prepared in a relatively dust controlled laboratory environment. The polymerization of the monomers prepared was also carried out in a dust controlled laboratory. The monomers were purified by activated charcoal treatment followed by vacuum distillation wherever

possible. Some of the monomers were purified by flash chromatography or column chromatography using silica gel (60-120 mesh size).

Initiators: The initiators used for free radical polymerization were IPP and BP. IPP was prepared in our laboratory and being highly unstable, was used after its percentage purity analysis directly without further purification. Details of its synthesis and characterization are given in Chapter IV. Commercially available moist benzoyl peroxide BP (make- M/s Loba Chemie) was recrystallized from chloroform methanol mixture and used after drying.

Plasticizers: Dioctyl phthalate DOP (make- M/s Loba Chemie GR grade) was first dried over 3A molecular sieves and then 0.1- 1% (wt% of monomer) of DOP plasticizer was used in polymerization process.

Spectral characterization: The monomers after synthesis were characterized by using different spectral techniques. IR spectra were recorded on Shimadzu FT-IR model spectrophotometer with KBr/ NaCl discs for liquids and KBr powder for solid compound. NMR spectra (^{1}H, ^{13}C, and DEPT) were recorded on Bruker 400 MHz spectrophotometer with CDCI$_3$, D$_2$O, and DMSO solvents as required and TMS as an internal standard. High resolution mass spectra were recorded at IISc, Bangalore on a ES-QTOF mass spectrometer. The progress of reaction was monitored by silica gel TLC glass plates and TLC silica gel 60 F254 aluminium sheets (make: Merck Specialities Pvt. Ltd.)

2.2.1.1 Synthesis of Triallyl Phosphate monomer: W. N. Lynwood *et. al.*[15] have synthesized triallyl phosphate for the first time by reacting allyl alcohol with phosphorus oxychloride at low temperature (-30 ^{o}C) in presence of pyridine. Scheme 2.1 depicts the synthesis of triallyl phosphate.
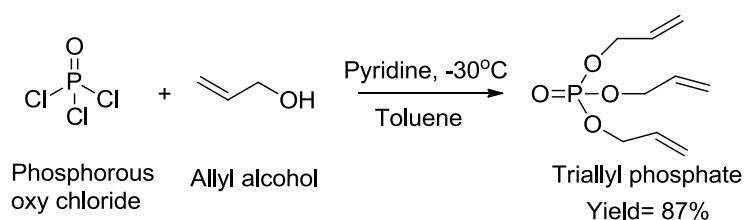
Scheme 2.1: Synthesis of Triallyl phosphate

In a typical experiment reacting vessel fitted with two pressure equalizing funnel, 23.10 g (27.05 mL, 0.398 mol) of allyl alcohol in 70 mL toluene was mixed homogenously and cooled down to -30 ^{o}C with the help of a Julabo cryostat. 17.01 g (10.4 mL, 0.1110 mol) of phosphorus oxychloride and 27.28 g (27.8 mL, 0.3449 mol) of pyridine were taken in separate addition funnel fitted to reacting vessel and at -30 ^{o}C, dropwise addition was carried out for a period of 3 hours. After complete addition, it was stirred for 12 hours in ice salt bath. The reaction was monitored by TLC followed by its workup to get crude product. Crude triallyl phosphate was vacuum distilled at 100 ^{o}C and 0.5 mm of Hg pressure. Triallyl phosphate obtained was in 87% yield. The structure of the monomer TAP was characterized by IR, ^{1}H, ^{13}C NMR and DEPT spectra as given in figure 2.5, figure 2.6, figure 2.7 and figure 2.8 (page no. 82-85). IR (KBr): 3086 cm^{-1}, 1150 cm^{-1} and 900-1050 cm^{-1}. ^{1}H NMR (400 MHz, CDCl$_3$) (ppm): 5.828-5.924 (m, 3H), 5.282-5.325 (d, 3H), 5.177-5.203 (d, 3H), 4.468-4.503 (t, 6H). ^{13}C-NMR (100 MHz, CDCl$_3$): 132.29, 118.50, 68.10.Unsaturation analysis proved the presence of 3 double bonds.
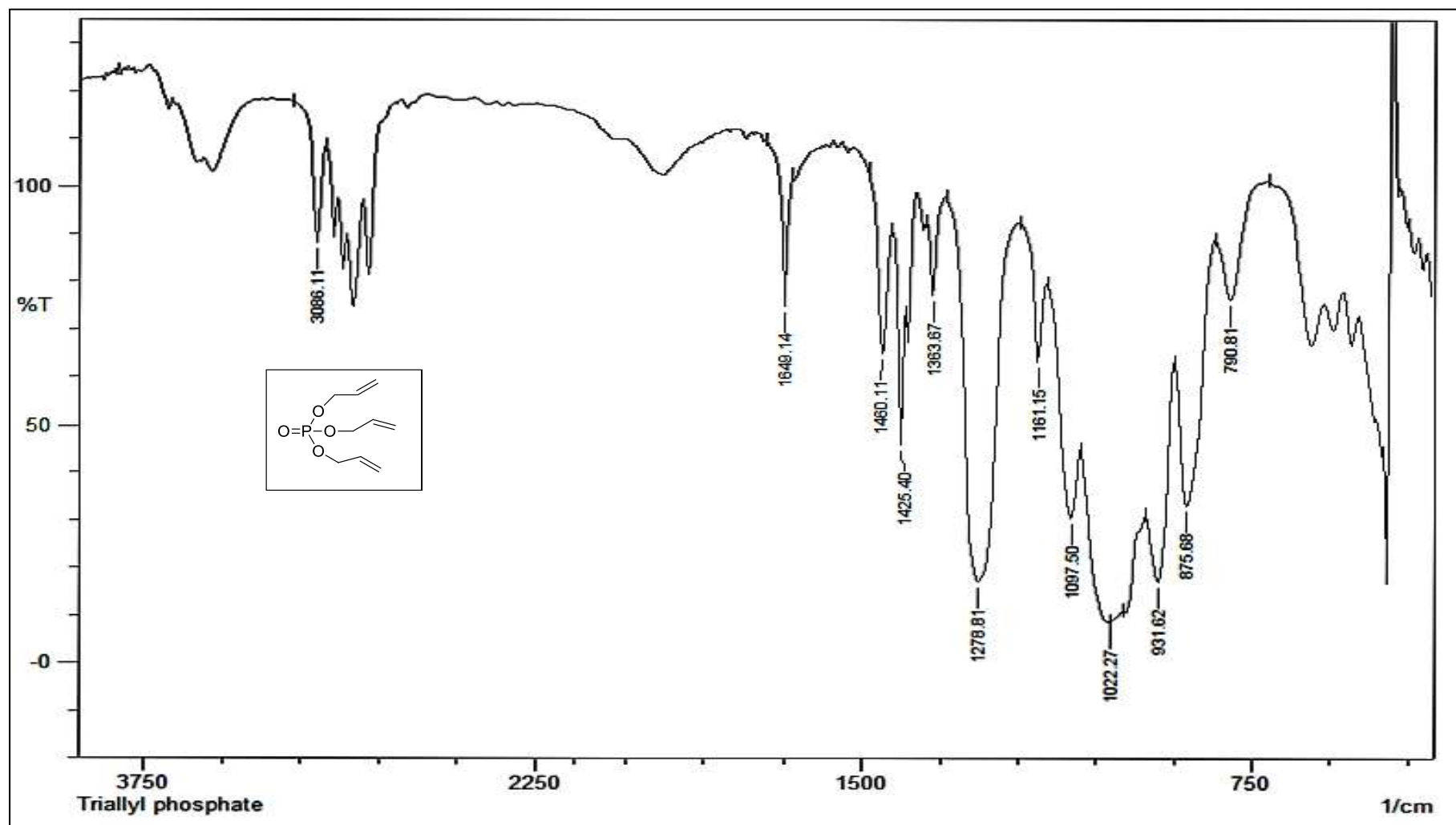
Figure 2.5: IR spectrum of triallyl phosphate (TAP)
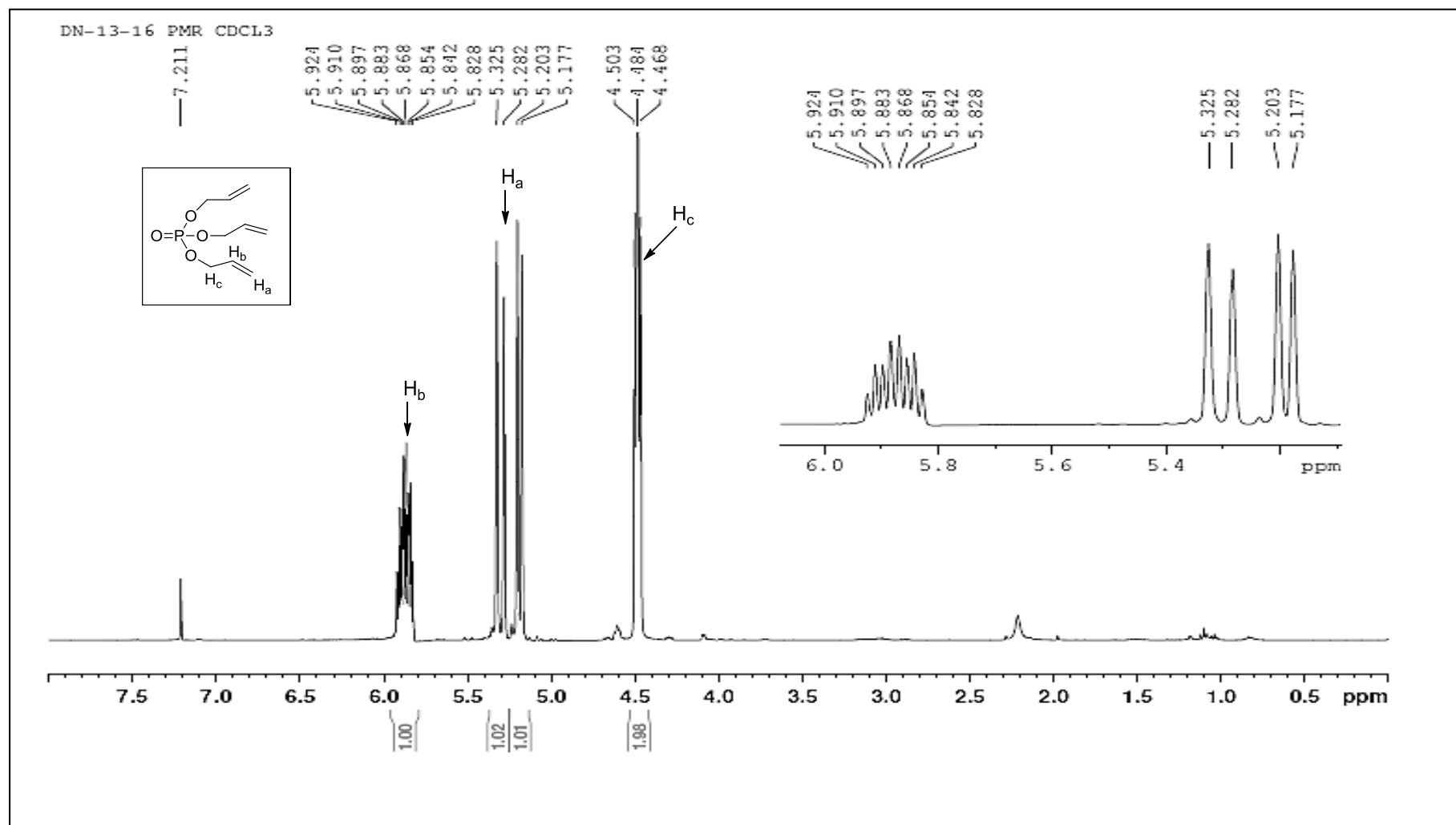
Figure 2.6: ^{1}H NMR of triallyl phosphate (TAP)
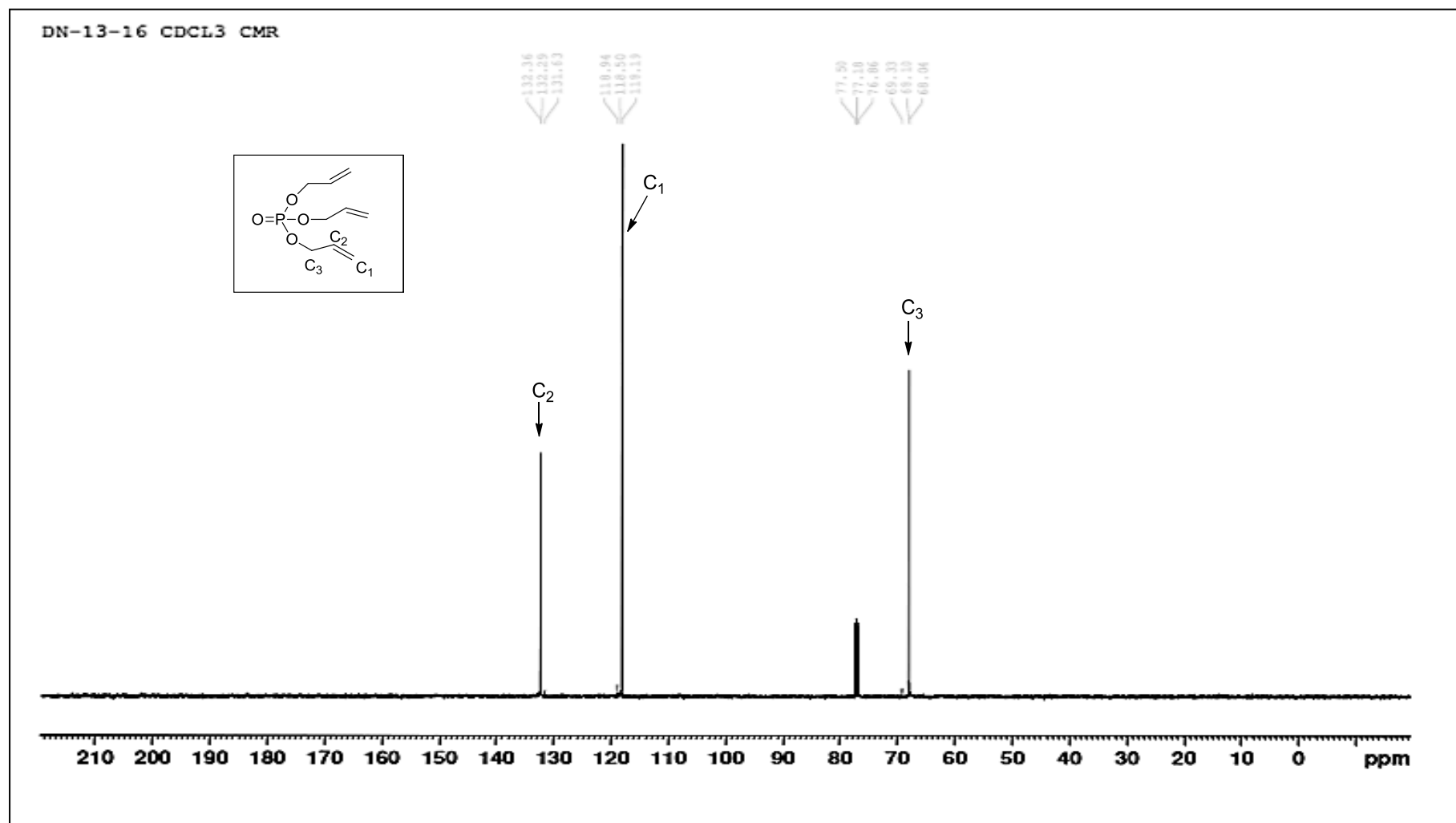
Figure 2.7: ^{13}C NMR of triallyl phosphate (TAP)
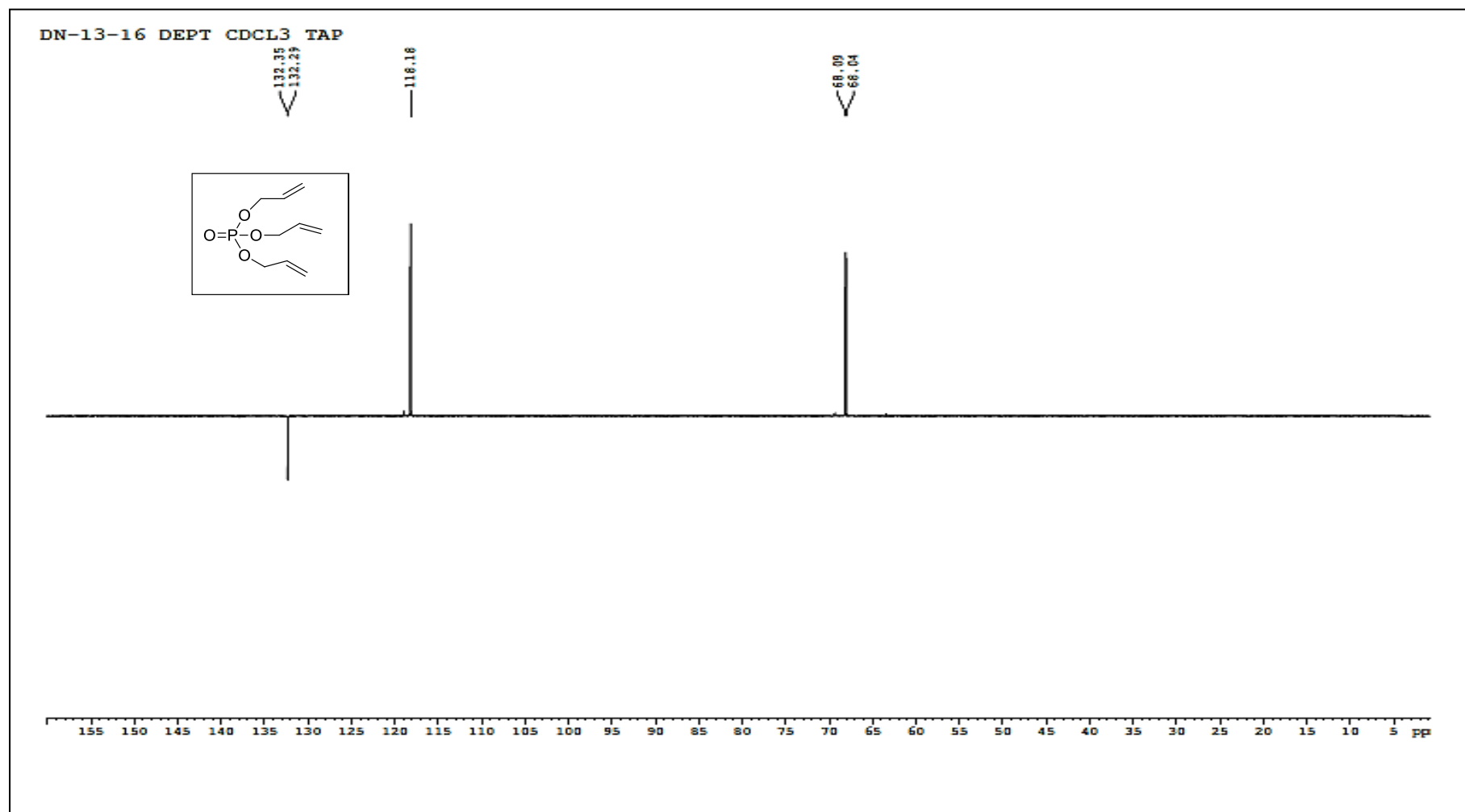
Figure 2.8: DEPT of triallyl phosphate (TAP)

2.2.1.2 Synthesis of 2,2-dimethylpropan-1,3-diyl diallylphosphoramidate (DMPDDP)[16]: It was synthesized in two steps. In the first step, 2, 2-dimethyl-1, 3-propanediol phosphoryl chloride (DPPC) was synthesized and was subsequently reacted with diallyl amine to obtain desired product in 52% yield (with respect to DPPC). The synthesis of desired product is given in Scheme 2.2 below.
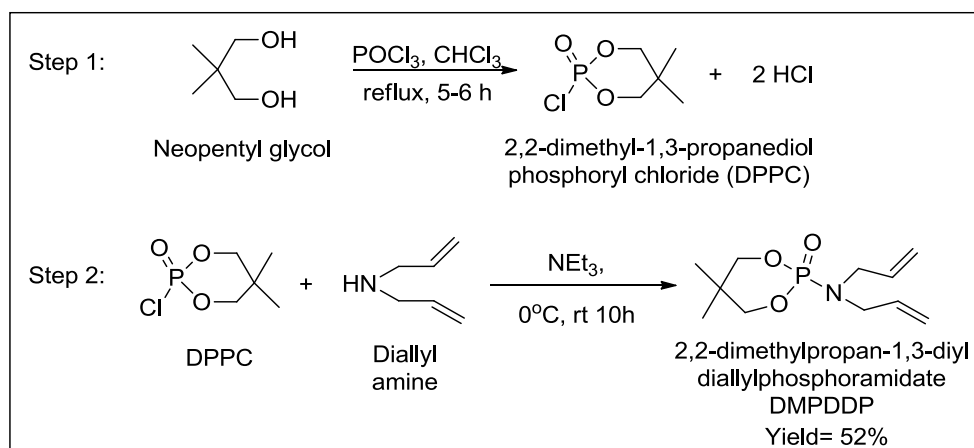
Scheme 2.2: Synthesis of 2,2-dimethylpropan-1,3-diyl diallylphosphoramidate.

Step 1: Synthesis of DPPC: In a three neck round bottom flask fitted with pressure equalizing funnel and condenser, 41.6 g (0.4 moles) of neopentyl glycol was dissolved in 300 mL chloroform. The reaction vessel was cooled to 0 ^{o}C in an ice bath, and 64.4 g (39.3 mL, 0.42 moles) of phosphorus oxychloride was added dropwise through pressure equalizing funnel. After complete addition, it was stirred for some time at 0 ^{o}C and then temperature was gradually increased to ambient temperature with constant stirring. Further it was refluxed for about 5 hours till no HCl gas was evolved. Then chloroform was removed over rotary evaporator till dryness and the white residue was washed with hexane (100 mL) and 3-4 times with ether. The product was dried under vacuum at 60 ^{o}C (68% yield). The solid product

was characterized by IR spectrum as shown in figure 2.9 (page no. 88). IR (KBr): 2976 cm^{-1}, 1469 cm^{-1}, 1303 cm^{-1}, 1004 cm^{-1}, 786 cm^{-1} and 551 cm^{-1}.

Step 2: Synthesis of 2,2-dimethylpropan-1,3-diyl diallylphosphoramidate: In a typical condensation reaction, to a dry 100 mL round bottom flask was added 2.0 g (0.0108 moles) of DPPC, 20 mL CHCl$_3$ and 2.26 g (3.11 mL, 0.0164 moles) of triethyl amine under nitrogen atmosphere. The reaction vessel was cooled to 0 ^{o}C and 1.53 g (1.94 mL, 0.01625 moles) of diallyl amine was added slowly with the help of pressure equalizing funnel with constant stirring. Once the addition was complete it was further stirred for 1 hour at 0 ^{o}C and then temperature was gradually brought to ambient temperature and stirred for 10 hours overnight at ambient temperature. The reaction was monitored by TLC and workup was carried out by washing reaction mixture with brine solution. The aqueous layer was extracted with dichloromethane (4 x 15 mL) and all combined organic phase was passed over dried Na$_2$SO$_4$. Finally, the crude product was obtained by removing organic solvent over rotary evaporator. Crude compound was purified by column chromatography using 30% EtOAc in petroleum ether to get yellow liquid in pure form. This monomer was characterized by IR and NMR spectra (figure 2.10- figure 2.13; page no. 89-92). IR (KBr): 3080 cm^{-1}, 1643 cm^{-1}, 1246 cm^{-1}, 1056 cm^{-1}and 1006cm^{-1}. ^{1}H NMR (400 MHz, CDCl$_3$) (ppm): 5.79-5.69 (m, 2H), 5.21-5.16 (dd, 4H), 4.34 (d, 2H), 4.79 (dd, 2H), 1.24 (s, 3H), 0.87 (s, 3H). ^{13}C-NMR (CDCl3, 100 MHz): 134.13, 117.73, 76.25, 47.45, 31.82, 22.32, 20.69. Unsaturation analysis proved the presence of 2 double bonds.
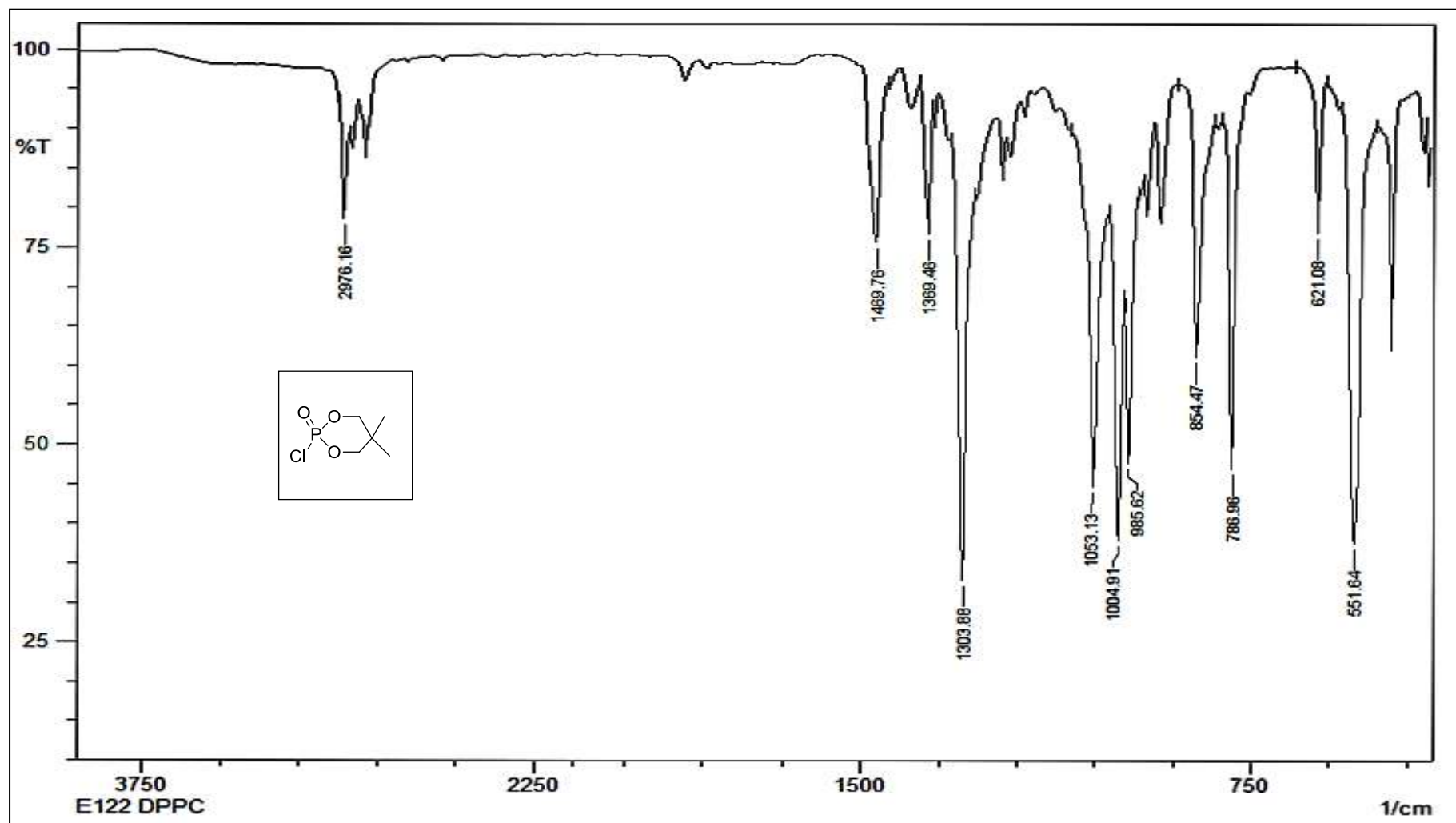
Figure 2.9: IR spectrum of 2,2-dimethyl-1,3-propanediol phosphoryl chloride (DPPC)
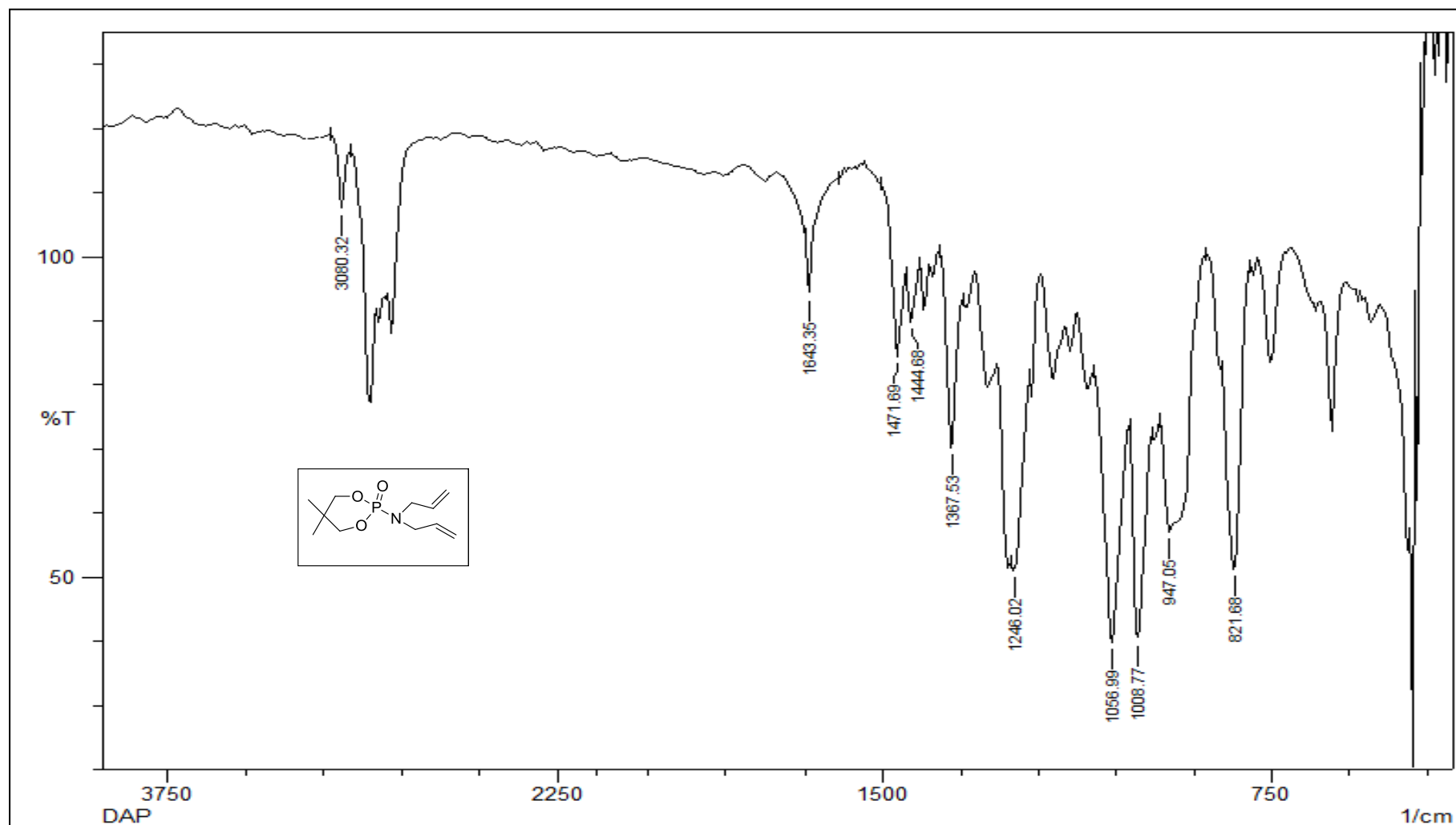
Figure 2.10: IR spectrum of 2,2-dimethylpropan-1,3-diyl diallylphosphoramidate (DMPDDP)
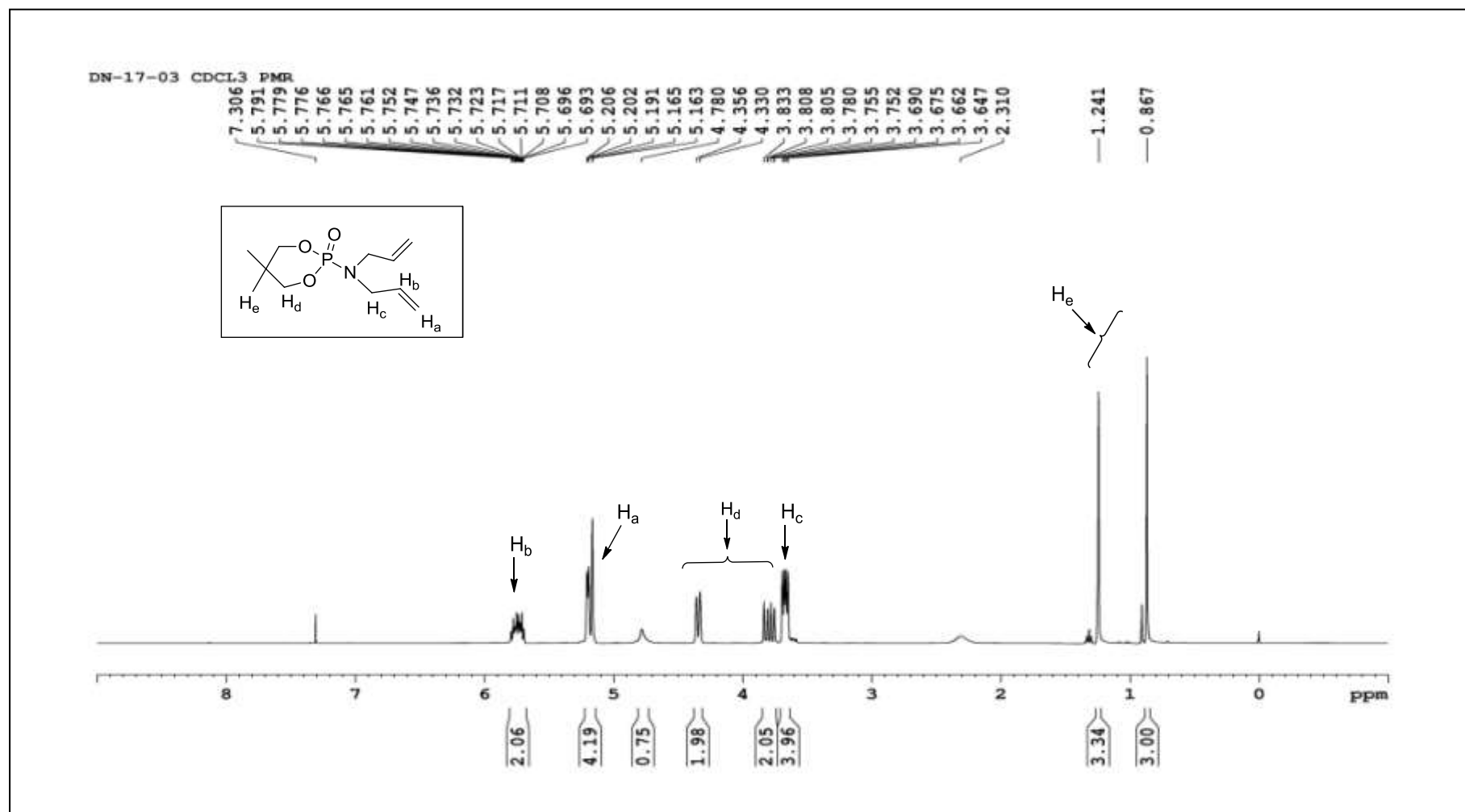
Figure 2.11: ^{1}H NMR of 2,2-dimethylpropan-1,3-diyl diallylphosphoramidate (DMPDDP)
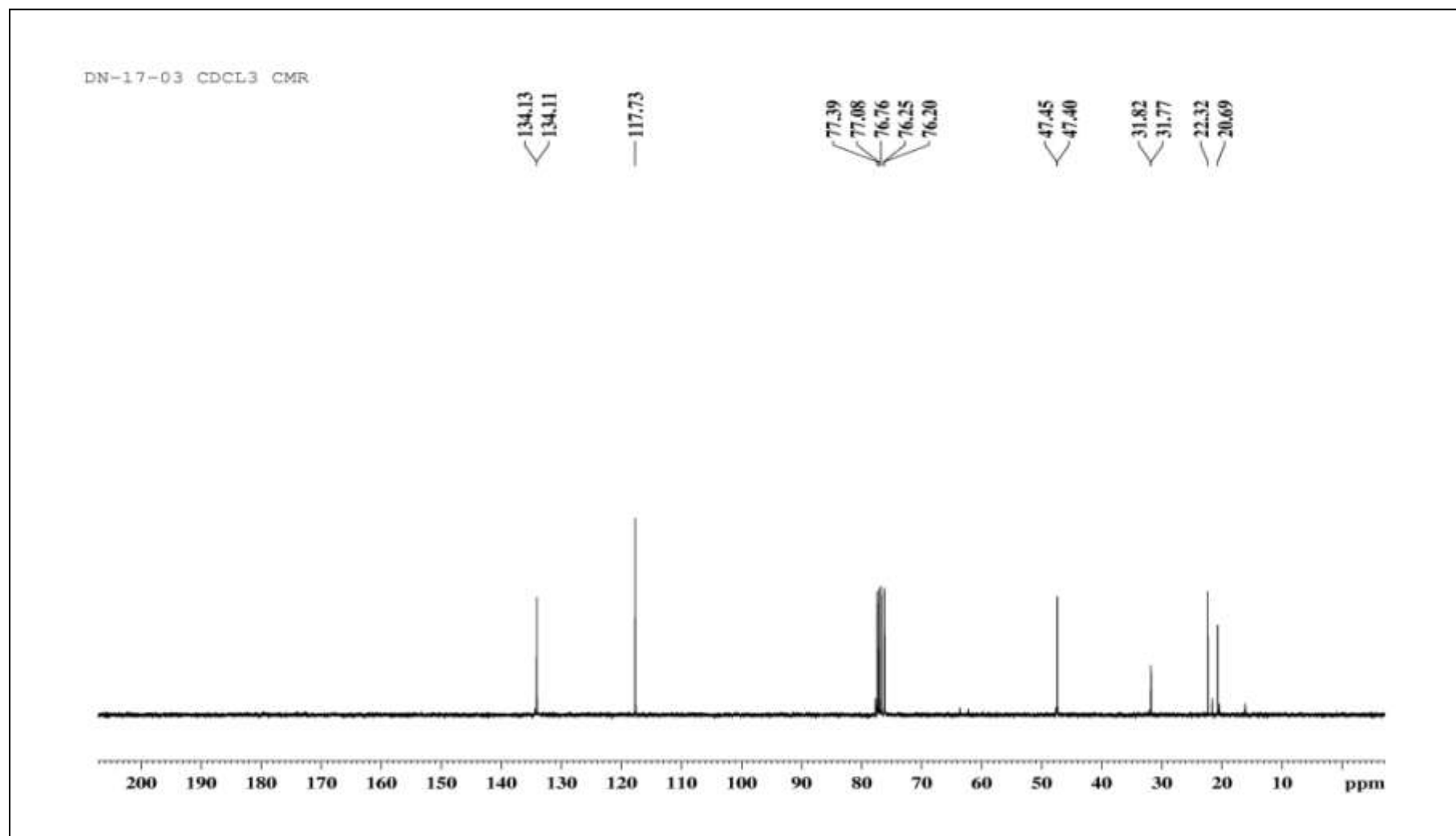
Figure 2.12: ^{13}CNMR of 2,2-dimethylpropan-1,3-diyl diallylphosphoramidate (DMPDDP)
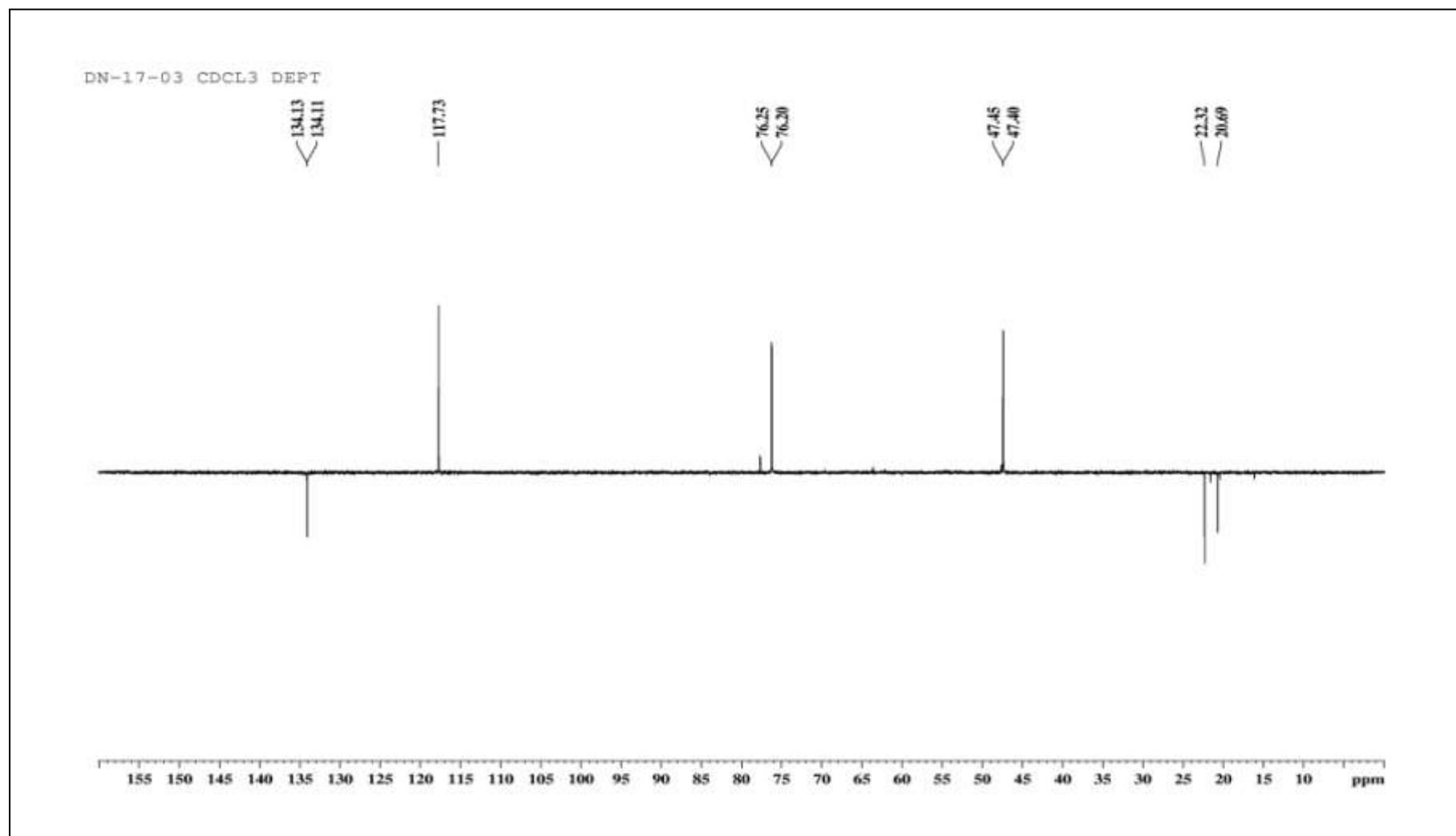
Figure 2.13: DEPT of 2,2-dimethylpropan-1,3-diyl diallylphosphoramidate (DMPDDP)

2.2.1.3 Synthesis of Pentaerythrityl bis (diallylphosphoramidate) (PEBDP)[17]:

This was also synthesized in two steps as shown below in Scheme 2.7. In first step, Spirocyclic Pentaerythritol bisphosphorate Disphosphoryl chloride (SPDPC) was synthesized and was subsequently reacted with 2 equivalents of diallyl amine in second step to obtain desired product in 52% yield.
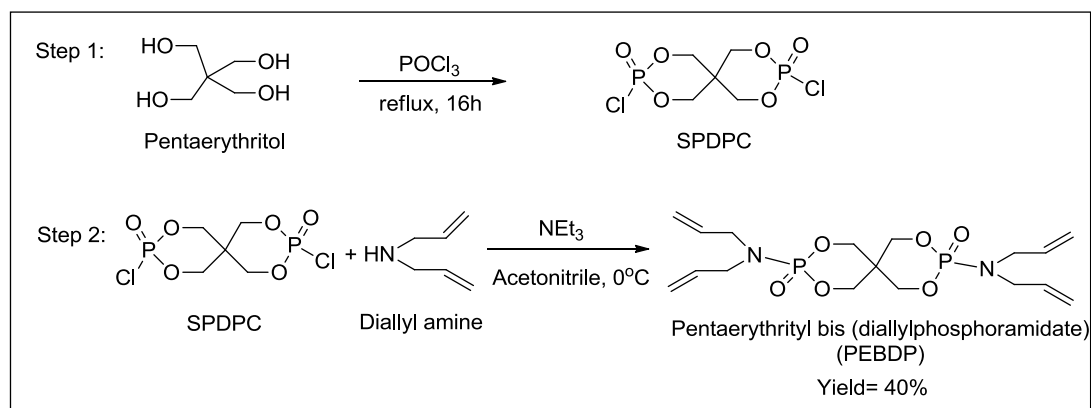
Scheme 2.7: Synthesis of Pentaerythrityl bis (diallylphosphoramidate) (PEBDP)

Step 1: Synthesis of SPDPC: A 3 neck 50 mL round bottom flask, equipped with dropping funnel, thermometer for temperature controlling, and reflux condenser was placed in an ice bath. 2.50 g (0.01836 moles) of pentaerythritol was added to this round bottom flask maintained at 15 °C. Six equivalents of phosphorus oxychloride (16.89 g, 0.11016 moles) was slowly added with the help of dropping funnel within 10 minutes maintaining lower temperature. After completion of addition, it was stirred for some time at 15 °C and then at ambient temperature. Further, it was refluxed for 16 hours at 85 °C. HCl was evolved during refluxing which was quenched in NaOH scrubber. Thereafter the mixture was heated and refluxed until no HCl gas was discharged from the reaction mixture. The crude product obtained was filtered and purified using chloroform and acetone solvents. The product was dried at 60 °C over rotary evaporator. White solid product was obtained in 70% yield. It was characterized by IR and NMR spectroscopy as shown in figure 2.14 and

figure 2.15 (page no. 95, 96). IR (KBr): 1306 cm^{-1} (vs, P=O), 1024 cm^{-1} (vs, P–O–C), 549 cm^{-1} (vs, P–Cl). ^{1}H NMR (400 MHz, d$_6$-DMSO) (ppm): 4.20–4.23 ppm (d,–CCH$_2$O–PO–, 8H).

Step 2: Synthesis of **Pentaerythrityl bis (diallylphosphoramidate) (PEBDP)**: Pentaerythrityl bis (diallylphosphoramidate) was synthesized by condensation process. In a round bottom flask, fitted with pressure equalizing funnel and magnetic stirrer, 3.76 g (4.77 mL, 0.0387 moles) of diallyl amine, 3.92 g (5.40 mL, 0.0387 moles) of triethyl amine as base and 20 mL acetonitrile were mixed together with the help of magnetic stirrer. The reaction mixture was cooled to 0 ^{o}C and by using pressure equalizing funnel 5.0 g (0.0168 moles) of SPDPC in 20 mL acetonitrile was added dropwise. After complete addition, it was stirred for an hour at 0 ^{o}C followed by stirring at room temperature for 5 hours. The reaction was monitored by TLC. The crude solid was filtered and purified with ethanol and dried over rotavap. The yield of the solid product obtained was 40% with respect to SPDPC feed. Spectral analysis of PEBDP was analyzed by IR and NMR spectroscopic techniques as shown in figure 2.16 and figure 2.17 (page no. 97, 98). The melting point of solid was found out to be 142 ^{o}C. IR (KBr): 3062 cm^{-1}, 1639 cm^{-1}, 1242 cm^{-1}, 1022 cm^{-1}. ^{1}H NMR (400 MHz, CDCl$_3$) (ppm): 5.76- 5.66 (m, HC=CH$_2$, 4H), 5.22-5.17 (dd, C=CH$_2$, 8H), 3.94 (d,–CCH$_2$O–PO–, 8H), 3.64 (d, O=P-N-CH$_2$-, 8H).
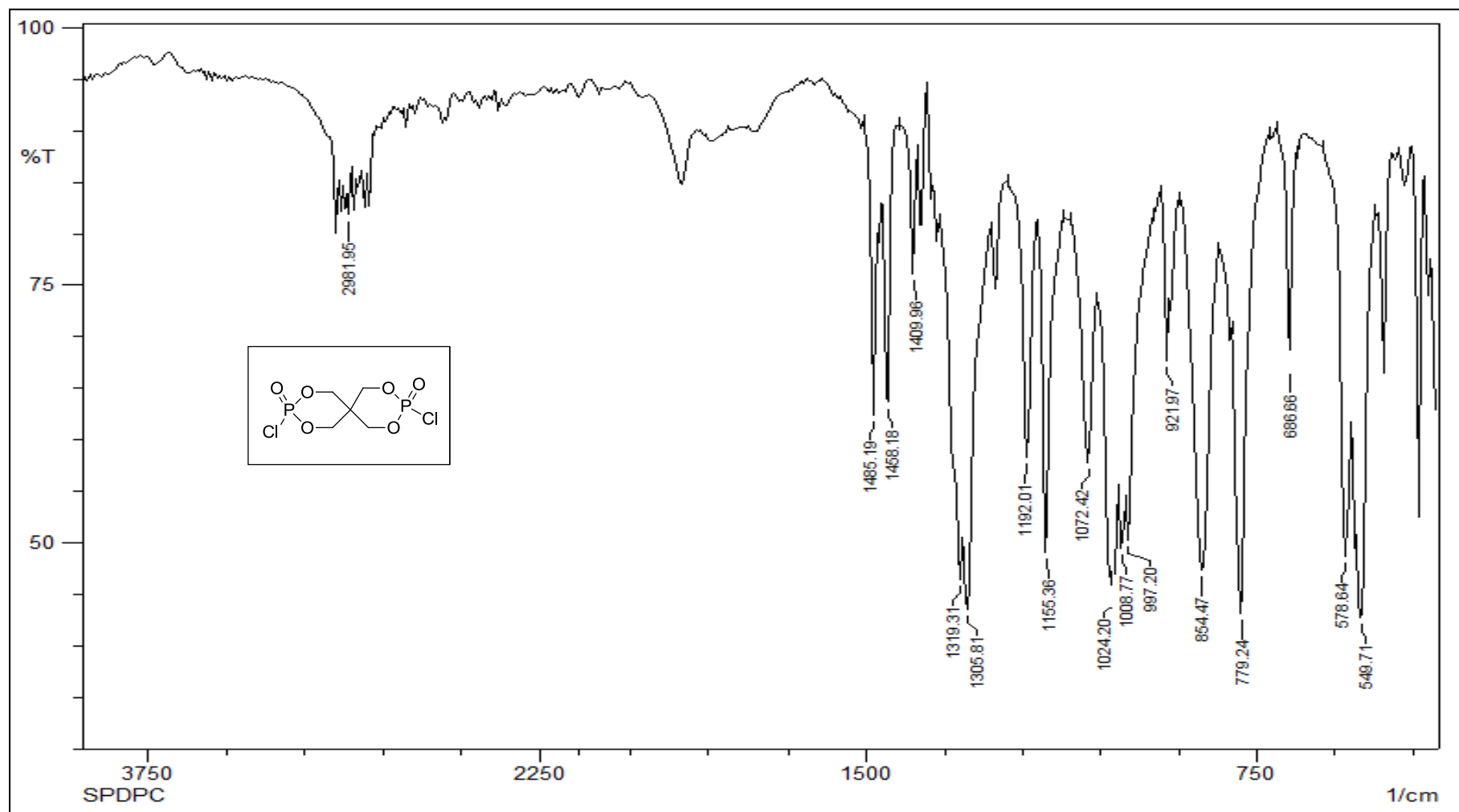
Figure 2.14: IR spectrum of Spirocyclic pentaerythritol bisphosphorate disphosphoryl chloride (SPDPC).
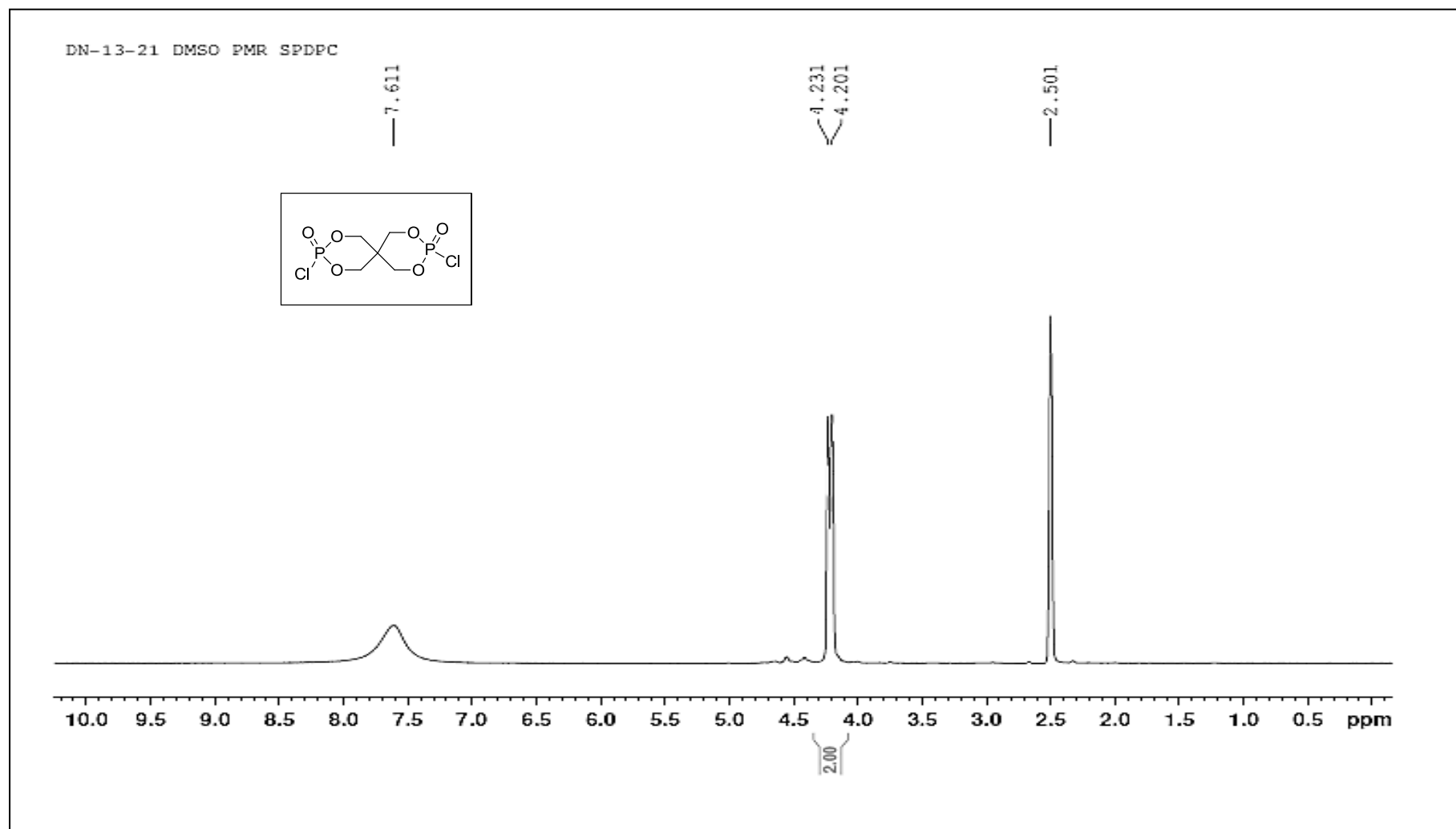
Figure 2.15: NMR spectrum of Spirocyclic pentaerythritol bisphosphorate disphosphoryl chloride (SPDPC).
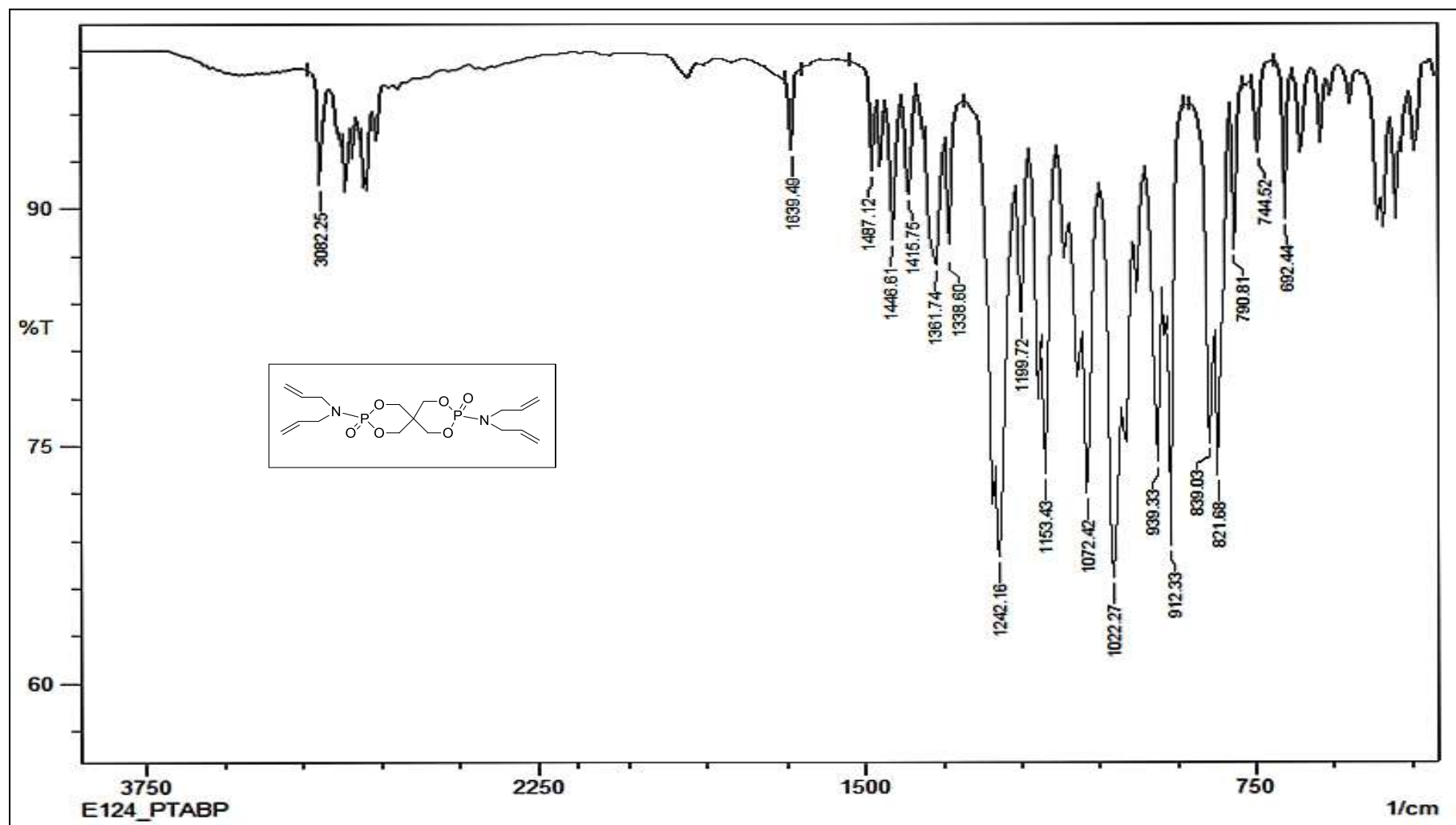
Figure 2.16: IR spectrum pentaerythrityl bis (diallylphosphoramidate) (PEBDP)
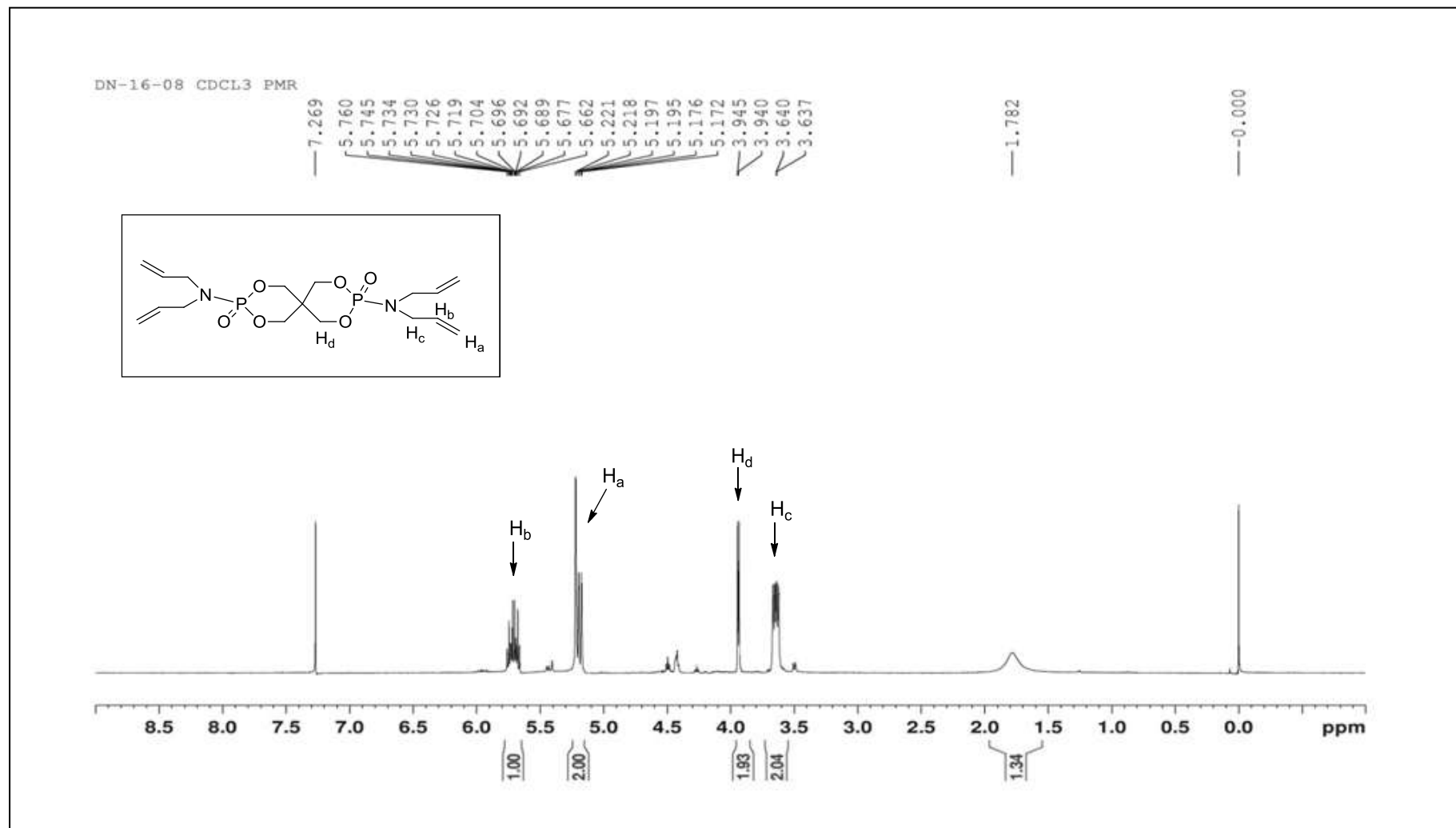
Figure 2.17: NMR spectrum of pentaerythrityl bis (diallylphosphoramidate) (PEBDP)

CHAPTER 2

Synthesis and characterization of ADC, NADAC, PETAC and AMPDAC was carried out as shown below.

2.2.1.4 Synthesis of ADC[18]: Allyl diglycol carbonate (ADC) was synthesized by two methods viz. condensation and transesterification processes. Detailed procedure of synthesis of ADC monomer is given in Chapter IV.

2.2.1.5 Synthesis of N-(Allyloxycarbonyl) diethanolamine bis (allyl carbonate) (NADAC)[19]: In a two neck round bottom flask fitted with pressure equalising funnel, drying tube and magnetic stirrer, 10.0 g (9.2 mL, 0.095 moles) of dry diethanolamine, acetone (100 mL) and 24.82 g (25.3 mL, 0.3139 moles) of pyridine were mixed homogenously with constant stirring. Reacting flask was cooled to -5 ^{o}C and then 37.83 g (33.33 mL, 0.3139 moles) of allyl chloroformate was slowly added to it by using pressure equalizing funnel. At 0 ^{o}C the reaction mixture was stirred for about 1 hour and then at room temperature it was stirred for another 2 hours. The reaction was monitored by TLC and workup was carried out. Initially, the solvent was removed under reduced pressure at room temperature. It was then acidified by 1:1 HCl and water. The reaction mixture was then suspended in ether (50 mL) and washed with brine water (6 x 20 mL) and dried over anhydrous sodium sulphate. Finally the solvent was removed under reduced pressure at room temperature. The crude product was distilled over vacuum at 180 ^{o}C internal temperature and 0.1 mbar pressure. The distilled product weighed 16.1 g was characterized by IR and NMR spectra (figure 2.18 and figure 2.19; page no. 101-102). Yield of the product obtained was 75% based on diethanolamine. Below scheme 2.8 depicts the synthesis of NADAC. IR (KBr): 3086 cm^{-1}, 1747cm^{-1}, 1701 cm^{-1}, 1649 cm^{-1}, 1255 cm^{-1}, 1070 cm^{-1}. ^{1}H NMR (400 MHz, CDCl$_3$) (ppm): 5.96–5.89 (m, 3H); 5.38-5.20 (dd, 6H); 4.63- 4.59 (d, 6H); 4.28 (t, 4H); 3.61 (t, 4H).
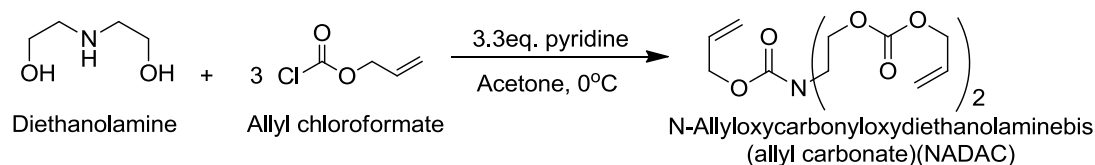
Scheme 2.8: Synthesis of NADAC

2.2.1.6 Synthesis of pentaerythritol tetrakis allyl carbonate (PETAC)[20]: In a three neck flask equipped with dropping funnel, thermometer and magnetic stirrer, 10 g (0.0734 moles) of pentaerythritol was suspended in 100 mL toluene. Reacting flask was cooled to 0 °C and 24.98 g (25.44 mL, 0.3158 moles) pyridine was added. 38.05 g (33.52 mL, 0.3158 moles) of allyl chloroformate was added drop by drop with vigorous stirring using dropping funnel. The temperature was strictly maintained below 5 °C during the course of addition. After complete addition of allyl chloroformate, the mixture was stirred for 1hr at 0 °C and then for 3 h at room temperature. The progress of reaction was monitored using thin layer chromatography. The reaction mixture was neutralized/ slightly acidified by using 50 mL 1N HCL and then washed it with 3×50 mL of water till it is neutral. The organic layer was dried with anhy. Na_2SO_4. The solvent was removed under vacuum to afford 26.02 g (75%) of crude product. The product obtained was purified by column chromatography using 3:7 EtOAc: Pet ether mixture to get 24.66g (70%) of the pure light yellow product as shown in scheme 2.9. It was characterized by IR and ^{1}H NMR spectroscopic techniques (figure 2.20, figure 2.21; page no. 103-104). IR (KBr): 3086 cm^{-1}, 1756 cm^{-1}, 1651 cm^{-1}, 1242 cm^{-1}, 968 cm-^{1}. ^{1}H NMR (400 MHz, CDCl$_3$) (ppm): 5.91–5.81 (m, 4H); 5.32-5.20 (dd, 8H); 4.54 (t, 8H); 4.18 (s, 8H).

Pentaerythritol tetrakis (allyl carbonate) PETAC
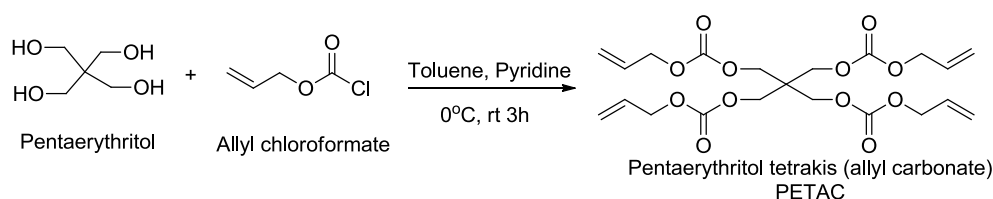
Scheme 2.9: Synthesis of PETAC
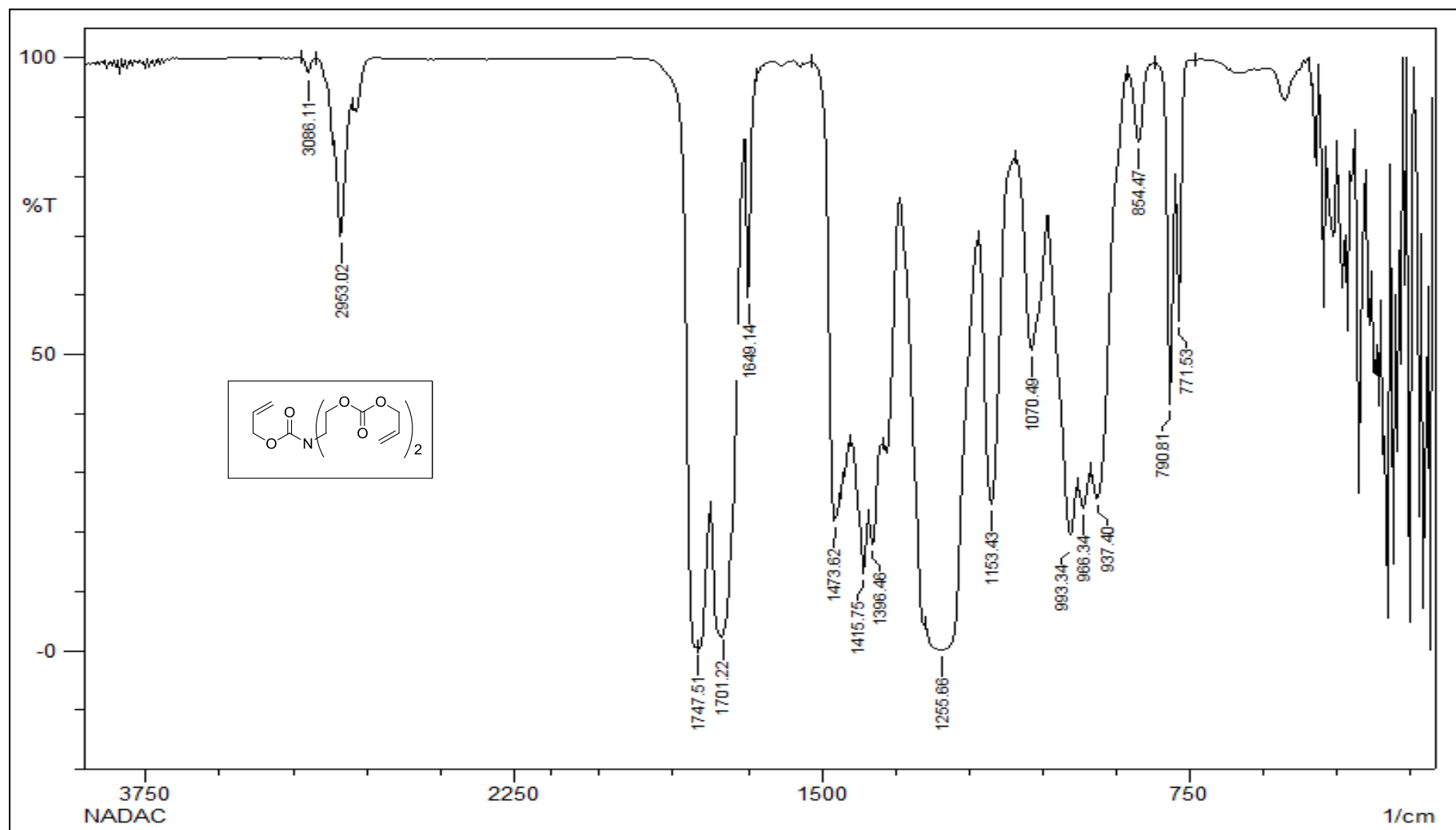
Figure 2.18: IR spectrum of NADAC
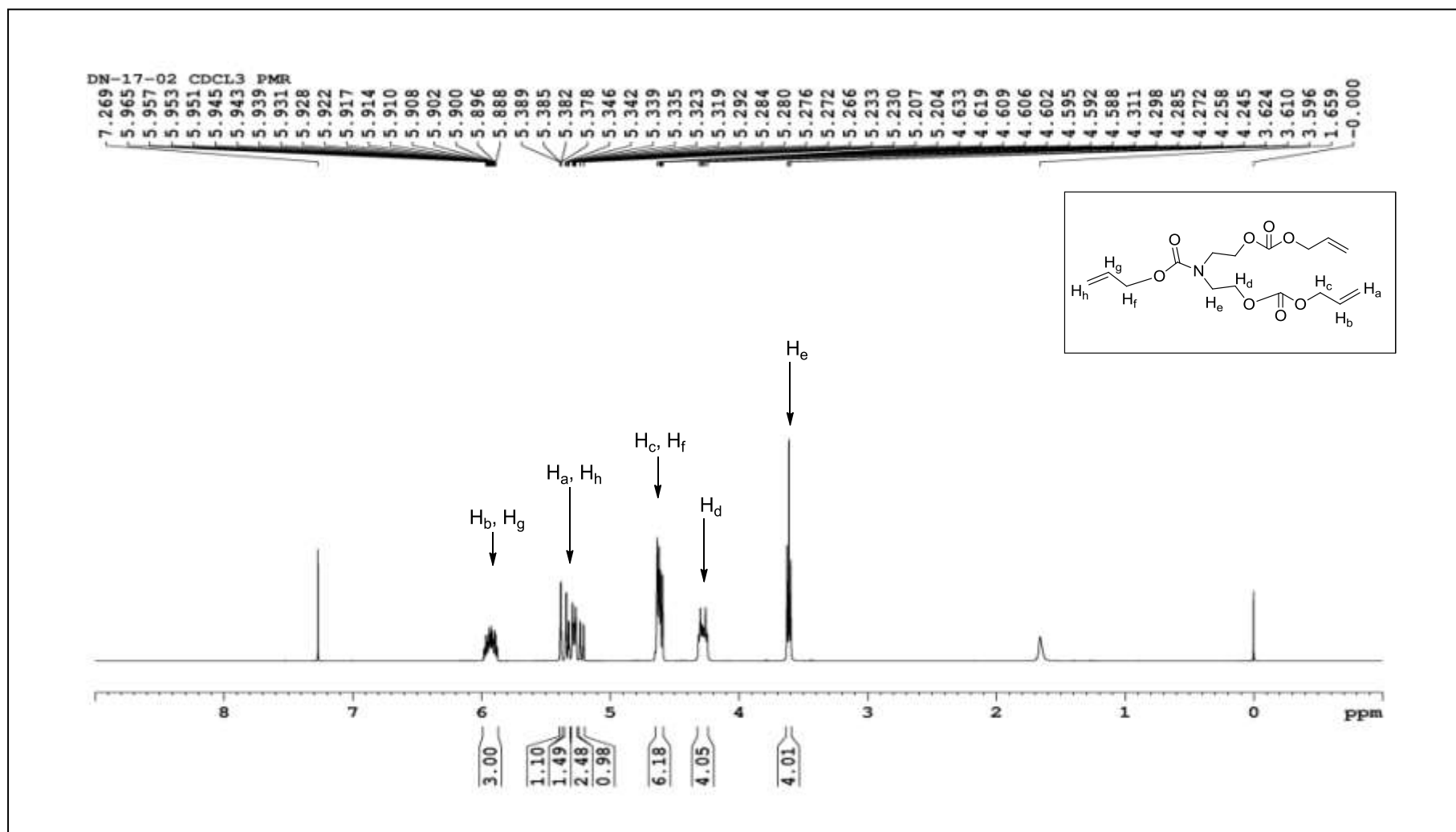
Figure 2.19: ^{1}H NMR spectrum of NADAC
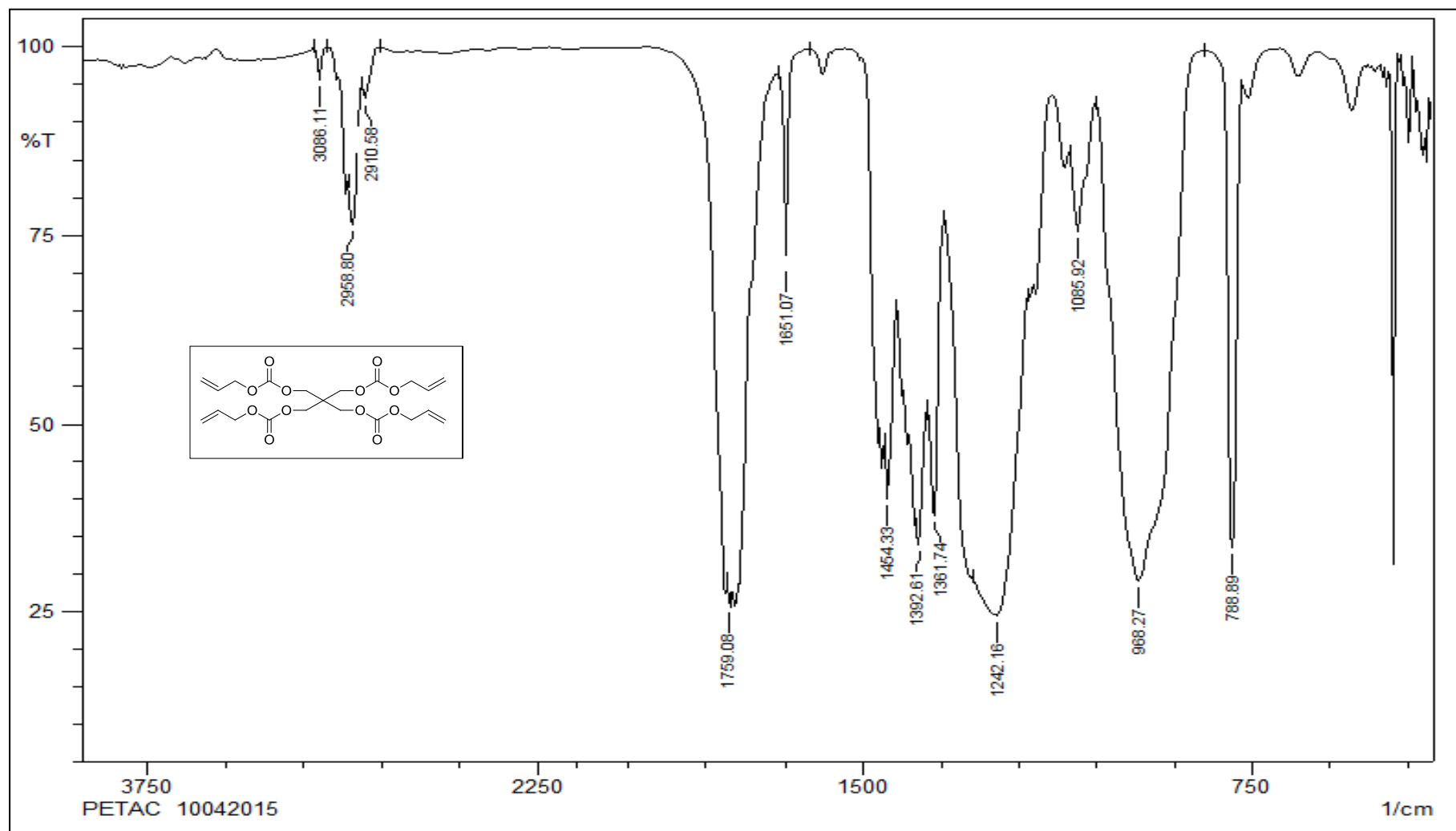
Figure 2.20: IR spectrum of PETAC
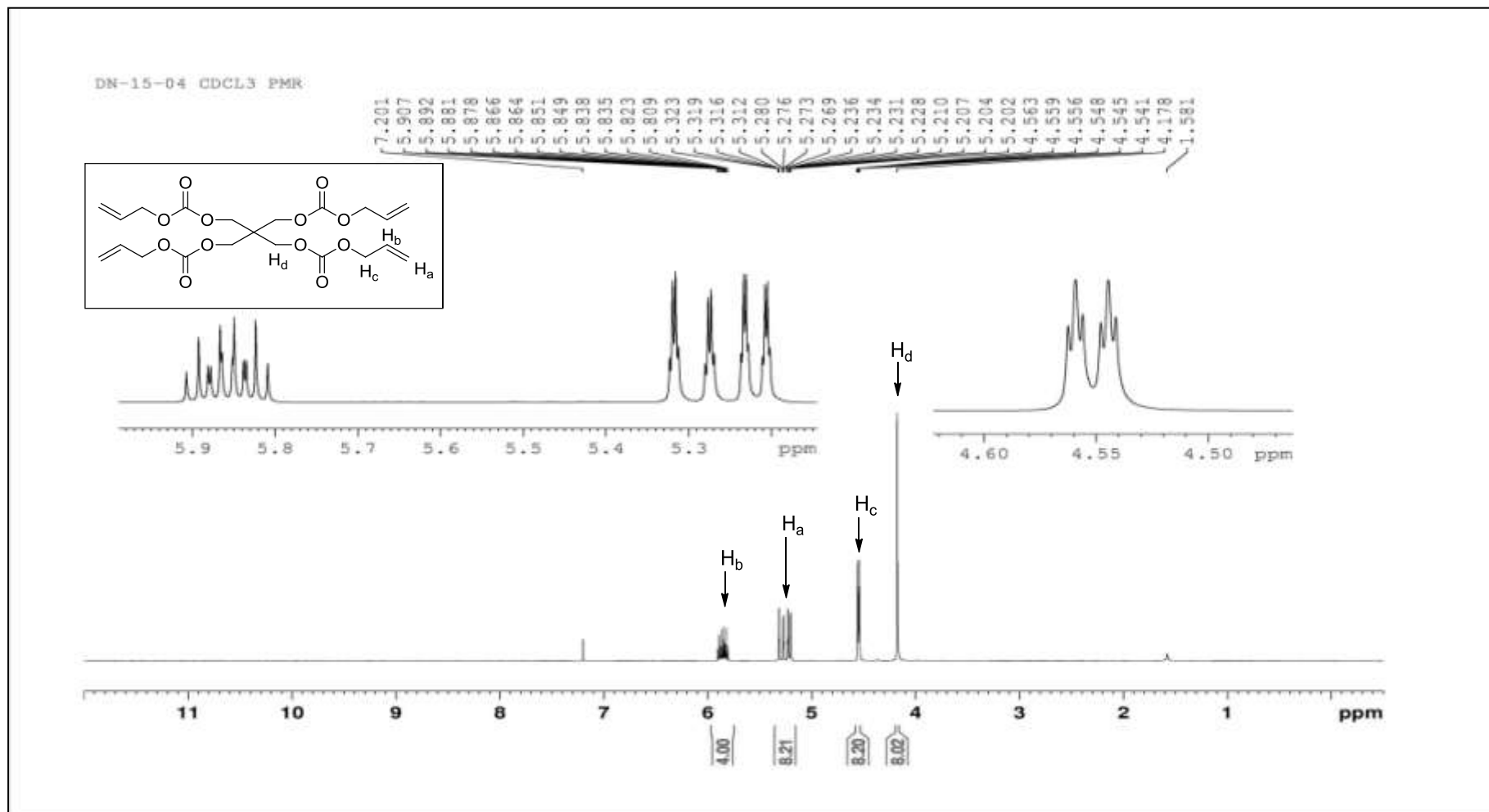
Figure 2.21: NMR spectrum of PETAC

2.2.1.7 Synthesis of Allyloxycarbonyl ammediol bis(allyl carbonate) (NAAAC): In a two neck round bottom flask equipped with dropping funnel and thermometer, 5 g (0.0476 moles) of 2-amino-2-methyl-1,3-propanediol (AMPD) was dissolved in 50 mL acetone. To this solution 12.41 g (12.64 mL, 0.1569 moles) of pyridine was added and cooled to $0\ ^{\circ}C$ with constant stirring. By using dropping funnel, 18.91 g (16.7 mL, 0.1569 moles) of allyl chloroformate was slowly added to the reaction flask over a period of 1 hour. Further, it was stirred for another 3 hours at an ambient temperature and was monitored by thin layer chromatography. After completion of reaction, acetone was removed from the reaction mixture over rotary evaporator and was treated with 30% HCl in water so as to neutralize the excess base. It was extracted in 50 mL of diethyl ether and washings of brine (5 x 20 mL) were given till it becomes neutral. Finally, organic layers were passed over anhydrous sodium sulphate and removed over reduced pressure to get desired product in 70% crude yield. Further, it was purified by column chromatography using 30% ethyl acetate in petroleum ether to produce pure light orange liquid in 68% yield. It was characterized by IR (figure 2.22; page 106) and NMR spectra (figure 2.23-figure 2.25; page no. 107-109). IR (KBr): 3375 cm^{-1}, 3086 cm^{-1}, 1745 cm^{-1}, 1730 cm^{-1}, 1651 cm^{-1}, 1255 cm^{-1} and 1080 cm^{-1}. ^{1}H NMR (400 MHz, CDCl$_3$) (ppm): 5.98–5.86 (m, 3H); 5.32-5.20 (dd, 8H); 4.54 (t, 8H); 4.18 (s, 8H). ^{13}C NMR (100 MHz, CDCl$_3$) (ppm): 154.59, 132.63, 119.16, 68.74, 65.34, 54.60, 19.00.
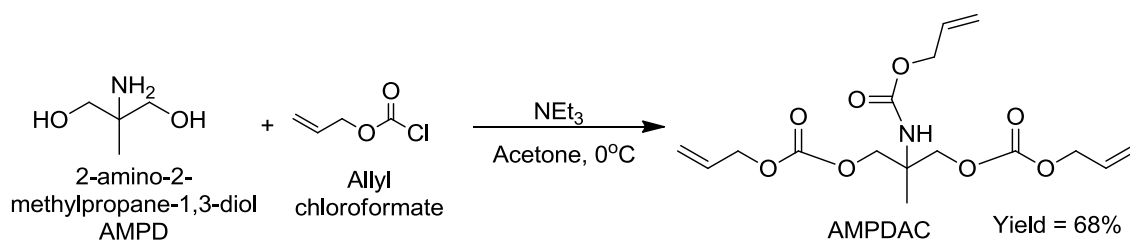
Scheme 2.10: Synthesis of Allyloxycarbonyl ammediol bis(allyl carbonate) (NAAAC)
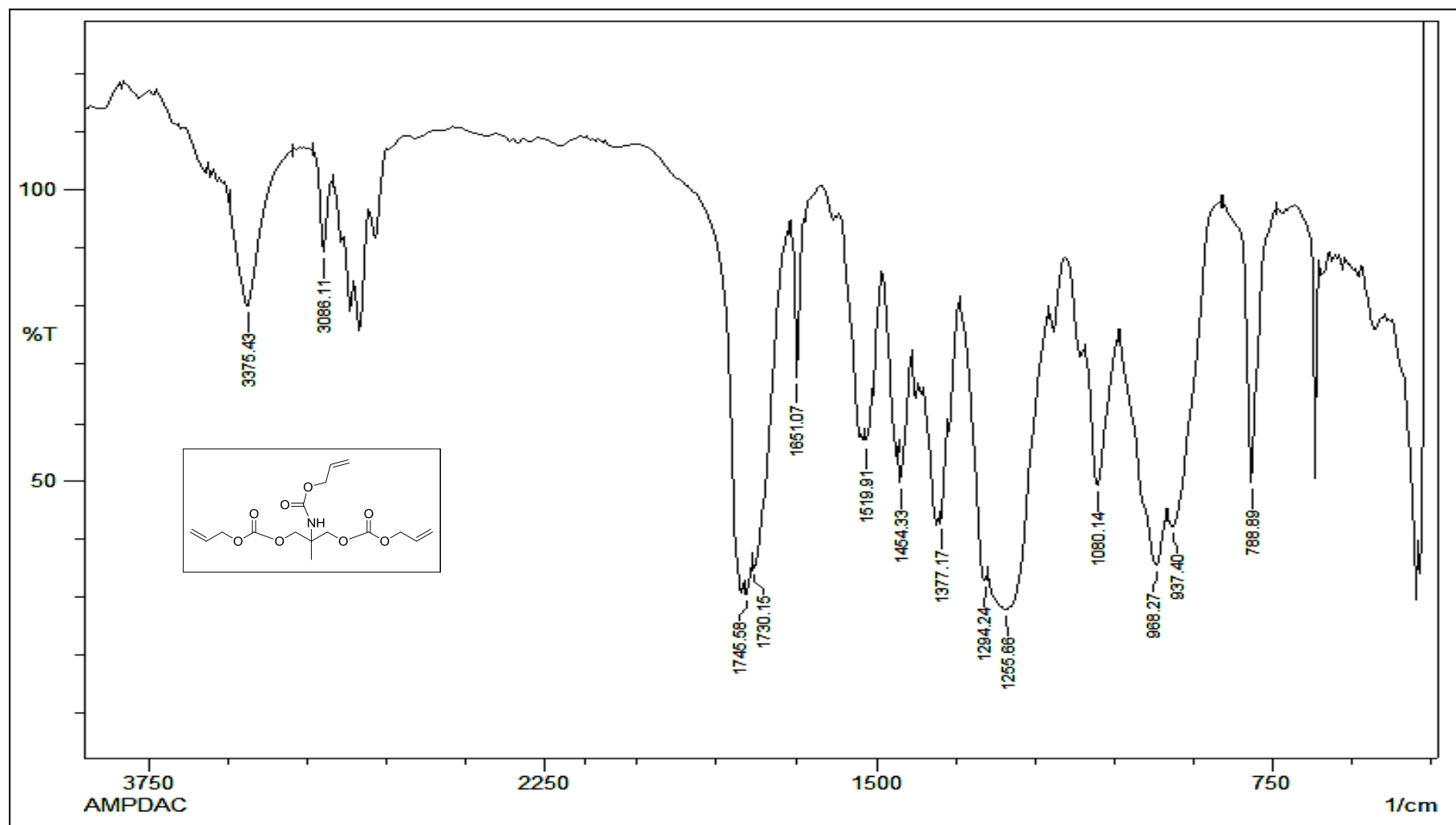
Figure 2.22: IR spectrum of Allyloxycarbonyl ammediol bis(allyl carbonate) (NAAAC).
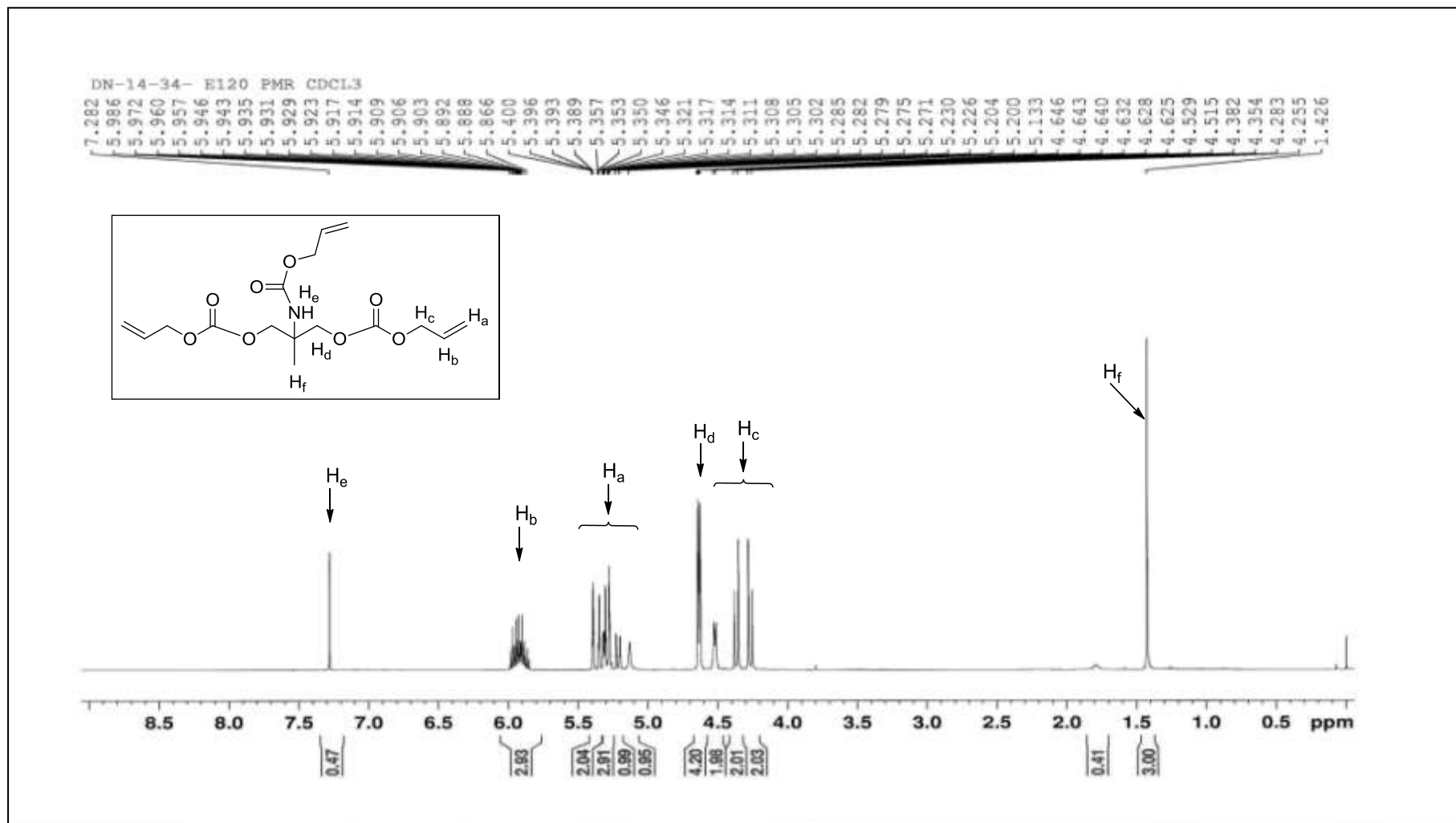
Figure 2.23: ^{1}H NMR spectrum of Allyloxycarbonyl ammediol bis(allyl carbonate) (NAAAC).
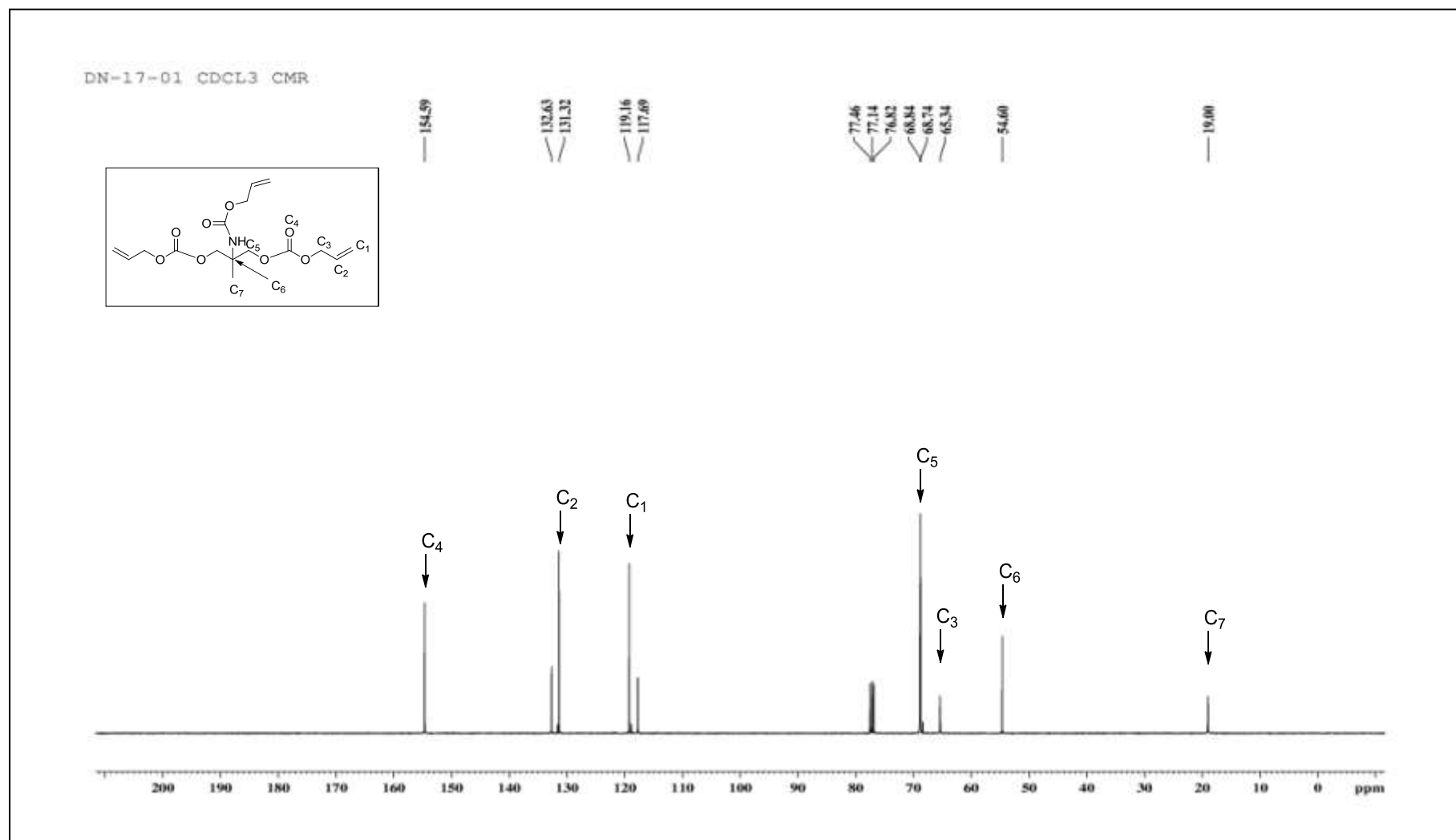
Figure 2.24: ^{13}C NMR spectrum of Allyloxycarbonyl ammediol bis(allyl carbonate) (NAAAC).
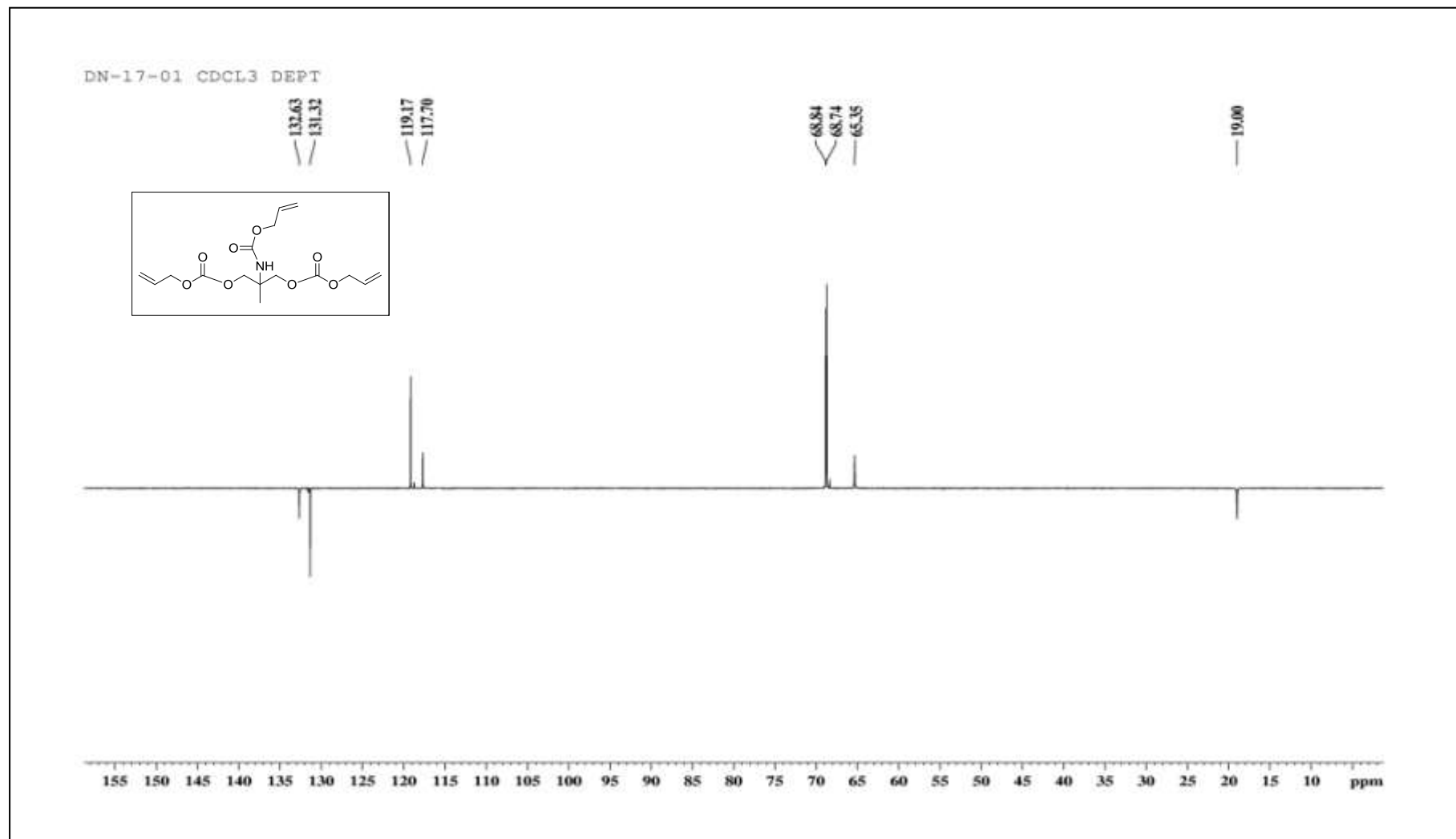
Figure 2.25: DEPT spectrum of Allyloxycarbonyl ammediol bis(allyl carbonate) (NAAAC).

CHAPTER 2

Preparation of SSNTD films by free radical polymerization[21]: We have already developed and standardized the casting of PADC films of size 25 cm x 15 cm. Also stepwise procedure from mould designing to mould filling have been discussed in Chapter 4. Triallyl phosphate was homopolymerized and copolymerized using initiators like benzoyl peroxide, isopropylperoxy dicarbonate (IPP) and plasticizer dioctyl phthalate. TAP monomer was first degassed and filtered through 0.45μ membrane. It was then mixed homogenously with initiator 3.3 wt. % of isopropyl peroxy dicarbonate (IPP) and 0.1 wt. % of dioctyl phthalate plasticizer. The prepared monomer mixture was filled into the mould and the polymerization was carried out by using 12 hour constant rate polymerization profiles developed for TAP and its copolymer with ADC by placing the mould into the polymerization assembly. Further analysis and preliminary dosimetric studies were carried out on the prepared polymeric materials. The percent polymerization of PTAP and poly (TAP-*co*-ADC) films was determined by Wij's method of unsaturation analysis[22].

2.2.2 Instrumentation and Techniques used for the preparation of polymeric detectors and their preliminary evaluation as track detectors:

In this section, various instruments and techniques used for preparing the thin films of polymeric detectors are described. Experimental methods used for study of polymerization kinetics and optimization of etching conditions are also mentioned. It may be noted that these were also used in case of all the polymeric detectors mentioned in the remaining chapters of this thesis.

2.2.2.1 General protocol for preparation of polymeric track detectors

Aiming at designing newer polymeric materials for solid state nuclear track detection, we followed a protocol for systematic testing of novel polymeric detectors

that was earlier proposed by us[23]. This included different stages viz., 1) initial studies for designing monomer/polymer, 2) developing constant rate polymerization profile by studying kinetics of polymerization, 3) optimization of initiator concentration, 4) optimization of etching condition, and finally 5) sensitivity at optimized initiator and etching conditions.

The monomers having two or more allylic linkage ($CH_2=CH-CH_2-$) undergo process of free radical polymerization and if the monomer functionality is more than two then a 3-D cross linked network can be obtained. Also, as compared to vinyl end group, allylic end group is easier to introduce into the monomer for its polymerization. Further, it is known from the literature that the insertion or addition of hetero atoms (N, O, S, and P) containing functional groups into the monomers can enhance its sensitivity towards radiation or charged particles. So if some functional moieties having hetero atoms are introduced between two allyl end groups then the polymer can become more radiation sensitive. Already, we have reported synthesis of monomers containing functional moieties like $–ONO_2$, -O-CO-O-, -N-CO-O-, O-SO-O-, $-O-SO_2-$ or a monomer with more than one type of functional group[24]. Then, to improve crosslinking density in a 3D polymeric network, branched monomers were used that can efficiently crosslinked[25]. Here, we have prepared some monomers containing phosphate, phosphamide linkage having two or more allylic groups as mentioned earlier which can form 3D polymeric network. These monomers were initially tested for free radical polymerization. Its copolymerization with different monomers viz. ADC, NADAC, PETAC, NAAAC were also carried out and the effect on radiation sensitivity was studied.

Based on our earlier experience, a protocol that is useful for track detector worker who want to synthesize and design a newer monomers/ polymers for track

detection is put forward. The brief description of the protocol is as given below and is followed for all the monomers and polymers prepared.

Step 1: Monomer synthesis and Initial studies of monomer /polymer:

a. Designing, syntheses and spectral characterization of the monomers: Based on the factors like radiation sensitive group effect, monomer functionality, extent of cross link and chain linking the two functionalities, the monomers were designed. The syntheses of the monomers were carried out by using different chemical processes. And all the monomers were characterized by Fourier Transform Infrared spectroscopy, ^{1}HNMR, ^{13}C NMR spectroscopy and Mass spectrometry.

b. *Stability of monomer using TG/DTA techniques:* A thermal study of the monomer offers a succinct plan about the polymerization conditions that can be used for polymerization of the monomer under study. The TG/DTA technique provides the maximum temperature above which monomer decomposes. This gives a brief idea of maximum temperature that can be used for polymerization. This is essentially done if the newly synthesized monomer is found to have some problems when heated during its polymerization.

c. Casting of a test polymer sample and its characterization: A test polymer is initially prepared to test the fittingness of the designed monomer for track detection. A homopolymer as well as a copolymer of the monomer under consideration with ADC are prepared by means of an appropriate heating profile. The polymeric films are than characterized with respect to the properties like color of the film, softness, % unsaturation left , average thickness and spectral properties.

d. Exposure to radiation source and etching in 6N NaOH at 70 °C: The polymer films so prepared is cut into small pieces of $1 \times 1 cm^2$ and exposed to [239]Pu source for

alpha particles and to ^{252}Cf source for fission fragments to study the track revelation properties of the polymer. The exposed and control films are then etched in 6N NaOH at 70 °C or related etching condition to reveal tracks. The etching condition is altered or varied if the polymer degrades or becomes opaque under above etching condition. The concentration of the etchant also varied if the problem persists

e. Bulk etch rate (V_b) determination: As mentioned in the Chapter-1, the bulk etch rate of the film is a very important part as it provides the rate at which the surface of the test polymer is removed. The track etch rate V_t should always be greater than the bulk etch rate of the polymer, that is the ratio of bulk etch rate to track etch rate should be less than 1 which is given as $V_b/V_t < 1$. During the etching process, the test polymer surface is removed layer by layer thereby reducing the film thickness.

Step 2: Kinetic study of polymerization:

Allylic polymerization suffers from certain disadvantages and this affects the quality of the polymeric detector. In order to overcome such problems Dial et al suggested a kinetic model for the Allyl Diglycol Carbonate (ADC) which is a tetrafunctional monomer. Applicability of the same to the newly synthesized allylic monomer is tested and a polymerization profile which can result in smooth polymerization of the monomer is calculated.

Step 3: Optimization of initiator concentration:

The quantity of initiator used during polymerization process determines the cross linking character in the polymer matrix. And the sensitivity of the detector in turn depends on the cross linking property of the polymer film. The density of crosslink's increases rapidly with increase in concentration of the initiator up to the maximum and then decreases with further increase in initiator concentration. Hence,

optimum initiator concentration is determined by studying the alpha sensitivity of polymer samples prepared using different initiator concentrations. The initiator concentration where the alpha sensitivity achieves a maximum value is the optimum initiator concentration for the polymeric detector material.

Step 4: Optimization of etching conditions:

By using different etching conditions the posts etch surface clarity of a film can be changed. For finding the optimum etching condition, first a 10" x 10" polymer film at optimized initiator concentration is prepared and around 10-15 pieces of films (size 1" x 1") are exposed to fission and alpha source. The exposed films are chemically etched in constant normality and varied temperature. Films are also etched changing the normality at constant temperature. Bulk etch rate after every etching time interval is noted along with the track appearance time. The optimum etching condition is one at tracks are developed within reasonable time and the surface of the film after etching remains clear with a moderate V_b.

Step 5: Determination of alpha sensitivity at optimized etching conditions:

At the selected optimum etching conditions, alpha sensitivity of the detector prepared using the optimized initiator concentration is determined.

Step 6: Other specific studies of the polymeric detector could then be carried out. However, this might require access to specific experimental facilities.

2.2.2.2 Study of allylic polymerization kinetics:

During free radical polymerization process, many steps like initiation, propagation, termination, decomposition of initiator etc occurs at faster rate. These processes are highly exothermic and there is increase in polymerization rate. Due to which there is

defect in the polymer matrix. Thus the polymeric films obtained for different batches show different properties. It is also known that during PADC polymerization there is 14% of shrinkage in the volume; which leads to the cracking of films.

So during polymerization, it becomes necessary to control the heat evolved and to carry out polymerization at low temperature over longer period of time. In order to overcome such problems faced during allylic polymerization to cast thin polymer films, Dial et. al. studied the kinetics of polymerization of ADC monomer using IPP initiator. The data obtained from kinetics study was utilised to derive a kinetic model. Heating temperature time profiles can be constructed by using the derived kinetic models. This heating profile endorse constant rate of initiator decomposition and constant heat evolution due to allylic polymerization. Dial et. al. had suggested use of constant rate polymerization profile based on the following set of kinetic equation below (Equation 2.1- 2.6). Dial et. al. had performed the kinetics of ADC monomer with IPP initiator (3.3 %) at three different set of temperature viz. 40, 50 and 60 °C to derived constant rate polymerization profile[26]. Mandrekar et. al.[24(a)] have successfully used these equations for kinetics of ADC polymerization using BP initiator at 60, 70 and 80 °C. Also he proved the suitability of the method to various monomers at a set of temperature.

$$K_4 = Z_3 e^{-E_3/RT} (M_0 - K_4 t) \sqrt{C_0 - \frac{K_4 t}{Z_1 e^{-E_3/RT}}} \tag{2.1}$$

$$E_1 = \frac{T_1 T_2}{T_1 - T_2} Log_e \frac{K_1}{K'_1} \tag{2.2}$$

$$K_1 = Z_1 e^{-E_1/RT} \tag{2.3}$$

$$K_3 = -\frac{1}{t}\left[\frac{1}{\sqrt{C_0 - \frac{M_0}{K_1}}} \log_e \frac{\sqrt{C_0 - \frac{M_0}{K_1} + \frac{M}{K_1}} - \sqrt{C_0 - \frac{M_0}{K_1}}}{\sqrt{C_0 - \frac{M_0}{K_1} + \frac{M}{K_1}} + \sqrt{C_0 - \frac{M_0}{K_1}}} - \frac{1}{\sqrt{C_0 - \frac{M_0}{K_1}}} \log_e \frac{\sqrt{C_0} - \sqrt{C_0 - \frac{M_0}{K_1}}}{\sqrt{C_0} + \sqrt{C_0 - \frac{M_0}{K_1}}} \right]$$

(2.4)

$$E_3 = \frac{T_1 T_2}{T_1 - T_2} Log_e \frac{K_3}{K'_3}$$

(2.5)

$$K_3 = Z_3 e^{-E_3/RT}$$

(2.6)

Where, K_4 is rate of polymerization, K_1 is the slope, K_3 is the rate of reaction, Z_1 and Z_3 are Arrehenius constants, E_1 and E_3 are corresponding energies of activations, M_0 and C_0 are initial concentrations of monomer and initiator respectively, R is gas constant. Temperature T at a given time *t* is calculated using this equation. These equations have also been employed to determine heating profiles for hexafunctional monomer and it may be interesting to study the rate of polymerization for monomers containing different functionalities and their effect on radiation sensitivity.

We have already extended this method successfully to many other allylic monomers and devised constant rate polymerization profiles for such monomers to cast thin (0.5 to 0.7 mm) detector films[25]. Constant rate polymerization results in a smooth evolution of heat and gives a polymer with more uniform bulk properties. We thought of extending this idea for newly prepared phosphate monomers and obtaining a constant rate polymerization profile for them. This methodology was extended by us to develop constant rate polymerization profile for hexafunctional allylic monomer containing phosphate functionalities i.e. for TAP monomer. Also for a mixture of ADC and TAP constant rate polymerization profile was developed. Kinetic study involves examination of change in the initiator and monomer

concentrations at different time intervals. At a particular constant temperature by using iodometric analysis, the initiator concentration was established and the unsaturation analysis was carried out by Wij's method. Detailed procedure for unsaturation analysis and IPP estimation is given in Chapter 4.

Starting with known concentrations of monomer and initiator, we determined change in their concentrations as a function of time. Residual monomer concentration was determined using ICl (Wij method) and peroxide concentration was determined by iodometric titration. A series of test tubes containing mixture of monomer and IPP initiator (3.3% by weight) were taken, and flushed with nitrogen gas and tightly sealed. Three such separate sets were placed in the water bath and after certain period of time each test tube was analyzed for its peroxide concentration and residual monomer concentration by iodometric titration. This way, the residual monomer concentration and peroxide concentration were determined as a function of time at 35, 45 and 55°C. By using both initiators IPP and BP kinetics of polymerization was studied for TAP and poly (TAP-*co*-ADC).

2.2.2.3 Preparation of polymeric detectors:

The techniques and instrumental requirements involved during the synthesis of the polymeric detectors are given below.

1. **Vacuum pump**: A high vacuum pump (Hindvac, India) was utilized to generate vacuum of the order of 0.1-0.2 mbar required to distill and purify high boiling monomers and also during the experiments related to the determination of alpha particle sensitivity of the polymers.

CHAPTER 2

2. **Mold design**: The details of assembling the mold and mold design are shown in Chapter 4. For analysis of newly designed monomer/ polymers, we prepared smaller moulds of 4" X 4" size.

3. **Polymerization assembly for free radical polymerization**: To carry out free radical polymerization, initially purified monomer is filtered through 0.45μ Ultipor N_{66} Nylon 6, 6 membrane (make PALL Life Sciences) to remove any suspended particles. It was further degassed by bubbling nitrogen gas for period of 30 minutes. After that appropriate amount of initiator and plasticizer are added to the monomer containing flask and the contents are homogenized by swirling. This polymerization mixture is then carefully injected into the previously assembled mold through the opening in the Teflon gasket. Care is taken not to trap any air bubbles which hinder the polymerization process. The mold is then sealed by using Teflon stopper and binder in such a way that there is no leakage. The mold is placed into heating assembly. It consists of polymerization bath attached to programmable Julabo temperature controller. The polymerization bath is coated with insulating foam so as to reduce loss of heat. The bath temperature was controlled by external using programmable Julabo water circulator (Julabo, F-25 HP, Germany) with a temperature control accuracy of $\pm$ 0.01 °C. The mold is kept horizontally into the polymerization bath (figure 2.26) and over the mold; sufficient weight is placed as shown in figure 2.26. The polymerization is carried out by using 12 or 24 hour constant rate polymerization temperature-time profile generated for desired monomer (in range of 45-95°C). After completion of the heating, the mold in polymerization vessel is cooled naturally for period of 12-14 hours. The polymerization could also be carried out using a polymer press designed for the

purpose. In this case, the Julabo water circulator was connected to the platens of the press for heating the molds. This arrangement is discussed in Chapter 4.

Figure 2.26: Cast polymerization assembly.

3. **Thickness measurements**: The thickness of the films prepared is measured by using elcometer 456 F Model S DFT electronic gauge (make Great Britain) (figure 2.27), over the entire surface of the films, randomly at 100 different points, for a film of size 10 cm x 10 cm. The instrument is also used to measure change in thickness of detector films while etching studies are performed.

Figure 2.27: Elcometer 456F thickness gauze

2.2.2.4 Preliminary evaluation of polymeric detectors

The techniques and instrumental requirements involved for the preliminary evaluation of the polymeric detectors are given below.

1.   Optical microscope: The particle tracks were counted after chemical etching using a trinocular optical microscope. The microscope (Axiostar, Carl Zeiss, Germany) had optical magnifications of 5x, 10x, 40x and 100x. To capture photographs of charged particles, the optical microscope is fitted with Tucsen

camera and by using IS software one can take still images of the tracks. One can also measure diameter of nuclear tracks by using this software.

Figure 2.28: Zeiss Optical microscope

2. **Exposure assembly**: By using the exposure assembly as shown below in figure 1.14, one can expose the polymer samples of size 1x 1cm^2 to desired source. The films are placed on the stage and the height can be adjusted by using the screw nuts. For lower energy particles, the exposure is performed at required distance from the source. The exposure assembly is as shown in the figure 2.29 below.
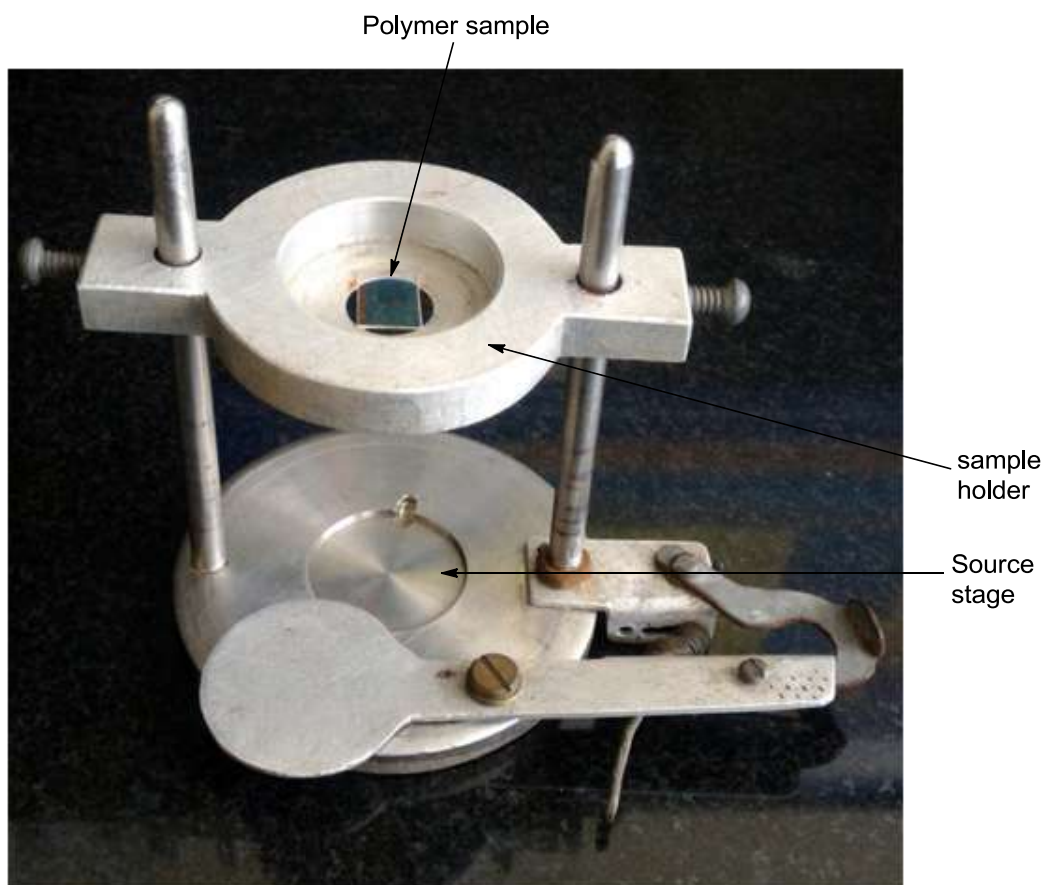
Figure 2.29: Polymeric film exposure assembly.

3. **Etching of the film**: The films exposed to radiation source are etched in glass etching bath as shown in figure 2.30. The bath is provided with a thermometer, hot water jacket, stainless steel stage and a magnetic stirrer. The apparatus is filled with etchant and heated by external circulation of hot water through the jacket. The polymer samples are placed in stainless steel cage. Once the etching temperature is attained the cage is placed into the etchant.

Figure 2.30: Glass assembly for chemical etching of polymeric detector.

4.   Determination of bulk etch rate: The bulk etch rate is the important parameter which is analyzed during the process of chemical etching. The bulk etch rate of the polymer can be determined by following methods

i.   Weight loss method: In weight loss method the weight of the test polymeric film before and after the chemical etching of the film is determined. It is also referred to as gravimetric method which has some limitation due to lack of exact mass measurement. The bulk etch rate is estimated by using formula

$$V_b = (M_2 - M_1) \, T_i \, / \, 2 \, M_1 \, t \qquad\qquad (1)$$

Where, initial mass of polymeric film is given by M_1 and M_2 is the final mass after 't' time interval. Initial thickness of polymeric film is given by T_i.

ii. ***Fission fragment track diameter method***: This is most oftenly used method for determination of bulk etch rate. In this method, the change in fission fragment diameter in the polymeric detector previously exposed to ^{252}Cf source upon etching is measured after certain time intervals. It is determined with the help of an optical microscope, camera and IS capture software. Further, the bulk etch rate of the polymeric detector is calculated by using the formula given below.

$V_b = D_f / 2\ t$ (2)

Where, D_f is the diameter of fission fragment track measured at time t.

iii. ***Change in thickness method:*** In this method, the thickness of the polymeric film is measured using thickness gauze over the entire area before and after chemical etching process. This method can be utilized only for detectors with uniform thickness. But, this method fails due to error caused by swelling of the polymer after chemical etching. So this method is not used at a large extent.

5. ***Counting of particle tracks under optical microscope***: The previously exposed film upon chemical etching are washed using distilled water 3-4 times and dried. The dry films are placed on the glass slide and kept on the microscope stage. The film is viewed through eye piece of optical microscope to observe nuclear tracks formed over the film by focusing and defocusing under the specified magnification (40x, 10x and 5x) and the numbers of tracks per view are counted. In a film of 1x1 cm^2 size, 100- 120 views were counted with the help of X-Y stage. The area under the observed view was determined for the given magnification and the track density (tracks /cm^2) was calculated using formula given below.

$$Track\ density = \frac{Total\ number\ of\ tracks\ counted}{Total\ number\ of\ views\ \times\ Area\ of\ the\ view}$$

6. **Sensitivity study**: To carry out sensitivity study of the polymers that can detect alphas as well as fission fragments, first these films are exposed to ^{252}Cf source at certain distance (3 cm or 5 cm) under high vacuum for 8-10 hours. After exposure these films are etched and change in track diameter is measured after specific etching time interval. In a typical setup, the polymeric films are attached on aluminium support and are exposed to ^{252}Cf source in a vacuum desiccator as shown in figure 2.31. The distance of 5 cm is kept between the source and the polymer. The films were exposed for 10 hrs under 0.5 mbar vacuum from high vacuum pump. Further by noting the diameters of alpha and fission tracks under optical microscope, alpha sensitivity is determined by using equation given below.

$$Alpha\ Sensitivity\ (S) = \frac{\{1 + (D_{\alpha}/D_f)^2\}}{\{1 - (D_{\alpha}/D_f)^2\}}$$

Where Diameter of alpha track is given by D_{α} and diameter of fission fragment track is given by D_f.

Polymeric detector

Vacuum
adaptor

Vacuum desiccator   Source
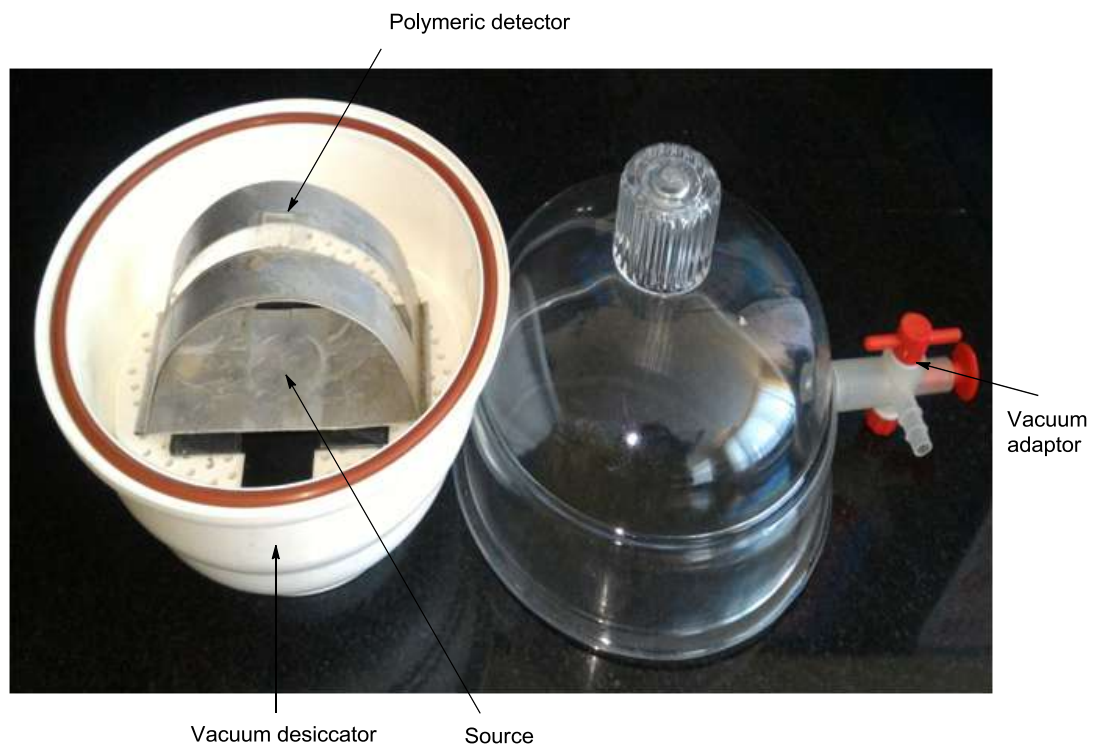
Figure 2.31: Exposure of polymeric film detector to ^{252}Cf source under vacuum for alpha sensitivity study.

As mentioned earlier, the bulk etch rate can be determined from weight change of the film before and after etching process by using equation 1. Also bulk etch rate V_b of the films can be determined from fission diameter by using equation 2.

$$Bulk\ etch\ rate\ V_b = {\{M_f - M_i\}T_i}\Big/{2M_i t} \qquad \text{------1}$$

$$Bulk\ etch\ rate\ V_b = {D_f}\Big/{2t} \qquad \text{------2}$$

Where M_f, is the final weight of the polymeric film after etching for time t. M_i and Ti is the initial weight and thickness of the polymeric film respectively.

2.3 Designing and synthesizing phosphorus containing monomers/polymers for SSNTD applications:

As mentioned previously, the literature survey indicates that the presence of radiation sensitive groups in the monomer increases the alpha sensitivity of a detector. In the commercially available CR-39 detector, the sensitivity is due to the presence of carbonate functionality and ether linkage. Our group have already prepared many polymeric detectors[18-20] consisting of various functional groups and hetero atoms and proved that the sensitivity of the detectors increases. Earlier reports indicated that there is no literature available using phosphorus containing polymer for nuclear track detection studies. Hence, we decided to prepare and analyze monomers/polymers with phosphate, phosphoramide functionalities. Particularly, we have prepared triallyl phosphate TAP (1), 2,2-dimethylpropan-1,3-diyl diallylphosphoramidate (DMPDDP) (2) and Pentaerythrityl bis (diallylphosphoramidate) (PEBDP) (3) monomers. The monomer (1) consists of one phosphate group attached to 3 allylic groups. The presence of three allyl groups should help in cross linking 3D polymeric network and phosphate linkage should

impart the radiation sensitivity property. Similarly in monomers (2) and (3) there are two and four allyl groups respectively that should form a hard polymer and also have phosphamide linkage that should impart the radiation sensitivity. These TAP was prepared by condensation of phosphorus oxychloride and allyl alcohol in presence of base at low temperature. DMPDDP and PEBDP were prepared by reacting diallyl amine with DPPC and SPDPC respectively at lower temperature. DPPC and SPDPC in turn, were prepared by refluxing neopentyl glycol and pentaerythritol respectively with phosphorus oxychloride. Further the prepared monomers were tested for their stability with initiators at elevated temperature.

It has been observed that vacuum distillation of the monomers gives pure and good quality polymeric films. Stability of the monomers to high temperature defines the type of conditions to be used for purification. These monomers have high boiling points and could not be purified by normal distillation. They sometimes get self polymerized or decompose upon heating even when subjected to vacuum distillation. So, techniques like flash chromatography or normal silica-gel column chromatography could be utilized for their purification. As no problems other than polymerization were observed, thermal studies using DSC or TG-DTA techniques were not carried out. Here, we have also considered the stability of other monomers that will be further used for copolymerization process. Table 2.1 depicts the stability purification techniques utilized for the prepared monomers.

Table 2.1: Stability of the monomers and their purification techniques

Monomer	Stability	Purification technique
TAP	Not stable under normal distillation	Vacuum distillation at 100 °C and 0.5 mbar pressure
DMPDDP	Not stable under normal	Column chromatography using 30%

	distillation	Ethyl acetate in petroleum ether
PEBDP	Solid compound, melting point 142 ^{o}C	Column chromatography using 3:7 mixture of Ethyl acetate-n-Hexanes 0.1-0.2mbar at 150-160 °C
ADC	Not stable at normal distillation condition	
PETAC	Polymerizes during vacuum distillation	Column chromatography using 8:2 mixture of n-Hexanes-ethyl acetate
NADAC	Polymerizes during vacuum distillation	Silica gel column chromatography using 3:7 ethyl acetate and n-hexane
NAAAC	Polymerizes during vacuum distillation	Column chromatography 30% ethyl acetate in petroleum ether

2.3.1   Cast polymerization of monomers to obtain test polymers:

The polymerization of monomers prepared is normally carried out using initiators like benzoyl peroxide (BP) or isopropyl peroxydicarbonate (IPP). BP is commercially available and used after recrystalization using ethanol and chloroform solvent mixture. Polymers prepared using BP requires higher curing temperature during polymerization. Polymers prepared using BP is less sensitive and decrease in sensitivity is due to loss of particle energy to ring vibration of benzene rings. Therefore, IPP is preferred for polymerization while casting detector films. It has lower decomposition temperature that allows initiation of the polymerization at lower temperature. Monomers having phosphate moieties are stable and can be polymerized using both IPP and BP initiators. The monomers containing phosphoramide groups are found to react on heating with IPP as well as BP initiators at higher temperature. The monomers form dark brown liquid upon heating with the initiators for longer period of time. The mixture of ADC and PEBDP with initiator decomposes to give brownish black coloured liquid upon heating at higher temperature. Table 2.2 gives the observations regarding gelation of the monomers.

Table 2.2: Stability studies for monomers in presence of initiators.

Monomer (w/w)	% IPP initiator	Temperature °C	Observation
TAP	4	50	Gelation in 2 hours, colourless hard polymer in 8 hours
DMPDDP	4	55	No gel formation up to 8 hours
TAP:ADC (1:1)	4	55	Yellow gel in 4 hours, light brown polymer in 12 hours
DMPDDP:ADC (1:1)	4	60	No gel formation even after 12 hours, dark brown liquid
PEBDP:ADC (1:1)	4	60	No gel formation even after 12 hours, dark brown liquid

From above Table it is clear that out of the three monomers prepared, only TAP can be cast polymerized. Rest two having phosphoramide linkage could not be polymerized using IPP/BP.

Cast polymerization of the monomers to prepare test polymers was done using suitable amount of initiator, following 12 hours constant rate polymerization profile developed for ADC[26]. The test polymerization is carried out so as to know whether it is suitable for track detection or not. It is also copolymerized with ADC, PETAC, NADAC and NAAAC monomers. The curing condition and amount of initiator used for test polymers is given in Table 2.3.

Table 2.3: Curing conditions used for polymerization of different test polymers.

Monomer (w/w)	Initiator used (wt. %)	Heating profile (Temperature range)
TAP	IPP (3.3)	ADC polymerization profile (45-95 °C)
TAP:ADC(1:1)	IPP (3.3)	ADC polymerization profile (45-95 °C)

TAP:PETAC (1:1)	IPP (4.0)	ADC polymerization profile (45-95 °C)
TAP:NADAC(1:1)	IPP (4.0)	ADC polymerization profile (45-95 °C)
TAP:NAAAC (1:1)	IPP (4.0)	ADC polymerization profile (45-95 °C)

All the polymeric films prepared were hard enough and transparent. Other physical properties of the test polymers are recorded in Table 2.4 below.

2.3.2 Initial Track detection and sensitivity studies of test polymers:

The test polymeric films were cut into pieces of size 1 cm x 1 cm and were exposed to ^{239}Pu alpha source and to a ^{252}Cf source for fission fragments. All the exposed films were etched in 7N NaOH at 70 ^{o}C. Copolymers of TAP with ADC, PETAC and NADAC showed charged particle tracks. However, hardly any tracks are shown by the homopolymer PTAP. The bond energy data indicates that the P-O bond is stronger than C-O or N-O bonds but the P=O bond is relatively weaker than C=O. Also it is known that the thermal and hydrolytic stability of P=O is more as compared to P=S and P=Se bonds[27]. Oxygen is more electronegative than phosphorus and the stability of P=O bond may be expected to depend upon the other substituents attached to phosphorus atom. In case of triallyl phosphate, due to presence of three electronegative oxygen atoms attached to the phosphorus, the P=O bond is expected to be shorter which results in its increased bond strength. Although, the bond energy of P=O bond is lesser than that of C=O bond, P=O bond in homopolymer PTAP may be expected to be strong enough to resist the alkaline hydrolysis during chemical etching which is well supported by its lower bulk etch rates (about 0.008 µ/hr) compared to that of PADC (0.016 µ/hr). It is also possible that lone pairs on oxygen of the phosphate group are held relatively strongly, so that ejection of these electrons (i.e. delta rays which cleave surrounding bonds thereby

forming tracks) is probably not sufficient resulting into formation of very less number of tracks when compared with PADC which has a carbonate link. We have noted that PTAP exposed to ^{239}Pu alpha particles at a distance of three centimetres from source hardly shows any alpha tracks when compared with PADC detector. Poly (TAP-*co*-NAAAC) after etching for 60 minutes became hazy white. This may be due to the presence of NH linkages in the polymer matrix. Even if the charged particle produces tracks in such cases, they will be deep inside the polymer. However, very slow etching rates will not permit development/observation of such tracks and the etching time required in such cases will be very high and practically not acceptable.

Table 2.4: Physical and track detection properties of the polymers

Polymer composition (w/w)	Avg. Thickness (μm)	Color and hardness before etching	Type of tracks revealed after chemical etching
TAP	580±10	Colorless hard film	No tracks seen
TAP:ADC(1:1)	600±10	Colorless hard film	Alpha and fission
TAP:PETAC (1:1)	578±10	Hard pale yellow film	Alpha and fission
TAP:NADAC(1:1)	615±10	Light brown hard film	Alpha and fission
TAP:NAAAC (1:1)	622±10	Hard brownish film	hazy white film

The post etch surface of the polymeric films and track revelation time in 6N NaOH at 70 $^{\rm o}$C was also determined and given below in Table 2.5. Initially, from the results obtained it is clear that, monomers containing phosphate-carbonate linkages reveal tracks after 2 hours of chemical etching. However, copolymers with higher concentration of triallyl phosphate cracked upon etching for longer period of time. Homopolymer PTAP also cracked soon after etching for 1 hour due to which tracks

could not be observed in it. Copolymers of TAP with PETAC as well as NADAC can develop tracks in 2 to3 hours and post etched surface was clear. Alpha sensitivity of copolymers poly (TAP-*co*-PETAC; 1:1 w/w) and poly (TAP-*co*-NADAC; 1:1 w/w) was found out to be low as compared to that with poly (TAP-*co*-ADC; 1:1 w/w). This may be due to higher cross linking network occurring in copolymers of monomers having hexafunctionality and octafunctionality. Due to which it becomes hard and strong enough. Poly (TAP-*co*-NAAAC) became opaque white upon etching.

Table 2.5: Track recording properties and post etched surface study of different test polymers of TAP.

Sr. No.	Composition of polymer (w/w)	*Time for track revelation in minutes in 6N NaOH at 70 °C		Alpha sensitivity	Post etched surface of polymers
		Alpha track	Fission fragment		
1	TAP homopolymer	-	-	-	Cracks developed
2	TAP-ADC (2:8)	140	120	1.25	Clear
3	TAP-ADC (3:7)	120	100	1.61	Clear
3	TAP-ADC (4:6)	120	100	1.40	Clear
4	TAP-ADC (1:1)	140	120	1.59	Clear
5	TAP-PETAC (1:1)	180	100	1.31	Clear
6	TAP-NADAC (1:1)	160	90	1.33	Clear
7	TAP-NAAAC (1:1)	Tracks could not be seen			Hazy white
8	PADC	120	90	1.28	Clear
9	CR-39	120	90	1.22	Clear

*Exposure: [239]Pu at 2 mm for 2 minute and [252]Cf at 2mm for 2 h; Etching condition: 6N NaOH at 70 °C

From the initial study regarding alpha sensitivity, it may be noted that some of the copolymers have higher sensitivity than that of the commercially available

CR-39 polymer. The sensitivity of the polymeric detectors can be enhanced by optimizing polymerization and etching conditions. The ratio of monomer mixture or monomer concentration also needs to be optimized first. The initiator concentration should be optimized to enhance the sensitivity property of polymers. First and foremost, the polymerization condition is optimized by performing the kinetics study of the polymerization.

2.3.3 Polymerization Kinetics of TAP monomer using IPP initiator:

Different amount of % IPP initiator (w/w) was mixed with TAP monomer and the mixture was flushed with dry nitrogen gas. The mixture was taken in test tubes and the time required for gel formation was noted at the specified temperature. The results are given in the Table 2.6 below. The gel formation for a hexafunctional monomer occurs at approximately 75% unsaturation. It was decided to study the kinetics of polymerization at 35, 45 and 55 °C.

Table 2.6: Time required for the gelation of TAP using different %IPP concentration at different temperature.

IPP concentration (% by weight)	Temperature °C	Time (h)	Remark
0.5	40	10	Mobile gel
	50	9	Immobile gel
	60	2	Immobile gel
1.5	40	10	Immobile gel
	50	3	Immobile gel
	60	1	Immobile gel
3.0	35	8	Mobile gel
	40	5	Immobile gel
	45	4	Immobile gel
	50	1.5	Immobile gel

	55	1	Immobile gel
	60	1	Immobile gel

Further, TAP monomer was mixed with 3.0% IPP initiator and was taken in a set of test tubes. The mixture was flushed with nitrogen and test tubes sealed with rubber stopper. The test tubes were placed in a constant temperature thermostat and were heated at a constant temperature. A test tube was removed after particular time interval and analyzed for its percentage unsaturation and initiator concentration with respect to time. The results of such analysis at three different temperatures are reported. The data for the temperature sets 35, 45, and 55 ^{o}C are given below in Table 2.7, 2.8, and 2.9 respectively.

Table 2.7: Peroxide and unsaturation contents for different time interval at 35 ^{o}C

Sr. No.	Time (h)	Unsaturation (%)	Peroxide (%)
1	0	100.00	3.13
2	1	97.83	3.06
3	2	94.95	3.04
4	3	91.39	2.87
5	4	87.47	2.84
6	5	85.63	2.82
7	6	84.37	2.73
8	7	83.45	2.77
9	8	80.05	2.68
10	9	79.76	2.66

Table 2.8: Peroxide and unsaturation contents for different time interval at 45 ^{o}C

Sr. No.	Time (h)	Unsaturation (%)	Peroxide (%)
1	0	100.00	3.10
2	0.5	98.08	3.02

3	1	95.12	2.95
4	1.5	92.69	2.88
5	2	89.70	2.87
6	2.5	86.08	2.80
7	3	83.29	2.70
8	3.5	82.17	2.62
9	4	80.72	2.66
10	4.5	78.34	2.54

Table 2.9: Peroxide and unsaturation contents for different time interval at 55 ^{o}C

Sr. No.	Time (h)	Unsaturation (%)	Peroxide (%)
1	0.00	100.00	3.14
2	0.10	97.14	2.97
3	0.20	94.21	2.82
4	0.30	91.81	2.86
5	0.40	89.04	2.74
6	0.50	87.93	2.75
7	0.60	85.87	2.69
8	0.70	84.22	2.68
9	0.80	82.85	2.67
10	0.90	80.41	2.51

The graphical representation of the results obtained in kinetic study is shown below in figure 2.32
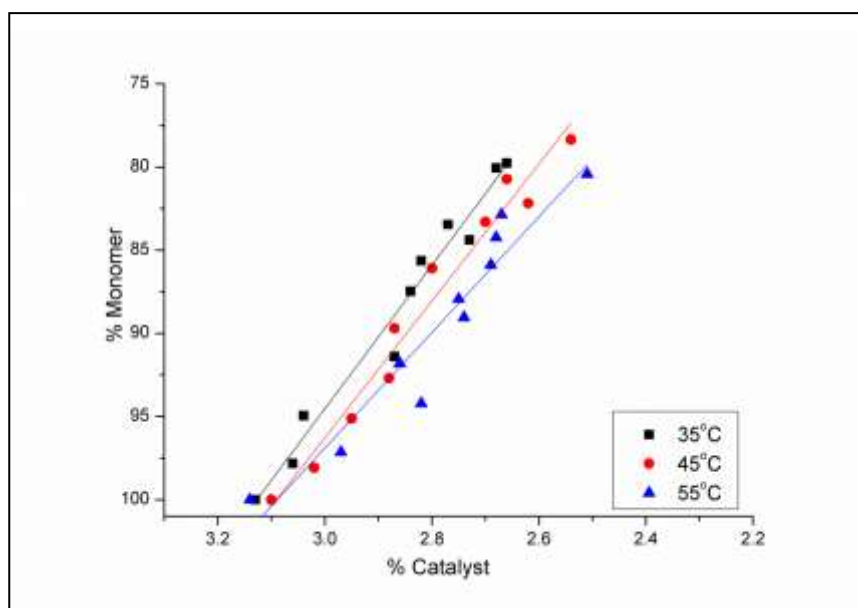
Figure 2.32: Graphical representation of the amount of initiator and unsaturation at 35, 45 and 55 °C in %monomer conversion for TAP.

The slopes obtained for three lines were

At 35 $^{\circ}$C, K_1= 43.12

45 $^{\circ}$C, K_1= 41.17

55 $^{\circ}$C, K_1= 34.80

The values obtained are in decreasing order and are above the limiting values for the slope. These values were then used to obtain the kinetic constants E_1, Z_1, E_3, and Z_3. The values are given below in Table 2.10.

Table 2.10: Values obtained for the constants given in the Dials equation.

Sr. No.	Constant	Value
1	R	1.986
2	E_1	-2135
3	E_3	22459
4	Z_1	0.133 E+1
5	Z_3	1.43 E+14

By using a FORTRAN program, Dial's equations were solved and a temperature time polymerization profile was calculated[26]. The profile obtained from the program was for 12 hours. 12 and 24 hour constant rate polymerization profile using IPP initiator is shown in figure 2.33.
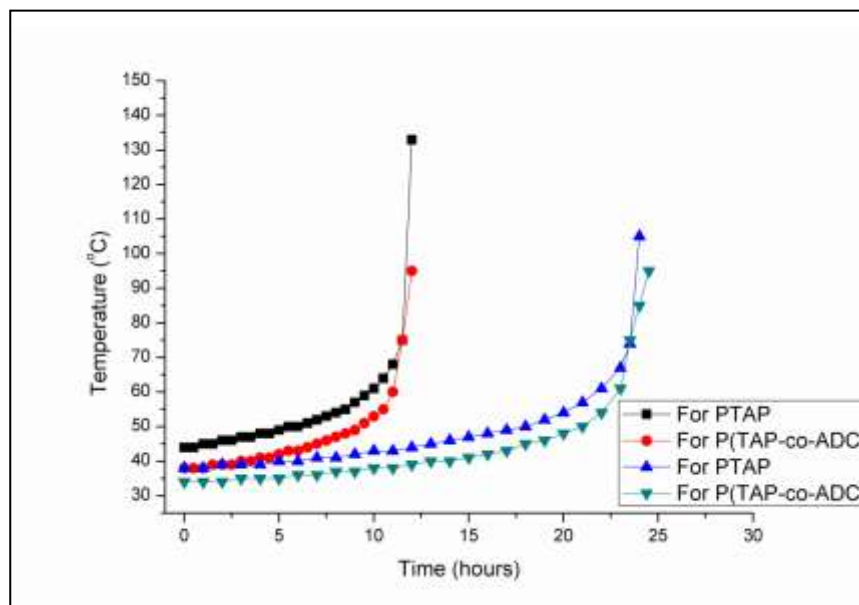
Figure 2.33: Constant rate polymerization profile for TAP and poly (TAP-*co*-ADC; 3:7 w/w) using 3.3% IPP.

To check the effectiveness of generated polymerization profile; the correlation study was also performed and found to be in good agreement with calculated polymerization profile for homopolymer. In correlation study, to see the efficacy of both 12 and 24 hour polymerization profile 12/ 24 test tubes were filled with monomer mixture and heated in programmable Julabo water bath. The constant rate polymerization profile developed for homopolymer PTAP was fed into the Julabo software and heating was started as per the profile. A test tube was removed after every hour and unsaturation analysis was carried out. The results obtained are given in the figure 2.34 below.
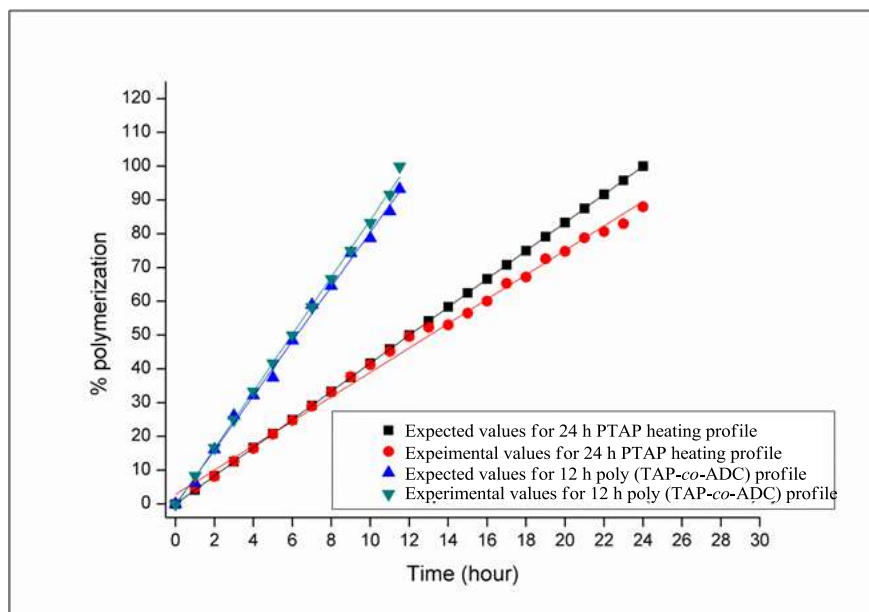
Figure 2.34: Verification of 24 hour polymerization profile for PTAP and 12 hour polymerization profile for Poly (TAP-*co*-ADC).

Figure 2.35: Verification of 12 hour polymerization profile for PTAP.

The correlation coefficient for 24 hour PTAP constant rate polymerization profile was found out to be 0.9980 but it may note that for the first 12 hours, the linear correlation coefficient was 0.9998. When correlation studies were carried out for 12 hour constant rate polymerization profile for PTAP (Figure 2.35), linear

correlation coefficient was 0.9931. As polymerization proceeds, more and more three dimensionally cross-linked polymer is formed which is increasingly insoluble in the solvent used for W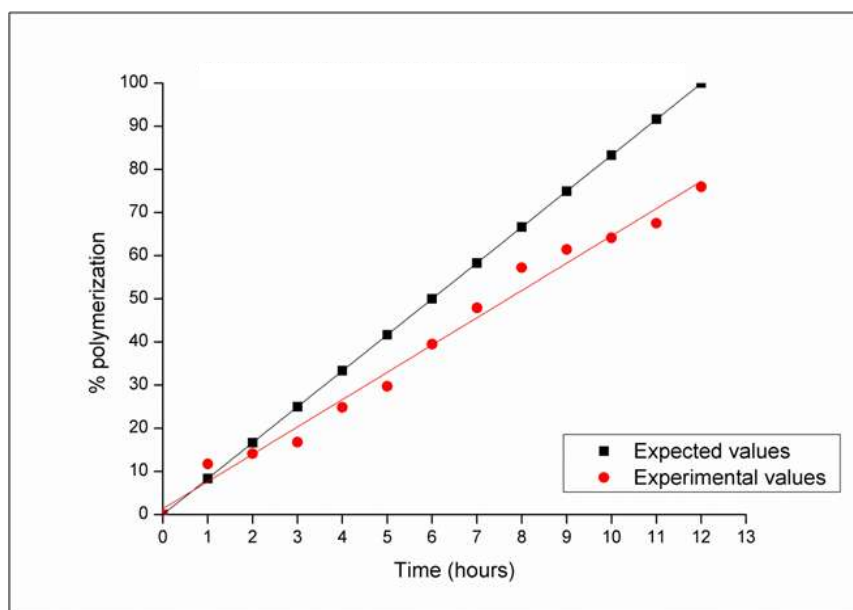ij method. This might result in lesser estimation of non-polymerized C=C bonds which might remain trapped in the rigid polymer structure.

2.3.4 Polymerization Kinetics of TAP:ADC (3:7 w/w) copolymer using IPP initiator:

The copolymer of ADC with TAP was found have higher alpha sensitivity than CR-39 detector. So the kinetics of polymerization using IPP initiator of the monomer mixture was carried out. In a TAP:ADC (3:7 w/w) monomer mixture 3.3% IPP initiator (w/w) was added and the mixture was flushed with dry nitrogen gas. The mixture was taken in test tubes and the time required for gel formation was noted at the specified temperature. The results are given in the Table 2.11 below. It was decided to study the kinetics of polymerization at 35, 45 and 55 °C. Time required for gel formation is given below.

Table 2.11: Time for gelation of 3:7 w/w TAP:ADC monomer mixture at specified temperatures.

Temperature	Time for gelation in hours	observation
35	11	mobile gel
45	3.45	immobile gel formed
55	1	immobile gel formed

At a temperature of 35, 45 and 55 $^{\circ}$C, the mixture of TAP:ADC (3:7 w/w) and 3.3% IPP mixture was heated. All test tubes were analyzed for initiator concentration as well as for unsaturation content. The results obtained at three different set of temperatures are given in Tables 2.12, 2.13 and 2.14 below

Table 2.12: Peroxide and unsaturation contents for different time interval at 35 $^{\circ}$C

Sr. No.	Time (h)	Unsaturation (%)	Peroxide (%)
1	0	100	3.31
2	1	96.79	3.23
3	2	92.73	3.1
4	3	89.53	3.07
5	4	86.39	3.01
6	5	81.19	2.95
7	6	77.53	2.91
8	7	75.38	2.86
9	8	73.18	2.72
10	9	70.29	2.63
11	10	68.39	2.42

Table 2.13: Peroxide and unsaturation contents for different time interval at 45 $^{\circ}$C

Sr. No.	Time (h)	Unsaturation (%)	Peroxide (%)
1	0	100.00	3.35
2	0.33	90.10	3.11
3	0.67	85.53	3.03
4	1	81.53	2.91
5	1.34	79.24	2.78
6	1.68	75.49	2.65
7	2.02	68.74	2.54
8	2.35	66.62	2.48
9	2.69	64.29	2.40
10	3.03	61.48	2.33
11	3.36	59.08	2.22

Table 2.14: Peroxide and unsaturation contents for different time interval at 55 $^{\circ}$C

Sr. No.	Time (h)	Unsaturation (%)	Peroxide (%)

1	0.00	100.00	3.34
2	0.10	87.56	2.89
3	0.20	81.35	2.64
4	0.30	72.37	2.28
5	0.40	65.16	2.14
6	0.50	61.88	2.06
7	0.60	54.57	1.89
8	0.70	50.74	1.82
9	0.80	46.52	1.72
10	0.90	45.52	1.66
11	1.00	45.35	1.57

The gelation of the monomer mixture occurs at 65% residual unsaturation.

The results obtained are represented in graphical manner in figure 2.36 below.
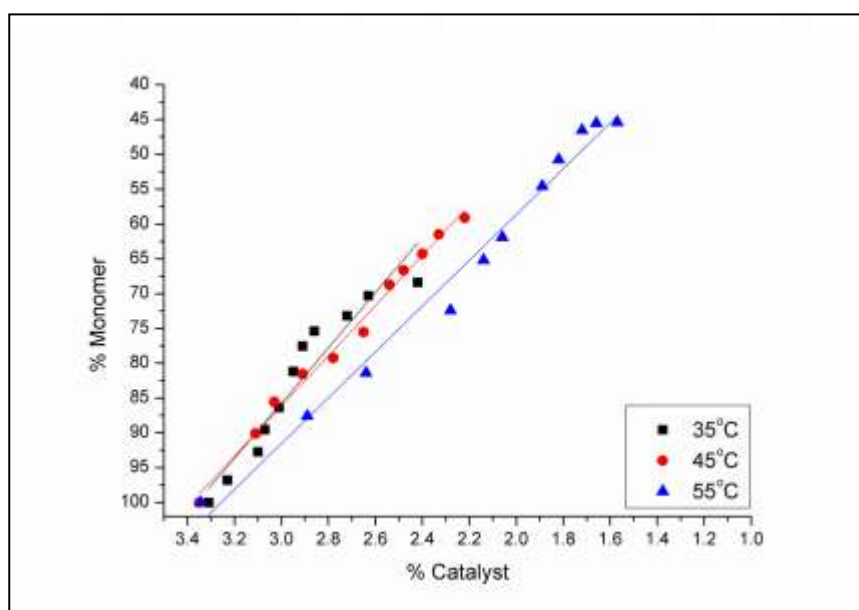

Figure2.36: Decomposition of IPP initiator in (TAP+ADC) monomer at 35, 45 and 55 °C.

The slopes (K_1) obtained for above figure 2.36 are given below:

K_1 = 39.71 at 35 °C

= 36.04 at 45 °C

= 32.92 at 55 °C

The values obtained are in decreasing order and are above the limiting values for the slope. These values were then used to obtain the kinetic constants E_1, Z_1, E_3, and Z_3. The values are given below in Table 2.15.

Table 2.15: Values obtained for the constants given in the Dials equation.

Sr. No.	Constant	Value
1	R	1.986
2	E_1	-1877.31 cal
3	Z_1	1.83
4	E_3	33238.31 cal
5	Z_3	1.16×10^{22}

By solving Dial's equations, a heating profile was calculated. The heating profile for copolymerization was calculated for 11 hours and the curve was smoothly extrapolated to obtain a 12 hour heating profile for TAP-ADC monomer mixture using IPP initiator as shown in figure 2.33. Also 24 hour heating profile for same mixture was generated. Both 12 and 24 hour constant rate polymerization profile for poly (TAP-*co*-ADC) are shown in figure 2.33.

The constant rate polymerization profile for poly (TAP-*co*-ADC) was also verified for its effectiveness. It is graphically represented in figure 2.34. The constant rate polymerization profile for poly (TAP-*co*-ADC), is supported well by the linear correlation coefficient (R^2) of 0.9989. This clearly indicates that the polymerization profile generated by us for copolymer is in good agreement with the kinetic model as proposed by Dial and co-workers and can be used for cast polymerization process.

2.3.5 Polymerization Kinetics of TAP:ADC (3:7 w/w) copolymer using BP initiator:

Kinetic study of TAP-ADC mixture using benzoyl peroxide (BP) initiator at 55, 65 and 75 ^{o}C was also carried out in similar fashion to generate 12 hour constant rate polymerization profile shown in figure 2.23. The time required for gel formation using 3.3% BP at different specified temperature was determined. The results are given in Table 2.16.

Table 2.16: Time for gelation of 3:7 w/w TAP: ADC monomer mixture at specified temperatures using BP.

Temperature ^{o}C	Time for gelation in hours	observation
55	8	immobile gel
65	3	immobile gel formed
75	1.5	immobile gel formed

Further, the kinetics was studied at 55, 65 and 75 ^{o}C temperature. The above monomer mixture was heated in a set of test tubes at particular temperature. All test tubes were analyzed for initiator concentration as well as for unsaturation content. The results obtained at three set of temperatures are given in Table 2.17, 2.18 and 2.19.

Table 2.17: Peroxide and unsaturation contents for different time interval at 55 ^{o}C

Sr. No.	Time (h)	Unsaturation (%)	Peroxide (%)
1	0	100.00	3.30
2	1	96.43	3.22
3	2	91.23	3.11
4	3	85.22	2.96
5	4	79.01	2.83
6	5	74.21	2.68
7	6	70.43	2.61
8	7	68.54	2.56
9	8	65.87	2.51

Table 2.18: Peroxide and unsaturation contents for different time interval at 65 $^{\circ}$C

Sr. No.	Time (h)	Unsaturation (%)	Peroxide (%)
1	0	100.00	3.35
2	0.37	97.64	3.32
3	0.73	94.33	3.28
4	1.10	91.05	3.19
5	1.47	85.71	3.01
6	1.83	82.50	2.96
7	2.20	81.34	2.86
8	2.57	80.73	2.81
9	2.93	75.72	2.60

Table 2.19: Peroxide and unsaturation contents for different time interval at 75 $^{\circ}$C

Sr. No.	Time (h)	Unsaturation (%)	Peroxide (%)
1	0.00	100.00	3.33
2	0.25	92.35	3.25
3	0.5	89.11	3.17
4	0.75	83.21	2.94
5	1	78.34	2.72
6	1.25	72.42	2.64
7	1.5	70.02	2.55
8	1.75	69.21	2.48
9	2	65.61	2.22

The gelation of the monomer mixture occurs at 79% residual unsaturation.

The results obtained are represented in graphical manner in figure 2.37 below.
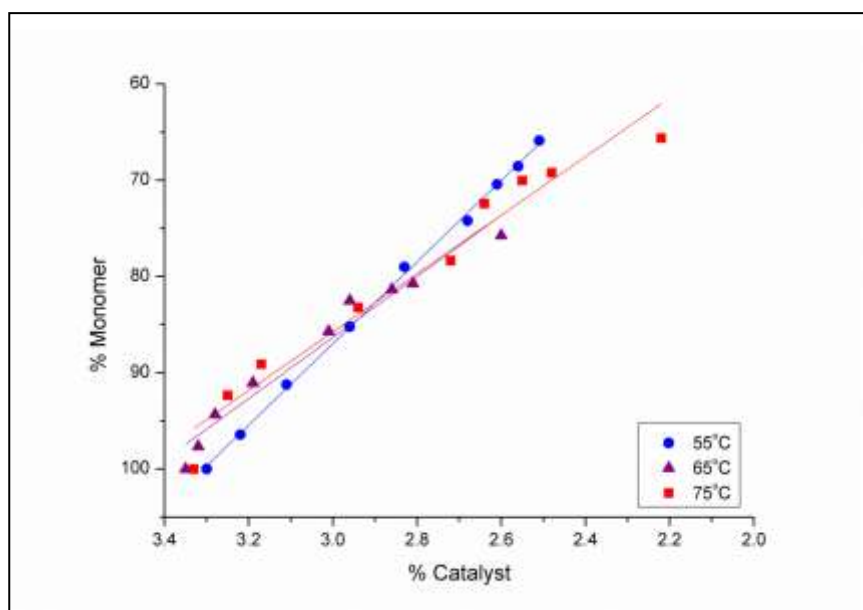
Figure 2.37: Decomposition of BP initiator in (TAP+ADC) monomer at 55, 65 and 75 °C.

The slopes (K_1) obtained for above figure 2.37 are given below:

K_1 = 42.40 at 55 °C

= 31.78 at 65 °C

= 30.39 at 75 °C

The values obtained are in declining order and are above the limiting values for the slope. These values were then utilized to obtain the kinetic constants E_1, Z_1, E_3, and Z_3. The values are given below in Table 2.20.

Table 2.20: Values obtained for the constants given in the Dials equation for TAP-ADC.

Sr. No.	Constant	Value
1	R	1.986
2	E_1	-3796 cal
3	Z_1	1.19×10^{-1}
4	E_3	17489 cal

| 5 | Z_3 | 1.37×10^{10} |

The constants E_1, E_3, Z_1 and Z_3 involved in Dial equation are given in Table 2.20 above. Dial in his work has already pointed out that the roots of kinetic equation become imaginary at the end of profile and hence it is sometimes not possible to calculate the values of polymerization temperature. This was also observed by us in this case. Hence, polymerization was continued at constant temperature of 100 °C after eight hours to complete twelve hour heating profile as seen from figure 2.38. The constant rate polymerization profile for poly (TAP-*co*-ADC) using BP initiator was also verified for its effectiveness. It is graphically represented in figure 2.39. It is supported well by the linear correlation coefficient (R^2) of 0.9897. This clearly indicates that the polymerization profile generated by us for copolymer using BP initiator is in good agreement with the kinetic model as proposed by Dial and co-workers and can be used for cast polymerization process.

Although, we have studied the kinetics of TAP-ADC co-polymerization using BP, we recommend the use of IPP for polymerization as it leads to good quality detector films. Also the background tracks like features are lesser in case of films prepared by using IPP as compared to that by using BP.
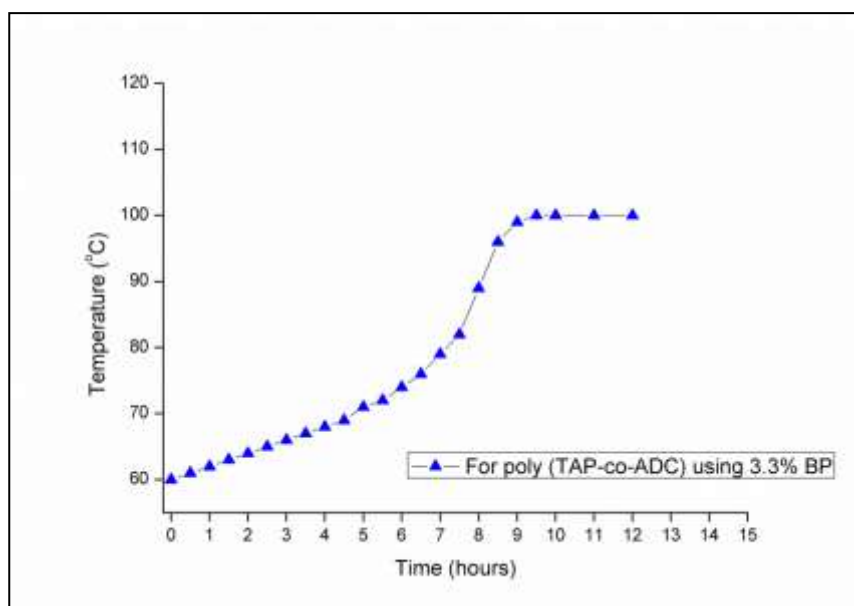
Figure 2.38: Constant rate polymerization profile for poly (TAP-*co*-ADC; 3:7 w/w) using 3.3% Benzoyl peroxide initiator
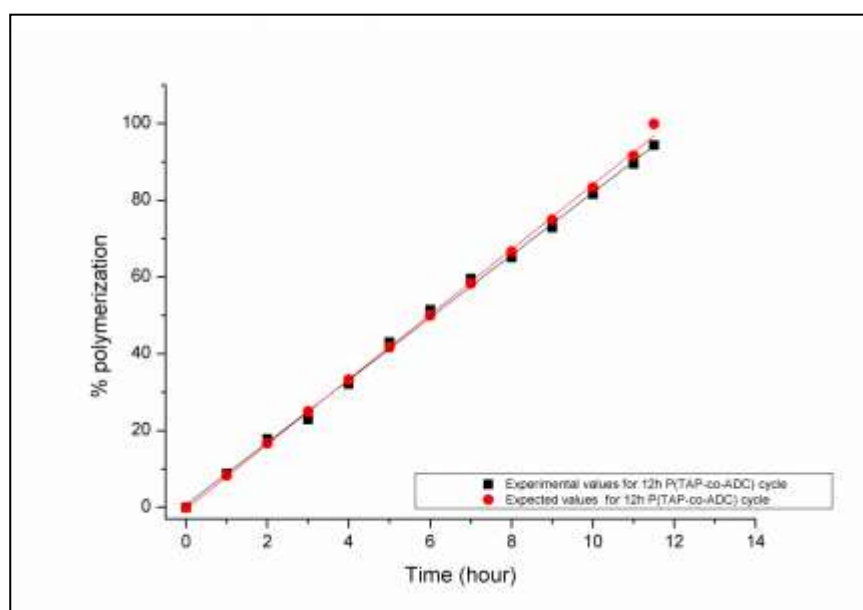

Figure 2.39: Verification of 12 hour polymerization profile for Poly (TAP-*co*-ADC) profile using 3.3% BP initiator.

Further, by using constant rate polymerization profile developed for both homopolymer and copolymer of TAP and ADC, optimization of monomer / catalyst concentration and etching condition was carried out.

2.3.6   Optimization of monomer concentration (TAP-ADC ratio):

The monomer prepared is first homopolymerized to find out its track detection properties. The various copolymers of ADC with TAP were prepared and their track detection properties were studied. TAP-ADC constant rate polymerization profile derived using 3.3% IPP was utilized for preparation of copolymers i.e. 1:9, 2:8, 3:7, 4:6 and 1:1 w/w monomer ratio. The polymers having higher ADC concentration (i.e. 6:4- 9:1 w/w ratio of TAP-ADC) were also prepared. The polymers were tested for the amount of unsaturation left after complete polymerization. Table 2.21 gives the physical properties of the various polymers prepared from TAP and ADC. All the copolymers prepared were light brown in color and could detect alpha and fission tracks.

Table 2.21: Physical properties of TAP homopolymer and copolymers with ADC

Sr. No.	Polymer composition TAP:ADC (w/w)	Thickness of Film (μm)	Residual Unsaturation (%)	% Polymerization
1	1:9	523.5	11.75	88.25
2	2:8	522.9	6.90	93.10
3	3:7	461.6	7.77	92.23
4	4:6	516.1	14.2	85.80
5	1:1	579.3	14.3	85.70
6	6:4	482.9	18.09	81.91
7	7:3	550.5	11.15	88.85
8	8:2	617.4	7.99	92.01
9	9:1	511.8	5.16	94.84
10	PTAP	580.9	4.7	95.30
11	PADC	450	5.02	94.98

Further, each of the films were cut into small piece of 1 x 1 cm^2 sizes and exposed to fission fragments from ^{252}Cf source and alpha particles from ^{239}Pu source

in close 0.2 cm distance. These films were etched in 7N NaOH at 70 $^{\circ}$C and compared with PADC/CR-39 detectors exposed under identical conditions. Homopolymer could not reveal any tracks even after etching for 180 minutes using identical etching condition. The time required for track revelation is given in Table 2.22 below.

Table 2.22: Time required to reveal alpha and fission fragment tracks in TAP-ADC polymers.

Sr.no	Composition of polymer TAP:ADC (w/w)	Alpha track development time (min)	Fission fragment track development time (min)
1	TAP	-	-
2	1:9	140	120
3	2:8	140	120
4	**3:7**	**120**	**100**
5	4:6	120	100
6	1:1	140	120
7	6:4	140	120
8	7:3	150	120
9	8:2	150	120
10	9:1	150	120
11	PADC	120	60
12	CR-39	120	60

From the track revelation studies it can be seen that the time required to reveal alpha tracks is more in polymers with higher concentration of TAP and for 3:7 (w/w) ratio of TAP: ADC, it is almost same as that of CR-39. Fission tracks in poly (TAP-*co*-ADC; 3:7 w/w) film were also revealed comparatively faster as compared to all other copolymers.

The sensitivity of the films were measured based on variation of alpha and fission track diameters and is given in Table 2.23.

Table 2.23: Sensitivity values and the post etch rate of different copolymers.

Sr. No.	Composition of polymer (w/w)	Alpha sensitivity	Remark
1	TAP	-	Cracks developed
2	TAP-ADC (1:9)	1.3	Hard, clear
3	TAP-ADC (2:8)	1.25	Hard, transparent
4	TAP-ADC (3:7)	1.68	Clear
5	TAP-ADC (4:6)	1.4	Clear
6	TAP-ADC (1:1)	1.59	Hard, light brown
7	TAP-ADC (6:4)	1.28	Clear
8	TAP-ADC (7:3)	1.25	brittle, few cracks developed
9	TAP-ADC (8:2)	1.21	Hard and brittle film
10	TAP-ADC (9:1)	1.12	brittle, few cracks developed
14	PADC	1.28	Clear
15	CR-39	1.22	Clear

From the data obtained it is clear that the alpha sensitivity of TAP-ADC copolymers with ratio 3:7, 4:6 and 1:1 is more as compared to commercially available CR-39 detectors. The sensitivity decreased with increase in concentration of TAP in the copolymers. Homopolymer PTAP could not reveal any tracks.

2.3.7 Optimization of initiator concentration:

Type of initiator and initiator concentration plays a very important role in casting polymeric films. The bulk property varies with type and concentration of initiator used. For nuclear track detection polymers preparation it becomes crucial to choose a initiator and its concentration as it directly affects the sensitivity and track

detection properties of detectors prepared. So to determine the optimum initiator concentration in a particular track detector, a series of polymer films with varying initiator concentration and optimized monomer concentration (ADC: TAP; 3:7 w/w) are prepared and subjected to alpha sensitivity analysis.

Alpha sensitivity becomes maximum for particular concentration of initiator which is considered as optimum initiator concentration. Alpha sensitivity of the polymers prepared was determined by track diameter method.

Optimization of initiator concentration for TAP: ADC 3:7 w/w copolymer: The optimization of monomer concentration studies revealed that the TAP: ADC; 3:7 w/w copolymer has a maximum sensitivity in the series of copolymers prepared of TAP and ADC. The cast polymerization of the monomer mixture (TAP:ADC; 3:7 w/w) with IPP initiator concentration of 2, 3, 3.3, 4, 5 and 6% w/w was carried out using 0.1% DOP plasticizer in all films. The physical properties of all the polymers prepared are given in Table 2.24.

Table 2.24: Physical properties of TAP: ADC 3:7w/w copolymers prepared using different IPP initiator concentration.

Sr. No.	IPP concentration wt. %	Thickness (μ)	Hardness
1	2	550	hard polymer
2	3	545	hard
3	3.3	483	hard
4	4	601	hard
5	5	560	Hard/brittle
6	6	554	Hard/brittle

The polymers prepared using 2-6% initiator concentrations are hard and are appropriate as track detectors. The polymers with 5 and 6% initiator are hard and brittle. Alpha sensitivity measurement studies were performed on all the copolymers.
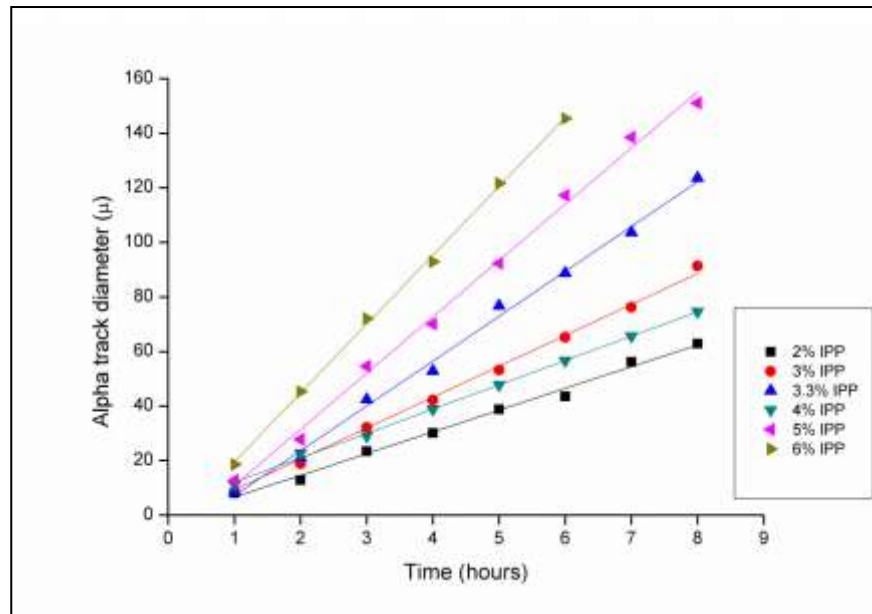

Figure 2.40: Variation of alpha track diameter in Poly (TAP-*co*-ADC) copolymers prepared using different initiator concentration
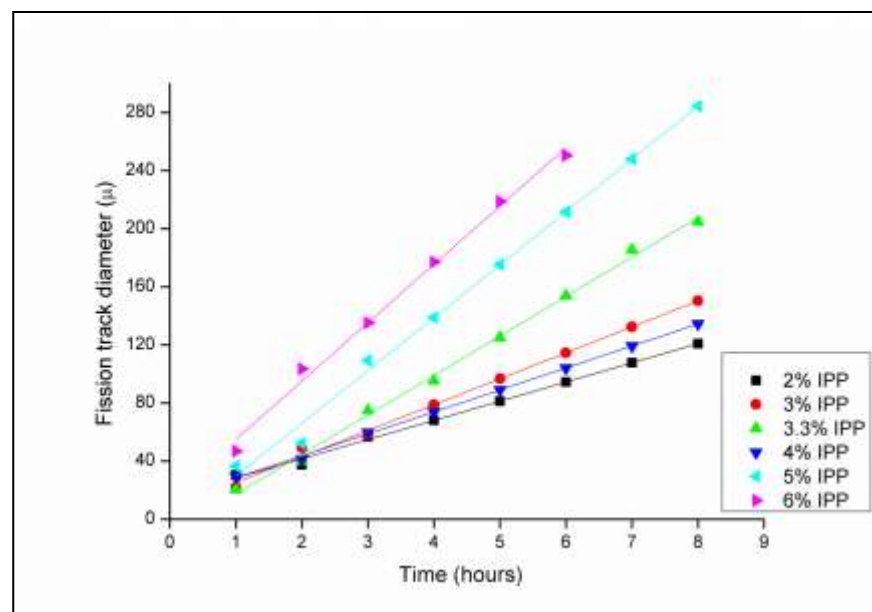

Figure 2.41: Variation of fission track diameter in Poly (TAP-*co*-ADC) copolymers prepared using different initiator concentration

The variation of alpha and fission track diameters in the polymers is depicted in the figures 2.40 and figure 2.41 respectively. It is clearly seen from the figures that there is linear increase in alpha as well as fission track diameter with etching time indicating uniformity in polymer structure. Post etched surface of all the films were clear till 5 hours of etching under 7N NaOH at 70 ^{o}C temperature. Detector films did not become soft throughout the etching process. The alpha sensitivity of the polymer films was found out by using the track diameters. The variation of alpha sensitivity in different polymers prepared using different initiator is shown in figure 2.42. Also the variation in bulk etch rates in these polymers is summarized in figure 2.43. It can be seen from figure 2.42, for the films prepared from 2, 5 and 6% IPP concentration bulk etch rate is almost constant and very low. Bulk etch rate of polymer with 4% IPP concentration is bit higher and that of polymer film prepared with 3.3% IPP concentration it is higher than all other.
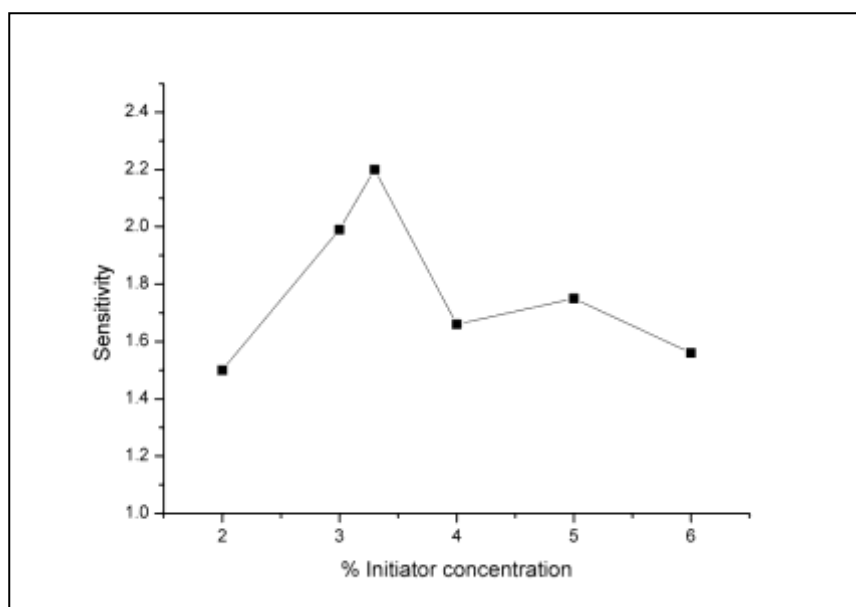
Figure 2.42: Variation of alpha sensitivity of poly (TAP-*co*-ADC, 3:7w/w) films with different initiator concentration.
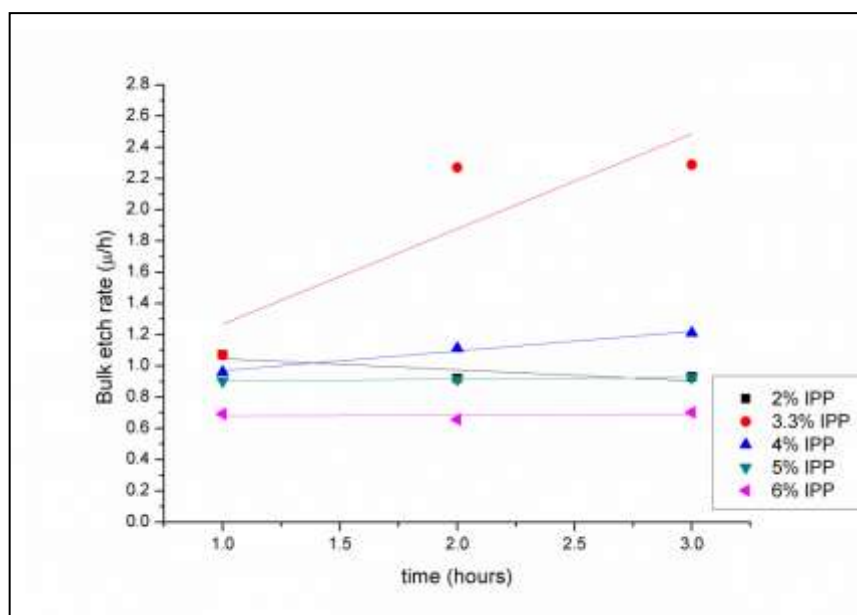
Figure 2.43: Bulk etch rate study of 3:7 Poly (TAP-*co*-ADC; 3:7 w/w) films with different IPP initiator concentration

For polymers prepared using different initiator concentration, there was large variation in alpha sensitivity. The films prepared using 2, 4, 5 and 6% IPP concentration were having similar alpha sensitivities and was approximately between 1.5–1.7. The film with 3.3 % IPP initiator had a maximum sensitivity of 2.20 and was the most sensitive amongst the copolymers prepared. The polymer with 3% initiator concentration had a maximum sensitivity of 1.99 which was determined after 4 hours of etching. The maximum alpha sensitivity obtained for different polymers is given below in Table 2.25.

Table 2.25: Maximum sensitivity observed for different polymers.

Sr. No.	IPP concentration (% by weight)	Maximum alpha sensitivity	Time (h) to attain maximum sensitivity
1	2	1.5	3
2	3	1.99	4
3	3.3	2.20	3
3	4	1.66	5

| 4 | 5 | 1.75 | 7 |
| 5 | 6 | 1.56 | 5 |

2.3.8 Optimization of Etching Conditions for TAP:ADC 3:7w/w copolymer:

Once the initiator concentration is optimized, the films with optimized initiator concentration were etched under different etching medium at different temperature and its post etch surface was analyzed so as to optimize the etching condition. For poly phosphate-carbonate polymeric films lower etchant concentration i.e. 4N or 5N NaOH solution could not reveal tracks at faster rate and films etched at higher etchant concentration (10 – 12N NaOH solution) cracked severely after 2 hours at 70 ^{o}C, so we considered 6-9N NaOH solution during optimization of etching condition. The time required for track development and post etch appearance of the surface was observed for TAP:ADC 3:7 w/w copolymer. The films were therefore etched at temperatures of 60, 70 and 80 °C. Table 2.26 gives the track revelation time under different etching condition for poly (TAP-*co*-ADC; 3:7 w/w) film.

Table 2.26: Time required for track development in the films poly (TAP-*co*-ADC, 3:7 w/w) at different temperature and different concentration of etching medium.

Etchant	Temperature (^{o}C)	Time required for track revelation in minutes		Post etch surface
		Alpha tracks	Fission fragments	
6N NaOH	60	240	120	Clear
	70	180	100	Clear
	80	120	60	Rough
7N NaOH	60	210	80	Clear
	70	**120**	**60**	**Clear**
	80	120	60	Clear

8N NaOH	60	150	60	Clear
	70	120	60	Cracks developed
	80	100	60	Cracks developed
9N NaOH	60	120	60	Rough surface
	70	110	50	film became brittle
	80	120	50	cracks seen

From the Table above the time required for track revelation was more when the film was etched at 6N NaOH at 60 °C. The films when etched in 6N NaOH solution at 80 °C, time required for revelation of alpha tracks was 120 minutes and that for fission fragments was 60 minutes but the post etch surface of the film was rough due to higher temperature condition. Time required to reveal alpha tracks and fission fragments was more when the films were etched in 7N NaOH solution at 60 °C. At etching condition of 7N NaOH and 70 °C, polymeric film revealed alpha tracks and fission fragments in 120 and 60 minutes respectively. The post etch surface after etching it in 7N NaOH at 70 °C was clear and tracks could be observed clearly. Further, upon increase in the etchant concentration and temperature, the post etch surface of the film became rough and even cracks were developed in some cases. When etched in 8N and 9N NaOH solution at 70-80 °C, post etch surface of the film was rough and tracks could not be viewed clearly under optical microscope. So we considered 7N NaOH and 70 °C temperature as optimum etching condition for poly (TAP-*co*-ADC) polymers.

Finally 3:7 poly (TAP-*co*-ADC) film was prepared using optimized initiator concentration and the sensitivity of the optimized film was determined at optimized etching condition i.e. 7N NaOH at 70 °C and compared it with indigenously prepared PADC and CR-39 films.

2.3.9   Sensitivity Studies under Optimized Conditions:

Poly (TAP-*co*-ADC; **3:7** w/w) film prepared using optimized conditions was exposed to ^{252}Cf source under 2 mm of Hg pressure at height of 5 cm from the source and for a period of 8 hours. These exposed films were then etched under optimized etching condition as a function of time and sensitivity at optimized condition was determined as reported below in Table 2.27. Also time required for track revelation in all developed polymers was observed at optimized condition and compared with commercially available CR-39 detector.

Table 2.27: Time required for alpha and fission tracks when etched under 7N NaOH medium at 70 ^{o}C and their sensitivity at different time interval.

Polymer composition TAP:ADC (w/w)	Time required to observe (minutes)		Maximum sensitivity ^{c} S after				
	alpha tracks[a]	fission fragments[b]	1 hour	2 hour	3 hour	4 hour	5 hour
1:9	120	60	1.3	1.44	1.7	1.47	1.48
2:8	120	60	1.25	1.32	1.54	1.83	1.41
3:7	**100**	**60**	**1.68**	**1.81**	**2.19**	**1.65**	**1.41**
4:6	120	60	1.4	1.62	1.68	1.89	1.67
1:1	120	60	1.59	1.76	1.6	1.64	1.73
6:4	120	60	1.28	1.49	1.58	1.67	1.17
7:3	120	60	1.25	1.33	1.36	1.24	1.19
8:2	120	60	1.21	1.26	1.36	1.2	1.21
9:1	120	60	1.12	1.21	1.26	1.21	1.18
PTAP	-	-	-	-	-	-	-
PADC	90	60	1.28	1.31	1.29	1.2	1.19
CR39	90	60	1.22	1.28	1.3	1.26	1.28

[a] films exposed to ^{239}Pu source at 1mm for 2minutes

[b] ^{252}Cf source at 1mm for 2hours

c films exposed to ^{252}Cf source at height of 5cm under 2mm of Hg vacuum for 8 hours

It is clear from the Table 2.27 that for poly (TAP-*co*-ADC; 3:7 w/w) attains maximum alpha sensitivity value. The alpha sensitivity of indigenous PADC and CR-39 is low as compared to that of phosphate-carbonate copolymers. The variation in alpha track diameter and fission track diameter as a function of etching time is shown in figure 2.44 below.

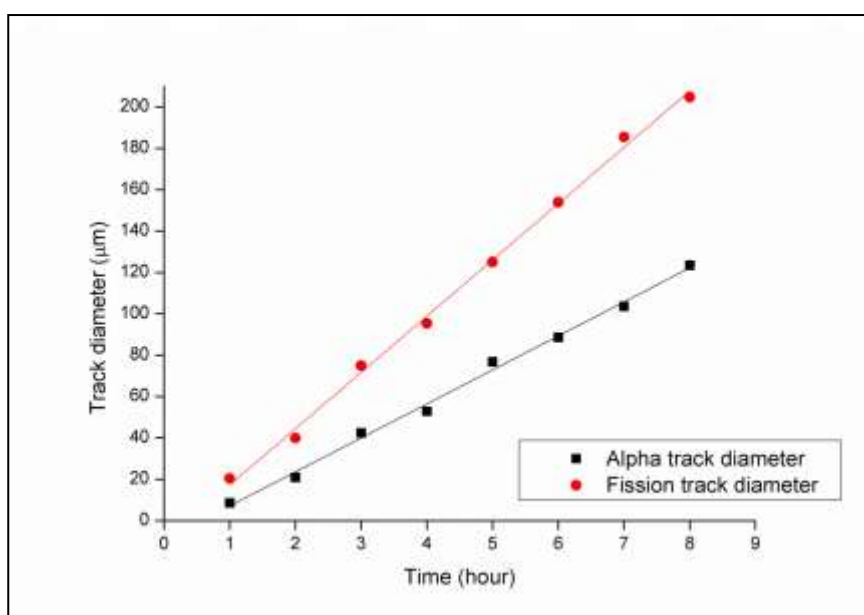**Figure 2.44:** Alpha particle and fission fragments growth in poly (TAP-*co*-ADC; 3:7 w/w) at optimized initiator concentration and etching condition i.e. 7N NaOH at 70 °C.

Also the alpha sensitivity of the poly (TAP-*co*-ADC, 3:7 w/w) prepared from 3.3% BP initiator was determined at optimized etching condition and compared it with that of polymer prepared using 3.3% IPP initiator as shown in Table 2.28.

Table 2.28: Alpha sensitivity of 3:7 Poly (TAP-*co*-ADC) film prepared using BP and IPP initiators.

Time hour	Alpha Sensitivity	Alpha Sensitivity
	BP	IPP
1	1.25	1.68
2	1.32	1.81
3	1.46	2.19
4	1.53	1.65
5	1.42	1.41

2.3.10 Alpha Track Detection Efficiency:

The optimized poly (TAP-*co*-ADC; 3:7 w/w) films along with CR-39 and indigenously prepared PADC were exposed to alpha particles from ^{239}Pu source for 5 minutes at a height of 3 cm. All these films were then etched in optimized etching condition for poly (TAP-*co*-ADC) polymer film i.e. 7N NaOH at 70 $^{\circ}$C and tracks were counted using optical microscope after every hour of time and alpha track detection efficiency of films was then measured. Figure 2.45 depicts the trend of number of alpha tracks as a function of time in optimized Poly (TAP-*co*-ADC) film, indigenously prepared PADC film and CR-39. It is clearly seen from the figure that trend of alpha track efficiency for all films are alike. Number of alpha tracks present in the copolymer after etching for certain period of time is more as compared to that of indigenously prepared PADC as well as CR-39 as reported in Table 2.29.

Table 2.29: Comparison of alpha sensitivity, alpha track detection efficiency of newly developed and optimized poly (TAP-*co*-ADC; 3:7 w/w) with indigenously prepared PADC and CR-39 films.

Sr. No.	Polymer detector	Alpha sensitivity*	Alpha tracks /cm^2
1	Poly (TAP-*co*-ADC; 3:7w/w)	2.19	19005
2	PADC	1.27	17025
3	CR-39	1.21	17100

* exposed to ^{252}Cf source at a height of 5 cm in 2 mm of Hg pressure for 8 hours.
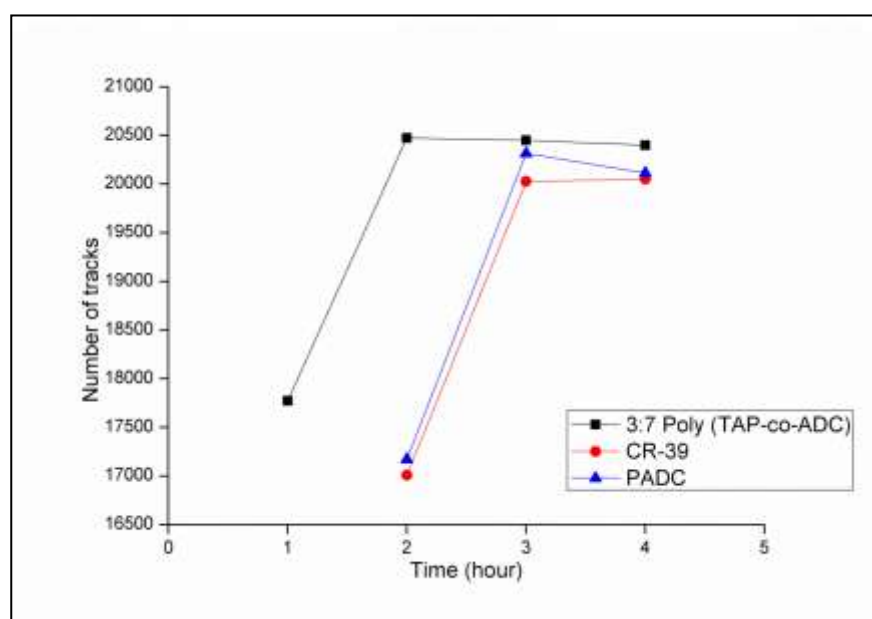
Figure 2.45: Comparison of alpha track detection efficiency in poly (TAP-*co*-ADC; 3:7 w/w) with PADC and CR-39.

2.4   Photomicrographs of optimized poly (TAP-*co*-ADC, 3:7 w/w) detector

Photographs of the tracks were recorded by using Tucsen ISH500 Camera and track diameters were determined by using its own imaging software i.e. IS Capture. Figure 2.46 depicts the fission fragments developed in the poly (TAP-*co*-ADC; 3:7w/w) detector when exposed to ^{252}Cf source at 1mm for 2 hour and subsequent etching for 1h. Alpha tracks can be revealed by the developed detector previously exposed to ^{239}Pu source at 1 mm for 2 minutes when etched for 2.5 h in optimized etching condition as shown in figure 2.47. Figure 2.48 show alpha tracks

as well as fission fragments formed in the detector when viewed under optical microscope with 40x magnifications. Figure 2.49 and Figure 2.50 shows alpha tracks developed in poly(TAP-*co*-PETAC; 4:6w/w) and poly(TAP-*co*-NADAC; 3:7w/w) respectively.
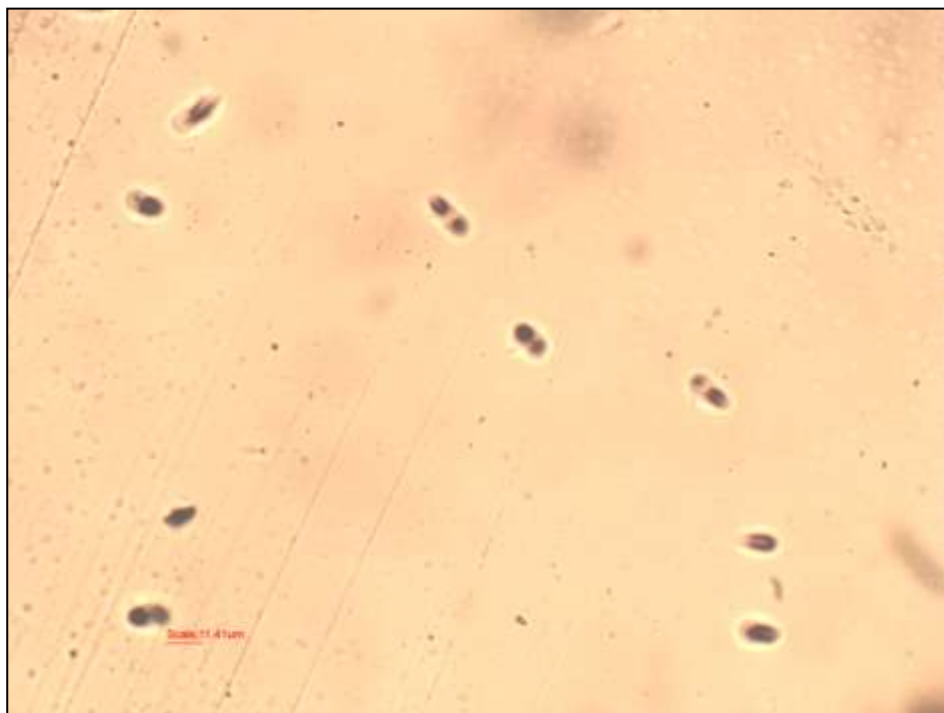
Figure 2.46: Fission fragments observed in poly (TAP-*co*-ADC; 3:7) detector when etched for 1 hour in 7N NaOH at 70 ^{o}C (40x magnification) (exposed to ^{252}Cf source at 1mm for 2 hour)

Figure 2.47: Alpha tracks observed in poly (TAP-*co*-ADC; 3:7 w/w) detector when etched for 2.5 hour in 7N NaOH at 70 ^{o}C (40x magnification) (exposed to ^{239}Pu source at 1mm for 2 minutes)
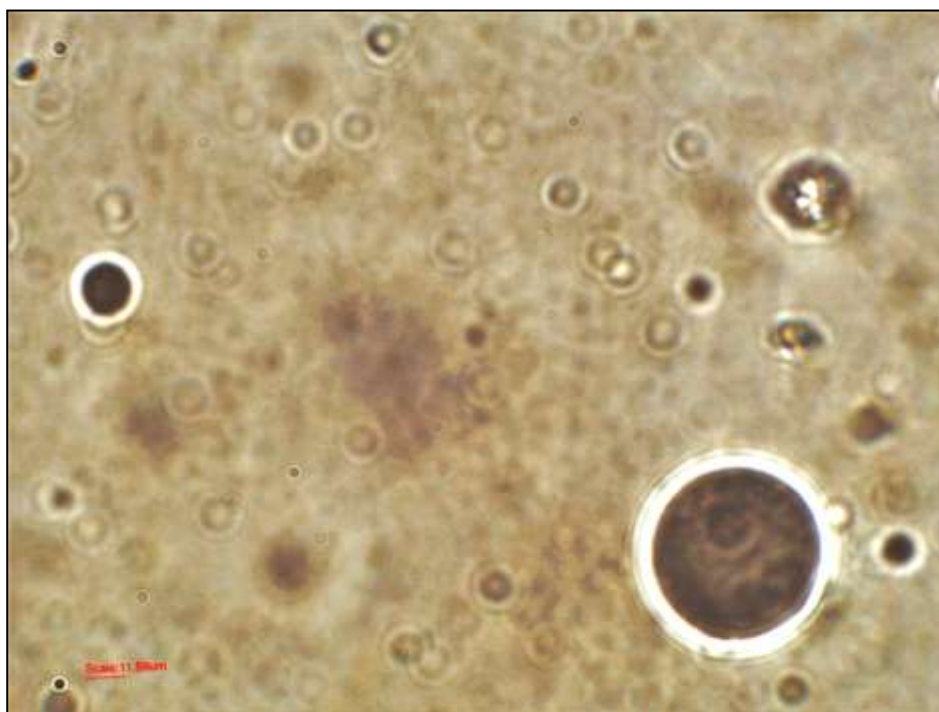
Figure 2.48: An alpha and fission tracks observed in Poly (TAP-*co*-ADC) (3:7 w/w) {Exposed to ^{252}Cf source at 5cm height in vacuum for 8 hours} after 2 hour of etching in 7N NaOH at 70 ^{o}C (magnification: 40X)

Figure 2.49: Alpha tracks observed in poly (TAP-*co*-PETAC; 4:6 w/w) detector when etched for 2 hour in 7N NaOH at 70 ^{o}C (40x magnification) (exposed to ^{239}Pu source at 2 mm for 5 minutes)

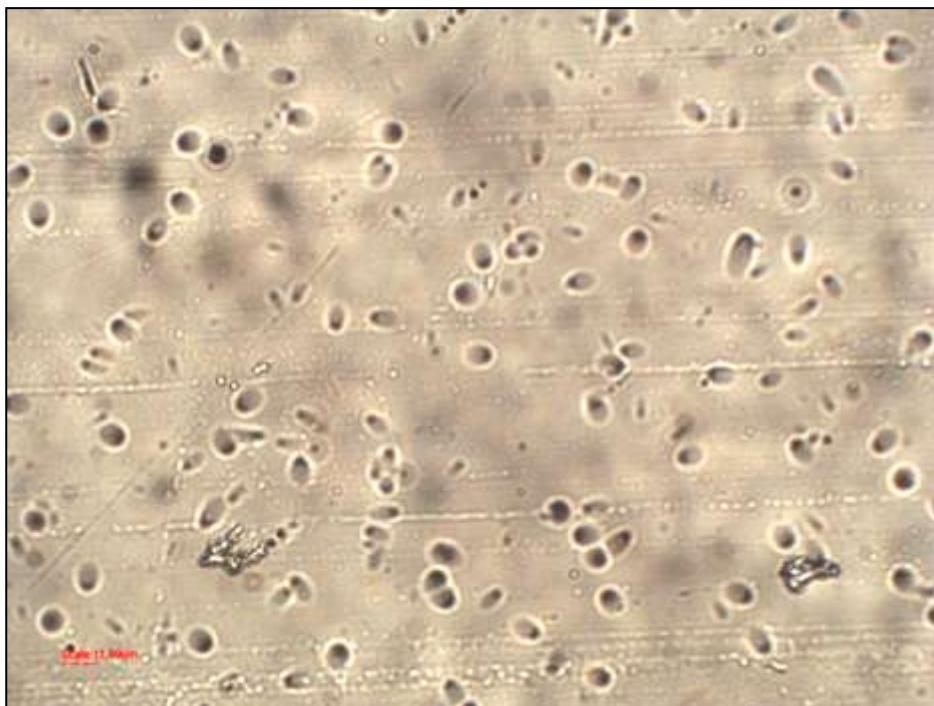**Figure 2.49:** Alpha tracks observed in poly (TAP-*co*-NADAC; 3:7 w/w) detector when etched for 4 hour in 7N NaOH at 70 ^{o}C (40x magnification) (exposed to ^{239}Pu source at 1 cm for 10 minutes)
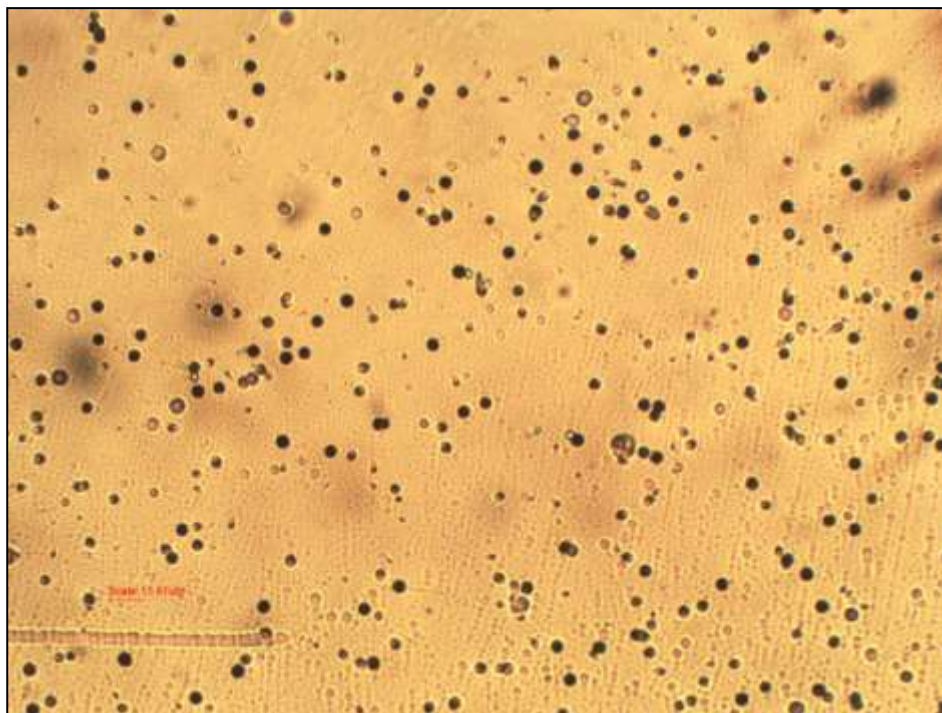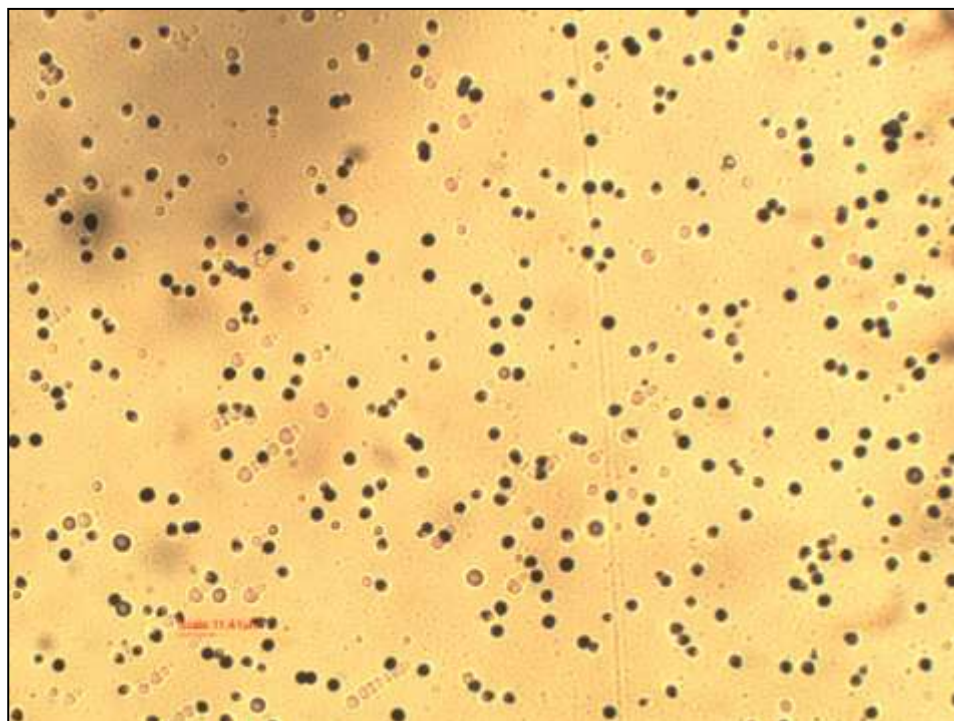
CHAPTER 2

2.5   Conclusion

We have successfully developed novel copolymers to be used as solid state nuclear track detectors. A homopolymer of triallyl phosphate (TAP) and a series of its copolymer with ADC (starting from 1:9 to 9:1 wt%) have been prepared out of which copolymers with a ratio of ADC:TAP in 2:8, 3:7, 4:6, 1:1, and 6:4 (wt%) show better sensitivity in comparison with indigenously prepared PADC film and commercially available CR-39. Kinetics of polymerization for homopolymer PTAP and copolymer poly (TAP-*co*-ADC; 3:7 w/w) have been studied using 3.3% IPP as well as 4% BP initiators to generate their constant rate polymerization profile as per Dial's methodology. The polymeric detector with 3:7 w/w ratio of TAP:ADC show maximum sensitivity of 2.19 which is higher than that of commercially available CR-39 detector i.e.1.25.

Besides increase in sensitivity the detector also show better alpha track efficiency as compared to that of CR-39. The detectors can reveal alpha as well as fission tracks under 7N NaOH solution at 70 ^{o}C temperature. PTAP homopolymer could not reveal tracks efficiently. PTAP film upon chemical etching under alkali metal hydroxides at 70 ^{o}C temperature produced cracks.

Copolymers of TAP with NADAC and PETAC were also prepared and tested for nuclear track detection. Out of which poly (TAP-*co*-NADAC; 1:1 w/w) and poly (TAP-*co*-PETAC; 1:1 w/w) showed better sensitivity than that of CR-39 detectors.

CHAPTER 2

2.6 References

1. (a) Clearfield, A. *Curr. Opin. Solid State Mater. Sci*. **1996**, *1*, 268–278. (b) Clearfield, A. *Curr. Opin. Solid State Mater. Sci*. **2002**, *6*, 495–506. (c) Clearfield, A. *J. Alloys Compd.* **2006**, *418*, 128–138.

2. (a) Plesu, N.; Ilia, G.; Pascariu, A.; Vlase, G. *Synth. Met.* **2006**, *156*, 230–238. (b) Chougrani, K.; Boutevin, B.; David, G.; Seabrook, S.; Loubat, C. *J. Polym. Sci., Part A: Polym. Chem.* **2008**, *46*, 7972–7984.

3. (a) Levchik, S. V.; Weil, E. D. *J. Fire Sci.*, **2006**, *24*, 345–364. (b) Schartel, B. *Materials*, **2010**, *3*, 4710–4745. (b) Chang, Y. L.; Wang, Y. Z.; Ban, D. M.; Yang, B.; Zhao, G. M. *Macromol Mater Eng*. **2004**, *289(8)*, 703–707.

4. (a) Ogliari, F. A.; da Silva, E. D.; Lima, G. D.; Madruga, F. C.; Henn, S.; Bueno, M.; Ceschi, M. A.; Petzhold, C. L.; Piva, E. *J. Dent.* **2008**, *36*, 171–177. (b) Avci, D.; Mathias, L. *J. Polym. Bull.* **2005**, *54*, 11–19. (c) Yeniad, B.; Albayrak, A. Z.; Olcum, N. C.; Avci, D. *J. Polym.* Sci., Part A: Polym. Chem. **2008**, *46*, 2290–2299. (d) Moszner, N.; Zeuner, F.; Pfeiffer, S.; Schurte, I.; Rheinberger, V.; Drache, M. *Macromol. Mater. Eng*. **2001**, *286*, 225–231.

5. (a) Monge, S.; Canniccioni, B.; Graillot, A.; Robin, J. J. *Biomacromolecules,* **2011**, *12 (6)*, 1973–1982. (b) Goda, T.; Ishihara, K. *Expert Rev. Med. Devices*, **2006**, *3*, 167–174.

6. (a) Parvole, J.; Jannasch, P. *Macromolecules*, **2008**, *41*, 3893–3903. (b) Jiang, F.; Kaltbeitzel, A.; Meyer, W. H.; Pu, H.; Wegner, G. *Macromolecules*, **2008**, *41*, 3081–3085. (c) Bock, T.; Muelhaupt, R.; Moehwald, H. *Macromol. Rapid Commun.* **2006**, *27*, 2065–2071.

7. (a) Popa, A.; Davidescu, C. M.; Negrea, P. Ilia, G.; Katsaros, A.; Demadis, K. D. *Ind. Eng. Chem. Res.*, **2008**, *47*, 2010–2017. (b) Graillot, A.; Faur, C.; Bouyer, D.; Monge, S.; Robin, J. J. *Water Sci. Technol.* **2013**, *67*, 1181-1187, doi: 10.2166/wst.2012.671. (c) Graillot, A.; Bouyer, D.; Monge, S.; Robin, J. J.; Faur, C. *J. Hazard. Mater.* **2012**, doi: 10.1016/j.jhazmat.2012.10.031.

8. (a) Tarascon, M.; Armand, M. *Nature* **2001**, *414*, 359–367. (b) Bruce, P.G.; Scrosati, B.; Tarascon, J. M. *Angew. Chem. Int Ed*. **2008**, *47(16)*,

2930–2946. (c) Iliescu, S.; Zubizarreta, L.; Plesu, N.; Macarie, L.; Popa, A.; Ilia, G. *Chem. Cent. J.* **2012**, *6*, 1–13.

9. Becker, A. *Health Phys.* **1966**, *12* (6), 769–785.

10. (a) Price, P. B.; Park, H. S.; Gerbier, G.; Drach, J.; Salamon, M. H. *Nucl. Instruments Methods Phys. Res. Sect. B Beam Interact. with Mater. Atoms* **1987**, *21* (1), 60–67. (b) Price, P. B.; Cook, L. M.; Markert, A. *Nature* **1987**, *325* (6100)*,* 137–138.

11. Shicheng, W.; Barwick, S. W.; Ifft, D.; Price, P. B.; Westphal, A. J.; Day, D. E. *Nucl. Instruments Methods Phys. Res. Sect. B Beam Interact. with Mater. Atoms* **1988**, *35* (1), 43–49.

12. Bonetti, R.; Chiesa, C.; Guglielmetti, A.; Migliorino, C. *Int. J. Radiat. Appl. Instrumentation. Part D. Nucl. Tracks Radiat. Meas.* **1991**, *18* (3), 325–327.

13. (a) Bonetti, R.; Guglielmetti, A.; Poli, G. *Radiat. Meas.* **1997**, *27* (1), 71–74. (b) Moody, K. J.; Hulet, E. K.; Wang, S.; Price, P. B.; Barwick, S. W. *Phys. Rev. C* **1987**, *36* (6), 2710–2712.

14. Armarego, W. L. F.; Perrin, D. D. *Purification of Laboratory Chemicals*; Butterworth Heinemann: 1996, *4th edition*.

15. Lynwood, W. N.; Robert, B. S. Allyl type phosphates and their preparation. USP 2,394,829, **1946**.

16. (a) Liu, H.; Xiong, Y.; Xu, W.; Zhang, Y.; Pan, S. *J. Appl. Polym. Sci.* **2012**, *125*, 1544–1551. (b) Dekorver, K. A.; Wang, X.; Walton, M. C.; Hsung, R. P. *Org. Lett.* **2012**, *14* (4), 1768–1771. (c) Hulst, R.; Robert W. J., Z.; Feringa, B. L.; Vries, N. K. de; Hoeve, W. ten; Wynberg, H. *Tetrahedron Lett.* **1993**, *34* (8), 1339–1342. (d) Stowell, J.; Liu, W. Phospharamide ester flame retardant and resins containing same. US 2010/0063169 A1, **2010**.

17. (a) Zhao, W.; Li, B.; Xu, M.; Yang, K.; Lin, L. *Fire Mater.* **2013**, *37*, 530–546. (b) Wang, L.; Jiang, J.; Jiang, P. *J. Polym. Res.* **2010**, *17*, 891–902. (c) Chen, D.; Wang, Y.; Hu, X.; Wang, D.; Qu, M.; Yang, B. *Polym. Degrad. Stab.* **2005**, *88*, 349–456. (d) Halpern, Y.; Mott, D. M.; Nlswander, R. H. *Ind. Eng. Chem. Prod. Res. Dev.* **1984**, *23* (2), 233–238.

(e) Yu Ju, Z.; Ye, Y.; Yi, R.; Liao, X. C.; Zhao, Y. F. *Chinese Chem. Lett.* **2008**, *19*, 277–278.

18. Nadkarni, V. S.; Tilve, S. G.; Mascarenhas, A. A. A. Indian Process Patent no. 19996627 20, **1999.**

19. Mascarenhas, A. A. A.; Tilve, S. G.; Nadkarni, V. S. *Des. Monomers Polym.* **2005**, *8* (2), 177–186.

20. Mandrekar, V. K.; Chourasiya, G.; Kalsi, P. C.; Tilve, S. G.; Nadkarni, V. S. *Nucl. Instruments Methods Phys. Res. B.* **2010**, *268* (5), 537–542.

21. Mascarenhas, A. A. A.; Mandrekar, V. K.; Kalsi, P. C.; Tilve, S. G.; Nadkarni, V. S. *Radiat. Meas.* **2009**, *44*(1), 50-56.

22. Vogel, A. I. *Elementary Practical Organic Chemistry Part III*; Longmann, London: 1958.

23. Nadkarni, V. S. *Indian J. Phys.* **2009**, *83* (6), 805-811.

24. (a) Mandrekar, V. K. Novel polymeric materials for nuclear track detection. [Ph.D. Thesis]. Goa, India, Goa University; 2010. (b) Mascarenhas, A. A. A. Development of plastic materials for nuclear track detection. [Ph.D. Thesis]. Goa, India, Goa University; 2007.

25. Mascarenhas, A. A. A.; Kolekar, R. V.; Kalsi, P. C.; Ramaswami, A.; Joshi, V. B.; Tilve, S. G.; Nadkarni, V. S. *Radiat. Meas.* **2006**, *41*(1), 23-30.

26. Dial, W. R.; Bissinger, W. E.; Dewitt, B. J.; Strain, F. *Ind. Eng. Chem.* **1955**, *47*(12), 2447-2451.

27. Corbridge D. Phosphorus: Chemistry, Biochemistry and Technology, 2015; 6th edition, (page 70-90).

CHAPTER 3

Development of sulfur containing polymeric materials for SSNTD applications

CHAPTER 3

3.1   Introduction

In the last more than a decade, sulphur containing polymers have gained increasing interest because of their remarkable properties that make them useful in a wide variety of applications. These polymers can be utilized as proton-conducting electrolytes, high performance engineering plastics, chemically stable ion-exchange membranes in electro-membrane processes[1], and optical, optoelectronic, and photochemical materials[2]. Some sulfur containing polymers are used in biomedical applications[3], e.g., sulfopolymers as biomembranes and blood-compatible materials, various polysulfates and polysulfonates as antithrombotic or antiviral agents. The presence of sulfur, mainly in the form of disulfide linking, plays a significant role in biopolymers. Polysulfates are extensively studied because of their potential biomedical applications. A naturally occurring sulfated polysaccharide "Heparin" has antithrombogenic properties so as to become useful in cardiovascular surgery[4]. Most of the polysulfates and sulfated polysaccharides are active against a broad range of enveloped viruses[5]. Also sulfated polysaccharides were found to be selective inhibitors of HIV-1 replication in cell culture. It offers promising features to anti-HIV drug patients.

Immense advances have been made regarding the synthesis of new types of sulfur containing polymers and modification of the properties of some polymers by adding sulfur fragments to the polymer[6]. Many sulfur containing polymers have been prepared and utilized in wide range of applications. Recently, both basic and applied research has been focused on developing the processability, solubility, mechanical strength, thermal and flame resistance in the polymers by incorporating sulfur moiety (sulfide, sulfoxide, sulfone) in the main-chain to widen the scope of technological applications of these materials. Commercially known polymers having sulfur

moieties are polysulfides and polysulfones which have a wide number of expensive industrial applications comprising mechanical parts, electrical components, biomedical equipment, and aerospace, etc[7]. The sulfur-containing polymers are also known with reference to their significance as optically active, liquid crystalline, and fuel cell materials. Several activities are in progress to take advantage of built-in sulfur moiety in the polymer backbone, as a result to ascertain their validity on the forefront of scientific investigations. By using different synthetic routes one can produce sulfur-containing polyamides, polyimides, poly (amide-imide) s, polybenzimidazoles, polyurethanes, and polyesters. These can be prepared by well known methods such as by the chemical modification of monomers and their polycondensation using different methods or by direct modification in the synthetic polymers. The property of polymers depends on the functional groups like sulfide, sulfoxide, sulfone, thiophene, thiourea, thiazol, etc present in it. The sulfur bearing groups affect the physical and chemical properties of polymers.

A series of sulfur-containing polyimides from 4, 4'-(*p*-phenylenedisulfanyl) dianiline and various dianhydrides via two-step polycondensation were developed by J. G. Liu and co-workers[8]. These sulfur-containing polyimides show a fine combination of properties including high thermal stability, good optical transparency in the visible region, high refractive indices, and low birefringence as given in scheme 3.1 below.
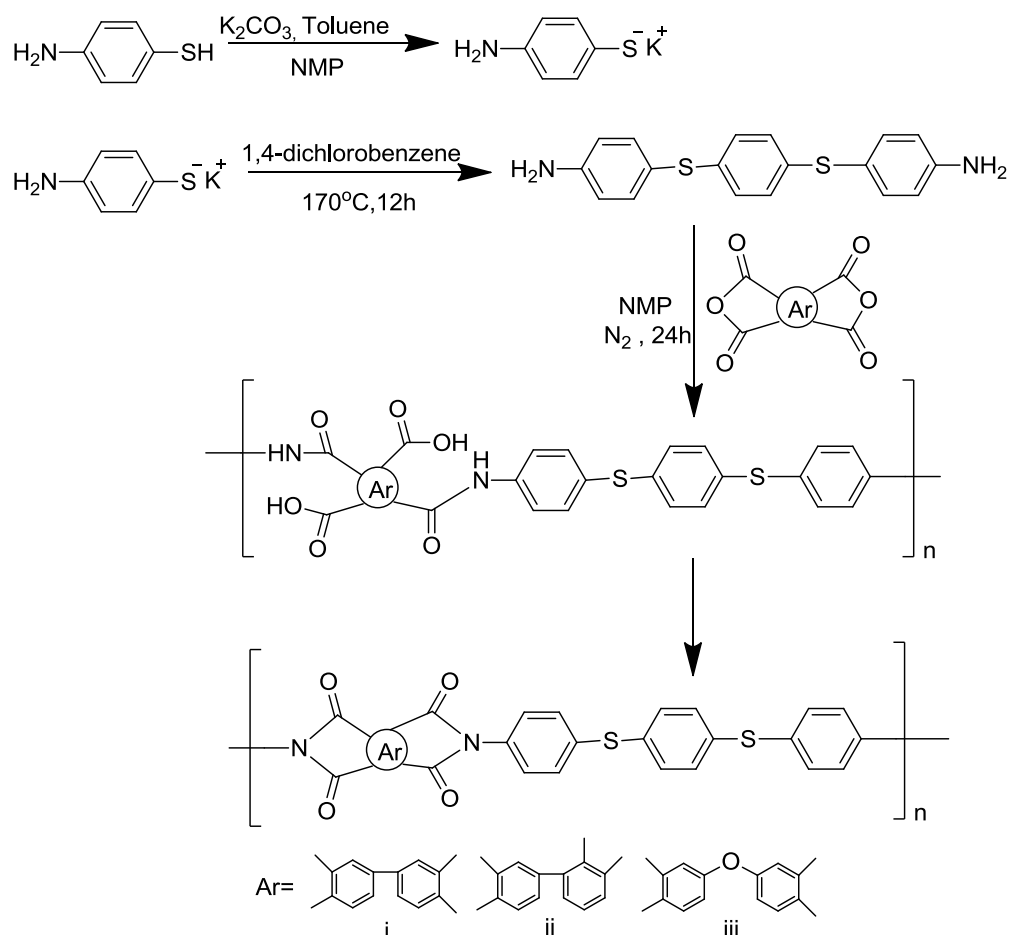
Scheme 3.1: Synthesis of sulfur containing polyimides conducted in N-methylpyrrolidone (NMP)

The earliest sulfur containing polymers that are commercially manufactured are polysulfides and polysulfones. Poly (phenyl sulfide) (PPS) was developed by Philips petroleum company[9]. PPS is useful for electrical components, precision mechanical parts etc. The manufactured part that uses PPS includes engine components, valves, exterior light reflectors, high pressure nozzles, coil bobbins etc[10]. Polysulfones (PSU) are group of aromatic resins having sulfone and ether moieties. Few commercially available structures of polysulfones are shown below in figure 1. These polysulfones[11] have excellent resistance towards stress cracking, good thermoplastic properties, high softening point, negligible water absorption, and high softening point. Also they have incomparable resistance to air oxidation at high

temperature due to presence of deactivating sulfone group in the backbone. Some of the polysulfones are capable of acting as antioxidants. They have interesting applications in synthetic membranes for blood dialysis, water treatments and food preservatives as polysulfones have advanced separating capacity. In the year 1966, Udel® PSU was the first industrially produced PSU resin. After that in 1972 PAS resin Radel® was commercialised. Polyether sulfone (PES) resin was first promoted by ICI in 1971.

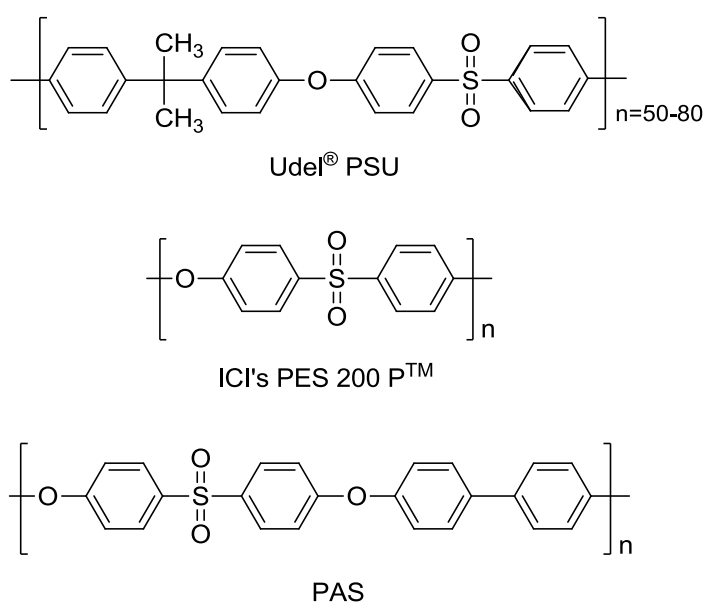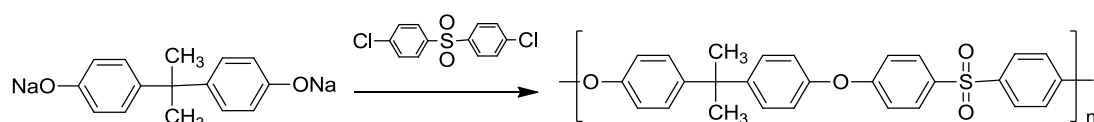Udel® PSU

ICI's PES 200 P™

PAS

Figure 3.1: Commercially available polysulfones

The polysulfones prepared from 4, 4'-dichlorodiphenyl sulfone and bisphenol-A by condensation process is rigid tough and has excellent insulation properties[12]. The polymer is self extinguishing. Synthetic route is shown in scheme 3.2 below.

Scheme 3.2: Synthesis of polysulfone prepared from bisphenol-A

Further, sulfone containing polymers like poly (urethane-sulfone), poly (ester-sulfone) and poly (carbonate-sulfone) have been synthesised and used as high barrier materials[13]. These sulfone containing polymers have approximately 50 times smaller CO_2 permeability coefficient as compared to that with corresponding polymers having no sulfone moieties in it. The CO_2 barrier properties of sulfone containing polymers are similar to that with commercial high barrier vinyl alcohol copolymers (EVAL). Shockravi *et. al.*[14] reported the synthesis and use of poly (sulfide-ether-amide)s and poly (sulfoxide-ether-amide)s for their improved solubility without losing their heat resistance. S. R. Rafikov[15] examined the effect of the composition of polymers containing sulfur as –S-, Ss, SO_2, SO and SH on their physicochemical, thermal, photochemical, radiation chemical and complexing properties. Among bisvinyl sulfones, divinyl sulfone (DVS) finds many applications in bioconjugation[16], proteomics[17] and in production of polysaccharide-based networks. Polysaccharides and DVS based hydrogel materials have been prepared for their use in controlled drug delivery systems and biocompatible biomaterials for biomedical applications. Also the potential of DVS as a cross-linker is exploited[18] for the invention of novel water-insoluble homo and hetero cyclodextrin-based polymers (CDPs) by cross-linking native α-cyclodextrin (α-CD), β-cyclodextrin (β-CD) and starch[19]. These materials have capabilities for the removal of a variety of some representative phenolic pollutants as sorbents and for bioactive compounds such as a model steroid hormone (progesterone) as encapsulating agents. Anna Kultys[20] in her review has described some methods of synthesis and properties of various newer sulfur containing polymers like polysulfides, polysulfoxides, polysulfonium salts, sulfopolymers, and polysulfates and their major applications. Polysulfoxides are utilized as functional polymers. They can be used as new polymeric oxidizing reagents,

compatibilizers, and polymer solvents. Polysulfonium salts are exploited as ion-exchange resins, polymer supports in peptide synthesis, polymeric reagents, or conducting and photochemical polymeric materials. Polymers with sulfonium salt moieties are also used as a catalyst to organic reactions.

Yet another interesting application of sulphur polymers is found in solid state nuclear track detectors (SSNTD). In the year 1978, B. G. Cartwright[21] *et al.* used commercially available CR-39 polymeric material for detection of charged particles and it showed very high sensitivity to many charged particles. Further M. Fujii[22] *et al.*, in the year 1990 prepared some copolymers of ADC with solid diethylene glycol bis (allyl sulfonate) (DEAS) in the ratio 90:10 wt% {SR-86(10)} and 80:20 wt% {SR-86(20)} and used as SSNTD, which showed higher alpha sensitivity then CR-39. However, these polymeric detectors were having short shelf life due to which they degraded within a week's time. In 1986, J Stejny[23] *et al.*, prepared copolymeric material by UV initiated bulk copolymerization of ADC with liquid sulfur dioxide that showed good alpha track recording property. However, the disadvantage of this copolymer was that it was having lower ceiling temperature so that it got de-polymerized to the monomer. V. K. Mandrekar[24] *et al.* extended the work of developing SR-86 detector, and designed homopolymer of DEAS and various copolymers with ADC in the higher concentration of DEAS as SSNTD which was not reported earlier by Fujii *et al.* The homopolymer containing sulfonate functionalities showed high sensitivity towards alpha track detection but due to its short shelf life the polymeric detector was unstable. Our group also reported some polysulphite-carbonate polymeric films for track detection applications[25]. Diallyl sulphite[26] (DAS) and allyl diglycol sulphite[27] (ADS) polymers have already been prepared by our group and utilized for nuclear track detection. As it was observed that sulfur functionalities containing polymeric materials show better alpha

sensitivity and they could reveal nuclear tracks in smaller time by chemical etching, we thought of preparing a series of allylic monomers containing sulfide, sulfonamide, sulfoxide, and sulfone functionalities, study their polymerization properties and test the corresponding polymers as nuclear track detectors. Following monomers (Figure 3.2) were thus considered for this study.
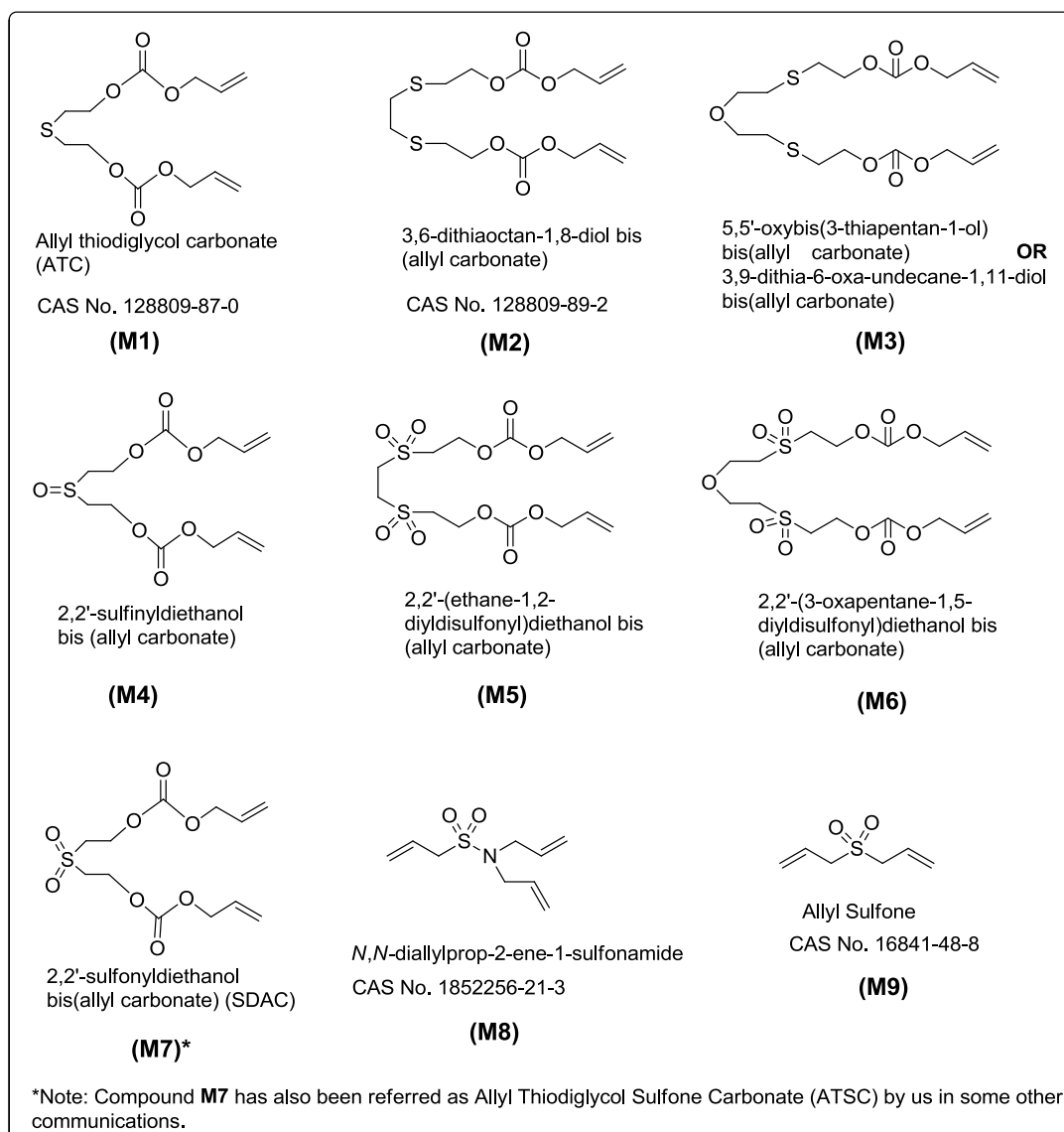

Figure 3.2: Sulfur containing allylic monomers as prepared.

It may be noted that out of these, monomers M1, M2, M8 and M9 are previously reported where as M3, M4, M5, M6 and M7 are novel monomers being reported by us for the first time.

Also copolymerization of above mentioned monomers with ADC using initiators viz. BP, IPP, AIBN were tested and thriving copolymers were used for nuclear track detection studies.

3.2   Experimental

3.2.1   Materials and Methods:

Chemicals used for the synthesis and purification of sulfur containing monomers were obtained from M/s Spectrochem, India, M/s Qualigens Fine Chemicals, India, and M/s Molychem, India. Dry solvents were used during reaction. Reagents used in chemical kinetics study were freshly prepared and used whenever required. Synthesis of monomers and polymerization process were carried out under dust controlled environment. The progress of reaction was monitored by thin layer chromatographic technique and the characterization of the synthesized monomers was carried out by different spectral techniques viz. IR, NMR, and HRMS. Mostly isopropyl peroxydicarbonate (IPP) initiator is prepared and utilized for polymerization process. Synthesis and characterization of IPP is given in chapter 4 (page no.322). Dioctyl phthalate (DOP) is used as plasticizer in polymerization process.

3.2.1.1   Allyl thiodiglycol carbonate (ATC) (M1): Allyl thiodiglycol carbonate was synthesised in two steps. In first step, β-thiodiglycol was prepared using sodium sulfide and 2-chloro ethanol followed by condensation of thiodiglycol with allyl chloroformate using pyridine in second step to prepare allyl thiodiglycol carbonate as shown in scheme 3.3.
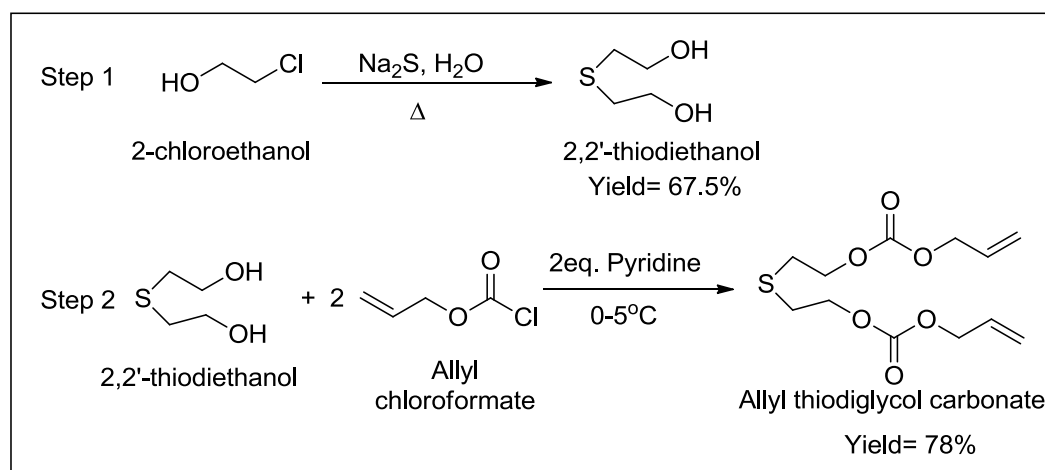
Scheme 3.3: Synthesis of Allyl thiodiglycol carbonate (ATC).

Step 1: Synthesis of β-thiodiglycol: β-thiodiglycol can be synthesized by treating ethylene chlorohydrin in water with sodium sulfide at room temperature[28]. In a 1 L three neck round bottom flask fitted with overhead mechanical stirrer and thermometer, 290 mL of 20% (60 g, 0.745 moles) 2-chloroethanol solution and 200 g of water was placed. The reaction assembly was placed in a cooling bath to maintain the temperature below 20 °C. To the reaction vessel, 32.1 g (0.411 moles) crystalline sodium sulfide was added in small portions. Addition was continued over a period of 2 hours maintaining the temperature between 30-35 °C. After complete addition of sodium sulfide, it was stirred for another 40 minutes. The mechanical stirrer was removed and the flask was fitted with a reflux condenser and the solution was set for reflux. The flask was heated till temperature of reaction mixture reached to 90-95 °C and held for another 45 minutes. It was then cooled to ambient temperature and neutralized to turmeric paper by adding drop by drop concentrated hydrochloric acid. It was then filtered and concentrated over rotary evaporator under reduced pressure and elevated temperature. Further, it was extracted by using hot absolute ethanol. The crude liquid product was vacuum distilled at reduced pressure of 0.2 mm of Hg and 80 °C. It was characterized by IR and NMR spectra (Figure

3.3a-b; page no.179-180). The yield of pure β-thiodiglycol was 180 g (67.5% based on 2-chloroethanol). The synthetic scheme 3.3 above depicts synthesis of β-thiodiglycol. IR (KBr): 3367 cm^{-1}, 2922 cm^{-1}, 1406 cm^{-1} and 1043 cm^{-1}. ^{1}H NMR (400 MHz, CDCl$_3$) (ppm): 3.69 (2H, t), 2.68 (2H, t).

Step 2: Synthesis of Allyl thiodiglycol carbonate: In a 100 mL two neck flask fitted with pressure equalizing funnel, 5.01 g (4.09 mL, 0.0409 moles) of β-thiodiglycol was dissolved in 50 mL acetone. 7.44 g (7.58 mL, 0.0941 moles) of pyridine was added and stirred constantly with the help of stirrer. It was placed in a cooling methanol bath and temperature was brought down to 0 ^{o}C. At 0 ^{o}C, 11.53 g (10.0 mL, 0.0941 moles) allyl chloroformate was added slowly to the reaction mixture with the help of pressure equalizing funnel. After complete addition of allyl chloroformate, it was stirred for another 1 hour at 0 ^{o}C followed by stirring at ambient temperature for 2 hours. Reaction was monitored by TLC and on completion workup was carried out using diethyl ether. Initially, acetone was removed over rotary evaporator and it was acidified by using 2N HCl solution. Further it was extracted in to diethyl ether solvent and washed with brine solution 4-5 times till it becomes neutral. The washings were also extracted using diethyl ether. The combined organic layers were passed over dry sodium sulphate and were concentrated over rota-vap to get crude liquid ATC product. It was vacuum distilled under 2 mm of Hg at 140 ^{o}C to obtain 78.0% of desired product. Spectral characterization of the purified ATC was carried out by IR and NMR spectral techniques (Figure 3.3c-d; page no. 181-182). The synthetic route is given in scheme 3.3. IR (KBr): 3084 cm^{-1}, 2951 cm^{-1}, 1747 cm^{-1}, 1649 cm^{-1}, 1388 cm^{-1} and 1257 cm^{-1}. ^{1}H NMR (400 MHz, CDCl$_3$) (ppm): 6.00-5.90 (m, 2H), 5.40-5.28 (dd, 4H), 4.65 (d, 4H), 4.32 (t, 4H), 2.86 (t, 4H).
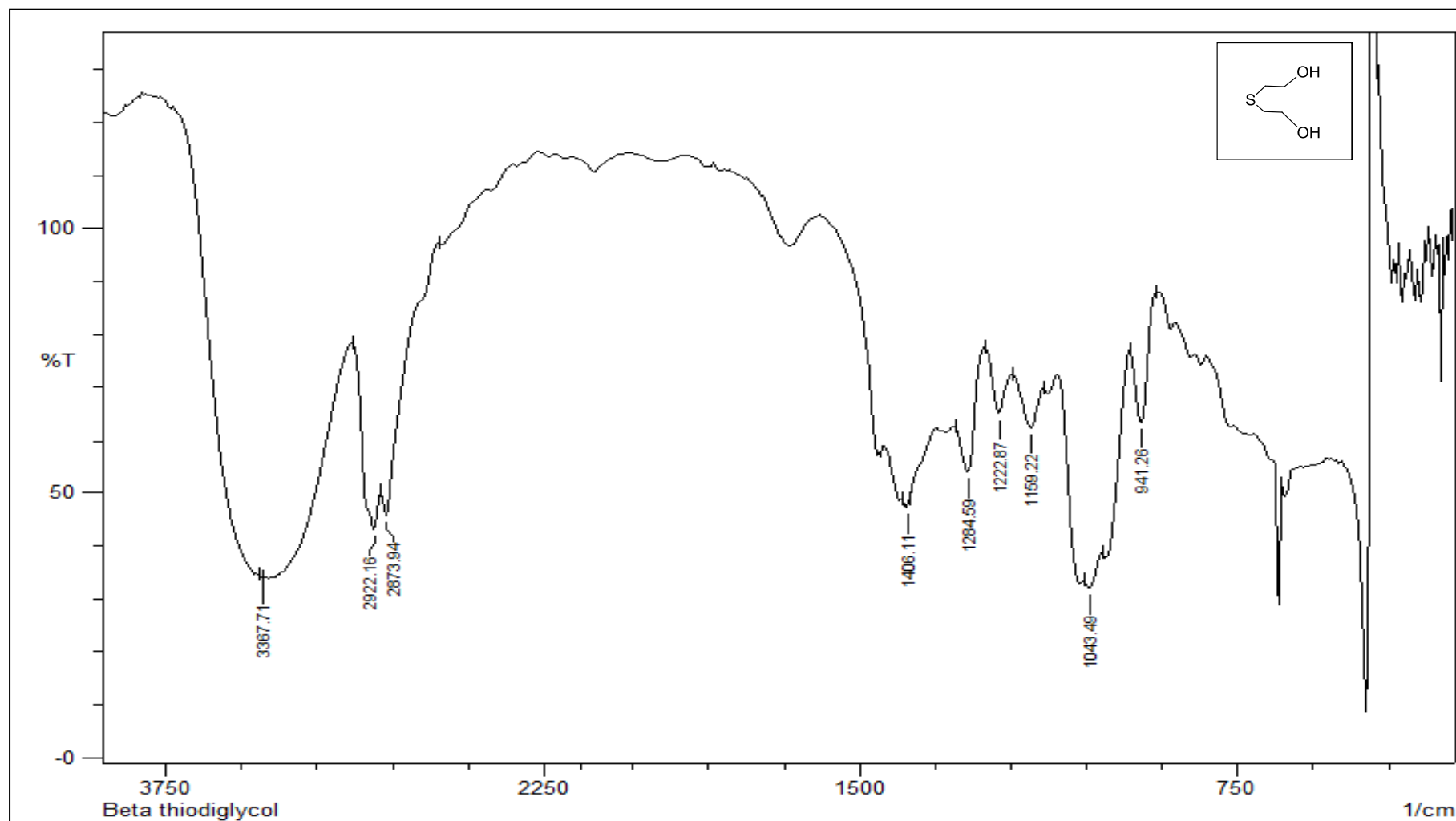
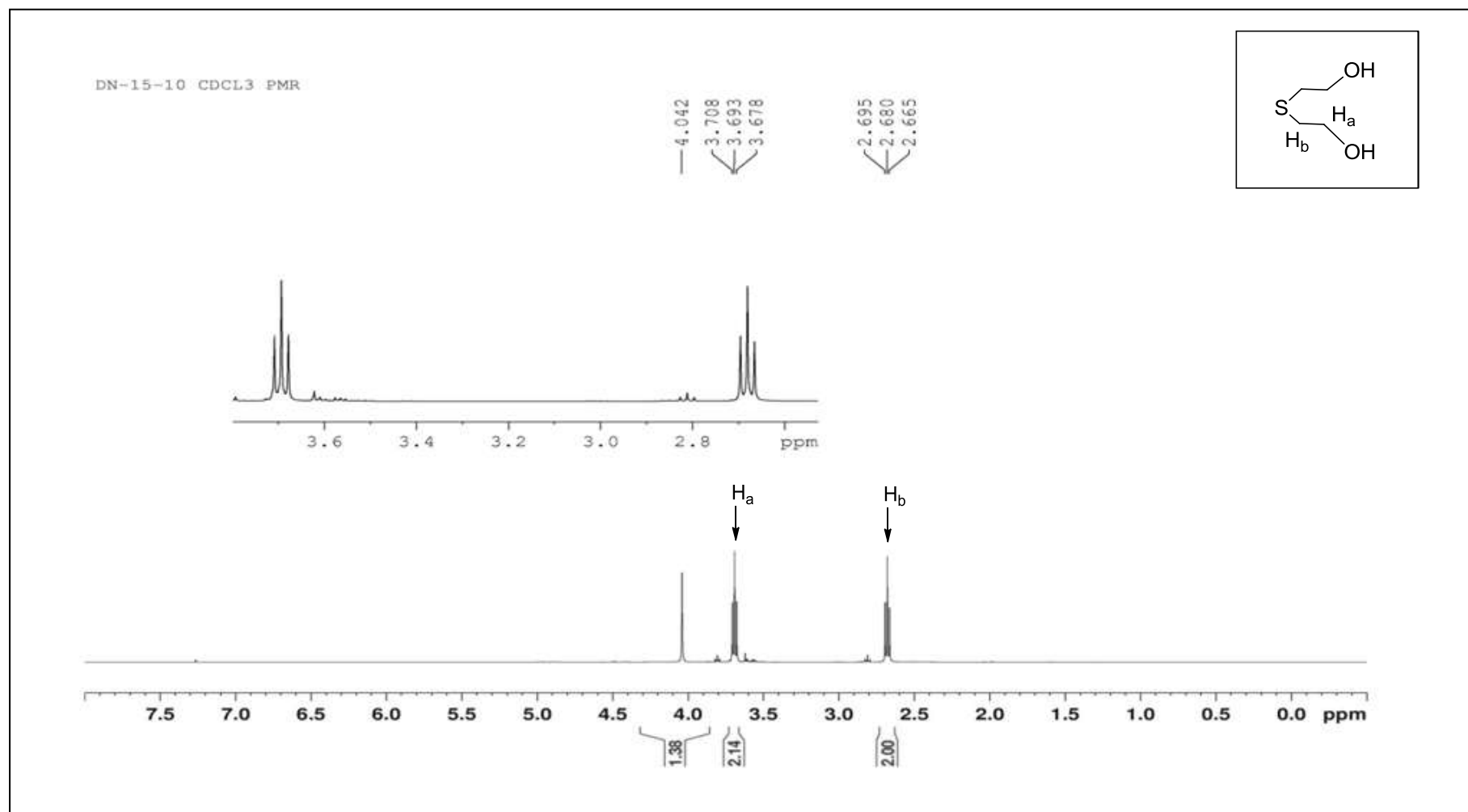**Figure 3.3 (a):** IR spectrum of β-thiodiglycol.

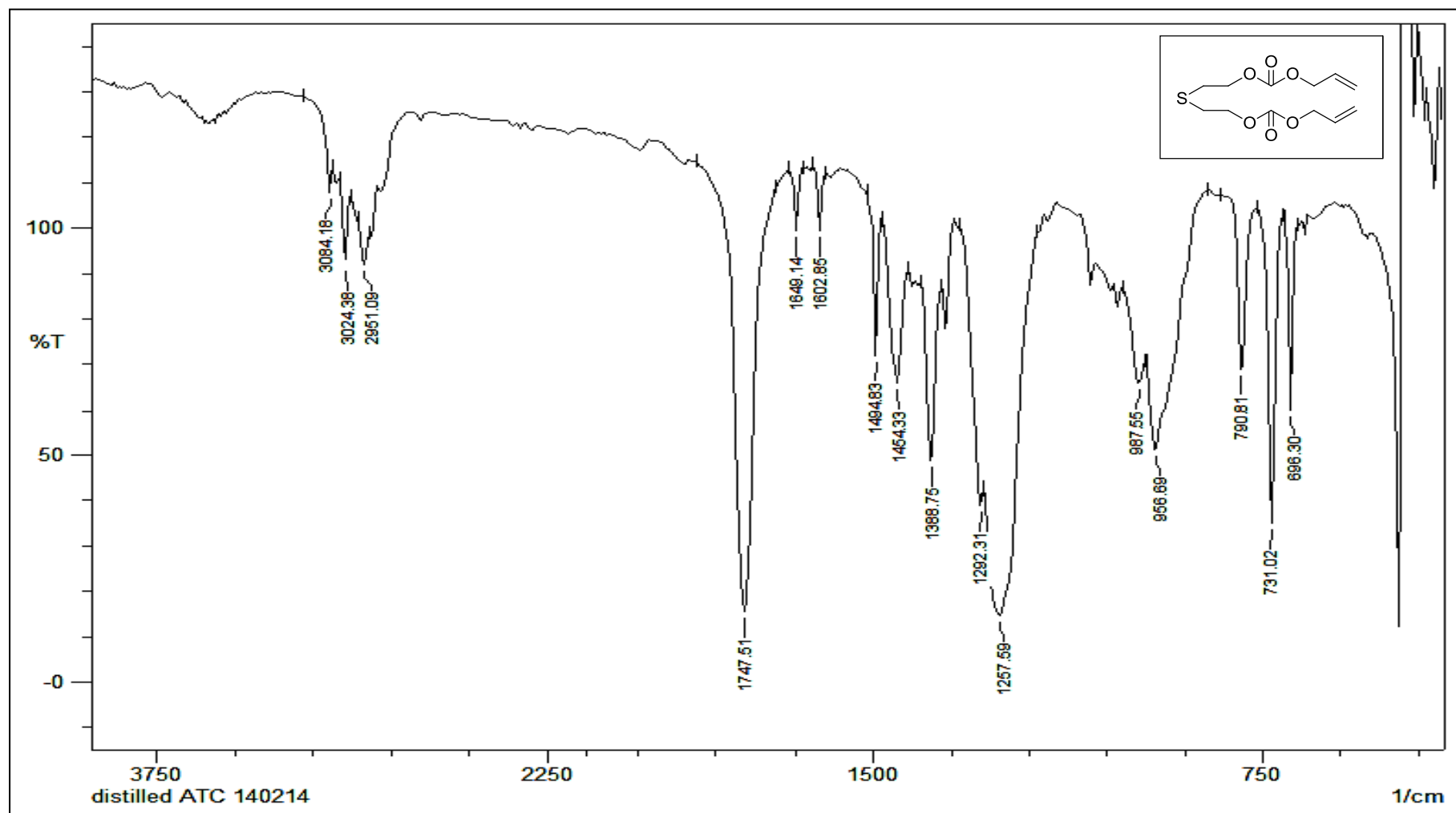**Figure 3.3 (b):** NMR spectrum of β-thiodiglycol.

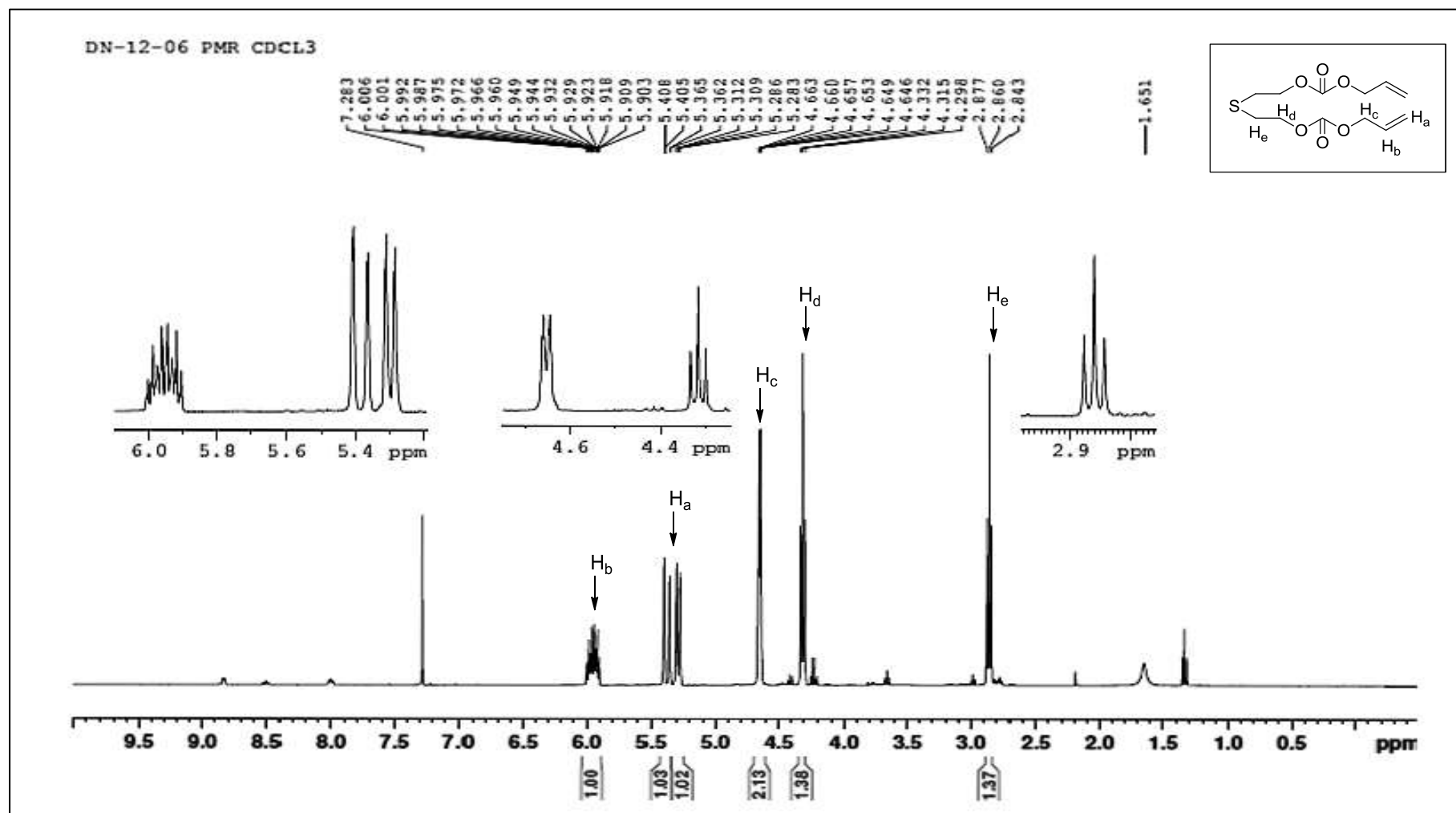**Figure 3.3 (c):** IR spectrum of Allyl Thiodiglycol Carbonate

Figure 3.3 (d): ^{1}H NMR spectrum of Allyl Thiodiglycol Carbonate

3.2.1.2   3,6-dithiaoctan-1,8-diol bis (allyl carbonate) (M2): This monomer was also prepared in two steps. Initially 1, 2-bis (2-hydroxyethyl sulfanyl) ethane was prepared using mercaptoethanol followed by condensation with allyl chloroformate using pyridine as base. The two step synthetic route is depicted in scheme 3.4 below.
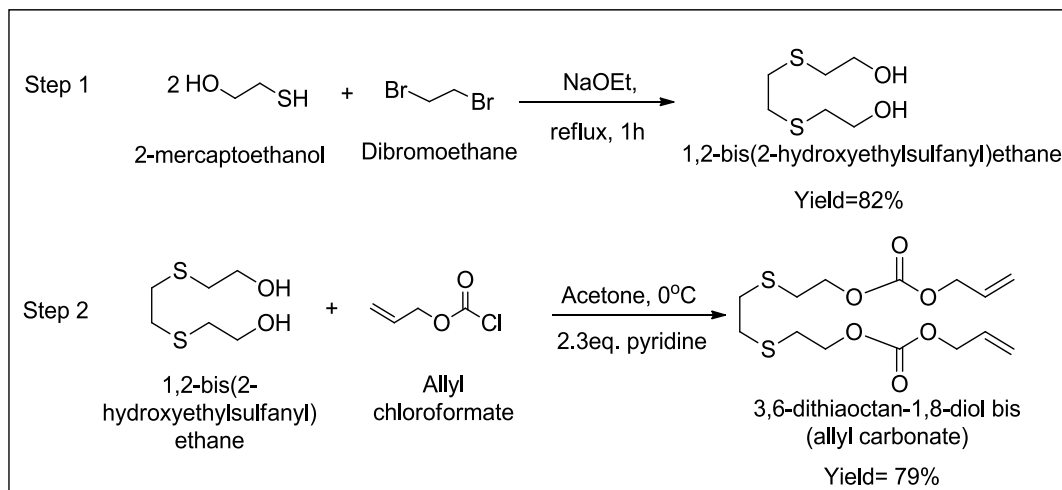
Scheme 3.4: Two step synthesis of 3,6-dithiaoctan-1,8-diol bis (allyl carbonate).

Step 1: Synthesis of 1, 2-bis (2-hydroxyethyl sulfanyl) ethane: Disulfide diol was prepared by reacting dibromoethane with 2 moles of 2-mercaptoethanol[29]. In a three neck, 250 mL flask equipped with double surface condenser at centre socket of the flask and the side necks with stoppers, 100 mL absolute ethanol was taken. To the stirred ethanol, 4.8 g (0.2087 moles) of small pieces of sodium were added in portions till it dissolved completely to get freshly prepared sodium ethoxide. 16.3 g (14.62 mL, 0.2087 moles) 2-mercaptoethanol was then quickly added and the reaction mixture was warmed. 19.58 g (9.00 mL, 0.1042 moles) 1, 2-dibromoethane was added dropwise using pressure equalizing funnel over a period of 1 hour keeping the mixture in warm condition. Further, it was refluxed for 1 h. After cooling back to ambient temperature, it was filtered through celite. The filtrate was concentrated to obtain crude white solid which was purified by column

chromatography using 19:1 chloroform-methanol to yield 15.5 g desired solid product (81.62%). The melting point of the solid was found out to be 61 $^{\circ}$C. It was characterized by IR and NMR spectroscopy (figure3.4a-c; page no. 185-187). IR (KBr): 3360 cm^{-1}, 2956 cm^{-1}, 1006 cm^{-1} and 656 cm^{-1}. ^{1}H NMR (400 MHz, CDCl$_3$) (ppm): 3.69 (t, 4H), 2.72 (s, 4H), 2.70 (t, 4H). ^{13}C NMR (100 MHz, CDCl$_3$) (ppm): 60.79, 35.33 and 32.06.

Step 2: Synthesis of 3,6-dithiaoctan-1,8-diol bis (allyl carbonate): In a round bottom flask, 0.5 g (0.0027 moles) of 1, 2-bis (2-hydroxyethyl sulfanyl) ethane was dissolved in 15 mL dried acetone and 0.498 g (0.51 mL, 0.0063 moles) pyridine was added. The reaction mixture was cooled to 0 $^{\circ}$C with constant stirring. At 0 $^{\circ}$C, 0.79 g (0.7 mL, 0.0063 moles) of allyl chloroformate was slowly added with pressure equalizing funnel. After complete addition, stirring was continued at 0 $^{\circ}$C for 1 hour and then at ambient temperature for another 1 hour. After monitoring the progress of reaction workup was carried out. The acetone was first removed using vacuum pump and the reaction mixture was acidified with 2N HCl solution. The mixture was extracted in diethyl ether and 3-4 brine water washings were given till it became neutral. Water washings were also extracted with diethyl ether and combined organic layers were passed over sodium sulphate. The solvent was removed over rota-vap to obtain 0.79 g (82.25%) crude liquid product. Chromatography of crude product eluting with 20% ethyl acetate in petroleum ether, gave 0.75 g pure pale yellow liquid (79.0 % yield) which was characterized by IR and NMR spectroscopy (figure3.4d-g; page no. 188-191). IR (KBr): 3084 cm^{-1}, 2953 cm^{-1}, 1747 cm^{-1}, 1649 cm^{-1}, 1388 cm^{-1} and 1257 cm^{-1}. ^{1}H NMR (400 MHz, CDCl$_3$) (ppm): 5.97-5.87 (m, 2H), 5.39-5.22 (dd, 4H), 4.62 (d, 4H), 4.26 (t, 4H), 2.84 (s, 4H), 2.76 (t, 4H). ^{13}C NMR (100 MHz, CDCl$_3$) (ppm): 154.71, 131.44, 116.99, 68.53, 66.81, 32.33, 30.29.
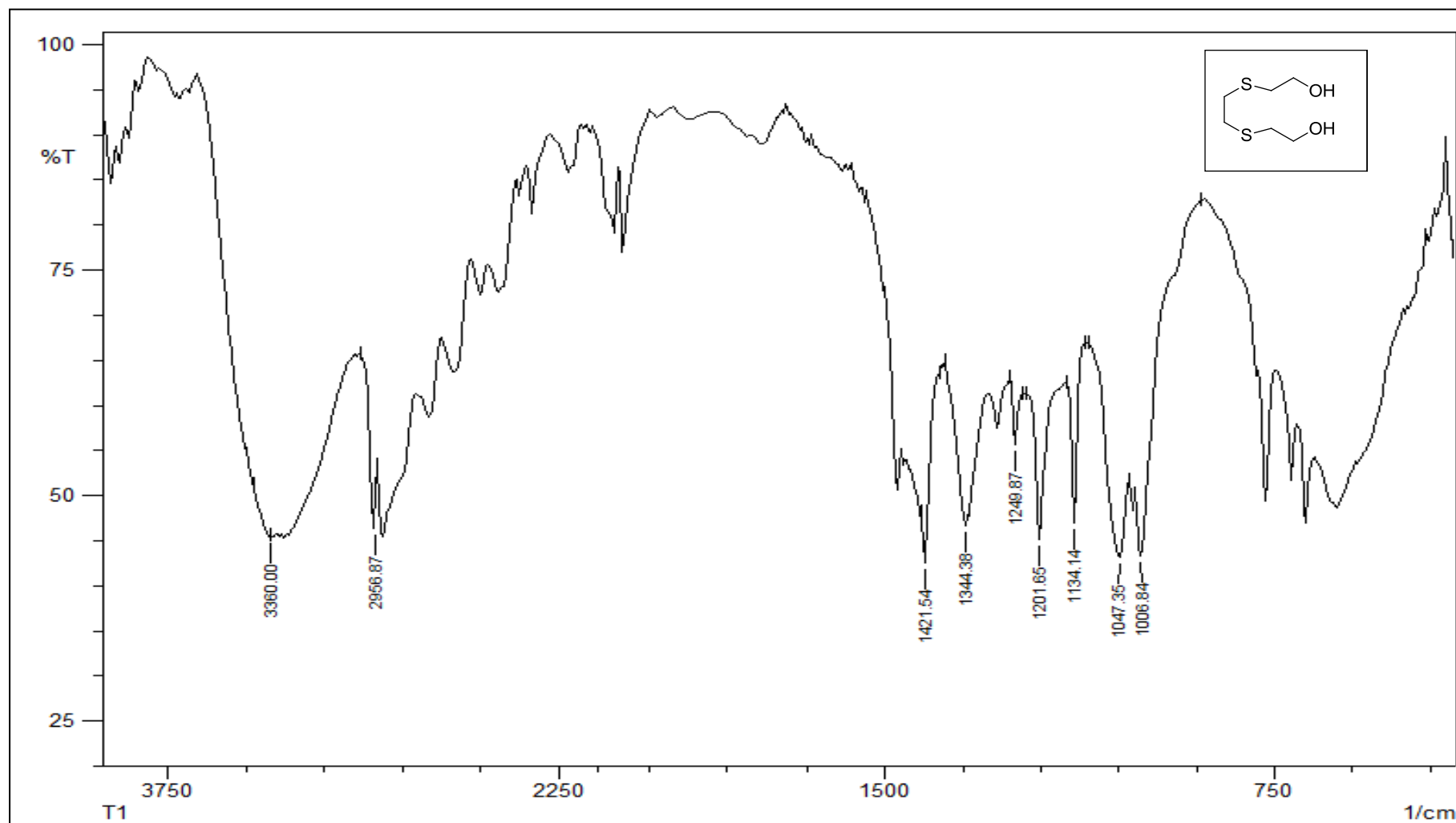
Figure 3.4 (a): IR spectrum of 1,2-bis(2-hydroxyethyl sulfanyl)ethane

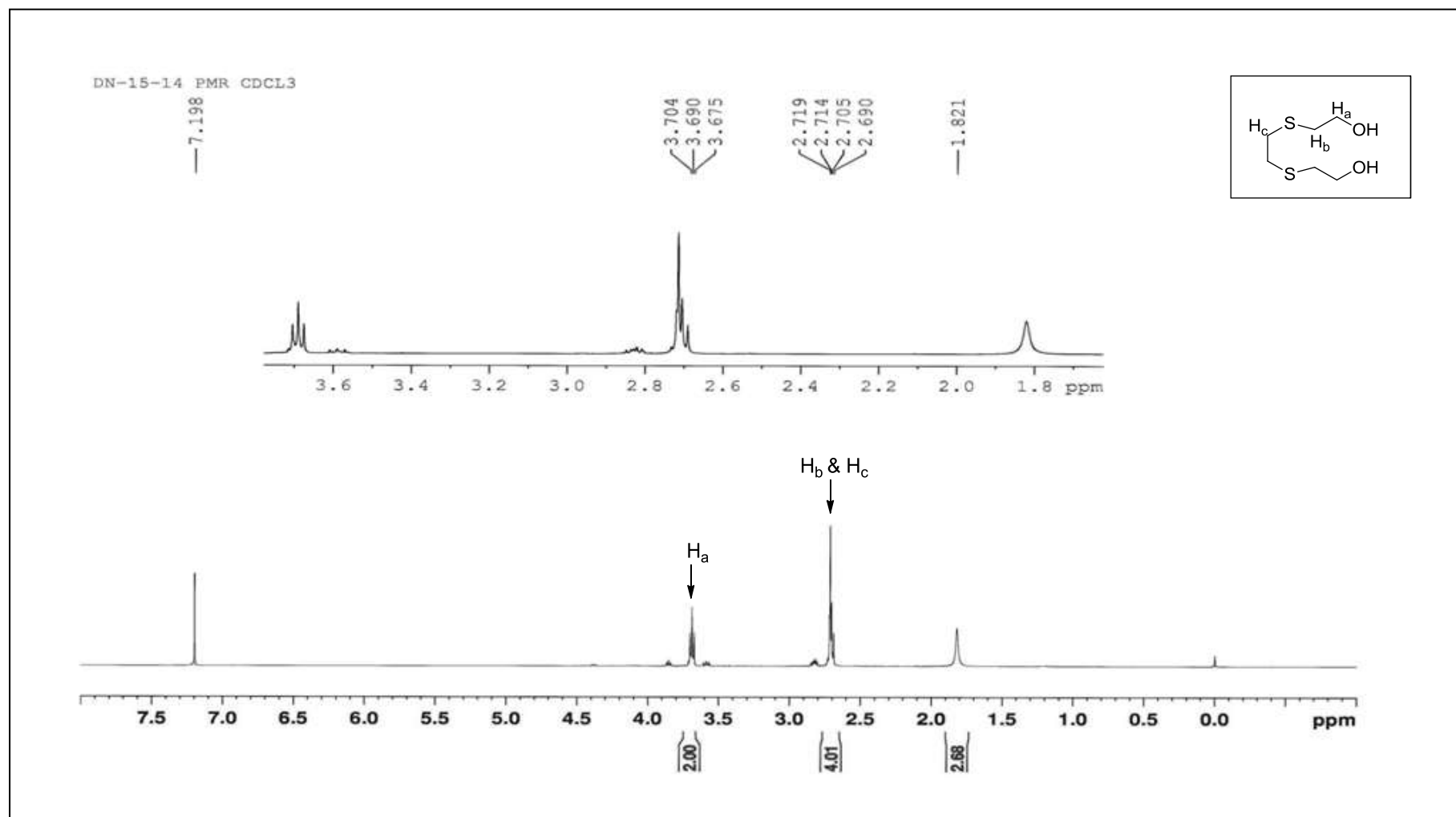**Figure 3.4 (b):** ^{1}H NMR spectrum of 1, 2-bis(2-hydroxyethyl sulfanyl)ethane

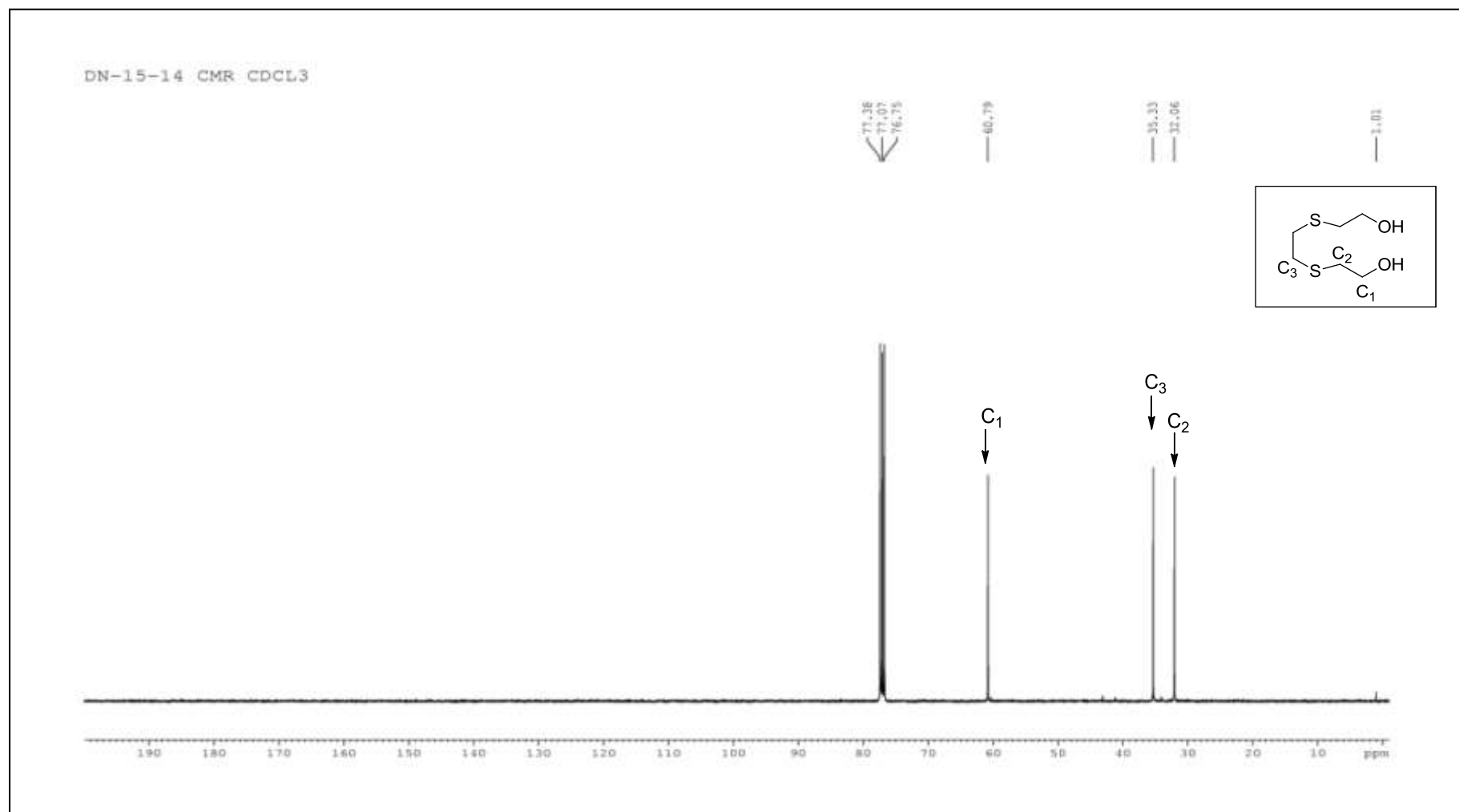**Figure 3.4 (c):** ^{13}C NMR spectrum of 1, 2-bis(2-hydroxyethyl sulfanyl)ethane
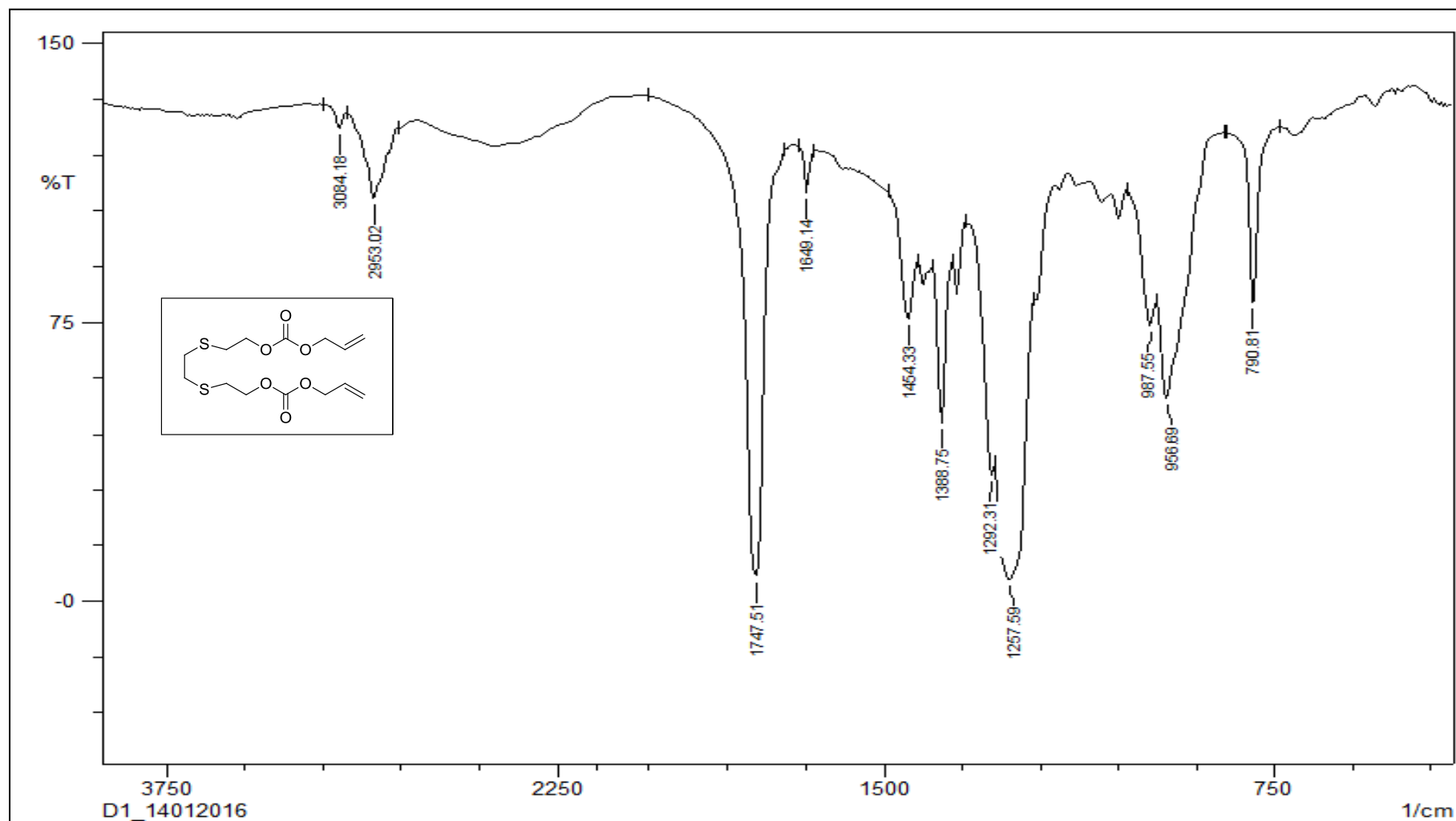
Figure 3.4 (d): IR spectrum of 3,6-dithiaoctan-1,8-diol bis (allyl carbonate)

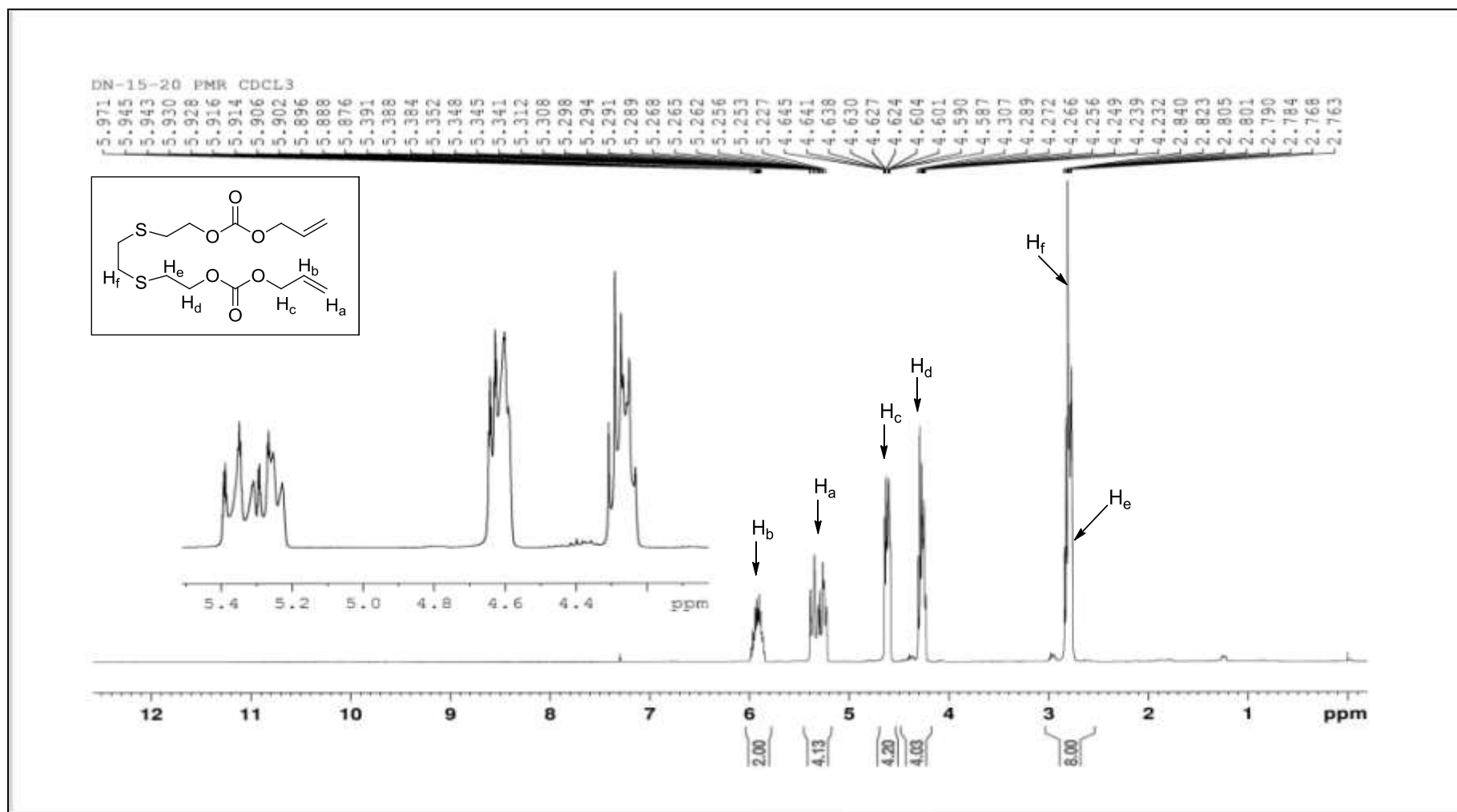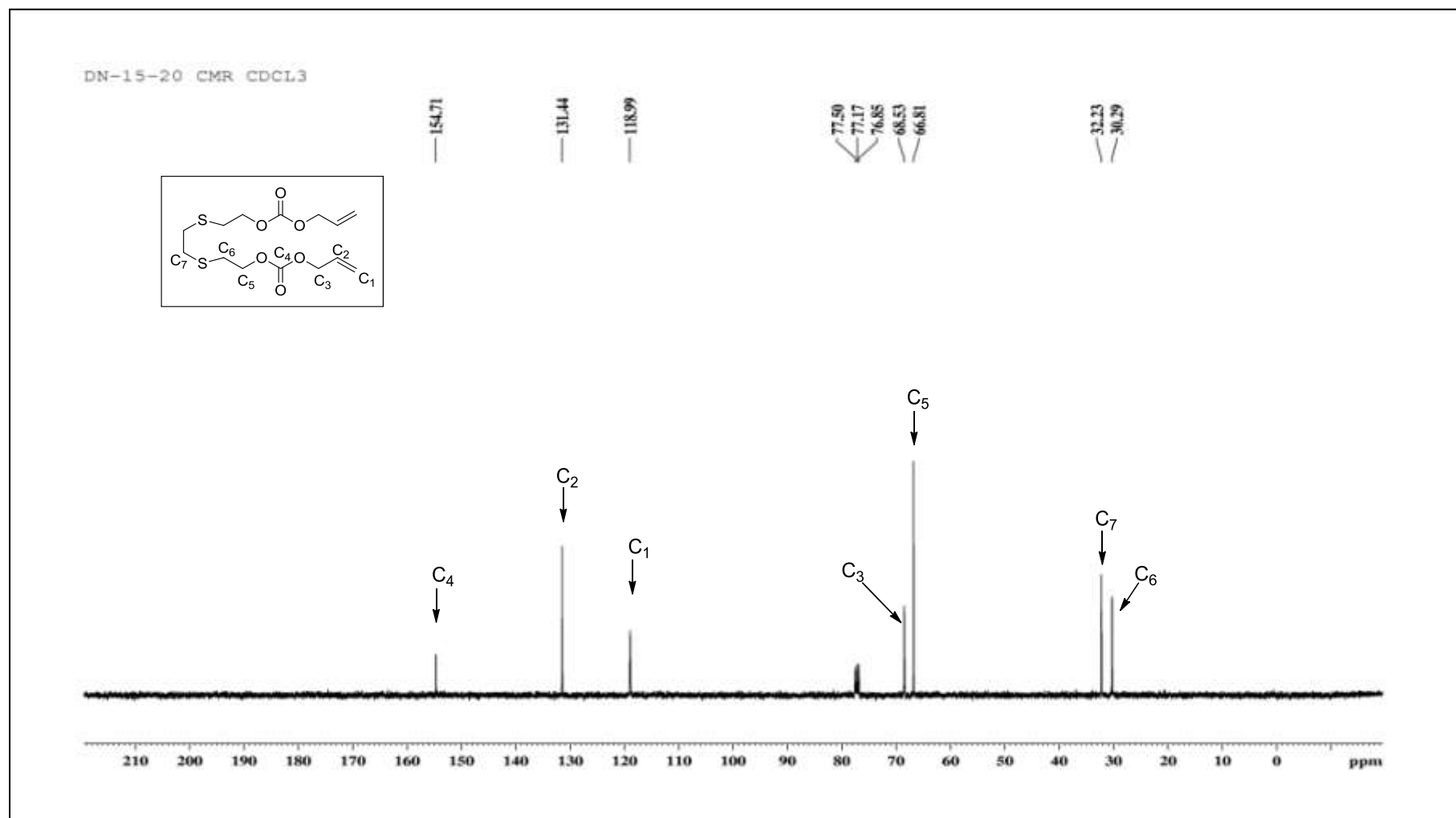**Figure 3.4 (e):** ^{1}H NMR spectrum of 3,6-dithiaoctan-1,8-diol bis (allyl carbonate)

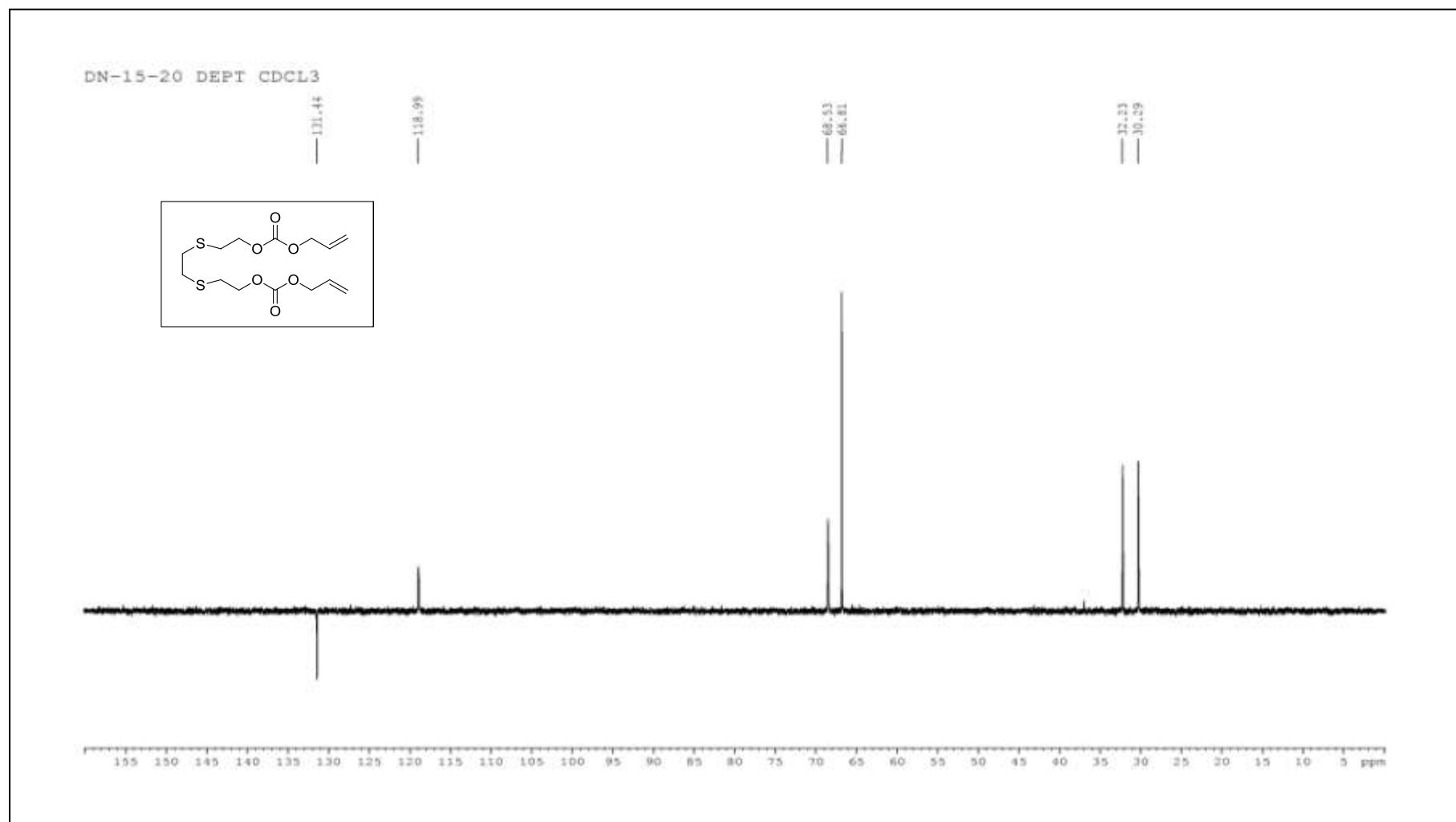**Figure 3.4 (f):**^{13}C-NMR spectrum of 3,6-dithiaoctan-1,8-diol bis (allyl carbonate)

Figure 3.4 (g): DEPT of 3,6-dithiaoctan-1,8-diol bis (allyl carbonate)

3.2.1.3   3,9-dithia-6-oxa-undecane-1,11-diol   bis(allyl carbonate) (M3):

This monomer was synthesised by condensation of 2, 2'- bis (2-hydroxyethylsulfanyl) diethyl ether with allyl chloroformate in presence of base. Following are the two steps involved in the synthesis of desired monomer and scheme 3.5 below depicts the synthetic route.
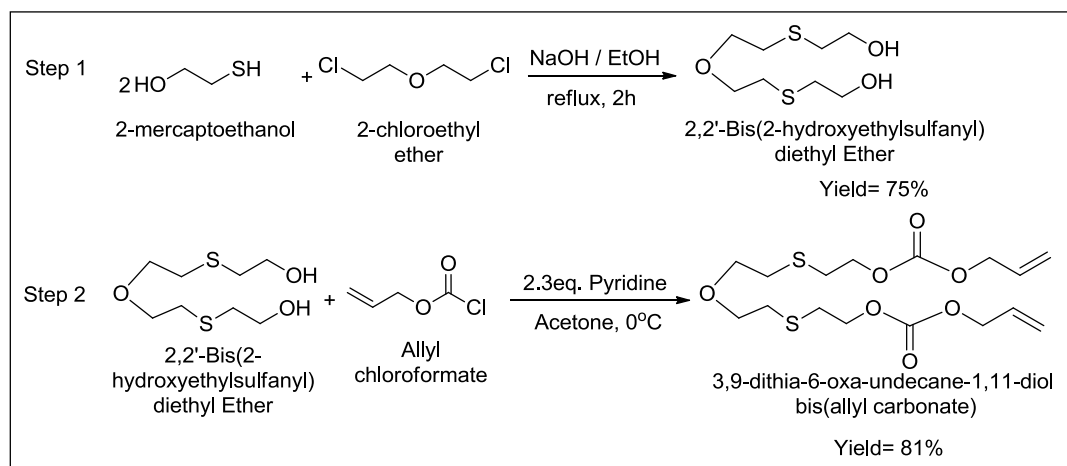
Scheme 3.5: Synthesis of 3,9-dithia-6-oxa-undecane-1,11-diol bis(allyl carbonate)

Step 1: Synthesis of 2, 2'-Bis (2-hydroxyethylsulfanyl) diethyl ether: In a two neck round bottom flask fitted with dropping funnel was added 0.8 g (0.02 moles) sodium hydroxide in 0.8 mL water and 6.5 mL absolute ethanol. 1.5 g (1.35 mL, 0.02 moles) of 2-mercaptoethanol was added to the reacting mixture and heated to 45 ^{o}C. Using dropping funnel 1.4 g (1.15 mL, 0.01 moles) of 2-chloroethyl ether was slowly added over a period of 20 minutes. Further, the reaction mixture was refluxed for 30 minutes and allowed to cool to ambient temperature. It was then filtered over celite and filtrate was concentrated over rotary evaporator to obtain crude product. Column chromatography was carried out to produce pure pale yellow liquid product. Yield of the product obtained was 75%. Spectral characterization was carried out using IR and NMR spectroscopic techniques (figure3.5a-b; page no. 194-195). IR (KBr):

3081 cm^{-1}, 2920 cm^{-1}, 1010 cm^{-1} and 690 cm^{-1}. ^{1}H NMR (400 MHz, CDCl$_3$) (ppm): 3.75 (t, 4H), 2.65 (t, 4H), 2.76 (t, 8H).

Step 2: Synthesis of 3,9-dithia-6-oxa-undecane-1,11-diol bis(allyl carbonate): In a two neck flask fitted with pressure equalizing funnel, 0.5 g (0.0022 moles) 2,2'-bis(2-hydroxyethylsulfanyl) diethyl ether was weighed and dissolved in 10 mL acetone. To this, 0.4 g (0.41 mL, 0.0051 moles) pyridine was added and mixture was cooled to 0 ^{o}C with constant stirring. At 0 ^{o}C, 0.61 g (0.54 mL, 0.0051 moles) allyl chloroformate was added dropwise. After complete addition the reaction mixture was stirred for 30 minutes at 0 ^{o}C and then at ambient temperature for another 30 minutes. Finally, after monitoring the progress of reaction by TLC, workup was carried out. Solvent from reaction mixture was removed till dryness and was slightly acidified with 2N HCl solution. It was then extracted into diethyl ether and the organic layer was washed with brine till it becomes neutral. The washings were also extracted using diethyl ether. Combined organic layers were passed over sodium sulphate and concentrated to get 0.73 g crude liquid product (83% yield) which was purified by column chromatography using 30% ethyl acetate in petroleum ether. The % yield of pale yellow liquid product obtained was 81.0% which was characterized by IR and NMR spectroscopy (figure 3.5c-f; page no. 196-199). IR (KBr): 3084 cm^{-1}, 2953 cm^{-1}, 1747 cm^{-1}, 1649 cm^{-1}, 1388 cm^{-1} and 790 cm^{-1}. ^{1}H NMR (400 MHz, CDCl$_3$) (ppm): 5.95-5.90 (m, 2H), 5.40-5.26 (dd, 4H), 4.63 (t, 4H), 4.29 (t, 4H), 3.65 (t, 4H), 2.84 (t, 4H), 2.76 (t, 4H). ^{13}C NMR (100 MHz, CDCl$_3$): 154.72, 131.54, 118.90, 70.77, 68.47, 66.84, 31.76, 30.74.
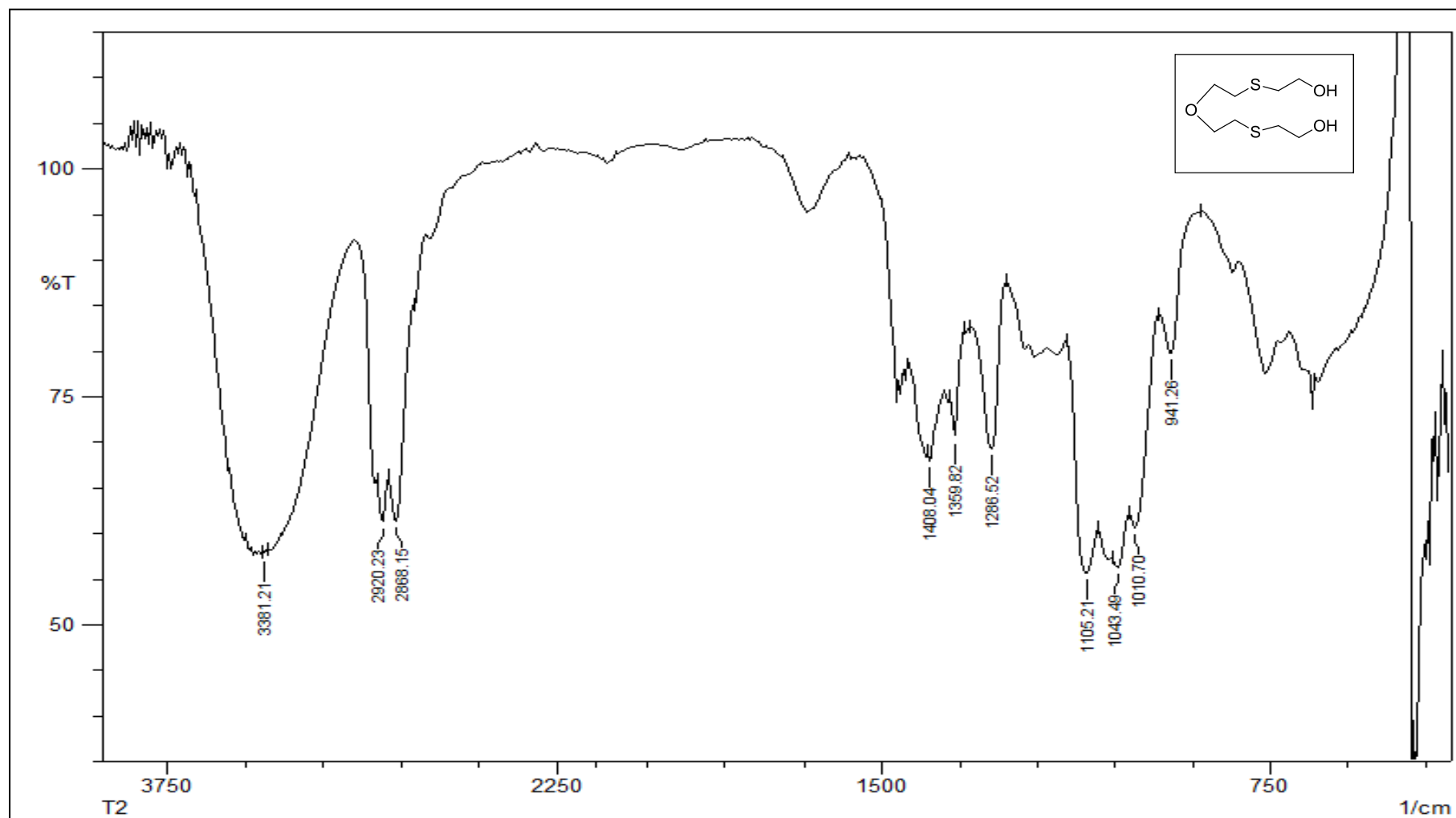
Figure 3.5 (a): IR spectrum of 2, 2'-Bis (2-hydroxyethyl sulfanyl) diethyl ether
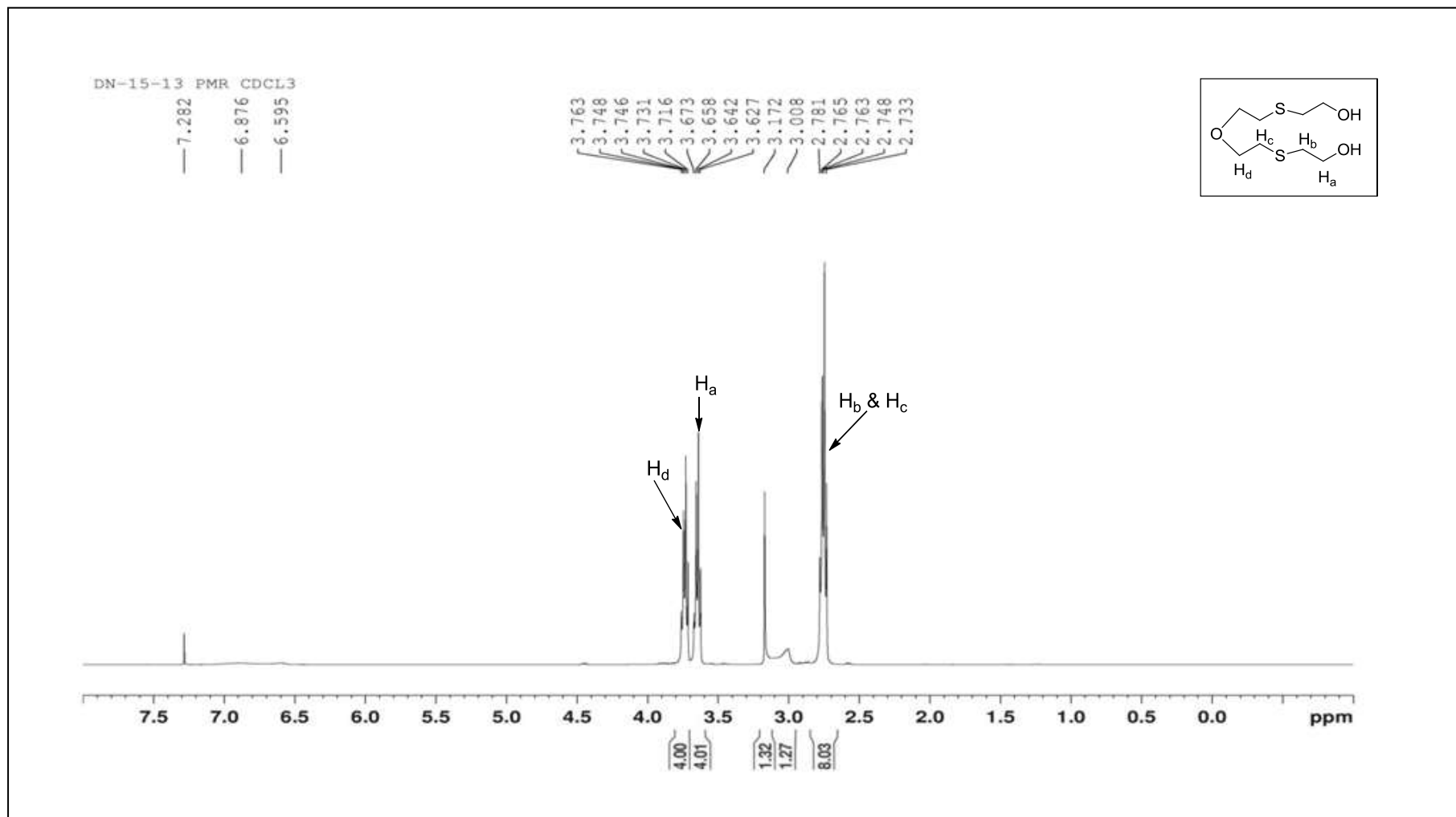
Figure 3.5 (b): NMR spectrum of 2, 2'-Bis (2-hydroxyethyl sulfanyl) diethyl ether
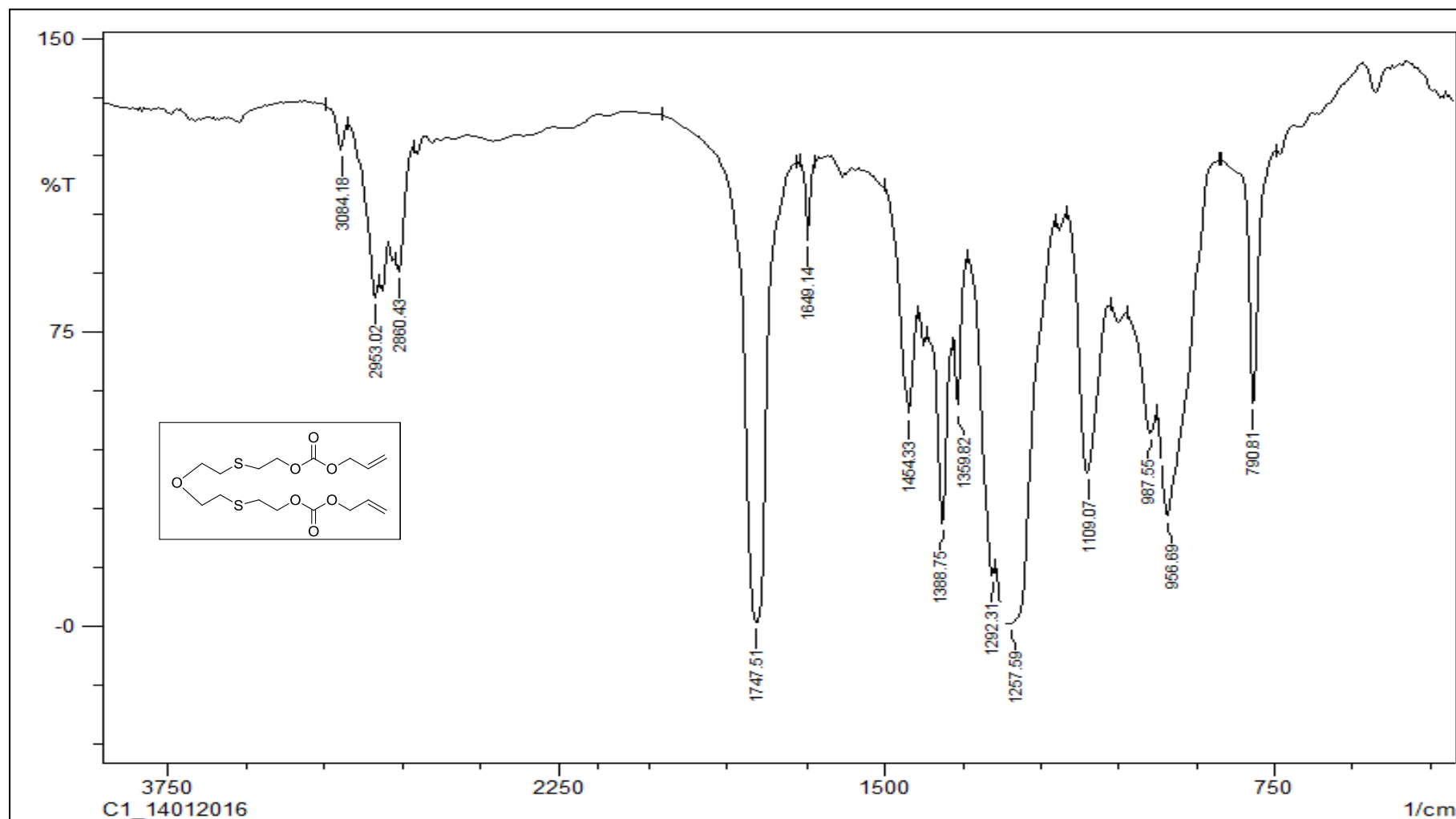
Figure 3.5 (c): IR spectrum of 3,9-dithia-6-oxa-undecane-1,11-diol bis(allyl carbonate)
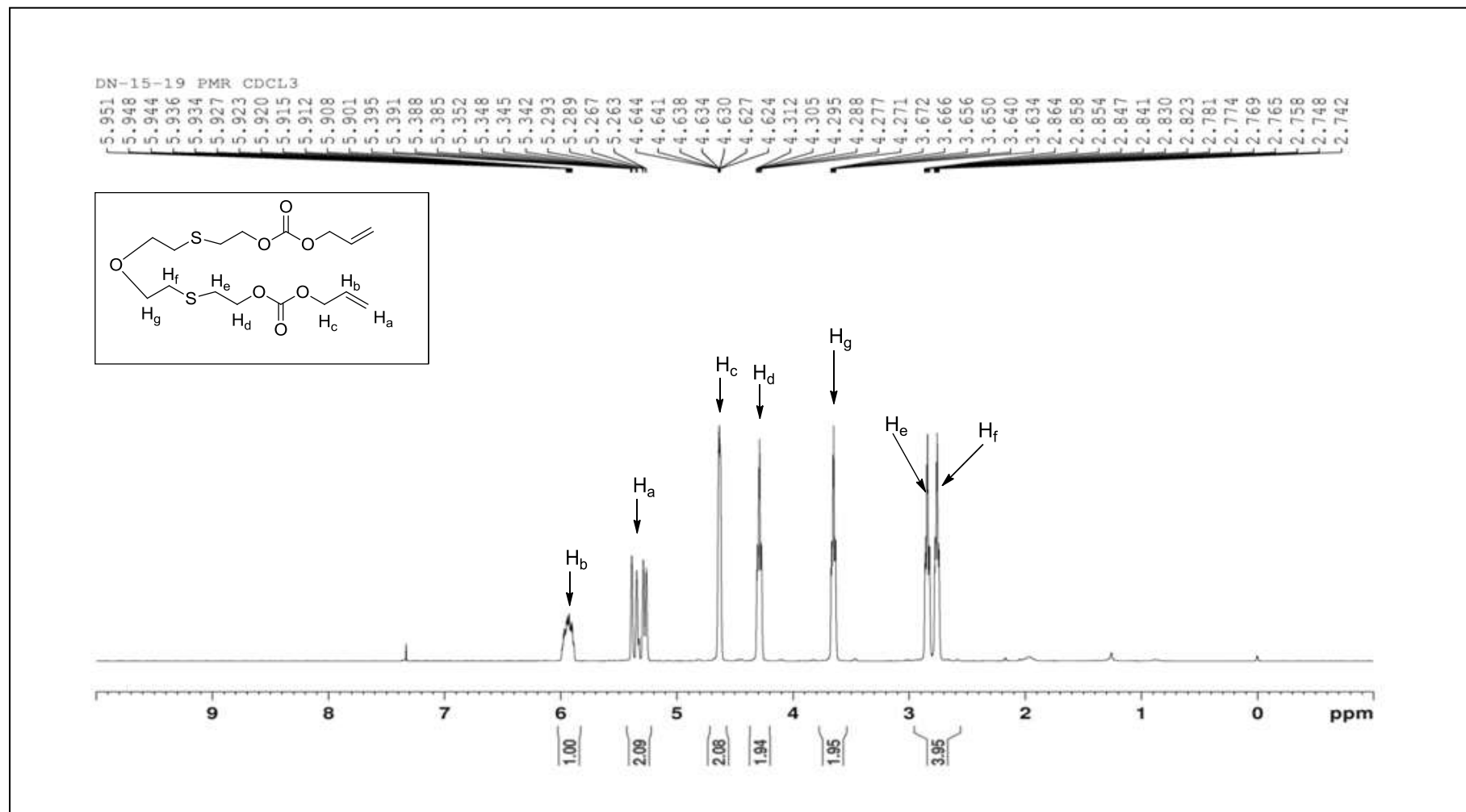
Figure 3.5 (d): NMR spectrum of 3,9-dithia-6-oxa-undecane-1,11-diol bis(allyl carbonate)
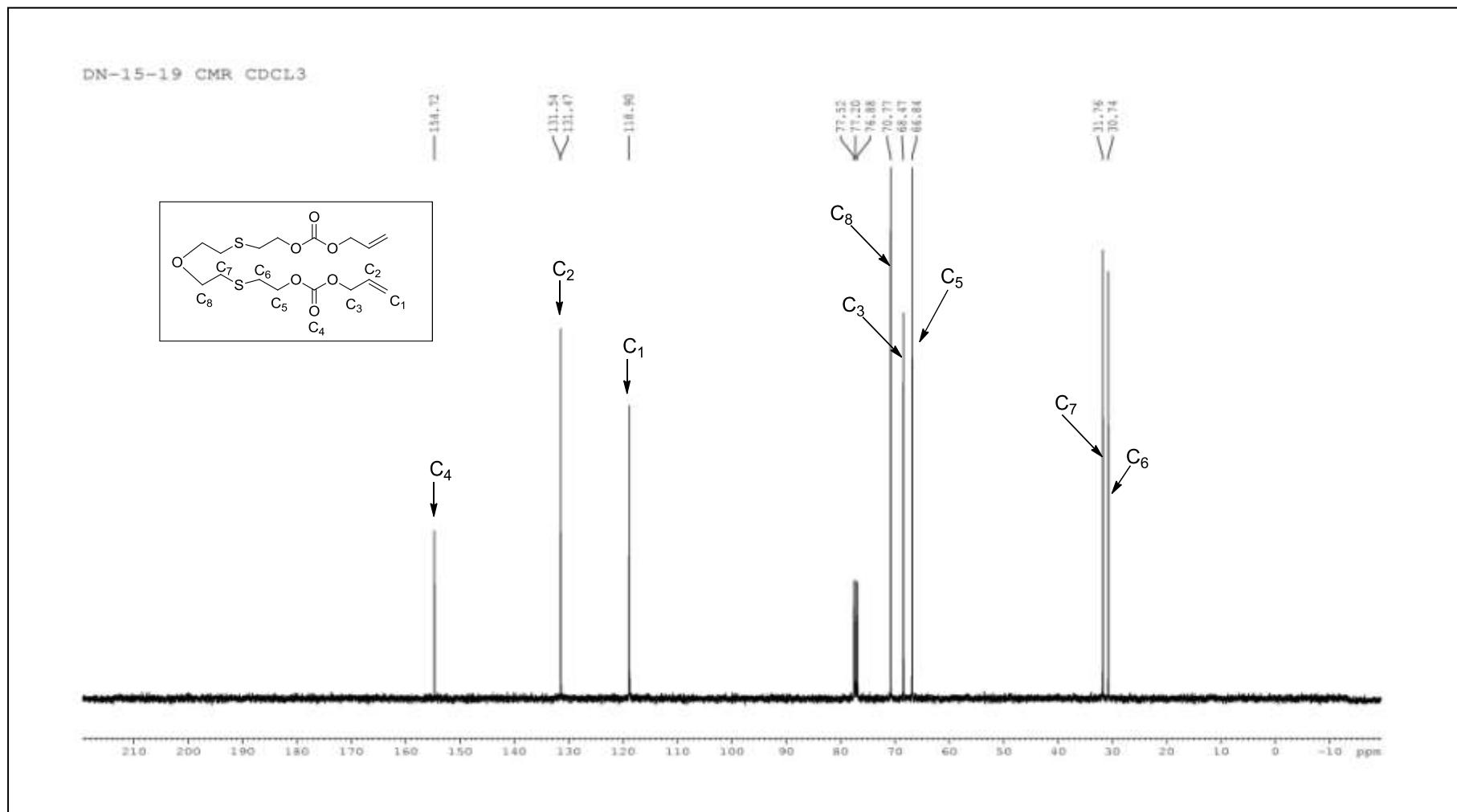
Figure 3.5 (e): ^{13}C-NMR spectrum of 3,9-dithia-6-oxa-undecane-1,11-diol bis(allyl carbonate)
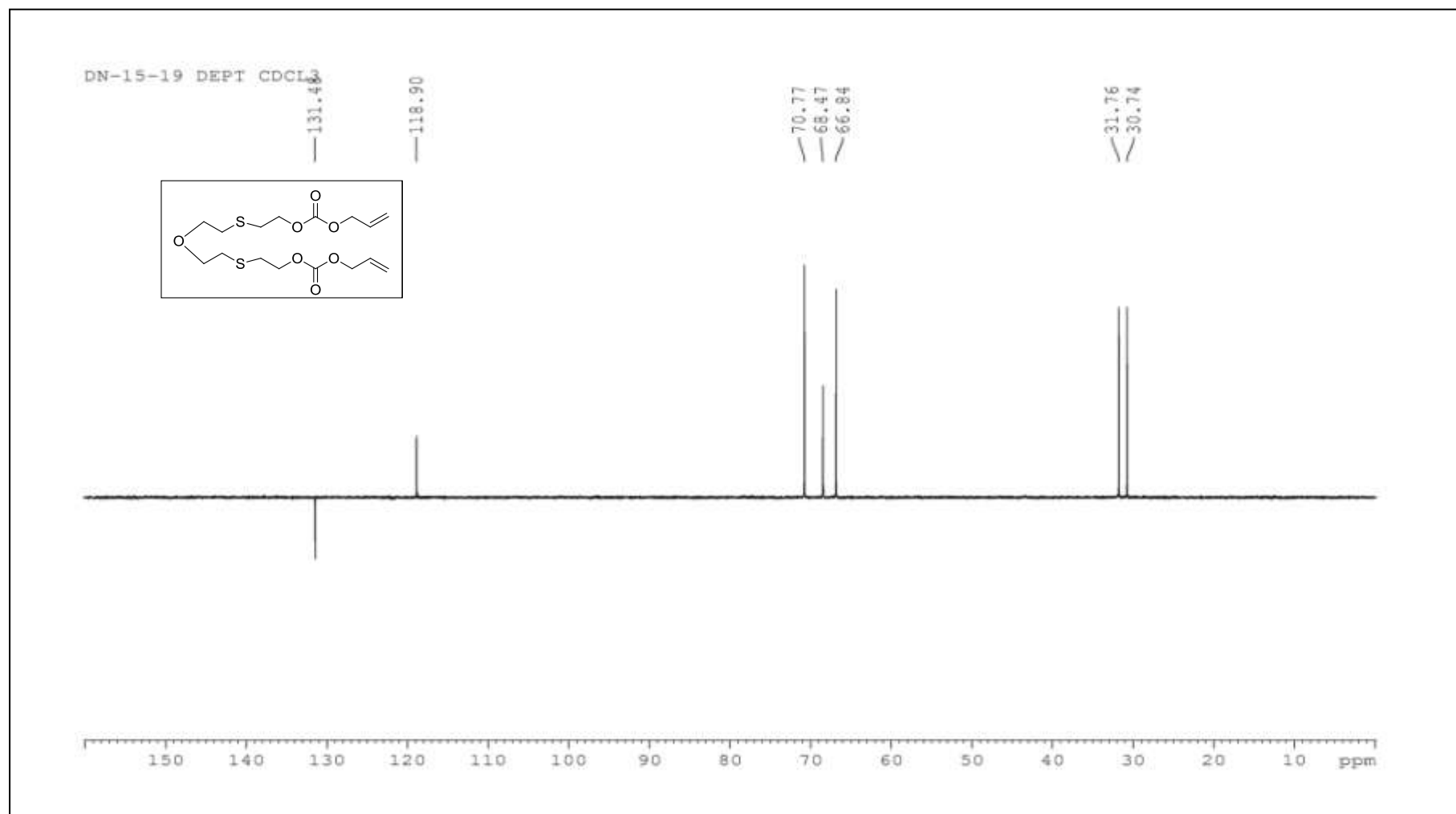
Figure 3.5 (f): DEPT of 3,9-dithia-6-oxa-undecane-1,11-diol bis(allyl carbonate)

3.2.1.4 **2,2'-sulfinyldiethanol bis (allyl carbonate) (M4):** This monomer was synthesised by condensation of allyl thiodiglycol sulfoxide with allyl chloroformate using triethyl amine at lower temperature. Initially oxidation reaction of thiodiglycol to thiodiglycol sulfoxide was carried out using hydrogen peroxide in acidic medium[30]. Stepwise synthesis of 2,2'-sulfinyldiethanol bis (allyl carbonate) is shown in scheme 3.6.
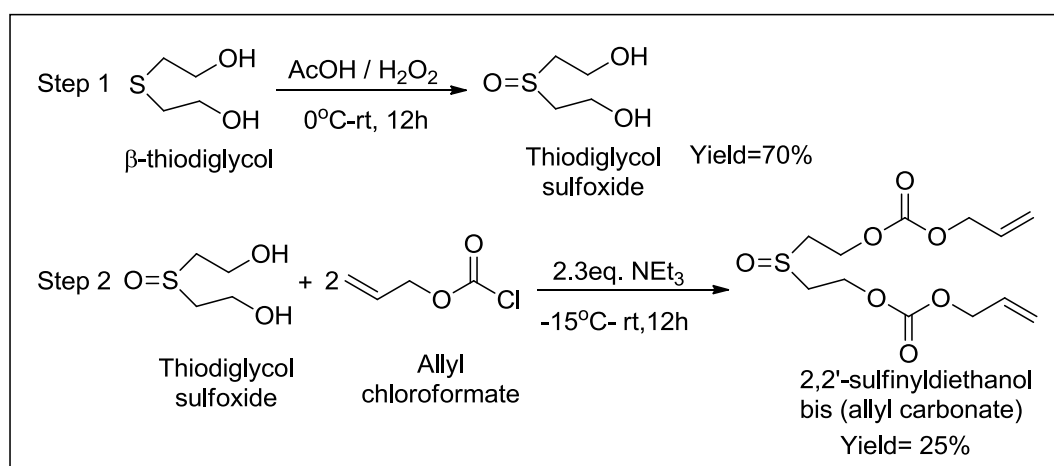
Scheme 3.6: Synthesis of 2,2'-sulfinyldiethanol bis (allyl carbonate) (M4)

*Step 1: Thiodiglycol sulfoxide:* In a two neck reacting flask fitted with pressure equalising funnel, 10.34 g (9.85 mL) glacial acetic acid and 10.01 g (10.30 mL, 0.0818 moles) of 27% H_2O_2 was mixed and cooled to 0-5 ^{o}C in methanol bath. To this cold reaction mixture, 10 g (8.2 mL, 0.0818 moles) of β-thiodiglycol was added dropwise with constant stirring. Care should be taken while adding reactant as it is highly exothermic reaction. Finally, after complete addition, the reaction mixture was stirred overnight for 12 hours at ambient temperature. The acetic acid and excess of hydrogen peroxide was removed over rotavap till dryness. A white solid was formed in the reaction flask which was filtered over Buchner funnel and was washed with diethyl ether, 4-5 times to remove traces of acetic acid. Finally, it was recrystallized from 1:1 methanol and acetone mixture to obtain 7.4 g of colorless

needles of desired product (yield 64.60%). Melting point was found to be 113 ^{o}C. It was characterized by IR and NMR spectra (figure 3.6a-b; page no. 202-203). IR (KBr): 3323 cm^{-1}, 2914 cm^{-1}, 1070 cm^{-1} and 1043 cm^{-1}. ^{1}H NMR (400 MHz, DMSO) (ppm): 3.76 (t, 4H), 2.90 (m, 2H), 2.78 (m, 2H), 2.50 (q, 2H).

Step 2: 2,2'-sulfinyldiethanol bis (allyl carbonate) (M4): In a 100 mL two neck flask fitted with dropping funnel, 2 g (0.0145 moles) of allyl thiodiglycol sulfoxide was suspended in 20 mL acetonitrile. 3.37 g (4.64 mL, 0.0333 moles) of triethyl amine was added and cooled to -5 ^{o}C with constant stirring. At -5 ^{o}C, 4.02 g (3.54 mL, 0.0333 moles) allyl chloroformate was added dropwise using dropping funnel. After the addition was complete, it was stirred for 1 hour at 0 ^{o}C and overnight at ambient temperature. Upon monitoring the progress of reaction by TLC, workup was carried out. Salt formed in the reaction flask was filtered off and acetonitrile was removed from the filtrate over rotavap and extracted in chloroform. Further, it was washed with brine water 4-5 times. The organic layer was passed over sodium sulphate and upon concentrating it crude liquid product was obtained. It was purified by column chromatography using 3:7 ethyl acetate and petroleum ether as mobile phase to get pure liquid compound. It was characterized by IR and NMR spectroscopy (figure 3.6c-f; page no. 204-207). The % yield of the liquid product obtained was 25%. IR (KBr): 3086 cm^{-1}, 2953 cm^{-1}, 1745 cm^{-1}, 1649 cm^{-1}, 1581 cm^{-1} and 1035 cm^{-1}. ^{1}H NMR (400 MHz, CDCl$_3$) (ppm): 5.98-5.88 (m, 2H), 5.40-5.28 (dd, 4H), 4.65 (dt, 4H), 4.60 (t, 4H), 3.15 (m, 2H), 3.05 (m, 2H). ^{13}C NMR (100 MHz, CDCl$_3$): 154.39, 131.15, 119.42, 68.93, 60.24, 51.54.
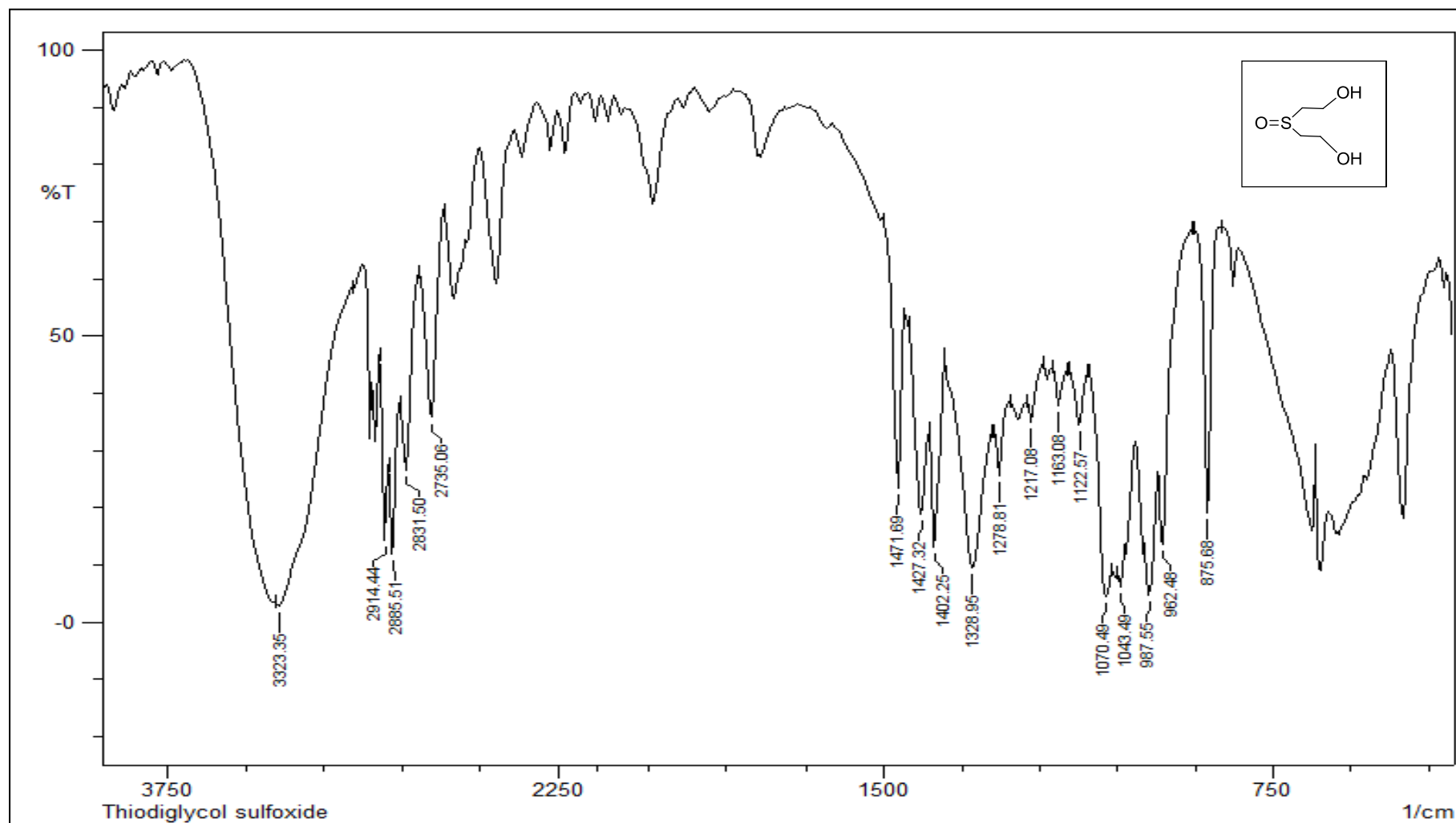
Figure 3.6 (a): IR spectrum of Thiodiglycol sulfoxide

Figure 3.6 (b): NMR spectrum of Thiodiglycol sulfoxide

Figure 3.6 (c): IR spectrum of 2,2'-sulfinyldiethanol bis (allyl carbonate)
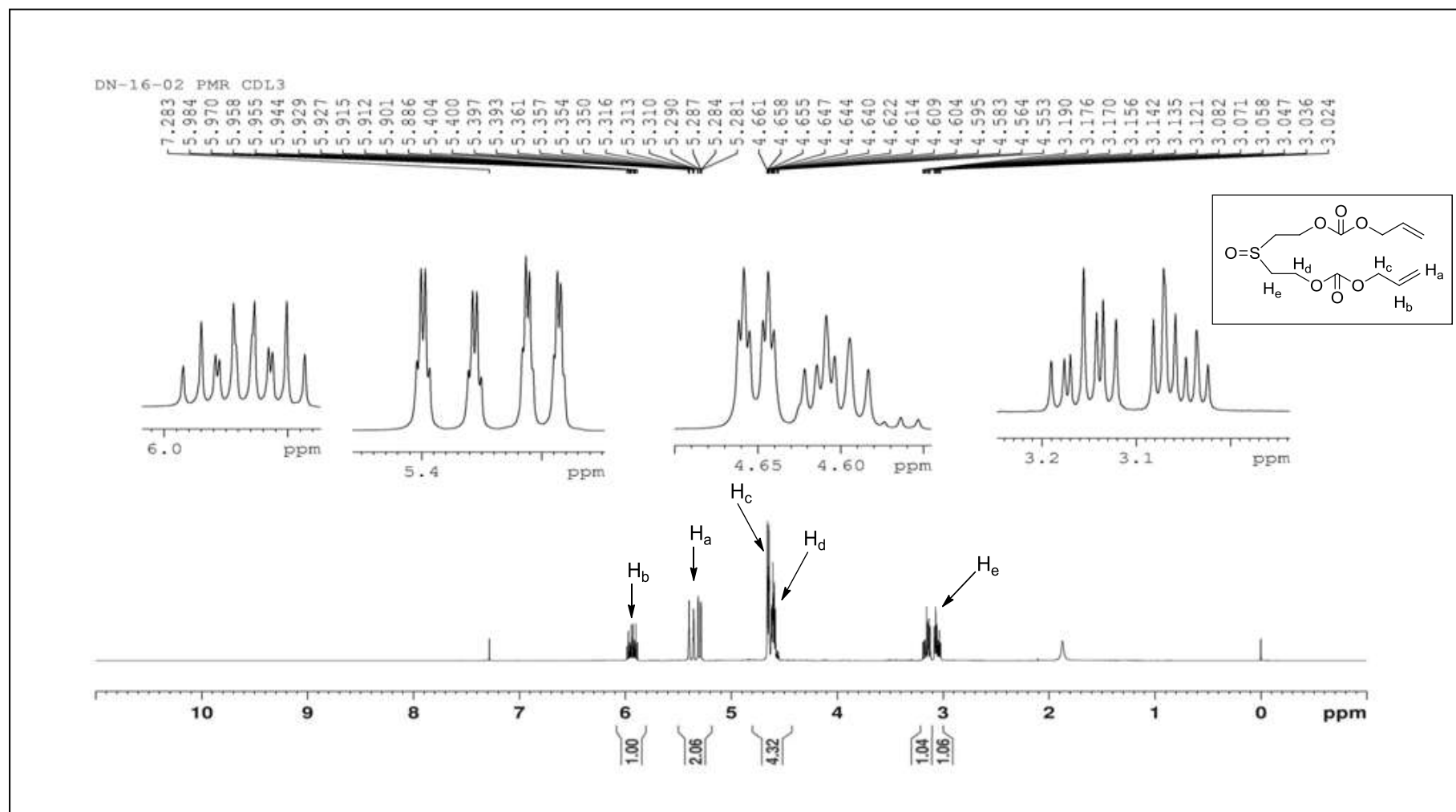
Figure 3.6 (d): NMR spectrum of 2,2'-sulfinyldiethanol bis (allyl carbonate)

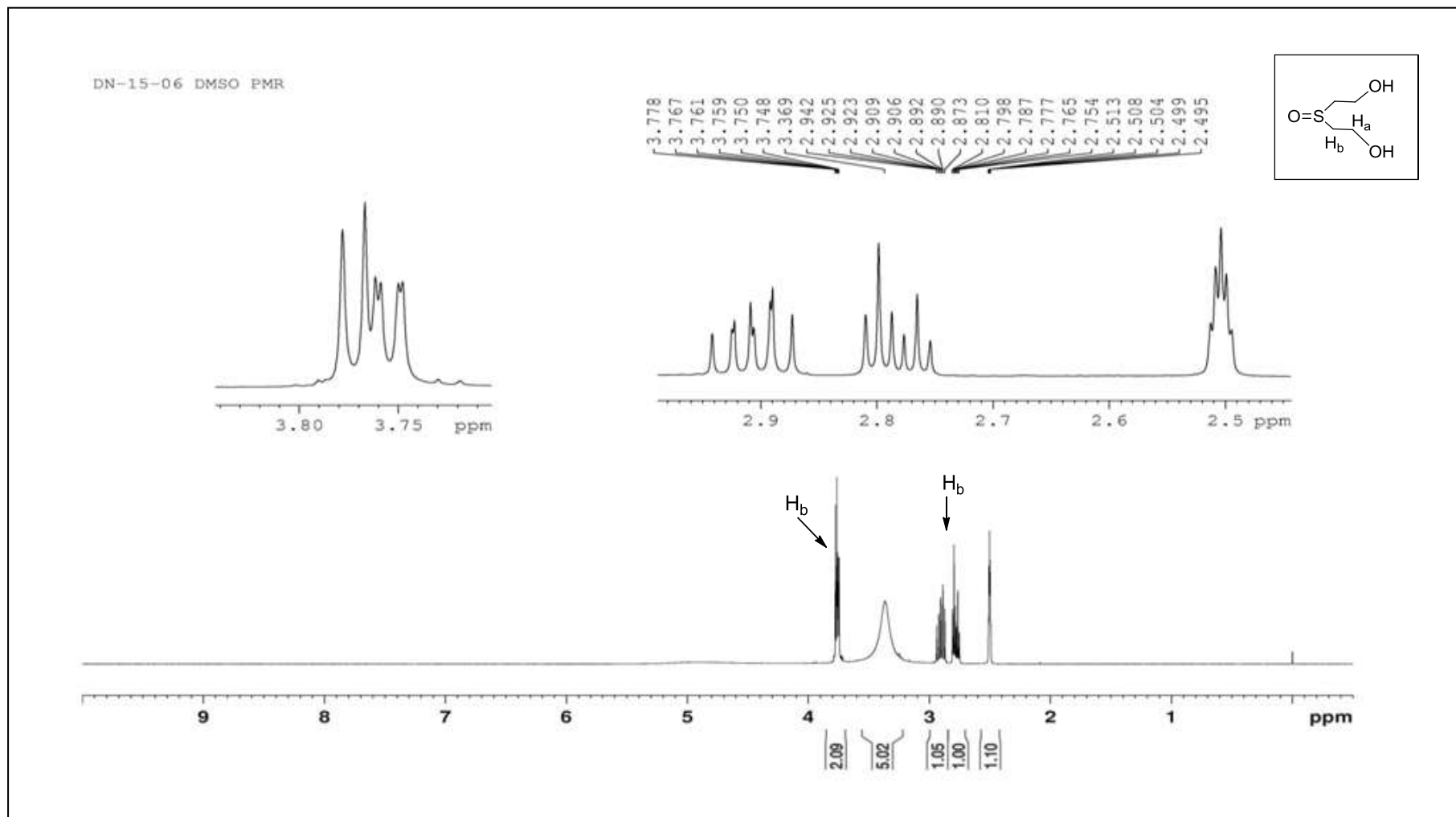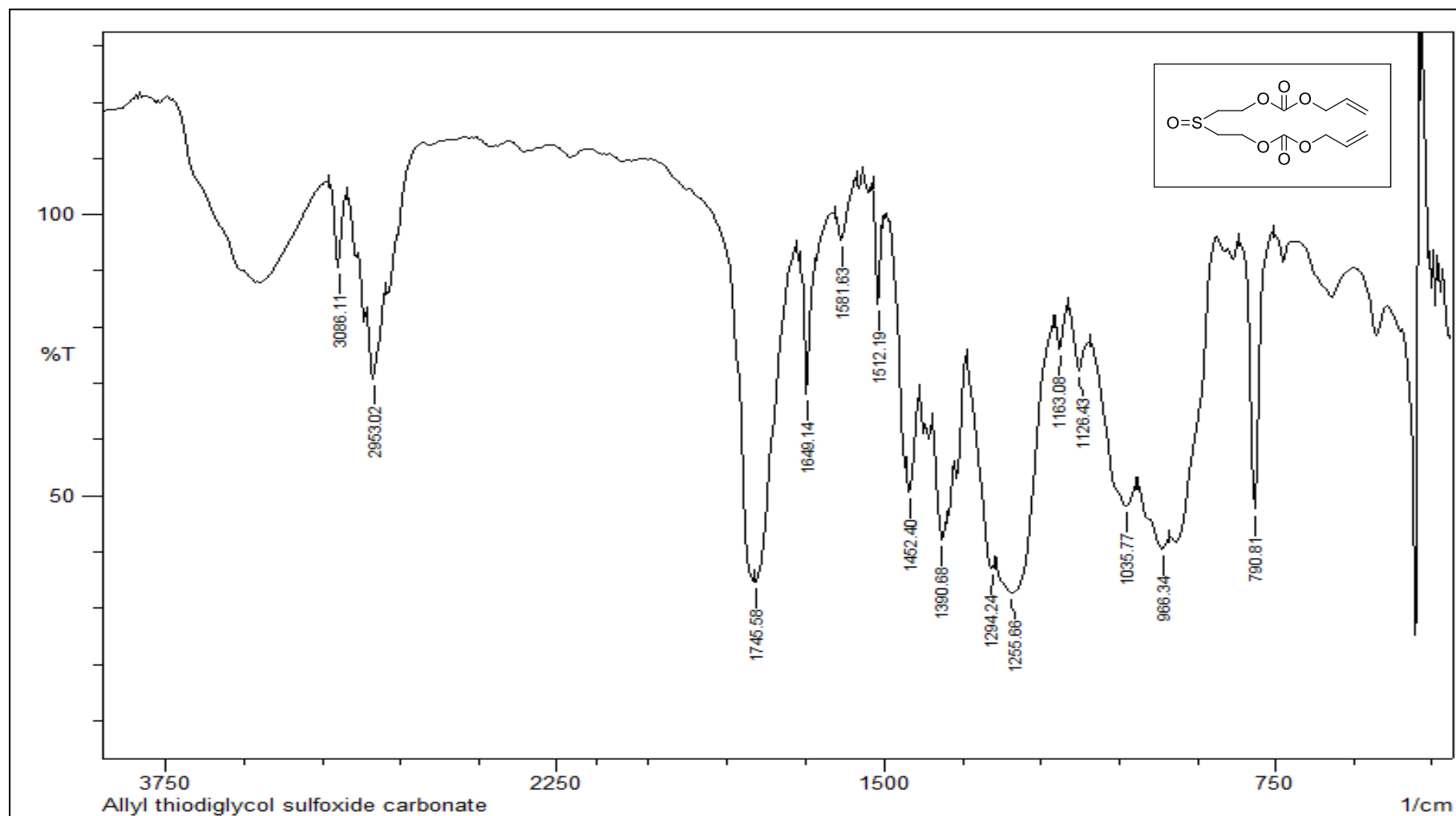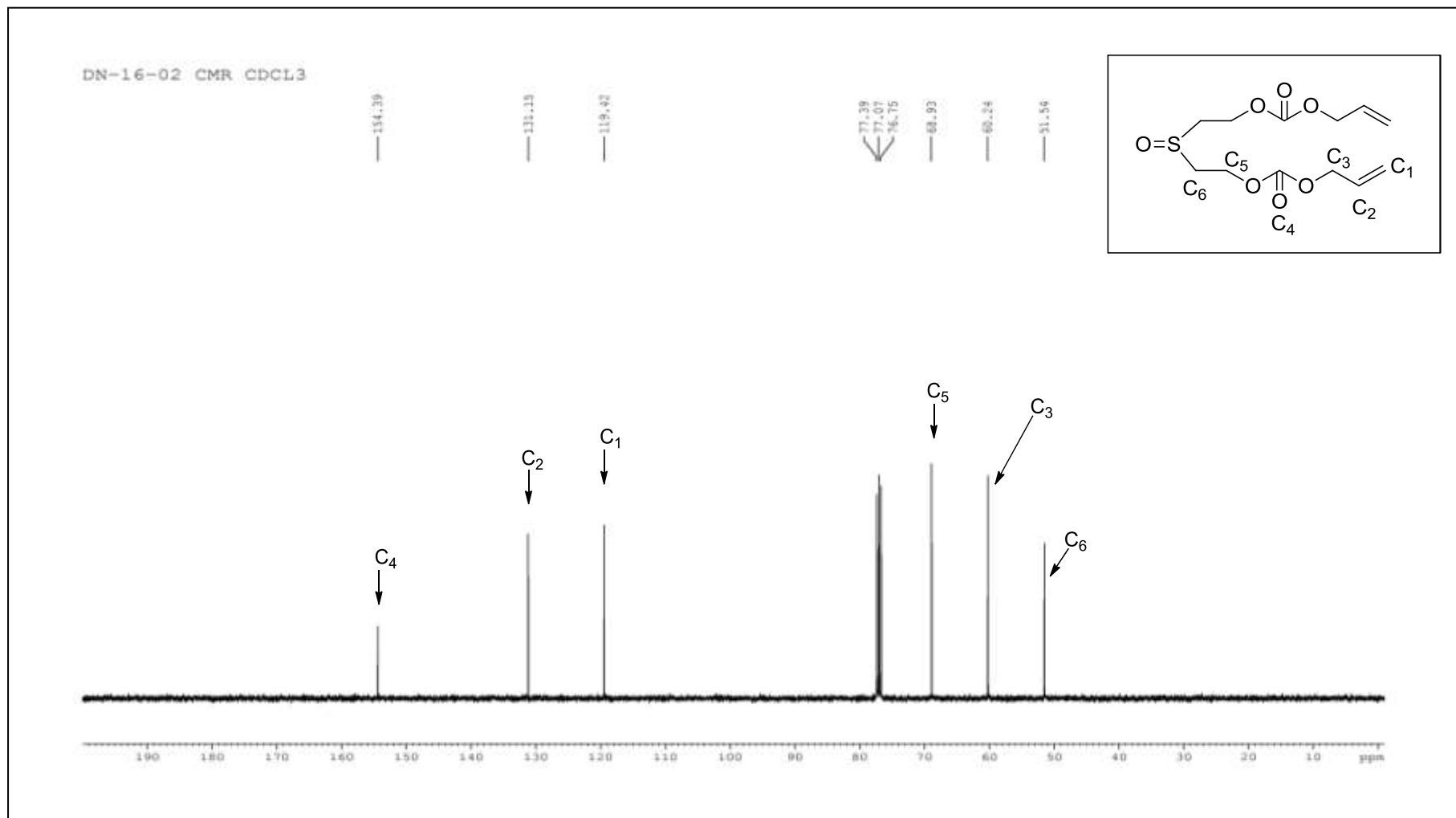**Figure 3.6 (e):** ^{13}C-NMR spectrum of 2,2'-sulfinyldiethanol bis (allyl carbonate)
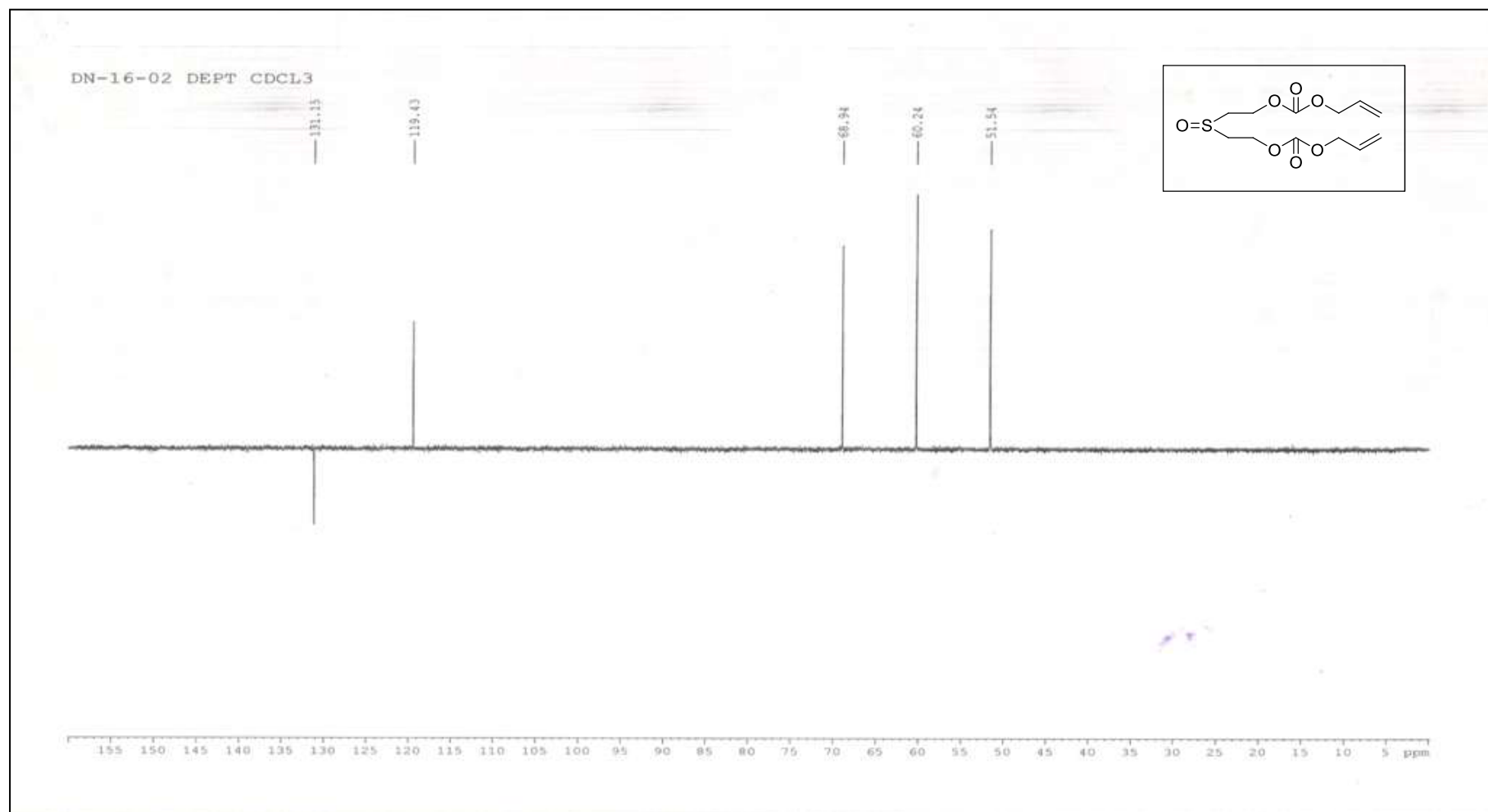
Figure 3.6 (f): DEPT of 2,2'-sulfinyldiethanol bis (allyl carbonate)

3.2.1.5   **2,2'-(ethane-1,2-diyldisulfonyl)diethanol bis (allyl carbonate)**

(M5): To prepare desired monomer (M5), two methods were utilized. In method 1, initially 1, 2- bis (2-hydroxyethylsulfanyl) ethane was oxidized to 1,2-bis(2-hydroxyethylsulfonyl)ethane using hydrogen peroxide (scheme 3.7). The oxidized product was subjected to transesterification process with diallyl carbonate but failed to synthesise desired monomer (M5) (scheme 3.8a). 1,2-bis (2-hydroxy ethylsulfonyl) ethane was further condensed with allyl chloroformate in presence base to give a very low yield (yield=15%) of monomer M5 as shown in scheme 3.8b.

In method 2, previously prepared monomer M2 was directly oxidised using hydrogen peroxide in acidic medium[31]. By this process 70% yield of desired monomer M5 was obtained.

3.2.1.5.1   Method 1: Synthesis of M5 monomer

Step1: Synthesis of 1,2-bis(2-hydroxyethylsulfonyl)ethane: In a 100 mL two neck flask fitted with reflux condenser and a dropping funnel 3.64 g (0.02 moles) 1,2-bis(2-hydroxyethylsulfanyl)ethane was stirred with 20 mL of trifluoroacetic acid. 12 mL (0.082 moles) of 27% hydrogen peroxide was added dropwise to the reaction flask over a period of 1 hour. After complete addition, mixture was refluxed for about 2 hours and then cooled to room temperature. Reaction was monitored by TLC before the workup was carried out. Trifluoroacetic acid and water was removed over rotary evaporator. Traces of acid were removed over high vacuum pump. It was purified by column chromatography using 12:1 chloroform-methanol solvent system. Pure white solid compound was obtained in 75% yield. Scheme 3.7 depicts the synthesis of 1,2-bis(2-hydroxyethylsulfonyl)ethane. It was characterized by IR and NMR spectra (figure 3.7a-b; page no.212- 213). IR (KBr): 3475 cm^{-1}, 2999 cm^{-1},

1336 cm^{-1} and 1143 cm^{-1}. ^{1}H NMR (400 MHz, D$_2$O) (ppm): 3.95 (t, 4H), 3.67 (s, 4H), 3.40 (t, 4H).
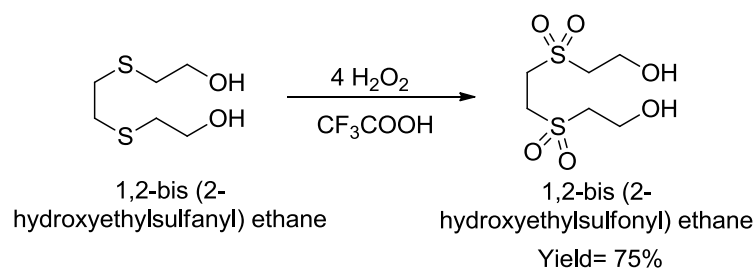
Scheme 3.7: Synthesis of 1, 2-bis(2-hydroxyethylsulfonyl)ethane.

Step 2: Synthesis of **2,2'-(ethane-1,2-diyldisulfonyl)diethanol bis (allyl carbonate) (M5)***:* A two neck round bottom flask was charged with 0.5 g (0.0027 moles) 1,2-bis(2-hydroxyethylsulfonyl)ethane and 10 mL acetone. To this, 0.498 g (0.51 mL, 0.0063 moles) pyridine was added and stirred. The reaction mixture was cooled to -5 ^{o}C and 0.76 g (0.67 mL, 0.0063 moles) allyl chloroformate was added dropwise using addition funnel with constant stirring. It was stirred for an hour at 0 ^{o}C after addition was complete followed by stirring at ambient temperature for 12 hours and the workup was carried out. Acetone was removed using rotary evaporator till dryness; it was acidified by using 2N HCl solution and extracted in diethyl ether. Further, brine water washings were given to the organic layer till it becomes neutral and finally the organic layer was passed over sodium sulphate. The crude solid product obtained was purified by column chromatography. Pure white solid was obtained in 15% yield i.e. very low as shown in scheme 3.8b. It was characterized by using IR and NMR spectral techniques.
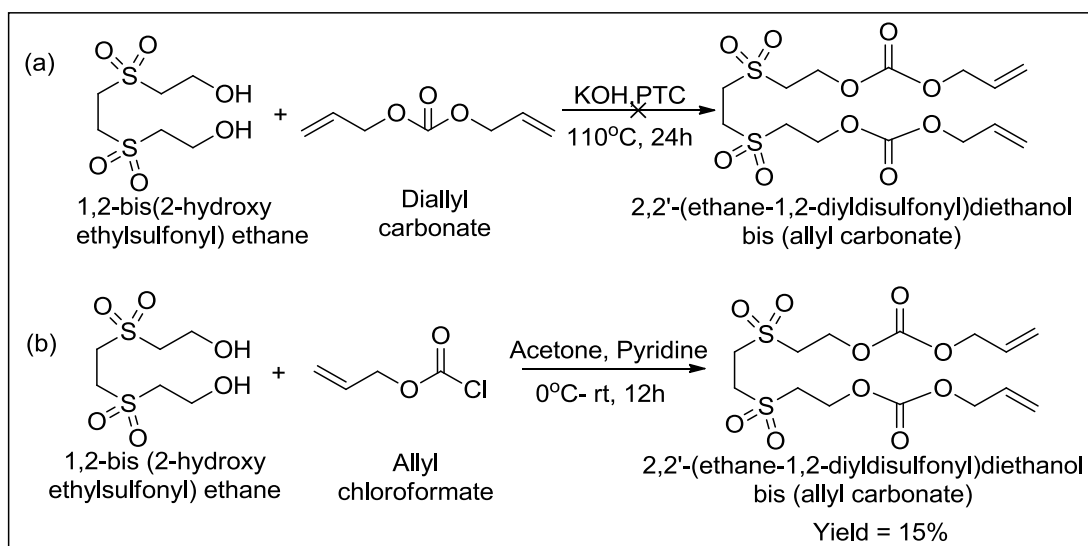
Scheme 3.8: Synthesis of 2,2'-(ethane-1,2-diyldisulfonyl)diethanol bis (allyl carbonate) via (a) Transesterification process (b) Condensation process

3.2.1.5.2 *Method 2: Synthesis of 2,2'-(ethane-1,2-diyldisulfonyl)diethanol bis (allyl carbonate) from 3,6-dithiaoctan-1,8-diol bis (allyl carbonate):* In a two neck flask, 0.13 g (0.3711 mmoles) of 3,6-dithiaoctan-1,8-diol bis (allyl carbonate) (M2) and 0.5 mL glacial acetic acid were added and cooled to 0 ^{o}C in ice bath. To the chilled reaction mixture 0.3 mL (2.2 mmoles) of 28% aqueous hydrogen peroxide was added dropwise. It was stirred for 20 hours at room temperature. The solid obtained in the reaction flask was treated with distilled water and decanted to remove acetic acid. It was filtered and washed with distilled water followed by 2-3 times washing with diethyl ether to remove any impurities. It was then dried over vacuum pump and kept in a vacuum desiccator overnight for drying. 0.107 g of the solid product was obtained (70% yield). Melting point of the compound was 90-92 ^{o}C. It was characterized by IR, NMR and HRMS spectral data (Figure 3.7c-g; page no. 214-218). The synthesis of 1, 2-bis (2-allylcarbonate ethylsulfonyl) ethane is depicted in scheme 3.9. IR (KBr): 3086 cm^{-1}, 2991 cm^{-1}, 1735 cm^{-1}, 1651 cm^{-1}, 1581 cm^{-1}, 1286 cm^{-1} and 1141 cm^{-1}. ^{1}H NMR (400 MHz, CDCl$_3$) (ppm): 5.98-5.88 (m,

2H), 5.41-5.36 (d, 2H), 5.33-5.30 (d, 2H), 4.65 (t, 4H), 4.59 (t, 4H), 3.60 (s, 4H),

3.45 (t, 4H). ^{13}C NMR (100 MHz, CDCl$_3$): 153.97, 130.91, 119.81, 69.27, 60.88,

52.95, 47.24. HRMS: (*m/z*) [M+Na]$^+$ calculated for C$_{14}$H$_{22}$O$_{10}$S$_2$Na: 437.0552;

found: 437.0552.
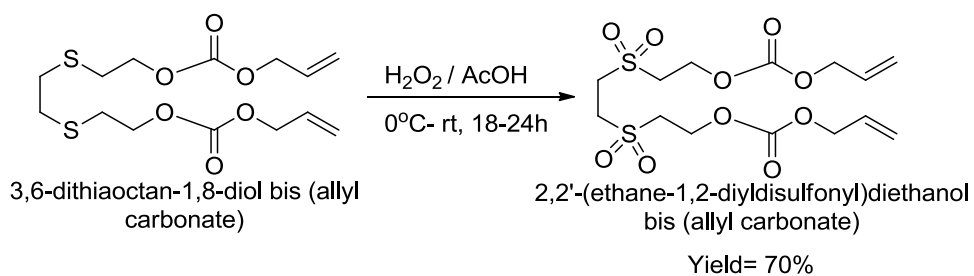
Scheme 3.9: Synthesis of 2,2'-(ethane-1,2-diyldisulfonyl)diethanol bis (allyl
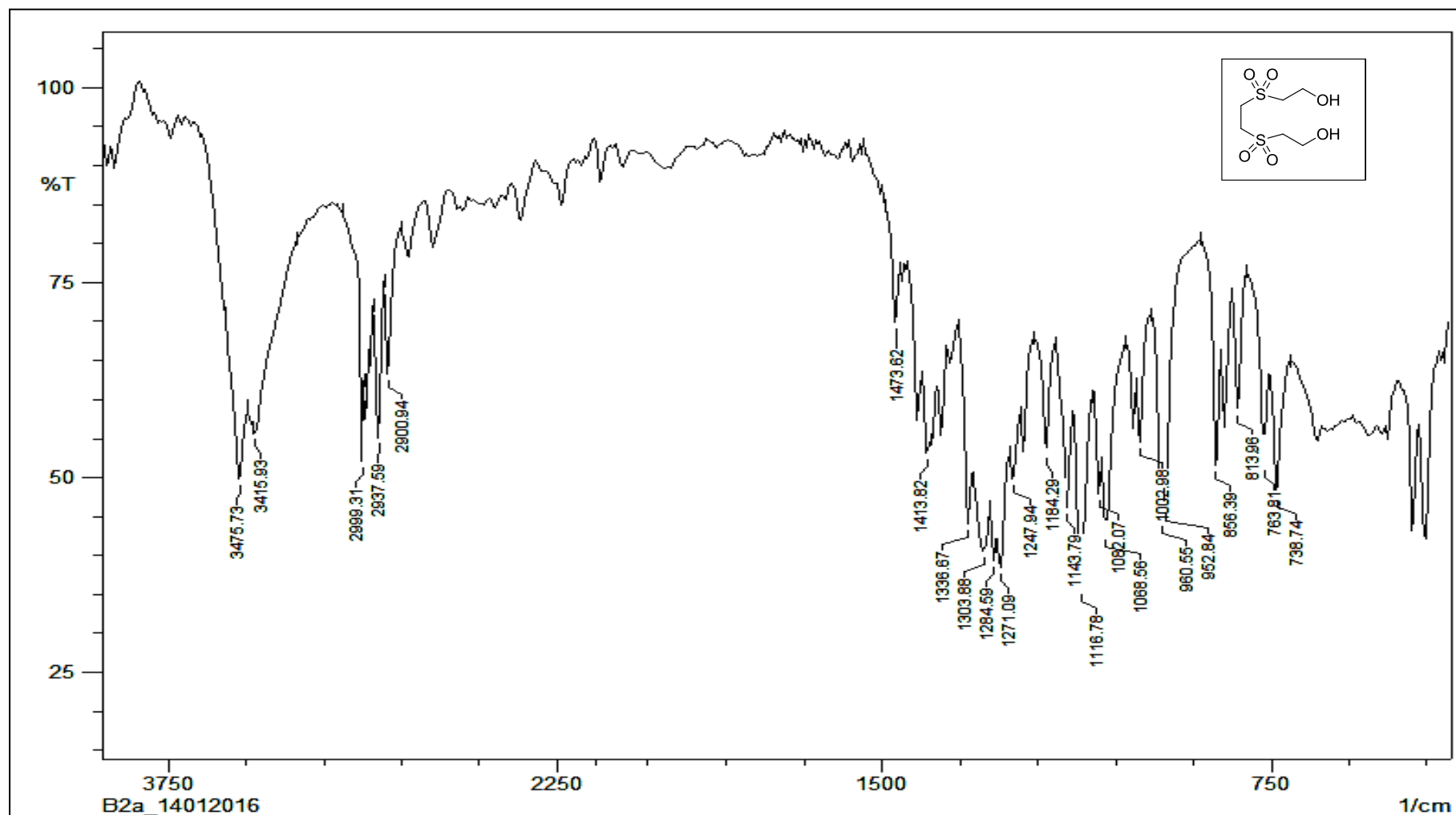
carbonate)

Figure 3.7 (a): IR spectrum of 1, 2-bis (2-hydroxyethylsulfonyl) ethane
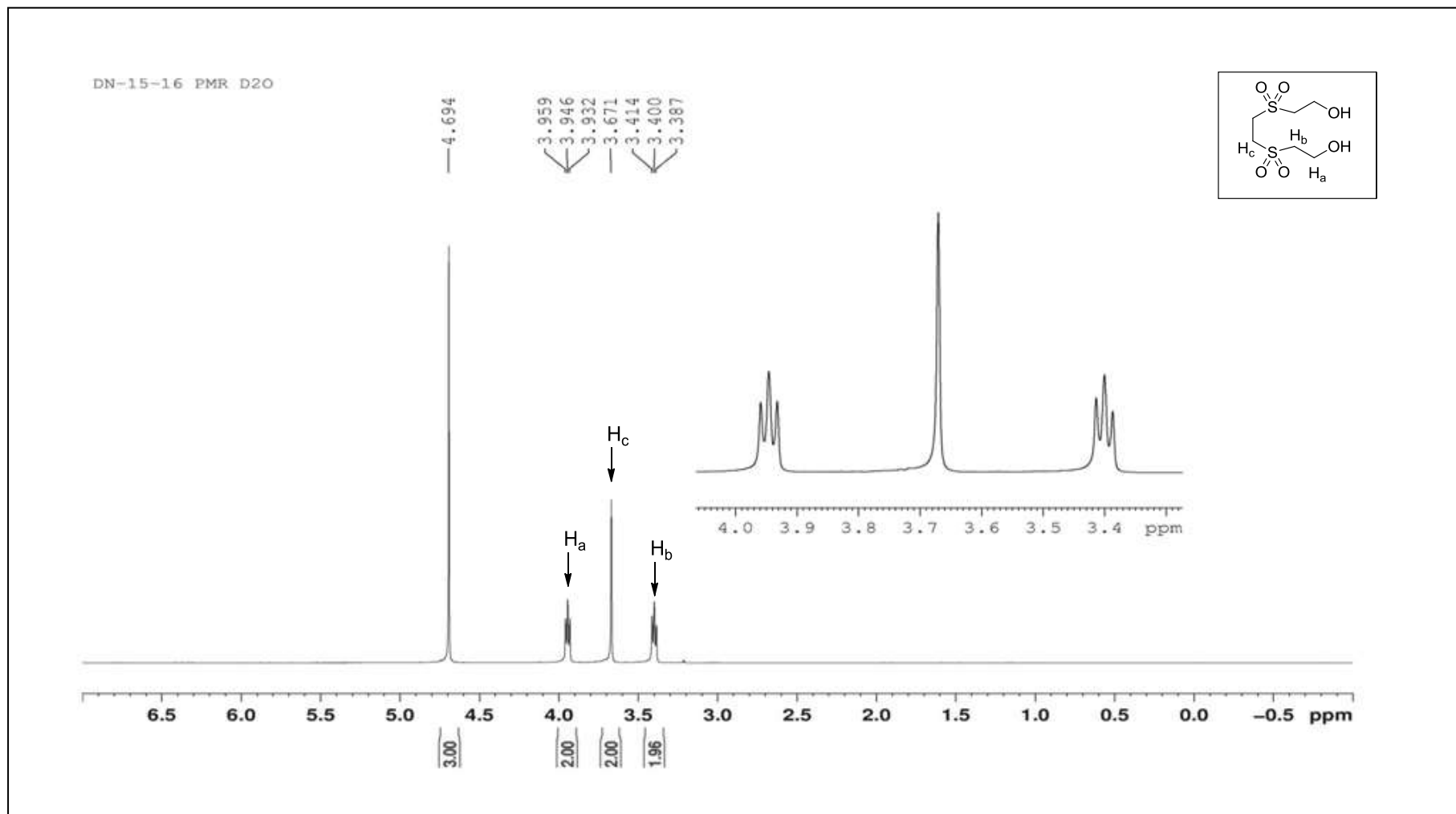
Figure 3.7 (b): NMR spectrum of 1, 2-bis (2-hydroxyethylsulfonyl) ethane
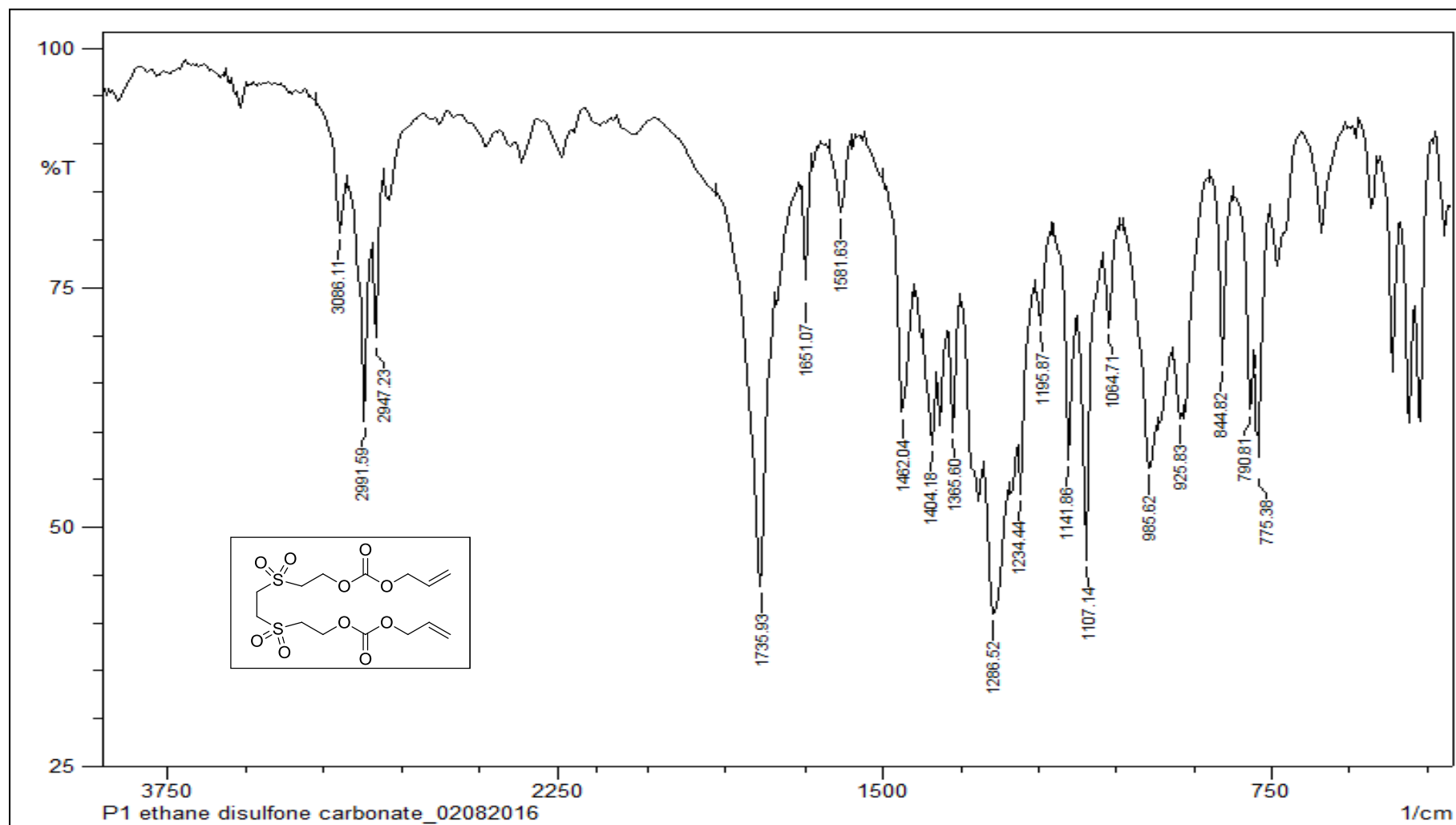
Figure 3.7 (c): IR spectrum of 2,2'-(ethane-1,2-diyldisulfonyl)diethanol bis (allyl carbonate)
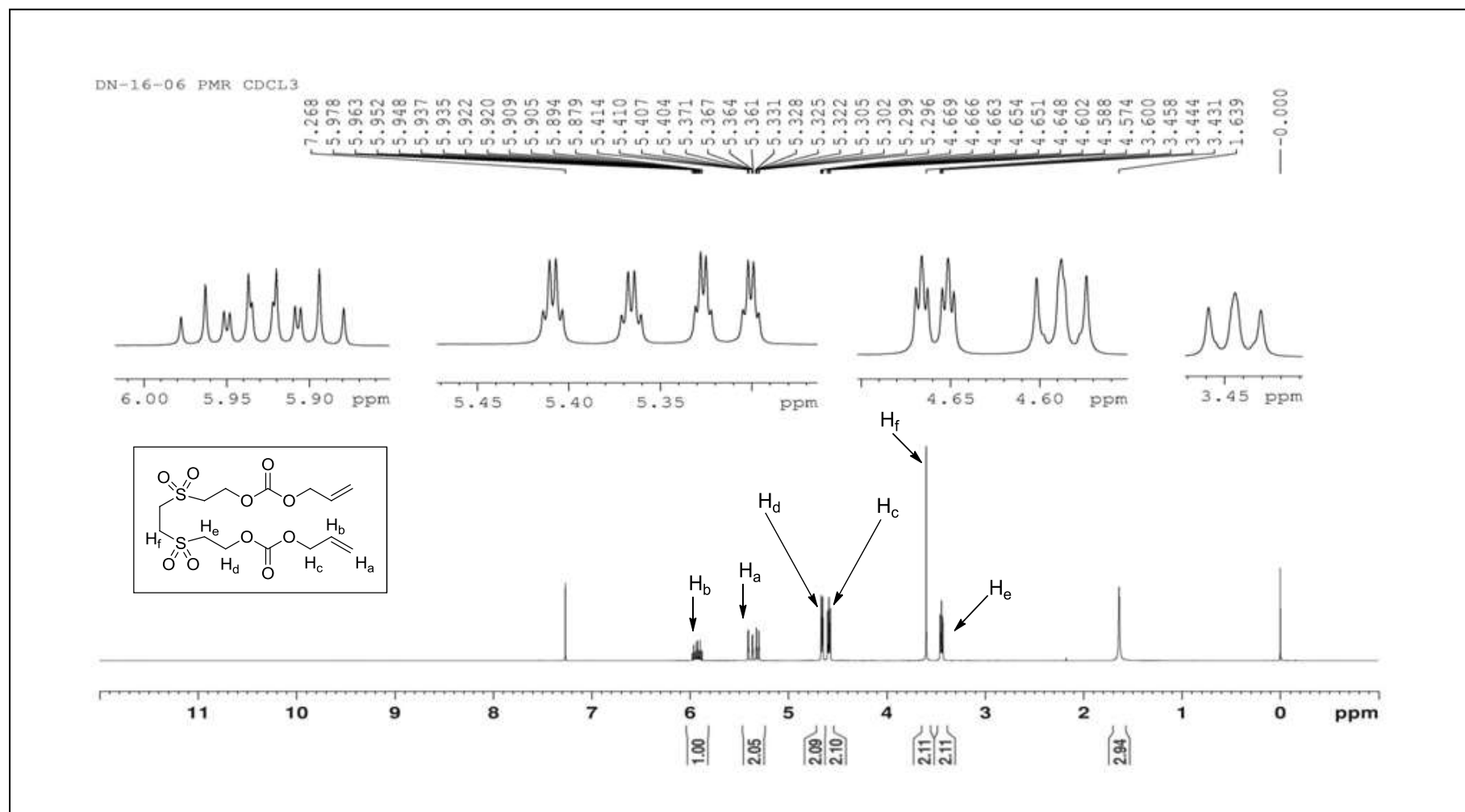
Figure 3.7 (d): NMR spectrum of 2,2'-(ethane-1,2-diyldisulfonyl)diethanol bis (allyl carbonate)
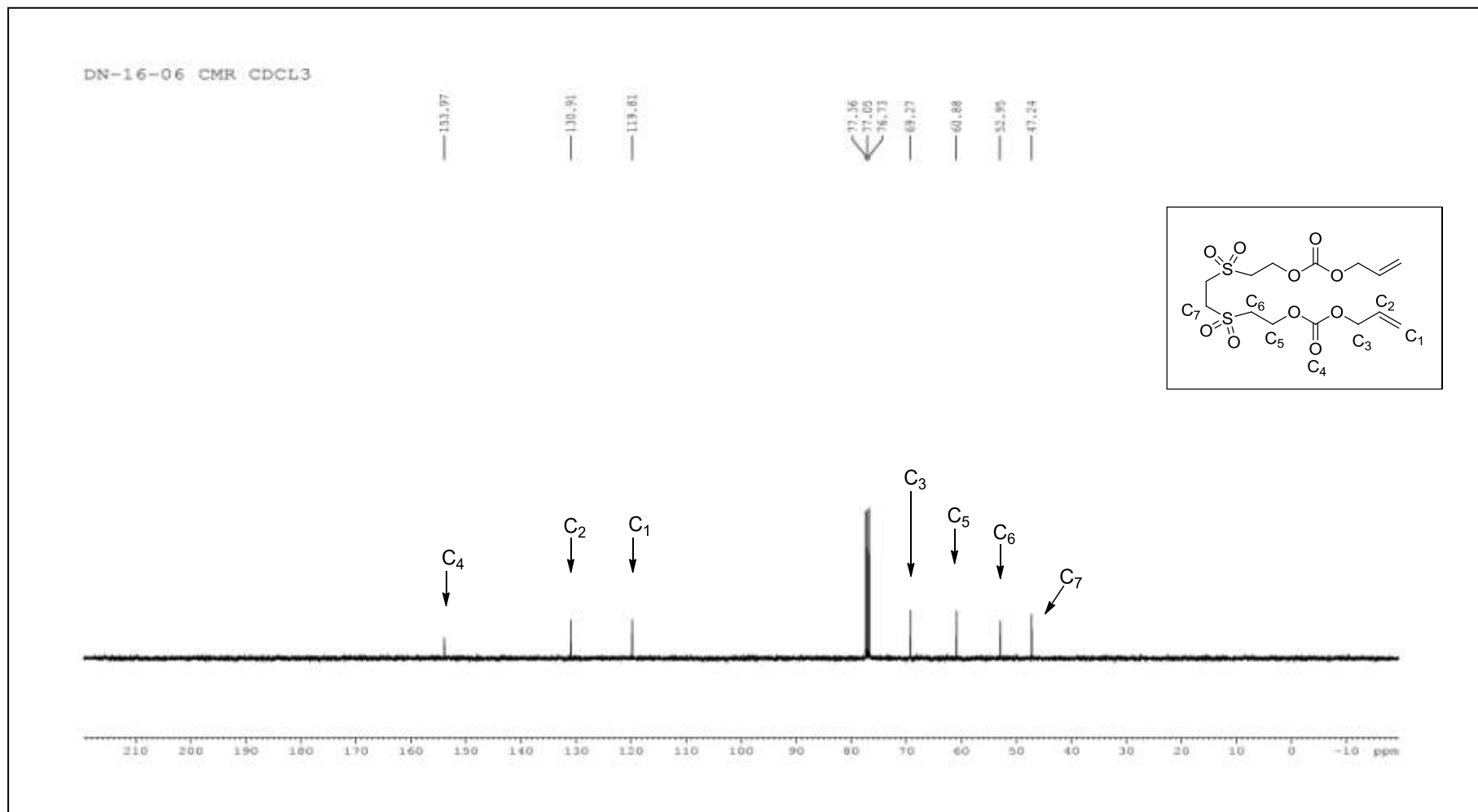
Figure 3.7 (e): ^{13}C-NMR spectrum of 2,2'-(ethane-1,2-diyldisulfonyl)diethanol bis (allyl carbonate)
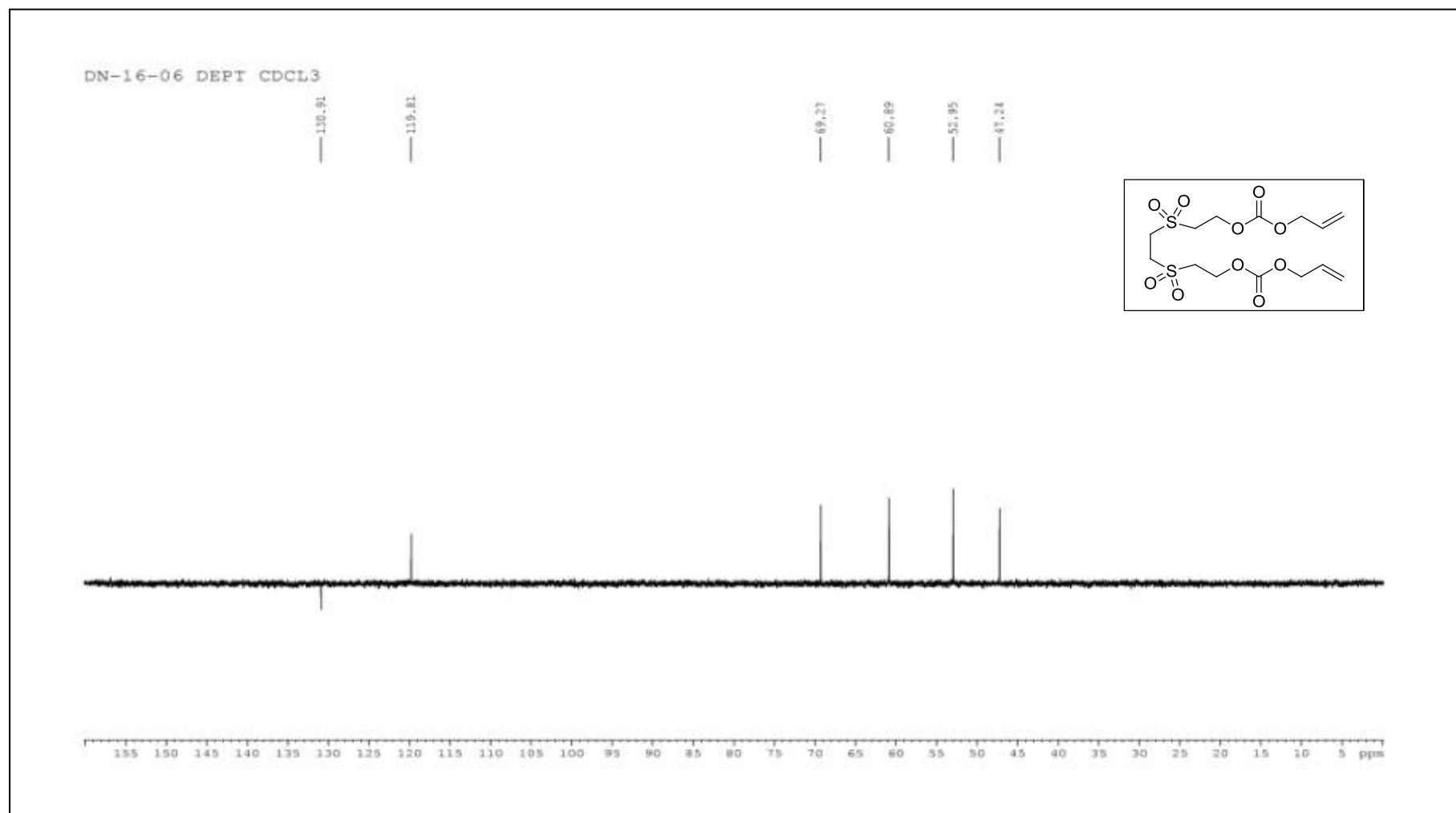
Figure 3.7 (f): DEPT of 2,2'-(ethane-1,2-diyldisulfonyl)diethanol bis (allyl carbonate)
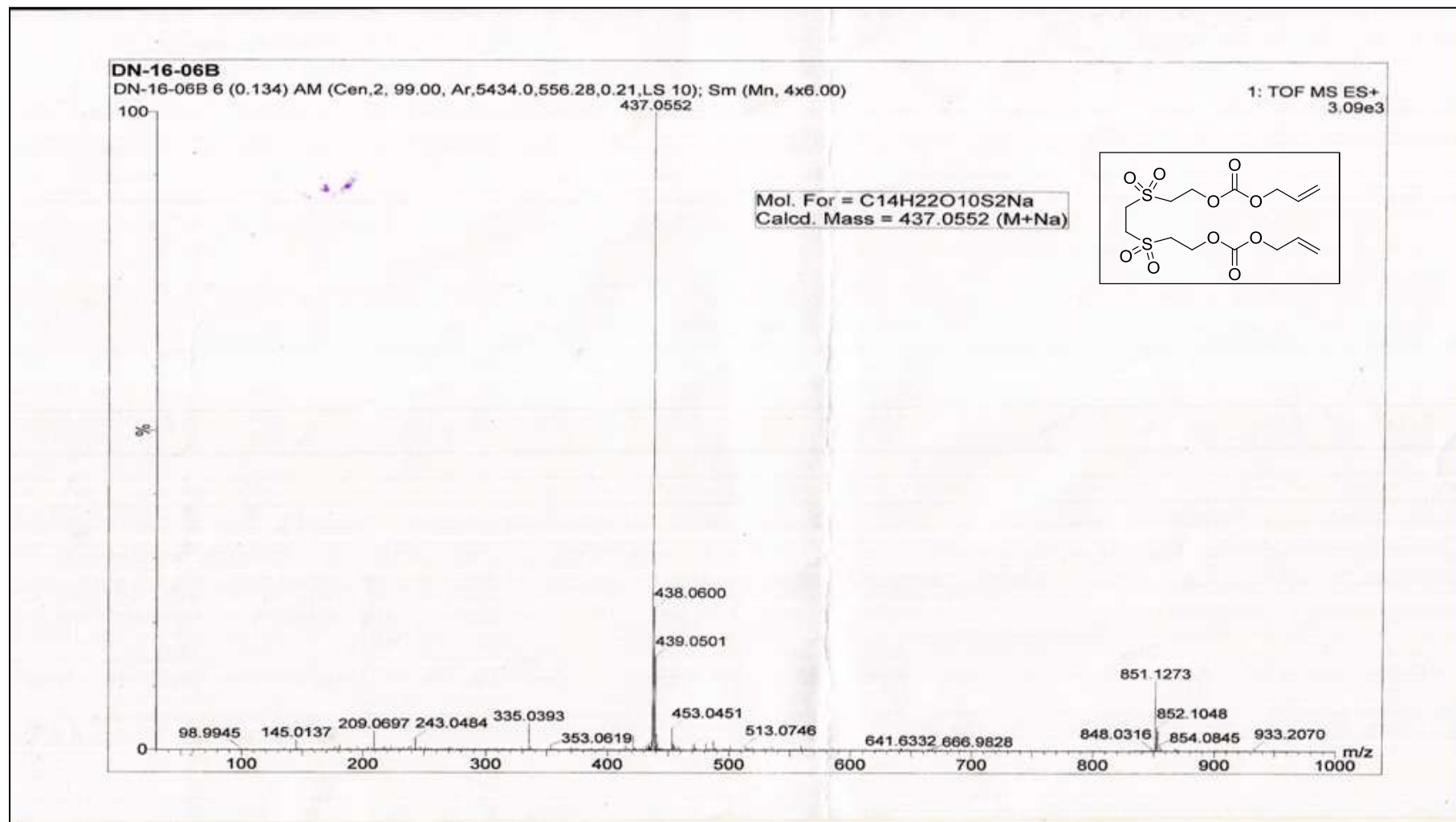
Figure 3.7 (g): HRMS of 2,2'-(ethane-1,2-diyldisulfonyl)diethanol bis (allyl carbonate)

3.2.1.6   2,2'-(3-oxapentane-1,5-diyldisulfonyl)diethanol   bis   (allyl

carbonate) (M6): Initially, the monomer was prepared in two steps viz. 1. Oxidation

of 2, 2'-bis (2-hydroxyethyl sulfanyl) diethyl ether to 2, 2'-bis (2-

hydroxyethylsulfonyl) diethyl ether followed by condensation of 2, 2'-bis (2-

hydroxyethylsulfonyl) diethyl ether with allyl chloroformate using base. But this

synthetic route gave very poor yield. The desired monomer was synthesised in good

yield by oxidizing 3,9-dithia-6-oxa-undecane-1,11-diol bis(allyl carbonate) with 4.1

moles of hydrogen peroxide in acidic medium.

3.2.1.6.1   Method 1: Synthesis of M6 monomer: Scheme 3.10 shows two steps

involved in synthesis of 2,2'-(3-oxapentane-1,5-diyldisulfonyl)diethanol bis (allyl
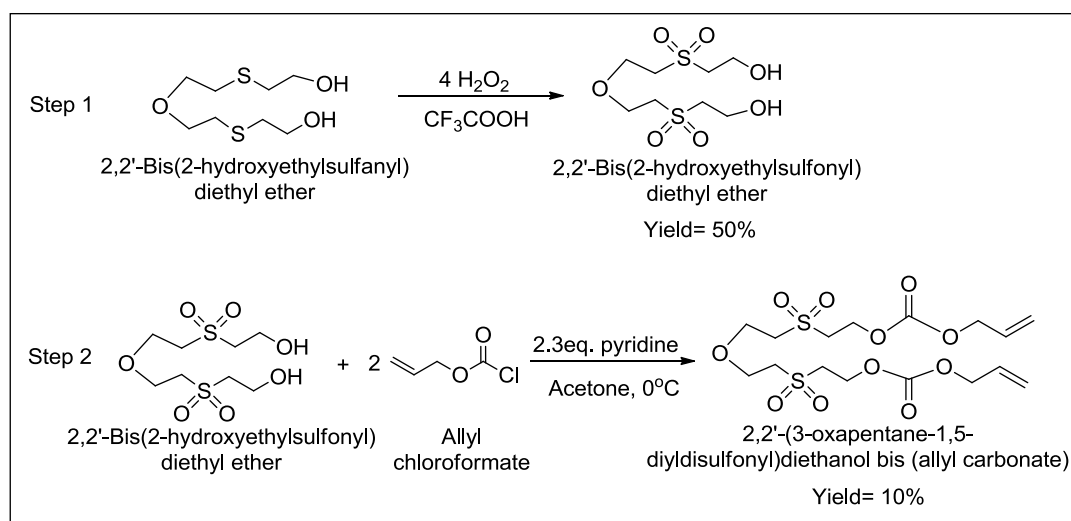
carbonate).

Scheme 3.10: Synthesis of 2,2'-(3-oxapentane-1,5-diyldisulfonyl)diethanol bis (allyl
carbonate)

Step 1: Synthesis of 2,2'-Bis(2-hydroxyethylsulfonyl)diethyl ether: In a 50 mL two

neck flask fitted with reflux condenser and a dropping funnel, 2.5 g (0.0110 moles)

2,2-bis(2-hydroxyethylsulfanyl)diethyl   ether   was   stirred   with   10   mL   of

trifluoroacetic acid. 6.74 mL (0.0456 moles) of 25% hydrogen peroxide was added

to the reaction flask over a period of 10 minutes using dropping funnel. It was refluxed for about 1 hour. Progress of reaction was monitored by TLC followed by removal of trifluoroacetic acid and water over rotary evaporator. Traces of acid were removed over high vacuum pump. Column chromatography using 9:1 dichloromethane-methanol solvent system gave a 1.6 g viscous liquid (50% yield). Scheme 3.10 depicts the synthesis of 2, 2'-Bis (2-hydroxyethylsulfonyl) diethyl ether. It was characterized by IR, NMR spectral techniques as shown in figure 3.8a-b (page no. 222-223). IR (KBr): 3498 cm^{-1}, 2931 cm^{-1}, 1315 cm^{-1}, 1122 cm^{-1}, 1066 cm^{-1}, and 723 cm^{-1}. ^{1}H NMR (400 MHz, D$_2$O) (ppm): 3.94-3.88 (d, 8H), 3.45-3.35 (8H), ^{13}C NMR (100 MHz, D$_2$O): 63.83, 56.11, 54.86, 53.88

Step 2: Synthesis of M6: In condensation process, 3.3 g (0.0114 moles) of 2, 2'-Bis (2-hydroxyethylsulfonyl) diethyl ether was charged into the two neck flask fitted with pressure equalizing funnel and was dissolved in 20 mL acetonitrile. 2.06 g (2.1 mL, 0.0261 moles) pyridine was added to the reaction flask and cooled to 0 ^{o}C. By using dropping funnel 3.14 g (2.8 mL, 0.0261 moles) allyl chloroformate was slowly added to this reaction mixture with constant stirring. It was stirred for an hour at 0 ^{o}C and then for 12 hours at ambient temperature. Workup was carried out in similar fashion and crude product obtained was purified by chromatographic technique giving 10% yield of pale yellow liquid. It was characterized by IR and NMR spectroscopic techniques. Scheme 3.10 shows two steps involved in synthesis of 2,2'-(3-oxapentane-1,5-diyldisulfonyl)diethanol bis (allyl carbonate).

3.2.1.6.2 Method 2: Synthesis of 2,2'-(3-oxapentane-1,5-diyldisulfonyl)diethanol bis (allyl carbonate) via oxidation process: In a round bottom flask, 0.0776 g (0.1967 mmoles) 3,9-dithia-6-oxa-undecane-1,11-diol

bis(allyl carbonate) i.e. (M3) was dissolved in 0.5 mL acetic acid and cooled to 0 $^{\circ}$C using ice bath. 0.15 mL (1.18 mmoles) of 28% aqueous hydrogen peroxide was slowly added to the previously cooled reaction mixture. It was stirred for 15 hours at room temperature. The progress of reaction was monitored by TLC followed by the workup. Equal amount of water and ethyl acetate was added to the reaction mixture and stirred for 20-30 minutes. The aqueous layer was thus extracted 2-3 times using ethyl acetate and later with chloroform. The extracted product in solvent was dried by passing over sodium sulphate. After removing solvent over rotary evaporator, 0.080 g of viscous liquid in pure form was obtained (85% yield). It was characterized by IR and NMR spectroscopy (figure 3.8c-g; page no. 224-228). Scheme 3.11 depicts the process of synthesis of 2,2'-(3-oxapentane-1,5-diyldisulfonyl)diethanol bis (allyl carbonate). IR (KBr): 3086 cm^{-1}, 1751 cm^{-1}, 1649 cm^{-1},1321 cm^{-1}, 1265 cm^{-1} and 1128 cm^{-1}. ^{1}H NMR (400 MHz, CDCl$_3$) (ppm): 5.98-5.88 (m, 2H), 5.40-5.35 (d, 2H), 5.33-5.29 (d, 2H), 4.65 (d, 4H), 4.56 (t, 4H), 3.98 (t, 4H), 3.47 (t, 4H), 3.34 (t, 4H). ^{13}C NMR (100 MHz, CDCl$_3$): 154.12, 131.10, 119.68, 69.09, 64.75, 61.26, 54.36, 53.72. HRMS: (m/z) [M+Na]$^{+}$ calculated for C$_{16}$H$_{26}$O$_{11}$S$_2$Na: 481.0814; found: 481.0814.
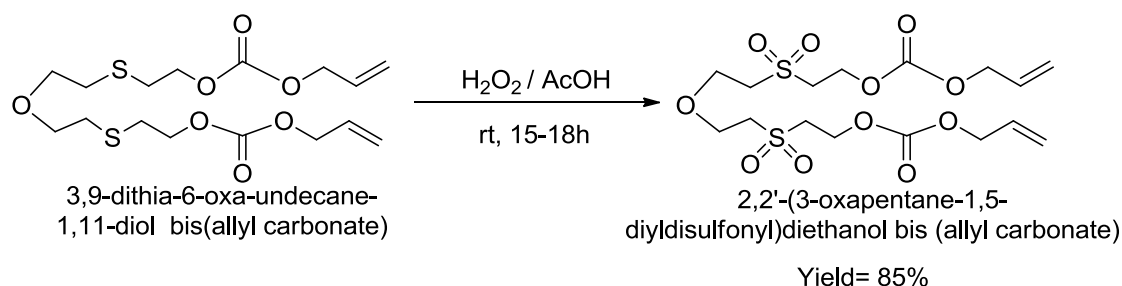
Scheme 3.11: Synthesis of 2,2'-(3-oxapentane-1,5-diyldisulfonyl)diethanol bis (allyl carbonate)
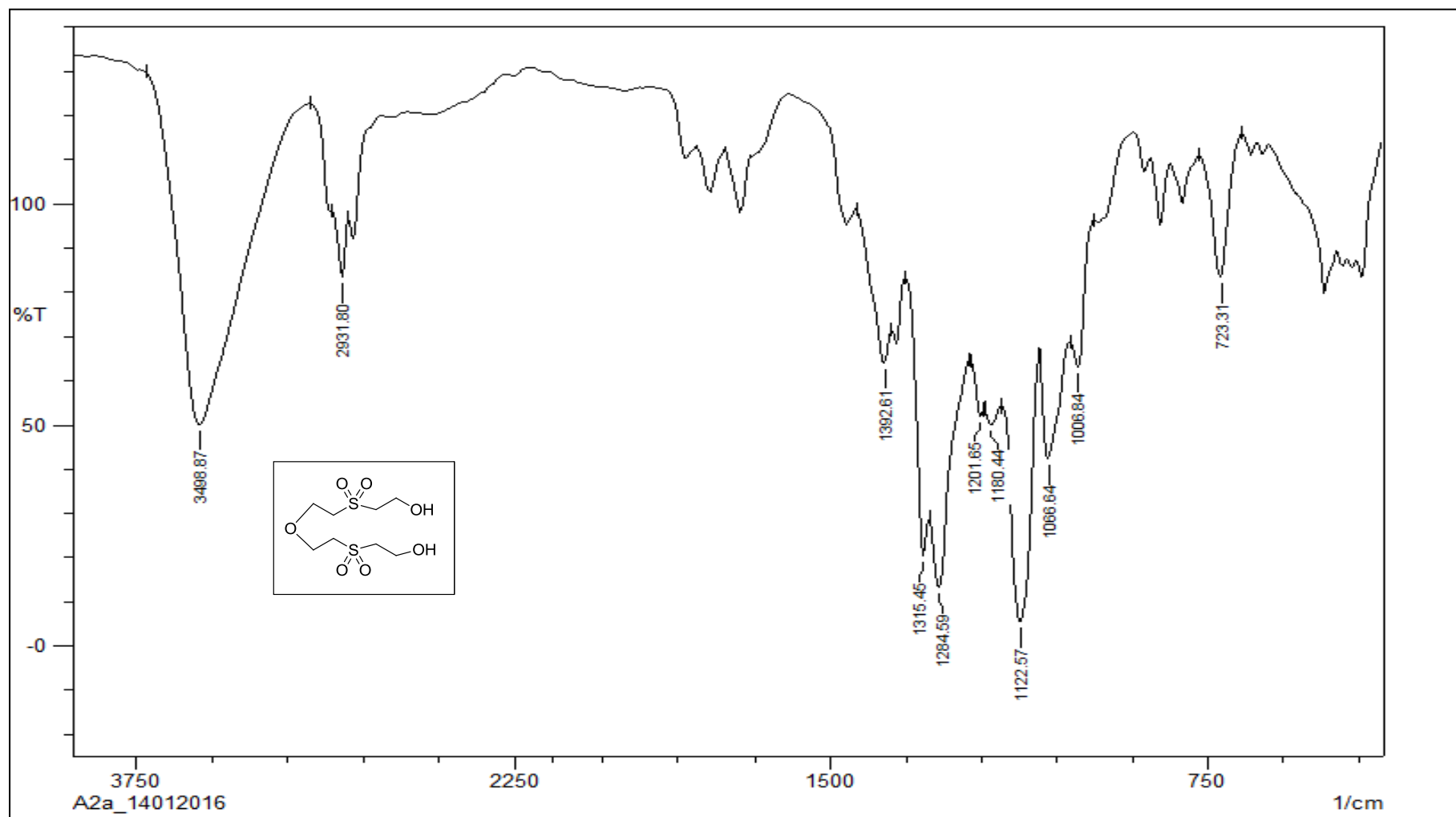
Figure 3.8 (a): IR spectrum of 2, 2'-Bis (2-hydroxyethylsulfonyl) diethyl ether

DN-15-18 PMR D20

4.696
3.941
3.938
3.930
3.917
3.909
3.889
3.877
3.459
3.447
3.381
3.369
3.357

H$_a$ & H$_d$

H$_b$ & H$_c$

1.00   1.01

9   8   7   6   5   4   3   2   1   0   ppm
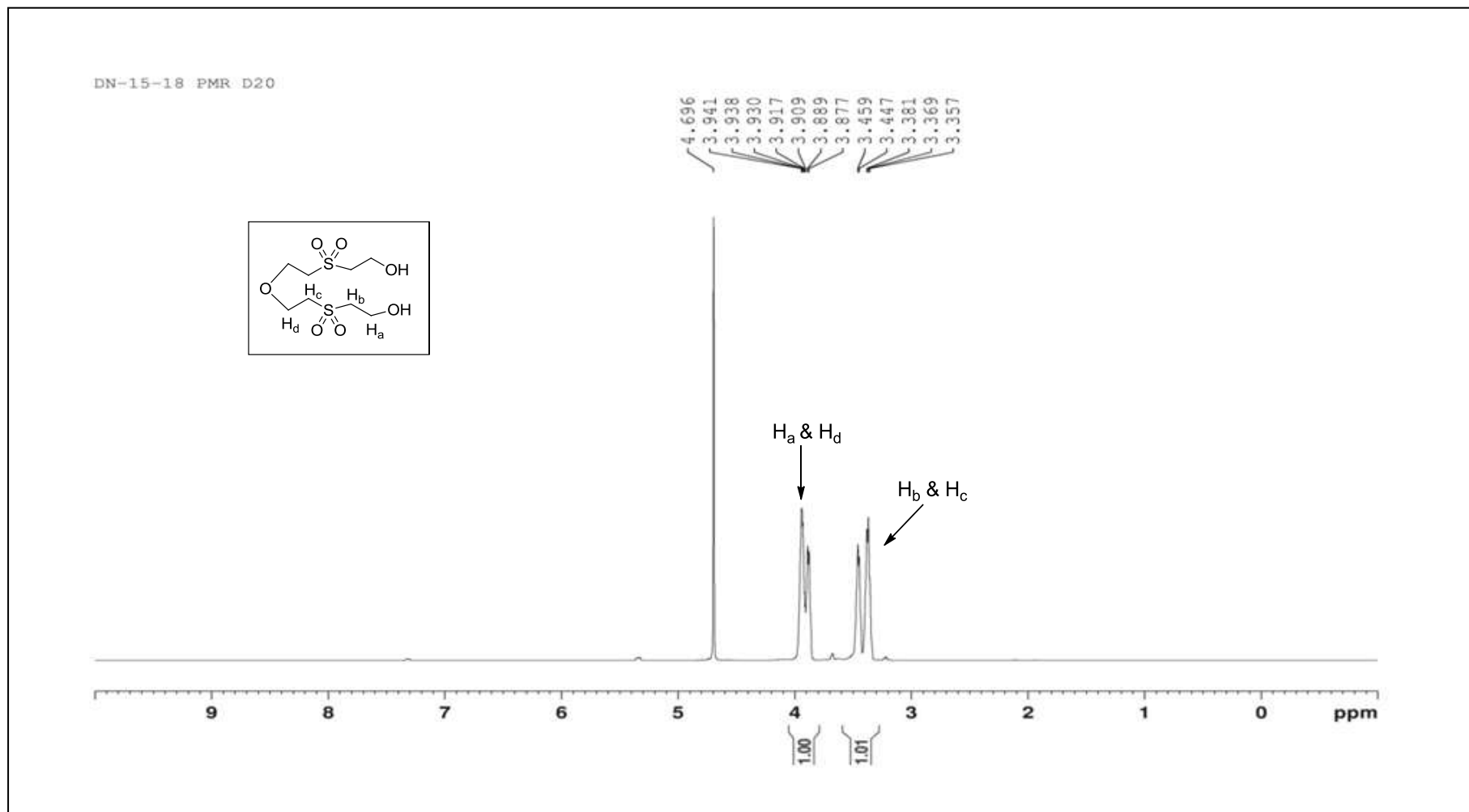
Figure 3.8 (b): NMR spectrum of 2, 2'-Bis (2-hydroxyethylsulfonyl) diethyl ether
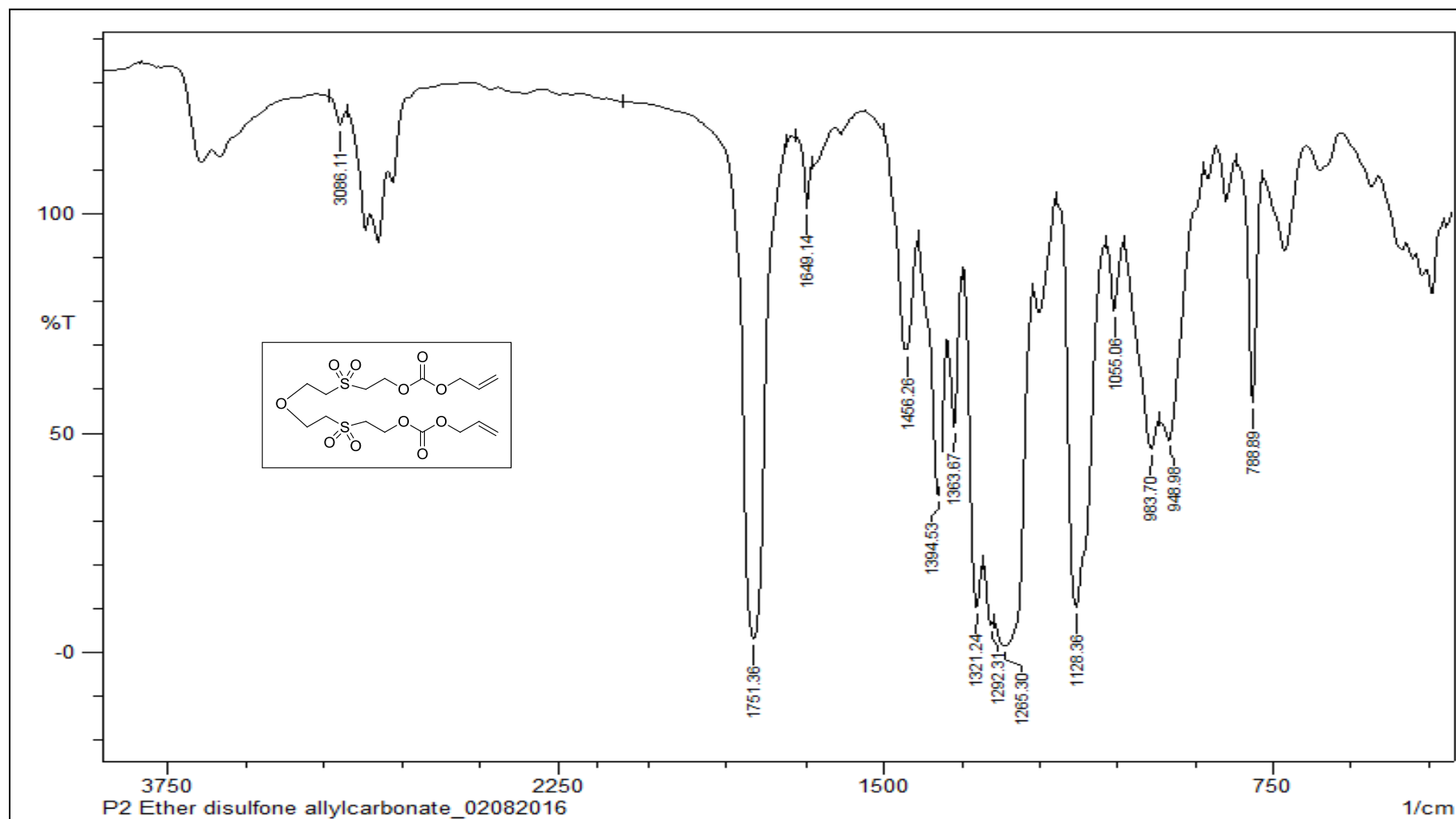
Figure 3.8 (c): IR spectrum of 2,2'-(3-oxapentane-1,5-diyldisulfonyl)diethanol bis (allyl carbonate)
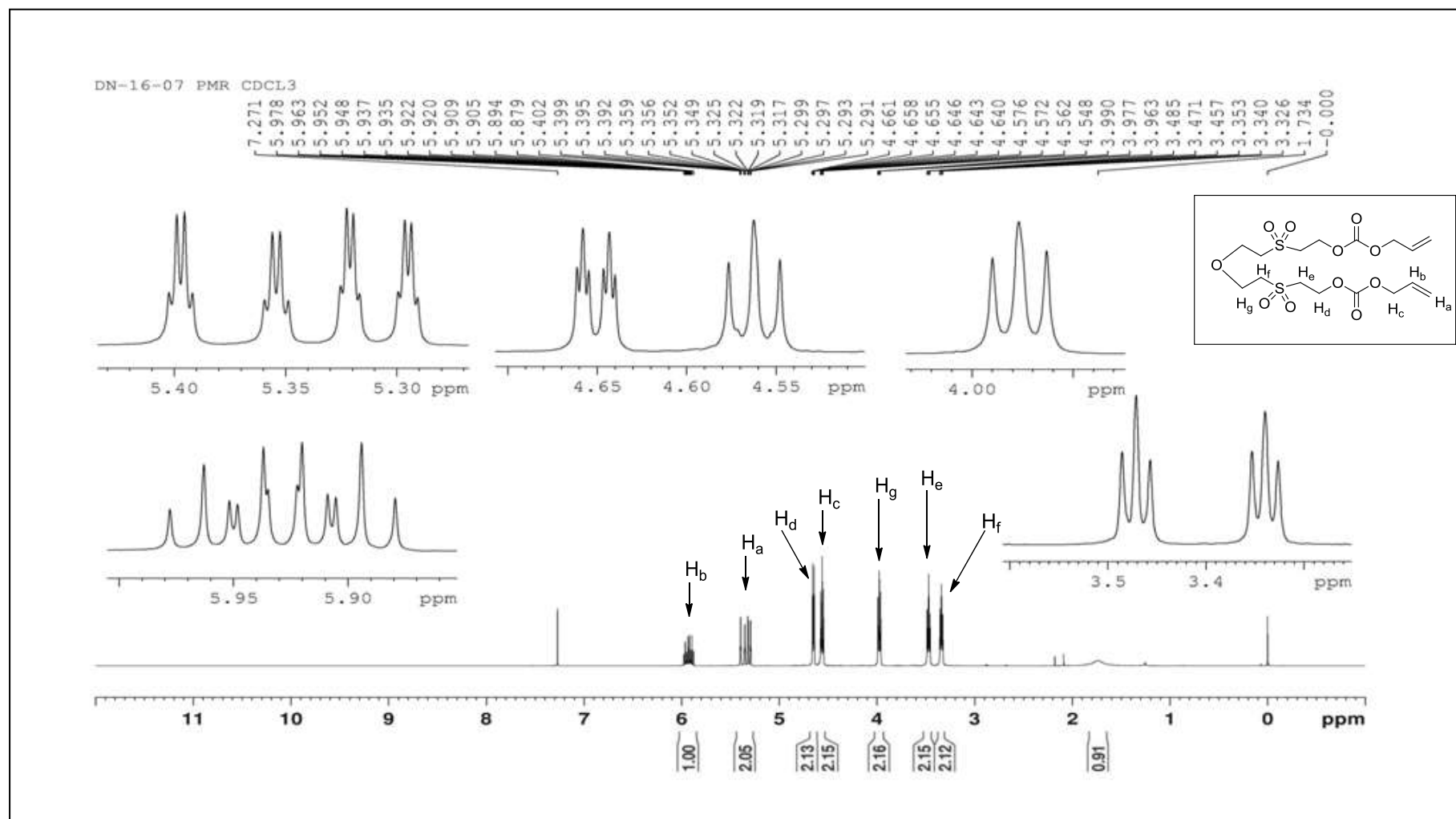
Figure 3.8 (d): ^{1}H NMR spectrum of 2,2'-(3-oxapentane-1,5-diyldisulfonyl)diethanol bis (allyl carbonate)
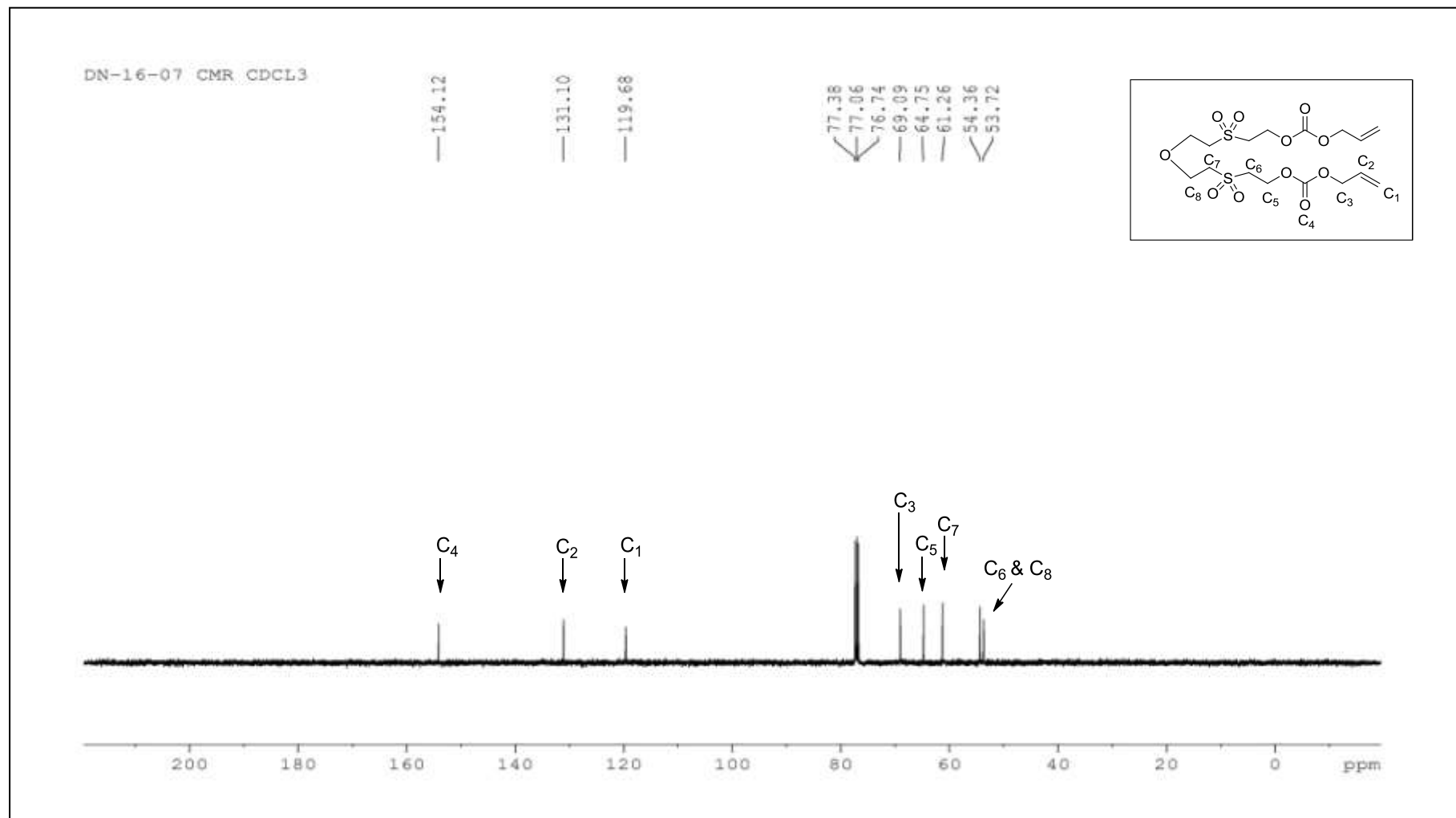
Figure 3.8 (e): ^{13}C NMR spectrum of 2,2'-(3-oxapentane-1,5-diyldisulfonyl)diethanol bis (allyl carbonate)
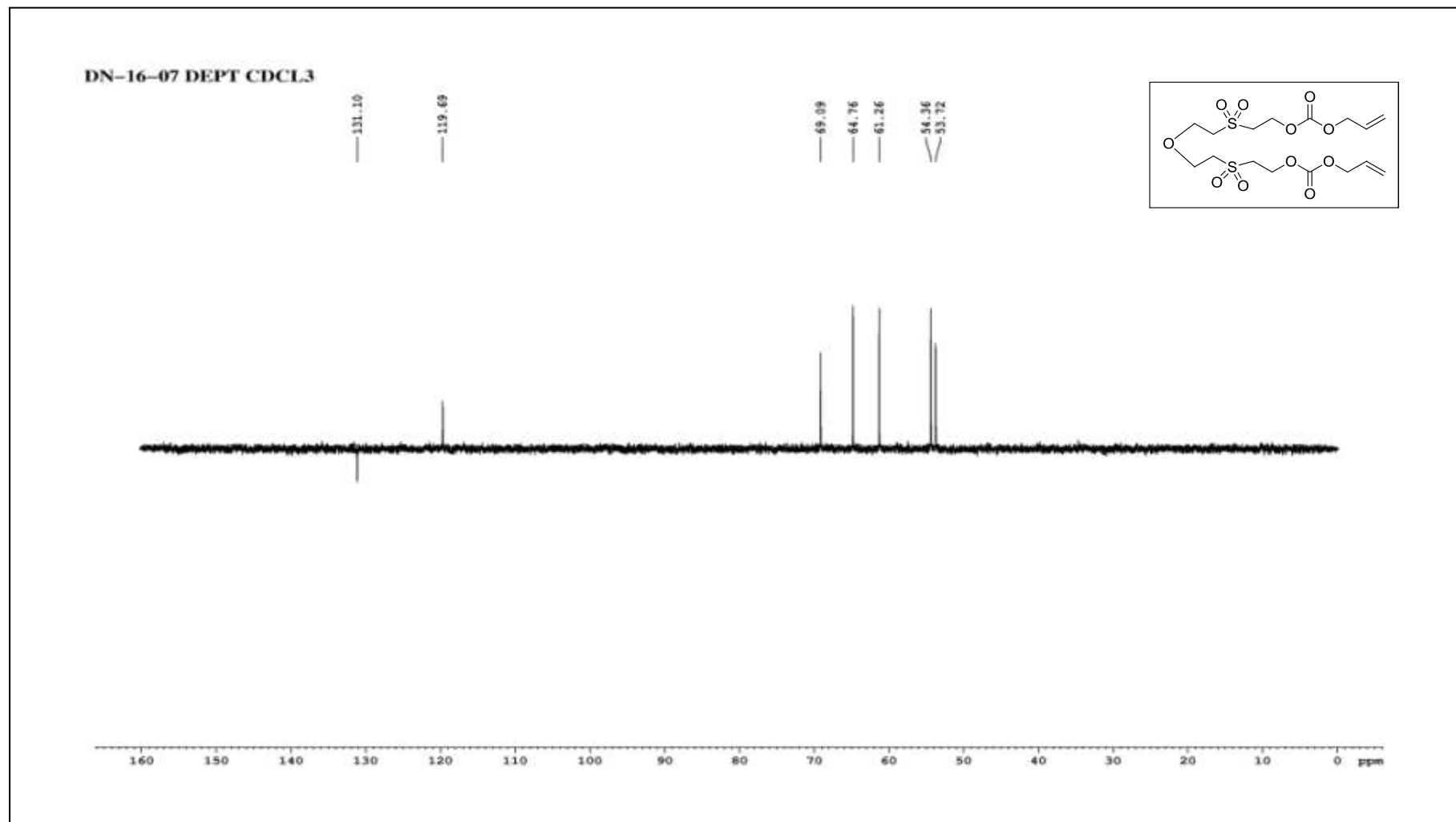
Figure 3.8 (f): DEPT of 2,2'-(3-oxapentane-1,5-diyldisulfonyl)diethanol bis (allyl carbonate)
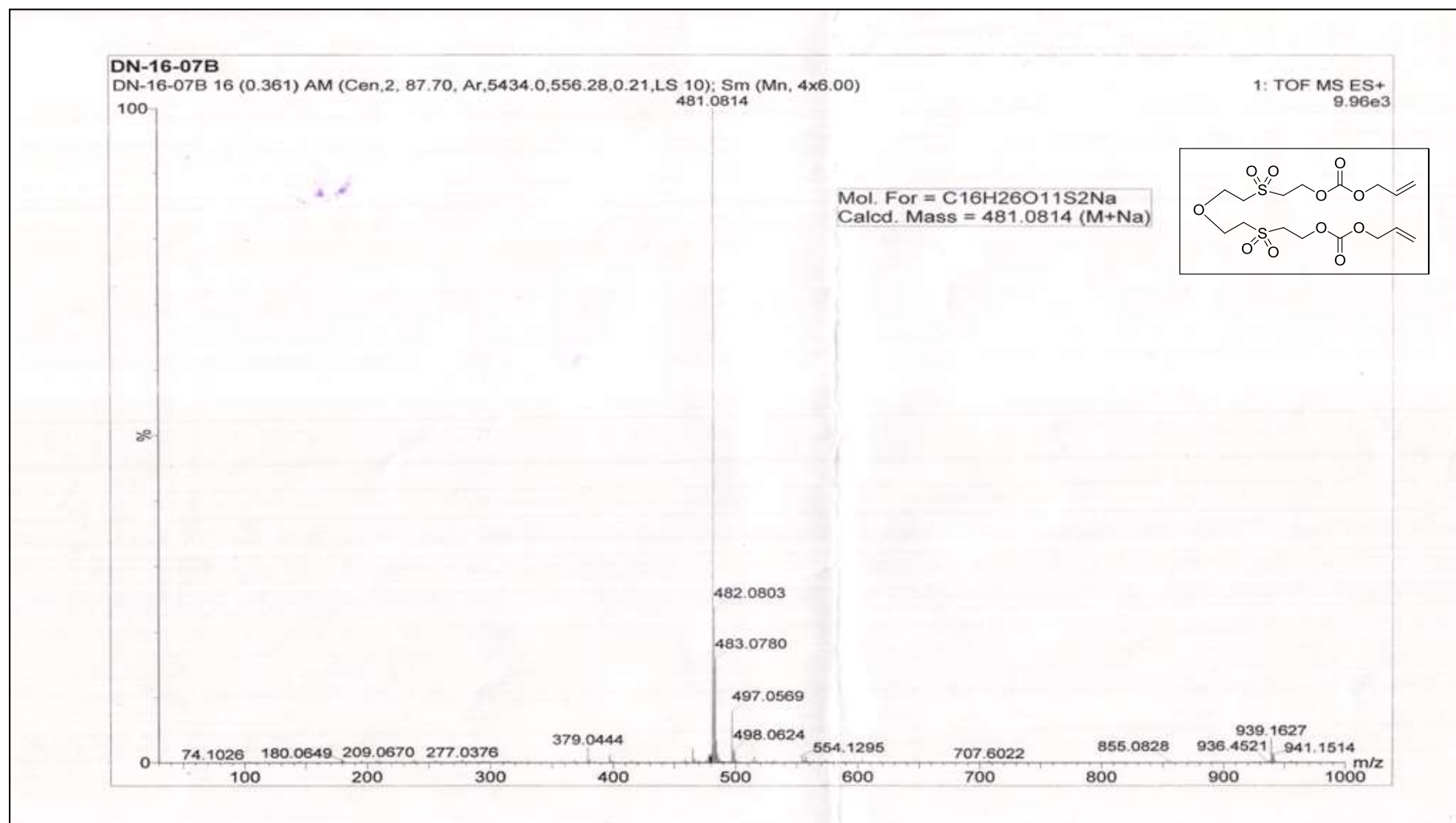
Figure 3.8 (g): HRMS of 2,2'-(3-oxapentane-1,5-diyldisulfonyl)diethanol bis (allyl carbonate)

3.2.1.7 **Synthesis of 2,2'-sulfonyldiethanol bis(allyl carbonate) (SDAC/ ATSC/ M7):** The monomer 2,2'-sulfonyldiethanol bis(allyl carbonate) was prepared in two steps i.e., oxidation of β-thiodiglycol to thiodiglycol sulfone followed by its condensation with allyl chloroformate using pyridine as base. It is schematically represented in scheme 3.12.
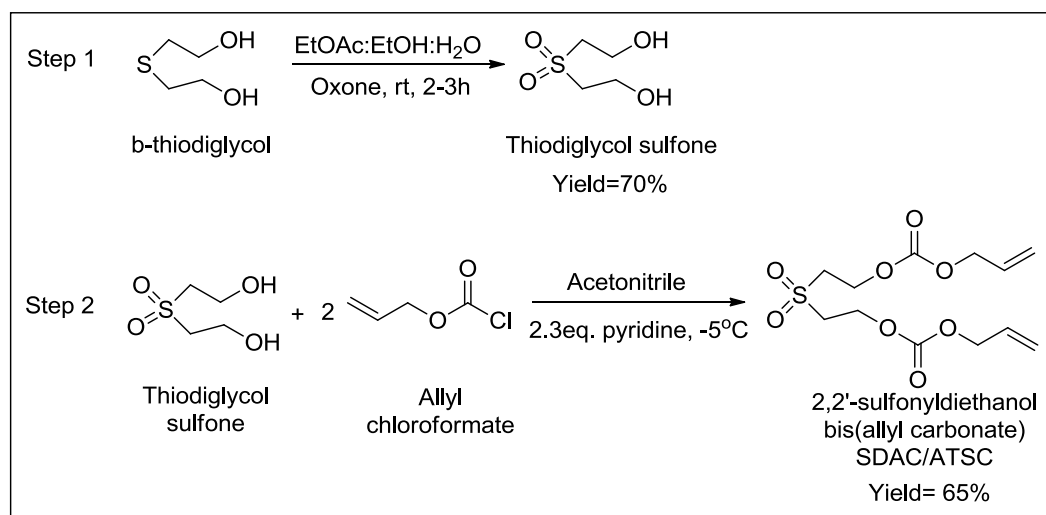
Scheme 3.12: Synthesis of 2,2'-sulfonyldiethanol bis(allyl carbonate) (M7)

Step 1: Synthesis of Thiodiglycol sulfone: β-thiodiglycol was oxidized to thiodiglycol sulfone using oxone[32]. 11.09 g (9.09 mL, 0.0908 moles) of β-thiodiglycol was dissolved in 20:10:1 mixture of ethyl acetate/ ethanol/ water by stirring. To this solution of thiodiglycol, 69.84 g (0.2272 moles) of oxone was added in small portions with vigorous stirring over a period of 3 hours. It was stirred for another 1 hour and then the reaction mixture was evaporated to dryness on a rotary evaporator. The solid obtained was extracted first by using ethyl acetate and then twice with dichloromethane. The product was concentrated by removing solvent over rotary evaporator to give 70% of liquid product. It was characterized by IR spectrum (figure 3.9a; page no. 231). IR (KBr): 3358 cm^{-1}, 2927 cm^{-1}, 1311 cm^{-1}, 1278 cm^{-1} and 1122 cm^{-1}.

Step 2: Synthesis of **2,2'-sulfonyldiethanol bis(allyl carbonate)** ***(SDAC):*** 5.64 g

(0.0366 moles) of thiodiglycol sulfone was weighed in a three neck round bottom

flask fitted with pressure equalizing funnel and thermometer pocket. 50 ml of

acetonitrile and 6.66 g (6.78 mL, 0.0842 moles) of dried pyridine were added into

the reaction vessel. The reaction vessel was placed into the cryogenic bath and its

temperature was lowered to -5 ^{o}C. Further, 10.15 g (11.51 mL, 0.0842 moles) of

allyl chloroformate was taken into a pressure equalizing funnel. As the temperature

of reaction mixture dropped down to -5 ^{o}C, allyl chloroformate was added dropwise.

Reaction was monitored by silica gel TLC. Thus, thiodiglycol sulfone was

condensed with allyl chloroformate in presence of pyridine as base to get 2,2'-

sulfonyldiethanol bis(allyl carbonate). The product obtained was purified by column

chromatography to get a pale yellow colored liquid with 65.2 % of yield w.r.t.

thiodiglycol sulfone. It was characterized by IR, NMR and HRMS spectral

techniques (Figure 3.9b-f; page no. 232-236). IR (KBr): 3086 cm^{-1}, 1749 cm^{-1}, 1327

cm^{-1}, 1130 cm^{-1} and 790 cm^{-1}. ^{1}H NMR (400 MHz, CDCl$_3$) (ppm): 5.90-5.80 (m,

2H), 5.33-5.27 (d, 2H), 5.25-5.21 (d, 2H), 4.58 (d, 4H), 4.52 (t, 4H), 3.37 (t, 4H). ^{13}C

NMR (100 MHz, CDCl$_3$): 154.07, 131.13, 119.37, 68.98, 61.03, 53.51. HRMS: (*m/z*)

[M+Na]$^+$ calculated for C$_{12}$H$_{18}$O$_8$SNa: 345.0620; found: 345.0622.
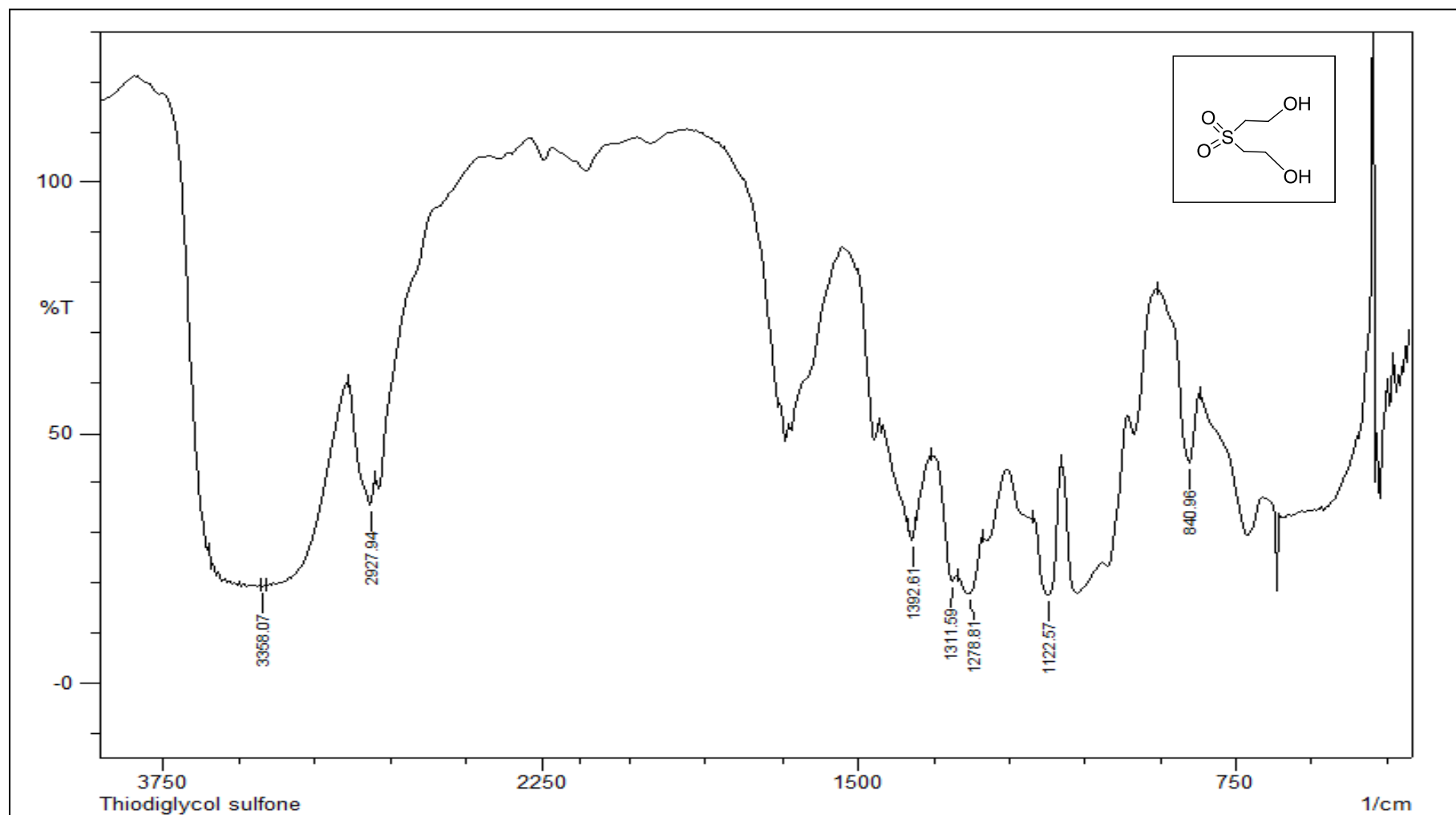
Figure 3.9 (a): IR spectrum of Thiodiglycol sulfone
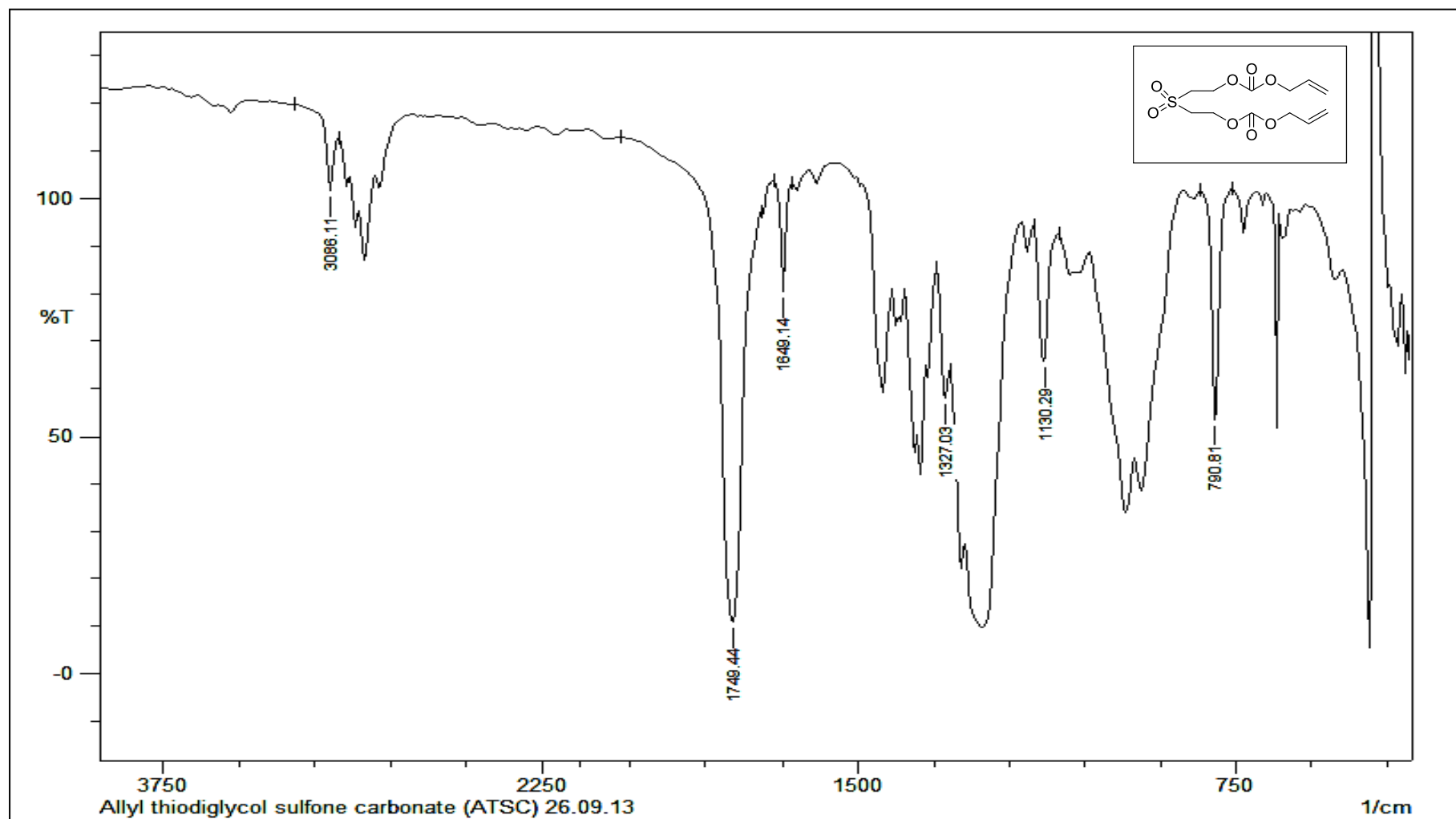
Figure 3.9 (b): IR spectrum of 2,2'-sulfonyldiethanol bis(allyl carbonate) (SDAC)
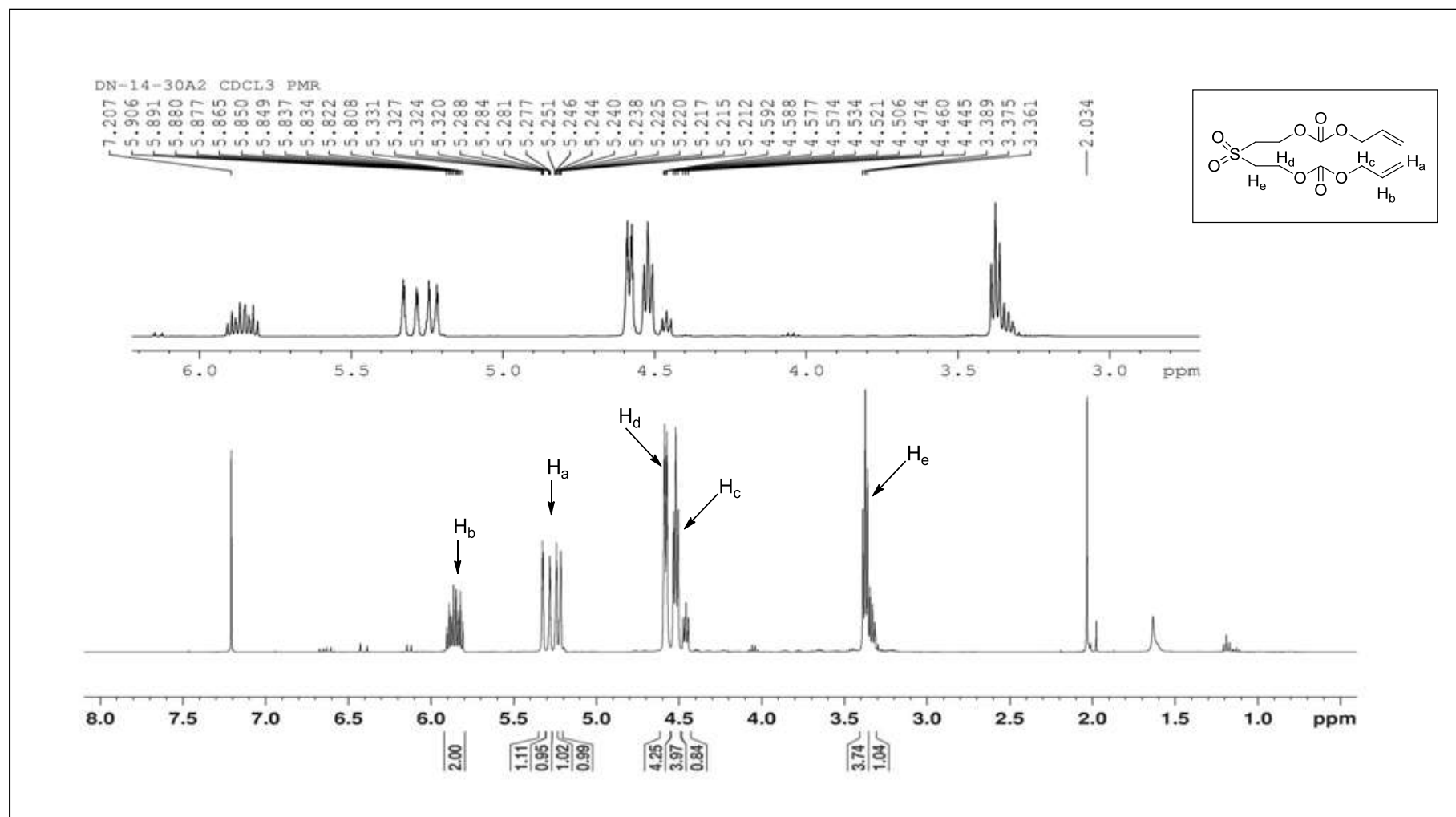
Figure 3.9 (c): ^{1}H NMR spectrum of 2,2'-sulfonyldiethanol bis(allyl carbonate) (SDAC)
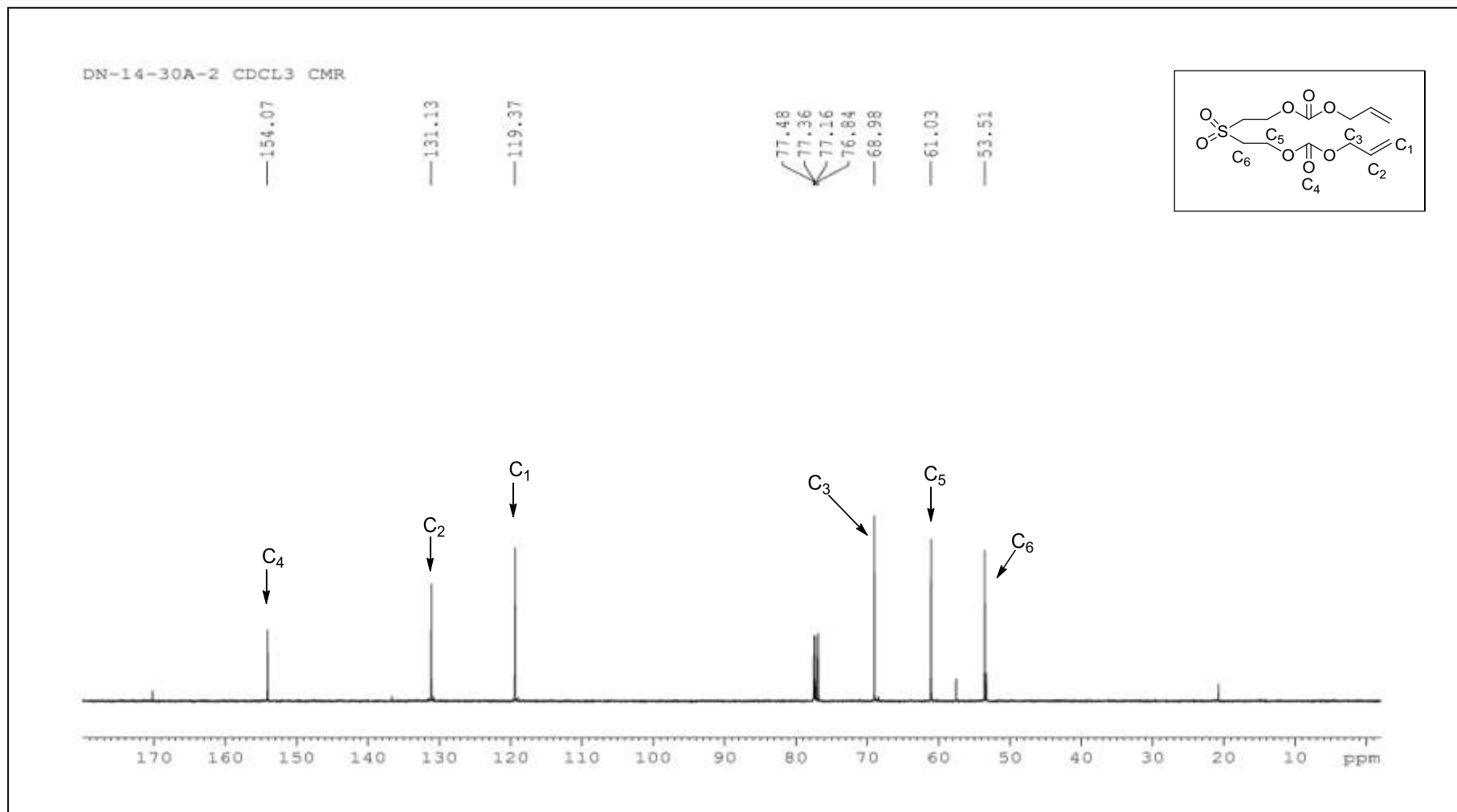
Figure 3.9 (d): ^{13}C NMR spectrum of 2,2'-sulfonyldiethanol bis(allyl carbonate) (SDAC)
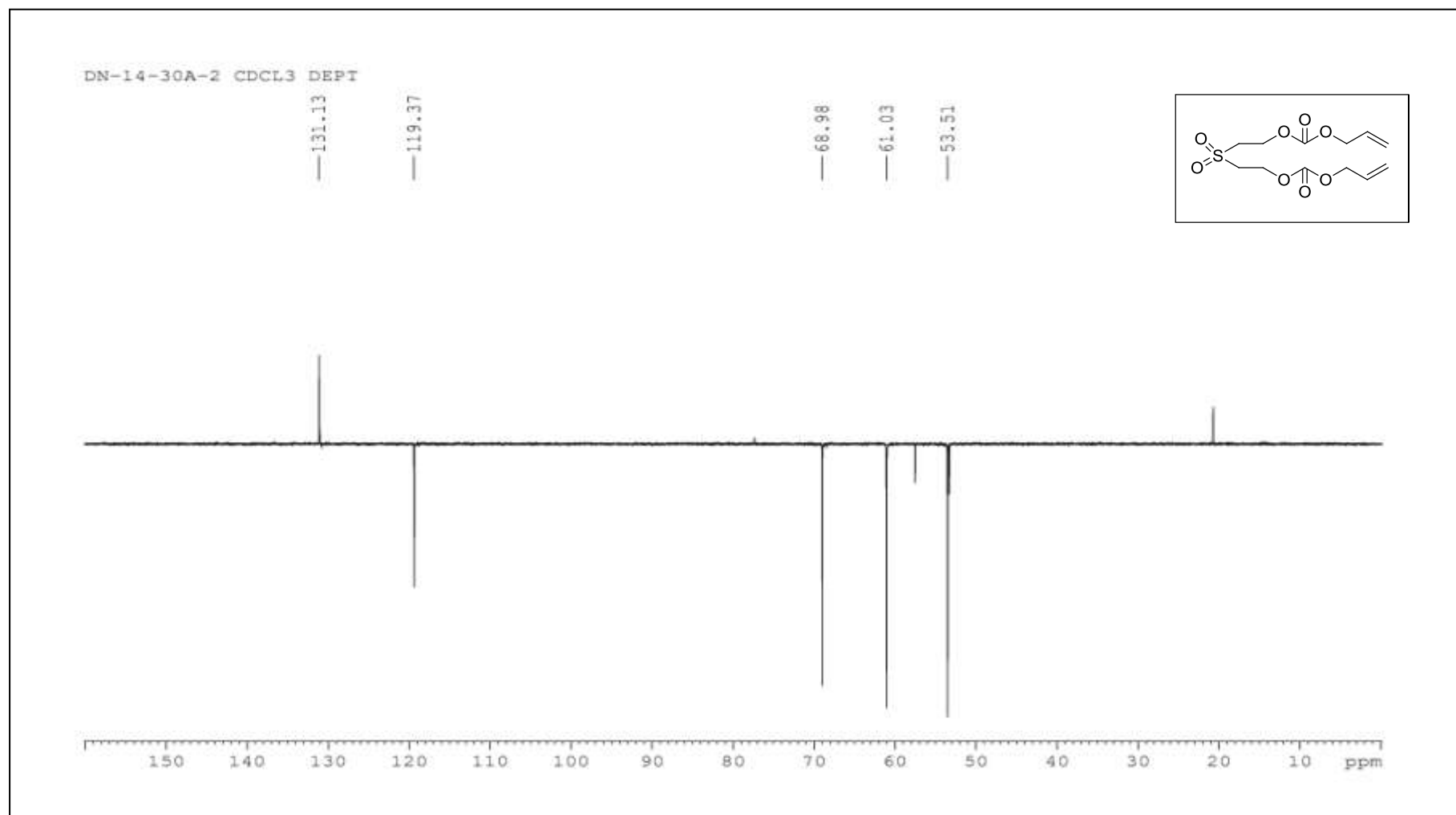
Figure 3.9 (e): DEPT of 2,2'-sulfonyldiethanol bis(allyl carbonate) (SDAC)
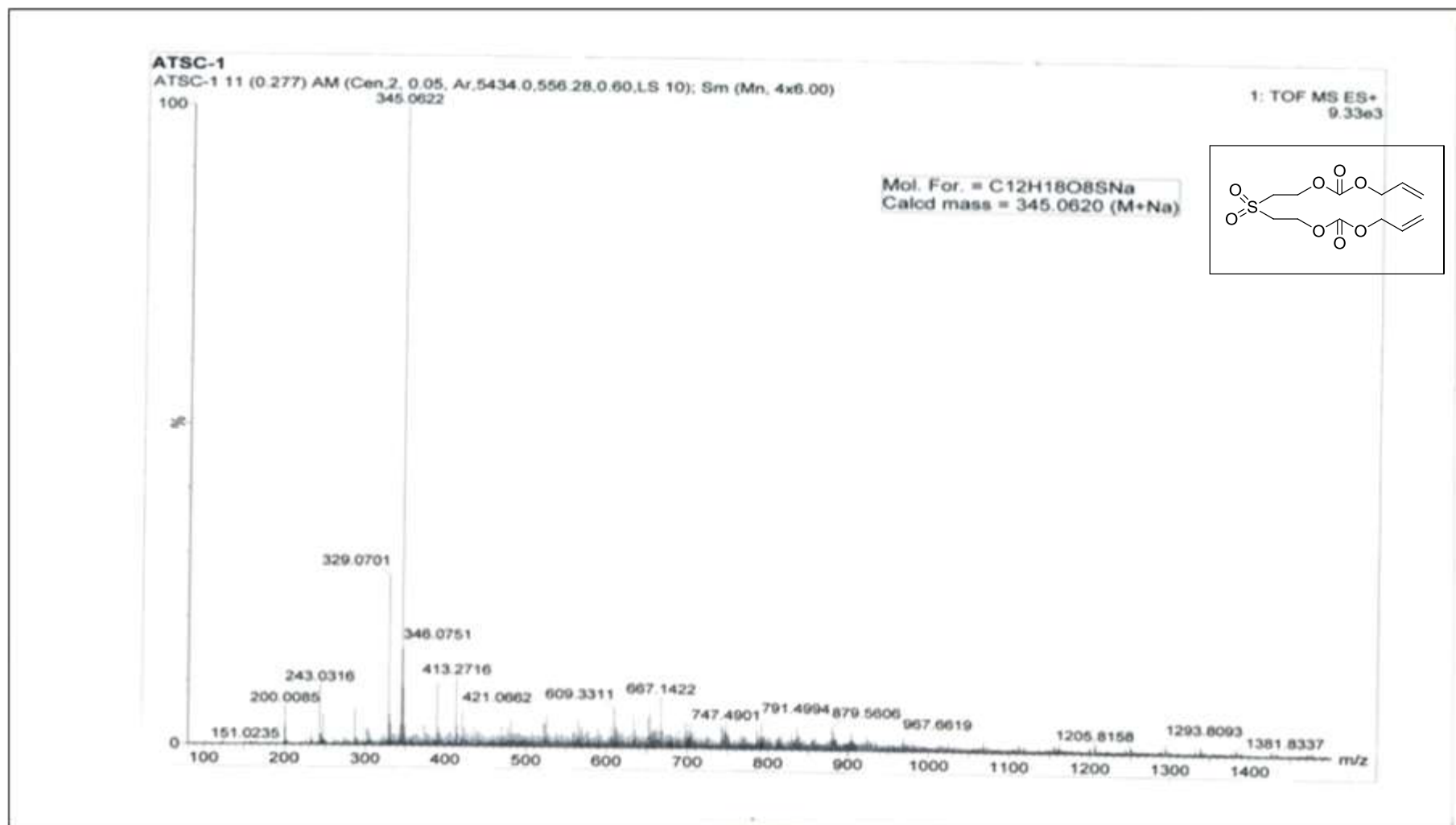
Figure 3.9 (f): HRMS of 2,2'-sulfonyldiethanol bis(allyl carbonate) (SDAC)

3.2.1.8 Hydrogenation of 2,2'-sulfonyldiethanol bis(allyl carbonate) (SDAC) by catalytic hydrogenation process: 0.405g (moles) of SDAC monomer was dissolved in a 25 mL ethyl acetate and 100 mg Pd/C (10%) catalyst was added to the reacting flask. The mixture was hydrogenated under H_2 atmosphere (40 psi) using Parr hydrogenation apparatus for 16 hours. The progress of reaction was monitored by TLC. The reaction mixture was filtered over whatman paper and was washed with ethyl acetate. Finally, the filtrate collected was concentrated to get 0.3665 g of dipropyl (sulfonyl bis(ethane-2, 1-diyl)) dicarbonate product in pure form. The product obtained was colorless liquid with 89.5% yield. It was characterized by IR and NMR spectra (figure 3.10a-d; page no. 238-241). Scheme 3.13 depicts the hydrogenation process of SDAC monomer. IR (KBr): 2970 cm^{-1}, 1745 cm^{-1}, 1325 cm^{-1}, 1132 cm^{-1} and 790 cm^{-1}. ^{1}H NMR (400 MHz, CDCl$_3$) (ppm): 4.58 (t, 4H), 4.13 (t, 4H), 3.44 (t, 4H), 1.74-1.66 (m, 4H), 0.96 (t, 6H). ^{13}C NMR (100 MHz, CDCl$_3$): 154.40, 70.26, 60.78, 53.65, 21.93, 10.11.

2,2'-sulfonyldiethanol bis(allyl carbonate)

H$_2$, Pd/C
EtOAc, 16h

dipropyl (sulfonylbis(ethane-2,1-diyl)) dicarbonate
Yield = 89%
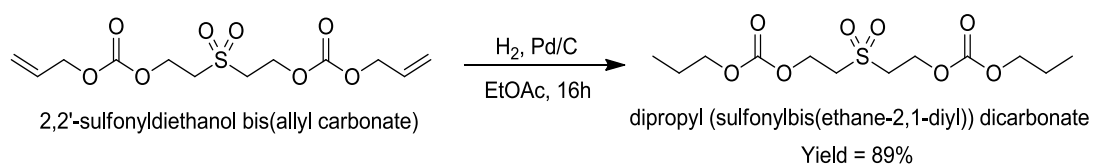
Scheme 3.13: Hydrogenation of 2,2'-sulfonyldiethanol bis(allyl carbonate) (SDAC)
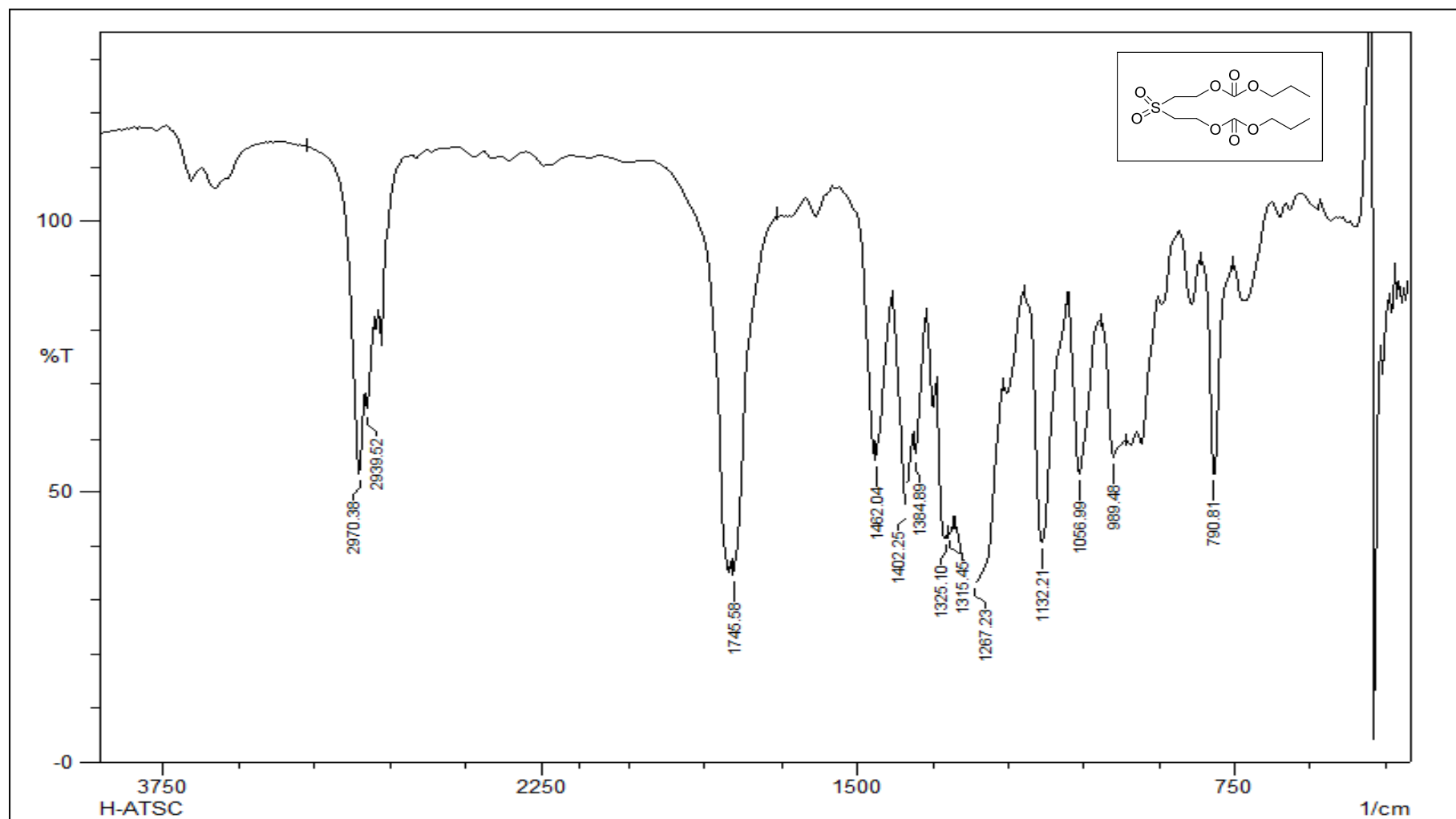
Figure 3.10 (a): IR spectrum of dipropyl (sulfonyl bis(ethane-2, 1-diyl)) dicarbonate
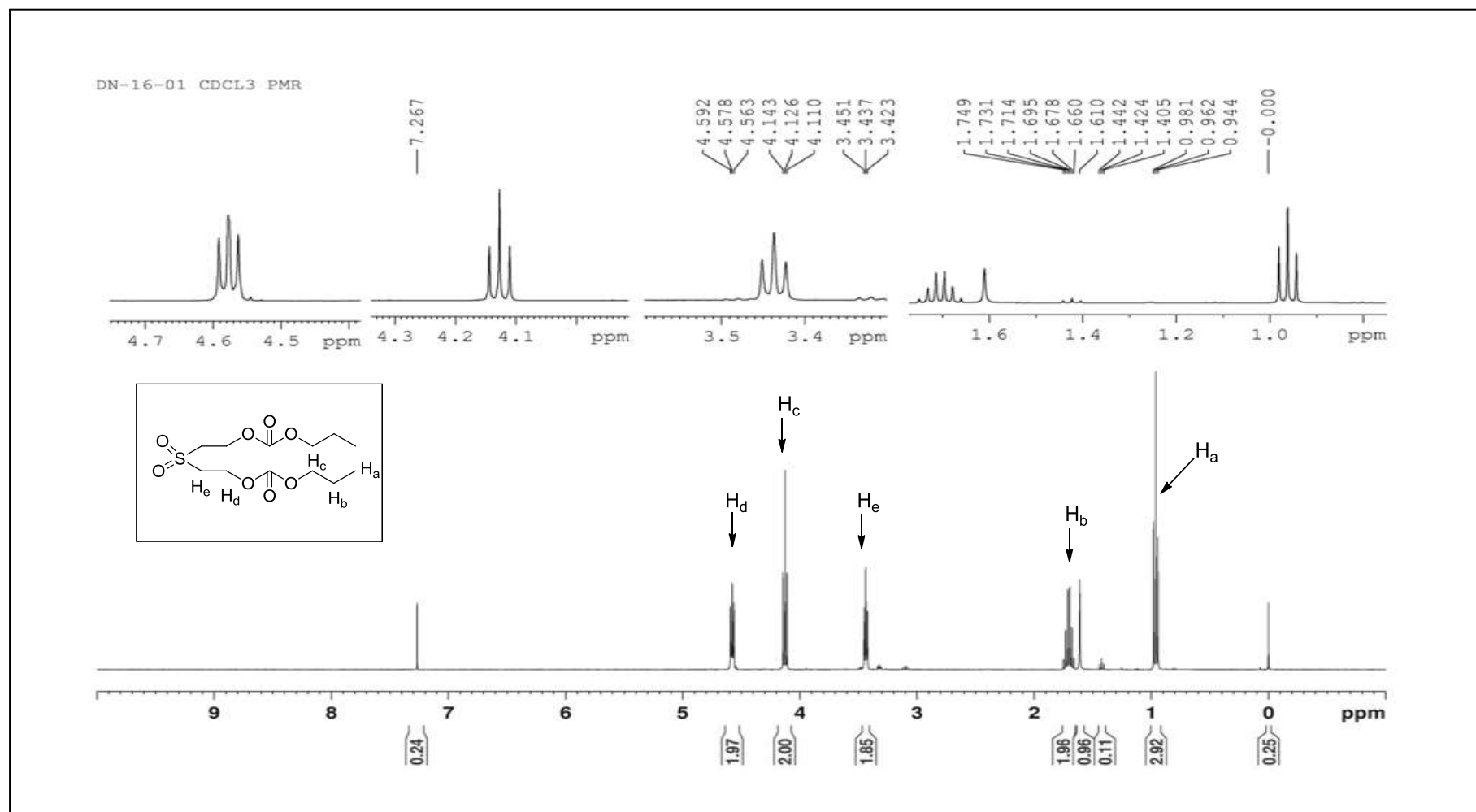
Figure 3.10 (b): ^{1}H NMR spectrum of dipropyl (sulfonyl bis (ethane-2, 1-diyl)) dicarbonate
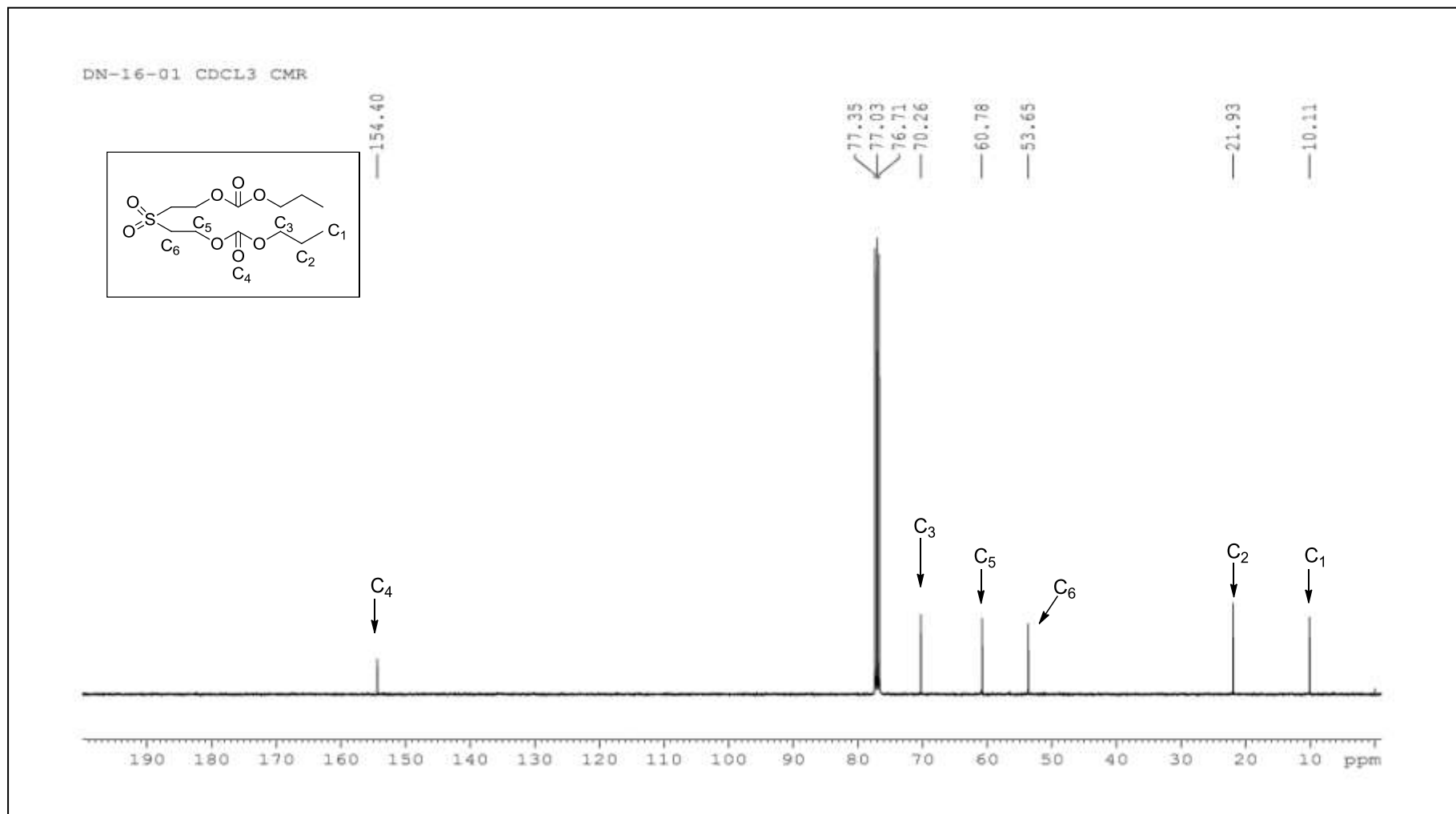
Figure 3.10 (c): ^{13}C NMR spectrum of dipropyl (sulfonyl bis(ethane-2, 1-diyl)) dicarbonate

DN-16-01 CDCL3 DEPT
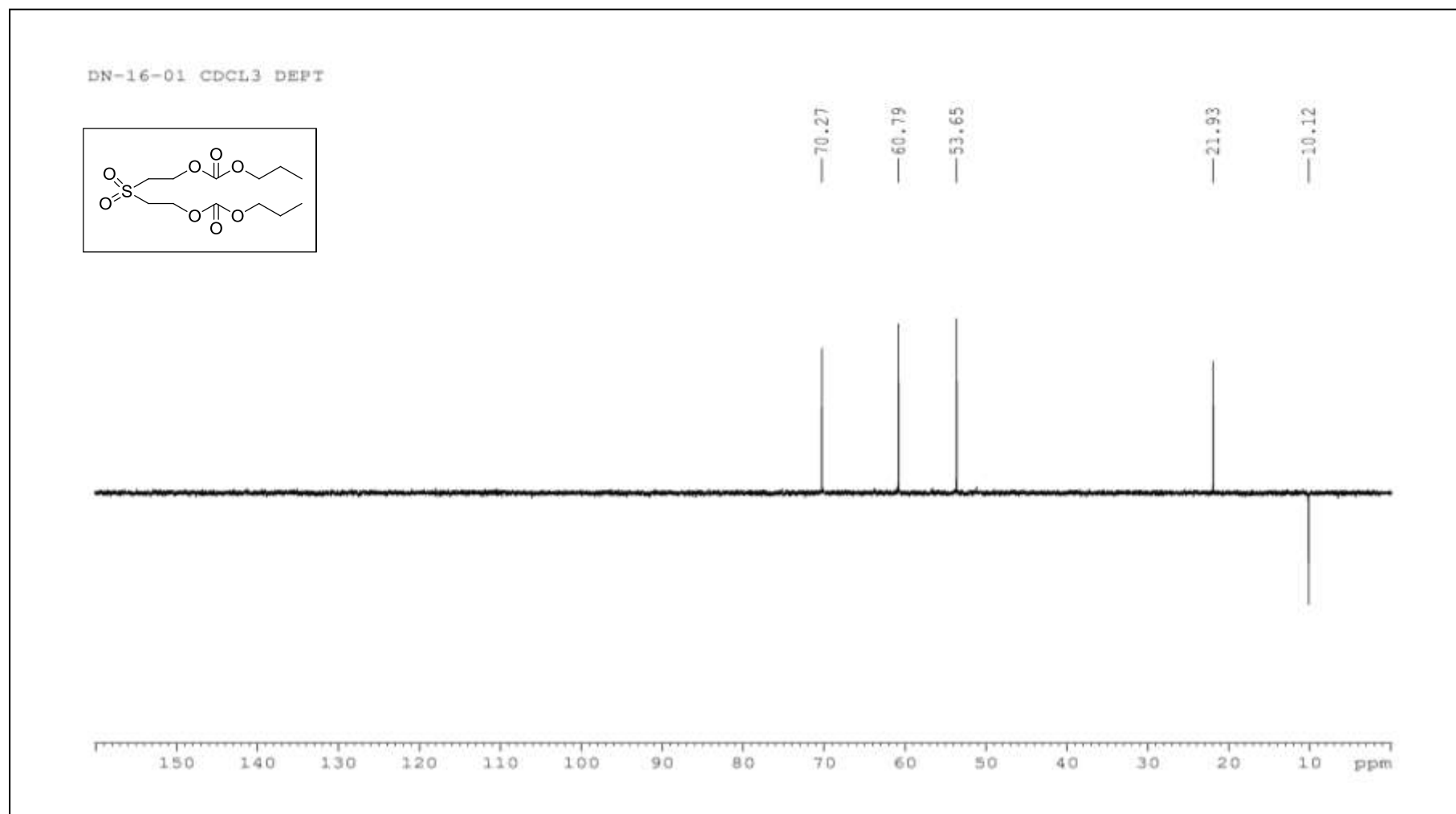
Figure 3.10 (d): DEPT of dipropyl (sulfonyl bis(ethane-2, 1-diyl)) dicarbonate

3.2.1.9 Synthesis of Triallyl sulfonamide (M8): The monomer was synthesised in 2 steps. Initially allyl sulfonyl chloride was prepared by known method[24, 33] and was slowly reacted with diallyl amine to synthesise triallyl sulfonamide in 60 % yield. The synthetic route is depicted in the scheme 3.14 below.
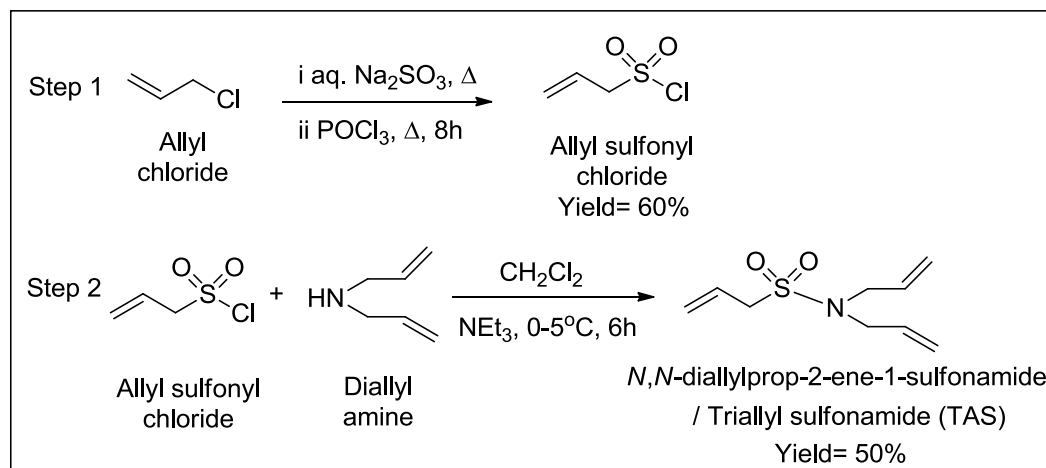
Scheme 3.14: Synthesis of triallyl sulfonamide

Step 1: Synthesis of allyl sulfonyl chloride: In a two neck flask, 82.35 g (0.6530 moles) of sodium sulphite (Na_2SO_3) was dissolved in 100 mL distilled water. 50 g (53.19 mL, 0.6534 moles) of allyl chloride was added slowly into the reacting vessel with constant stirring. During addition temperature was maintained below 50 ^{o}C. After the addition was complete, the reaction mixture was heated to 60 ^{o}C for 7 hours. It was cooled to room temperature and water was removed over rotary evaporator till dryness. The sodium allyl sulfonate obtained was recrystallized from water-ethanol (1:4) mixture. Further 10.6 g (0.07314 moles) of sodium allyl sulfonate was taken into round bottom flask fitted with reflux water condenser. 11.22 g (6.84 mL, 0.07314 moles) phosphorus oxy chloride was added into the flask and heated to 120 ^{o}C with constant stirring for 8-9 hours. This mixture was then poured into the ice flakes present in 500 mL beaker with dynamic stirring. It was further extracted in diethyl ether (4 x 20 mL). Crude product was obtained after removing

ether over rota-vap. It was vacuum distilled at 60 ^{o}C to get pure colourless liquid allyl sulfonyl chloride in (6.5 g) 60% yield. IR spectrum of the prepared pure compound is shown in figure 3.11a (page no. 244). IR (KBr): 3093 cm^{-1},2985 cm^{-1}, 1639 cm^{-1}, 1373 cm^{-1} and 1193 cm^{-1}.

Step 2: Synthesis of Triallyl sulfonamide: 1.0 g (0.0103 mL, moles) diallyl amine and 1.14 g (1.57 mL, 0.0113 moles) triethyl amine were stirred together along with 10 mL dichloromethane in a reacting flask at 0 ^{o}C using an ice bath. 1.59 g (1.19 mL, 0.0113 moles) allyl sulfonyl chloride was slowly added using dropping funnel with constant stirring. After complete addition of allyl sulfonyl chloride, the reaction mixture was stirred for another 3 hours. The salt formed in the reaction flask was filtered off and filtrate was washed with brine water 3-4 times and extracted in dichloromethane. The organic extract was passed over anhydrous sodium sulphate and was concentrated over rotary evaporator to obtain 54% of crude product. 51.3% of pure pale yellow liquid was obtained after column chromatographic purification. IR, NMR spectral data confirmed the synthesis of triallyl sulfonamide compound (figure 3.11b-e; page no.245-248). IR (KBr): 3082 cm^{-1}, 1641 cm^{-1}, 1340 cm^{-1} and 1139 cm^{-1}. ^{1}H NMR (400 MHz, CDCl$_3$) (ppm): 5.87-5.65 (m, 3H), 5.33 (d, 2H), 5.16 (d, 4H), 3.76 (d, 4H), 3.65 (d, 2H). ^{13}C NMR (100 MHz, CDCl$_3$): 132.92, 125.89, 123.55, 119.18, 57.83, 49.46.
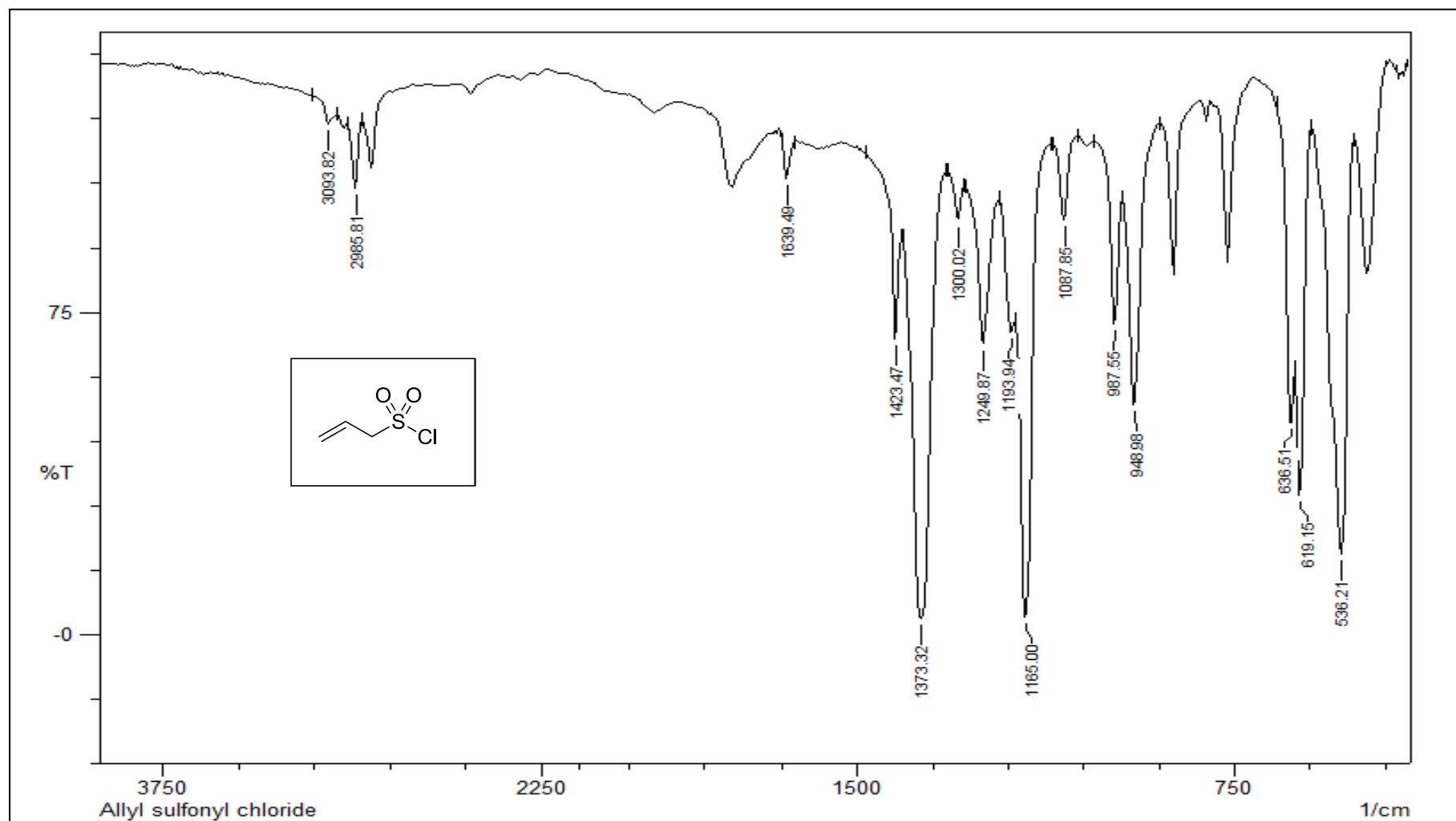
Figure 3.11 (a): IR spectrum of Allyl sulfonyl chloride
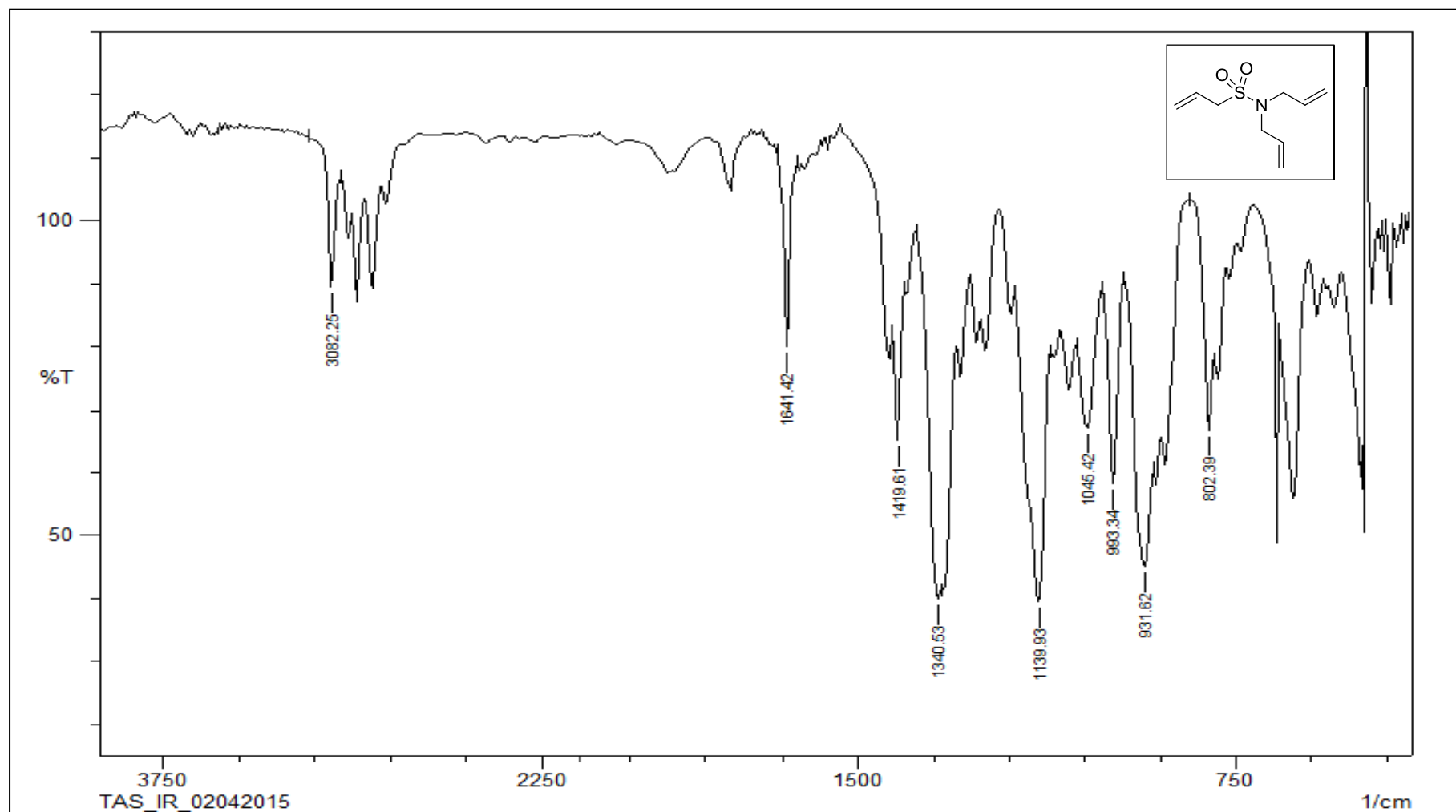
Figure 3.11 (b): IR spectrum of Triallyl sulfonamide
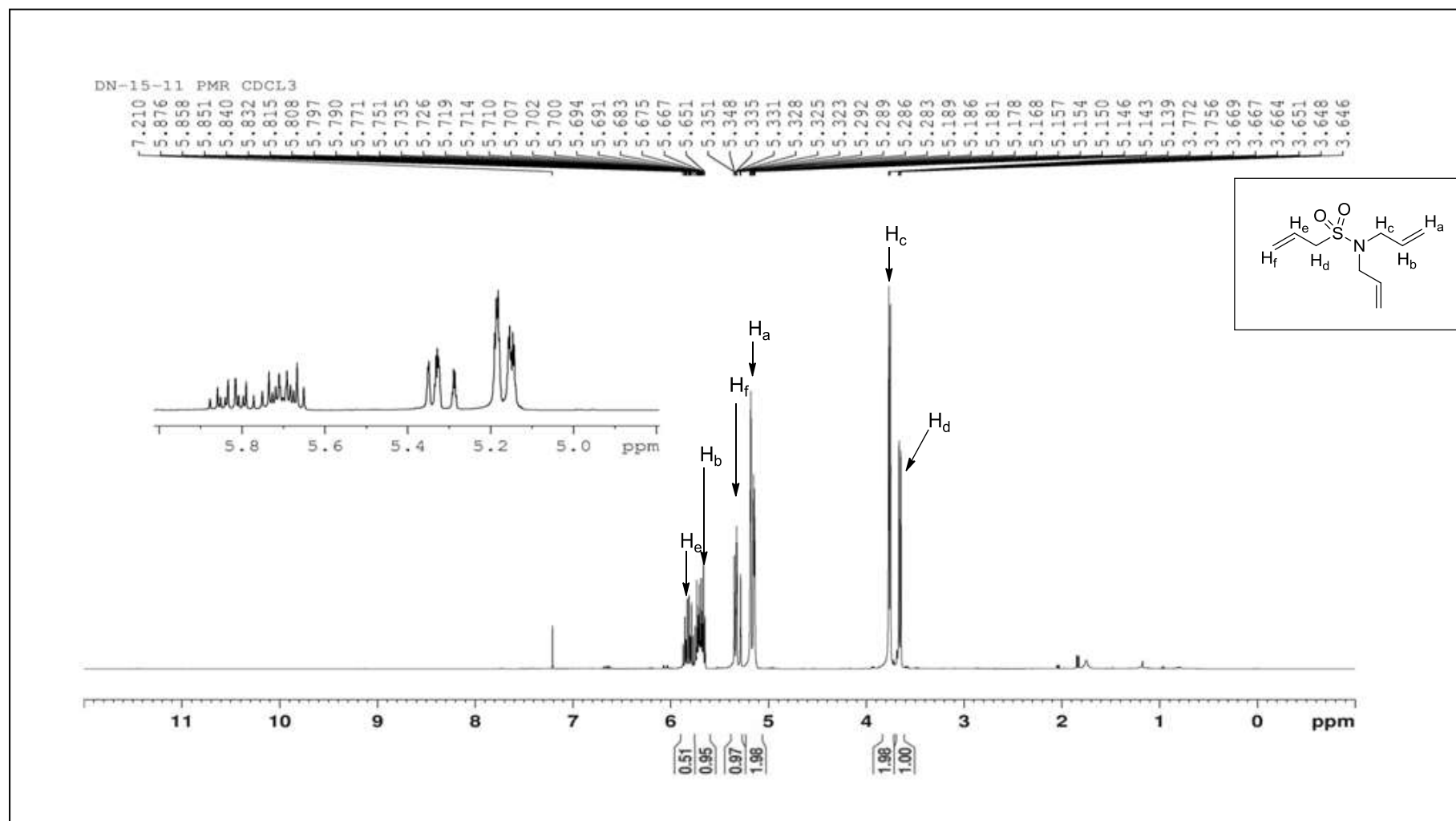
Figure 3.11 (c): ^{1}H NMR spectrum of Triallyl sulfonamide
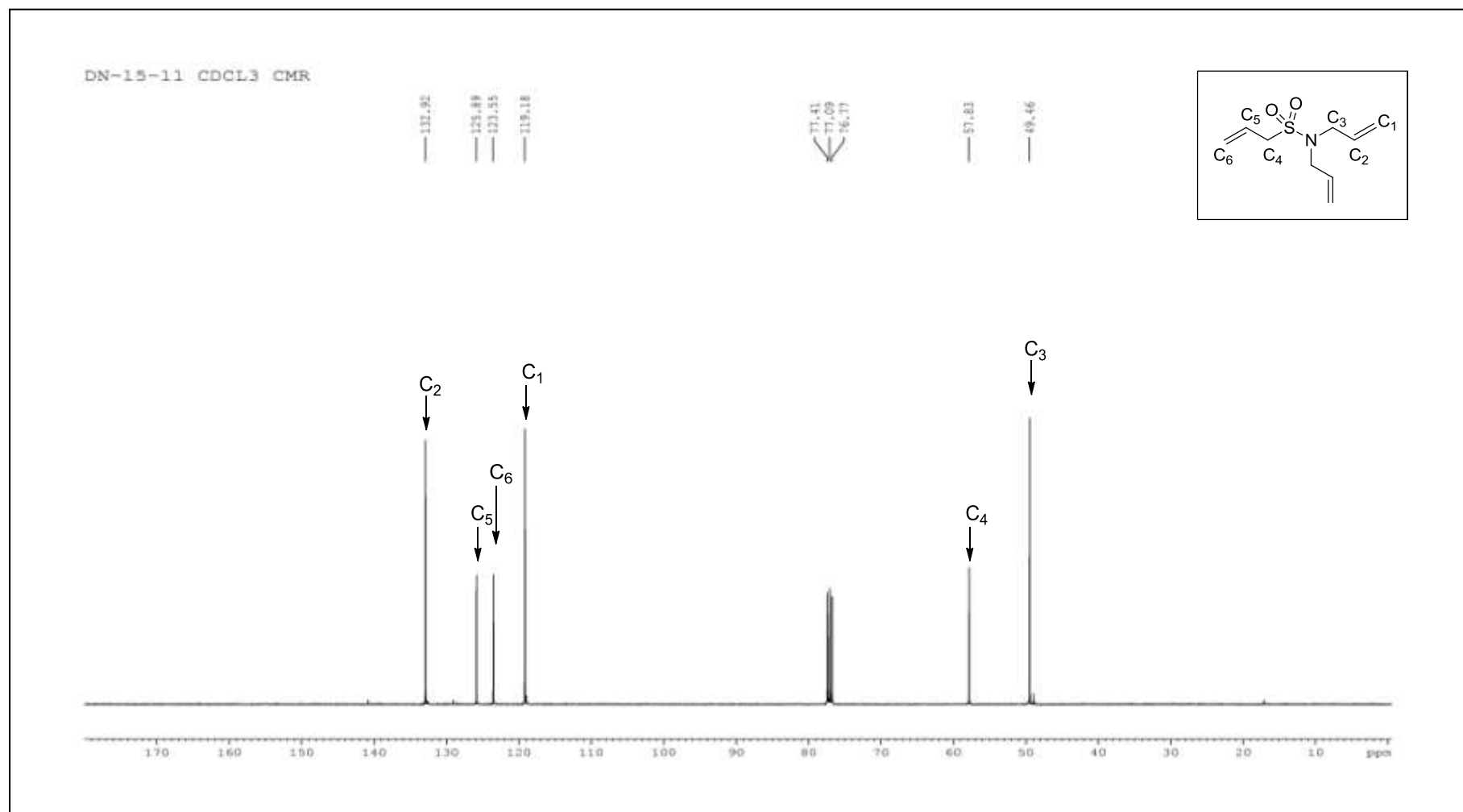
Figure 3.11 (d): ^{13}C NMR spectrum of Triallyl sulfonamide
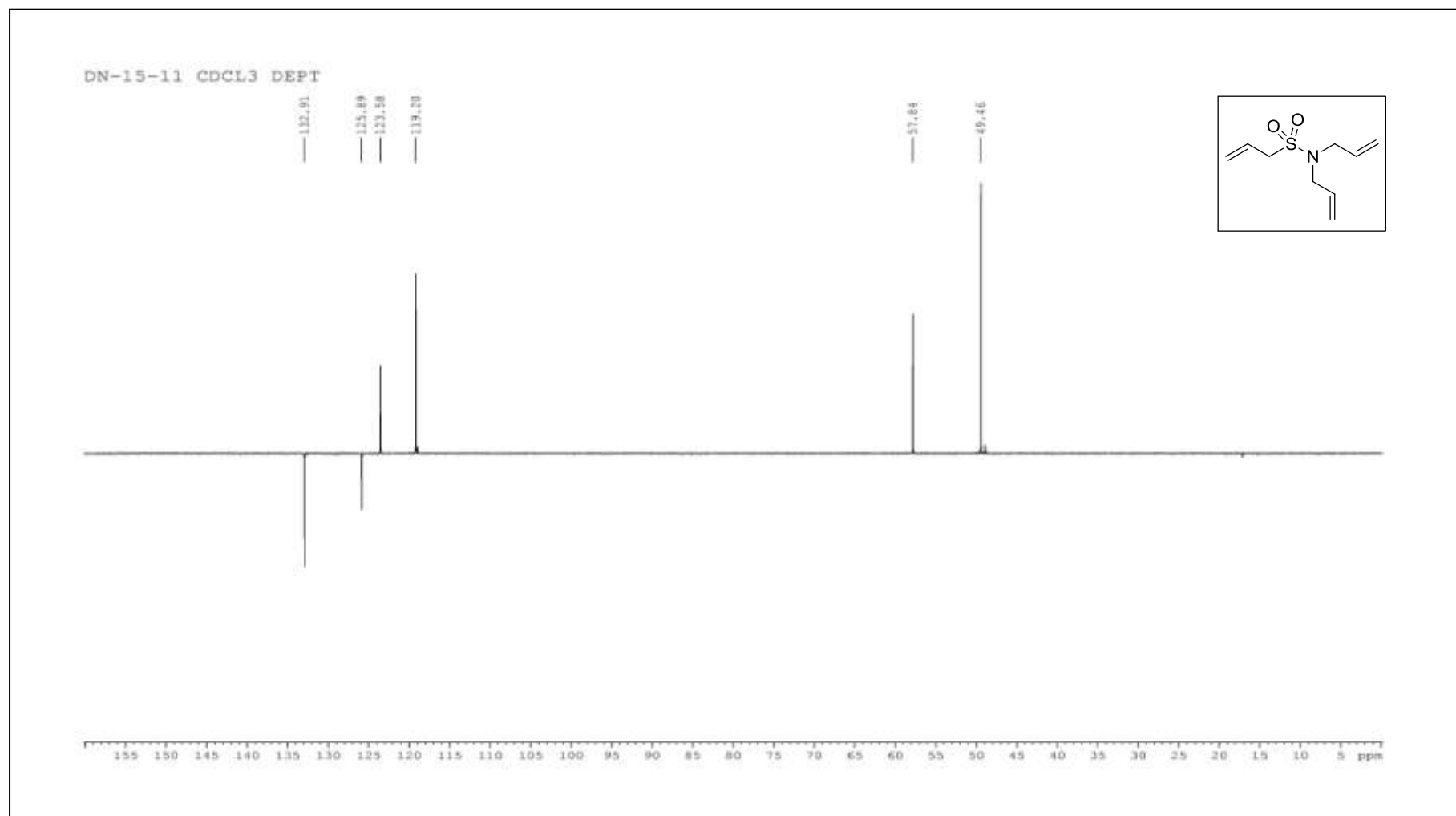
Figure 3.11 (e): DEPT of Triallyl sulfonamide

3.2.1.10 **Synthesis of Allyl sulfone[34] (M9):** Allyl sulfone was prepared from sodium hydroxymethanesulfinate commonly known as Rongalite. 7.7 g (0.0499 moles) of Rongalite was ground using mortal and pestle and suspended in a 50 mL DMF solvent. The suspension was stirred at room temperature. To this, 6.9 g (0.050 moles) K_2CO_3, 0.161 g (0.050 moles) tetrabutylammonium bromide (PTC) and 12.68 g (9.06 mL, 0.1049 moles) allyl bromide was added. The reaction mixture was stirred at room temperature for about 100 hours (4 days) and quenched with cold water. The aqueous content was extracted with diethyl ether (5x 15mL) and washings with brine were given to the organic layer several times. Finally dried by passing over anhydrous sodium sulfate and concentrated. Crude product obtained was purified by column chromatography using 1:9 ethyl acetate-petroleum ether mobile phase. Pure colourless liquid was obtained in 50.2 % yield which was characterized by IR and NMR spectroscopy (figure 3.12a-d; page no. 250-253). Scheme 3.15 below shows synthesis of allyl sulfone. IR (KBr): 3088 cm^{-1},1639 cm^{-1}, 1317 cm^{-1} and 1132 cm^{-1}. ^{1}H NMR (400 MHz, CDCl$_3$) (ppm): 5.98-5.87 (m, 2H), 5.52 (d, 2H), 5.45 (d, 2H), 3.72 (d, 4H). ^{13}C NMR (100 MHz, CDCl$_3$): 124.90, 124.81, 55.96.
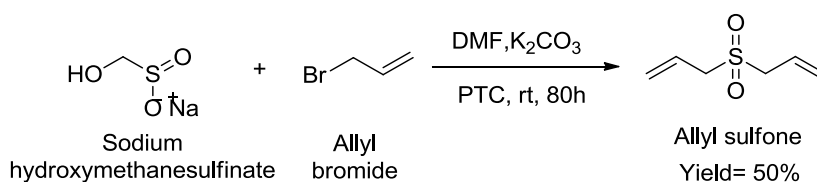
Scheme 3.15: Synthesis of Allyl sulfone.
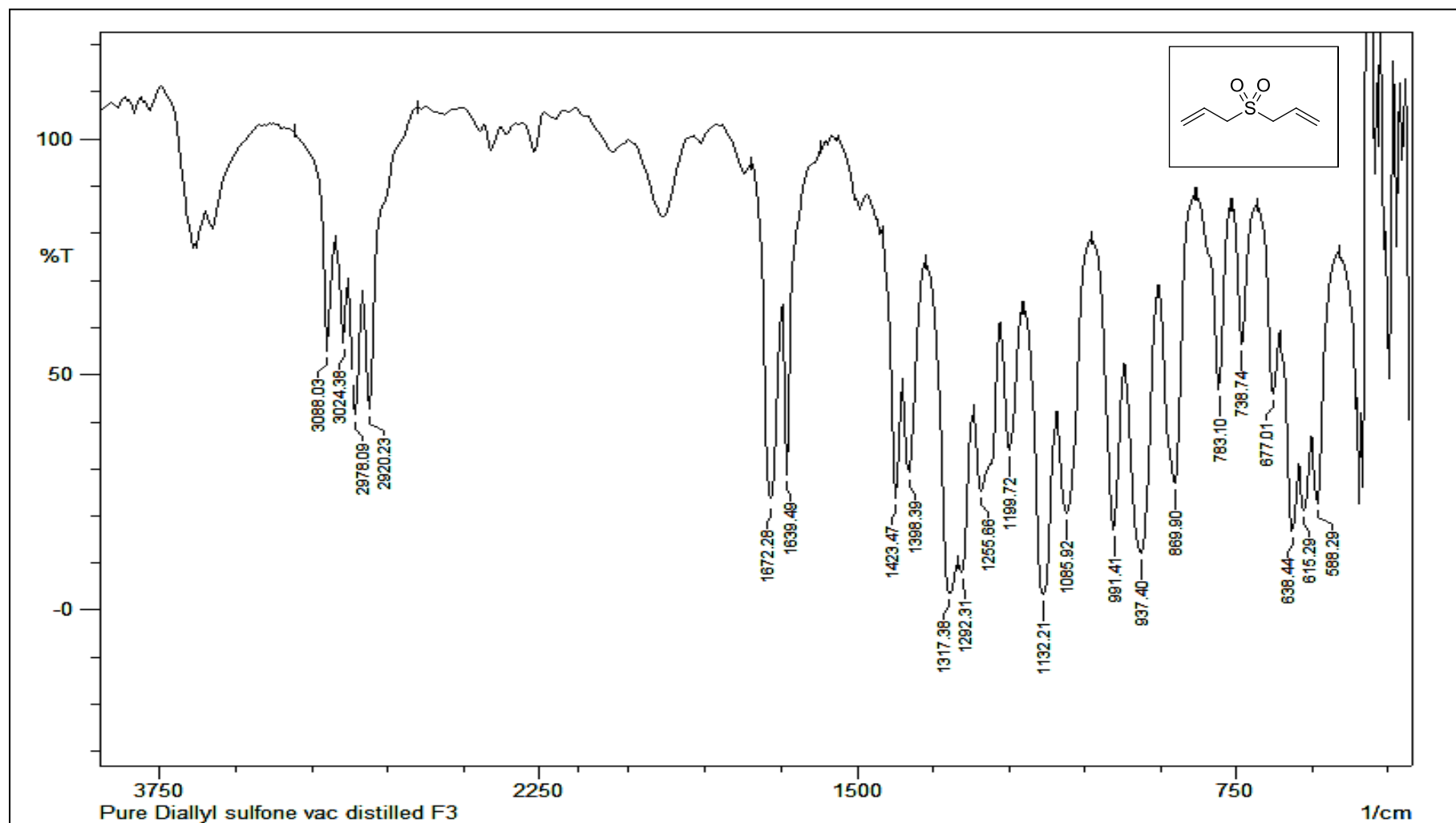
Figure 3.12 (a): IR spectrum of Allyl sulfone
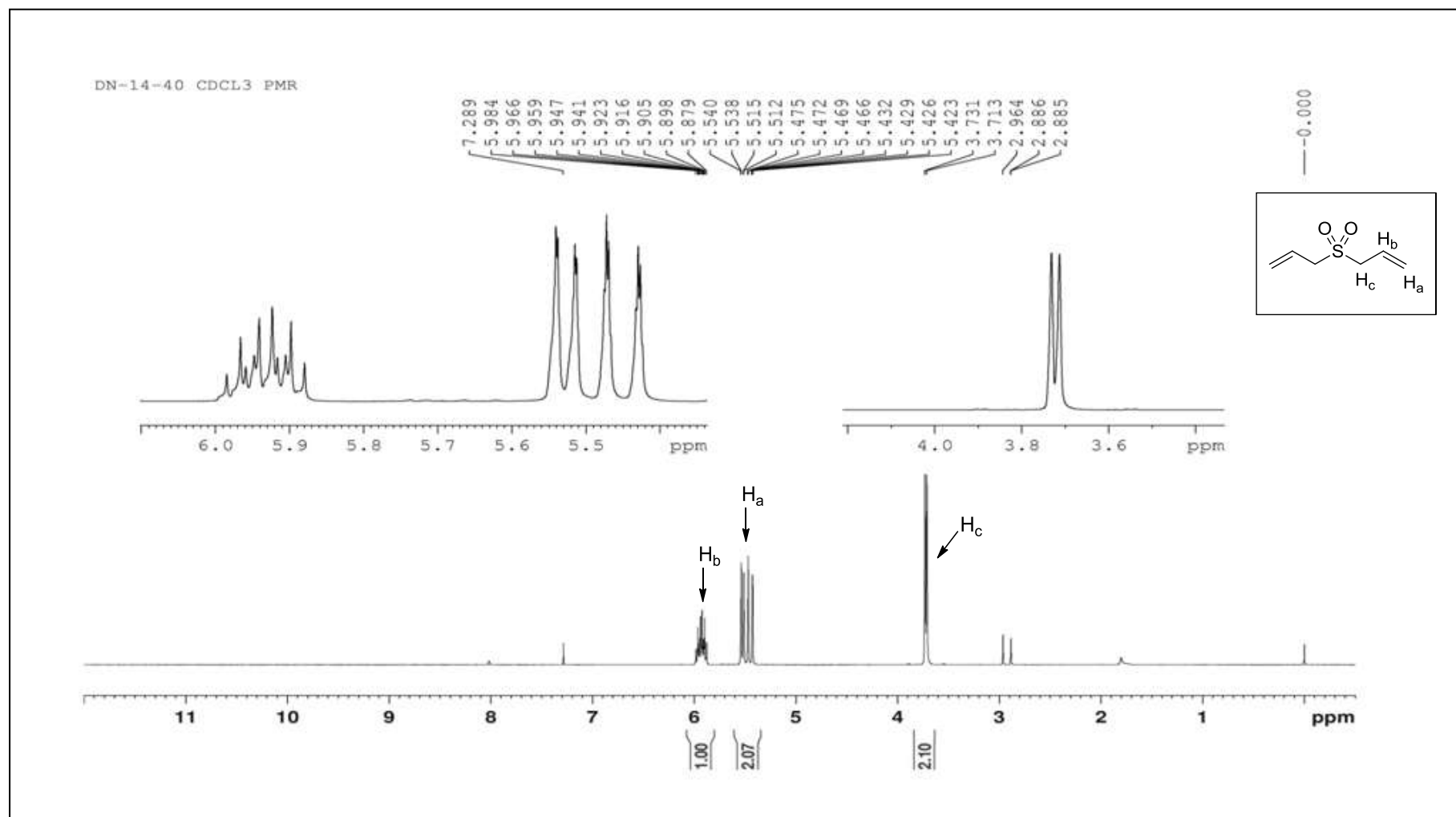
Figure 3.12 (b): ^{1}H NMR spectrum of Allyl sulfone
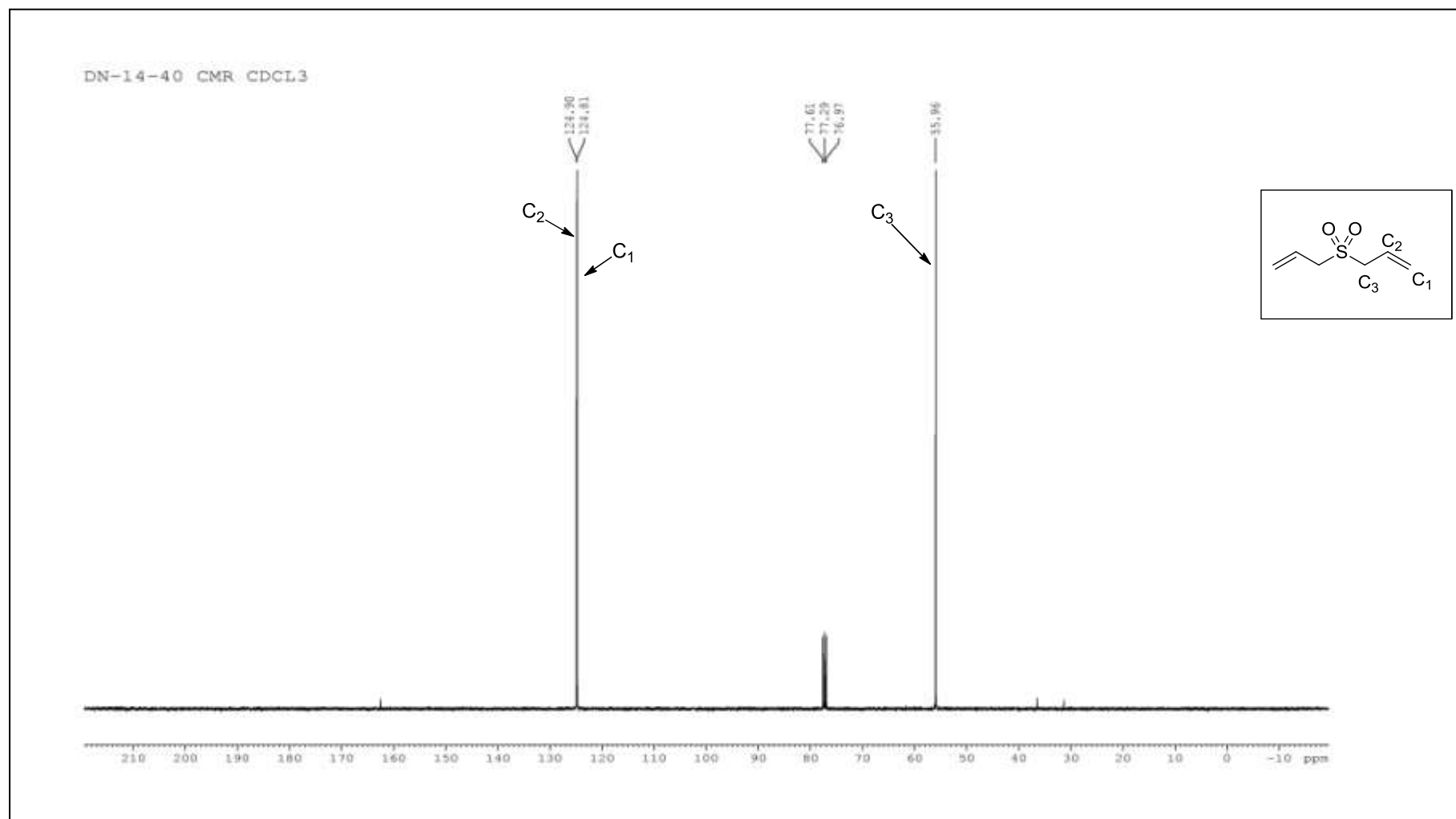
Figure 3.12 (c): ^{13}C NMR spectrum of Allyl sulfone
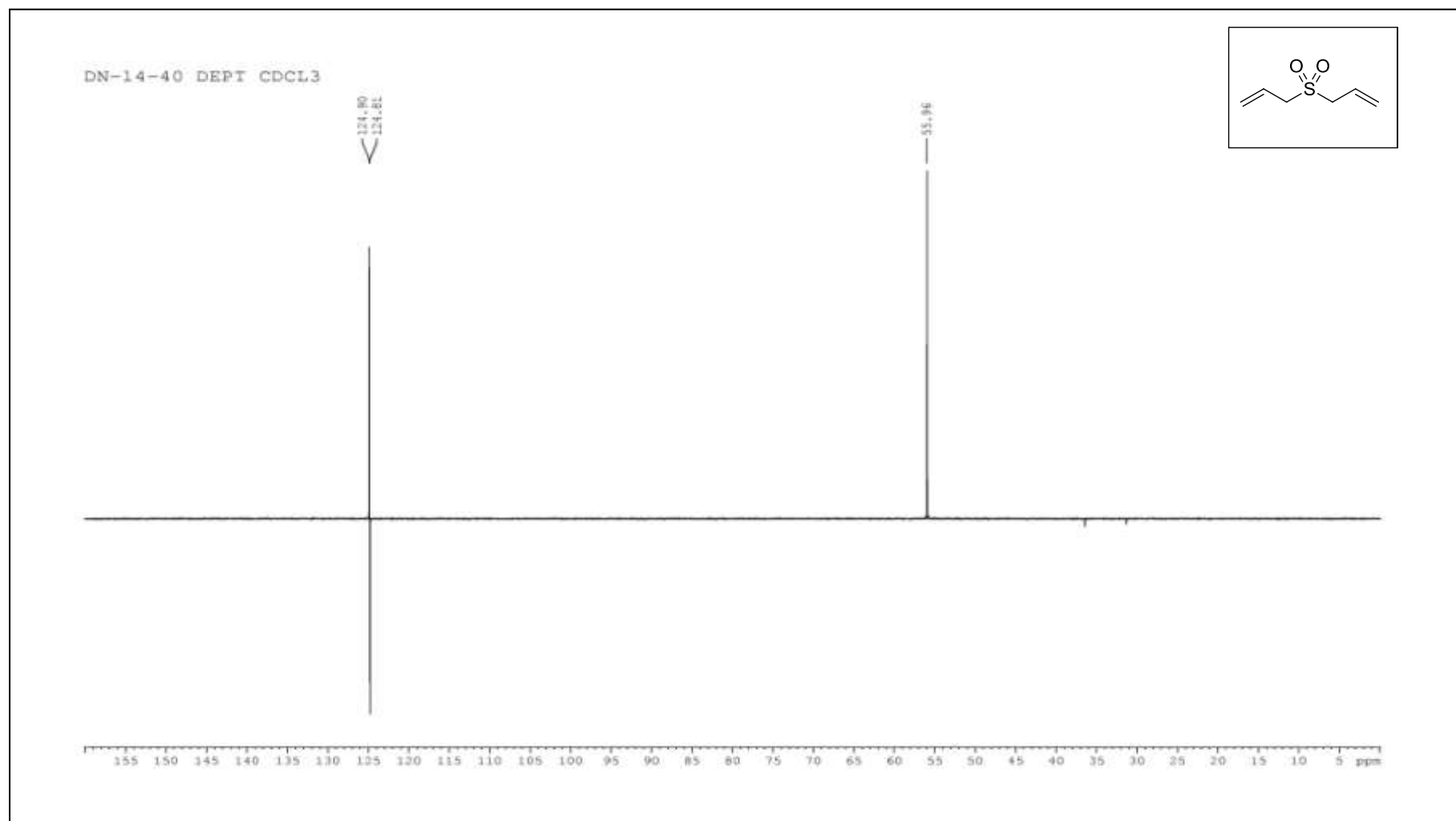
Figure 3.12 (d): DEPT of Allyl sulfone

3.3   Results and Discussion

It is known fact that the radiation sensitivity of any polymeric radiation detector mostly depends upon the functional groups like carbonate (-O-CO-O-), carbamate (-N-CO-O-), nitrate (O-NO_2), sulfonate (O-SO_2-), etc. The presence of ether linkage (-C-O-C-), 3D cross-linked network in the polymer also enhances the radiation sensitivity. As per prior knowledge, radiation sensitivity increases with the change in functional groups in following order carbonate < carbamate < nitrate esters < sulfonate.   Thus, by altering the functionality in monomer unit one can improvise radiation sensitivity. It is seen that polysulfonate material show best results as track detector but its shelf life is very limited[24(a)]. The shelf life of this detector was less due to the presence of more labile sulphonate moiety. Sulfonic esters are a class of organic compounds with the general formula R-SO_2-OR. Sulfonic esters are considered good leaving groups in nucleophilic aliphatic substitution. As mentioned previously, polymers of diethylene glycol bis(allyl sulfonate) undergo decomposition when stored under atmospheric conditions and have no good shelf life[24, 35]. They are relatively stable if stored away from air or moisture and under refrigeration. It appears that the atmospheric oxygen readily combines with the sulfonate moiety where sulfur has oxidation state of +4, to form presumably more stable sulfates where sulfur is present in +6 oxidation state. Analogy could also be drawn to the fact that, in humans, sulphite oxidase enzyme converts sulphites formed during the sulfur metabolism into relatively stable sulphates. In organic sulfonates, the carbon-oxygen bond is cleaved easily under the nucleophilic attack due to electron attracting action of the sulfonyl group[36].   However, sulfones have sulphur in oxidation state of +2 and are characterized by greater stability and require extreme conditions for conversion to sulfonates or sulfates[37]. This is probably due to the negative charge on

the oxygen atoms of sulfonyl group which hinder the nucleophilic attack[36]. The higher stability of ATSC/SDAC polymers may be probably due to these reasons. . In an attempt to develop more efficient plastic track detectors using various sulfur containing functional groups, we have synthesized a few monomers containing sulfide, sulfoxide, sulfone, sulfonamide functional groups along with allylic or allylic carbonate ends. The synthesized monomers were to be cast polymerized into thin, transparent films for examining them as charge particle detectors. Further, the designed polymers have been tested for track detection analysis and were then optimized as per the previously developed protocol by our group[38] for systematic development of polymeric detectors. Alpha sensitivity and alpha track efficiency studies of the developed polymeric materials were carried out.

3.3.1 Designing of sulfur containing monomers/polymers for SSNTD applications:

The presence of hetero atoms in the monomer alters the alpha sensitivity of the detector so prepared. There are reports signifying that the radiation sensitivity of polymeric detectors containing sulfur moieties has been enhanced[19-24]. Also, it was observed that some of these polymers like diallyl sulphite (DAS), allyl diglycol sulphite (ADS) and Diethyleneglycol bis (allyl sulfonate) (DEAS) could reveal nuclear tracks in short period of time i. e. 20-30 minutes[39] but these polymers were not sufficiently stable at room temperature. Since polymers with sulfur functionalities like $-OSO_2-$, $-O(SO)O-$, $-SO_3-$ are known to give better radiation sensitivity, we thought of synthesizing the monomers as shown in figure 3.2 (page no. 175) for nuclear track detection studies.

CHAPTER 3

Thermoplastic thiodiglycol polycarbonates are known in literature for their use in production of polyurethane plastics[40] and for other optical materials[41]. However, we prepared monomers containing sulfide and allyl carbonate functional moieties which would give thermosetting plastics. Thus, allyl thiodiglycol carbonate (ATC) was prepared by reacting β-thiodiglycol with allyl chloroformate. It consists of sulfide linkage along with two allyl carbonate groups. Similarly monomers M2 and M3 were prepared by reacting allyl chloroformate with disulfide dihydroxy ethane and disulfide dihydroxy diethyl ether respectively. These monomers have sulfide linkage; ether functional group and allyl carbonate end groups. Further, sulfoxide containing allylic monomer, 2,2'-sulfinyldiethanol bis (allyl carbonate) (M4) was synthesised in two steps (scheme 3.6; page no. 200). The polysulfone polycarbonates are also well known in the literature[42]. Then sulfone containing allylic monomers viz. 2,2'-sulfonyldiethanol bis(allyl carbonate) (SDAC), 2,2'-(ethane-1,2-diyldisulfonyl)diethanol bis (allyl carbonate) (M5), 2,2'-(3-oxapentane-1,5-diyldisulfonyl)diethanol bis (allyl carbonate) (M6) and Allyl sulfone (M9) were prepared. SDAC was prepared by oxidising β-thiodiglycol to thiodiglycol sulfone followed by its condensation with allyl chloroformate at low temperature using pyridine. Two methods were opted for the synthesis of Monomer M5. In the first method disulfide dihydroxy ethane was oxidised to disulfone dihydroxy ethane which was subjected to transesterification process with diallyl carbonate but could not gave desired product. Then condensation of disulfone dihydroxy ethane with allyl chloroformate was carried out using base at lower temperature which led to desired product but in very low yield (Scheme 3.8a, b; page no. 210). The solid monomer M5 was obtained in good yield by oxidation of M2 using hydrogen peroxide in acidic medium (Scheme 3.9; page no. 211). Similarly monomer M6 was

synthesised by oxidation of M3 in very good yield (scheme 3.11; page no. 221). Condensation process gave product in 10% yield (Scheme 3.10; page no. 219). Allyl sulfone (M9) was synthesized by reacting allyl bromide with sodium hydroxymethanesulfinate in presence of base and phase transfer catalyst (PTC) at elevated temperature. Also, triallyl sulfonamide (M8) was prepared by reacting allyl sulfonyl chloride with diallyl amine. All the monomers prepared have two or more than two allylic functionalities. The presence of two allyl groups should help in free radical polymerization using initiators like benzoyl peroxide (BP), diisopropyl peroxydicarbonate (IPP), azobisisobutyronitrile (AIBN), etc. These monomers were then analysed further for their interaction with different initiators at high temperature.

Vacuum distillation is generally employed to get pure monomers that give high quality, transparent polymeric films. Most of the prepared monomers have high boiling points and could not be distilled at atmospheric pressure. Vacuum distillation of many of them was also difficult and the distilled monomers failed to undergo polymerization using 3-4 % of IPP initiator. So column chromatographic technique was utilised for monomer purification. Stability, techniques of purification and % yield of product obtained is given in table 3.1. Only ATC monomer was vacuum distilled and rests all the monomers were purified by column chromatographic techniques as some of them got decomposed during vacuum distillation. Vacuum distillation of SDAC was tried out at 10 mm of Hg pressure and 220 $^{\circ}$C temperature but few drops of the monomer got collected and remaining got decomposed in flask due to overheating for longer period.

Table 3.1: Stability of the monomers and their purification techniques.

Sr. No.	Monomer	Stability	Purification technique	% Yield (pure monomer)
1	Allyl Thiodiglycol Carbonate (ATC/M1)	Unstable under normal distillation	Vacuum distillation at 140°C and 2 mbar pressure	78.0
2	3,6-dithiaoctan-1,8-diol bis (allyl carbonate) (M2)	Could not be distilled using vacuum upto 5 mm of Hg.	Column chromatography using 20% Ethyl acetate in petroleum ether	79.0
3	5,5'-oxybis(3-thiapentan-1-ol) bis(allyl carbonate) (M3)	Could not be distilled using vacuum upto 5 mm of Hg.	Column chromatography using 30% Ethyl acetate in pet ether	81.0
4	2,2'-sulfinyldiethanol bis (allyl carbonate) (M4)	Could not be distilled using vacuum upto 5 mm of Hg.	Column chromatography 3:7 using ethyl acetate and petroleum ether as mobile phase	25.0
5	2,2'-sulfonyldiethanol bis(allyl carbonate) (SDAC/ ATSC/ M7)	Could not be distilled using vacuum upto 5-10 mm of Hg.	Column chromatography 30% ethyl acetate in petroleum ether	60.5
6	2,2'-(ethane-1,2-diyldisulfonyl)diethanol bis (allyl carbonate) (M5)	Solid, Melting point is 90-92 °C	Column chromatography 3:7 using ethyl acetate and petroleum ether as mobile phase	70.0
7	2,2'-(3-oxapentane-1,5-diyldisulfonyl) diethanol bis (allyl carbonate) (M6)	-	Column chromatography using 3:7 ethyl acetate and n-hexane	85.0

| 8 | N,N-diallylprop-2-ene-1-sulfonamide TAS (M8) | Unstable at normal distillation - | Column chromatography with 20% ethyl acetate in petroleum ether | 51.3 |
| 9 | Allyl sulfone (M9) | Unstable at normal distillation | Column chromatography using 1:9 ethyl acetate-petroleum ether mobile phase | 50.2 |

3.3.2 Free radical polymerization of the monomers for test polymers

To check the suitability of the designed monomers for nuclear track detection, test polymers were prepared first. Different initiators were used for testing polymerization of the prepared monomers. Interaction with IPP was tested first and other initiators BP, AIBN were used only if no gelation occurred with IPP. The interaction of monomers with different initiators was checked at an elevated temperature as noted in table 3.2 below. The temperature was chosen depending on type of initiator used.

Table 3.2: Interaction of various monomer compositions with initiators

Sr. No.	Monomer composition (wt. by wt.)	Initiator used	Temperature (^{o}C)	Time (h)	Observation/Remark
1	ATC (M1)	10%IPP/ 10%BP/ 5%AIBN	60 80 80	16	No gelation occurred, Not polymerizable.
2	ATC:ADC (1:9, w/w)	4%IPP/ 4%BP	60 80	12	No gel formation, Not polymerizable.
3	ATC:ADC (1:1, w/w)	4%IPP/ 4%BP	60 80	12	No gel formation, Not polymerizable

4	ATC:TAP (1:1 w/w)	4%IPP/ 4% BP	60 80	12	No gelation, Not polymerizable.
5	ATC:PETAC (1:1 w/w)	6% IPP 4%BP	60 90	12	No Gelation, Not polymerizable.
6	M2	4% IPP 4%BP	65 80	5	No gelation, Not polymerizable.
7	M2:ADC (1:1, w/w)	4% IPP 4%BP	65 80	5	No gel formation, Not polymerizable.
8	M3	4% IPP 4%BP	60 80	6	No gel formation, Not polymerizable.
9	1:1 M3:ADC	4% IPP 4%BP	60 80	6	No gel formation, Not polymerizable.
10	M4	4% IPP	55	5	Gelation occurred, may be polymerizable
11	M4:ADC (1:1, w/w)	4% IPP	55	5	Gelation occurred, may be polymerizable
12	SDAC	4% IPP	55	6	Gel formation occurred, polymerizable.
13	SDAC:ADC (1:1, w/w)	4% IPP	55	6	Gel formation occurred, polymerizable.
14	SDAC:PETAC (1:1, w/w)	4% IPP	60	6	Gel formation occurred, polymerizable.
15	SDAC:NADAC (1:1, w/w)	4% IPP	60	6	Gel formation occurred, polymerizable.
16	SDAC:TAP (1:1, w/w)	4% IPP	60	6	Gel formation occurred, polymerizable.
17	M5:ADC (1:1, w/w)	4% IPP	60	6	Gel formation occurred,

					polymerizable.
18	M6	4% IPP	60	6	Gel formation occurred, polymerizable.
19	M6:ADC (1:1, w/w)	4% IPP	60	6	Gel formation occurred, polymerizable.
20	M8	4% IPP 4%BP	60 80	6	No Gelation, Not polymerizable.
21	M8:ADC (1:1, w/w)	4% IPP 4%BP	60 80	6	No Gelation, Not polymerizable
22	M9	4% IPP 4%BP	60 80	6	No Gelation, Not polymerizable.
23	M9:ADC (1:1, w/w)	4% IPP 4%BP	60 80	6	No Gelation, Not polymerizable.

It is clear from above table that, sulfide, disulfide ethane or disulfide ether containing monomers i.e. ATC, M2 and M3 respectively could not be polymerized using IPP or BP or AIBN initiators even at elevated temperature. Their combination with ADC, PETAC or TAP monomers also could not form any gel leading to polymer. Triallyl sulfonamide M8 and its mixture with ADC in presence of IPP initiator decomposes to give brownish liquid at 80 ^{o}C temperature. Allyl sulfone (M9) also decomposed upon heating with IPP initiator at 60 ^{o}C leading to brown liquid after 12 hours. Sulfoxide-carbonate, sulfone-carbonate containing monomers that is M4, SDAC, M5 and M6 formed gel upon heating with 4% IPP initiator. Their mixture with other monomers viz. ADC, PETAC, NADAC etc. could also be polymerized.

All the above sulfone-carbonate monomers were then cast polymerized using appropriate amount of IPP initiator to prepare test polymers. The polymerization was carried out using 12 hour constant rate polymerization profile developed for ADC.

CHAPTER 3

These monomers are also copolymerized with ADC, PETAC, and NADAC monomers. The constant rate polymerization profile and amount of initiator used for test polymers is given in Table 3.3. The prepared test polymers were used to investigate track detection property.

Table 3.3: Curing conditions used for polymerization of different test polymers.

Sr. No.	Monomer (wt. by wt.)	Initiator used (Concentration in wt.%)	Heating profile (Temperature range)
1	M4	IPP (4.0)	ADC polymerization profile (45-95°C)
2	M4:ADC (1:1)	IPP (4.0)	ADC polymerization profile (45-95°C)
3	SDAC (M7)	IPP (3.3)	ADC polymerization profile (45-95°C)
4	SDAC:ADC (1:1)	IPP (3.3)	ADC polymerization profile (45-95°C)
5	SDAC:PETAC (1:1)	IPP (4.0)	PETAC polymerization profile (40-98°C)
6	SDAC:NADAC (1:1)	IPP (4.0)	NADAC polymerization profile (42-91°C)
7	SDAC:TAP (1:1)	IPP (4.0)	TAP polymerization profile (42-110°C)
8	M5:ADC (1:1)	IPP (3.3)	ADC polymerization profile (45-95°C)
9	M6	IPP (4.0)	ADC polymerization profile (45-95°C)
10	M6:ADC (1:1)	IPP (4.0)	ADC polymerization profile (45-95°C)

All the polymeric films prepared were hard and clear except poly (2,2'-sulfinyldiethanol bis (allyl carbonate)) and poly (M4-*co*-ADC), which were soft.

Average thickness and other properties of the prepared test films are reported below in table 3.4.

3.3.3   Initial track detection studies of designed polymers:

All the prepared polymeric films were cut into small pieces of 1 cm^2 and were exposed to alpha particles from a ^{239}Pu source and to a ^{252}Cf source for fission fragments. The exposed polymeric films were etched in 6N NaOH at 70 ^{o}C. Poly (2,2'-sulfinyldiethanol bis (allyl carbonate)) and poly (M4-*co*-ADC) being soft could not reveal charged particles after etching for 1 hour. Homopolymer of PSDAC and M6 revealed charged particles. Copolymers of SDAC with ADC, PETAC and NADAC showed charged particle tracks and also copolymer of M6 with ADC showed nuclear tracks. Poly (SDAC-*co*-TAP) could not reveal tracks and became opaque white after etching for 1 hour.

Table 3.4: Physical and track detection properties of the polymers

Sr. No.	Polymer composition (Wt. by wt.)	Avg. Thick-ness (μm)	Color and hardness before etching	Time to observe alpha tracks	Type of nuclear tracks revealed after chemical etching
1	M4	580±10	Colorless soft film	-	No tracks seen
2	M4:ADC (1:1)	612±10	Colorless soft film	-	No tracks seen
3	SDAC	529±10	Hard colorless film	1	Alpha and fission
4	SDAC:ADC (1:1)	537±10	Hard colorless film	1	Alpha and fission
5	SDAC:PETAC (4:6)	532±10	Hard colorless film	6	Alpha and fission
6	SDAC:NADAC (1:1)	530±10	Hard colorless film	6	Alpha and fission

7	SDAC:TAP (1:1)	556±10	Hard colorless film	-	-
8	SDAC:TAP (9:1)	540±10	Hard colorless film	-	-
9	SDAC:TAP (9:1)	564±10	Hard colorless film	-	-
10	M5:ADC (1:9)	558±10	Hard colorless film	5	Alpha and fission
11	M6	551±10	-	5	Alpha and fission
12	M6:ADC (3:7)	523±10	Hard colorless film	4	Alpha and fission
13	SDAC:ADC: PETAC (1:1:1)	518±10	Hard colorless film	4	Alpha and fission
14	SDAC:ADC: NADAC (1:1:1)	508±10	Hard colorless film	5	Alpha and fission
15	SDAC:PETAC: NADAC (1:1:1)	550±10	Hard colorless film	5	Alpha and fission

Since SDAC based polymers appeared to be very much promising and rapidly revealing the alpha tracks, we then carried out optimization studies of SDAC homopolymer and its copolymers with ADC, for further analysis to produce better nuclear track detectors. So, the time required for alpha and fission track revelation by PSDAC and its copolymers with ADC was determined and compared with indigenously prepared PADC and commercially available CR-39 detectors. The post etched surface and bulk etch rate of the polymers was also observed upon etching in 6N NaOH at 70 $^\circ$C as given in table 3.5. From the results obtained it is clear that, monomers containing sulfone-carbonate functionalities can reveal nuclear tracks within 1 minute of chemical etching. Homopolymer PSDAC as well as copolymers of SDAC with ADC revealed alpha and fission tracks very quickly. Post etched surface of all polymers was clear except for PSDAC which became hazy after longer

etching time. Bulk etch rate for PSDAC and poly (SDAC-*co*-ADC) was very high as compared to that of CR-39.

Table 3.5: Track recording properties and post etched surface study of different test polymers of SDAC.

Sr. No.	Composition of polymer (Wt. by wt.)	*Time for track revelation in minutes in 6N NaOH at 70°C		Post etched surface of polymers	Bulk etch rate V_b (μ/min.)
		Alpha track	Fission fragment		
1	SDAC homopolymer	1	0.5	Clear	39.5
2	SDAC-ADC (1:9)	2	1	Hard, transparent	0.4642
3	SDAC-ADC (2:8)	1	0.5	Clear	1.97
4	SDAC-ADC (3:7)	1	0.5	Clear	4.28
5	SDAC-ADC (4:6)	1	0.5	Clear	9.37
6	SDAC-ADC (1:1)	1	0.5	Clear	14.21
7	PADC (indigenous)	120	90	Nil	0.06 μ/h
8	CR-39 (commercial)	120	90	Nil	0.08 μ/h

*Exposure: ^{239}Pu at 2mm for 2minute and ^{253}Cf at 2 mm for 2 h; Etching condition: 6N NaOH at 70 ^{o}C

From the initial studies it was clear that the PSDAC and poly (SDAC-*co*-ADC) polymeric films are rapidly detecting nuclear tracks. In order to identify the best performing detector composition in this series, we need to optimize the polymerization conditions, etching conditions and initiator concentration etc[38]. Polymerization condition could be optimized by performing kinetics study during polymerization but before kinetics study, catalytic hydrogenation of SDAC monomer was carried out to check the effect of Wij's reagent that is used for

unsaturation analysis on sulfone moiety. It is important to note whether sulfone functionality reacts with the Wij's reagent or is neutral to the Wij's reagent. Hydrogenation of SDAC monomer was carried out in a catalytic hydrogenation apparatus using activated Pd/C and ethyl acetate solvent for 16 hours. The product obtained (H-SDAC) was pure and directly characterized by IR and NMR spectra. The unsaturation analysis of the same was performed and compared with SDAC and ADC monomers. Unsaturation analysis showed that SDAC and ADC have 2 double bonds each and for hydrogenated product there are no double bonds.

Table 3.6: Unsaturation values of SDAC, H-SDAC and ADC monomers.

Samples	Unsaturation
SDAC – Sample 1	1.96
SDAC – Sample 2	2.12
SDAC – Sample 3	2.01
H-SDAC – Sample 1	0.00
H-SDAC – Sample 2	0.00
H-SDAC – Sample 3	0.06
ADC – Sample 1	1.96
ADC – Sample 2	2.15

It is clear from the table 3.6 that sulfone moiety does not react with Wij's reagent and so one can safely perform kinetic study of polymerization of SDAC monomer as well as of the poly (SDAC-*co*-ADC) polymers to generate constant rate polymerization profiles by extending the Dial's kinetics model[43].

3.3.4 Polymerization kinetics of SDAC monomer using IPP initiator:

CHAPTER 3

As the test polymers PSDAC and its copolymer showed good radiation sensitivity and etching property as compared to that with commercial CR-39[TM] we extended the Dial's model to study the polymerization of tetrafunctional SDAC monomer. We have already applied Dial's kinetics model to various tetrafunctional allylic monomers as well as to allylic monomers having higher functionality[39]. To begin with the kinetics of polymerization, time required by SDAC monomer for gel formation at different temperature was noted. SDAC monomer was mixed with 3.3% IPP initiator and the mixture was bubbled with dry nitrogen gas. The mixture was taken into 3 different test tubes and tightly stoppered all three test tubes. Each test tube was placed in a waterbath maintained at 40, 50 and 60 ^{o}C separately. Time required for gel formation was determined and recorded in table 3.7 below. At this set of temperature, kinetics was carried out.

Table 3.7: Time required for the gelation of SDAC monomer.

% IPP concentration (by wt.)	Temperature ^{o}C	Time (h)	Remark
3.3	40	8	Mobile gel
	50	6	Immobile gel
	60	3	Immobile gel

A set of sealed test tubes filled with 0.5 g of SDAC monomer and 3.3% IPP initiator were heated at specified temperature and analysed for unsaturation and IPP concentration left after certain time interval. The percent unsaturation and initiator concentration remaining at different temperatures i.e. at 40, 50, and 60 ^{o}C for different time intervals are given in tables 3.8, 3.9 and 3.10.

Table 3.8: Peroxide and unsaturation contents for different time interval at 40 ^{o}C

Sr. No.	Time (h)	Unsaturation (%)	Peroxide (%)
1	0	100	3.31
2	1	98.83	3.23
3	2	93.12	3.14
4	3	89.43	3.06
5	4	82.37	3.00
6	5	80.21	2.94
7	6	75.45	2.85
8	7	71.18	2.78
9	8	70.34	2.70

Table 3.9: Peroxide and unsaturation contents for different time interval at 50 ^{o}C

Sr. No.	Time (h)	Unsaturation (%)	Peroxide (%)
1	0	100.00	3.33
2	1	88.92	3.15
3	2	82.63	3.01
4	3	71.16	2.80
5	4	60.18	2.63
6	5	55.52	2.55
7	6	46.34	2.41
8	7	35.50	2.10
9	8	30.15	1.73

Table 3.10: Peroxide and unsaturation contents for different time interval at 60 ^{o}C

Sr. No.	Time (h)	Unsaturation (%)	Peroxide (%)
1	0.00	100.00	3.32

2	0.25	91.10	3.01
3	0.50	82.23	2.81
4	0.75	65.18	2.31
5	1.00	53.36	1.98
6	1.25	42.32	1.69
7	1.50	35.23	1.52
8	2.00	32.14	1.37
9	2.50	30.22	1.20

From the table 3.8-3.10, it is clear that the rate of polymerization increases with increase in temperature. The graphical representation of the results obtained during kinetics of SDAC monomer is shown below in figure 3.13.
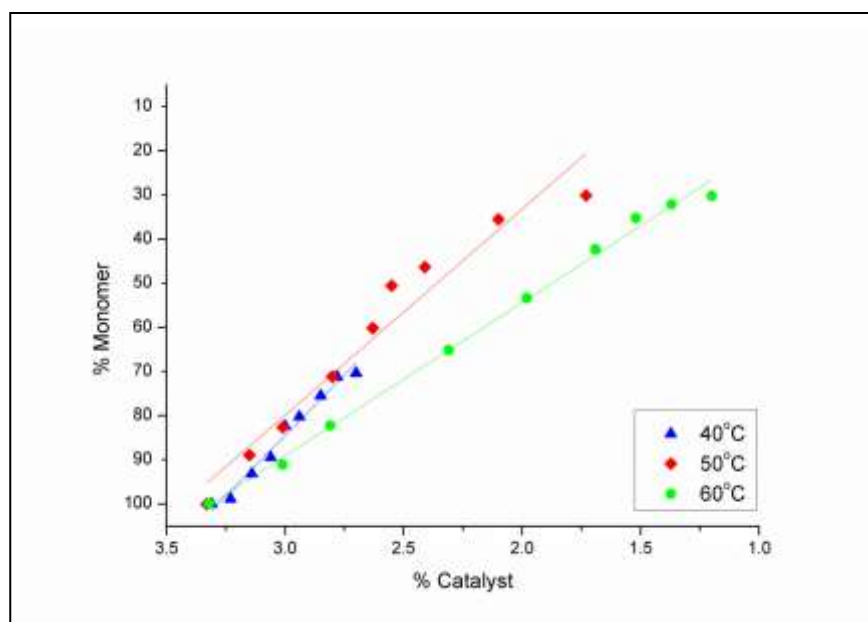
Figure 3.13: Graphical representation of the amount of initiator and unsaturation at 40, 50 and 60°C for SDAC.

The slopes obtained for three lines were:

At   40 $^{\circ}$C, K_1=   54.64

         50 $^{\circ}$C, K_1=   46.47

60 ^{o}C, K$_1$=   34.74

The K$_1$ values of the graph obtained was above the limiting values for the slope. These K values were used in solving Dials equation to obtain the kinetic constants E$_1$, Z$_1$, E$_3$, and Z$_3$. The kinetic constants obtained after solving the Dial's equations are given in the table 3.11.

Table 3.11: Values obtained for the constants given in the Dials equation.

Sr. No.	Constant	Value
1	R	1.986
2	E$_1$	-4664.1 cal
3	E$_3$	28347.3 cal
4	Z$_1$	3.03 E-02
5	Z$_3$	1.67 E+18

By solving Dial's equations, a constant rate polymerization profile was calculated for SDAC homopolymer. The heating profile was developed for 10.5 hours only as the roots of Dial's equation become imaginary after this time. Further, it was extrapolated smoothly to obtain 12 hours heating profile. This smooth extrapolation was done keeping in mind the fact that the residual unsaturation of polymer becomes negligible if the polymer is heated at about 95 ^{o}C towards the end of polymerization[43]. The constant rate polymerization curve obtained is as shown in figure 3.14.
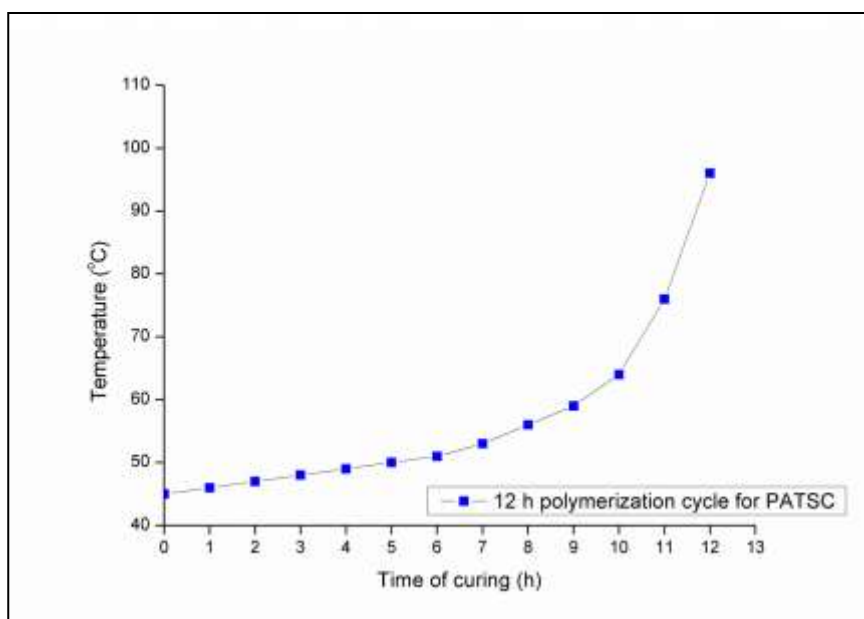
Figure 3.14: 12 hour constant rate polymerization profile for PSDAC using 3.3% IPP.

The constant rate polymerization profile obtained for SDAC polymerization was verified for its effectiveness. SDAC monomer along with IPP initiator was heated in a programmable bath using above developed constant rate polymerization profile and after every hour, unsaturation analysis were carried out to determine % polymerization. Graphically the linear correlation coefficient of experimental values with expected values for 12 h constant rate polymerization profile was determined. It is graphically represented in figure 3.15. The constant rate polymerization profile developed for PSDAC is supported well by linear correlation coefficient (R^2) of 0.9991. This implies that the developed polymerization profile for SDAC polymerization is in good agreement with the kinetic model given by Dial and co-workers and can be used for cast polymerization process.
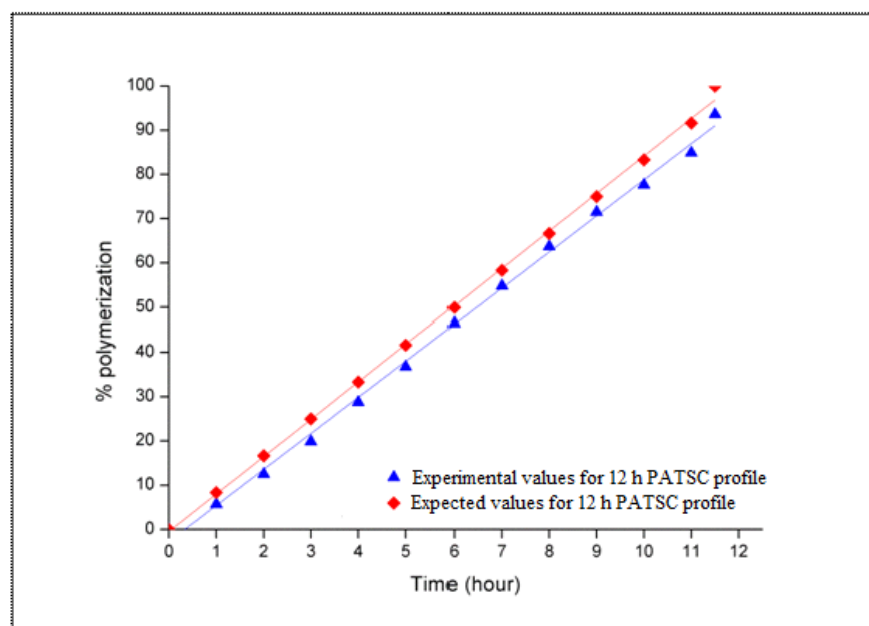
Figure 3.15: Verification of 12 hour polymerization profile for PSDAC using 3.3% IPP.

3.3.5 Polymerization kinetics of SDAC: ADC (4:6 w/w) copolymer using IPP initiator:

It is known that copolymers of an allylic monomer using ADC show better radiation sensitivity. Poly (SDAC-*co*-ADC) showed enhanced radiation sensitivity as noted in terms of alpha sensitivity. Hence, it is necessary to carry out kinetics study of polymerization of SDAC and ADC monomers using 3.3% IPP initiator[39]. The time required for gel formation using 3.3% IPP initiator at specific temperature was determined. The results of gel formation are given in table 3.12. Further analysis was carried out using same set of temperatures.

Table 3.12: Time required for the gelation of Poly (SDAC-*co*-ADC; 4:6 w/w) using IPP at different temperature.

% IPP concentration	Temperature ^{o}C	Time (h)	Remark
	40	8	Mobile gel

3.3	50	7	Immobile gel
	60	2.5	Immobile gel

A set of test tubes containing the monomer mixture and IPP was heated at 40, 50 and 60 ^{o}C temperature separately. The test tubes were analysed for unsaturation content as well as initiator content remaining after specific time interval. The results found out at three different temperatures are given in table 3.13, 3.14, and 3.15.

Table 3.13: Peroxide and unsaturation contents for different time interval at 40 ^{o}C

Sr. No.	Time (h)	Unsaturation (%)	Peroxide (%)
1	0	100	3.31
2	1	96.23	3.22
3	2	92.15	3.13
4	3	88.92	3.09
5	4	85.84	3.00
6	5	80.73	2.93
7	6	75.77	2.85
8	7	72.86	2.79
9	8	70.03	2.73

Table 3.14: Peroxide and unsaturation contents for different time interval at 50 ^{o}C

Sr. No.	Time (h)	Unsaturation (%)	Peroxide (%)
1	0	100.00	3.33
2	1	86.22	3.01
3	2	77.71	2.82
4	3	65.56	2.58
5	4	56.48	2.37
6	5	49.67	2.21
7	6	43.96	2.05
8	7	38.65	1.92

| 9 | 8 | 33.24 | 1.70 |

Table 3.15: Peroxide and unsaturation contents for different time interval at 60 $^{\circ}$C

Sr. No.	Time (h)	Unsaturation (%)	Peroxide (%)
1	0.00	100.00	3.32
2	0.25	83.76	2.89
3	0.50	77.17	2.68
4	0.75	65.43	2.39
5	1.00	54.64	2.09
6	1.25	48.86	1.85
7	1.50	42.51	1.60
8	2.00	37.14	1.41
9	2.50	31.45	1.30

The results obtained for kinetics of SDAC-ADC monomer mixture are represented in a graphical manner in figure 3.16.
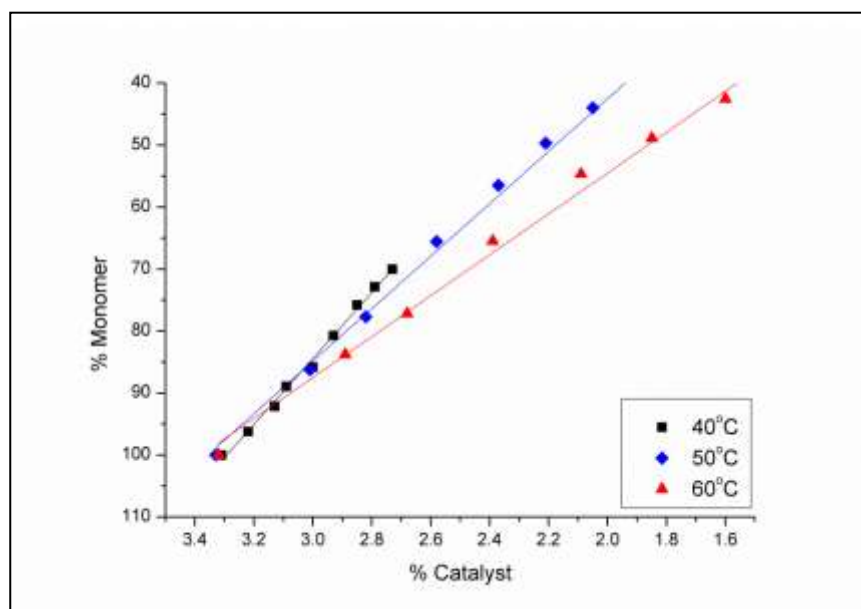
Figure 3.16: The amount of initiator and unsaturation present at 40, 50 and 60°C for SDAC+ADC mixture.

It is clear from table 3.13-3.15 that the polymerization rate increases with increase in temperature. Gelation of the mixture took place between 70-80 $^{\circ}$C of unsaturation.

The slopes obtained for three lines were

At   40 $^{\circ}$C, K_1=   53.22

        50 $^{\circ}$C, K_1=   42.36

        60 $^{\circ}$C, K_1=   32.99

From the K_1 values, kinetic constants were generated which in turn used to generate constant rate polymerization profile. The kinetic constants E_1, Z_1, E_3 and Z_3 are given in table 3.16 below.

Table 3.16: Values obtained for the constants given in the Dials equation for poly (SDAC-*co*-ADC).

Sr. No.	Constant	Value
1	R	1.986
2	E_1	-4937.15 cal
3	E_3	28321.13 cal
4	Z_1	1.87 E-02
5	Z_3	1.73 E+18

By using a FORTRAN program Dial's equation was solved and constant rate polymerization profile was generated. It was noted that for time more than 10 hours, roots of equations proposed by Dial became imaginary and hence smooth extrapolation of the profile to reach about 95 $^{\circ}$C at the end of 12 hours was done. The constant rate polymerization profile developed for poly (SDAC-*co*-ADC) using IPP initiator is represented graphically in figure 3.17. It was also verified for its effectiveness.
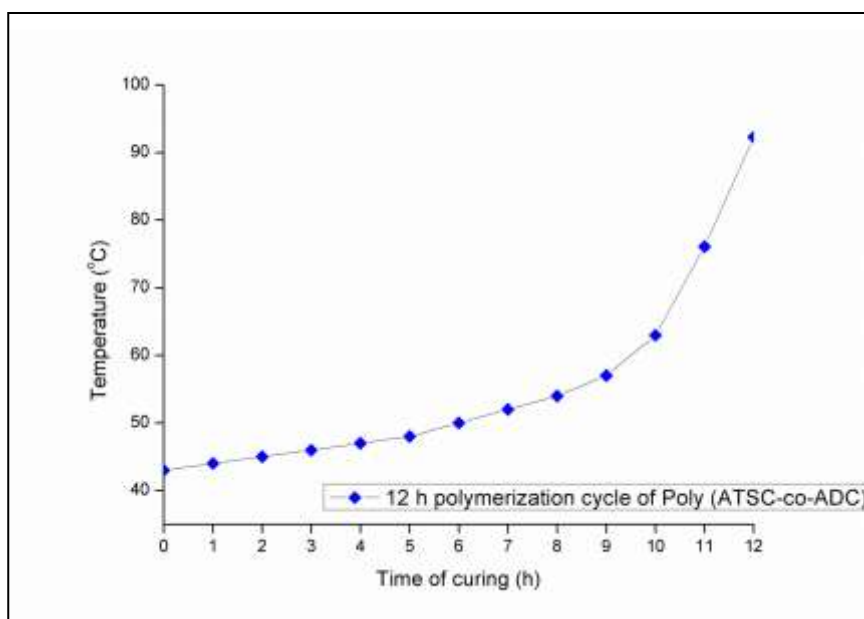
Figure 3.17: 12 hour constant rate polymerization profile for poly (SDAC-*co*-ADC; 4:6 w/w) using 3.3% IPP initiator

A correlation of calculated and theoretical rates of polymerization was done and is shown in figure 3.18. The linear correlation coefficient (R^2) for % polymerization as a function of time for SDAC:ADC (4:6 w/w) monomers with IPP initiator are close to one i.e. 0.9990, which implies that developed constant rate polymerization profile could be used practically to polymerize the monomer mixture.
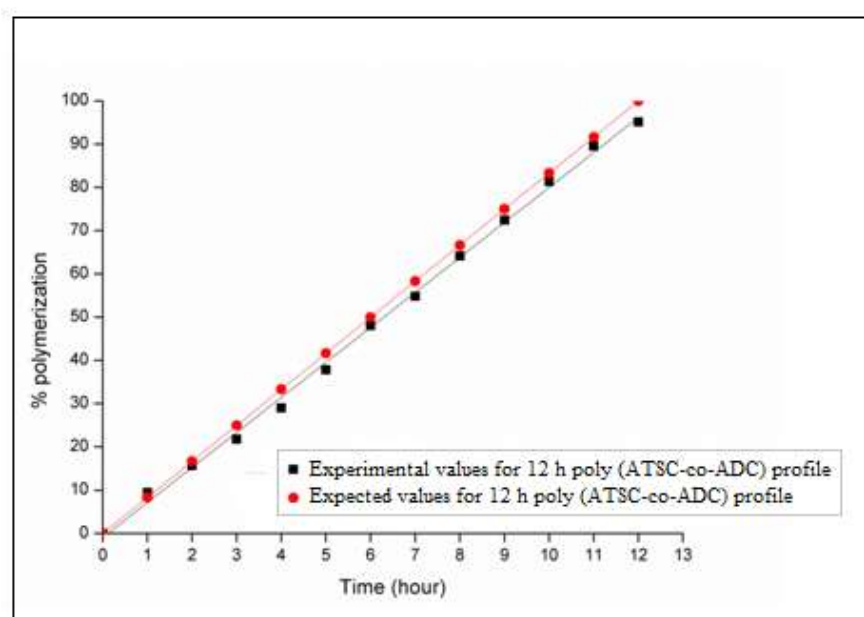
Figure 3.18: Verification of 12 hour polymerization profile for poly (SDAC-*co*-ADC; 4:6 w/w).

The developed constant rate polymerization profile was used for preparation of PSDAC and poly (SDAC-*co*-ADC) polymeric films and for their further optimization studies.

3.3.6   Optimization of composition of SDAC:ADC copolymer: It is known from the literature that for a given monomer, copolymers with ADC monomer have higher sensitivity as compared to that of corresponding homopolymer[22, 23]. This is due to presence of higher cross-links and/ or higher concentration of functional groups in copolymeric films. Optimization of monomer composition was carried out to find the optimum composition of copolymer which shows maximum alpha sensitivity.

A series of copolymers of SDAC with ADC in different w/w ratio were prepared using 3.3% IPP initiator. The polymerization of the monomer mixture was executed by using 12 hour constant rate polymerization profile derived for poly (SDAC-*co*-ADC) polymer. Also, PSDAC homopolymer was prepared using 3.3% IPP initiator. Physical parameters of PSDAC and the different copolymers are recorded in table 3.17. Unsaturation analysis of all films were also carried out and noted in table 3.17.

Table 3.17: Physical properties of SDAC homopolymer and copolymers with ADC.

Sr. No.	Polymer composition ADC:SDAC (wt/wt)	Thickness of Sample film (μm)	%Residual Unsaturation after polymerization	% Polymerization
1	1:9	542.5	4.57	95.43
2	2:8	551.9	6.86	93.14

3	3:7	518.1	7.69	92.31
4	4:6	532.5	4.77	95.23
5	1:1	551.3	6.55	93.45
6	6:4	521.1	12.11	87.89
7	7:3	633.7	10.44	89.56
8	8:2	541.7	9.68	90.32
9	9:1	646.4	8.79	91.21
10	PSDAC	624.9	6.55	93.45
11	PADC	450.8	3.46	96.54

Each piece of the prepared polymeric films was exposed to ^{239}Pu alpha source at a distance of 1 mm from the source for 5 minutes and to ^{252}Cf source for fission fragment at a distance of 1 mm from the source for 2 hours separately. The exposed films were etched in 6 N NaOH at 70 ^{o}C. Time required for revelation of alpha and fission fragments was observed and compared with that of PADC and CR-39 as given in table 3.18.

Table 3.18: Time required to reveal alpha and fission fragment tracks in SDAC-ADC polymers.

Sr.no	Composition of polymer (w/w) (SDAC:ADC)	Alpha track development time (seconds)	Fission fragment development time (seconds)
1	SDAC	30	5
2	1:9	120	60
3	2:8	60	30
4	3:7	60	30
5	4:6	60	30
6	1:1	50	30
7	6:4	50	30
8	7:3	50	30
9	8:2	45	15
10	9:1	45	15
11	PADC	120 minutes	60 minutes
12	CR-39	120 minutes	60 minutes

CHAPTER 3

From the track revelation studies, it is observed that homopolymer as well as copolymers of SDAC revealed alpha and fission fragment tracks in few seconds to a minute. The alpha sensitivity of all copolymers along with homopolymer PSDAC was calculated after noting the alpha and fission track diameters[39]. The bulk etch rate and post etched surface of the polymeric film was also determined and reported in table 3.19.

Table 3.19: Sensitivity values and the post etch rate of different copolymers

Sr.no	Composition of polymer (wt. by wt.)	Alpha sensitivity	Bulk etch rate V_b (μ/min)	Remark
1	SDAC	1.52	25.49	Clear
2	SDAC-ADC (1:9)	1.45	2.97	Hazy film
3	SDAC-ADC (2:8)	1.48	3.78	Clear
4	SDAC-ADC (3:7)	1.64	6.04	Clear
5	SDAC-ADC (4:6)	1.65	10.32	Clear
6	SDAC-ADC (1:1)	1.59	11.30	Clear
7	SDAC-ADC (6:4)	1.52	12.51	Clear
8	SDAC-ADC (7:3)	1.45	12.42	Clear
9	SDAC-ADC (8:2)	1.51	11.21	Clear
10	SDAC-ADC (9:1)	1.47	15.45	Clear
14	PADC	1.28	0.06 μ/h	Clear
15	CR-39	1.22	0.11 μ/h	Clear

Clearly from the results obtained, alpha sensitivity of homopolymer PSDAC and all copolymers was found to be greater than that of PADC and CR-39 detectors. Among all copolymers, poly (SDAC-*co*-ADC) with 3:7 and 4:6 w/w ratio had maximum alpha sensitivity. Hence, we considered optimum SDAC-ADC copolymer concentration to be 4:6 (w/w).

3.3.7 Optimization of initiator concentration for SDAC: ADC 4:6 w/w copolymer: The optimization of monomer composition studies revealed that the SDAC:ADC 4:6 w/w copolymer has a maximum alpha sensitivity as compared to a series of copolymers prepared. For initiator optimization study, we prepared poly (SDAC-*co*-ADC; 4:6 w/w) polymeric films using different IPP concentration following the polymerization profile just derived. The physical properties of the polymeric films are recorded in table 3.20.

Table 3.20: Physical properties of SDAC: ADC 4:6w/w copolymers prepared using different IPP initiator concentration.

Sr. No.	IPP concentration	Thickness microns	Hardness	Track detection properties
1	2	-	Soft gel (soft film)	Nil
2	3	562	Hard polymer	Alpha and fission
3	3.3	542	Hard	Alpha and fission
4	4	462	Hard	Alpha and fission
5	5	559	Hard	Alpha and fission
6	6	520	Hard	Alpha and fission
7	7	506	Hard	Alpha and fission

Out of the set of polymers prepared using 2-7 % w/w IPP initiator concentrations, polymeric film prepared using 2% (by wt.) was soft. Others were hard and suitable for track detection analysis. Alpha sensitivity studies of the copolymeric films were carried out.
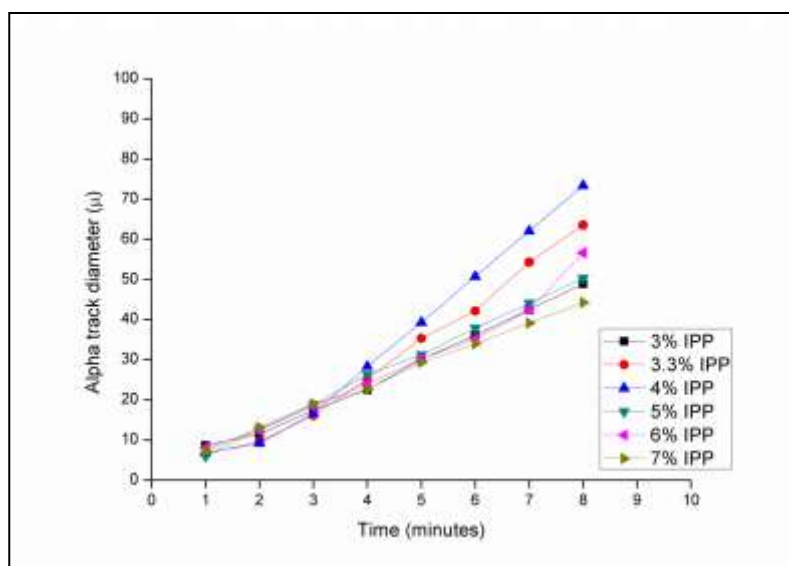
Figure 3.19: Variation of alpha track diameter in Poly (SDAC-*co*-ADC; 4:6 w/w) copolymer prepared using different initiator concentration.
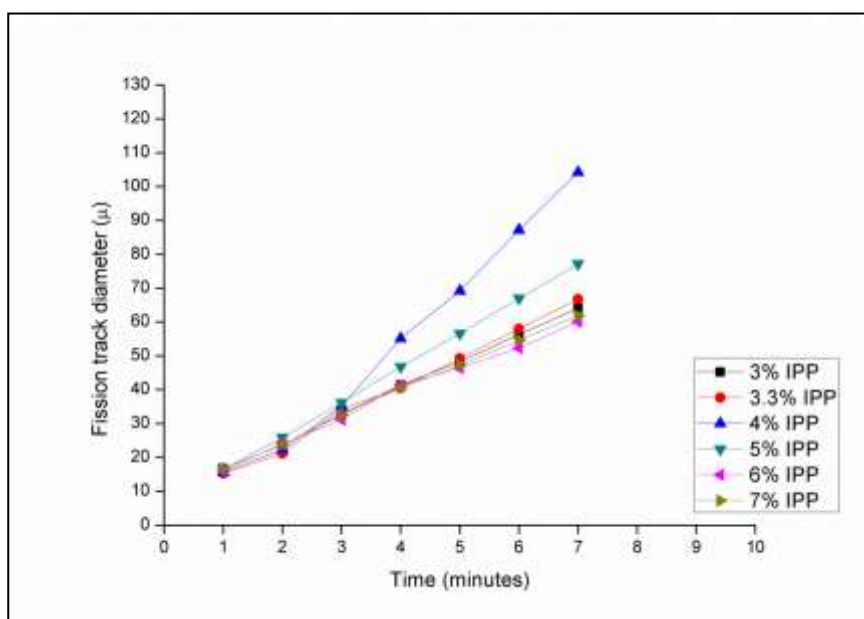
Figure 3.20: Variation of fission fragment diameter in Poly (SDAC-*co*-ADC; 4:6 w/w) copolymer prepared using different initiator concentration.

Alpha as well as fission track diameters were measured after etching for interval of one minute. The variation in alpha and fission track diameters with time is represented graphically in figure 3.19 and 3.20. The film with 4% initiator show

maximum increase in alpha as well as fission track diameter with time (minutes). Post etched surface of all film was clear, but after etching for 15-20 minutes films became thin and soft. Alpha sensitivity of the films was determined. The variation of alpha sensitivity as a function of initiator concentration is shown in figure 3.21. Variation in bulk etch rate in these copolymers is given in figure 3.22. The bulk etch rate is almost steady indicating smooth etching process and in turn sufficiently uniform polymer. The film with 4% w/w IPP initiator had a maximum alpha sensitivity of 2.75 just after 4 minutes of etching and was the most sensitive copolymer. All other copolymers attained maximum sensitivity after 4 minutes only. The maximum alpha sensitivity of all other copolymer is reported in table 3.21 below.
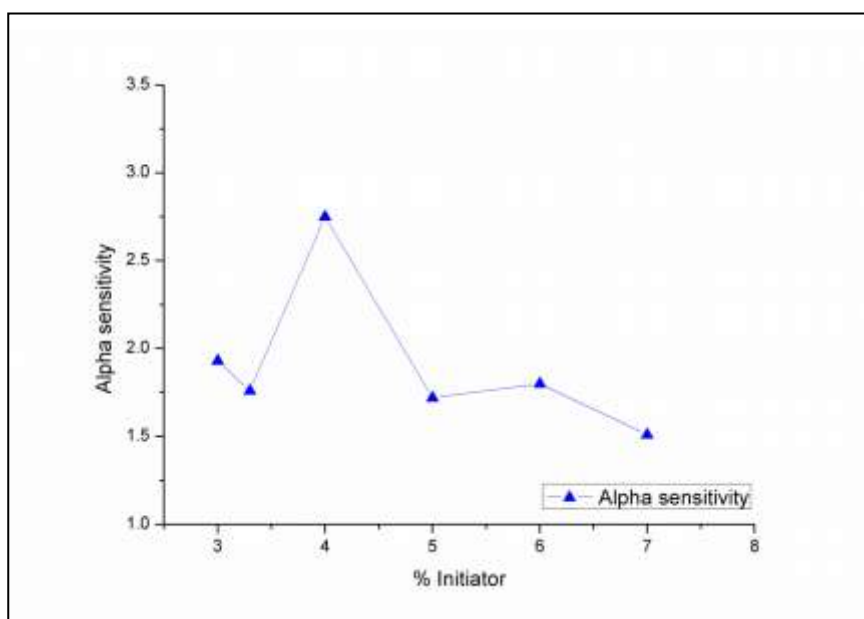
Figure 3.21: Variation of alpha sensitivity of poly (SDAC-*co*-ADC, 4:6 w/w) films with different initiator concentration.
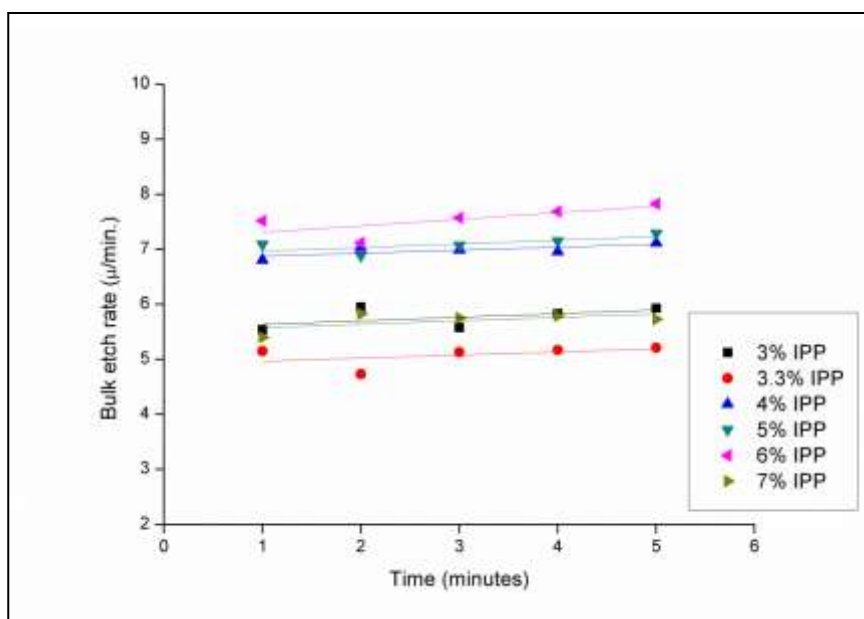
Figure 3.22: Bulk etch rate study of Poly (SDAC-*co*-ADC; 4:6 w/w) films prepared using different IPP initiator concentration (V_b in m/min.).

Table 3.21: Maximum alpha sensitivity observed for poly (SDAC-*co*-ADC;4:6 w/w) with different IPP concentration.

Sr. No.	w/w% IPP concentration	Maximum alpha sensitivity	Time to attain maximum sensitivity (minutes)
1	3	1.93	4
2	3.3	1.76	4
3	4	2.75	4
4	5	1.72	4
5	6	1.80	4
6	7	1.51	4

3.3.8 Optimization of Etching conditions for PSDAC and poly (SDAC-*co*-ADC; 4:6 w/w):

It is known fact that etching conditions affects the response of plastic track detector towards charged particles. It alters many track detection properties of nuclear track detectors. The main condition for the track development in a material is $V_t/V_b > 1$; thus, it is very important to know both bulk etch rate V_b as well as track etch rate V_t which are altered by temperature as well as concentration of etchant. The main factors affected by etching conditions are: a) Bulk etch rate and track etch rate and b) The track development time in detector which is also important factor; necessity for rapid track development is one of the major and practical requirements that will help differentiate tracks from background track like feature. c) Alteration in etching conditions alters the alpha sensitivity of the polymeric detector. d) Post etched surface of the films. This should be transparent to do further analysis under optical microscope.

The optimization of etching condition is carried out by varying temperature at a constant etchant concentration and by changing etchant concentration at constant temperature. Though there is no specific rule the bulk etch rate as well as post etched surface appearance will determine the optimum etching condition for particular detector. Homopolymer PSDAC and poly (SDAC-*co*-ADC; 4:6 w/w) were prepared using optimized initiator concentration and were used for optimization of etching conditions.

Table 3.22: Time required development of alpha tracks and fission fragments in the films PSDAC at different temperature and different concentration of etching medium.

Sr no	Normality N	Temperatu-re ^{o}C	Time for fission, alpha track detection (minutes)$^{\#}$	Observations and Remark
1	0.5	60	30, 45	Hard, opaque white film
		70	10, 15	Hard but whitish film after 30 minutes of etching
2	1	50	30, 40	Hard, white film after 50 minutes of etching
		60	15, 20	Hard, white film after 45 minutes of etching
		70	4, 5	Whitish film after 10 minutes of etching
3	2	50	10, 20	white film after 50 minutes of etching
		60	6, 10	Clear, transparent film after 30 minutes of etching
		70	2, 4	Clear and transparent film
4	3	50	5, 15	Clear and transparent film even after 20 minutes of etching
		60	6, 8	Clear and transparent film even after 20 minutes
		70	1,1	clear film even after 10 minutes of etching
5	4	50	8, 10	whitish film after 40 minutes of etching
		60	2, 3	Hard and transparent film
		70	1, 1	Hard and transparent film
6	6	70	5, 30 (seconds)	Film becomes thin and soft after 5 minutes of etching

Exposure: # films exposed to ^{252}Cf source at a distance of 5 cm for 8 hours.

Since poly (sulfone-carbonate) and poly (sulfone-*co*-carbonate) polymeric detectors could reveal charged particles rapidly within few seconds using 6N NaOH at 70 ^{o}C, we considered lower concentrations for etching studies. Initially optimised films were cut into 1 cm^{2} pieces and each piece of PSDAC and poly (SDAC-*co*-ADC) were exposed to ^{239}Pu source for alpha particles and ^{252}Cf source for fission fragments and each piece were etched in boiling water for 3 hours. But this condition didn't reveal any tracks. Then exposed films were etched in 0.1N NaOH solution at 70 ^{o}C. After 2 hours of etching PSDAC developed some track like pits but both films became opaque white after 2 hours of etching. Exposed films were etched in 0.5N – 6N NaOH solution at 50, 60 and 70 ^{o}C temperature and time required for development of alpha as well as fission fragments was recorded also post etched surface appearance was observed for both PSDAC and poly (SDAC-*co*-ADC; 4:6 w/w) detectors and noted in a table 3.22 and 3.23. It is observed that, PSDAC could reveal charged particles even in 0.5N NaOH at 70 ^{o}C within 10-15 minutes but film had turned opaque. Tracks were observed under optical microscope. Poly (SDAC-*co*-ADC; 4:6 w/w) could not reveal any tracks in 0.5 N NaOH at 70 ^{o}C. In 1N NaOH solution, both detectors could reveal tracks but homopolymer became opaque after 30-40 minutes of etching at 50 and 60 ^{o}C. In 1N NaOH at 70 ^{o}C temperature, PSDAC could reveal tracks in 5 minutes with clear post etched surface. Post etched surface for both detectors was clear when they were etched in 2-6 N NaOH at 50-70 ^{o}C temperature as mentioned in table 3.22 and 3.23. In a process of optimizing the conditions for chemical etching, we have observed that alpha tracks could also be revealed in PSDAC polymeric material using even 1N NaOH in a reasonable time of five minutes at 70°C. Further, it was concluded that 3N NaOH at 60 ^{o}C temperature was the best and optimum condition for these detectors as at this condition both

detectors could reveal tracks in 6-10 minutes. But to compare radiation sensitivity and other track detection characteristics of PSDAC and poly (SDAC-*co*-ADC) polymeric detectors with that of indigenously prepared PADC and commercially available CR-39™ detectors, we considered 6N NaOH at 70 ^{o}C i.e. optimized etching conditions of CR-39™.

Table 3.23: Time required development of alpha tracks and fission fragments in the films Poly (SDAC-*co*-ADC; 4:6 w/w) at different temperature and different concentration of etching medium.

Sr. No.	Normality N	Temperature ^{o}C	#Time for fission; alpha track detection (minutes)	Post etch rate surface
1	1	50	70; 105	Clear and transparent
		60	30; 40	whitish film after 2 hours
		70	10; 15	Not etched beyond 30 minute
2	2	50	30; 45	White film after 45 minutes
				white film after 40 minutes
		60	10; 15	etching
		70	4; 6	became blur after 30minutes
3	3	50	15; 30	Transparent till 45 minutes
		60	7; 10	Transparent film
		70	1.5; 3	Hard and transparent film
5	4	50	12;25	Fogy white after 50 minutes
				Whitish hard film after 20
		60	4;8	minutes of etching
		70	1;3	Transparent till 8 minutes
				Not etched beyond 30
6	5	50	9;20	minutes of etching
		60	5;8	Not etched beyond 15

				minutes
		70	2;3	Not etched beyond 5 minutes
			30; 60	Film becomes slightly white
4	6	70	(seconds)	after 10 minutes of etching

Exposure: # films exposed to ^{252}Cf source at a distance of 5 cm for 8 hours.

The optimised PSDAC and poly (SDAC-*co*-ADC) detectors which were previously exposed to alpha and fission fragment sources were etched in 6N NaOH at 70 ^{o}C etching condition. Maximum alpha sensitivity and time required to reveal alpha and fission fragments at this condition was determined as reported in table 3.24.

Table 3.24: Time required for alpha and fission tracks when etched under 6N NaOH medium at 70 ^{o}C and their alpha sensitivity.

Polymer composition SDAC:ADC w/w	Time required to observe (seconds)		Alpha sensitivity[c] after 4 minutes of etching
	alpha tracks[a]	fission fragments[b]	
1:9	120	60	1.50
2:8	60	30	1.42
3:7	50	30	1.95
4:6	50	30	2.75
1:1	50	30	1.52
6:4	50	30	1.45
7:3	50	30	1.43
8:2	45	20	1.39
9:1	45	20	1.55
PSDAC	30	5	1.62

[a] films exposed to ^{239}Pu source at 1 mm for 2 minutes

[b] ^{252}Cf source at 1 mm for 2 hours

[c] films exposed to ^{252}Cf source at height of 5 cm under 2 mm of Hg vacuum for 8 hours

3.3.9 **Study of track detection properties at optimized conditions:** Different copolymers of SDAC with PETAC and NADAC and also ternary copolymers of SDAC were prepared using optimised conditions. Copolymer of disulfone dicarbonate (M6) with ADC was also prepared. All these detectors were analysed for alpha sensitivity and time required to observe tracks through naked eyes was compared with that of CR-39. Table 3.25 gives bulk etch rate, alpha sensitivity and time to observe tracks via naked eyes for developed copolymers and CR-39 when chemically etched in 6N NaOH at 70 ^{o}C.

Table 3.25: Comparison of time required to observe tracks through naked eyes in designed copolymers of SDAC and in CR-39.

Sr. No.	Polymeric detector composition (w/w)	Alpha track revelation time (minutes)*	Bulk etch rate V_b (μ/min.) *	Time to observe alpha autoradiographs by naked eyes (minutes)*	Alpha sensitivity
1	PSDAC	0.5	39.2	50 seconds	1.94
2	SDAC:ADC (4:6)	0.83	8.1	1.5	2.75
3	M6:ADC (3:7)	2	2.96	3	1.56
4	SDAC:PETAC (4:6)	5	5.60	6	1.62
5	SDAC:NADAC (4:6)	6	2.61	15	1.58
6	SDAC:ADC: NADAC (1:1:1)	2	3.13	6	1.52
7	SDAC:ADC: PETAC (1:1:1)	2	3.60	6	1.45
8	CR-39	60	0.20	180	1.22

*all films were exposed to [239]Pu source in close contact for 5 minutes.

From the table 3.25, it is clear that all the copolymers of SDAC have higher sensitivity and can reveal tracks in few minutes.

3.3.10 Sensitivity studies of PSDAC and poly (SDAC-*co*-ADC) at the optimized conditions.

PSDAC and poly (SDAC-*co*-ADC; 4:6 w/w) were prepared using previously optimized conditions and each piece was exposed to ^{252}Cf source at 5 cm height under vacuum of 2 mm of Hg for 8 hours for alpha sensitivity study. These films were etched in 6N NaOH at 70 ^{o}C. Alpha sensitivity was measured as a function of time and was compared with that of CR-39. Table 3.27 gives alpha sensitivity and bulk etch rate of PSDAC poly (SDAC-*co*-ADC; 4:6 w/w) and CR-39 at different etching time. Alpha sensitivity of optimized poly (SDAC-*co*-ADC; 4:6 w/w) film under optimized etching condition (3N NaOH at 60 ^{o}C) at different time interval was determined and reported in Table 2.26.

Table 2.26: Alpha sensitivity of optimized poly (SDAC-*co*-ADC; 4:6 w/w) film detector etched in 3N NaOH at 60 ^{o}C for different time interval

Etching time (minutes)	Alpha Sensitivity
9	1.51
10	1.5
11	1.6
13	1.66
15	**2.36**
20	1.76
25	1.63
30	1.6

Table 3.27: Comparison of alpha sensitivity of PSDAC, Poly (SDAC-*co*-ADC; 4:6 w/w) at different etching time interval

Polymeric detectors	Etching Time	$V_b = D_{ff}/2t$ (μ/min.)	Sensitivity S
PSDAC Etching condition: 6N NaOH at 70 ^{o}C	(seconds) 15	20.64	1.42
	20	45.67	1.23
	30	38.16	1.22
	40	25.49	1.95
	50	30.62	1.34
Poly(SDAC-*co*-ADC; 4:6 w/w) Etching condition: 6N NaOH at 70 ^{o}C	(minutes) 2	7.41	1.37
	3	7.35	1.67
	4	7.11	1.98
	5	8.42	2.00
	6	7.47	2.75
	7	10.1	2.14
CR-39 Etching condition: 6N NaOH at 70 ^{o}C	(In Hour) 1	0.12	1.18
	2.5	0.10	1.14
	3	0.06	1.15
	4	0.07	1.20
	5	0.08	1.17

Maximum alpha sensitivity of PSDAC and poly (SDAC-*co*-ADC) was found out to be 1.95 and 2.84 respectively which was much better than that of CR-39. The designed novel polymer could also reveal fast neutrons in 2- 2.5 minutes when

etched in 6N NaOH at 70 ^{o}C. The maximum alpha sensitivity of optimised polymeric detector was reported in table 3.28.

Table 3.28: Alpha sensitivity and fast neutron revelation time of newly developed polymeric detectors and indigenously prepared PADC and CR-39 detectors

Sr. No.	Polymer detector	Maximum alpha sensitivity*	Fast neutron revelation time (minutes)
1	PSDAC	1.95 (after 1.2 minutes of etching in 6N NaOH at 70 ^{o}C)	2.5
2	Poly (SDAC-*co*-ADC; 4:6w/w)	2.75 (after 4 minutes of etching in 6N NaOH at 70 ^{o}C)	2.5
3	PADC	1.27 (after 180 minutes of etching in 6N NaOH at 70 ^{o}C)	4.0 h
4	CR-39	1.21 (after 240 minutes of etching in 6N NaOH at 70 ^{o}C)	4.0 h

* exposed to ^{252}Cf source at a height of 5 cm in 2 mm of Hg pressure for 8 hours

3.3.11 Alpha track detection efficiency of PSDAC and poly (SDAC-*co*-ADC; 4:6 w/w): Alpha track detection efficiency of the polymers was measured at three different exposure conditions and compared with that of CR-39.

A.   Exposure condition: ^{239}Pu source at distance of 1cm for 35 seconds.

In first case, each piece of detectors was exposed to ^{239}Pu, alpha source at a distance of 1 cm for 35 seconds. All these exposed films were etched in 6N NaOH at 70 ^{o}C and after specific time tracks were counted under optical microscope. Control films

were also etched for same time and background tracks were counted. Alpha track detection efficiency with this exposure condition is reported in table 3.29.

Table 3.29: Alpha track detection efficiency of PSDAC, poly (SDAC-*co*-ADC; 4:6 w/w) and CR-39 detector

Sr. No.	Film	Etching time	V_b by weight loss method (μ/min)	Total tracks registered /cm^2	Alpha tracks/ cm^2
1	PSDAC	50 sec.	35.43	11443	10633
	control PSDAC	50 sec.	27.83	810	
2	P(SDAC-*co*-ADC)	1 min.	7.74	11998	11660
	P(SDAC-*co*-ADC) control	1 min.	6.73	339	
3	CR39	3 h	0.08	11551	9821
	control CR39	3 h	0.06	1730	

B.   Exposure condition: ^{239}Pu source at distance of 2 cm for 60 seconds.

These detectors were exposed to alpha radiographs at distance of 2 cm for 60 seconds and etched in 6N NaOH at 70 ^{o}C temperature. Alpha track detection efficiency at this exposure condition is given in table 3.30.

Table 3.30: Alpha track detection efficiency of PSDAC, poly (SDAC-*co*-ADC; 4:6 w/w) and CR-39 detector

Sr. No.	Film	Etching time	V_b by weight loss method (μ/min)	Track registration cm^{-2}	Net alpha tracks/ cm^2
1	PSDAC	10 sec.	45.57	6594	6050
	control PSDAC	10 sec.	25.53	544	
2	P(SDAC-*co*-ADC)	70 sec.	7.55	7040	6702

	P(SDAC-*co*-ADC) control	70 sec.	6.74	338	
3	CR39 control CR39	3 h 3 h	0.05 0.06	7332 1729	5603

C.   Exposure condition: ^{239}Pu source at distance of 2 mm for 10 seconds.

Similarly all three films were exposed to alpha source at 2mm for just 10 seconds and etched in 6N NaOH at70 ^{o}C. Alpha track detection efficiency at this exposure condition was calculated and given in table 3.31.

Table 3.31: Alpha track detection efficiency of PSDAC, poly (SDAC-*co*-ADC; 4:6 w/w) and CR-39 detector

Sr. No.	Film	Etching time	V_b by weight loss method (μ/min)	Track registration cm^{-2}	Net alpha tracks/ cm^2
1	PSDAC control PSDAC	40 sec 40 sec.	41.31 49.80	5310 702	4608
2	P(SDAC-*co*-ADC) P(SDAC-*co*-ADC) control	100 sec. 100 sec.	7.21 7.39	4735 1203	3532
3	CR39 control CR39	3.5 h 3.5 h	0.06 0.12	6054 2774	3280

It is clear from above results that track efficiency of the designed novel polymeric detectors is greater than that of commercially available CR-39 detector. These polysulfone-carbonate detectors developed alpha tracks in few minutes whereas CR-39 took 3-3.5 hours to develop alpha tracks during track detection efficiency studies.

3.4 Photomicrograph of optimized poly (sulfone-carbonate), poly (sulfone-*co*-carbonate) detectors:

All photographs were captured using Tucsen ISH500 camera with IS capture software. Photomicrographs of all poly (sulfone-carbonate) detectors are shown in following figures. Exposure condition and time of etching in 6N NaOH at 70 $^{\circ}$C etching condition is mentioned with respective figures.
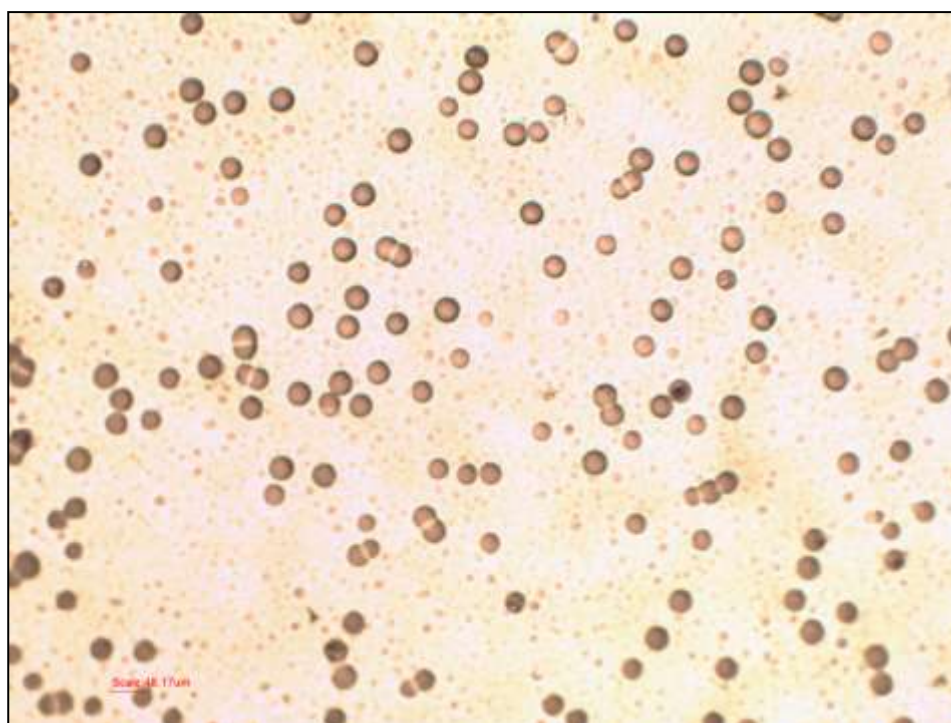
Figure 3.23. PSDAC polymeric detector: Exposed to alpha autoradiograph from ^{239}Pu source at 1 cm for 30 seconds and chemically etched for 50 seconds (**a**-under 10x magnification)
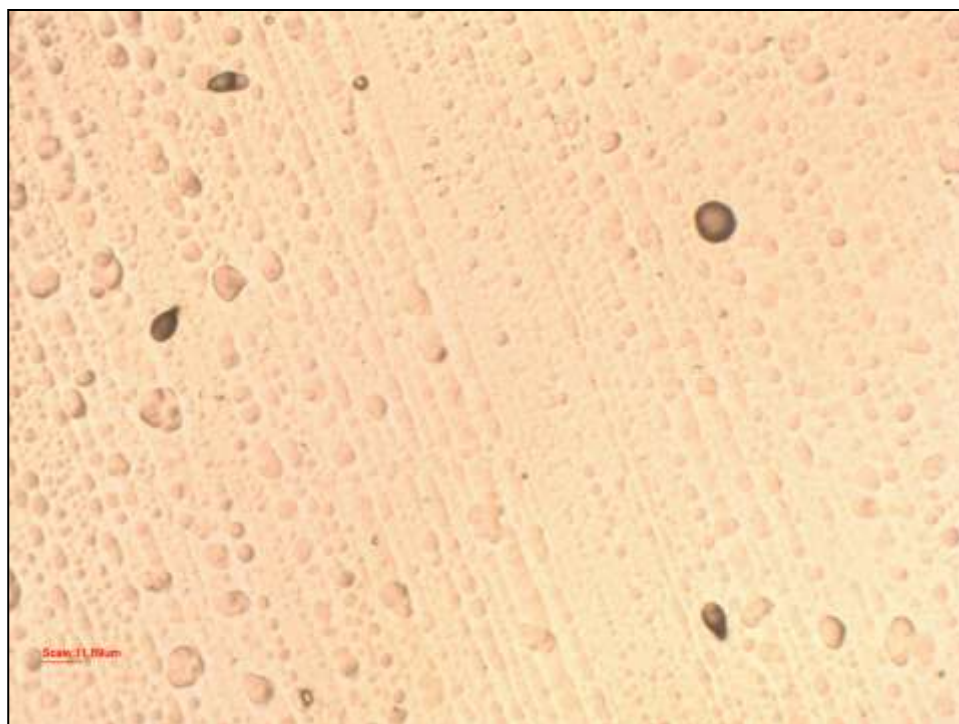
Figure 3.24. PSDAC polymeric detector: Exposed to ^{252}Cf source for fission fragments at 1 mm for 2h and chemically etched for 10 seconds (viewed under 40x magnification)
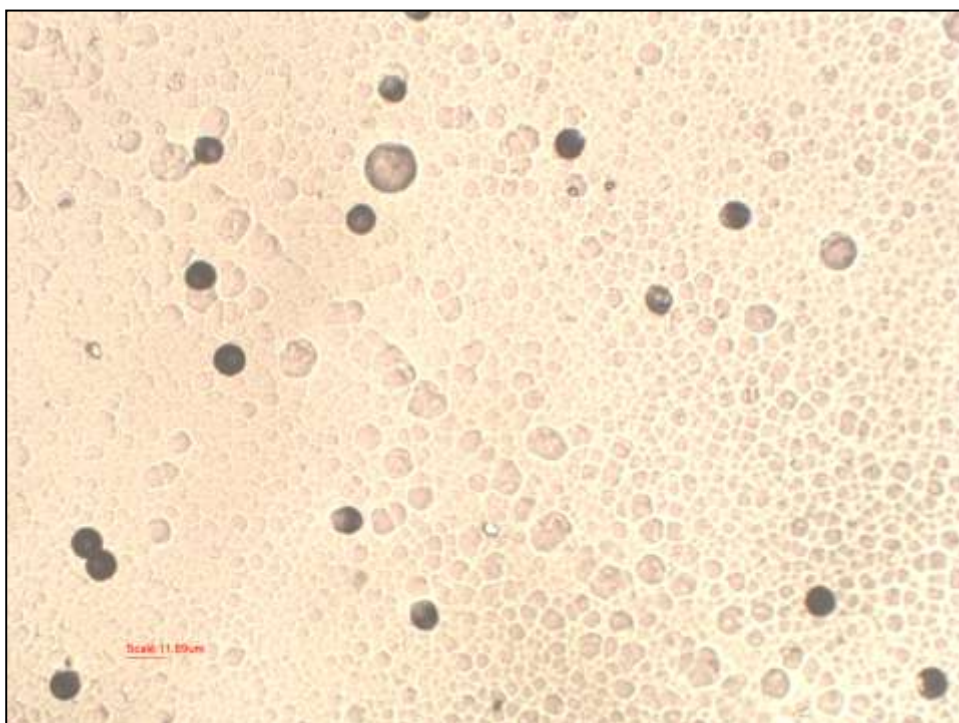
Figure 3.25. Poly (SDAC-*co*-ADC; 4:6 w/w) detector: Exposed to ^{239}Pu source for alpha tracks at 1 cm for 30 seconds and chemically etched for 50 seconds (viewed under 40x magnification)
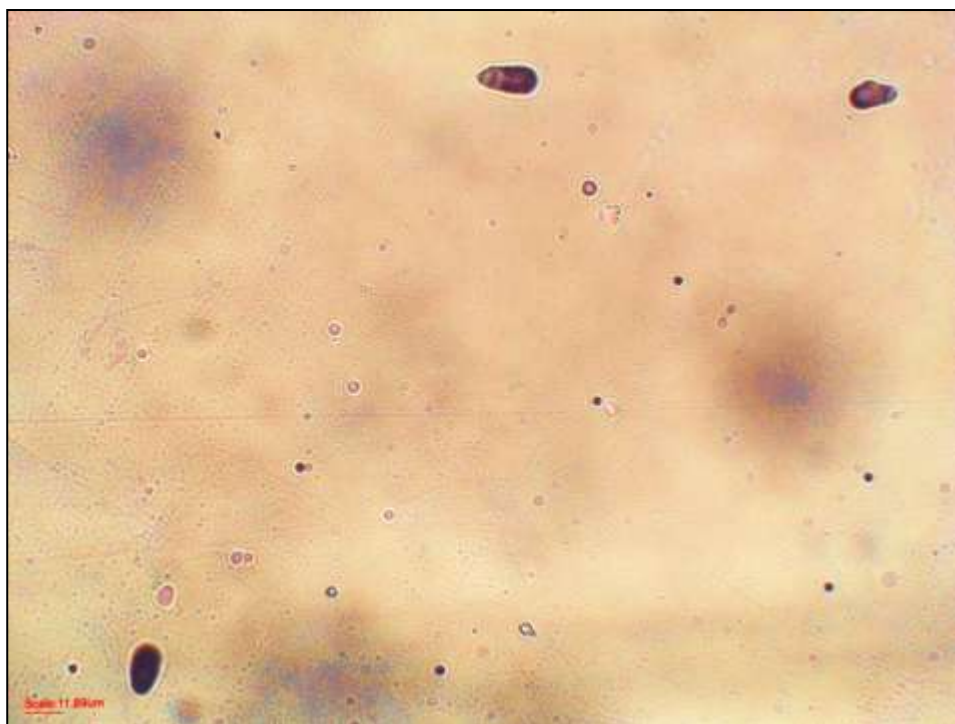
Figure 3.26. Poly (SDAC-*co*-ADC; 4:6 w/w) detector: Exposed to ^{252}Cf source for fission fragments at 1 mm for 2h and chemically etched for 30 seconds (viewed under 40x magnification)
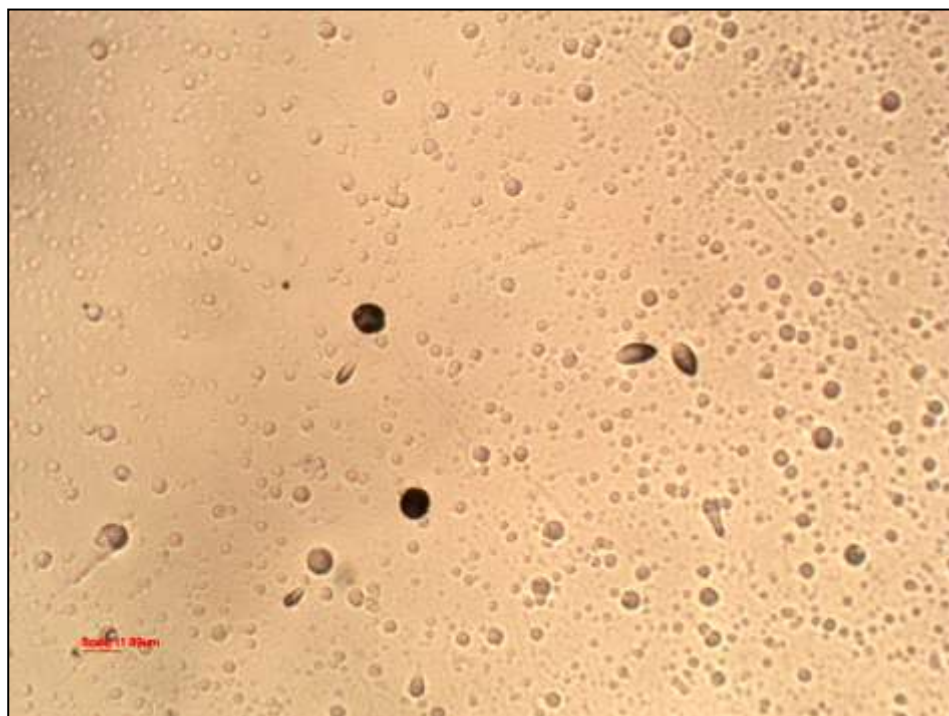
Figure 3.27. Poly (SDAC-*co*-ADC; 4:6 w/w) detector: Exposed to fast neutron from ^{252}Cf source for 3h and chemically etched for 2 minutes (viewed under 40x magnification)
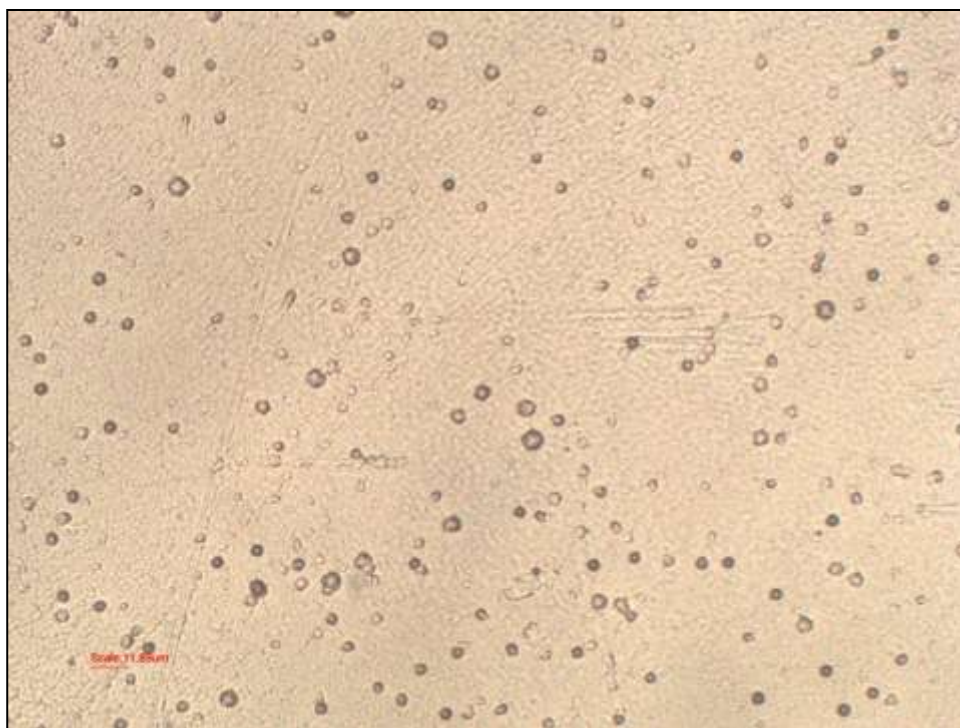
Figure 3.28.   Poly (SDAC-*co*-PETAC; 4:6 w/w) detector: Exposed to ^{239}Pu source at 1 mm distance for 5 minutes and chemically etched for 6 minutes (viewed under 40x magnification)
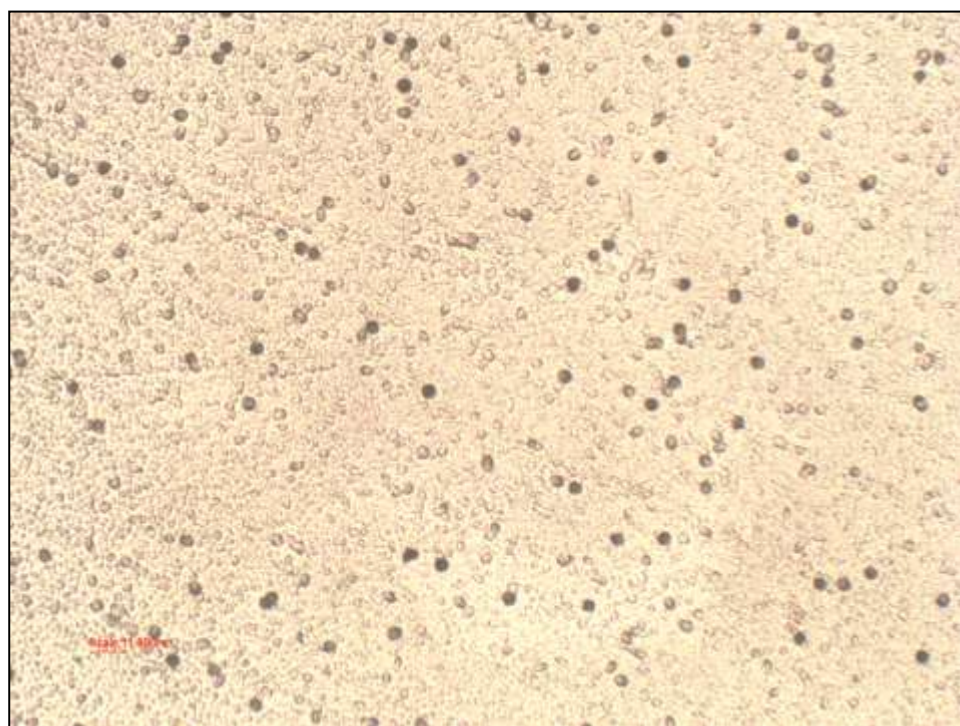
Figure 3.29.   Poly (SDAC-*co*-NADAC; 4:6 w/w) detector: Exposed to ^{239}Pu source at 1 mm distance for 5 minutes and chemically etched for 6 minutes (viewed under 40x magnification)
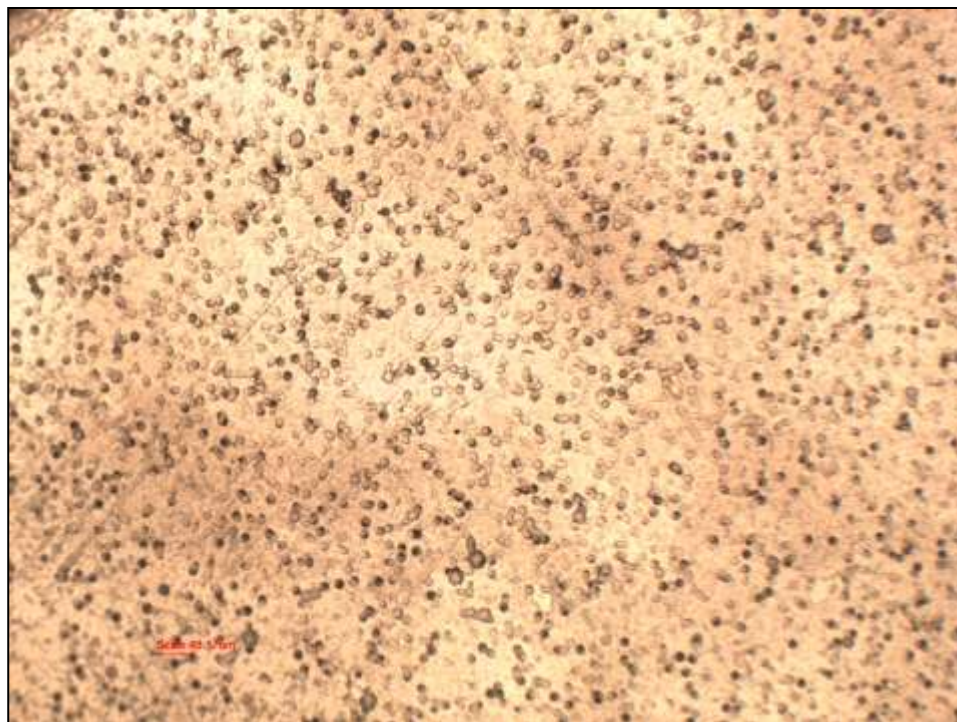
Figure 3.30. Poly (SDAC-*co*-ADC-*co*-PETAC; 1:1:1 w/w) detector: Exposed to ^{239}Pu source at 1 mm distance for 5 minutes and chemically etched for 6 minutes (viewed under 10x magnification).
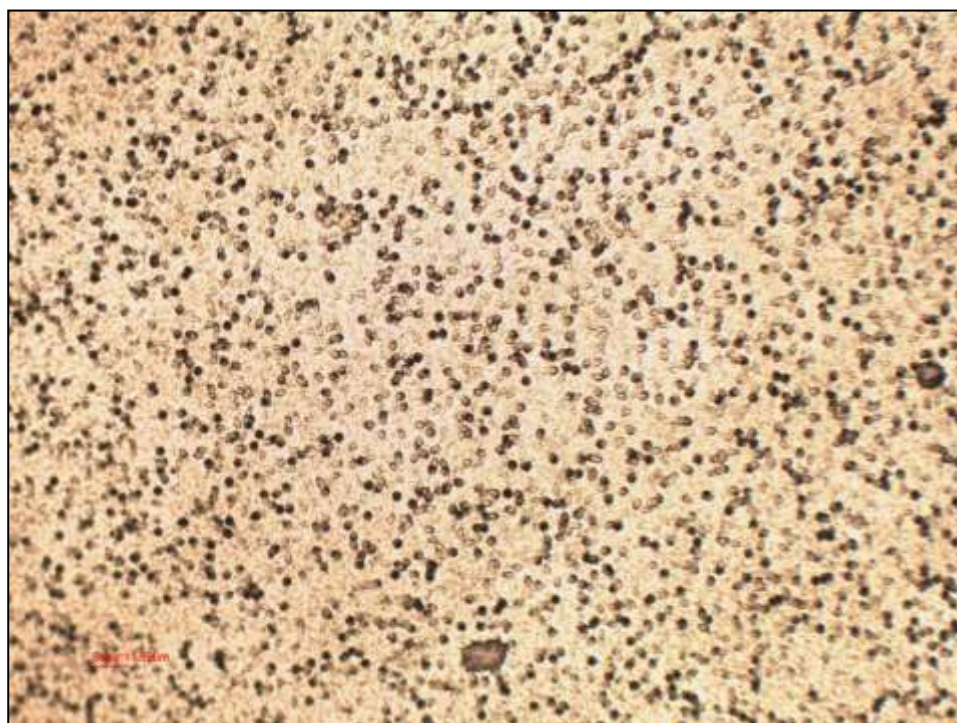
Figure 3.31. Poly (SDAC-*co*-ADC-*co*-NADAC; 1:1:1 w/w) detector: Exposed to ^{239}Pu source at 1 mm distance for 5 minutes and chemically etched for 6 minutes (viewed under 40x magnification)
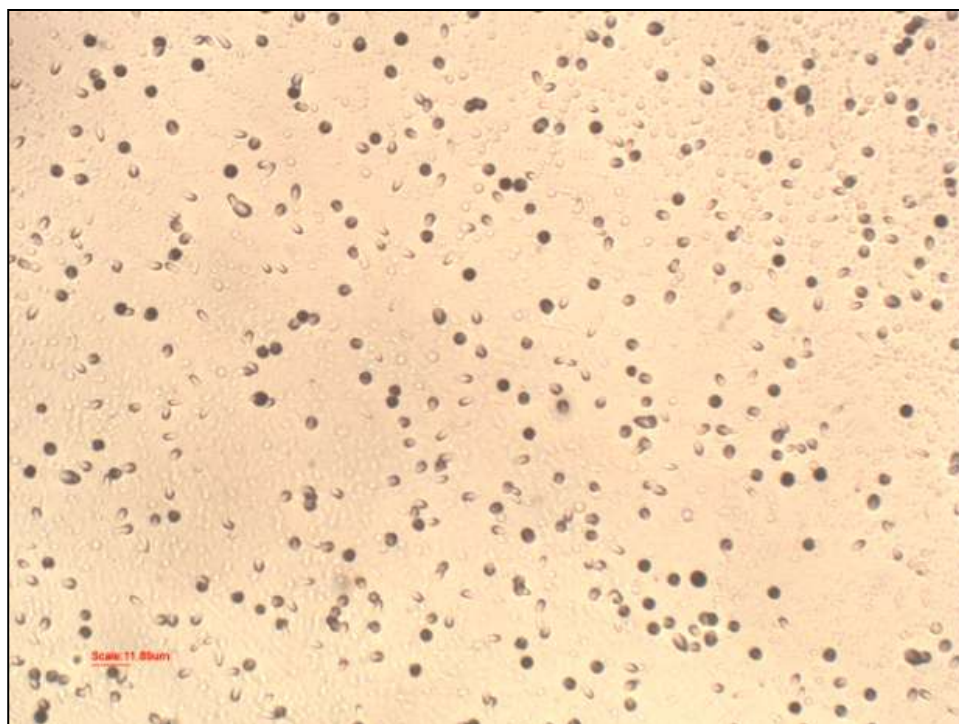
Figure 3.32. Poly (**M6**-*co*-ADC; 1:3 w/w) detector: Exposed to ^{239}Pu source at 1mm distance for 5 minutes and chemically etched for 2 minutes (viewed under 40x magnification) (**M6**- 2, 2'-Bis (2-allylcarbonate ethylsulfonyl) diethyl ether)
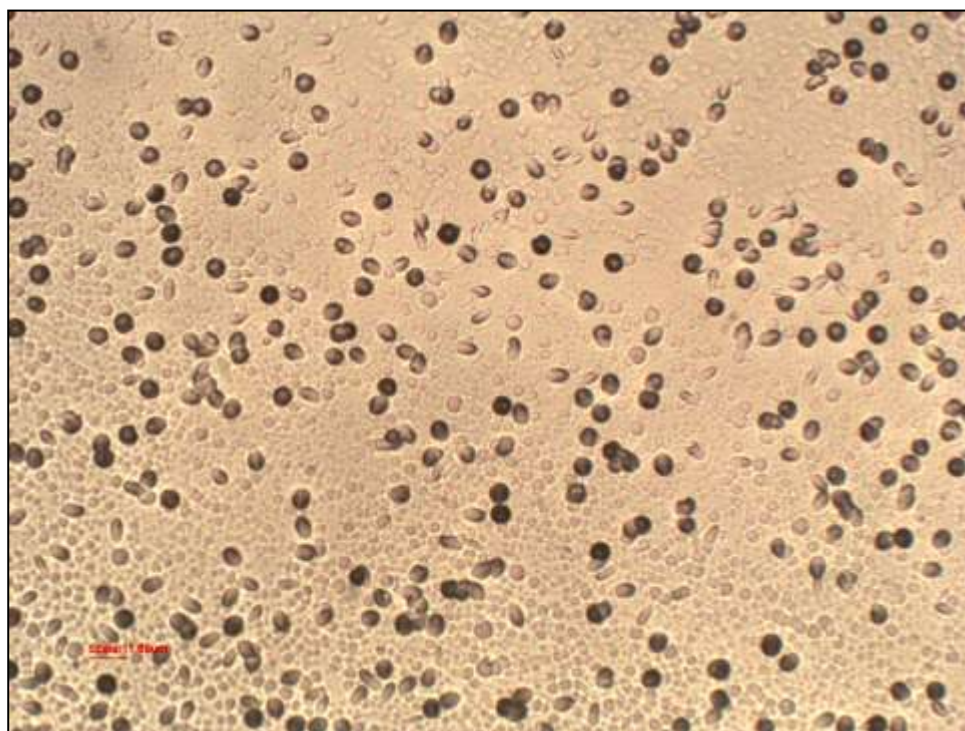
Figure 3.33. Poly (**M6**-*co*-ADC; 1:3 w/w) detector: Exposed to ^{239}Pu source at 1mm distance for 5 minutes and chemically etched for 3 minutes (viewed under 40x magnification)

3.5   Conclusion:

We have successfully prepared four novel sulfone-carbonate polymers for Solid state nuclear track detection. Of these four, PSDAC and poly (SDAC-*co*-ADC; 4:6 w/w) detectors have been optimised as per the protocol developed. Kinetics of polymerization has been studied so as to generate constant rate polymerization profile for homopolymer PSDAC as well as its copolymer. PSDAC and poly (SDAC-*co*-ADC; 4:6 w/w) film detectors show alpha sensitivity of 1.95 and 2.75 respectively. PSDAC detector can reveal alpha as well as fission fragment tracks using 0.5N NaOH at 70 ^{o}C etching condition within 10-15 minutes and poly (SDAC-*co*-ADC; 4:6 w/w) can reveal alpha as well as fission fragment tracks using 1N NaOH at 70 ^{o}C within 10 minutes. Both these detectors can reveal fission fragments in 5-20 seconds and alpha tracks in 30-50 seconds when etched in 6N NaOH at 70 ^{o}C. Nuclear tracks in these films were developed sufficiently and could be observed through naked eyes just in 2-4 minutes of etching in 6N NaOH at70 ^{o}C where as commercial detector CR-39 takes 2-3 hours. Alpha track detection efficiency of both newly designed polymeric detectors is superior as compared to that of commercially available CR-39 detector.

The PSDAC homopolymer and poly (SDAC-*co*-ADC, 4:6 w/w) copolymer could also reveal recoil proton tracks when exposed to fast neutrons from a ^{252}Cf source within 2-3 minutes when compared with CR-39 which took minimum 7 hours for the same.

It was also noted that copolymers of ADC with novel monomers M5 and M6 revealed the alpha tracks within 5 minutes of chemical etching using 6N NaOH at 70°C. Thus, sulfone-carbonate polymers of this type appear to be very promising nuclear track detectors for rapid revelation of nuclear tracks by chemical etching.

3.6   References:

1. (a) Eisenberg, A.; Hird, B.; Moore, R. B. *Macromolecules* **1990**, *23*, 4098-4107. (b) Perusich, S. A.; Avakian, P. Keating, M. Y. *Macromolecules* **1993**, *26*, 4756-4764. (c) Belomoina, N. M.; Rusanov, A. L.; Yanul, N. A.; Kirsh, Y. E. *Vysokomol. Soedin. Ser. B* **1996**, *38* (2), 355-378.

2. (a) Tsuchida, E.; Yamamoto, K.; Shouji, E.; Haryono, A. *Chem. Commun.* **1996**, *17*, 2091-2092. (b) Haryono, A.; Miyatake, K.; Tsuchida, E. *Macromol. Chem. Phys.* **1999**, *200*, 1257-1267. (c) Morishima, Y. *Trends Polym. Sci.* **1994**, *2*, 31-33.

3. (a) Grasel, T. G.; Cooper, S. L. *J. Biomed. Mater. Res.* **1989**, *23*, 311-338. (b) Okkema, A. Z.; Visser, S. A.; Cooper, S. L. *J. Biomed. Mater. Res.* **1991**, *25*, 1371-1395. (c) Silver, J. H.; Marchant, J. W.; Cooper, S. L. *J. Biomed. Mater. Res.* **1993**, *27*, 1443-1457. (d) Silver, J. H.; Hart, A. P.; Williams, E. C.; Cooper, S. L.; Charef, S.; Labarre, D.; Jozefowicz, M. *Biomaterials* **1992**, *13*, 339-344. (e) Santerre, J. P.; ten Hove, P.; VanderKamp, N. H.; Brash, J. L. *J. Biomed. Mater. Res.* **1992**, *26*, 39-57. (f) Skarja, G. A.; Perry, D. W.; Rathbone, R. L.; Rubens, F. D.; Brash, J. L. *J. Biomed. Mater. Res.* **1997**, *34*, 427-438. (g) Skarja, G. A.; Brash, J. L. *J. Biomed. Mater. Res.* **1997**, 34, 439-455. (h) Takahara, A.; Okkema, A. Z.; Wabers, H.; Cooper, S. L. *J. Biomed. Mater. Res.* **1991**, *25*, 1095-1118. (i) Yung, L. L.; Lim, F.; Cooper, S. L. *Trans. Soc. Biomater.* **1995**, *18*, 78.

4. (a) Jozefowicz, M.; Jozefonvicz, J. *Pure Appl. Chem.* **1984**, *56*, 1335-1344. (b) Hovingh, P.; Piepkorn, M.; Linker, A. *Biochem. J.* **1986**, *237*, 573-581.

5. (a) Clercq, E. D. *Biomed. Pharmacother.* **1996**, *50*, 207-215. (b) Witvrou, M.; Clercq, E. D. *Gen. Pharmacol.* **1997**, *29*, 497-511.

6. Kausar, A.; Zulfiqar, S.; Sarwar, M. I. *Polym. Rev.* **2014**, *54* (2), 185–267.

7. (a) Garbassi, F.; Po, R. "Engineering thermoplastics, overview", In Encyclopedia of Polymer Science and Technology, Kroschwitz, J.; Mark, H., Eds.; Wiley: Hoboken, NJ, **2003**, pp 383–387. (b) Polk, M. "High performance fibers", In Encyclopedia of Polymer Science and Technology, Kroschwitz, J.; Mark, H., Eds.; Wiley: Hoboken, NJ, **2003**, p 214.

8. Liu, J. G.; Nakamura, Y.; Shibasaki, Y.; Ando, S.; Ueday, M. *Polym. J.* **2007**, *39*, 543–550.

9. Edmonds, J. T.; Hill, H. W. *U.S.* Patent 3,354,129. assigned to Phillips Petroleum Company, 1967.

10. (a) Lopez, L. C.; Wilkes, G. L. *J. Macromol. Sci Part C.* **1989**, *29* (1), 83–151. (b) Fahey, D. R.; Ash, C. E. *Macromolecules* **1991**, *24*, 4242–4249.

11. (a) Rao, V. L. *J. Macromol. Sci. Rev. Macromol. Chem. Phys.* **1999**, *C39*, 655–711. (b) Carborundum, A. *Engineering Thermoplastics,* CRC Press: Florida, USA, 2010.

12. Sorenson, W. R.; Campbell, T. W. Preparative Methods of Polymer Chemistry*,* Interscience Publishers: 1968, 2nd edn.

13. Zhang, T.; Litt, M. H.; Rogers, C. E. *J. Polym. Sci. Polym. Phys.* **1994,** *32*, 1671-1676.

14. Shockravi, A.; Mehdipour-Ataei, S.; Abouzari-Lotf, E.; Yousefi, E. *Eur. Polym. J.* **2006**, *42*, 133–139.

15. Rafikov, S. R. *Polymer Science U.S.S.R.* **1980**, *21*, 2780–2792.

16. Morales-Sanfrutos, J.; Lopez-Jaramillo, J.; Ortega-Munoz, M.; Megia-Fernandez, A.; Perez-Balderas, F.; Hernandez-Mateo, F.; Santoyo-Gonzalez, F. *Org. Biomol. Chem.* **2010**, *8*, 667–675.

17. Lopez-Jaramillo, F. J.; Hernandez-Mateo, F.; Santoyo-Gonzalez, F. Vinyl sulfone: A Multi-purpose Function in Proteomics. In *Integrative Proteomics*; Eastwood Leung, H. C., Ed.; InTech: Rijeka, Croatia, 2012, pp. 301–326.

18. Morales-sanfrutos, J.; Lopez-jaramillo, F. J.; Elremaily, M. A. A.; Hernández-mateo, F.; Santoyo-gonzalez, F. *Molecules* **2015**, *20*, 3565–3581.

19. Santoyo-González, F.; Hernandez-Mateo, F.; Morales-Sanfrutos, J. Polymeric Adsorbents Based on Polysaccharides and Cyclodextrins for Water Purification. ES Patent 2334756 A1, March 2010.

20. Kultys, A. "Sulfur-containing polymers", In Encyclopedia of Polymers Science and Technology, vol. 4, 3rd edition; Mark, H. F., Ed.; Wiley: Hoboken, NJ, 2003.

21. Cartwright, B. G.; Shirk, E. K.; Price, P. B. *Nucl. Instruments Methods* **1978**, *153* (2), 457–460.

22. Fujii, M.; Yokota, R.; Atarashi, Y. *Int. J. Radiat. Appl. Instrumentation. Part D. Nucl. Tracks Radiat. Meas.* **1990**, *17* (1), 19–21.

23. Stejny, J.; Portwood, T. *Int. J. Radiat. Appl. Instrumentation. Part D. Nucl.*

Tracks Radiat. Meas. **1986**, *12* (1), 59–62.

24. (a) Mandrekar, V. K.; Tilve, S. G.; Nadkarni, V. S. *Radiat. Phys. Chem.* **2008**, *77* (9), 1027–1033. (b) Nadkarni, V. S. *Proceedings of the 15th SSNTD-15,* Tehry, Jun 21-23, **2007** (c) Mandrekar, V. K.; Tilve, S. G.; Nadkarni, V. S. *Proceedings of the 15th SSNTD-15,* Tehry, Jun 21-23, **2007**.

25. Mandrekar, V. K.; Kotkar, S. M.; Tilve, S. G.; Nadkarni, V. S. *Novel high sensitivity poly (sulphonate-carbonate) nuclear track detector-I : poly (PECS-co-ADC).* **2009**, 40.

26. (a) Mandrekar, V. K.; Tilve S. G.; Nadkarni, V. S. *NSRP-2007,* Chennai, **2007**, 277. (b) Van Woerden, H. F. *Chem. Rev.* **1963**, *63*(6), 557-571. (c) Bissinger, W. E.; Kung, F. *J. Am. Chem. Soc.* **1947**, *69*, 2158-2163.

27. (a) Mandrekar, V. K.; Tilve, S. G.; Nadkarni, V. S. *Proceedings of the Trombay Symposium of Radiation and Photochemistry,* Trombay. **2007**. (b) Mandrekar, V. K. Tilve, S. G.; Nadkarni, V. S. *Proceedings of the 23rd International Conference of Nuclear Track Society,* Beizing, **2006**.

28. Faber, E. M.; Miller, G. E. *Org. Synth.* **1932**, *12*, 68-67.

29. Timperley, C. M.; Black, R. M.; Bird, M.; Holden, I.; Mundy, J. L.; Read, R. W. *Phosphorus. Sulfur. Silicon Relat. Elem.* **2003**, *178* (9), 2027–2046.

30. (a) Reichstein, T.; Goldschmidt, A. Constituents of the adrenal cortex. III. The sulfur containing compound, C. A. 30, 4174.4. (b) Tramier, B.; Delourme, R.; Fresenel, P. Sulphoxides. US4108866A, 1978.

31. Reisenauer, H. P.; Schreiner, P. R.; Romanski, J.; Mloston, G. *J. Phys. Chem. A* **2015**, *119*, 2211–2216.

32. Lodwig, Wu, R.; Schmidt, S. N.; Williams, J. G.; R. F.; Silks, L. A. *J. Label. Compd. Radiopharm.* **2012**, *55* (6), 211–222.

33. Karsh, S.; Freitag, D.; Schwab, P.; Metz, P. *Synthesis.,* **2004**, *10*, 1696.

34. Kotha, S.; Khedkar, P.; Ghosh, A. K. *European J. Org. Chem.* **2005**, *16*, 3581–3585.

35. Fujii, M.; Yokota, R.; Atarashi, Y.; Hasegawa, H. *Nucl. Tracks Radiat. Meas.* **1991**, *19*, 171–176.

36. Kharasch, N. *Organic Sulfur Compounds* (Elsevier, 2013).

37. Patai, S.; Rappoport, Z.; Stirling, C. *The Chemistry of Sulphones and Sulphoxides In The Chemistry of Functional Groups*; John Wiley and Sons,

1988.

38. Nadkarni, V. S. *Indian J. Phys.* **2009**, *83* (6), 805-811.

39. Mandrekar, V. K. Novel polymeric materials for nuclear track detection. [Ph.D. Thesis]. Goa, India, Goa University; 2010.

40. Krimm, H.; Buysch, H. J.; Schnell, H. Thiodiglycol Polycarbonates, US 4054597, 1976.

41. Shingo, M.; Toshihiro, N.; Yasuji, K. Difunctional polymerizable carbonate compounds for optical materials and manufacture thereof. JP02072154, 1990.

42. Fox, D. W.; Gallucci, R. R.; Peters, E. N.; Smith, G. F. Thermoplastic polycarbonate-polysulfone carbonate molding compositions. US 4489181 A.

43. Dial, W. R.; Bissinger, W. E.; DeWitt, B. J.; Strain, F. *Ind. Eng. Chem.* **1955**, *47* (12), 2447–2451.

44. Mascarenhas, A. A. A. Development of plastic materials for nuclear track detection. [Ph.D. Thesis]. Goa, India, Goa University; 2007.

CHAPTER 4

Development of PADC polymeric track detectors for the personnel neutron dosimetric analysis and attempt towards its commercialization.

CHAPTER 4

4.1   Introduction

The Atomic Energy Regulatory Board (AERB) which is a regulatory body in India, has mandated that every occupational worker, who is involved in the use/handling of the radioactive sources, must be periodically monitored for the purpose of radiation protection. Such a purpose could be effectively served using polymeric track detectors. So there exists a need for the development of solid state nuclear track detectors within the country for use in various applications like neutron monitoring.

As per directives of various Regulatory Authorities all over the world personnel neutron monitoring has become essential. It is therefore employed in vicinity of radioactive sources, nuclear reactors, particle accelerators, neutron generators and fuel reprocessing plants. Personnel neutron monitoring involves the evaluation of magnitude of unwanted effects on the personnel working in vicinity of neutrons/nuclear radiation by way of noting the neutron dose which the personnel has received from time to time. The biological effect of neutrons depends upon energy of neutrons and can be different from the effect produced by gamma rays under identical dose conditions. This obviously needs a method that is suitable in the working environment of the personnel.

There are many techniques for neutron dosimetry [1 (a-c)] based on classical concepts like elastic scattering, neutron activation and absorptive reactions. For experimental neutron detection, gas filled proportional counters, scintillation neutron detectors working with liquid organic scintillators, crystals, plastics, glass and scintillation fibres etc. are used to detect a spectrum of neutron energy. The various types of neutron dosimeters which are in use at present have different detection mechanisms, merits and demerits. Most of them are passive and require some

development processes to note the dose. For last more than four decades, Solid State Nuclear Track Detectors[2] (SSNTD) have been employed for radiation dosimetry in general and neutron dosimetry in particular. They produce etchable tracks inside the detector as a result of charged particles produced due to interaction of neutrons with detector material. For detection of neutrons, they work mainly thorough two mechanisms- registration of fission fragment tracks due to radiators placed in contact with SSNTD and registration of recoil particles (alphas, protons) produced by direct interaction of neutron with detector material. As detectors and radiators used are comprised of organic polymers, the elastic recoils of elements like H, C, O and N give rise to tracks in detector materials along with some tracks due to non-elastic (n, p) and (n, α) processes.

In 1978, Cartwright[3] et al discovered the proton registration properties of CR-39 (PADC) polymer and since then PADC has remained a material of choice in personnel neutron monitoring [4 (a-c)]. CR-39 satisfies most of the requirements of an ideal track detector and is found to show proton sensitivity over a wide range of energies. It is preferred for personnel neutron monitoring owing to its larger cross-section for (n, p) scattering, greater ranges of recoil protons, greater possibility of neutron energy transfer to protons. Further, these tracks could be developed using chemical etching or electrochemical etching[5] or a suitable combination of both and many reports are available about this in the literature. It is also possible to automate the process of track counting in the present days.

PADC detector film is widely used in monitoring fast neutron doses because of its sensitivity to neutrons through (n, p) reactions, excellent optical properties that facilitate the analysis and sufficiently high shelf life. For thermal neutrons, boron or doped PADC could be used through ^{10}B (n,α) ^{7}Li reaction. However, these detector

films are procured only through import procedure (commercially available as CR-39) as it is not manufactured in India at present. If this could be developed, it would be an import substitution and foreign currency resources could also be saved.

With this view in mind, a MOU based project was evolved between Bhabha Atomic Research Centre (BARC) and Goa University on development of solid state nuclear track detectors for charged particle dosimetry. This was mainly focused on the scale-up of process for the preparation of PADC as our research group had previously studied the processes to develop ADC monomer on laboratory scale and cast polymerized the same to get detector films of size upto 4" x 4". The MOU was mainly focused on scale up of the existing polymeric film casting process to a stage of casting PADC detector films of size 10"x10" or 11"x11" and its standardization followed by its dosimetric evaluation at BARC laboratories.

4.2   Materials and Methods

All the chemicals used in synthesis of monomers and initiators were obtained from different suppliers (M/s Molychem, M/s Spectrochem, M/s Loba Chemie) as per their availability. Allyl alcohol, dimethyl carbonate, diethylene glycol were purified by appropriate distillation procedures[6] before their further use. Solvents used were dried using standard procedures before use. The reaction products/ monomers were characterized by TLC and various spectroscopic techniques (IR, PMR, and CMR) as per requirements.

Monomers: The ADC monomer used in the study was synthesized in our laboratory by maintaining dust free environment to the extent possible. The polymers prepared from such monomers synthesized in a dust free environment had a lesser background track like features seen under microscope. The monomers were

purified by vacuum distillation at elevated temperature. Initial treatment with activated charcoal was also given to the monomer synthesised so as to remove any coloured impurities.

Initiators: The initiators used for free radical polymerization were IPP and BP. IPP was prepared as and when it was required as it is highly unstable and decomposes on standing for longer period of time. IPP was prepared and estimated for its purity just prior to its use for polymerization. Second initiator i.e. BP is commercially available with M/s Loba Chemie. It was recrystallized from chloroform methanol mixture and used after drying. BP is, however, not much recommended as it needs higher temperature for initiation of the polymerization and presence of aromatic rings in its structure might cause some problems towards radiation sensitivity.

Plasticizers: Commercially available dioctyl phthalate (M/s Loba chemie) of "GR" grade was used after its purification i.e. washings with 1 % aq. NaOH solution followed by washing with sufficient quantity of water and drying over anhydrous Sodium sulphate.

Spectral Characterization: The monomer after its synthesis and purification was characterized using various spectral techniques. Infra red spectra were recorded on Shimadzu FT-IR spectrophotometer with NaCl discs for liquid samples and KBR-compound powdered mixture for solid samples. ^{1}H and ^{13}C spectra were recorded on Bruker 400 MHz NMR instrument with CDCl$_3$ / DMSO as solvent and TMS as an internal standard.

4.2.1   Monomer Synthesis: Scale-up process

The synthesis of Allyl Diglycol Carbonate (ADC) monomer could be carried out using two different routes; first based on phosgene [7 (a, b)] and the other based on transesterification [8 (a-d)]. The first route was developed during the discovery of ADC in the year 1945 and is used to synthesize ADC in a relatively faster process. The second route, on other side, requires somewhat longer time. It is also to be noted that while using the first route, possibilities exist of getting a slight colour to the ADC monomer. This colour may not affect quality of detector film but may be a problem if the PADC polymer is to be used for optical or particularly ophthalmic applications. Both routes have all the possibilities of formation of certain by-products and hence require appropriate purifications steps. We have used both the routes in the present work.

I.   ADC via transesterification process:

ADC can be synthesised by transesterification of DAC with diethylene glycol at 110 ^{o}C temperature using KOH and phase transfer catalyst (PTC).

Diallyl carbonate (DAC): Diallyl carbonate was first prepared by D. E. Adelson et al[9] in year 1950 and copolymers with other allyl esters were prepared and used for laminations, coatings and glass substitutes. This was also synthesised by using different methods [10 (a-h)]. This was also prepared and standardised by A. A. A. Mascarenhas et.al [8d, 11] in our laboratory on small scale. We have tried and succeeded in scaling up this synthesis to prepare 500 g of DAC in a single batch. 895 g of allyl alcohol (1050 mL, 15.4 moles) and 280 mL cyclohexane was taken in 2 L, 5-neck round bottom flask fitted with overhead stirrer and thermometer. The distillation assembly was setup using fractionating column and addition funnel. The mixture was stirred vigorously and heated to attain 60 ^{o}C temperature. Once temperature was

reached to 60 ^{o}C, 6.96 g KOH (i.e. 1.5% by weight of DMC) and 1.0 g PTC were added to the mixture. Further, dropwise addition of 463.5 g (434 mL, 5.2 moles) of dimethyl carbonate (DMC) was commenced using a dropping funnel. Simultaneously, temperature was gradually raised to 70 ^{o}C. After completion of addition over a period of 2-3 hours, the azeotropic mixture of methanol and cyclohexane was taken out by azeotropic distillation process for 7 hours. The excess of allyl alcohol and dimethyl carbonate was removed by normal distillation process. The unreacted allyl alcohol and dimethyl carbonate could be recycled in the new batch of DAC monomer synthesis. The reaction was monitored by TLC (10 mL, 100% pet ether) and it was completed after 10 hours. After completion of reaction, it was cooled and workup was carried out using diethyl ether. Initially around 100 mL brine water was added to the semi solid reaction mass. It was then extracted into 100 mL of diethyl ether and brine washings (8 x 25 mL) were given till it become neutral. Finally the extract was dried by passing it over bed of 7-8 g anhydrous sodium sulphate. The combined washings were also extracted using (6 x 15 mL) diethyl ether and passed over sodium sulphate. Finally the crude product was distilled out at reduced pressure of 1.0×10^{-2} mbar and 39 ^{o}C to get 540 mL of pure Diallyl carbonate in 72.81% yield with respect to dimethyl carbonate. Transesterification of allyl alcohol and dimethyl carbonate in presence of base catalyst gives DAC (scheme 4.1). Infrared spectrum and NMR spectrum of DAC is given in figure 4.1 and figure 4.2 respectively . The structure of DAC was characterized by following spectral data. IR ν_{max} (KBr): 3088 cm^{-1}, 1747 cm^{-1}, 1249 cm^{-1} and 968 cm^{-1}. ^{1}H NMR (Bruker 400MHz, CDCl$_3$) (ppm): 5.93 (m, 2H), 5.40 (d, J=18.4, 2H), 5.36 (d, J=11.6, 2H), 4.66 (d, 4H).
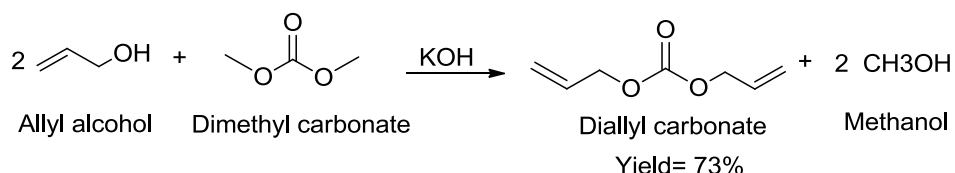
Scheme 4.1: Synthesis of Diallyl carbonate

Allyl diglycol carbonate: 40 g of diethylene glycol (0.3773mol) and 428.61 g of DAC (3.02 mol) were taken into the three neck flask fitted with thermometer and nitrogen gas inlet tube from both side arms and at centre overhead stirrer was connected with help of which reaction was mixed vigorously. Initially, nitrogen was bubbled through reaction mixture and then flow was maintained at 120-150 bubbles/minute. Further, the temperature was gradually increased to 65 ^{o}C. At 65 ^{o}C temperature, 1.2 g KOH and 1.5 g PTC were added to the reaction flask. Then temperature was increased to 75 ^{o}C and held for 30 minutes with constant stirring. After that it was gradually increased to 90 ^{o}C and kept constant for 3 h with vigorous stirring. Temperature was then increased to 95 ^{o}C, the N_2 flow rate was also increased so that allyl alcohol formed in reaction was distilled out. Excess DAC was removed in another 0.5 h. After four hours of reaction, it was cooled to ambient temperature and monitored by TLC (10 mL, 2:8 EtOAc: Pet ether). Further once reaction was complete workup was carried out using diethyl ether.

Workup: Initially 40 mL brine was added to the cooled reaction mixture and taken up into 500 mL separating funnel. 50 mL of diethyl ether was added and product was extracted into it. It was then washed with brine (6 x 15 mL) till it is neutral checked by pH paper. The organic layer was passed over bed of 10 g anhydrous Na_2SO_4 into the flask. Product was extracted from washings using diethyl ether (4 x 15 mL). Finally the crude product was obtained by removing diethyl ether and excess DAC at

reduced pressure and 39 ^{o}C temperature. The crude ADC was vacuum distilled at 2.0 x 10^{-2} mbar pressure and 160 ^{o}C to yield pure ADC. The yield obtained of pure ADC was 80.0 g (theoretical yield=103.3 g); 77.44%. Scheme 4.2 depicts synthesis of ADC via transesterification process. Infrared spectrum and NMR spectrum of ADC is given in figure 4.3 and figure 4.4 respectively (page no. 317-318). The structure of ADC was characterized by following spectral data. IR ν_{max} (KBr): 3086 cm^{-1}, 1748 cm^{-1}, 1649 cm^{-1} and 1258 cm^{-1}. ^{1}H NMR (400MHz, CDCl$_3$) δ 5.95 (m, 2H), 5.40 (d, J=18.8, 2H), 5.30 (d, J=11.6, 2H), 4.65 (d, J=8.0, 4H), 4.31(t, 4H), 3.75 (t, 4H).
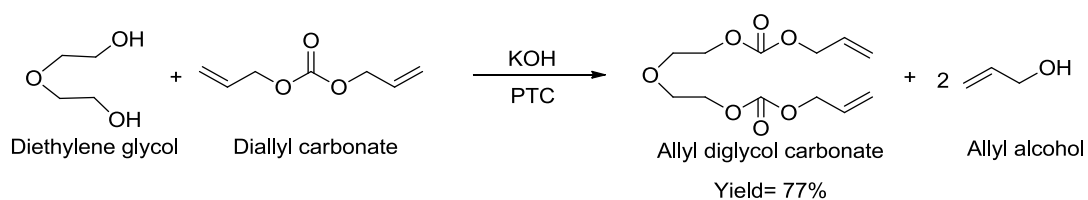
Scheme 4.2: Synthesis of Allyl diglycol carbonate

II.   ADC via chloroformate/condensation method:

In this method, allyl chloroformate (either commercially available or prepared by reacting allyl alcohol and phosgene or triphosgene) are condensed with diethylene glycol to form ADC monomer.

In a two neck round bottom flask fitted with pressure equalising addition funnel and overhead stirrer, 50 g of diethylene glycol (0.4712 mol) was dissolved in 100 mL acetone and to this 90 mL of pyridine (88.38 g, 1.117 mol) was added and kept in a methanol bath for cooling. Once the temperature of reaction mixture reached to -5 ^{o}C, 115 mL of allyl chloroformate was added dropwise into the reaction flask over a period of 2 hours with vigorous stirring. After complete addition it was stirred at same temperature for 1 hour and then at ambient temperature for 1 hour. After

completion of reaction monitored by TLC (10 mL, 2:8 EtOAc: Pet ether), workup was carried out.

Workup: Initially the acetone was removed over rotavap and the solid mass remained was acidified with 10 mL of 1:1 HCl: water. Further it was taken in 500 mL separating funnel and extracted in 50 mL of diethyl ether. The organic layer was washed with brine (5 x 15 mL) till neutral. Finally organic layer containing product was passed over bed of 10g sodium sulphate. Combined washings were treated with diethyl ether (5 x 10 mL) to extract product from washings. Finally, crude ADC was vacuum distilled at 2.0 x 10^{-2} mbar pressure at 160 ^{o}C to yield pure ADC. The yield obtained of pure ADC was 95.0 g (theoretical yield=129.2 g); 73.53%. Scheme 4.3 depicts synthesis of ADC via condensation process. Infrared spectrum and NMR spectrum of ADC is given in figure 4.5 and figure 4.6 respectively The structure of ADC prepared via condensation route was characterized by following spectral data. IR ν_{max} (KBr): 3086 cm^{-1}, 1747 cm^{-1}, 1649 cm^{-1} and 1257 cm^{-1}. ^{1}H NMR (400MHz, CDCl$_3$) (ppm): 5.98-5.88 (m, 2H), 5.36 (d, 2H), 5.27 (d, 2H), 4.63 (d, 4H), 4.30(t, 4H), 3.73 (t, 4H).
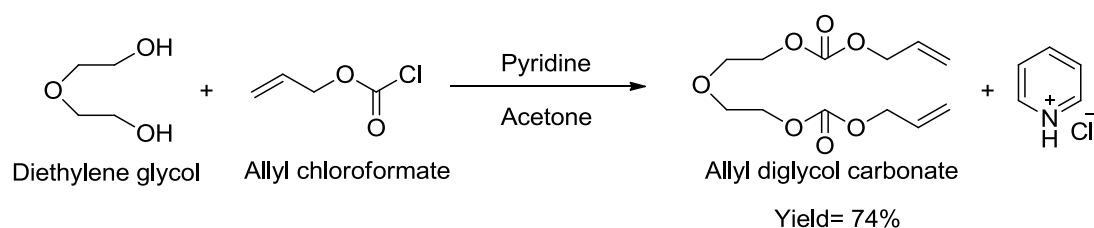
Scheme 4.3: Synthesis of ADC using condensation process

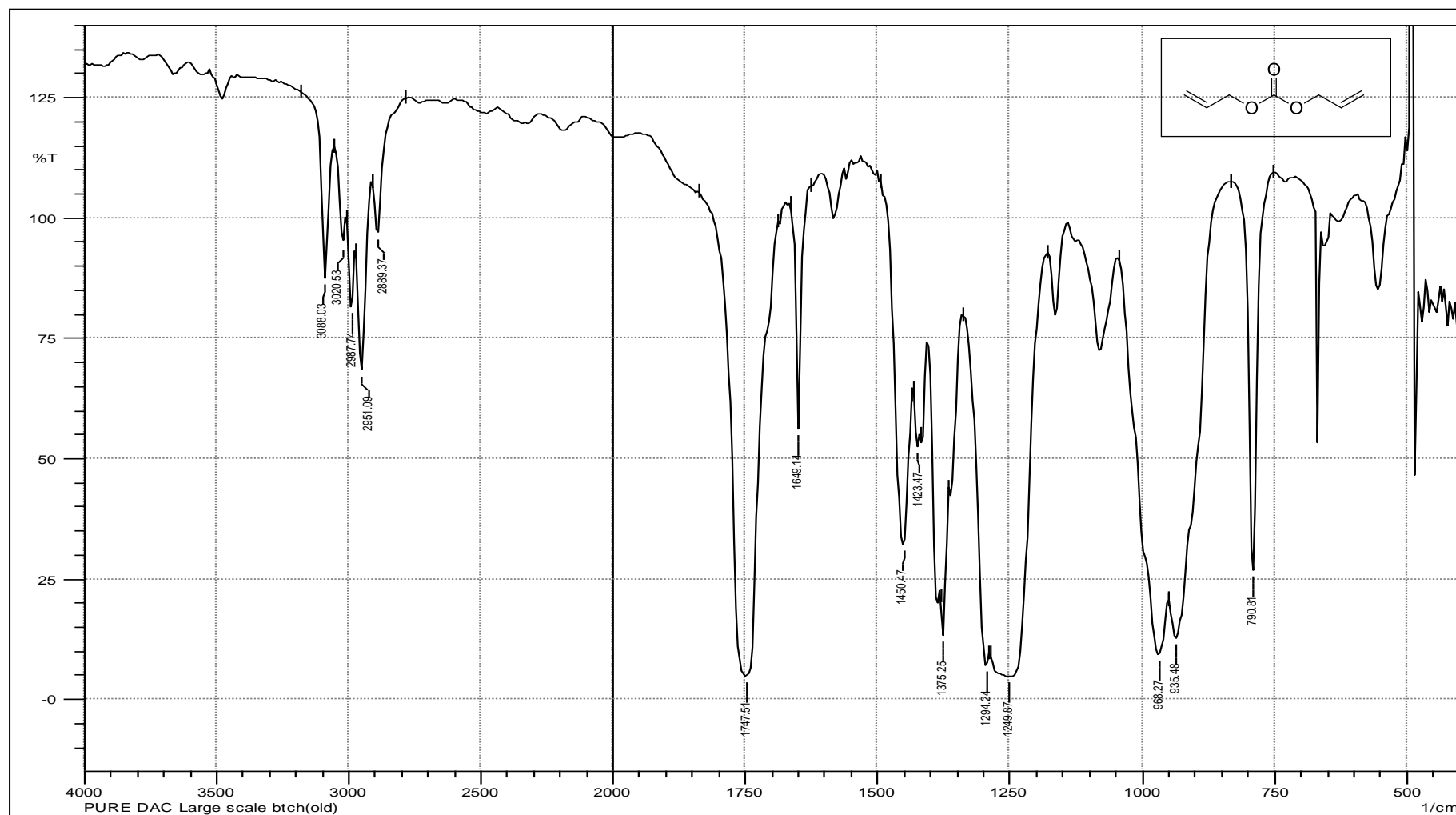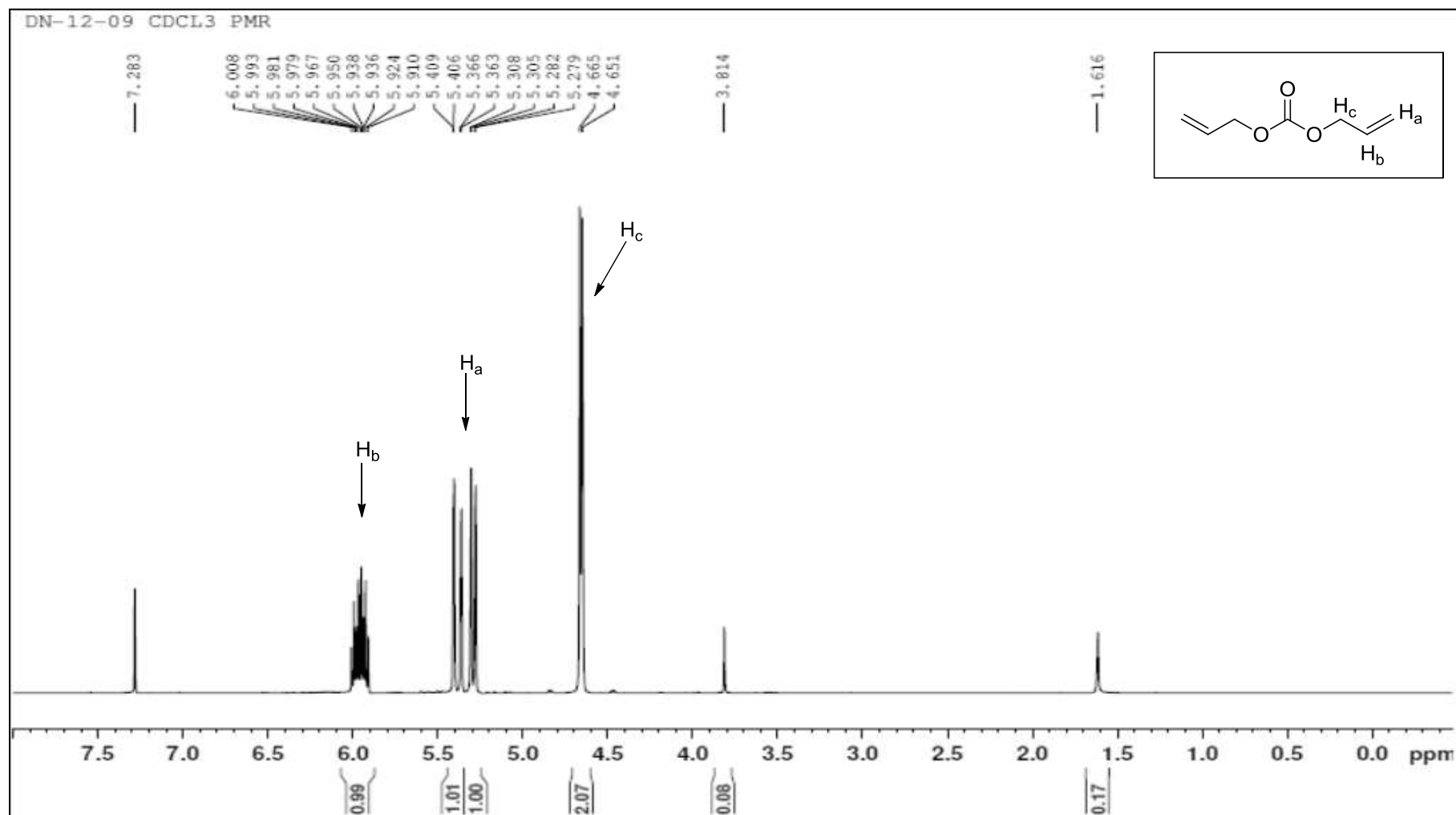**Figure 4.1:** IR spectrum of Diallyl carbonate (DAC)
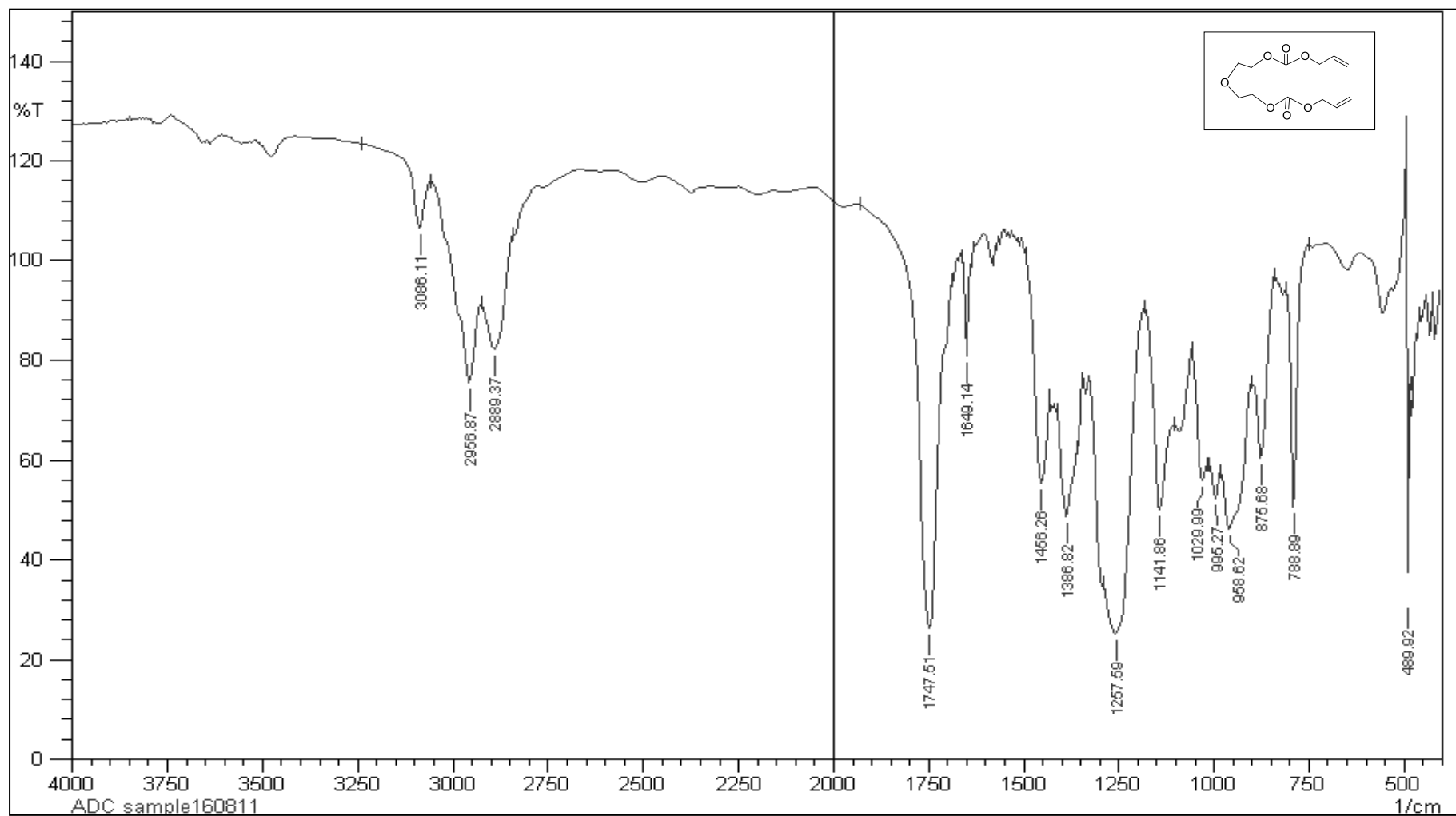
Figure 4.2: ^{1}H NMR spectra of DAC

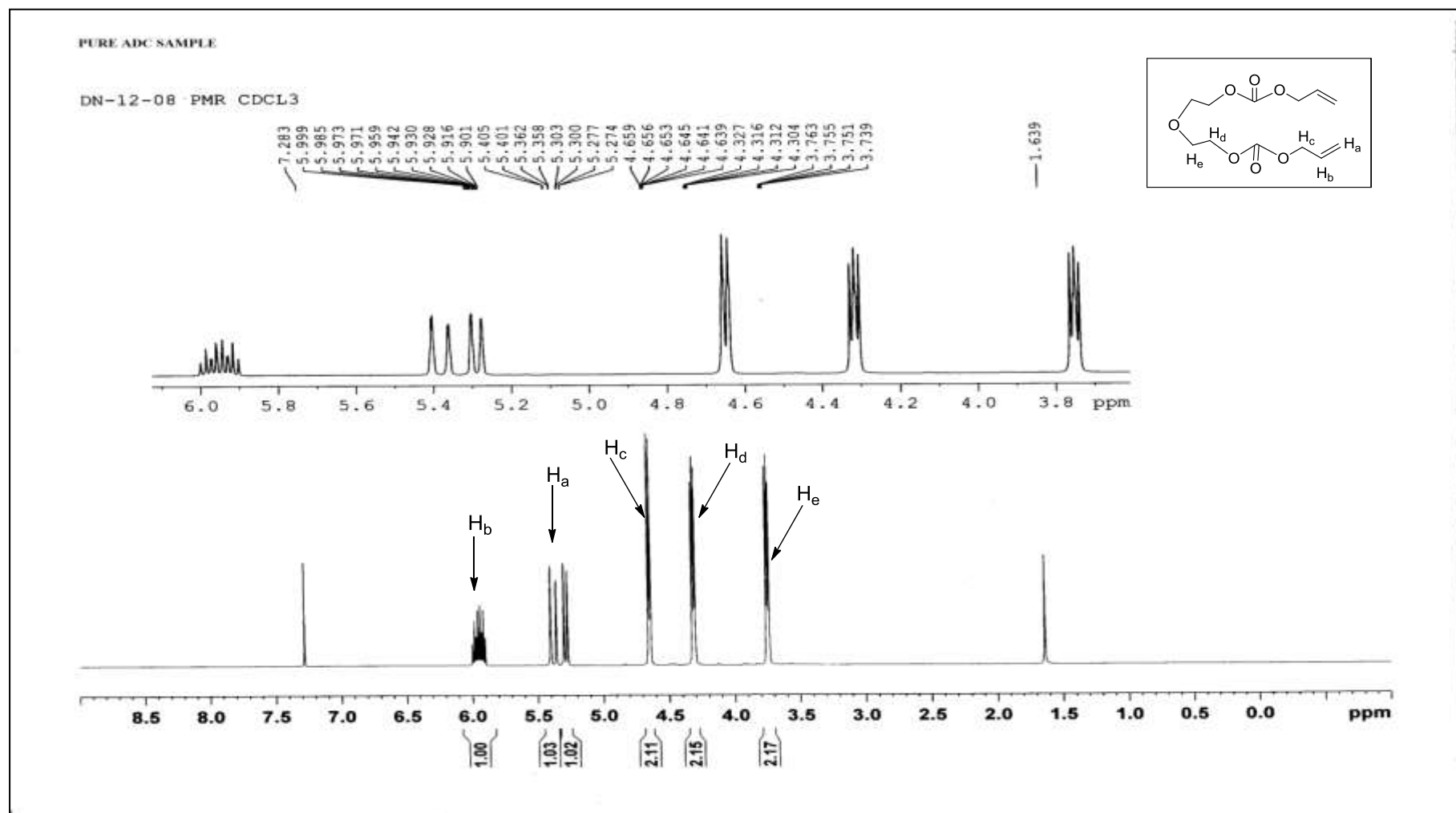**Figure 4.3:** IR spectrum of ADC sample via transesterification route

Figure 4.4: ^{1}H NMR spectrum of ADC sample via transesterification route
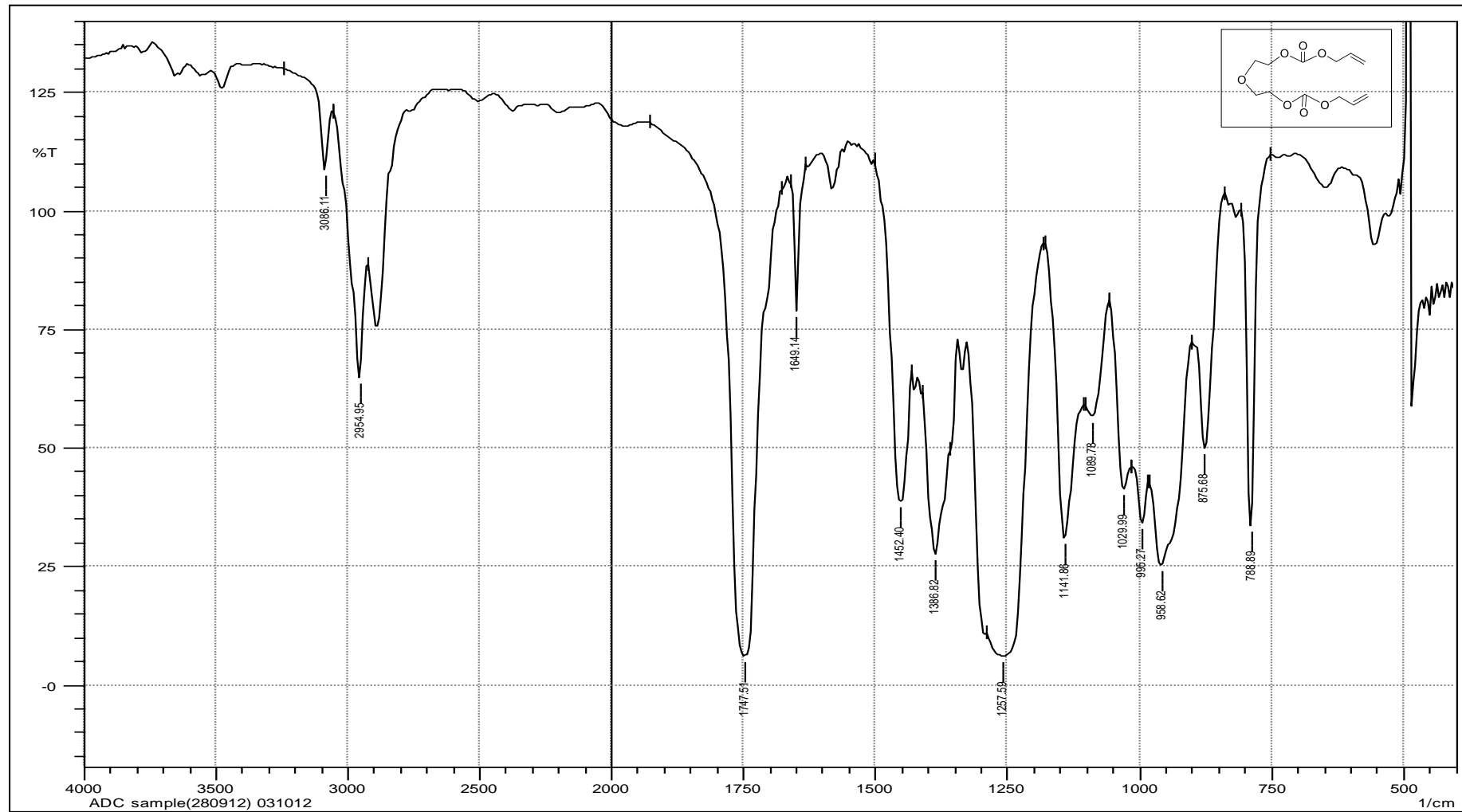
Figure 4.5: IR spectrum of ADC sample prepared by condensation process
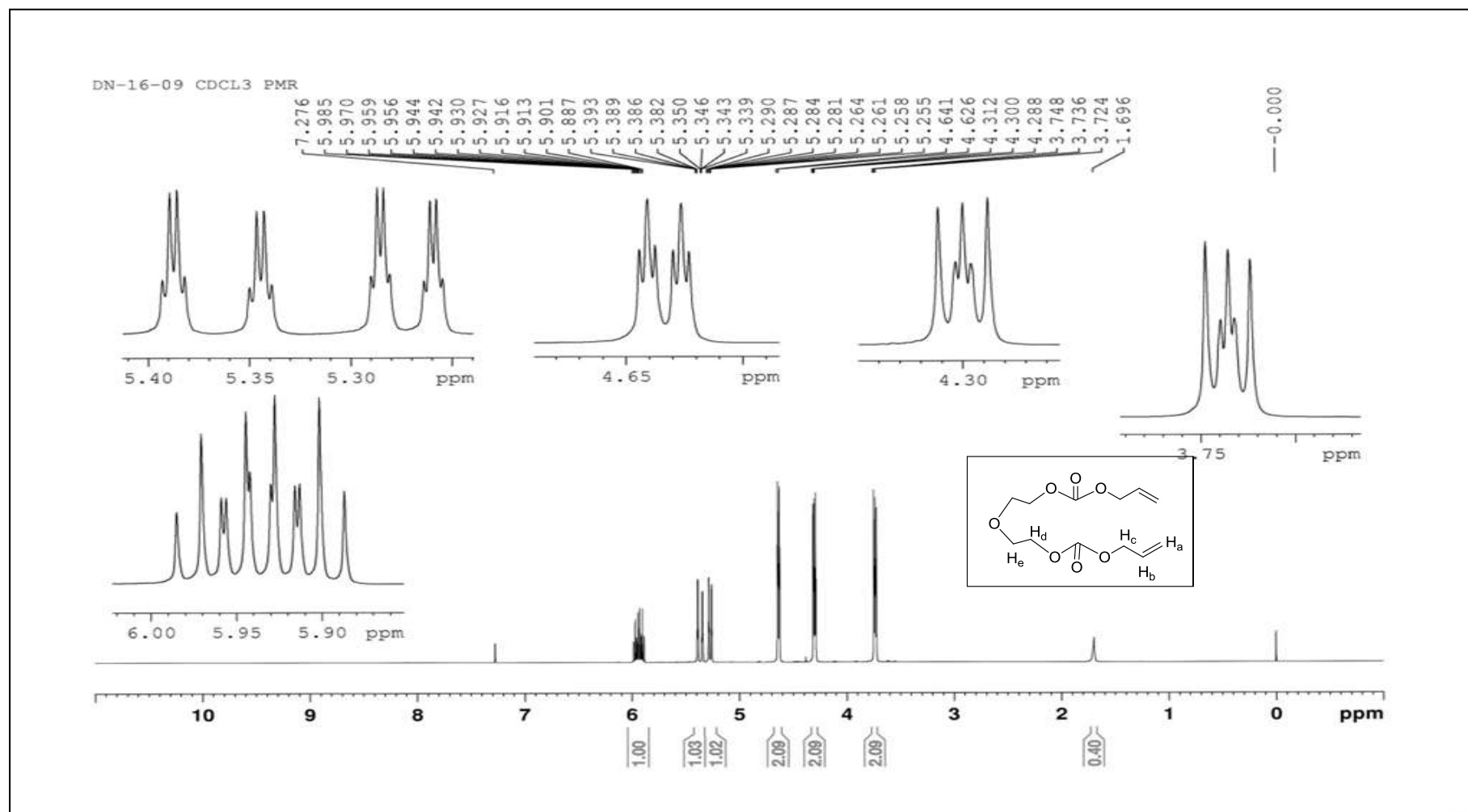
Figure 4.6: ^{1}H NMR spectrum of ADC sample prepared by condensation process

4.2.2 Synthesis of Isopropyl Chloroformate (IPCL) [12, 13]: The initiator isopropyl peroxydicarbonate (IPP) used during the polymerization of ADC is highly unstable compound and its commercial supply is not possible as it is not much stable above 0°C. Further, in larger quantities, its transportation could result in explosions. IPP is synthesized from an intermediate IPCL, which in turn, is synthesized from isopropyl alcohol and phosgene/ triphosgene. Triphosgene is a relatively stable compound that can be transported and generates 3 mol of phosgene in situ under suitable conditions. The synthesis of IPCL is described below in scheme 4.4.

In a two neck round bottom flask 18.56 g (0.0632 mol) of triphosgene was weighed and dissolved in 150 mL dichloromethane. The neck of flask was fitted with rubber septum so that the phosgene generated does not leak out. It was then stirred and cooled to 0^0C. To this stirred reaction mixture, 13.6 g (13.8 mL, 0.172 mol) of pyridine was injected to generate phosgene gas and simultaneously 10 g (12.7 mL, 0.172 mol) of isopropyl alcohol was injected through the rubber septum into the reaction flask with the help of another syringe. Care must be taken while adding the base. Excess pyridine at once should not be added; it may lead to generation of large amount of phosgene gas and may also lead to some accident. After completion of addition, reaction mixture was stirred for 1.5 hour at 0^0C. Slowly the septum was removed and reaction mixture was quenched with ice flakes followed by workup. The reaction mixture was washed with 6×25 mL of ice cold water and the organic layer was dried over anhydrous Na_2SO_4. Reaction mixture from two such batches was mixed and was concentrated by distilling out dichloromethane at 50 ^{o}C, by fractional distillation. This crude product was vacuum distilled at 40 ^{o}C with very low vacuum to afford pure isopropyl chloroformate in 60-70% yield. IR and NMR spectrum of the product was recorded and reported in figure 4.8 and figure 4.9

respectively (page no.324-325). Gas chromatogram (GC) was also recorded and shown in figure 4.7. The GC of IPCL was taken in toluene (1:1 ratio). Sample injected was IPCL and toluene in 1:1 v/v ratio. At retention time of 1.07 minutes toluene peak was observed (as confirmed previously). The peak at retention time of 1.20 minute was due to IPCL. The temperature program used in gas chromatographic technique for IPCL sample was as follows; Injector temperature =150 ^{o}C, Oven temperature = 150 ^{o}C, Detector temperature = 160 ^{o}C. Thus, the only additional peak is at retention time of 0.95 minute with about 1.9% was attributed to the impurity indicating that purity of IPCL prepared was sufficiently high. The structure of IPCL was characterized by following spectral data. IR ν_{max} (KBr): 2988 cm^{-1}, 1774 cm^{-1}, 1089 cm^{-1}and 692 cm^{-1}, ^{1}H NMR (400 MHz, CDCl$_3$) (ppm): 5.01(m, 1H), 1.31 (d, 6H)

Scheme 4.4: Synthesis of Isopropyl chloroformate
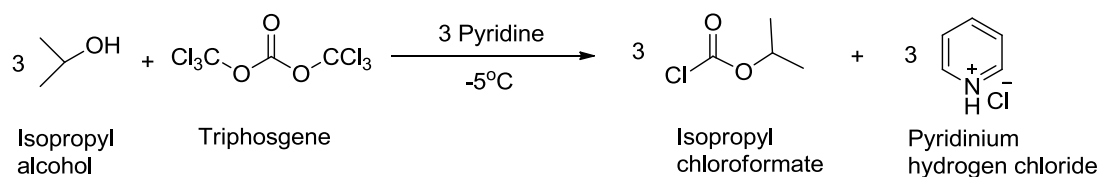
4.2.3   Synthesis of Isopropyl peroxydicarbonate (IPP)[14]: IPP was prepared in two steps as shown in scheme 4.5. First sodium peroxide was prepared and then IPCL was condensed with freshly prepared sodium peroxide. Initially, 1.5 g (0.0375 mol) of NaOH was dissolved in little water and was cooled to 0 ^{o}C and H$_2$O$_2$ was added to it drop by drop, maintaining the temperature below 5 ^{o}C with continuous stirring to get Na$_2$O$_2$. It was directly used for next reaction without further purification. Meanwhile, 5 g (0.0408 mol) of IPCL was weighed and kept for cooling at 0 ^{o}C. Once it attains 0 ^{o}C, Na$_2$O$_2$ was added drop wise to IPCL maintaining temperature between 3-7 ^{o}C, the mixture was stirred vigorously for 1

hour at 0 °C temperature and then it was extracted in dichloromethane. It was passed over anhydrous Na_2SO_4. Further it was characterized by IR spectrum as shown in figure 4.8 (page no.326). IR ν_{max} (KBr): 2987 cm^{-1}, 1796 cm^{-1}, 1209 cm^{-1} and 1093 cm^{-1}. Then its percentage purity was determined by volumetric titration using sodium thiosulphate and iodine monochloride. Percent purity of IPP above 75% was used for cast polymerization. Being very unstable at room temperature, it was stored safely under refrigerated condition below 0 °C.

Step 1: $H_2O_2 + 2NaOH \longrightarrow Na_2O_2 + H_2O$

Step 2: Isopropyl chloroformate $\xrightarrow[0-5^oC]{NaOONa}$ Isopropylperoxydicarbonate
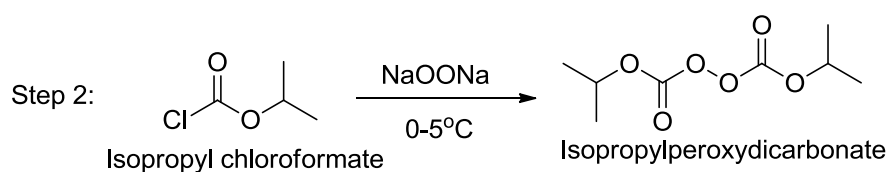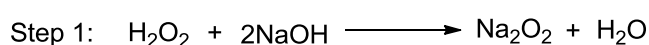
Scheme 4.5: Synthesis of diisopropyl peroxydicarbonate (IPP)
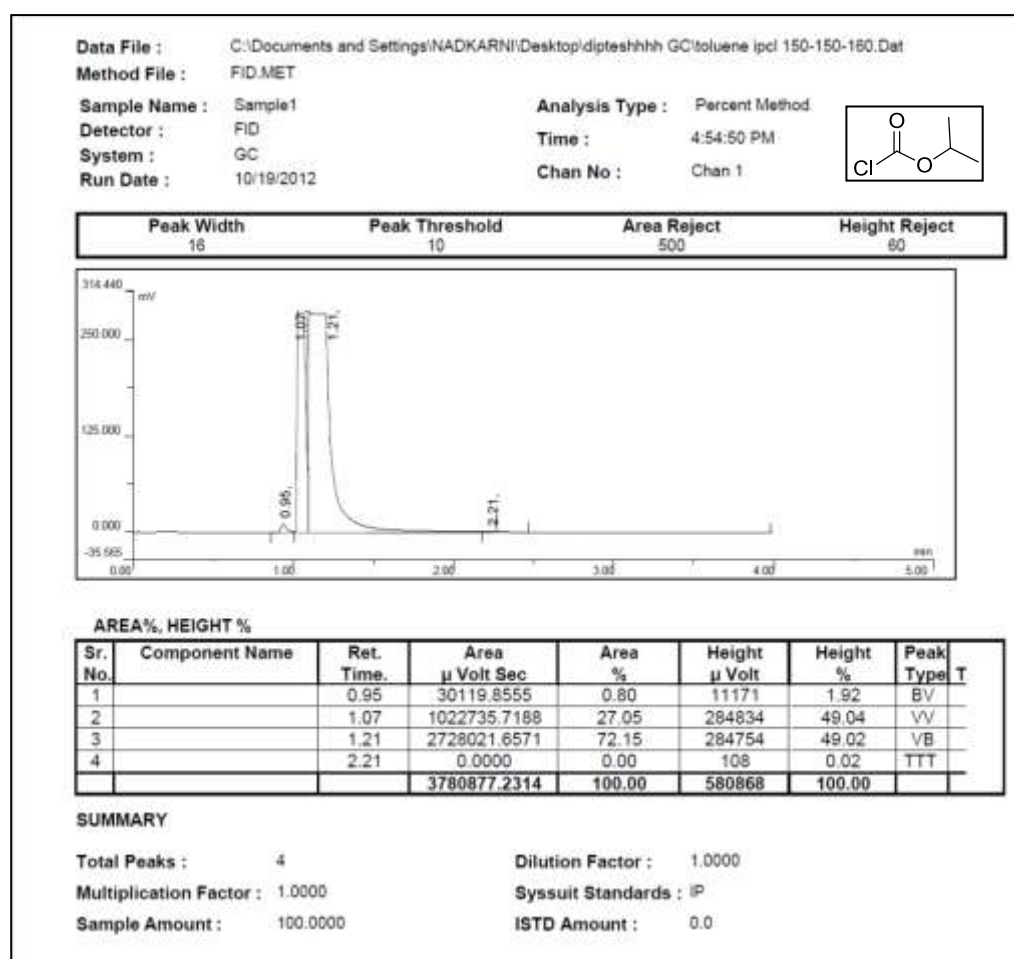
Figure 4.7: Gas Chromatogram of IPCL
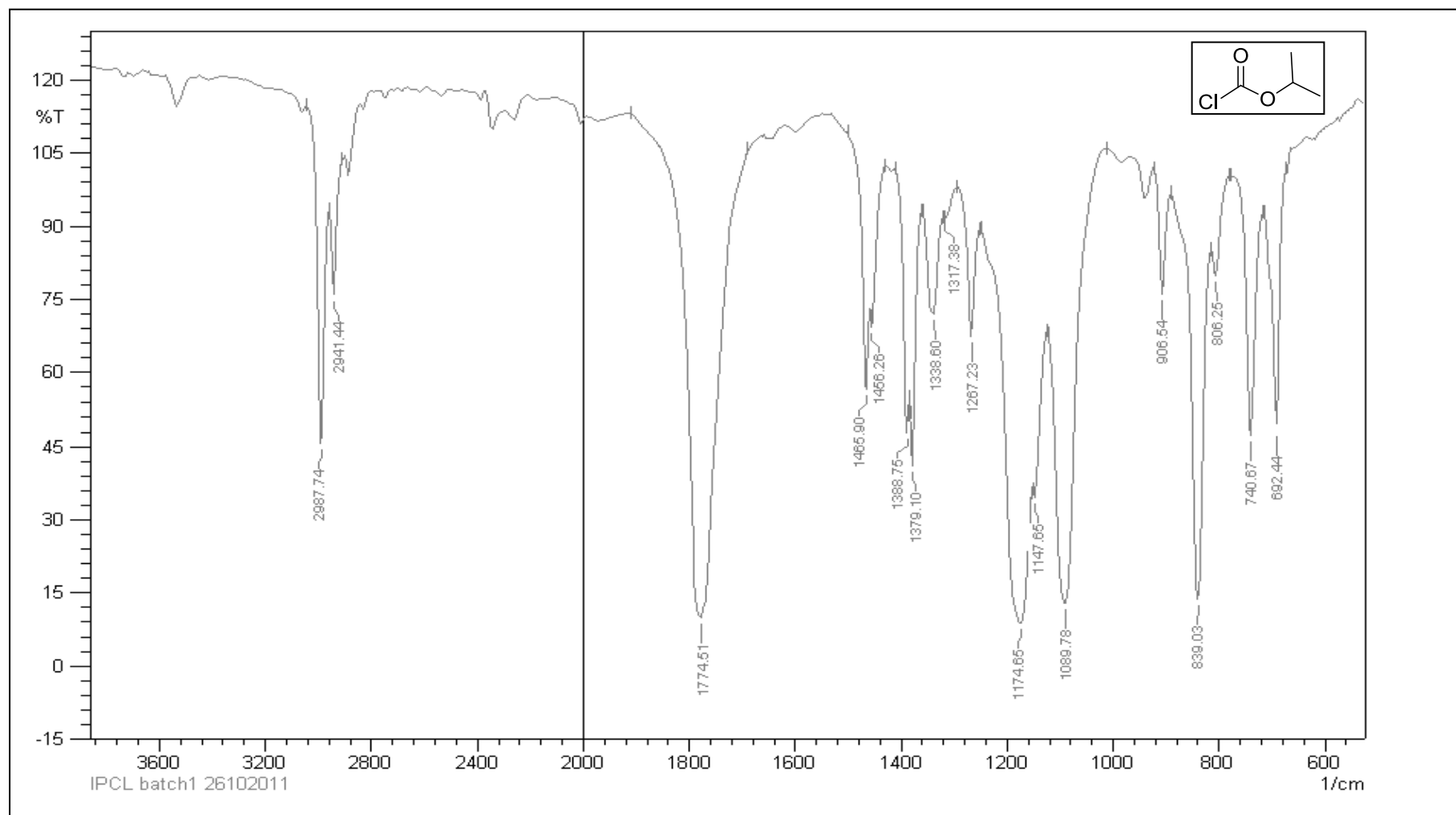
Figure 4.8: IR spectrum of isopropyl chloroformate (IPCL)

DN-13-10 CDCL3 PMR
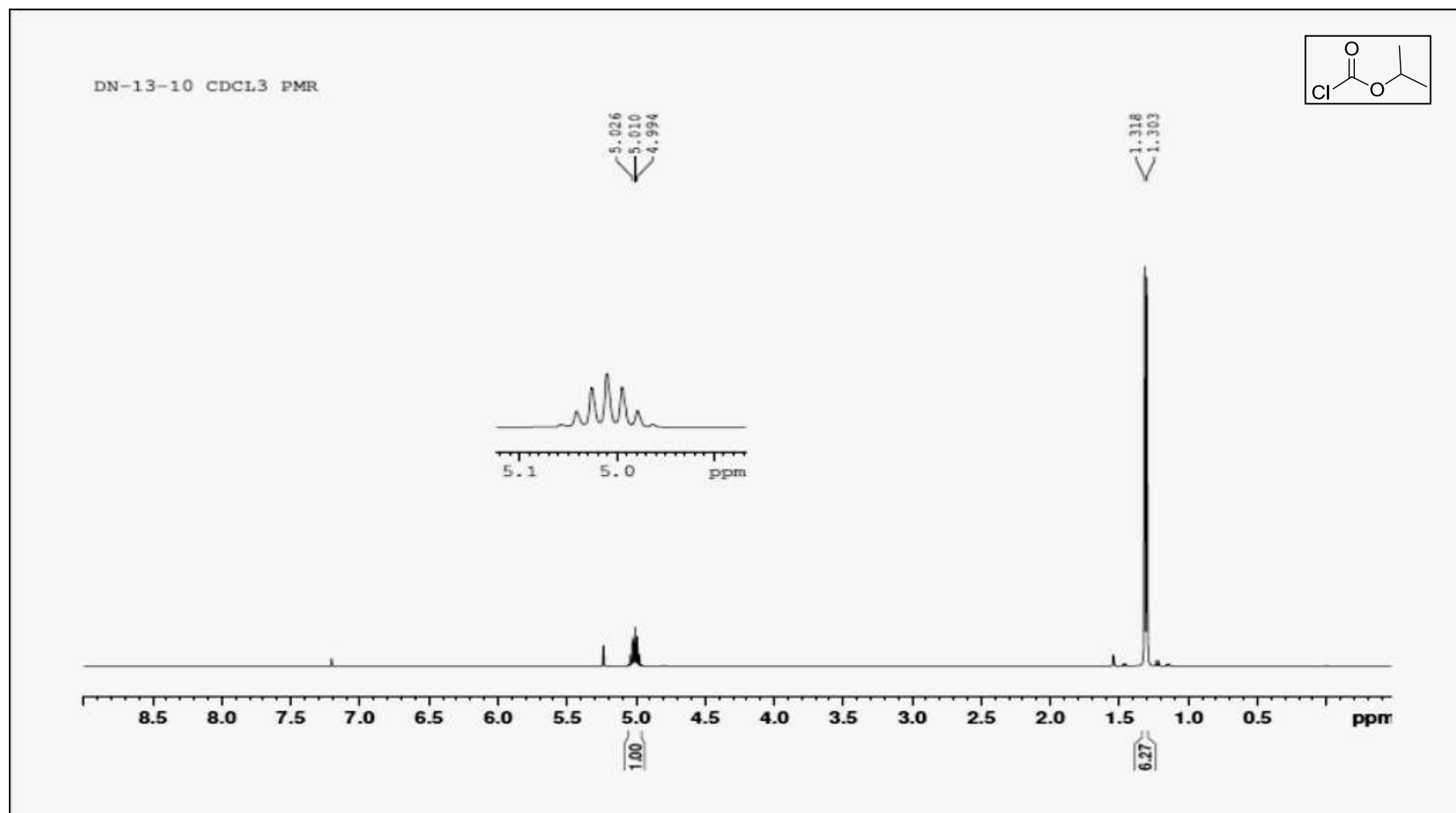
Figure 4.9: ^{1}H NMR spectrum of isopropyl chloroformate (IPCL)
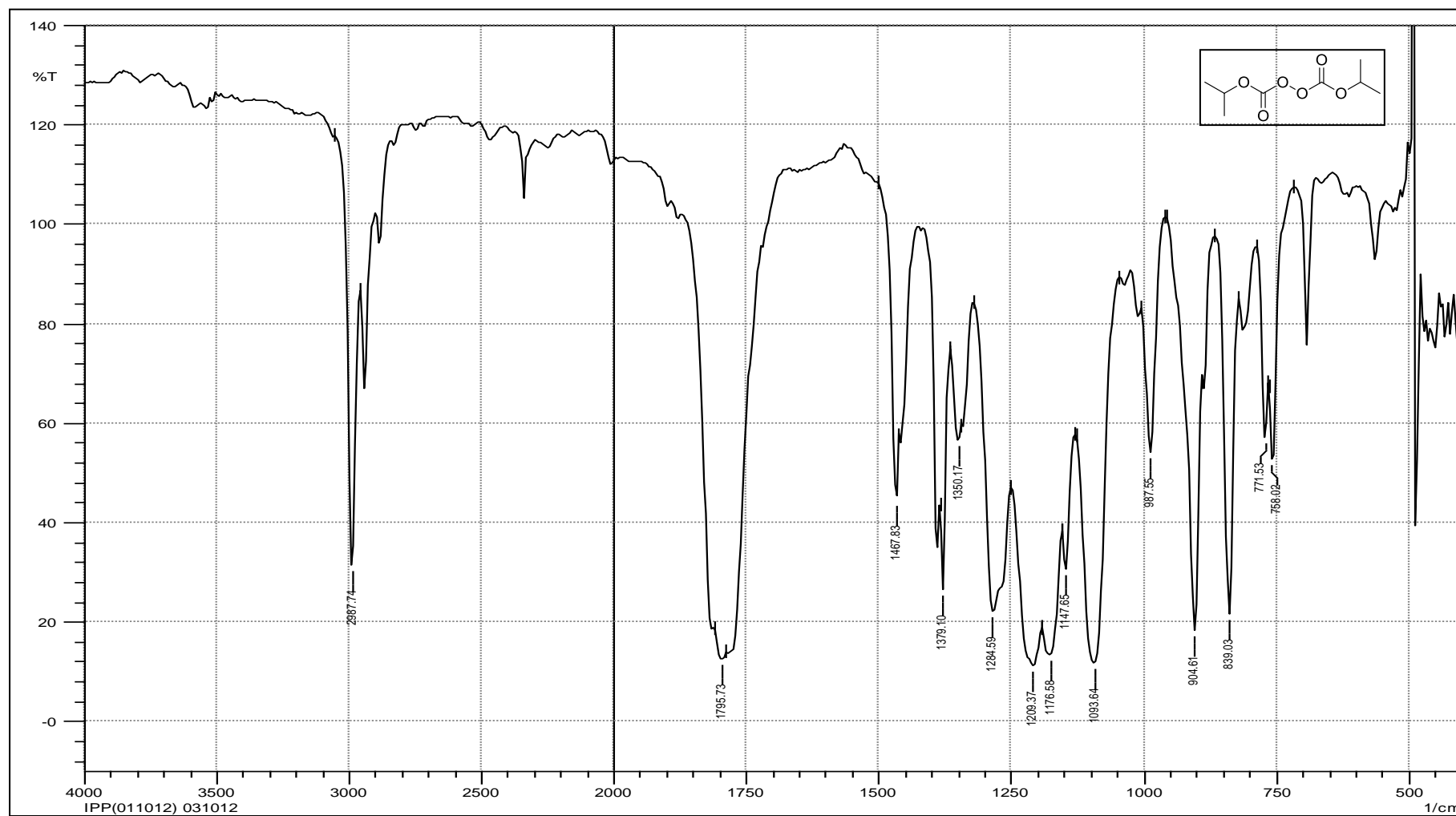
Figure 4.10: IR spectrum of diisopropyl peroxydicarbonate (IPP)

4.3 Results and Discussion

Aiming at the development of PADC films of larger dimensions (10"x10" in size), we first thought of optimizing monomer synthesis via both routes. Synthesis of precursor of initiator i.e. IPCL was also tried to optimise for large scale synthesis as mentioned above in scheme 4.1 to scheme 4.7. Further casting of films was carried out and modifications were done over several trials during polymerization. Some of the equipments used during the process of polymerization are discussed in this section.

4.3.1 Equipments used during scale-up of polymerization processes.

1.   Polymer press: The polymer press was designed by M/s Techno Search Instruments, Mumbai after discussions with us about the requirements. However, it was based on their similar polymer press model used for casting small films from thermoplastic materials, already commercially available with them.

Figure 4.11 shows the photograph of the polymer press before modification and figure 4.11a shows its schematic arrangement. It can be seen that it consisted of two metallic flats (platens) positioned parallel to each other. In the original hydraulic press, the bottom platen could be raised with hydraulic pressure against the top platen whose position was adjustable with a screw. Three heating blocks that could be placed in between the top and the bottom platen and hot water circulated between them using inter connected water lines. These blocks had water lines inside them so that hot water could be circulated externally. Polymer press was connected to the programmable circulating water bath (make Julabo. Two moulds could be kept in the space between these three blocks. Sensor was inserted into the middle block to measure the temperature of the blocks. The pressure applied to the mould could be

noted using gauge fitted to the hydraulic pump of the press. It is to be noted that the hydraulic pressure up to 2 tonnes could be applied although such high pressure is not required for casting polymer films.

This gave us detector films with good surface but they were getting cracked. Around 30-40 films of smaller size (~ between 6 x 6" to 10" x 10") were tried but all were formed in broken/ severely cracked condition. Some of them were tested for alpha tracks registration and they showed good alpha tracks after etching chemically.

Figure 4.11: Original design of the polymer press
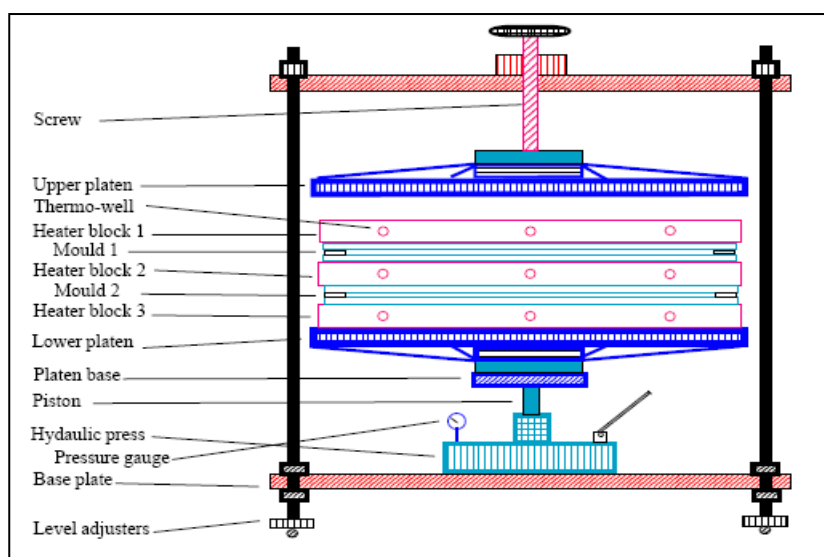
Figure 4.11a: Schematic presentation of the press (First design)

After careful observations we noted that the platens (especially the bottom one) had sufficient play that could result into non-uniform contact with the top platen thereby resulting into uneven pressure being applied on the heating blocks/ polymerization moulds held in between. Polymerization trials were taken by changing applied pressure, time of polymerization, different glasses for moulds etc. It was observed that-

a. PADC films obtained were cracked severely.

b. The cracking of films appeared to be due to uneven pressure exerted by

   platens on the moulds.

Although broken, these PADC detector pieces were sent to Radiological Physics and Advisory Division (RP&AD), BARC for further analysis of its radiation sensitivity.

1.1 Modification of the polymer press: The polymer press had some faults in its design due to which it could not give us good intact PADC films. There was play in platens of the press, the pressure exerted on to platen was uneven, also the platens were made of mild steel and they were sufficiently heavy. All these problems probably led to failure in getting intact films. So we requested the manufacturer of the press to do necessary modifications in the press.

Initially, they modified the base to minimize the play. Since this was not much effective, the press was fitted with level adjuster; carried out surface grinding of both the platens. After these changes in the press, it was observed that extent of cracking was reduced. It appeared that further repairs should be carried out in order to completely eliminate the pressure imbalance between the platens.

It was suggested that the required pressure being small in quantity, one could better apply it using a screw system instead of hydraulic system. It was noted that there is some inherent play possible with the bottom platen of the hydraulic press.

Thus, it was decided to replace the hydraulic pump with stationary base platen and pressure may be applied using only the top platen fitted with a screw system. Thus, the hydraulic pump and pressure gauge was removed and heating blocks were placed on rigid support. The heating filaments were inserted into the blocks and heating was controlled by controller. This could serve as a secondary heating system (we never used this as hot water circulation proved to be efficient). The water was circulated through the blocks to maintain the uniform temperature between two blocks where the filled mould was placed for polymerization. The programmable Julabo water bath was used to keep the moulds at constant temperature for longer period of time.

All the framework of polymer press was modified by subjecting its components like base plates, rods etc. to surface grinding so as to fit them in a manner that results into perfectly parallel disposition of the parts that are actually pressurize the polymer mold. Three additional heating blocks with machined and parallel surfaces, made of aluminium (14 mm thick) were fabricated to replace the originally supplied heating blocks which had certain imperfections. Similarly, the original heating blocks were made of mild steel and thus, were heavier and we faced some difficulties in handling them within the restricted space within the press. This modified press system gave us films with better surface and negligible cracks. The modified press system is shown in figure 4.12 and Figure 4.12a shows its schematic arrangement.

Figure 4.12: Modified polymer press with auxiliary heating controller
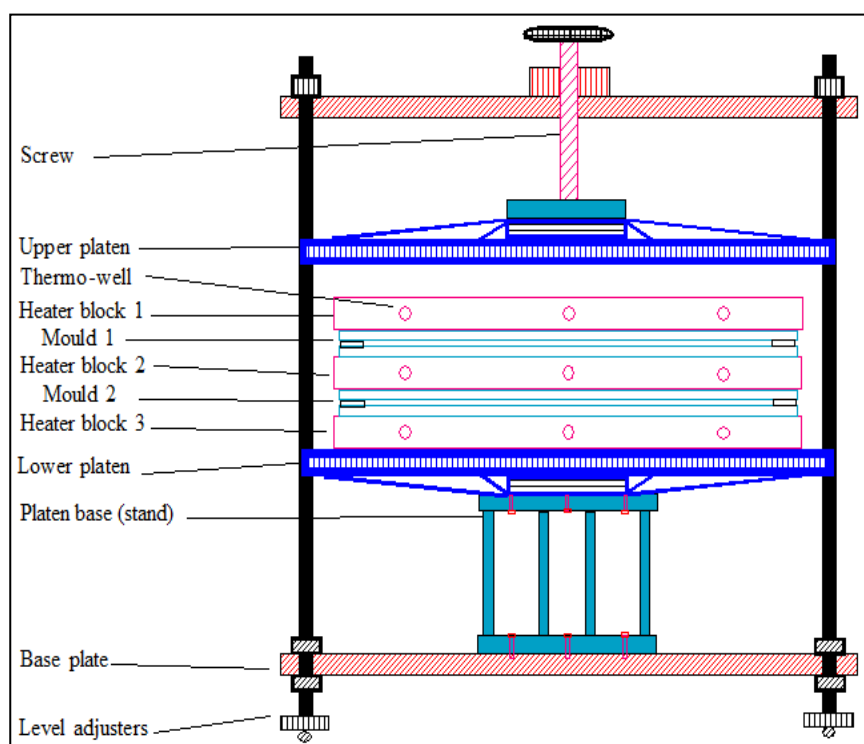
Fig. 4.12 a: Modified polymer press (Schematic representation)

2. **Syringe pump:** Syringe pump (Model 11 Plus, Harvard) was used to fill the moulds with monomer since monomer required to inject into the mould were viscous and was in large amount. Also, it was used to filter the solvents, monomers etc.

Syringe pump has facilities available for suction /delivery of liquids through a syringe, from/to a reservoir at pre-set suction or delivery rates. Figure 4.13 shows a photograph of the syringe pump used.

Figure 4.13: Syringe pump used for filling the moulds.

4.3.2   Details of synthesis for scale-up process.

At initial stages of the work of scaling up of the synthesis, we tried to optimize the synthesis of the ADC monomer on small scale. The transesterification route involved two steps, so more time was required for small scale preparation of desired quantity of ADC. So as stated previously, we decided to optimize the method with the synthesis on a larger scale. We also used other method for the synthesis of ADC, based on allyl chloroformate and diethylene glycol (as described above). A series of experiments were carried out for optimizing it on larger scale for both routes. The ADC monomer prepared was analysed based on its physical and chemical properties like colour, purity, unsaturation etc.

Characterization of monomers and polymers: Apart from use of monitoring methods like TLC and some spectroscopic methods to prove structure of the chemicals/ intermediates during their syntheses, we also used some other qualitative/quantitative methods to ascertain the purity of the materials synthesized. These are briefly described below.

The estimation of unsaturation and purity of initiator[15]: The amount of unsaturation left or the amount of monomer converted to the polymer can be estimated by Wij's iodometric estimations. This method could also be used to get an idea of the purity of monomer itself. The solutions of Wij's reagent (iodine monochloride in acetic acid), 0.1N $Na_2S_2O_3$, 10% KI solution, 0.1N KIO_3 solution, and starch indicator were prepared using the standard methods. The reagents were standardized wherever required. Similarly, estimation of peroxide content using iodine gives an idea about the purity of initiator.

Peroxide estimation[16]: A known quantity of initiator (30-50 mg) was dissolved in acetic anhydride and treated with solid KI. The mixture was swirled and kept in dark for 30 minutes. Then the mixture was diluted with glacial acetic acid and water. The liberated iodine was titrated against standard 0.01N $Na_2S_2O_3$ solution using starch indicator. The chemical reactions involved in the reaction are

R-CO-O-O-CO-R + KI $\longrightarrow$ I_2 + R-CO-O$^-$K$^+$

$Na_2S_2O_3$ + I_2 $\longrightarrow$ $2NaI$ + $Na_2S_4O_6$
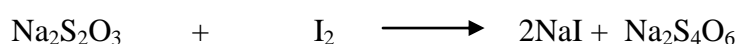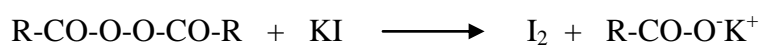
From the relation,

2000 mL of 1N $Na_2S_2O_3$ equals molecular weight of initiator used. The relation can be suitably used to find out the amount of initiator in the sample. The method can be used to determine the amount of initiator left during the kinetics of

polymerization study. Here, 1 g of monomer containing the initiator is dissolved in acetic anhydride and treated with potassium iodide. Further testing remains same as mentioned above. From the relation, the amount of initiator can be determined by using the relation,

$$X \text{ g} = \frac{\text{Burette reading x Normality of } Na_2S_2O_3 \text{ x Molecular weight}}{\text{Sample weight x 2000}}$$

Determination of Unsaturation: This involved a back titration of liberated iodine with standardized 0.1N $Na_2S_2O_3$ solution. A known amount of monomer (30-50 mg) was dissolved in chloroform and a known amount of ICl in acetic acid was added. The mixture was kept in the dark for 1 hour and after 1 hour, 5 mL of 20% KI solution was added to that mixture. The liberated iodine was than titrated against standard 0.1N $Na_2S_2O_3$ solution using starch indicator till end point and burette reading was recorded. The chemical reactions involved in the process are

$$-CH_2\text{-}CH{=}CH_2 \ + \ ICl \ \longrightarrow \ -CH_2\text{-}CHCl\text{-}CH_2I \ + \ -CH_2\text{-}CHI\text{-}CH_2Cl$$

$$ICl \ + \ KI \ \longrightarrow \ I_2 \ + \ KCl$$

$$Na_2S_2O_3 \ + \ I_2 \ \longrightarrow \ 2NaI + Na_2S_4O_6$$
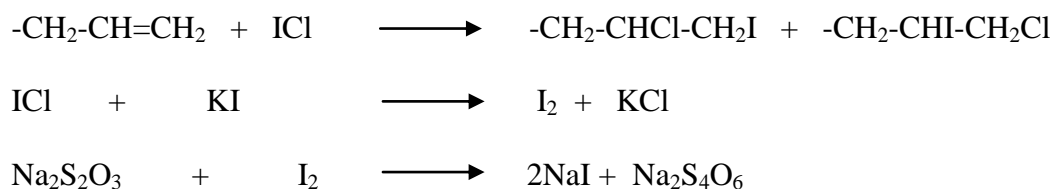
From the relation, 2000 mL of 1N $Na_2S_2O_3 = 1I_2 = n$ X C=C that is the molecular weight of the monomer, n is the number of double bonds.

This method is utilized to estimate the unsaturation amount during the kinetic studies. Approximately 40 mg of the monomer and initiator mixture is dissolved in chloroform and examined as per the procedure. By using following relation, the number of unsaturation was determined.

$$\text{No. of C=C} = \frac{(\text{Blank -Main reading}) \text{ x Normality of } Na_2S_2O_3 \text{ x Molecular weight}}{\text{Sample weight x 2000}}$$

CHAPTER 4

After confirming the unsaturation of ADC sample (minimum acceptable index of unsaturation for ADC is 1.95, theoretical is 2) and % purity of IPP initiator (minimum required purity 75% and above) both are in acceptable required limit, polymerization is carried out. The unsaturation analysis of intermediates like DAC, ADC monomers prepared by different method were studied simultaneously and compared with authentic ADC sample. It may be noted that the authentic ADC sample was also synthesised by us in the laboratory, repeatedly purified by vacuum distillation till index of unsaturation reaches as close as possible to 2 which is the index for pure ADC. It was also confirmed by matching its IR and NMR spectra with recorded spectra available in the literature. Needless to say that, if a sample of DAC or ADC was not showing the index of unsaturation within acceptable limits, it was purified repeatedly till these conditions are satisfied.

Different initiators can be utilised for free radical polymerization of the monomers. The two initiators used for polymerization were benzoyl peroxide (BP) and diisopropyl peroxydicarbonate (IPP). Several experiments were carried out to optimise the synthesis of precursor of the IPP initiator and also synthesis of IPP initiator was optimised on 5-6 g scale. For the preparation of IPP initiator which was again a two step synthesis as given previously, we first optimised the synthesis of IPCL on small scale and later on large scale and stored it in a refrigerator. IPCL prepared can be stored in refrigerator safely and can used over period of 2 months. To optimise IPCL synthesis on large scale it took a considerable time. It may be noted that IPCL synthesis using isopropyl alcohol and triphosgene works best in a specific solvent only but its purification from this solvent is time consuming process. The industrial synthesis of IPCL is faster process as they probably use phosgene gas.

As IPP is not stable at ambient temperature, it was prepared and analysed just before the polymerization process and stored at 0 $^{\circ}$C in refrigerator.

4.3.3 Preparation of PADC polymer

Many vinylic and allylic monomers suffer from volume shrinkage during polymerization.   It is well known fact that during polymerization process, ADC undergoes about 14% volume shrinkage. This causes the PADC film to bend inside the mould and leads eventually to a broken film or even a powder. This was avoided by pressurizing the mold periodically so that the mold plates are brought closer to each other thereby stopping the bending of the film. Since, we have fabricated a polymer press, it was necessary to get a few idea of the pressure to be actually used. Excess of pressure could result into breakage of glass plates of the molds itself.

The process of polymerization involved following steps:

 A. Assembling the mold

 B. Filling the mold with a mixture of monomer, initiator, and plasticizer.

 C. Actual polymerization which involves heating the filled molds with the help of polymer press and programmable circulating water bath.

The experiments towards the polymerization are briefly described below:

Initially, we used a polymerization mold assembled using a Teflon gasket and two optical glass plates from Asahi Glass (11.25" x 11.25" x 0.25"). The Teflon gasket with inner window of 10" x 10" was sandwiched between the two glass plates using some high quality binder. The monomer containing IPP initiator (~45 mL) was filled inside the mold using the syringe pump. It was observed that the glass sheets used started cracking while opening the molds after polymerization. So, we shifted to Schott Glass which was found to be relatively better.

CHAPTER 4

A.   **Assembling the mould and Mould design**[17 (a-g)]**:** An optical glass plates (from Schott, Germany) of the above mentioned size were used to assemble the mold. These plates were cleaned with solvents and then wiped with anti-dust cloth to assure that plates are clean and dust free. Commercial Teflon sheet (500 microns or 700 microns thick as per requirement) was heated under pressure to remove the wrinkles on its surface. It was then cut in a square shaped gasket having a width of one inch and a small opening as shown in figure 4.14. The gasket was sandwiched between two cleaned glass plates using binder. The mold was initially kept under polymer press overnight for pressing so that there is no leakage during the filling of monomer and polymerization. It was found that during filling of monomer in the mold, always the bubbles get trapped in it at the opening which could result in cracking as well as colouring of films. Therefore, we modified the design of Teflon gasket by keeping tapering at the opening lengthwise and height wise as shown in figure 4.14a, 4.14b and we increased the width to around 1.5- 2.0 cm to avoid leakage. This resulted in a smooth filling of the mold eliminating trapping of the bubbles. The mould assembly used for polymerisation is shown in the above said figures.
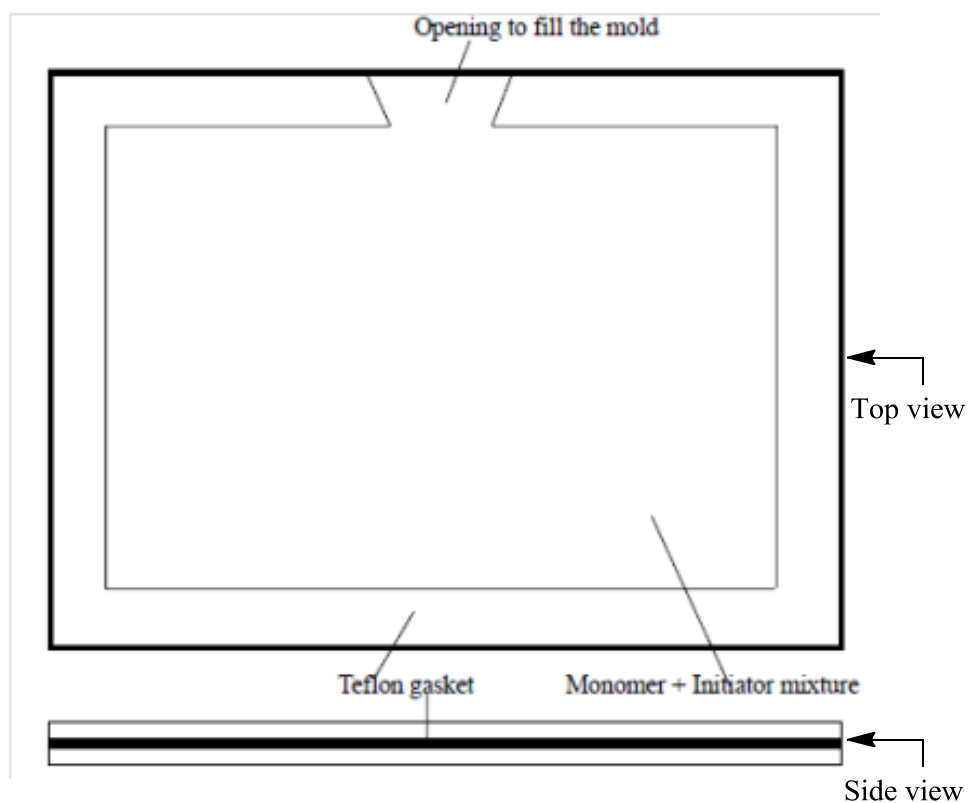
Figure 4.14:   Original design of the gasket and mould
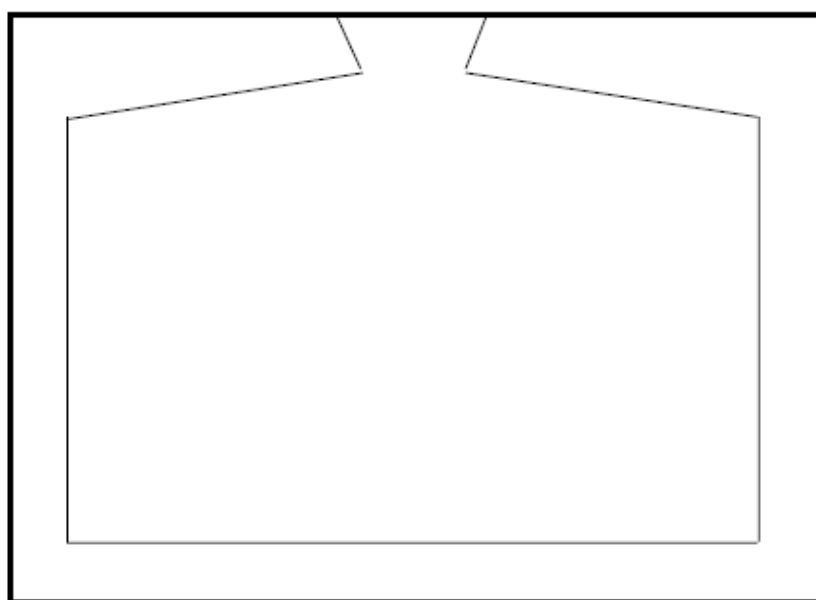
Figure 4.14 a: Modified design of the mould for horizontal filling.
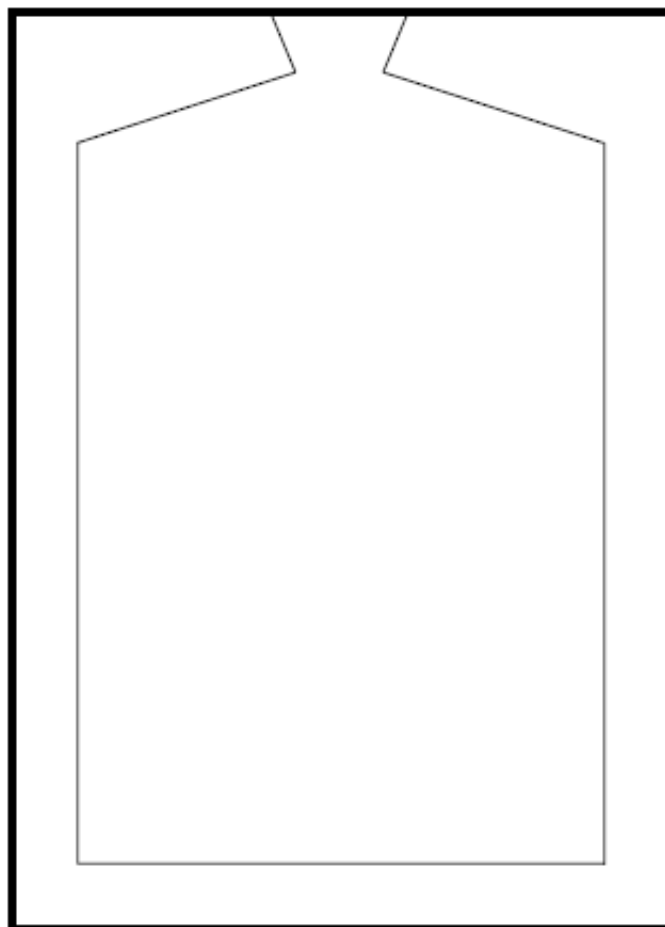
Figure 4.14 b: Mould that may be used with vertical filling.

B.   Filling the mold: Purified monomer was first filtered through a Teflon filter of 500 μm and than through 200 μm filter to remove suspended particles/ solids if any. The monomer was subjected to vacuum for about 10 minutes and then dry nitrogen was flushed for about 20 minutes. The process was repeated twice to completely remove the dissolved oxygen from the monomer. Initiator and the plasticizer were added to the flask and the contents were homogenized by swirling it. The polymerization mixture was carefully injected into the mold through the opening in the Teflon gasket avoiding the formation of air bubbles and the opening was sealed. This is shown below in the figure 4.15.

Figure 4.15: Filling a polymerization mould with syringe pump.

The volume of ADC required to fill a given mould can be calculated by knowing the size of inner window of the gasket and its thickness. In practice, about 1 to 1.5 mL in excess than this calculated amount is sufficient. This is indicated in Table 4.1 below.

Table 4.1: Volume of ADC required for filling a mould.

Sr. No.	Size of the mould (cm)	Size of the gasket (cm)	Calculated amount of ADC for 0.05 cm gasket (mL)	Calculated amount of ADC for 0.07 cm gasket (mL)
1	20 x 20	18 x 18	16.20	22.68
2	25 x 25	22 x 22	24.20	33.88
3	20 x 30	17 x 27	22.95	32.13
4	28 x 28	24 x 24	28.80	40.32

C.   Heating the mold (Polymerization): The mold containing monomer was placed in a Polymer press for heating which was connected to Julabo HL water bath and the heating was started. The molds were slightly pressurized during polymerization. After completion of 50-55% polymerization, pressure was increased slightly (by clockwise rotation of the screw) on to the mold and polymerization cycle was continued till completion of 12 hours. The mold was opened after cooling it to room temperature overnight (natural cooling took about 12 hours) followed by placing it in warm water for 2-3 hours to obtain an unbroken film of PADC with fine surface.

We conducted a few trials to arrive at a process that resulted in crack-free PADC films. Some photographs of cracked PADC films obtained during initial trials are shown in Figure 4.16 below to give an idea of severity of cracking.
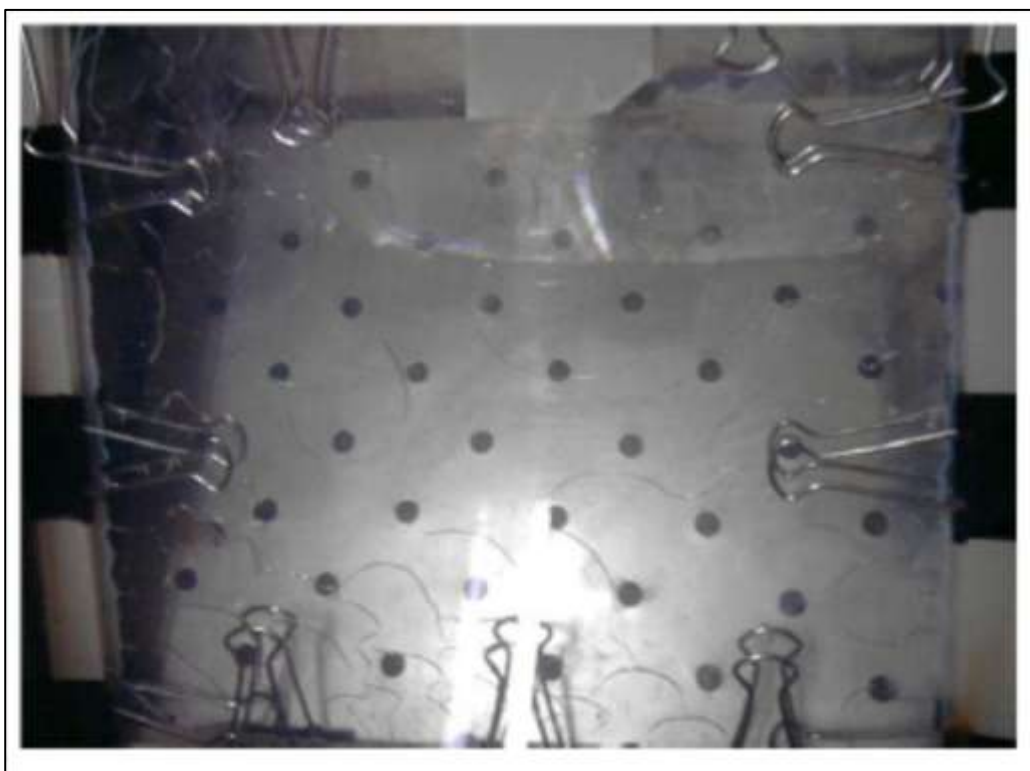
Figure 4.16:   Photograph indicating cracked PADC films

As mentioned previously, the allylic or vinyl polymerization process is strongly exothermic and hence auto-acceleration of polymerization is possible especially when an immobile gel starts forming from the monomer. Such a gel is definitely poor conductor of heat and hence if too much heat is evolved suddenly, a crack may be observed at that place. In order to avoid such problems a process of constant rate polymerization was suggested by Dial et al. They studied the kinetics of ADC polymerization[18] and proposed a set of kinetic equations using which one could calculate the temperature of polymerization bath that should be maintained at a given time under constant rate conditions. This avoids excess of heating of the mold at any given time and there is smooth evolution of heat during polymerization so that unwanted effects are almost avoided. Based on our previous studies[19], we decided to use heating profile generated for ADC polymerization for 12 hours and 24 hours as given in the table 4.2 and table 4.3 below.

Table 4.2: 12 hour time-temperature heating profile for ADC monomer

Sr. No.	Time in hours	Temperature in ^{o}C
1	0.0	42.76
2	1.0	43.57
3	2.0	44.47
4	3.0	45.46
5	4.0	46.59
6	5.0	47.87
7	6.0	49.38
8	7.0	51.21
9	8.0	53.51
10	9.0	56.65
11	10.0	61.76
12	11.0	72.00
13	12.0	90.00

14	13.0	95.00

Table 4.3: 24 hour time-temperature heating profile for ADC monomer

Sr. No.	Time in hours	Temperature in ^{o}C
1	0.0	42.76
2	1.0	43.57
3	2.0	44.47
4	3.0	45.46
5	4.0	46.59
6	5.0	47.87
7	6.0	49.38
8	7.0	51.21
9	8.0	53.51
10	9.0	56.65
11	10.0	61.76
12	11.0	72.00
13	11.5	80.00
14	12.0	80.00
15	13.0	80.00
16	14.0	80.00
17	15.0	80.00
18	16.0	80.00
19	17.0	80.00
20	18.0	80.00
21	19.0	80.00
22	19.5	80.00
23	20.0	85.00
24	20.5	85.00
25	21.0	90.00
26	22.0	90.00
27	23.0	90.00
28	23.5	95.00

29	24.0	95.00

It may be noted that 24 hours profile is not exactly similar to the 12 hour one. There are reports available indicating that heating the films around 80-90°C for longer time removes residual unsaturation and generates a PADC that is very smooth towards prolonged etching[20]. Hence, after the end of normal 12 hour profile, one may hold the moulds at constant temperature of 80°C for about 8 hours, followed by slowly raising the temperature further upto 95°C for the remaining period till 24 hours of heating is over.

We have already described modifications made in the design of the mold. In spite of this there was problem of uneven pressurising of the mold as evidenced from more adhesion of the PADC films at the centre of the mold. Hence, we modified the top platen of the polymer press in such a way that pressure was more evenly distributed and can be applied on the mold from top of press. This gave us good results and intact films were formed with this further modified polymer press. The intact PADC film made after polymer press modification is given in figure 4.17. Figure 4.18 shows the change made in the top platen design of the polymer press.

Figure 4.17: Photographs of intact PADC film (dimensions 10"x10").
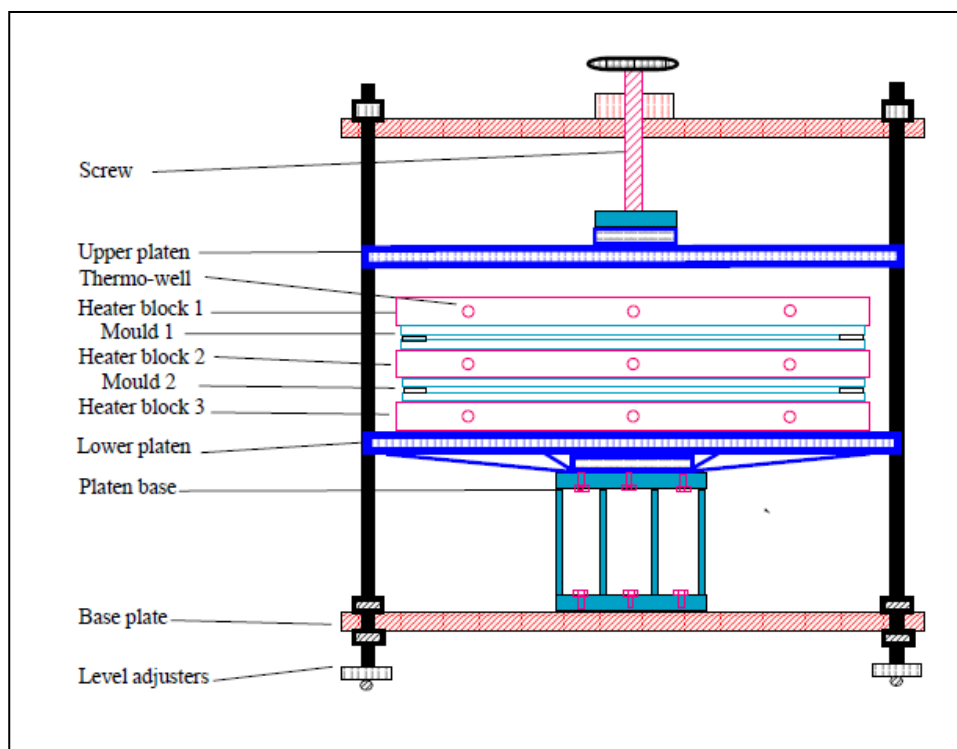
Figure 4.18: Change in the top platen design of the polymer press.

Later, we tried the polymerization directly using a water bath and found that good results are obtained even by this method. A typical water bath was fabricated for polymerization. A rectangular steel bath of size 20" x 15" was fitted with circular copper coil with around 20 windings as shown in figure 4.19. The inlet and outlet of the coil was connected to the Julabo HL programmable bath. The whole vessel was insulated with the black foam such that there is no loss of heat during polymerization. This vessel was used as a polymerization bath. The mould stand was placed inside the bath so that one can stack about three moulds one over other for polymerization. We noted that by using a larger sized bath fabricated as described in the foregoing discussion, it is possible to use this method to cast more detector films in a single polymerization experiment. Thus, unbroken detector films of the size 10"

x 10" of thickness 500 or 700 microns in sufficient number were cast as per our main objective and were sent to BARC for further studies. The results of are given below.

4.3.4   Parameters for dosimetric characterization of indigenous PADC sheets.

Minimum detection Limit (MDL): The dose equivalent at which signal is significantly greater than the background is called "Minimum detectable limit" of a dosimetric system. The unit of MDL is milli Sievert (mSv). It is represented by the equation below[21].

$$\text{MDL} = N_B \times 3\sigma$$

Where, N_B is the calibration factor (mSv/tracks cm^{-2}) for PADC detector, σ is the standard deviation of the background signal (number of tracks per cm^2 of unirradiated detectors) obtained from the average of the 20 unirradiated and processed detectors.

Dose linearity: Linearity in the response of PADC detector with increase in dose equivalent.

4.3.5   Testing and characterization of indigenous PADC sheets.

PADC sheets developed in different phases were tested for the dosimetric parameters such as MDL, sensitivity and signal to noise ratio. Based on these observations improvements in polymerization process were carried out to develop a dosimetric grade PADC sheet.

4.3.5.1   Phase I: In the initial testing, two sheets (labelled as A & B) of thicknesses 530 micron and 600 micron were used. The sheets obtained were very brittle and broken during removal from glass moulds. For their neutron sensitivity

studies, each film was cut into nine and fifteen pieces of size 3 x3 cm. The results are shown in Table 4.4. It was observed that, in sheet A, the background tracks were very high. Although the background of sheet B was comparable to reference CR-39, its sensitivity to neutrons was poor with signal to noise ratio of 1.6 as compared to 7.5 of reference CR-39.

Table 4.4: Preliminary testing of indigenous PADC with reference CR-39 in phase I

Sheet label	Thickness (μm)	Average background track density (tracks cm^{-2})	*Total average track density (tracks cm^{-2} mSv^{-1})	*Net Track density (tracks cm^{-2} mSv^{-1})	Signal to noise ratio
Reference CR-39	635±30	27±6	229±12	202±3.1	7.48
Sheet A	530±45	1006±54	850±462	-----	----
Sheet B	600 ±62	24±3	64±16	40±4	1.66

Note: * counts are average of three detectors.

4.3.5.2   Phase II: In phase-II, the PADC films were prepared after the rectification of the polymer press carried out to maintain uniform pressure and temperature. Two sheets (labelled C and D) were analysed in this phase. Sheet C and D were of 800 micron in thickness. Again nine pieces of 3 x 3 cm were made from each sheet for further analysis. The results on the track density of the control (unirradiated) and exposed detectors are shown in Table 4.5. Signal to noise ratio of sheet C was found to be comparable to that of reference sheet and but for sheet D the signal to ratio was poor. Based on these results, it was decided to prepare more number of sheets of thickness 600 micron to generate good data on neutron sensitivity and MDL.

CHAPTER 4

In the second lot of phase II, three sheets (labelled as E to G as shown in Table 4.5) were prepared as per the requirements from previous testing. The results are shown in the Table 4.5. It was observed that the signal to noise ratio of sheet F was close to reference CR-39 but other sheets were not of dosimetric grade in terms of sensitivity. In this phase, sheets were prepared with uniform surface having no cracks but their sensitivity was not similar to that of reference CR-39. Further, in order to have PADC sheets with higher neutron sensitivity, it was decided to use less amount of plasticizers i.e. 0.1% DOP as compared to the presently tested sheets which had 1% DOP. 3.3% of IPP initiator was used and its quantity was not varied.

Table 4.5: Results of the neutron sensitivity and background track density of sheets in phase II

Sheet label	Thickness (μm)	* Average background track density (tracks cm^{-2})	*Total average background track density (tracks cm^{-2} mSv^{-1})	*Net Track density (tracks cm^{-2} mSv^{-1})	Signal to noise ratio
Sheet C	800±25	24 ± 12	202 ±7	74±14	3.08
Sheet D	800±30	20 ± 7	109 ± 8	37±20	1.85
Sheet E	600±34	607±67	798±27	95±72	0.15
Sheet F	500±46	97±36	487±10	195±37	2.01
Sheet G	600±30	93 ± 46	118 ± 38	10.4±59	0.11
Reference CR-39	625±34	54±9	250 ±8	196±12	3.63

Note: * counts are average of three detectors.

4.3.5.3   Phase III: In the final phase III of testing, two batches comprising of eight and six intact sheets with dimensions 240 x 130 cm were used.   These sheets were physically clear, transparent and strong. These sheets were cut into 3 x 3 cm

pieces and thicknesses of these pieces were measured at all the four edges. They showed varying thicknesses as shown in Table 4.12. These films were divided into two groups based on the thicknesses so that appropriate voltage for etching can be applied. In the first group, eight sheets labelled from H, to M with thickness 520 ± 31 micron and in second group, sheet N and O with thickness 730 ± 28 micron were placed. For these two groups, the etching voltages were 1150V and 1600V respectively based on average thickness keeping the electric field strength at 22 kVcm^{-1}. A total of 108 detectors were utilised for testing. Out of 108, 53 detectors were kept as control and 55 were exposed to 2 mSv neutron dose equivalent. In order to observe the consistency of their neutron sensitivity/response, etching of these detectors were carried out in groups of equal numbers of control and exposed (3 detectors each) at a time.

Table 4.6 shows the results on the neutron sensitivity and background tracks of these detectors. Only J and N sheets of first group showed acceptable control, exposed track density and good signal to noise ratio (>3) as compared to rest films. Sheets H and M showed high background (>100 tracks/cm^2) and signal was less. Sheet O was unsatisfactory due to its negligible sensitivity. In case of sheet I, K and L the signal to noise ratio was poor (around 1.5), they were not of dosimetric grade. Only in sheet N and O, the average signal to noise ratio was around 3.0 near to the reference CR-39 detector used in neutron monitoring. Sheets N and O, could produced consistent results in two trials of processing. All sheets tested in this lot were polymerized with 12 h constant rate polymerization cycle. In order to improve the performance of the detector further, it was therefore decided to increase the constant rate polymerization cycle duration to 24 h.

Table 4.6: Results on track density and signal to noise ratio of eight PADC sheets in phase III

Sheet label	Thickness (μm)	Etching Voltage (V)	* Average background Track density (tracks cm^{-2})	*Net Track density (tracks cm^{-2}mSv^{-1})	Signal to noise ratio	No. of detectors with acceptable control (30-100 tracks cm^{-2})	No. of detectors acceptable based on signal to noise ratio(>3.0)	Performance of the sheet
H	505±48	1150	270 ± 156	156.3± 40	0.58	0	0	unsatisfactory
I	494±25	1150	98 ± 47	119.3±30	1.22	3	0	Not dosimetric grade
J	550±50	1150	37 ± 26	143.2±20	3.86	3	3	Dosimetric grade
K	482±55	1150	154 ± 102	194.9±60	1.26	1	0	Not dosimetric grade
L	560±38	1150	85.6± 16.8	136 ± 18	1.6	5	6	Not dosimetric grade
M	530±56	1150	45.8 ± 11.9	39 ± 13.0	0.7	3	10	Unsatisfactory
N	750±37	1600	33 ± 5	136.5±8	4.09	4	3	Dosimetric grade
O	710±58	1600	273 ± 44	18.6±40	0.07	0	0	unsatisfactory

Note: *counts are average of three experiments with five detectors. All the sheets were polymerized with 12h curing cycle.

In the second batch, six sheets were labelled from P to U. In order to investigate the variation in background with respect to the two surfaces of the sheet, the top and bottom surface were marked as S1 and S2. Sheets were cut into 3 x 3cm and thickness was measured at all the four edges. They were divided into three groups based on their thicknesses. Sheet P and T were placed in one group, sheet Q and R were placed in second group and sheet S and U were placed in third group as shown in table 4.7 along with their etching voltages. Sheets T and U were polymerized with 24 h constant rate polymerization cycle while the rest were

prepared with 12 h constant rate polymerization cycle. Three PADC detectors were irradiated with S1 side and three with S2 side and etched along with control (also etched on both sides) for background and sensitivity. The film surface with lower background was identified and that particular surface was used for further studies on reproducibility of results and dose linearity. Out of 142, 54 detectors were kept as control and 88 were exposed to different doses.

Table 4.7 provides the details of results like track density, background track density and signal to noise ratio etc. for each sheet with respect to its side. The average results of three etchings carried out to verify the consistency in sensitivity of the sheets is also shown. In sheet P and Q, S2 side showed lower background. However, the MDL was around 0.4 and 0.3 mSv respectively. The signal to noise ratio was around 4.7. Although, the background and signal to noise ratio was acceptable, the MDL was high, due to which the sheets could not be used for low dose measurements as required in personnel monitoring. These sheets can be used in high dose measurements as in experiments. They are considered to be satisfactory. Sheet R showed dosimetric quality on S2 side. The S1 side was satisfactory. All the other sheets from S to U were tested and found to be of dosimetric grade (criteria for dosimetric quality is signal to noise ratio should greater than 3 and MDL ≤0.2mSv). Both sides of the sheets from S-U were acceptable as they have lower background track density and high signal to noise ratio. The MDL was upto 0.2 mSv as required for personnel monitoring. These sheets were promising as they fit the acceptance criteria.

Sheets R and S were prepared using 12 h curing cycle where as T and U were polymerized with 24 h curing cycle. The sheets exhibit good dosimetric characteristics as that of reference CR-39 detector. As quality of PADC sheet

depends on the purity of the monomer, the most important ingredient of PADC, it is essential to have severe checks on the purity of monomer. As observed from table 4.6, in case of 12 h curing, out of eight sheets only two were of dosimetric quality and in table 4.7, out of four sheets, two were satisfactory and two were dosimetric grade. In case of 24 h curing, only two sheets were prepared and both have dosimetric quality. Therefore, it can be predicted that 24 h curing has better chance of providing dosimetric grade sheets due to prolonged and slow polymerization which leads to sheets with uniform surface. The sheets prepared with 24 h curing cycle were found out to be promising for neutron personnel monitoring.

This continuous improvement in constant rate polymerization cycle over a period of three years had finally succeeded in producing dosimetric grade PADC which can be used for neutron monitoring. Sheets of larger size using a large polymer press can now be polymerized without cracking. Uniformity of the sheets could also be maintained.

Table 4.7: Results of last lot of six PADC sheets in Phase III

Sheet label	Thickness (μm)	Curing details (h)	Etching Voltage (V)	Sheet side with less bkg.	*Average background Track density (tracks cm^{-2})	*Net Track density (tracks cm^{-2} mSv^{-1})	Signal to noise ratio	MDL (mSv)	Performance of the sheet
P	470±48.2	12	1050	S2	58 ± 40	275.9 ± 63	4.7	0.4	satisfactory
Q	540±57.9	12	1200	S2	53 ± 27	255.4 ± 29	4.8	0.3	satisfactory

R	5405±2.2	12	1200	S1	54 ± 26	233.8 ± 5	4.4	0.3	Good dosimetric quality on S2 side
				S2	46 ± 19	260.4 ± 44	5.7	0.2	
S	560±53.4	12	1250	S1	69 ± 14	217.7 ± 8	3.2	0.2	Good dosimetric quality
				S2	52 ± 16	276.9 ± 28	5.3	0.2	
T	480±9.46	24	1050	S1	29 ± 7	256.7 ± 10	9.0	0.08	Good dosimetric quality.
				S2	46 ± 17	239.6 ± 19	5.2	0.2	
U	570±46.1	24	1250	S1	60 ± 3	215.0 ± 29	3.6	0.04	Good dosimetric quality.
				S2	32 ±8	264.7 ± 33	8.3	0.09	

Note:*counts are average of three experiments with five detectors. Sheets labelled P, Q, R, S were polymerized with 12h curing cycle whereas sheets labelled T and U were polymerized with 24h curing cycle.

4.4   Conclusion

A method for casting unbroken PADC sheets of size 10" x 10" and thickness of 500-800 microns has been developed. This requires ADC monomer and IPP initiator of high purity as characterized by minimum index of unsaturation of 1.95 for ADC monomer and minimum of 70% purity for IPP initiator. Polymerization moulds made of toughened Pyran S (Schott) glass with thickness between 6-8 mm should be used. Teflon was used as gasket material. The gasket shape was modified so as to avoid trapping of air in the mould. The process involves gradually heating the filled polymerization mould in a polymer press whose heating is controlled using a programmable circulating water bath for a suitable period like 12 hours, 24 hours or more. Cast polymerization for longer period of time resulted in good quality detector films. Detector film thickness was also found to vary because of the variation in thickness of both gasket material and glass sheets which were procured

externally. The entire process of evaluating an indigenous PADC sheet starting from detector preparation, irradiation, etching and counting has been standardized.

It was observed that polymerization using 24 hours curing cycle results in better quality dosimetric grade detector sheets. Curing cycle of 24 h could produce PADC sheets with MDL of 0.1 mSv and signal to noise ratio of 8.0 which is similar to reference CR-39. We feel that these details could be used to produce PADC detector films suitable for the personnel neutron monitoring programme.

CHAPTER 4

4.5   References:

1. (a) Griffith, R. V; Hankins, D. E.; Gammage, R. B.; Tommasino, L.; Wheeler, R. V. *Health Phys.* **1979**, *36* (3), 235–260. (b) Nakamura, T. *Indian J. Pure Appl. Phys.* **2012**, *50* (July), 427–438. (c) Alevra, A. V. *Radioprotection* **1999**, *34* (3), 305–333.

2. Durrani, S. A. *Radiat. Meas.* **2008**, *43*, *Supplement 1*, S26–S33.

3. Cartwright, B. G.; Shirk, E. K.; Price, P. B. *Nucl. Instruments Methods* **1978**, *153* (2), 457–460.

4. (a) Harrison, K. G.; Tommasino, L. *Radiat. Prot. Dosimetry* **1985**, *10* (1–4), 219–235. (b) Matiullah; Ahmad, A.; Durrani, S. A.; Kudo, K. *Nucl. Instruments Methods Phys. Res. B* **1990**, *51* (October), 76–84. (c) Tanner, R. J.; Bartlett, D. T.; Hager, L. G. *Radiat. Meas.* **2005**, *40* (2–6), 549–559.

5. Piesch, E.; Al-Najjar, S. A. R.; Ninomiya, K. *Radiat. Prot. Dosimetry* **1989**, *27* (4), 215–230.

6. Bassett, J.; Denney, R. C.; Jeffery, G. H.; Mendham, J. *Vogel's Textbook of Quantitative Inorganic Analysis*, 4th Edition; 1978.

7. (a) Muskat, I. E.; Strain, F. Carbonic acid esters of polyhydroxy compounds. U.S. Patent 2,370,567, 1945. (b) Dial, W. R.; Gould, C. Method of casting resins. U.S. Patent 2,379,218, 1945.

8. (a) Ugo, Romano EPO Appl.No. 0035304/1981 (Chem Abstr.,98, 142969). (b) Ugo Romano GB 2 098 984/1981 (Chem Abstr., 96, 69576). (c) M. Pellegrina, Y. Proux, EP 72325 (Chem. Abstr. 99, 6486). (d) Nadkarni, V. S.; Tilve, S. G.; Mascarenhas, A. A. A. An Improved Process for Preparation of carbonates. IP196627, 2005.

9. Adelson, D. E.; Dannenberg, H. Copolymers of allyl esters. USP 2,514,354, 1950.

10. (a) Hoffman, W. A. *J. Org. Chem.* **1982**, *47* (26), 5209–5210. (b) Holt, T.; Simpson, W. *Proc. R. Soc. London A Math. Phys. Eng. Sci.* **1956**, *238* (1213), 154–174. (c) Fukui, K.; Yoneda, S.; Takayama, H.; Kitano, H. *J. Soc. Chem. Ind. Japan* **1960**, *63* (12), 2146–2148. (d) Fischer, K. D.; Himmele, W. D.; Kaibel, G. D. I.; Barl, M. D.; Schneider, K. D. Dialkyl carbonate esters production by ester interchange of dimethyl carbonate and alcohol, using (cyclo)paraffin as entrainer for methanol. DE 2749754, May 10, 1979. (e) Doya,

M.; Ohkawa, T.; Kamihara, Y. Preparation of diallyl carbonate from allyl alcohol and urea. JP 10259165 A 19980929., 1998. (f) Barneis, Z.; Broeir, Y.; Bittner, S., Synthesis of carbonates and carbamates from dialkylazodicarboxylates. *Chem. Ind. (London)* **1976**, *(12)*, 526-527. (g) Altuglu, S.; Preparation of allyl carbonate using sodium hydroxide. 1980-3042271, 19801108., 1981. (h) Nefedov, B. K.; Sergeeva, N. S.; Eidus, Y. T. Synthesis of symmetrical unsaturated mono- and polycarbonates by carbon monoxide carbonylation of allyl alcohol in the presence of mercury acetate. *Izv. Akad. Nauk SSSR, Ser. Khim.* **1973**, (1), 137-138.

11. Mascarenhas, A. A. A. Development of plastic materials for nuclear track detection, Goa University, 2007, PhD Thesis.

12. Pasquato, L.; Modena, G.; Cotarca, L.; Delogue, P.; Mantovani, S. *J. Org. Chem.* **2000**, *65*, 8224-8228.

13. *US Pat.* 2 592 058, 1952.

14. Strain, F.; Bissinger, W. E.; Dial, W. R.; Rudoff, H.; DeWitt, B. J.; Stevens, H. C.; Langston, J. H. *J. Am. Chem. Soc.* **1950**, *72* (3), 1254–1263.

15. Vogel, A. I. *Elementary Practical Organic Chemistry Part III*; 1958.

16. Nozaki, K. *Ind. Eng. Chem. Anal. Ed.* **1946**, *18* (9), 583-583.

17. (a) Fowler, P. H.; Clapham, V. M.; Henshaw, D. L.; O'Sullivan, D.; Thompson, A. In *Solid State Nuclear Track Detectors Proceedings of the 10th International Conference, Lyon, 2–6 July*; Francois, H., Massue, J. P., Schmitt, R., Kurtz, N., Monnin, M., Durrani, S. A., Eds.; Pergamon, 1980; pp 437–441. (b) Henshaw, D. L.; Griffiths, N.; Landen, O. A. L.; Austin, S. P.; Hopgood, A. A. In *Proceedings of 11th International Conference on Solid State Nuclear Track Detectors, Bristol*; Fowler, P. H., Clapham, V. M., Eds.; Pergamon: Amsterdam, 1982; pp 137–140. (c) Henshaw, D. L.; Griffiths, N.; Landen, O. A. L.; Benton, E. V. *Nucl. Instruments Methods* **1981**, *180* (1), 65–77. (d) Turner, T. W.; Clapham, V. M.; Fews, A. P.; Henshaw, D. L. In *Proceedings of international conference on Solid State Nuclear Track Detectors,Bristol*; Fowler, P. H., Clapham, V. M., Eds.; Pergamon: Amsterdam, 1982; pp 141–144. (e) Portwood, T.; Turner, T. W.; Fews, A. P. *Nucl. Tracks Radiat. Meas.* **1984**, *8* (1), 155–158. (f) Manzoor, S.; Khan, H. A.; Matiullah; Tufail, M.; Qureshi, A. A.; Ansari, F.; Shoaib, R.; Lembo, L. *Int. J. Radiat. Appl. Instrumentation. Part D. Nucl.*

Tracks Radiat. Meas. **1988**, *15* (1), 207–210. (g) Stejny, J.; Carrell, J.; Palmer, M. J. *Radiat. Meas.* **2000**, *32* (4), 299–305.

18. Dial, W. R.; Bissinger, W. E.; DeWitt, B. J.; Strain, F. *Ind. Eng. Chem.* **1955**, *47* (12), 2447–2451.

19. Mandrekar, V. K. Novel Polymeric Materials for Nuclear Track Detection, Goa University, 2010, Ph.D Thesis.

20. Kinoshita, K.; Price, P. B. *Rev. Sci. Instrum.* **1980**, *51* (1), 32.

21. Pal, R. R.; Jayalakshmi, V.; Sathian, D.; Chaurasiya, G.; *IEEE Transactions on Nuclear Science,* **2009**, *56,* (6), 3774-3778.